

# Northumbria Research Link

Citation: Risdonne, Valentina (2022) Materials and techniques for coating of the nineteenth-century plaster casts. A scientific and archival investigation of the Victoria & Albert museum cast collection. Doctoral thesis, Northumbria University.

This version was downloaded from Northumbria Research Link:  
<http://nrl.northumbria.ac.uk/id/eprint/49513/>

Northumbria University has developed Northumbria Research Link (NRL) to enable users to access the University's research output. Copyright © and moral rights for items on NRL are retained by the individual author(s) and/or other copyright owners. Single copies of full items can be reproduced, displayed or performed, and given to third parties in any format or medium for personal research or study, educational, or not-for-profit purposes without prior permission or charge, provided the authors, title and full bibliographic details are given, as well as a hyperlink and/or URL to the original metadata page. The content must not be changed in any way. Full items must not be sold commercially in any format or medium without formal permission of the copyright holder. The full policy is available online: <http://nrl.northumbria.ac.uk/policies.html>

**MATERIALS AND TECHNIQUES  
FOR COATING OF THE  
NINETEENTH-CENTURY  
PLASTER CASTS.  
A SCIENTIFIC AND ARCHIVAL  
INVESTIGATION OF THE  
VICTORIA & ALBERT MUSEUM  
CAST COLLECTION.**

V RISDONNE

PhD

Volume 2 of 2

2022



**MATERIALS AND TECHNIQUES  
FOR COATING OF THE  
NINETEENTH-CENTURY  
PLASTER CASTS.  
A SCIENTIFIC AND ARCHIVAL  
INVESTIGATION OF THE  
VICTORIA & ALBERT MUSEUM  
CAST COLLECTION.**

VALENTINA RISDONNE

A thesis submitted in partial fulfilment of the requirements of  
the University of Northumbria at Newcastle for the degree of  
Doctor of Philosophy

Research undertaken in the Faculty of Arts, Design & Social  
Sciences and in collaboration with the Victoria & Albert  
Museum

Volume 2 of 2

January 2022



**VOLUME 2**

List of contents	III
<b>Appendices</b>	<b>1</b>
Appendix 1. Plaster cast collections around the World	3
Appendix 2. A summary timeline of the V&A Museum	17
Appendix 3. Historical technical literature	21
Appendix 4. Patents	69
Appendix 5. V&A casts	87
Appendix 6. V&A analysis reports	103
Appendix 7. V&A museum environment	405
Appendix 8. Calculations	415
Appendix 9. Additional tables and figures	431
<b>Glossary</b>	<b>483</b>





## APPENDICES



## APPENDIX 1. PLASTER CAST COLLECTIONS AROUND THE WORLD

---

Collection	Created	Reference
State museums, Collection of Antiquities, Kassel (DE)	1603	
Royal Academy of Fine Arts of San Fernando, Madrid (ES)	1649	Frederiksen & Marchand (2010)
National School of Fine Arts, Paris (FR)	1666	
Collection of casts of Geneva School of Fine Arts (CH)	1751	
Filippo Farsetti Collection, Venezia (IT)	1752	Androsov (1991)
The Royal Danish Academy of Fine Arts Copenhagen (DK)	1754	
Collections of the Archaeological Institute, University of Göttingen (DE)	1767	Fittschen & Bergemann (1990)
The Royal Academy London (UK)	1768	
Mantova Academy (IT)	1769	
Brera Academy of Fine Arts in Milan (IT)	1775	Valli (2008)
Collection of casts from the University of Geneva (CH)	1778	Grange (1992)
The Royal Academy of Fine Arts Stockholm (SE)	1780	
Cast collection of the Dresden Sculpture Collection (DE)	1784	
National Museum of Stockholm (SE)	1784	
Museum of Scientific Research of the Academy Fine Arts, Petersburg (RU)	1788	
National School of Plastic Arts. Academia San Carlos, Mexico City (MX)	1791	
The Louvre Museum's moulding workshop, Paris (FR)	1794	Rionnet (1996)
Pennsylvania Academy of Fine Art, Philadelphia (US)	1805	
Bern Collection of Antiquities (CH)	1806	
Crawford Municipal Art Gallery (IE)	1818	
National Museum, Prague (CZ)	1818	Frederiksen & Marchand (2010)
Gipsformerei, Berlin (DE)	1919	

Academic Art Museum, Bonn (DE)	1820	
Higher Institute of Art Adolfo Venturi, Modena (IT)	1821	
Maastricht Academy of Visual Arts (NL)	1823	
Plaster cast collection, Kaliningrad (RU)	1824	
Sir John Soane's Museum, London (UK)	1827	Dorey et al. (1992)
Observatory of Sciences of the Universe, University Lyon 1 (FR)	1830-40	
Collection of casts, Château de Pierrefonds (FR)	1833	
Antonio Canova Museum and Gipsoteca, Possagno (IT)	1836	Hemingway (2002)
Phrenology museums, Paris (FR)	1836	
Sculpture collection. Faculty of Fine Arts, University of Lisbon (PT)	1836	
Museum Schloss Hohentübingen (DE)	1836	
Brussels phrenological museum (BE)	1839	Barthel (1841)
David d'Angers Gallery (FR)	1839	Huchard (1984)
Collection of casts from the University of Leipzig (DE)	1840	
Antoine Vivenel Museum, Compiègne (FR)	1841	
Art Museum, Uppsala University (SE)	1841	
Manufacture of Christian Art. The Sainterie De Vendevre-Sur-Barse (FR)	1842	Poulat (1980)
Collection of antiquities at the Kunsthalle zu Kiel (DE)	1843	
Institute of Art and Design, Birmingham (UK)	1843	
Schinkel Museum, Building Academy Berlin (DE)	1844	
Archaeological Museum of the University, Robertinum, Halle (DE)	1845	
Cast Gallery Ashmolean Museum, Oxford (UK)	1845	Kurtz (2000)
Glasgow School of Art (UK)	1845	
Collection of casts from the former University's Archaeological Institute, Jena (DE)	1846	
Museum of casts in Athens (GR)	1846	
Institute of Anatomy. University Rene Descarte Paris 5(FR)	1847	
Collection of casts from the archaeological institute of the University of Heidelberg (DE)	1848	

State Lindenau Museum Altenburg (DE)	1848	
Thorvaldsens Museum Copenhagen (DK)	1848	
L. Bartolini Works, Gallery of the Academy of Florence (IT)	1850	
Villa Medici: The French Academy in Rome (IT)	1850	Delivre (1991)
Academy of Fine Arts, Vienna (AT)	1851	Hagen (2007)
Glyptothek Gemäldegalerie of the Academy of Fine Arts Vienna (AT)	1851	Hagen (2007)
Crystal Palace, London (UK)	1851	Kenworthy-Browne (2006)
The archaeological collection of the University of Zurich (CH)	1852	Zindel (1998)
Collection of casts from the archaeological institute of the University of Hamburg (DE)	1852	
City College of New York (US)	1852	
University College Cork (IE)	1855	
Collection of Antiquities Friedrich-Alexander, University Erlangen (DE)	1857	
Catholic Institute of Vaucouleurs (FR)	1860	
Museum of Natural Sciences of Aix-en-Provence (FR)	1860	
The Nicholson Museum, Sydney (AU)	1860	Trendall (1941)
Plaster casts Museum. University of Urbino (IT)	1861	Gasparri (1990)
Cast collection Catholic University of Leuven (BE)	1864	Driessche (2016)
Collection of seal casts from the General Archives of the Kingdom, Bruxelles (BE)	1864	Laurent (2003)
Collection of casts, Louvain-la-Neuve Museum (BE)	1864	
Collection of casts from the Archaeological Seminar of the University of Marburg (DE)	1866	
Vassar college plaster cast collection (US)	1866	
Rollet Museum of the City of Baden (AT)	1867	Firla (1999)
The collection of mathematical models, Technical University of Vienna (AT)	1868	
Archaeological Collection, Institute for Classical Archaeology, University of Vienna (AT)	1869	Meyer (2008)
Museum of casts of classical sculptures in Munich (DE)	1869	Bildwerke et al. (1909)

Museum of casts and original collection. Institute for Classical Archaeology, Innsbruck (AT)	1869	Dietrich (2001)
Casting workshop of the Royal Museums of Art and History, Bruxelles (BE)	1870	Rousseau (1926)
Men's cabinet and antique collection Winterthur (CH)	1870	
Metropolitan Museum of Art, New York (US)	1870	Robinson (1913)
Art Institute of Chicago (US)	1871	Emerson (1907)
Lorenzi. Art casts, Arcueil (FR)	1871	
Museum Of Funeral Art. Former Atelier Ernest Salu (BE)	1872	
Strasbourg Gypsothèque (FR)	1872	Morinière (2015)
Archaeological plaster cast collection of the University of Rostock (DE)	1873	
Department of Art History, University of Helsinki (FI)	1873	Nikula (2003)
The Cast Collection of Ancient Sculpture, Faculty of Arts, Charles University (CZ)	1873	Dufkova (1987)
Victoria and Albert Museum. The Cast Courts (UK)	1873	Baker (1982)
Institute for Mathematics, Martin Luther University (DE)	1875	
Museum of Ethnology. Anthropological Collection, Dresden (DE)	1875	
Museum of Fine Arts, Boston (US)	1876	Cambareri (2011)
National Museum of artistic reproductions, Madrid (ES)	1877	Almagro (1989)
National Museum of sculpture, Valladolid (ES)	1877	
Auckland War Memorial Museum. Russel's Cast collection (NZ)	1878	
Collection of Angkor Wat casts. Guimet Museum, Paris (FR)	1878	
The National History Museum at Frederiksborg Castle, Hillerød (DK)	1878	
Allard Pierson Museum, Amsterdam (NL)	1879	
Anatomy Museum of the Otago Medical School (NZ)	1879	
Educational collection of the former Institute of Zootechnics of UCL (BE)	1881	
City of architecture (formerly: Musée des Monuments Français) Paris (FR)	1882	
Mount Holyoke College Art Museum (US)	1882	

Museum of Classical Archaeology. Cast Collection, Cambridge (UK)	1883	
Archaeological Museum of the Westphalian Wilhelm University - Collection of casts of ancient sculptures (DE)	1884	Dierichs (1999)
Museum of Invertebrate Paleontology, Lawrence (US)	1884	
Collection of antique and medieval casts from the Faculty of Letters of Bordeaux (FR)	1886	
Royal museums of art and history. Museum of moulds, Brussels (BE)	1886	Rousseau (1897)
Telfair Academy Museum (US)	1886	
The Wilcox Museum, Lawrence (US)	1886	
Dijon Museum of Fine Arts (FR)	1887	
Gipsoteca of the Department of Archaeological Sciences. Faculty of Literature, University of Pisa (IT)	1887	Donati (1999)
Sculpture Hall Basel. Collection of casts in the Museum of Antiquities (CH)	1887	
Slater Memorial Museum, Norwich (US)	1887	
The caves of Conjoux (BE)	1887	
Collection of Casts from the University of Franche-Comté, Besançon (FR)	1889-92	
Auguste Fraikin Museum (BE)	1890	
Museum of casts of the University of Montpellier III (FR)	1890	
Classical art museum. La Sapienza University of Rome (IT)	1892	Morricone (1981)
Collection of casts from the Institute of Art and Archaeology, Paris (FR)	1891	
Oriental Institute University of Chicago (US)	1891	
Museum of the Certosa di Pavia: Gipsoteca (IT)	1892	
P. Caproni & Brother, Cast Factory (US)	1892	
Altgeld Model Collection. University of Illinois: Campus Tours (US)	1893	
Museum of moulds, University of light Lyon 2 (FR)	1893	
Peabody Museum of Archaeology and Ethnology. Harvard University (US)	1893	
Blanton Museum of Art. The William J. Battle collection of Plaster Cast, Austin (US)	1894	
Haenecour workshop (BE)	1894	

Laurence Hutton Collection of Life and Death Masks (US)	1894	
Wright Museum of Art. Beloit College. Fischer collection (US)	1894	
Rodin Museum, Meudon (FR)	1895	
Royal Casting Collection Copenhagen (DK)	1895	
The Cast Gallery University of Missouri, Columbia (US)	1895-1902	
Museum of Fine Art of Budapest (HU)	1896	
Casts from the Egyptian collection of the Royal Museums of Art and History (BE)	1897	Van Rinsveld (1997)
Royal Museum of Central Africa (BE)	1897	
The University of Costa Rica, Plastic Arts School (CR)	1897	
State Museum of A.S. Pushkin, Moskov (RU)	1898	
Vincenzo Vela Museum, Ligornetto (IT)	1898	
Cesare Lombroso Museum of Criminal Anthropology, Turin (IT)	1899	
Collection of casts, Museum of Fine Arts of Anger (FR)	End 19th c.	
Faculty of Mathematics Rijksuniversiteit Groningen (NL)	End 19th c.	
Gipsoteca of the State Institute of Art, Florence (IT)	End 19th c.	Hubbard (2002)
Laboratory of mathematics of the Université de Franche-Comté, Besançon (FR)	End 19th c.	
Museum of Copies at the National Museum of Fine Arts in Santiago (CL)	End 19th c.	
The University of Tokyo. Architecture Department (JP)	End 19th c.	
The University of Tokyo. Graduate School of Agricultural and Life Sciences (JP)	End 19th c.	
University of Iowa collection, Iowa City (US)	End 19th c.	
Flaubert and History of Medicine Museum (FR)	Beginning 20th c.	Vimont (1994)
Gipsoteca of the University Museums of the University of Pavia (IT)	1900	
Gipsoteca of the Foundation Pietro Vannucci of the Academy of Fine Arts of Perugia (IT)	1900	
Schola Graphidis Art Collection (HU)	1900	
The University of California. Bay Area Casts (US)	1902	
Villa Kerylos, Beaulieu-sur-Mer (FR)	1902-08	

Harvard Arts Museum: Busch-Reisinger Museum (US)	1903	
Cast Collection of the Maryland Institute College of Art (US)	1904	Basile (2014)
Ethnological Museum of the National Museums in Berlin (DE)	1906	
Gipsoteca of the Museum of Archaeological Sciences and Art, University of Padua (IT)	1906	Menegazzi (2008)
Carnegie Museum of Art. Hall of architecture and sculpture (US)	1907	
Sergey Merkurov Museum (AM)	1907	
Edinburgh College of Art (UK)	1911	Smailes (1991)
Museum of Roman Civilization, Rome (IT)	1911	
Ivan Tsvetaev Educational Art Museum, Moskov (RU)	1912	
Gipsoteca Davide Calandra, Savigliano (IT)	1913	
Dihigo Museum. University of Havana (CU)	1919	
Feste Rosenberg, cast collection of medieval sculptures (DE)	1920	
Museum of Antiquities, Department of Classics, Lund University (SE)	1920	
Collection of casts of ancient sculptures from the Humboldt University of Berlin (DE)	1921	
Collection of casts, Universite Laval Quebec (CA)	1922	
Ernesto de la Cárcova Museum of Comparative Sculpture (AR)	1923	
Museum of Greco-Roman Sculptures, Tata (HU)	1923	
Museum of Art of the National University of Colombia (CO)	1926	
Museum of Artistic Reproductions of Bilbao (ES)	1927	
Cast Museum, Thessalonique (GR)	1928	
Medardo Rosso Museum (IT)	1928	
Collections of casts, Université Libre de Bruxelles (BE)	1930	
Constantin Meunier Museum, Bruxelles (BE)	1930	
Map of Rome / University of Caen (FR)	1930	Royo (2006)
Museum of Comparative Sculpture, Mafra (PT)	1934	
Glyptotek. Croatian Academy of Sciences and Arts, Zagreb (HR)	1937	

Museum of Mankind, Paris (FR)	1937	
Ivan Mestrovic Foundation, Zagreb (HR)	1946	
Bourdelle Museum, Paris (FR)	1949	
University of Aarhus Museum of Antiquities (DK)	1949	
Greek, Etruscan and Roman plaster casts collection, Perugia (IT)	1960	
Collection of casts from the University of Provence (FR)	1962	Jockey (1999)
Cast collection of the Archaeology Institute of the University of Salzburg (AT)	1970	
Deposit of works of art from the City of Paris (FR)	1972	
University of Saskatchewan Museum of Antiquities (CA)	1974	
The archaeological collection of the University of Trier (DE)	1975	
Gipsoteca Libero Andreotti, Pescia (IT)	1976	
Gipsoteca Uno Gera, Ripatransone (IT)	1976	
Le Paradis, Fontes d'art de Sommevoire (FR)	1980	
Harry Elstrom workshop. Catholic University of Leuven (BE)	1980-84	
Archaeological collection, University of Freiburg (DE)	1981	
Pierluigi Gherardi Sketches Museum, Lucca (IT)	1984	
Bouchard Museum, Paris (FR)	1985	
Versailles Gypsothèque (FR)	1985	Martinez (2000)
Collection of antique sculptures from the Free University of Berlin (DE)	1988	
Fork Museum, Mortar (BE)	1989	
Fairfield University (US)	1991	Schwab (2017)
H, C. Andersen Museum, Rome (IT)	1992	Di Majo & Perrella (2001)
International Collection Alexander Schubert (living and death masks), Bochum (DE)	1994	
Museum of sculptures by the sea, Scheveningen (NL)	1994	
Plaster Museum in Corneilles, Paris (FR)	1996	
George Mason University Cast Collection, Fairfax (US)	2004	
The Museum of the Memory of the Walls (FR)	2000	

The Institute of Classical Architecture and Classical America (US)	2004	
Aynhoe park (UK)	2005	Frederiksen & Marchand (2010)
Giuseppe Mozzanica Foundation (IT)	2007	Mozzanica & Cimoli (2007)
Museum Vaals (NL)	2009	
The Cassero for nineteenth and twentieth-century Italian sculpture (IT)	2010	
A. Canova - A. Tadolini workshop, Rome (IT)		
Academy of Fine Arts of Naples, Gipsoteca (IT)		Cassese (2013)
Archaeological Museum of Pompeii (IT)		
Archaeological study collection at the Ernst Moritz Arndt University (DE)		
Carrara Academy, Gipsoteca (IT)		Russo (1996)
Cast collection of the Institute for Archaeology at the University of Graz (AT)		
Château de Blois Museum (FR)		
Civic Archaeological Museum of Bologna (IT)		
Collection of casts, Archaeological Institute of the Johann Wolfgang Goethe University, Frankfurt (DE)		Mandel (1994)
Collection of casts from Johannes Gutenberg, University Mainz (DE)		
Collection of mathematical models, University of Pavia (IT)		
Faculty of Theology. Victor Schultze Institute for Christian Archaeology and Church Art (DE)		
Felice Calchi workshop, Roma (IT)		
Fossil Hominid Cast Collection, University of Alberta (CA)		
Gipsoteca A. Malfatti. Museum of modern and contemporary art of Trento and Rovereto (IT)		
Gipsoteca at the National Academy of San Luca, Rome (IT)		Villari (2003)
Gipsoteca of the Castello Svevo, Bari (IT)		
Gipsoteca of the Civic Museum, Castello of Udine (IT)		
Gipsoteca of the school of drawing and the school of painting, Pavia (IT)		

Gipsoteca of the Sculpture Laboratory of Front (IT)

Goethe National museum (DE)

Graduate School of Mathematical Sciences. Tokyo University (JP)

Historic Center of the National Archives, Seals service, Paris (FR)

Knauf Museum, Iphofen (DE)

Seidl (2005)

Manchester University Museum (UK)

Mathematics department, Coimbra University (PT)

Mathematical Institute Georg-August, University of Göttingen (DE)

National Glyptothek of the National Gallery, Alexandros Soutzos Museum (GR)

Frederiksen & Marchand (2010)

National Museum of Science and Technology (IT)

Norbert Hintz Collection, Ahrensfelde (DE)

Palestine Exploration Fund (UK)

Parthenon Project. City University of New York (US)

Philadelphia Penn Museum, Hominid fossil casts collection (US)

Pier Pander Museum, Leeuwarden (NL)

Plaster cast collection of the Institute for Classical Archaeology, Saarland University (DE)

Plaster cast collection of the University of Melbourne (AU)

Prof. Andrea Chiesi workshop (IT)

The Rutgers State University of New Jersey, New Brunswick (US)

The Giust Gallery of Caproni Museum Reproductions (US)

The Mesoamerican Maudslay Casts (UK)

Tokyo University of the Art (JP)

The University of Arizona. Collection of mathematical models (US)

The University of Cape Town. Plaster cast collection (ZA)

Tietze (1998)

The University of Edinburgh. School of History and Classic. Teaching Collection (UK)

## REFERENCES

- Almagro, M. J. (1989). El Museo Nacional de Reproducciones Artísticas: necesidad de su reorganización. Objetivos y finalidad. *Boletín de La ANABAD*, 39(2), 297–322. ISSN: 0210-4164
- Androsov, S. (1991). *La Collezione Farsetti. Alle Origini Di Canova: Le Terrecotte Della Collezione Farsetti, Catalogo Della Mostra (Roma, 1991-1992)*, (S. Androsov, G. Nepi Scirè Ed.), Venezia: Marsilio, 15–22.
- Baker, Malcolm. (1982). The History of the Cast Courts. V&A Masterpieces Series. <http://www.vam.ac.uk/content/articles/t/the-cast-courts/> (last accessed: 27/03/2021)
- Barthel, N. A. (1841). *Quelques vérités importantes, sociales politiques et religieuses; précédées d' une notice sur le prototype de la phrénologie perfectionnée, confectionné & adressé à l' exposition des produits de l' industrie nationale belge, à Bruxelles, en aout 1841*, Perichon.
- Basile, J. (2014). Facsimile and Originality: Changing Views of Classical Casts in Arts Education and Art History. *International Journal of the Arts in Society: Annual Review*, 8(1).
- Bildwerke, M. für A. K., Buschor, E., & Sieveking, J. (1909). *Kurze Beschreibung des Kgl. Museums für Abgüsse Klassischer Bildwerke in München*. Kastner & Callwey.
- Cambareri, M. (2011). Italian Renaissance sculpture at the Museum of Fine Arts, Boston: the early years. *Sculpture and the Museum*. 95–114. London: Routledge.
- Cassese, G. (2013). *Accademie/Patrimoni di Belle Arti*. Roma: Gangemi Editore spa.
- Delivre, J. (1991). La collection des plâtres de la Villa Médicis. *Science et Technologie de La Conservation et de La Restauration Des Oeuvres d'art et Du Patrimoine*, 2, 103–111.
- Di Majò, E., & Perrella, C. (2001). *Yinka Shonibare: be-muse: Soprintendenza speciale alla Galleria nazionale d'arte moderna e contemporanea, Museo Hendrik Christian Andersen*, Roma.
- Dierichs, A. (1999). Abgüsse-modelle-originale: Munster: Das archaologische museum der westfälischen Wilhelms-Universität. *Antike Welt*, 30(1), 13–19.
- Dietrich, F. (2001). *Das Museum von Abgüssen und Originalen antiker Kunst des Institutes für Klassische Archäologie der Universität Innsbruck*.
- Donati, F. (1999). *La gipsoteca di arte antica*. Pisa: ETS.
- Dorey, H., Thornton, P., & Dorey, H. (1992). *A Miscellany of Objects from Sir John Soane's Museum*. London: Merrell Publishers Limited. ISBN-13: 978-1858946498
- Driessche, B. Van Den. (2016). Fernand Mayence et les moulages en Belgique: un musée universitaire (1927) et une reconstitution architecturale spectaculaire (1933). *In Situ. Revue Des Patrimoines*, 28.
- Dufkova, M. (1987). Le musée de moulages de sculptures grecques et romaines à Hostinné, Tchécoslavie. *Le Moulage: Actes Du Colloque International 10*, 173–179.

- Emerson, A. (1907). *Illustrated Catalogue of the Antiquities and Casts of Ancient Sculpture in the Elbridge G. Hall and Other Collections: Early Greek art*. Art Institute of Chicago.
- Firla, M. (1999). Die Afrikaner-Büsten im Rollettmuseum Baden bei Wien. Eine österreichisch-baden-württembergische Sammlung. *Tribus*, 48, 67–94.
- Fittschen, K., & Bergemann, J. (1990). *Verzeichnis der Gipsabgüsse des Archäologischen Instituts der Georg-August-Universität Göttingen: Bestand 1767-1989*. Archäologisches Institut.
- Frederiksen, R., & Marchand, E. (2010). *Plaster casts: making, collecting and displaying from classical antiquity to the present* (Vol. 18). Berlin: de Gruyter.
- Gasparri, C. (1990). *IL museo dei gessi*. Università degli studi di Urbino, Istituto Statale d'arte.
- Grange, D. (1992). Une collection genevoise méconnue: les moulages d'après l'antique: notice historique. *Antike Kunst*, 35(H. 2), 142–145.
- Hagen, B. (2007). The cast collection at the Academy of Fine Arts in Vienna. *Visual Resources*, 23(1–2), 7–19.
- Hemingway, C. C. (2002). On the sculptural technique of Antonio Canova and his plaster casts. *Sculpture Review*, 51(4), 18–23.
- Hubbard, G. (2002). A tour of the plaster collection at the State Art Institute of Florence. *Sculpture Review*, 51(4), 24–29.
- Huchard, V. (1984). *Galerie David d'Angers*. Musées d'Angers.
- Jockey, P. (1999). *Brèves observations sur la collection de moulages de l'Université de Provence*.
- Kenworthy-Browne, J. (2006). Plaster Casts for the Crystal Palace, Sydenham. *Sculpture Journal*, 15(2), 173–198.
- Kurtz, D. C. (2000). *The reception of Classical art in Britain: An Oxford story of plaster casts from the antique* (Vol. 1). Archaeopress Oxford.
- Laurent, R. (2003). *Inventaire de la collection de moulages de sceaux des Archives générales du Royaume. I. Moulages n 1 à 1000*. National Archives of Belgium.
- Mandel, U. (1994). *Begegnungen: Frankfurt und die Antike: Hauptband; Frankfurt am Main; Arbeitskreis Frankfurt und die Antike Die Abgusssammlung des Städelschen Kunstinstitutes und ihre Erweiterung als Sammlung des Archäologischen Instituts der Universität*.
- Martinez, J.-L. (2000). Les moulages en plâtre d'après l'antique du musée du Louvre: une utopie du XIX e siècle. *GABORIT, Jean-René, CUZIN, Jean-Pierre, PASQUIER, Alain. D'après l'antique. Cat. Expo., Paris, Musée Du Louvre*, 16, 78–82.
- Menegazzi, A. (2008). La Gipsoteca del Museo di Scienze Archeologiche e d'Arte dell'Università di Padova: l'esposizione e la fruizione. *Gipsoteche, Realtà e Storia*.
- Meyer, M. (2008). *The collection of the Institute of Classical Archaeology, University of Vienna*.

- Morinière, S. (2015). La gypsothèque de l'Université de Strasbourg : quand les statues parlent d'elles-mêmes. *Archimède : Archéologie et Histoire Ancienne*, 2, 78–93. <https://halshs.archives-ouvertes.fr/halshs-01587435>
- Morricone, M. L. (1981). *Il Museo dei gessi dell'Università di Roma*. Istituto poligrafico e zecca dello Stato.
- Mozzanica, G., & Cimoli, A. C. (2007). *Giuseppe Mozzanica, 1892-1983: la scultura*. Silvana.
- Nikula, R. (2003). *Helsingfors universitets skulptursamling: historia och bakgrund*.
- Poulat, E. (1980). Durand (Jean) Une manufacture d'art chrétien. La "Sainterie" de Vendevre-sur-Barse (1842-1961). *Archives de Sciences Sociales Des Religions*, 49(2), 255–256.
- Rionnet, F. (1996). *L'atelier de moulage du musée du Louvre (1794-1928)* (Vol. 28). Réunion des musées nationaux Paris.
- Robinson, E. (1913). *The Metropolitan Museum of Art. Catalogue of the Collection of Casts*.
- Rousseau, H. (1926). *Catalogue sommaire des moulages, (Musées royaux du Cinquantenaire à Bruxelles)*. Brussel.
- Rousseau, Henry. (1897). *Notes illustrées sur l'art monumental et les moulages typiques du Musée des Echanges*. Victor Chevalier.
- Royo, M. (2006). Rome et l'architecte. *PUC, Caen*.
- Russo, S. (1996). *La Gipsoteca dell'Accademia di Belle Arti di Carrara*. Lions Club Massa e Carrara Host.
- Schwab, K. A. (2017). *Fairfield University Museum - Plaster Cast Collection Introduction*. <https://www.fairfield.edu/museum/collections/plaster-casts/> (last accessed: 27/03/2021)
- Seidl, M. (2005). *Knauf-Museum: Reliefsammlung der großen Kulturepochen*. JH Röll Verlag.
- Smailes, H. E. (1991). A history of the statue gallery at the trustees' academy In Edinburgh: The acquisition of the Albacini casts in 1838. *Journal of the History of Collections*, 3(2), 125–143.
- Tietze, A. (1998). Classical casts and colonial galleries: the life and afterlife of the 1908 Beit Gift to the National Gallery of Cape Town. *South African Historical Journal*, 39(1), 70–90.
- Trendall, A. D. (1941). *A Guide to the Principal Casts of Greek and Roman Sculpture in the Nicholson Museum*. University of Sydney.
- Valli, F. (2008). Gessi dell'Accademia di Brera: storia e didattica. *Gipsoteche. Realtà e Storia*.
- Van Rinsveld, B. (1997). Une maquette monumentale au Musée du Cinquantenaire: Le complexe funéraire de Djoser à Saqqara. *Bull. R. Mus. Art Hist. Brussels*, 68, 43–54.

- Villari, A. (2003). Dall'antico e dal moderno: la gipsoteca dell'Accademia di San Luca (1804–1873). *Le 'Scuole Mute' e Le 'Scuole Parlanti': Studi e Documenti Sull'Accademia Di San Luca Nell'Ottocento*, 136.
- Vimont, J.-C. (1994). Phrénologie rouennaise: les collections retrouvées. *Bulletin de La Société Libre d'émulation de La Seine-Maritime*, 39–58.
- Zindel, C. (1998). *Verzeichnis der Abgüsse und Nachbildungen in der archäologischen Sammlung der Universität Zürich*. Archäologisches Institut der Universität Zürich.

## APPENDIX 2. A SUMMARY TIMELINE OF THE V&A MUSEUM

---

<b>1835-1836</b>	Committee of Arts and Manufactures is selected
<b>1837</b>	Foundation of the Government School of Design of Ornamental Arts in Somerset House, London
<b>1844</b>	First Sculpture acquisition
<b>1851</b>	The Great Exhibition in Crystal Palace in Hyde Park
<b>1852</b>	Museum of Manufactures is established  Henry Cole appointed general superintendent of the Department of Practical Art  The Department, including the Museum of Manufactures and the School of Design, moves into Marlborough House  The Circulation Department is established.
<b>1853</b>	Department of Practical Arts become Department of Science and Art  Museum of Manufactures renamed the Museum of Ornamental Art  Publication of the National Course of Art Instruction  John Charles Robinson appointed first curator ("Superintendent of Art Collections)
<b>1855</b>	Building works begin on the South Kensington site
<b>1857</b>	South Kensington Museum opens  The cast collection of the Architectural Museum is taken on loan  Acquisition of the Michelangelo's David cast
<b>1862</b>	Opening of the North and South Courts  The loan exhibition takes place in the South Court
<b>1864</b>	Loan of the Raphael Cartoons from the Royal Collection  Robinson's campaign in Spain  Acquisition of the Trajan's Column cast
<b>1866</b>	Brucciani make the cast of the Portico de la Gloria
<b>1867</b>	15 European princes sign the 'International Convention of promoting universally Reproductions of Works of Art'
<b>1869</b>	Central Lecture Theatre block opened  The cast collection of the Architectural Museum moves to the new Architectural Museum in Tufton Street

<b>1872</b>	Official opening of the Bethnal Green Museum
<b>1873</b>	Opening of the Architectural Courts Retirement of Henry Cole
<b>1874</b>	Science School building completed Philip Cunliffe Owen appointed director
<b>1876</b>	Foster bequest
<b>1879</b>	Collections of the India Museum largely transferred to the South Kensington Museum
<b>1882</b>	Jones bequest
<b>1884</b>	Art library building completed Schreiber gift
<b>1888</b>	Opening of the Imperial Institute
<b>1890</b>	Creation of the Museum Association
<b>1893</b>	Art Museum and science collection was given separate directors John Middleton appointed director of the Museum
<b>1896</b>	Caspar Purdon Clarke appointed director of the Museum Division of the Museum into five curatorial departments by material
<b>1897</b>	Government Select Committee set up to investigate the South Kensington Museum
<b>1899</b>	Foundation stone for the new Aston Webb building laid by Queen Victoria South Kensington Museum renamed the Victoria and Albert Museum
<b>1900</b>	Ionides bequest Donaldson gift
<b>1901</b>	The Glasgow International Exhibition opened showcasing a selection of reproductions of the sculptured stones of Scotland aided by Circulation Department grants
<b>1904</b>	Dundee museum's acquisition of casts aided by Circulation Department grants
<b>1905</b>	Arthur Banks Skinner appointed director Aberdeen museum's acquisition of casts aided by Circulation Department grants
<b>1908</b>	Committee on Re-arrangement formed
<b>1909</b>	Opening of the Aston Webb building Cecil Harcourt Smith appointed director
<b>1910</b>	Salting Bequest
<b>1916</b>	The cast collection of the Architectural museum return to the V&A

<b>1922</b>	Brucciani & Co. is taken over by the Board of Education, run as a V&A's service and renamed Department of Sale of Casts
<b>1924</b>	Eric Maclagan appointed director
<b>1937</b>	The fire of Crystal Palace, many casts are moved to the V&A
<b>1939</b>	The museum closed at the start of World War II due to fear of bombing
<b>1940</b>	The museum reopens with limited display
<b>1945</b>	Leigh Ashton appointed director
<b>1947</b>	Apsley House, the nineteenth-century residence of the Duke of Wellington, placed in the care of the V&A
<b>1948</b>	The division into Primary and Secondary Gallery Announced
<b>1955</b>	Cross Gallery (housing the Indian Collection) closes
<b>1956</b>	Trenchard Cox appointed director Hildburgh bequest
<b>1967</b>	John Pope-Hennessy appointed director
<b>1974</b>	Roy Strong appointed director
<b>1975</b>	Bethnal Green Museum relaunched as the Bethnal Green Museum of Childhood
<b>1978</b>	Final closure of Regional Services (formerly Circulation Department)
<b>1983</b>	The Henry Cole Wing (previously the Royal College of Science building) opened V&A accorded trustee status under the National Heritage Act
<b>1987</b>	The Theatre Museum opens in its new premises in Covent Garden
<b>1988</b>	Elizabeth Esteve-Coll appointed director
<b>1989</b>	Reorganization of the Museum's curatorial departments
<b>1995</b>	Alan Borg appointed director
<b>2001</b>	Mark Jones appointed director
<b>2011</b>	Martin Roth appointed director
<b>2014</b>	Reopening of the Weston Cast Court
<b>2016</b>	Opening of the Victoria and Albert Museum at Dundee
<b>2017</b>	Tristram Hunt appointed director
<b>2018</b>	Reopening of the Ruddock Family Cast Court and Chitra Nirmal Sethia Gallery

## REFERENCES

- Baker, Malcolm. (1982). *The History of the Cast Courts*. V&A Masterpieces Series. <http://www.vam.ac.uk/content/articles/t/the-cast-courts/> (last accessed: 27/03/2021)
- Foster, S. M., (2015). Circulating agency: the V&A, Scotland and the multiplication of plaster casts of 'Celtic crosses', *Journal of the History of Collections*, 27(1), 73–96, <https://doi.org/10.1093/jhc/fhu008>
- Hubbard, C. (2015). Conservation of the Weston Cast Court at the V&A. <https://www.pmsa.org.uk/news/2019/5/2/conservation-of-the-weston-cast-court-at-the-vampa>
- Scala (Ed.). (1991). *The Victoria and Albert Museum*. ISBN-13: 978-0863503344
- Wainwright, C., & Gere, C. (2002). The making of the South Kensington Museum I: The Government Schools of Design and founding collection, 1837–51. *Journal of the History of Collections*, 14(1), 3–23. <https://doi.org/10.1093/jhc/14.1.3>
- Whitehead, C. (2005). Henry Cole's European Travels and the Building of the South Kensington Museum in the 1850s. *Architectural History*, 207–234. <http://dx.doi.org/10.1017/S0066622X00003786>
- Williamson, P. (1996). *European sculpture at the Victoria and Albert Museum*. London: Victoria and Albert Museum Publishing. ISBN-13: 978-1851771738

## APPENDIX 3. HISTORICAL TECHNICAL LITERATURE

---

### Appendix 3 List of Contents:

Pollio, V. (1914). <i>The ten books on architecture</i>	22
Cennini, C. (1859). <i>Il libro dell'arte, o trattato della pittura</i>	23
Cellini, B. (1967). <i>The treatises of Benvenuto Cellini on goldsmithing and sculpture</i>	24
Smith, G. (1810). <i>The laboratory or School of Arts</i>	25
Merrifield, M. P. (1846). <i>The art of fresco painting: as practised by the old Italian and Spanish masters, with a preliminary inquiry into the nature of the colours used in fresco painting, with observation and notes</i>	26
Westwood, J. O. (1876). <i>A descriptive catalogue of the fictile ivories in the South Kensington Museum: with an account of the continental collections of classical and mediaeval ivories</i>	27
Frederick, F. F. (1899). <i>Plaster casts and how they are made</i>	28
Millar, W. (1899). <i>Plastering, plain &amp; decorative. A practical treatise on the art &amp; craft of plastering and modelling, including full description of the various tools, materials, processes and appliances employed</i>	29
Bankart, G. P. (1908). <i>The art of the plasterer. An account of the decorative development of the craft, chiefly in England from the XVIth to the XVIIIth century, with chapters on the stucco of the classic period and of the Italian renaissance, also on scraffito, pargeting</i>	34
Kemp, W. (1912). <i>The practical plasterer. A compendium of plain and ornamental plaster work</i>	36
Auerbach, A. (1961). <i>Modelled sculpture and plaster casting</i>	41
Wager, V. H. (1963). <i>Plaster casting for the student sculptor</i>	45
Meilach, D. Z. (1966). <i>Creating with plaster</i>	47
Chaney, C. (1973). <i>Plaster mold and model making</i>	51
de Jonge, L. (1985). <i>The art of doing: plaster techniques</i>	52
Piva, G. (2010). <i>Manuale pratico di tecnica pittorica</i>	54
Turco, T. (1990). <i>Il Gesso. Lavorazione, trasformazione, impieghi</i>	59

## POLLIO, V. (1914)

### THE TEN BOOKS ON ARCHITECTURE

(TRANSLATION OF DE ARCHITECTURA, 30-15 BC)

Vitruvius' *De Architectura* defines many techniques and provides numerous theoretical (symmetry and harmony) and practical (materials and techniques) rules related to the practice of the Architect.

In Book VII, Chapter II, the author defines the ancient technique of treating the lime for making stucco.

*1. [...] we must treat stucco work. This will be all right if the best lime, taken in lumps, is slaked a good while before it is to be used, so that if any lump has not been burned long enough in the kiln, it will be forced to throw off its heat during the long course of slaking in the water, and will thus be thoroughly burned to the same consistency. When it is taken not thoroughly slaked but fresh, it has little crude bits concealed in it, and so, when applied, it blisters. When such bits complete their slaking after they are on the building, they break up and spoil the smooth polish of the stucco. [205]*

In the same book, Vitruvius also illustrates the many pigments good to be used on frescos. In the following book (VIII) he describes how water should be chosen for these types of work.

## CENNINI, C. (1859)

### IL LIBRO DELL'ARTE, O TRATTATO DELLA PITTURA

Cennini's treatise focuses on painting techniques. Nevertheless, some sections of the treatise are worth mentioning as related to gesso preparations.

#### Capitolo CX. Perfetta colla a temperar gessi da ancone, o ver tavole.

*[...] Egli è una colla che si fa di colli di carte di pecora e di cavretti, e mozzature delle dette carte. Le quali si lavano bene, mettonsi in mole un di innanzi le metti a bollire; con acqua chiara fa' bollire tanto, che torni delle tre parti l'una. E di questa colla voglio, che quando non hai colla di spicchi, che adoperi sol di questa per ingessare tavole o vero ancone; chè al mondo non puoi avere la migliore. [...]*

#### Capitolo CXV. In che modo si debbe ingessare un pino di tavola, a stecca, di gesso grosso.

*[...] Poi abbi gesso grosso, cioè volterrano, ch'è purgato, ed è tamigiato a modo di farina. Mettine uno scodellino in su la prieta proferitica, e maina con questa colla bene; per forza di mano, a modo di colore. [...]*

#### Capitolo CXVI. Come si fa il gesso sottile da ingessare le tavole.

*[...] Ora si vuole che tu abbi d'un gesso il quale si chiama gesso sottile; il quale è di questo medesimo gesso, ma è purgato per bene un mese, e tenuto in mole in un mastello. Rinnuova ogni dì l'acqua, chè quasi si inarsisce, ed escene fuori ogni focor di fuoco, e viene morbido come seta. Poi si butta via l'acqua, fassene come pane, lasciarsi asciugare; e di questo gesso si vende poi dalli speziali a noi dipintori. E di questo gesso si adopera a ingessare, per mettere d'oro, per rilevare, e fare di belle cose. [...]*

#### Capitolo CXVII. Come s'ingessa un'ancona di gesso sottile, e a che modo si tempera.

*[...] Come tu hai ingessato di gesso grosso, e raso bene pulito, e spianato bene e diligentemente, togli di questo gesso sottile; a pane a pane mettilo in una catinella d'acqua chiara; lascialo bere quant'acqua e' vuole. Poi 'l metti a poco a poco in su la prieta proferitica, e senza mettervi altr'acqua dentro, perfettissimamente il macina nettamente. Poi 'l metti un pezzo di pannolino, forte e bianco; e così fa tanto, che n'abbi tratto un pane. Poi rinchiudi in questo panno e strucalo bene, che l'acqua n'esca fuori quanto più si può. [...]*

#### Capitolo CXIX. A che modo dèi temperare e macinare gesso sottile da rilevare.

*[...] Ancora son molti che macinano il gesso sottile pur con la colla e con acqua. Questo è buono per ingessare dove non è ingessato di gesso grosso, che vuol essere più temperato. Questo cotal gesso è molto buono a rilevare foglie e altri lavori, si come è molte volte per bisogno. Ma quando fai questo gesso da rilevare, mettivi dentro un poco di bolo armenico, tanto che gli dia un poco di colore. [...]*

## CELLINI, B. (1967)

### THE TREATISES OF BENVENUTO CELLINI ON GOLDSMITHING AND SCULPTURE

Cellini treatise is for the use of the sculptor. Amongst the rest, a paragraph is dedicated to the use of plaster and the making of the gesso moulds.

*[...] There are many ways of making the gesso moulds. The best [...] is to make as many small pieces as when put together would make a complete man. These small pieces must be made with great care, and while the gesso is moist you fit into each of them an iron wire bent double and projecting out the gesso much like a little ring, to be capable of holding a thread through it. [...] when you have thus fitted all your little undercut pieces into the mother mould, you grease the whole mould with **soft lard** and proceed to give it what has technically termed the lasagna [...]*

SMITH, G. (1810)

THE LABORATORY OR SCHOOL OF ARTS

*[...] the method of taking of casts of figures and busts is most generally by the use of plaster of Paris, i.e. alabaster calcined by a gentle heat. The advantage of using this substance, preferably to others, is, that notwithstanding slight calcination reduces it to a pulverine state, it becomes again a tenacious and cohering body, by being moistened with water, and afterwards suffered to dry; by which means either a concave or a convex figure may be given by a proper mould or model to it when wet and retained by the hardness it acquires when dry, and from these qualities, it is fitted for the double purpose of making both casts, and moulds for forming those casts. [...]*

*To impress Basso Rilievo, or Medals, in Imitation of Ivory. [...] Take of prepared clay one pound, fine plaster of Paris eight ounces, white starch eight ounces; mix these together, and beat up the mixture with the white of six or eight eggs; put to it three ounces of clear gum Arabic; stir it well together to a paste, and put so much of the dry mixture to it as will knead it like dough; [...] Then take one pound of fine parchment glue; the finest gum-tragacanth and gum-Arabic, of each four ounces; let them boil in clear pump-water, and filter through a clean rag; stir into the aforesaid power of wood [...] you may mix it, if you will, with a little beaten amber: for a red colour, use Brazil ink; [...]*

## MERRIFIELD, M. P. (1846)

### THE ART OF FRESCO PAINTING: AS PRACTISED BY THE OLD ITALIAN AND SPANISH MASTERS, WITH A PRELIMINARY INQUIRY INTO THE NATURE OF THE COLOURS USED IN FRESCO PAINTING, WITH OBSERVATION AND NOTES

Merrifield in this book presents a collection of directions as written by the 'old Italian and Spanish masters' on the techniques for fresco painting. In Vol. ii, 638, describes the grey *stucco* used by Italian masters for modelling replicas of their works executed in marble, and for their preliminary studies preparatory to cutting the marble, previous to the revival of the white *stucco-duro* by Giovanni da Udine:

*[...] "take 5 lbs. of finely powered travertine (and if you would have it finer and more delicate take fine marble instead of travertine), and 2 lbs. of slaked lime, mixed together with water, and stir and beat them well together to a fine paste, and execute what works you please with it, either by forming it with your hands or in moulds, and dry in the shade. "and if you wish to colour it white, when the work is dry enough to be tolerably firm but not quite dry, **grind white lead with water**, in the same way colours are ground, **and flour**, of finest quality of sifted lime and apply it with a pencil, and it will be very white, and effectually resist water. "and if you wish to colour it with other colours, **let the work dry perfectly, and then colour it; but these colours will not resist water like the white, because they do not incorporate or unite so well as that does with the materials of which the work is composed.**" "if then you wish the colours to resist water, apply on the work the above-mentioned composition (which is to be used in the manner described) and paint it with **oil colours**. You may also colour the *stucco* with colours ground up dry, but these will not be so bright as if they were applied afterwards. [...]*

WESTWOOD, J. O. (1876)

A DESCRIPTIVE CATALOGUE OF THE FICTILE IVORIES IN THE SOUTH  
KENSINGTON MUSEUM: WITH AN ACCOUNT OF THE CONTINENTAL  
COLLECTIONS OF CLASSICAL AND MEDIAEVAL IVORIES

*[...] At first, gutta-percha was alone used, but as it was found that after being softened in hot water it hardened again too rapidly to allow a large ivory to be properly pressed, it was advisable to mix a certain quantity of wax with the gutta-percha, which caused it to retain its softness for a longer period. The prepared gutta-percha is then to be placed in hot water, and then it has become as soft as putty it is to be moulded by the hand into a flattened plate rather larger than the ivory to be moulded. The face of the ivory must be wetted with cold clear water, or better still, must be washed over with soft soap applied with a camel's hairbrush, and whilst wet the gutta-percha is to be placed upon it and pressed by the thumb carefully so as to force the gutta-percha into all the deeper cut parts of the ivory. It is then allowed to harden and cool and must then be lifted with great care from the ivory. Of course, this is a delicate operation with old or deeply cut ivories, but it is very rare indeed that any injury has happened to the latter, as the wax in the composition allows a small amount of elasticity. With undercut ivories, the undercut parts must be guarded and the plaster cast, when made from the gutta-percha mould, must be undercut by hand to represent the original; but it is better to use gelatine to make the moulds from undercut ivories. [...] On being removed from the ivory the mould is ready to receive the fluid plaster of Paris of the finest quality for the cast, but when a number of copies are required it has been found advisable to have an electrotype made of the mould so that every subsequent cast might be as fresh as the one first made. In order to give the cast a greater similarity to ivory, as well as to harden the surface of the casts, they are dipped in warm fluid **stearin**. [...]*

FREDERICK, F. F. (1899)

PLASTER CASTS AND HOW THEY ARE MADE

Calcining and setting. [...] For the finer grades of plaster the heavier and denser varieties of gypsum are selected. This is broken into small lumps, placed in a furnace or kiln, and, according to one method, heated to about 80 °C. This heat is continued for about four hours and then increased to 100 or 110 °C and maintained for eight hours. Allowing twelve hours to cool, the plaster [...] is pulverized [...]. When fresh from the furnace or kiln the plaster sets quickly into a solid and rather hard mass, but with time and exposure to the atmosphere, or from being kept in a damp room, it gradually absorbs moisture and soon fails to set properly. [...]

Materials for casting. The moulder should be provided with two grades of plaster. A fine grade [...] for surfaces, and a larger quantity of a cheaper grade for strengthening moulds and casts. [...] In a bottle having a large mouth put one-half pint of alcohol. Add to this as much powdered shellac as the alcohol will “cut”. [...] The liquid plaster of a cast will not separate from the set plaster of a mould unless separated by a film of oil, soap or other “separation”. A 4-ounce bottle of sweet oil will cover a large area and is the best separation to apply to oiled, painted and shellacked surfaces in ordinary work. Equal quantities of lard and tallow [...]. For washing moulds, any soap will answer, but for a soap separation [...]: Put one pint of water on to boil and cut into this as much white castile soap as will dissolve. [...] Clay water for a clay separation is simply clay and water up to the consistency of cream.

Types of moulds. Waste mould, Piece mould, Elastic mould, Gelatine is “animal jelly, obtained by the prolonged action of boiling water on the organic tissues of the bones, tendons and ligaments, the cellular tissues, the skin and the serous membranes. Glue and size are coarser varieties of gelatine prepared from the hoof, hides etc.” The author suggests working only with glue (“the best white glue”), or with glue and molasses (“proportion of 16 ounces of glue to 14 ounces of molasses) and consider the gelatine the best material for elastic moulds (eventually mixed with molasses, “4 ounces of molasses to 16 ounces of gelatine). As for the previous techniques, the cast from which the elastic mould is made must be oiled, shellacked or painted. Wax mould, one part of rosin and three parts of white wax. Or melt paraffin wax and add a little sweet oil and whiting.

Tints and coatings. **Light yellow or buff** is easily obtained **by linseed oil**, which tints the plaster, makes it resistant to water and durable and hard. The oil can be applied with a **slightly tint (e.g. yellow ochre, raw sienna)** or a wax-like surface can be obtained (immersing the cast in warm oil for ten or twelve hours). The best white paint is **zinc white ground in oil, thinned with turpentine**. [...] **White lead thinned with turpentine** is preferred by many to zinc white. [...] Lead does not have the whiteness of the zinc, but it can be applied much more quickly. **The ivory-like finish** can be given in many ways for example rubbing the surface with **paraffin** or **wax candle** and polishing with silk. **Beeswax** with an equal amount, or a little more, of **turpentine**, gives a good finish. **Glue and shellac** can be applied as follows: brush the cast with several coats of hot glue sizing – the first being quite thin. Allow this to dry thoroughly and cover it with one or more coat of white shellac. Mr F. D. Millet invented a medium size for use in wax painting with the same materials of the ancient encaustic painting: **melt 1 ounce of pure white wax and 2 ounces of Venice turpentine in a jar placed in boiling water. Add, stirring gradually, about half pint spirits turpentine, or enough to make it flow freely.** The cast may be tinted as well as the first layer of the mould. Gilding is often unsuccessful, but possible: gold leaf can be applied to any painted or shellacked surface and gold paint can be used for the details. Plaster cast could also be **bronzed by the use of bronze paint (mastic varnish and bronze powder)** or **silvered by covering with finely ground mica powder mixed with colloidal**. A smooth surface can be obtained by mixing the plaster with a weak solution of **gum Arabic**. It will have a marble appearance if saturated with milk. **Melted stearin** can be applied. The finest quality of plaster mixed with turpentine can be used as a paint.

## MILLAR, W. (1899)

## PLASTERING, PLAIN &amp; DECORATIVE. A PRACTICAL TREATISE ON THE ART &amp; CRAFT OF PLASTERING AND MODELLING, INCLUDING FULL DESCRIPTION OF THE VARIOUS TOOLS, MATERIALS, PROCESSES AND APPLIANCES EMPLOYED

Millar introduces this volume with a 'Glimpse' to the history of plaster casting. The following Chapter features a wide description of materials, from plaster to lime, used by the plasterer. However, the description seems to be focussed on mortars and cements and their properties.

Bassett's Plaster Company. According to Millar:

*[...] In 1899, H. A. Bassett, a Birmingham plasterer, obtained a patent for an improvement in a cementitious plaster for plastering walls and ceilings. The composition consists of dry glue, linseed oil, carbonate of soda, plaster, sawdust, white china clay, sand and borax. [...]*

A great number of patents is mentioned by Millar; however, they are mostly related to the plastering of walls and ceilings. Examples of decorative patterns are also showed by Millar, including some remarkable decoration in English Mansions. A chapter describes the art of modelling and casting with plaster.

Squeezing wax. [...] used for taking an impression of metal, wood, stone or plaster models for reference purposes. The surface of the model should be dusted with **French chalk** to prevent adhesion and discoloration of the model. [...] The squeeze is then filled with plaster, thus producing a replica of the model. [...] **English recipe: take ½ lb. of pure beeswax, 1 lb. of lard and 1 gall of linseed oil, melt over a slow fire, then sprinkle in 1 lb. of flour, and stir well, then pour the whole out on a slate or bench and knead all together. [...]** **French recipe: take 1 lb. of pure beeswax, 1 and ½ lb. of lard and 1 gall of olive oil, dissolve over a slow fire, and add sifted whiting until of the desired consistency. [...]** **Belgian recipe: take ¾ lb. of beeswax, ¼ lb. of Burgundy pitch, and dissolve over a slow fire, and add ¾ pint of olive oil, gradually stir in equal parts of flour and fine sifted whiting until of the desired consistency. [...]** **Austrian recipe: take 2 parts of beeswax, 1 part of suet and 1 part turpentine, dissolve and add fine whiting as before.**

Casting Wax. [...] Wax combined with other materials is used for casting silver or bronze models, also for piece moulding. The Italian artists use a casting wax made simply of beeswax, Venice turpentine, and finely sifted wood ashes. [...]

Moulding wax. [...] is used for making moulds for plaster casting. It consists of 1 part pure beeswax, and from 1 to 2 parts of powdered resin, dissolved in a metal pot, over a slow fire, or on a hot plate. [...] The quantity of resin varies according to the quality of the wax. A rich wax will carry more resin than a poor one. Poor wax is improved by adding from 1 to 3 oz. of mutton suet, or best white tallow, to each pound of wax. [...]

Waste wax moulding. [...] Waste moulds are used to save the expense of piece moulding clay models, where one cast only is required for making a moulding piece, or for cleaning up the cast before being permanently moulded. Plaster is used for waste moulding models on the round and similar works. Wax is used for small, flat, and delicate work. [...]

Plaster waste moulding. [...] Plaster waste moulding is a method used for moulding clay models on the round to obtain a cast or a moulding piece. A waste mould derives its name from the fact that it must be broken or wasted before the cast can be extracted, whereas a number of casts can be obtained from a piece or safe mould. If the clay is firm, it can be carefully coated with thin shellac and then oiled. The shellac must be brushed on with a soft fine brush, so as not to injure the modelling. This gives more freedom in moulding and less fear of injuring the model when fixing the clay fences. [...]

Plaster piece moulding. [...] A piece mould derives its name from being made up of a number of pieces which placed together form the complete mould. Piece moulds are used for reproducing metal, terra-cotta, concrete, wax, or plaster casts from original models that are on the round or undercut, and where it is impracticable to mould them in one piece or two pieces, such as a front and back mould. If the seams formed by the joints of the pieces are carefully taken off a cast produced from a well-made piece mould, it will be a fair facsimile of the original model. Plaster lends itself more freely and is more adaptable for forming a piece mould than either wax, clay, sulphur, or metal. Its quick setting powers and unshrinkable and plastic nature, combined with its fine and smooth surface, seems to be expressly designed by Dame Nature for this purpose. [...] The surface of models that are seasoned with linseed oil or shellac is generally oiled with sweet oil. Suet solution is also an excellent compound for oiling models. It can be brushed on so as to leave a very thin coat on the surface of the model. This is an advantage, as the thinner the coat of oil is, the sharper and truer will the plaster piece turn out. Suet solution does not soil the model but tends to indurate it and season the plaster pieces. [...]

Oiling plaster moulds. [...] Plaster piece moulds are generally oiled with a mixture of Russian tallow and sweet oil. Lard with and without sweet oil is sometimes used. The addition of paraffin oil to these oils renders them softer, cleaner, and free to work. Softsoap alone also mixed with sweet oil, is preferred for some purposes. Plaster being of a porous nature, and containing a proportion of lime, is easily affected by soap, fats or oils. The fatty acids unite with the lime and render the face of the mould and cast sticky. This causes dust to accumulate, and in time to form crusts in the deeper recesses, which are difficult to remove. German plaster moulder overcomes this by the use of finely separated stearic acid. one part of stearic acid (or stearine) is melted in a water bath, and about 5 parts of alcohol or benzene is added, in which it dissolved to a clear solution. [...]

Suet solution. [...] suet solution is an excellent compound for oiling models when plaster piece moulding. It will also be found a ready and useful oil when casting in wax and sulphur moulds. Suet solution is made by dissolving fresh mutton suet by gentle heat, then adding as much paraffin oil as will keep it in a soft cream state when cold. [...]

Soap solution. [...] This solution, or soap water, is made by reducing soft soap with boiling water to a creamy consistency. It is used for plaster waste moulding, also for the joints when plaster piece moulding, and several other shop purposes. Soap water should not be used for washing old or dry plaster moulds or casts, as it leaves a thin sticky film which attracts and retains dust. They should be dry dusted, and then washed with warm water and wiped. They are then ready for oiling. [...]

Stearic impervious solution. [...] when casting special works, such as antique and classical figures. This solution will be found useful when plaster piece panels, &c. By its use, sharp, clean, and white casts are obtained. **A neutral soap of stearic acid and caustic soda is prepared and dissolved in about ten times its weight of hot water. The models and moulds are coated by being either brushed with or immersed in this solution.** [...] It is rendered impervious, and permits the moulds or casts to be washed, even with lukewarm soap water. **Stearate of potassium is only soluble in hot water. As already mentioned, soap water leaves a film on the surfaces of moulds, which attract dust. The same difficulty is presented by plaster that has been impregnated with a solution of alum and stearine. A solution made with stearate of alumina in benzole behaves in the same way. The plaster can also be made impermeable to water by washing it with a solution of oleic acid in benzine. This is applied cold, and the casts must not be washed with soap water, as it would take up the oleic acid. The best way is to wipe**

them with a cloth moistened with the acid. The stearic acid and caustic soda solution give the best results, and it may be used for waterproofing plaster casts. [...]

Oiling wax moulds. [...] Olive or sweet oil is generally used for oiling wax moulds and gives good results for general purposes. Russian tallow, lard, and mutton suet are also used for oiling wax moulds as well as for plaster moulds. Animal fats are too hard to work freely. If they are thinned down by adding paraffin oil, as already described, they work cleaner and more freely. The fats should be dissolved by heat, and then sufficient paraffin oil added until of a creamy consistency. Chalk oil is also used for wax moulds. Moulds composed of rich wax will yield a few casts without oiling by simply brushing with soap water and then rinsing. [...]

Rubber varnish. [...] Dissolve India rubber shavings in naphtha in a close vessel by means of gentle heat (or a hot-water bath), then strain the liquid off into bottles, and keep them corked until required for use. Before varnishing the mould with this solution, the surface must be dried by dusting with French Chalk, to absorb any surface oil or moisture which would prevent the varnish from adhering to the glue surface. [...]

Copal varnish. [...] A good varnish is made by mixing 1 gill of Copal varnish with about 1 oz. of patent driers. The latter is thinned down with turpentine before mixing with the copal varnish. The mould is dusted as before, and then varnished, and allowed to stand until dry. [...]

Shellac varnish. [...] This is made as follows — 100 parts water, 12 parts best hard shellac, and 4 parts of borax, are dissolved altogether in close vessels by gentle heat and continued stirring. The vessel is then covered, and the liquid allowed to cool, after which it is poured into bottles which are well corked. This is used alone or mixed with a small portion of linseed oil and a few drops of turpentine. The whole mass is then well incorporated, and it will dry in fifteen or twenty minutes. Glue and jelly moulds that are used for casting with hot plaster or Portland cement are apt to become soft and sticky at the prominent or weak parts. In this case, the moulds should be allowed to stand in a cool place until the parts are firm. They are then revarnished or washed with bichromate of potash as already described. Varnished moulds are oiled with chalk oil. [...]

To paint the cast as required. [...] Use **water-colour** when a dry surface is to be imitated, **oil-colours** when the surface is moist. The water-colour may require several coats. Finally, an edging of black velveteen or other material will hide the irregular margin and give a finish. [...]

Polishing plaster cast. [...] plaster casts can be made to take a high polish. Those which are to be polished by friction with other substances should be made as hard as possible. The plaster should be gauged firm and used expeditiously. When a soft gauged plaster is necessary to allow it to be run into closed up moulds, the cast may be partly hardened by dusting the back with dry plaster to absorb the moisture. Gauging with alum water hardens plaster but causes it to set too quick for manipulation in certain kinds of moulds. This may be overcome by adding size water (which also hardens plaster) to the gauging water. The setting may be regulated to any required degree. Casts intended to be polished should be covered with paper or cloths until dry and kept in a dry and warm place. The following are the best-known methods for polishing plaster casts — **To 4 lbs. of clean water add 1 oz. of pure curd soap, chipped and dissolved in a glazed pot; next, add 1 ½ oz. pure white beeswax cut into thin slices. When it is all properly mixed, it is fit for use.** The figure must be dried and suspended by a string. It is then dipped into the liquid varnish, and when taken out, allowed to stand for about three minutes; stir up the varnish, and then dip the figure again. Cover it up in a dry place, free from all dust, for six or seven days, after which take some soft rag or cotton wool, and gently rub the figure until it has received a brilliant gloss. [...] Another way — **Plaster casts soaked in olive oil in which white wax has been dissolved by heat, or casts soaked in dissolved paraffin wax, will when dry, take a fine polish. The casts should be hot when put into the hot solution. The polishing is done with French chalk and cotton wool. If the polished casts are left in a smoky room, they will acquire the appearance of old ivory.** Plaster casts can be made to assume any colour by dissolving in the water for gauging any desired colour in powder.

**Another way — Soak the casts in a hot solution of white beeswax and glycerine. When dry, polish with French chalk and cotton wool or sable hairbrushes. Another way — Take clean skimmed milk, and with a clean soft brush coat the figure until it will absorb no more. Gently blow off all superfluous milk from the face of the object, and lay it in a place perfectly free from dust. When dry, it will have the appearance of polished marble. A great deal depends on the amount of care bestowed on the skimming of the milk. Plaster gauged with milk and water will enable the casts to be polished. Another way — Plaster casts thoroughly dry and brushed with two coats of clear linseed oil, and kept for a while in a smoky room, will take a good polish, and acquire the appearance of old ivory. Another way — Dissolve ½ oz. of soft soap in 1 quart of water, and then incorporate 1 oz. of white wax. The cast is dipped in or brushed over with this mixture. When dry, it may be polished with a soft rag and French chalk. Another way — is to give the cast a thin coating of white shellac, then paint over this a good coating of boiled soft soap and polish when dry with a soft dry rag. Another way — A beautiful varnish for plaster casts may be made by fusing ½ oz. of tin and ½ oz. of bismuth in a crucible. Melt together, then add ½ oz. of mercury. When perfectly combined, take the mixture, allow it to cool, and add the white of an egg. The casts must be dry, and free from stains or dust. Another way — The cast must be perfectly dry, and free from scratches and dust. Give it a coat of linseed oil, and allow it to stand until dry, after which give another coat, and French polish in an ordinary way. If a figure or bust is required to be white, make smooth with white size, and varnish with hard white varnish. Another way — Take 2 parts stearine, 2 parts Venetian soap, and 1 part of pearl ash. Grate the stearine and soap and mix with 30 parts of a solution of caustic potash. Boil this for thirty minutes, stirring all the time. Add the pearl ash dissolved in a little clean rainwater, and boil for five minutes. Stir until cold and mix with more ley until it is quite liquid. Before use, it should be allowed to stand for a few days, keeping it properly covered up. Let the figure be clean and well dried. Coat with a soft brush or sponge until the figure will absorb no more. Allow it to stand well covered up and give another coat. When dry, rub with soft rags or a brush. This will give a beautiful polish. The liquid may be kept for years if properly covered up. Should the surface not have the required degree of gloss, the operation must be repeated. This liquid has the property of hardening the plaster. Another way — Take a clean cast, well dried, and coat with white wax. Place it before a fire until the wax is absorbed. A good polish may then be obtained by friction. Another way — Plaster may be polished with French chalk until it shines like glass. The cast when nearly dry is dusted with the finest French chalk, and gently rubbed with cotton wool. Repeat the dusting and rubbing until a bright polish is obtained, taking care that the chalk does not cake and injure the face of the cast. When perfectly dry, it may be dusted and rubbed again to give a good finish. For deep parts in a cast, where it is difficult to use the wool, use a camel hairbrush. French chalk can be used as a help in the final polish in most of the other methods described. [...]**

**Washable plaster casts. [...] In 1878, F. von Dechend, of Bonn, obtained a patent for “making plaster casts washable without injury.” The process consists of two distinct operations. One consists in the application of a solution of borax and alum to harden the plaster, and the finishing operation consists in the application of insoluble precipitates, by which the minutest pores are filled up and the surface rendered hard. Salts of barium, calcium, and strontium are suitable for obtaining insoluble precipitates without forming spots. A method of performing the process may be done as follows — A hot saturated solution of borax is spread with a brush over the cast any required number of times; next hydrochlorate of barytes, likewise in the form of a hot solution, is laid on with a brush, then soap solution is likewise applied hot, any excess being removed with hot water. [...]**

**Jacobsen prepares casts which retain no dust and can be washed with lukewarm soap-water, by immersing them or throwing upon them in a fine spray a hot solution of a soap prepared from stearic acid and soda lye in ten times its quantity, by weight, of hot water.**

Shellhass recommends the coating of plaster of Paris casts with a compound of finely powdered mica and collodion prepared as follows —The mica, rendered perfectly white by boiling with hydrochloric acid or calcining, is ground very fine, sifted and elutriated, and then mixed with dilute collodion to the consistency of oil - paint, and applied with a soft brush. Casts coated in this way possess a silvery lustre, have the advantage of being indifferent to sulphurous exhalations and can be washed without injury.

Waterproofing plaster casts – Another result of the prize offered by the German Government are the two following experiments made by Dr Reissig, of Darmstadt, in his endeavour to render plaster casts washable, and at the same time to preserve the sharpness of outline. He found this could be affected (1) by converting the lime sulphate into baryta sulphate and caustic or carbonate of lime, or (2) by changing the lime sulphate into lime silicate by means of potash silicate.

*[...] Of the two methods, the former is preferable, being simpler, more economical, and more easily carried out. The lime sulphate is changed into baryta sulphate and caustic lime by means of baryta water. Exposure in the air subsequently changes the caustic lime into lime carbonate. This is best worked by using a zinc vessel with a zinc grating 1 ½ m from the bottom, and a close-fitting lid, which must be nearly three parts filled with soft water, 54 to 77° Fahrenheit. To every 25 gallons of water add 8 lbs. fused oil or 14 lbs. crystallised pure hydrated barium oxide and 0.6 lb. lime which has been slaked in water. The solution stands about 4° Beck (10241 sp. Gr.). When the baryta water is clear, the casts may be immersed being previously suspended by cords. The dipping should be affected with rapidity. Hollow casts after being saturated are filled with the solution and suspended in the bath, and the vessel is closed from two to twelve days, according to the silicate Stratum required. Then remove the cover and the scum, draw the casts out by means of the cords, rinse with lime water, drain and wipe with soft rags. Do not handle them and leave them to dry in a warm place. The solution can be used again by adding more baryta and lime. 2. To harden by means of the silicate of potash solution, convert the lime sulphate into lime silicate by using a diluted solution of potash Silicate containing free potash. Make a 10 per cent solution of caustic potash in water, heat to the boiling point, adding pure silicic acid (free from the iron) as long as it continues to dissolve. After cooling the solution deposits silicated potash and alumina. Leave it in well-stoppered glass bottles to Settle. Before using, throw in some pieces of pure potash, or add about 2 per cent of the potash solution. To indurate the casts, dip them when cold for a few minutes into the solution, or apply it by means of a sponge. When the chemical reaction is finished, remove the excess of the solution by means of soap and water, and subsequently rinse with warm pure water. When thoroughly dry, the plaster casts can be washed with cold soap and water, with the addition of oil of turpentine, taking care that the sponge used to be thoroughly clean. Then rinse with clean water. [...]*

## BANKART, G. P. (1908)

### THE ART OF THE PLASTERER. AN ACCOUNT OF THE DECORATIVE DEVELOPMENT OF THE CRAFT, CHIEFLY IN ENGLAND FROM THE XVITH TO THE XVIIIITH CENTURY, WITH CHAPTERS ON THE STUCCO OF THE CLASSIC PERIOD AND OF THE ITALIAN RENAISSANCE, ALSO ON SCRAFFITO, PARGETING

Bankart draws a brief history of the *stucco duro* in Italy since the Roman period, starting from the description of the difference between *travertino* and *peperino*, also citing old recipes from ancient books.

*[...] Stucco has for its base carbonate of lime, generally the burnt limestone or chalk of the rocks and hills. [...]*

*Vitruvius. [...] the stucco of those days was far more carefully compounded than it is now. The lime was very carefully selected, burnt with wood, and subjected to a very gradual process of slaking for a long time before it was used. It was constantly beaten with heavy sticks and chopped up with a heavy hammer or axe. It was also subjected to frost and was mixed with fine sharp sand and white marble dust, which made it capable of receiving a fine polish. It has always been known to be necessary to toughen and regulate its setting qualities; and the ingredients in his times were: - juice of figs, rye dough, hogs' lard, curdled milk, blood, &c., also two other important things of which we are sparing now, viz. time, and the greatest care. [...]*

*Pliny mentions the use of figs juice, a very viscid sap, as being mixed with the stucco of his days. White of eggs and blood are also mentioned as having been used to retard the setting of the plaster. [...]*

*Elm bark and hot barley water (tannin and size) were mixed in the stucco used in the Justinian's Church of the Baptist, Constantinople. [...]*

*In later times at Rochester Cathedral, about the end of the ninth century, bullocks' blood was mixed in the stucco and mortar. [...]*

*In 1280, at Rockingham Castle, melted wax was used. [...]*

*On Queen Eleanor's Cross, Charing Cross, London, erected in the thirteenth century, the whites of eggs and strongest wort of malt were mixed with the lime and Calais sand. [...]*

*About 1324-1327, in King Edward II's work at Westminster pitch, was mixed in the stucco and mortar. Wax, pitch, urine, beer, and size were also extensively used at that time for the same purpose. [...]*

*Professor Middleton tells of 'six strikes of malt to make mortar, to blend with the lime, and temper the same, and 350 eggs to mix with it,' viz. to seven quarter of lime. [...]*

*Mons. A. Darcel, director of the Cluny Museum, mentions the use of urine, in the sixteenth century, at Rouen. [...]*

*In India and Ceylon sugar, and saccharine fruit juices, rice gluten, and other like compounds are used for increasing the hardness and retarding the setting process of the stucco. [...]*

Mrs Merrifield is also quoted by Bankart.

Bankart then proceeds with a description and historical review of the *Stucco Duro* of the Italian Renaissance and its use for the Arabesque. Following a chapter is dedicated to the Italian technique of sgraffito. The author also describes the techniques of 'wattle and dab'

and ‘pargetting or parge-work’. Bankart illustrates examples of remarkable *Stucco-Duro* used in English Palaces, such as Nonesuch Palace (between Epsom and Cheam) and the Palace in Hardwick (Derbyshire).

Bankart thinks that the art of the plasterer was introduced in England by Henry III, who brought in the Country plasterers from many different Countries, which inspired the local craftsmen. At that time the local workmen were not quite ready to learn the sophisticated technique of *Stucco Duro*, being used to ordinary plaster, or mortar, composed of lime, hair, and sand, such as covered the walls and the ceilings, and was used for ornamental purposes also, both inside and outside the building. These changed along the centuries, especially under the influence of Italian and French workers. The plasterworks on English Houses of the seventeenth century is highly celebrated.

Bankart also describes the importance of plasterwork in Scotland during the sixteenth century. Designs of plasterworks in Scottish Mansions and Castles are shown. Irish plasterworks, according to Bankart, seem to traceable only so far back as about 1740.

Bankart dedicates a chapter to the work of the brothers Robert and James Adam, architects, lived and work in the eighteenth century. They designed and executed between them an immense number of plasterworks.

*[...] The colouring of modelled surfaces of stucco-duro in the past reveals the employment of ‘tempera’ (dry powdered colour with the yolk of an egg) as the most successful and permanent medium known so far. The surface of the plaster must have its suction allayed to some extent by the application of a **hot solution of shellac** or similar preparation, before the application of the colouring matter. **Wax colours, spirit fresco**, and other media have been used, but with unsatisfactory results. The coatings and colouring which were applied to the walls 3500 years before Christ speak to us of their durability and the approval and acceptance of plaster as the material in which the rough walls of those days could be most suitably clothed. [...]*

## KEMP, W. (1912)

### THE PRACTICAL PLASTERER. A COMPENDIUM OF PLAIN AND ORNAMENTAL PLASTER WORK

Kemp provides definitions for the materials and many different recipes for making preparations used by the plasterer.

Blue lias lime. [...] Hydraulic lime formed by calcining rocks of the blue lias formation. Portland cement is obtained from this stone. [...]

Cement. [...] Occasionally employed by the plasterer, as plaster and cement have similar purposes. Cement provides a hard, non-porous surface, capable of resisting the influence of the weather. Kemp describes Portland cement, artificial hydraulic lime, Roman cement, Medina cement, Martin's cement, Metallic cement, Mastic cement, Atkinson's cement, Selenitic cement and Robinson's cement. [...]

Chromolith. [...] Finishing material, produced by the Adamant company, used for walls of buildings. [...]

Lime. [...] Prepared by burning various natural rocks or stones and varies in nature in different localities according to what species of mineral is readily accessible to supply the kiln. Ordinary limestone is a calcareous stone, frequently containing a certain proportion of alumina (or clay) – called 'pure' - or ferruginous – 'mixed' – constituent. The limestone is calcined or burned in a proper kiln, and if it has been properly heated, the resulting product falls into powder on being slaked, or having water applied to it, and is mixed with water and sand (and sometimes hair) in certain proportions, forms a strong plaster and durable cement. Lime in its burnt state is called 'quicklime', has strong caustic properties, but after being exposed to the air absorb carbonic acid gas and become mild and weak. Lime containing argillaceous constituents and is known as 'hydraulic lime' 'Fat' limes are mostly employed for internal plastering. [...]

Plaster of Paris. [...] Calcined gypsum, or sulphate of lime. It can be in two qualities, coarse and fine. The former is used for gauging or mixing with common lime and hair plaster in order to accelerate its setting. The latter is employed for moulding, casting, finishing coats of delicate work etc. [...]

Sand. [...] Essential for the production of a good plaster that the sand is of the proper kind (siliceous nature, clean and of a sharp, gritty character). Sea sand is unsuitable because of the salt that would absorb the humidity from the atmosphere, which makes the plaster damp, also might cause white efflorescence. [...]

Water. [...] Should be as pure as procurable, and especially free from those salts, which absorb moisture from the atmosphere. [...] Amalgamation of lime or cement, sand, hair and water in certain proportions to produce mortars, plasters cements ready for application. These can be coarse, fine, gauged, putty and various kind of so-called stucco and cement.

Coarse Stuff. [...] Mortar composed of from 1 to 1 ½ parts of sand to 1 of slaked lime (by measure) with the addition of short animal hair. The proportion of sand varies and can be from coarse to fine. A bushel of this mixture should weight from 14 lbs. to 15 lbs. Hair in the proportion of 1lb. to 2 cubic feet of stuff for superior works and 1 lb. to 3 feet for ordinary works. Hair should be of the ox, clean, unbroken, and not too short. The sand is usually heaped up and the lime is mixed with water so that the liquid is about the thickness of cream and is then poured into the centre of the circle of sand. The hair is next added and the whole mass well worked together until it is intimately amalgamated. The mixture should be then left for several weeks to cool that is until the lime is thoughtfully slaked, and its heating entirely killed. [...]

Fine Stuff. [...] Pure lime slaked with a small proportion of water into a smooth paste, and subsequently further diluted with water until it is of the consistency of cream. It is then permitted to remain until the slaked lime has subsided and the superfluous water has either been run off or allowed to evaporate. It can be mixed with hair for some uses. [...]

Plasterer's Putty. [...] Made dissolving pure lime in water and then running it through a hair sieve. It is quite the same as the fine stuff but the sieve makes it finer. Gauged Stuff: also called 'putty and plaster' is composed of from  $\frac{3}{4}$  to  $\frac{2}{3}$  plasters' putty and  $\frac{1}{4}$  or  $\frac{1}{5}$  of plaster of Paris. This mixture is used for the finishing coat and running cornices. The addition of the plaster causes this to be a very quick setting mixture. The weather has considerable influence on the setting of the plaster of Paris; the proportion of the latter is increased if the weather is damp. Too great a proportion of plaster, however, causes a tendency to crack in the work.

[...] Stucco is a somewhat an indefinite term used loosely for various mixtures of the nature of plaster, into whose composition common and hydraulic limes enter. Common Stucco. 3 or 4 parts of clean, sharp sand, to 1 of hydraulic lime, gauged as before directed. Troucelled Stucco. To produce a surface which will be subsequently painted, and where a smoother face is required.  $\frac{3}{4}$  of fine stuff without hair and  $\frac{1}{3}$  of very fine clean sand. Bastard Stucco. as the last description but with the addition of hair. Rough Cast. sand, grit or gravel, well washed to remove clay or dirt, mixed with hydraulic lime and water in a condition of slaking. [...]

Kemp dedicates a chapter to the architectural plasterer.

[...] In architecture, plaster and stucco are considered covering coats (renderings) added to a structure already existing. The preparation for their application would vary depending on the surfaces upon which these are spread: brickwork, lathing or wire netting. [...] Kemp describes various techniques: laying, pricking up, two-coat work, lathing, floating and set and pargetting. Kemp gives instructions and examples of motifs for moulding for the plasterer for cornices.

A section of the book is dedicated to the ornamental plaster.

[...] To produce an ornamental object in plaster it is necessary to have a model. This could be something already existing of which it is permissible to take a copy in squeezing-wax or it might be a new ornamental design in which case the model is made of clay, modelling.

The workroom and stand. Firm bench or table, good light.

Tools for modelling. Made of hard material, spatulas of different shapes, saws and measuring tools.

Materials. For modelling, are clay and wax. Pottery clay or kaolin is frequently used (£3 per ton, or 4s. 6d. or 5s. per cwt., at 1d. per lb). The colour of the clay is not as important as much as the texture. It should be pure clay. Some modellers add a bit of sand. Wax is usually employed for small and delicate work. Ordinary wax with the admixture of some ingredients to render it softer and more pliable. It can be purchased or made: clear wax 200 parts, Venice turpentine 26, lard 13, levigated bole Armenian 145. Mix and knead well underwater. [...]

Modelling practice. Kemp provides some tips for the beginners and examples of patterns.

[...] Having modelled the ornamental design in clay, we can reproduce it in plaster of Paris. We need to obtain a mould of it. Three ways of doing this: the mould can be made itself of plaster, or of moulding wax or some elastic substance or composition. [...]

Plaster moulding and casting. [...] The model is well brushed over with oil. Some good plaster of Paris mixed with a small portion of red ochre to reach the consistency of pudding batter. Good plaster means fresh plaster made of sound gypsum, sweet healthy odour and

set crisp and hard in from ten to twenty minutes after mixing. The plaster is gradually sprinkled in cold water with the left hand while the right stirs the mixture. The clay model is completely covered with a layer of plaster, taking care that the plaster goes into the undercuts and that no air bubbles are enclosed. When this layer of coloured plaster is set quite hard, it is to be washed over with clay-water to facilitate the breaking up and removal of the mould after casting. More plaster is then mixed for the backing, coarser plaster is applied all over the coloured coat. Some nail can be embedded to strengthen the mould. When the plaster has set perfectly hard, the work is to be turned over and the clay model is broken up and carefully picked out. For small or delicate models is better to mould in wax, meting ½ lb. of beeswax, ½ lb. of black resin, and 6 oz. of tallow together. The model has a border wall of clay built around it. The moulding wax is then poured on hot and when cold the clay is carefully picked and if necessary, washed out. For elastic moulds, one part of good glue and two parts of molasses (treacle), by weight, are melted together in a large glue pot and poured over the model after the latter has been prepared similarly to that just described for wax moulds. When the compo has quite set it can be carefully lifted without destroying the model. [...]

Casting. [...] It is differently carried out depending on the mould material. A plaster mould should have its surface washed and brushed. The mould is then placed in a vessel with water until soaked, taken out and drained but not wiped. The best quality of plaster should be poured in making the plaster equally cover the surface. The surface coat is then backed with coarse plaster and if necessary, strengthen with iron rods varnished or painted. When the plaster has set perfectly hard, it is performed the 'knocking out' (removal of the mould from the cast). The coloured plaster can be removed bit by bit. [...]

Waterproofing plaster casts. [...] Dr W. Reissing, of Darmstadt was offered prize by the Prussian Minister of Commerce and Industry for a method of preparing plaster casts well to be washed. It is as follow: make plaster casts washable maintaining the sharpness of outline, it is necessary to **convert the lime sulphate into either baryta sulphate and caustic or carbonate lime** (1) or into **lime silicate**, by means of **potash silicate** (2). (1). Gypsum, lime sulphate is covered by baryta water converted into baryta sulphate (which is totally insoluble) and caustic lime which is later converted into lime carbonate by the contact with the air (a large zinc vessel is required with a tight-fitting cover, in each vessel is a grating of a strip of zinc. This vessel is filled ⅔ with soft water at 54° to 77° F (12° to 25 °C) and every 25 gallons of water is added 8 lbs. or 14 lbs. crystallised pure hydrated barium oxide, also 0.6 lb. lime, previously slaked into water. The solution stands about 4 becks (1.0241 sp. Gr.) as soon as the baryta water gets clear it is ready to receive the casts. They are wrapped in suitable places with cords and after removing, the scum from the baryta bath are dipped in as rapidly as possible, and then allowed to rest upon the grating. Hollow casts are first saturated by rapid motions, then filled with the solution and suspended in the bath with the open part upwards. The zinc vessel is covered, and the casts are left in it for one to ten more days, depending on the thickness of the waterproof stratum required. After taking off the cover and removing the scum, the plaster casts are rinsed off with lime-water, allowed to drain and wiped off with cotton and left to dry dust-free warm place. (2). Conversion of the lime sulphate into lime silicate, an extremely durable and hard insoluble compound. Using a dilute solution of potash silicate containing free potash. 10% solution of caustic potash in water, heat to boiling in a suitable vessel and then add pure silicic acid (free from iron) as soon as it continues to dissolve. On standing the cold solution usually throws down some highly-silicated potash and alumina. It is left in a well-stoppered glass vessel to settle. Just before using it is well to throw in a few bits of pure potash or to add 1 or 2% of the potash solution. The casts are silicate by dipping them (cold) for a few minutes into the solution or applying the solution by means of a well clean sponge or as a fine spray. When the chemical reaction is finished the excess of the solution is best removed with some warm soap-water or a warm solution of stearin soap and this is finally removed with still warmer pure water. It is not advisable to leave the casts too long into the potash solution the fresher and purer the gypsum, and the more porous is the cast. Washing must be done with a clean sponge, well soaped, cold water they cannot be washed until thoughtfully dry and saturated with carbonic acid from the air the addition of some oil of turpentine to the soap is useful, as it bleaches the casts on standing. [...]

Stucco. [...] Rendering was not in use in the past. The Italian 'stucco' used for internal work was introduced and widely used in the UK. Stucco is not durable especially when not taken care of the constituent material. The weather deteriorates stucco and disintegrated it, making it fall off in patches. The Italians use plaster of different qualities for the various coat, which they lay on. They first apply a coat of coarse material and then they lay a second coat, which contains a larger proportion of lime than the first and it is finer. The stucco for finishing coat is a very superior description of plaster. Where a very superior stucco is required, the dust of the powdered Carrara marble or other white marble is often added. Alabaster of gypsum (sulphate of lime) in a powder state is also sometimes mixed with plaster in place of the marble dust. This third and final coat of stucco should be well and carefully trowelled to present a perfectly level and smooth surface. Colour can be imparted to this stucco by mixing certain **metallic oxides and earths** in it. When stucco is composed of plaster of Paris instead of lime lukewarm size water is very generally employed for gauging it dissolving some **fish glue** or **gum Arabic** in the water to make the mix more homogenous and avoid porosity of the surface and when the plaster is polished enabling a superior degree of gloss. The polishing can be done by rubbing with a piece of very fine-grained limestone and water washing the surface with a sponge. The stucco can be finished by friction with rubber of stout felt dipped in fine **Tripoli powder and oil** followed by alight rubbing with a felt charged with oil only.

Decorated ceilings. Both the Italians and French-produced excellent work of this character but we have little notable English works until the latter part of the eighteenth century. Robert Adams (1768-1820) great plasterwork designs.

Scagliola. Or fake marble, discovered in Italy and very much used in France. Henry Holland first brought it to England. French receipt:

[...] purest gypsum (alabaster, carbonate limestone), break-in small pieces and calcine. The calcined powder is passed through a very fine sieve and mixed to be used with a solution of Flanders glue, isinglass etc. when the powdered gypsum is prepared and mixed for the work, the plaster is applied over the prickled up coat of lime and hair and then coated with the species of tinted plaster necessary to the imitation of the special marble. [...] The colours used for affresco are suitable. [...] To polish use pumice-stone and a sponge. Then polish with Tripoli and charcoal and fine soft linen and then with felt dipped in a mixture of oil and fine Tripoli and then pure oil. [...]

Stucco duro and gesso. Early renaissance Italian techniques. Stucco duro, hard stucco,

[...] used by the ancient Romans, mentioned by Vitruvius. Well burned slaked lime, fine sand, finely ground unburned limestone or white marble dust. All gauged with water and mixed and beaten until homogenous and plastic. [...] Gesso is a compound of [...] the finest gypsum (plaster of Paris) procurable, or in thereof fine whiting, mixed with glue size. Gesso is mixed to about the thickness of good cream and is applied with a brush. Almost universally adopted as a base for gilding. [...]

Sgraffito. Plaster decoration for mural surfaces but little known or practised in this country. Graffiato, sgraffiato, sgraffito means scratched. On plaster or porcelain, linear ornamentation. The plasterer lay different coloured plaster layers and then a white one and then they cut the outline to expose the colours.

Whitewash, distemper, kalsomine etc. Whitewashing is the application of coloured washes to walls, distempering, kalsomine (US). Kemp describes many techniques to do so, with many materials for starch to size and different pigments.

Fine stuff or putty. [...] Take the best lime procurable, dissolve in water, and pass through a hair sieve. Gauged stuff: take 3 parts fine lime, 1 part of plaster of Paris, gauge lime, with water, and add plaster. Alternatively, 4 parts lime and 1 plaster of Paris. [...]

Modelling Wax. [...] Take 200 clear wax, 26 Venice turpentine, 13 lard, 145 precipitated bole Armenian, mix and knead well in water. [...]

Moulding wax. [...] Take ½ lb. bee's wax, ½ lb. black resin, and 6 oz. Tallow. Melt and mix. [...]

Plaster cast to toughen. [...] Place the cast in a **hot solution of glue** for a sufficient time to allow the cast to be well saturated. This will toughen the plaster so that a nail may be driven in without causing it to split. [...]

Rough stuff. [...] Take 16 parts sharp sand, 4 of good lime putty, and 1 of bullock's hair. Riddle sand through a ¼-inch mesh sieve, beat hair well with a flat lath until fibres are well separated or let it soak in water for forty-eight hours. Add sand to putty and mix intimately then add hair and thoughtfully incorporate let it stand for a time before using. This is suitable for the first coat. [...]

Size. [...] Melt good glue in the usual way and pour out the contents of the glue pot into a vessel filled with boiling water, stirring well until the solution is of one consistence. [...]

Stucco (common). [...] Take 1 part of hydraulic lime, 8 or 4 parts of clean sharp sand, gauge. [...]

Stucco duro. [...] Take 2 parts good lime, 1 ½ part fine sand and 1 part pounded fine marble, gauge, and mix well and beat up with lath or piece of the stick until well amalgamated and plastic. [...]

AUERBACH, A. (1961)

## MODELLED SCULPTURE AND PLASTER CASTING

Auerbach describes the techniques for plastering starting from the use of clay for modelling.

*[...] Clay is soft plastic earth formed for the most part as a result of the wearing down and decomposition of rocks containing aluminous minerals, such as granite. Many other ingredients can be present, among them oxide of iron. If clay contains iron it turns red when burned. Firing potters' clay is the king generally used for modelling. The moist form of clay is usually recommended for beginners as the addition of water to the powder can be troublesome. It is usually sold in quantities of seven and fourteen pounds, or by the hundredweight. Clay must, of course, be kept in a constantly damp state for use and contained in a suitable receptacle. A large strongly made wooden box, lined on the inside with zinc or lead and with a hinged lid, tightly fitting and similarly lined, is usual for storing large quantities of clay (clay bin). A well-damped and not too light cloth should be placed on top of the moist clay before the lid is closed down. Clay may be used almost indefinitely. It improves rather than deteriorates with use, but after use, it should be broken into small pieces before being put back in the bin. If it hardens, it will be necessary to pour water over it until almost covering it and left like this for about 24hrs. any surplus water should be then drained off. Tools, sculpting exercises and how to build the armature is also described by the author. [...]*

*On plaster casting. [...] In order to make a replica of the work in plaster, it will be necessary to take from the clay model exact moulds, which may then filled, or coated all over inside, with a sufficient thickness of liquid of plaster of Paris, to take the impress of the mould precisely as it sets. It must then be possible to remove the moulds, leaving the replica of the clay model – now in plaster – standing freely. A waste mould is so-called, because its removal from the plaster cast within, involves breaking away the mould piece by piece; the mould is then destroyed in the process and it is only possible to obtain one replica of the original model by this method. It is none the less the most usual method for sculptors to employ, in giving permanence to their work in clay. It is a very exact and simple method and the mould may be made directly on to the surface of the clay, without the use of any dressing such as would be necessary for preparing it for gelatine moulding, for instance. To make a waste mould of a head it would be necessary to make the mould in two pieces, so that one piece may be easily removed, and the clay and armature extracted from the other half, without injury to either piece. It will be important later to have sufficient access to the interior face of both halves of the mould, in order to clean them thoroughly and remove any clay left in the undercuts, and also to prepare the surface before they are put together again, so that fresh plaster may be poured in to for the replica, or cast, of the clay model. There are two chief methods of waste-moulding ahead. The mould may be divided by making a pot-lid – that is to say, a more or less circular or oval piece, some 5 to 7 inches in diameter, may be made at the back of the head and the rest of the head can then be moulded in one piece – or the mould can be divided by a line running over the top of the head and down both sides of it, on or behind the ears preferably, and down the side of the neck to the base; so that the moulds may be made both sides of this line and contiguous to each other upon it. [...]*

*Materials and equipment for waste-moulding a head. [...] Plaster of Paris is made by burning Gypsum – a whitish mineral consisting of sulphate of lime and water. This burning or calcinating drives off the water and reduces the gypsum into a fine powder, which as Plaster of Paris, will again solidify into a hard material when suitably mixed with the right quantity of water. Different quality of plaster may be obtained. The pink or light brown, coarse builders' plaster is no use for casting. The superfine quality which is used for casting sculpture is made from picked raw material and is pure white in colour. It is usually called 'Fine' or 'Superfine Dental Plaster'. It is sold in seven-pound bags, fourteen-pound bags or by the hundredweight. The chemical action by which water and plaster of Paris combine into a hard substance makes the plaster very sensitive to moisture. It absorbs moisture from*

*the air with extreme readiness and must therefore be kept in an air-tight tin for storage, or it will become soon useless. Once the chemical action has taken place it is useless for casting. Its speed of setting decreases as it absorbs moisture from the air, up to the point where it is altogether spent and quite useless. The first necessity is a bowl or bowls in which to mix the plaster. For this purpose, an ordinary white earthenware kitchen basin is excellent. At least two plaster tools will be necessary, one large and one small. These tools are made of steel. One end of the large one must be a spatula which is usually made slightly flexible, the other end is shaped like a thin leaf with the point turned up and is quite rigid. As for the modelling tools, there is a vast assortment of shapes to be obtained. A large kitchen spoon will be required to mix the plaster. A soft, long-haired brush will be used in cleaning out and preparing the inside of the empty mould. Some pure green **soft-soaps** which can be bought at any chemists and a very small quantity of pure **olive oil** will be used for the same purpose. Some string cord, with which to tie the moulds together before filling them, should be obtained. A strong knife will be necessary to trim the edges of the mould. Some powder colour – **yellow ochre, burnt umber, or light red** – will be used to tint the first coat of plaster. Some very thin brass sheeting must be bought to be cut into strips that will be used to make a fence dividing the two halves of the mould. A good supply of water near to hand will be very important. [...]*

*Waste-moulding the head.* [...] It will be first necessary to make a fence on the model with the strips of brass sheeting to divide the mould into two halves. As soon as the front mould has been made and when the plaster has set, the fence will have to be removed. The outer edge of the mould will have to be trimmed clean with a knife and a little of the surface around it will have to be smoothed also. Pour some freshwater into the earthenware bowl, filling it about 2/3 of its capacity. Into this water put some of the powder colour so that the first coat of plaster in contact with the model can be differentiated from the subsequent coats because of its different tint when the moulds are being chipped off the cast later on. [...] Mixing the plaster. [...] Now take and a handful of plaster from the bag and quickly but steadily, sift it through the fingers into the coloured water, using a slightly circular motion to spread it fairly evenly. Repeat the operation very speedily until the plaster forms a little mound just above the surface of the water in the centre of the bowl. Then take the spoon and plunging it right down to the bottom of the bowl stir or rather beat the plaster and water together without bringing the spoon to the surface (to avoid air bubbles). Leave the plaster standing for a few moments and then the plaster is ready to be poured on the clay model. Leave the first coat of plaster as rough as possible so that the next coat will adhere to it. This coat should be approx. ¼ inch thick. As soon as the head is covered with the first coat, the plaster should be left to set not more than 15 minutes. Take a brush with a little clay water and daub patches of the plaster with it here and there over the surface. This is done so that when the outer coat of white plaster mould is finally being chipped away, they will come away very freely from this first coloured-plaster coating. Now mix the plaster as before, but without adding any colour to the water and continue to build up the outside of the mould all over. This second coat of plaster should be rather thicker than the first coat, particularly over prominent parts such as the nose, chin, eyebrows and around the outside edge of the mould touching the brass fence. While this second coat is setting, take some lengths of iron and bend them as nearly as possible to the shape of the mould. Mix another bowlful of plaster, but this time let it stand until quite thick, then fix each iron quickly into position on the outside of the mould by placing a good solid blob of plaster at each end of the iron. Another way of fixing the irons is to use some 'scrim' (hessian canvas used by plasterers) and cut them into strips. Dip these strips into a bowl of mixed plaster and when fully soaked, twist it loosely around the iron. Then with some fairly thick plaster build up the outside of the moulds with a final coat. The completed plaster mould should be, roughly, not less than ¾ inch average thickness and should be built up to the full depth of the fence all-around at the edges and the base, where it needs to be strong. Once the plaster has set and the mould has been cleaned up and prepare for opening it, take up a wooden mallet or a light hammer and a broad, blunt chisel. Do not try to force the opening operation. Once the mould seems to loosen, move it patiently. Remove the clay and thoroughly clean the mould. When the mould is clean a mixture may be made putting a tablespoonful of the soft soap into a cup nearly full of very hot water and stirring until this dissolve. A small teaspoonful of the olive oil should be added to the mixture, which must be thoroughly stirred together again. The mould should

*be lathered with this mixture all over for about 20 minutes until the mould has repeatedly been treated all over. The surface now should be sufficiently saturated to be just non-absorbent for water and having something like an egg-shell finish rather than a high gloss. The two halves of the mould should now be put together and tied in position with a rope. Plaster is inclined to swell as it sets hard. In filling the mould, the objective will be to make a hollow cast not much more than an inch thick all over. Begin by mixing, carefully, a bowlful of plaster as before, and pour this into the open end of the mould. Shake the mould round rather vigorously, this operation is called 'rolling the mould'. Repeat this operation at once, the plaster will soon begin to thicken, and the operation should be repeated until it does so. Then mix another bowlful of plaster, pour it into the mould and repeat as before. If skilful rolled, a very thin coating of plaster should cover the entire surface of the mould. When it is not possible to roll the mould, there is another way of filling the mould. This is to fill each half of the mould separately and then, when they are put together and tied as before, to run liquid plaster into the combined mould down each side. Once the mould has been filled, it should be left standing for at least one hour to let the plaster set properly. When the plaster has had a good time to set thoroughly, lay the mould on some soft material and start chipping away the plaster mould with a very blunt chisel and a light mallet. Do this slowly and carefully. The coloured plaster will indicate when we are close to the cast. [...]*

The figure and works in relief. The author suggests some exercises for the student sculptor: modelling, casting, building the armature. As for the waste-moulding the figure, the process is similar to the one described for the head, although it is more complicated. The process involves making the moulds in many pieces. The simplest figure mould usually consists of three pieces. Care should be taken in deciding how to divide the moulds and where to place the brass fences, but apart from this, the rest of the operation is very similar to the one described before.

Finishing and colouring plaster casts. [...] *Plaster will pick up dust from the atmosphere on its outer surface, often leaving the recesses considerably lighter in tone. A cast in its natural untreated state can be cleaned by being entirely soaked for the best part of the day in a receptacle of water. The water should cover it entirely and dust marks may be gently sponged away while it is still underwater. Usually, however, it is far better to treat a new cast in some way which will give it a more permanently attractive surface, once the cast is hard and free from moisture. A new cast will usually take some weeks at least to dry out thoroughly in the atmosphere. To give to the plaster, the **appearance of bronze**, it can be applied some sort of coloration and finish which can be almost indistinguishable from the bronze itself. **Although it would be preferable and no doubt more aesthetically honest to have the work cast in metal, to give such finish to the plaster will, after all, leave it with an appearance almost indistinguishable from the final one intended by the sculptor when he first made his model in clay.** Nearly every sculptor has his own recipe for colouring plaster, to give to it much the effect of actual bronze. Some of these methods are based on the dry colouration which chemically treated bronze can give, when the action of the chemicals first raises light corrosion or Verdigris (happening when sal-ammoniac or dilute nitric acid or any other chemicals, are applied to the surface of the metal). To give something of these effects to the plaster cast there are innumerable recipes existent. A coat or coating of **powder-colour** mixed with **milk or casein**, followed by some slight polishing with cotton wool which has been dabbed into some **talca (French chalk)** is one method. Painting the cast with a fairly opaque coat of **poster colour** and then with a more transparent coat of **lighter colour** is another. Give the plaster cast a coat of **white Polish (thinnest forms of shellac varnish** – it can be diluted with **methylated spirits** if it has thickened). When this has dried thoroughly, pour some of the polish into a saucer and mix into it some **burnt amber** and give the cast a not too thick but free coating of this mixture. Work quickly and do not attempt to make the colour run too evenly. Now get some good **gold-bronze powder** of a full rich warm colour. Using a little of the white polish as a vehicle a dragging fresh bronze powder into it, touch up all the prominences of the cast with the gold bronze. If this operation has been carried out successfully, the cast will now have very*

much the appearance of a real bronze before being treated for colour. But it will look somehow coarse and raw. Then get a lump of **beeswax** and shred it finely into the top of tin or another small receptacle, with a knife. Just cover this pile of wax shreds with some turpentine and leave it to soak overnight. By the next morning, the wax should have dissolved, turning the mixture into a thickish and nearly transparent, somehow jelly-like substance. The wax may be dissolved more quickly by heating it with the **turpentine**, but this is dangerous for the vapours. Into this solution, mix whatever colour you have in mind for the final bronze. Artists' **oil colour** straight from the tube will serve well here; a **Prussian blue with burnt sienna** will give a rich green base with immense depth of tone whether it verges toward the olive or the blue side. Modification to the colour can, of course, be made by adding some **yellow ochre** or **viridian**. The whole mixture should be transparent rather than opaque. It is best to use a hog's hairbrush for this operation and to spread the coloured wax very evenly and not too thickly, by stippling hard over the whole surface and into all the crevices. This will be shiny when wet and will become matt when dry. It can be then polished with a very soft cloth. When it is completely dry another polishing can be made with **French chalk**. If beeswax is not available almost **any wax in paste form** – not liquid – will serve. To simulate the terracotta finish. **Venetian, light or Indian red** are often used to simulate the appearance of terracotta. It is better to give the cast a coat of **white polish** first and when this is completely dry, to work over this surface with poster colours or any other thin distemper colours. Start by applying the main colour desired opaquely and then work over the top of this colour with very thin washes, glazes or scumbles of lighter colours, finally using just a little French chalk and a wad of cotton wool to give the very slightest polish to the prominences. Alternatively, a little powder colour mixed with some **glue size** to hold it together and a little **gilders' whitening** (or a touch of **Titanium white**), making a sort of very thin coloured gesso. To apply a coat or coatings, of **white polish** alone, is the simplest method of giving a slightly ivory and polished appearance to the cast. A little **raw umber, yellow ochre** or another colour may be added to the polish to give variety and warmth. A thin top coating of the **beeswax dissolve in turpentine** may be applied **over the dry shellac** and then given a slight polish with some dressing of **French chalk**. The cast may be waxed without the coat of shellac first and if the top surfaces are a little polished when the wax is dry it will greatly improve the appearance of the cast. Another method of giving some translucency to plaster and protecting it from absorbing dust is to give it some coating of ordinary commercial **boiled linseed oil**. This will turn slightly yellow but also it will darken vary considerably with time. **Plaster may be stained or painted, stippled or glazed; it may be left near its natural colour or darkened to give the glow of bronze or the sheen and colour of ebony; it may be left matt or it may be polished. If you happen to have a great love for smooth surfaces you may work all over the cast with steel tools and glass-paper until it has nearly the fine surface of marble itself; if you have built your model so that its final form and texture expresses to perfection the development of your plastic idea, you may leave it exactly as it cast. Your colouring and finishing of the surface of the cast should always be directed towards the realization of the sculptural idea as a unified end.** One other prime method is to add powder colour when the plaster is being mixed to form the cast. This has some difficulties as picking the tone as when dry the colour will be different and it is difficult to do retouches. [...]

WAGER, V. H. (1963)

## PLASTER CASTING FOR THE STUDENT SCULPTOR

Treating the model. No treatment is necessary if casting from clay, plasticine or wax. Shellac the model to prevent the mould from adhering when casting from plaster. White beeswax and turpentine brushed on while hot and then washed off with turpentine when casting from marble. Shellac to be then removed with methylated spirit when casting from unpolished wood.

Types of Moulds. Waste mould is destroyed in the process when only the one cast is required. Plaster applied to the model and when set, the model is withdrawn. The mould created is filled with fresh plaster and broken away. Jelly mould the resiliency of the material permits making casts with undercuts, no fear of adherence of mould and cast. Many casts can be made, but the jelly can only be kept for a short time. Piece mould is for multiple casts, can be kept indefinitely. Various pieces of moulds are made and carefully fitted together. Pieces are held together by a casing of plaster. These moulds are imperative where moulds must be kept in stock over a period and for huge objects.

Releasing agents. A solution with soap can be made by boiling two large tablespoons of best black soft soap in a pint of water. This is then to be used cold. Shellac them while damp, with two coats. Then grease with olive oil mixed with tallow.

Closing the pores. White shellac, an ounce in a pint of methylated spirit, can be brushed or used to dip. Dextrin, an ounce of powder dissolved in a pint of water, can be brushed or used to dip. Size of white beeswax and glycerine (two ounces of beeswax heated and melted into half a pint of glycerine and thinned with turpentine). Clean skimmed milk can be used until the cast saturated. Clear linseed oil can be brushed on. A solution of two parts of stearin, two parts of Venetian soap and one part of pearl ash. Grate the stearin and soap and mix with thirty parts of a solution of caustic soda. Boil for half an hour, stirring well all the time. Add the pearl ash dissolved in a little rainwater and boil for another five minutes. Stir cold and mix with more caustic soda until it is liquid. Allow standing for seven days well covered up. Can keep the solution indefinitely. Brush onto the cast. Polish when dry with silky material. Second coat if not satisfied. Litharge and linseed oil (for external plasterworks, boil six parts of linseed oil, one part of litharge and one part of wax. Brush on hot, when dry second coat. Allow to dry and then polish). Wax and turpentine (stearin or paraffin wax dissolved in turpentine, 1 ounce to half-pint, apply on a dry plaster cast. When dull polish appears, it has absorbed sufficient wax. Polish briskly with a pad of cotton wool when dry. A little yellow ochre, raw umber or black, applied sparingly just before the final polish, will give an old ivory effect. Rub colour well into hollows and wipe off high spots. A

final polish with French chalk will give a good lustre). French chalk (excellent final polishing agent. Use with a pad of cotton wool).

Bronzing and colouring. Need powder colour, burnt umber, emerald green, lamp black, reds and blues and a medium for floating these on. Use a gold size (thinned with turpentine and linseed oil) or shellac. Need metal powders, bronzes, golds, coppers, medium cellulose lacquer or shellac. After bronzing, wax to protect.

Varnish. Half an ounce of tin and half an ounce of bismuth in a crucible. Melt together and then add half an ounce of mercury. When fusion is complete allow to cool and add the white of an egg. Brush on, dry, polish.

MEILACH, D. Z. (1966)

## CREATING WITH PLASTER

Meilach describes the preparation and the use of plaster, the tools used by the plasterers and the techniques to make sculptures with plaster. The techniques for plaster casting and few technical notes are also present.

*Prepare and Use Plaster. [...] Plaster comes as a white powder and must be mixed with water at room temperature. The water-to-plaster ratio varies, generally one part of water and two of plaster. A plaster object made from a plaster mould must be thoughtfully waxed so the two forms will separate when dry. Vaseline is the most easily available separating medium; it may be melted with carbon tetrachloride to simplify the spreading. Automobile paste wax, tincture of green soap and some grease-cutting detergents will also do the job. The separating medium may be removed by washing it with hot water. Waste plaster should never be poured down a drain! Always place the room-temperature water in the mixing bowl first. (too hot water, the plaster will set too quickly, cold water will retard setting). Sift the plaster through your fingers and into the water slowly and evenly to break down any lumps. Allow the plaster to soak for about two minutes to permit time for a film of water to surround most of the plaster grains. When the plaster is absorbed using a spatula or your hands to mix. Stir gently until there are no lumps. be careful not to enclose the air bubble into the mixture. If the mixture is too thick, more water may be added. If it is too thin, adding more plaster will weaken the final cast because the first solution of plaster already will have begun its chemical action. The ideal mixture has a creamy, pouring consistency. When the mix has been sufficiently stirred, tap the bowl gently on the worktable so that the excess air bubbles will come to the top. As the plaster continues to absorb the water, its crystals harden and interlock quickly, resulting in the 'setting' action. The plaster tends to expand slightly and become warm as it hardens. [...]*

*Tools. [...] There is a great variety of simple tools that can be used by the plasterer. It is possible to make impressions, add textures, dig holes and gouges, sand, smooth and scratch lines into plaster until the last moment. Spatulas, scrapers, saw-toothed instruments and chippers are finishing tools. Wet sponge to wash and smooth. Many instruments to create interesting designs. All tools should be immersed in water as you use them and washed immediately after use. [...]*

*Casting with Plaster. [...] Moulds can be made of sand, clay, cardboard, plaster and new plastic materials. From some mould, only one casting can be made, from others, the casting can be duplicated many times. [...]*

*Sand casting. [...] A sand mould may be used only once because the process of casting destroys it. Each sand casting produces an individual piece of sculpture. Sandcasting only requires a bag of sand and a few pounds of plaster, a box to hold the sand. Sand should be moist enough, so pattern edges hold up. Simple tools are used to create impressions and design. When the sand mould is complete, plaster is mixed about the consistency of heavy syrup, so it flows easily from a spoon without breaking down the design of the mould. If deep areas exist, fill these first, then continue to fill the mould until the plaster is level with the top of the sand. The casting should be allowed to dry overnight; the sand is then spooned away from the sculpture around the edges. The plaster is carefully cleaned, and the loose sand particles are brushed away. [...]*

*Clay casting. [...] Plasticine clay is one of the most functional materials for preparing negative moulds. It has a wax base and will not stick to plaster. Water-based clays are not satisfactory. The negative design is made in a slab of clay. The plaster will fill in the impression and the design left by the object will appear in the plaster casting. Clay is easier to work with when it is softened by kneading or placing it in a warm oven. Plaster is mixed*

to a creamy consistency and poured over the clay to about a three-quarter-inch dept. after the cast dries thoroughly; separate the clay from the plaster. [...]

Plaster Sculpture. [...] Sculpture usually falls into three classes: in the round, relief and intaglio. Traditionally sculpture in the round may be developed in two methods: chiselling or carving a design from a block of the material – subtractive method – and the other is the additive method, which involves building up a form by adding material over support called the armature. [...]

Sculpting from a block. [...] Vermiculite added to the plaster mixture gives the material a texture. It also makes the block lighter in weight and easier to carve. [...]

Building on an armature. [...] Wire, plastic, twigs, and many other materials can be used for the armature. An armature gives strength to the plaster and permits the plaster to dry more readily because the form is more hollow than solid. [...]

Relief sculpture. [...] Reliefs are of three kinds: high relief, in which the figures project boldly; low or bass-relief, in which they project slightly; and intaglio, in which the figures are sunk into the background. [...]

Duplicating with Plaster. [...] There are two basic methods of duplicating: the piece mould and the waste mould. [...]

The piece mould. [...] Consist in several small portions, planned so that each piece can be taken from the original then put together somewhat to make the mould for the new cast. Usually, the piece mould is made from an original sketch model of clay or plaster. The new casts sculpture may be made of plaster, bronze or other metal. The model must be carefully studied to determine where the sections will be made. Then one section at the time is outlined with plasticine clay as a 'fence'. The model is greased thoroughly with a separating medium. Plaster is poured into the clay fence and built up. Each section is made individually so it fits perfectly against the section next to it. All the mould pieces are then greased thoughtfully and assembled and tied together. The cast material is poured into the mould through an opening left at the top and allowed to harden. Each piece of the mould is then carefully removed and the finished cast results. Many identical casts can be made from one-piece mould over and over. [...] The waste mould. [...] The waste mould is used when the sculptor wants to cast a clay model in plaster. He's not interested in saving the clay model but wants the more permanent plaster reproduction. The waste mould is easier than the piece mould. In the process, both the plaster mould and the clay model are destroyed. If you want to duplicate a head made of clay you will need some 1- by 3-inch pieces of copper, aluminium or similar material to separate one half of the model from another (shims). Mix a small batch of plaster, using blue coloured water and apply a thin coat of the plaster over the entire clay model. Then add white plaster and built up the surface of at least 2-inch thickness. After the plaster has dried thoughtfully carefully separate the mould with a sharp instrument at the seam made by the shims. Dig out all the clay and you will have a perfect negative. Leave a hole at one end. Now grease the negative mould and seal the seam and tie the mould together tightly with coarse canvas or a rope dipped in plaster. Pour plaster into the mould tapping gently to eliminate the air bubbles. After the cast dries remove the ties and begin to chip away the plaster mould carefully. When you reach the blue plaster, you are close to the cast and must be careful. [...]

Technical Notes. Types of Plaster:

Plaster of Paris. [...] setting times 6 to 9 minutes. Must be mixed in small quantities because it sets so rapidly. It tends to be slightly lumpy. It is fragile because it dries quickly and quite hard. However, it is easy to carve. [...]

Casting Plaster. [...] setting time: 25 to 30 minutes. The most widely used plaster in fine arts, white and fine-textured. It mixes quickly without trapping air bubbles or forming lumps. It contains a surface hardening additive which helps resist chipping and cracking and reduces paint absorption. [...]

White art plaster. [...] setting time 25 to 35 minutes. Mainly for ornamental plaster, similar to casting plaster, softer and a bit more porous. [...]

Moulding Plaster. [...] setting time 25 to 35 minutes, there are no hardening additives, softer and not so strong as the ones described so far. More porous so requires **sealing with clear lacquer, white shellac** or decorating. Easy to carve but not durable. [...]

Portland cement. [...] setting time 3 hrs. when mixed with water it forms a paste which binds together materials such as sand and gravel. After drying the result product is called concrete. [...]

Latex-silicone. [...] Liquid: this is a hardening agent that is mixed with Portland cement instead of water. Stronger, lighter and more resistant than Portland cement mixed with water. [...]

Variables affecting Plaster. Because of its chemical properties, many factors affect the reaction of the plaster. Frequent problems are lumps, weak casts, erratic setting times and surfaces that are soft, chalky or full of air hole.

Contamination. The bowls and tools have to be kept clean to avoid contamination.

Improper storage. Plaster should be stored in a dry space in closed, heavy paper bags or metal or fibre drums with tight covers. Plaster which has been exposed to moisture will start crystallising and become lumpy. plaster containing lumps should never be used.

Mixing time (overmixing and undermixing). The purpose of mixing is to dry each particle of plaster and to force the air bubbles to escape. When not all the particles are wet, undermixing occurs and the plaster resulting will not be strong and the surface may be soft and chalky. Overmixing causes the plaster crystals to dissolve into the water more quickly, speeding up the setting process. An excess air bubble is also the result of overmixing.

The temperature of the water. [...] plaster sets more quickly when the water between 95° and 105° Fahrenheit is used because the point of maximum solubility of gypsum in water lies between these temperatures. Room temperature is the safest to use. [...]

Contamination in the mixing water. [...] Some waters contain alum or an electrolyte in solution which, when mixed with plaster, may cause rapid setting. In general, water that is satisfactory for drinking is best for mixing with plaster. [...]

Fasteners and retarders. Purposely speed up or slow down the setting. They will weaken a cast.

Adding texture to a plaster. The bone-white texture can be considerably varied by three methods: setting a foreign texture on to the surface before the plaster is dry, glueing the texture onto the hard-dry surface or adding the textured material to the dry plaster before it is mixed.

[...] Fine silica sand, coarse sand, crushed coloured glass and others, sprinkled on the top of the wet plaster for texture. Adding a few teaspoons of baking soda to the mixture causes a chemical reaction; the plaster dries with a sponge-like, bubbly texture. When vermiculite is added to the mix, an interesting, rough, masculine texture results and the weight of the finished piece is reduced considerably. The block becomes softer and grey. Sawdust, marble chips, terrazzo, sand and used coffee grounds may also be mixed with plaster to vary the texture. Generally, the texture material should be in a maximum ratio of three parts

to one part of the plaster. For extra hardness, add a solution of half-and-half glue water to the mixture. [...]

Colouring and finishing. [...] Fresco technique involves adding a painting medium to fresh, wet plaster. First, a design is made and transferred to the drywall. A thin layer of wet plaster is spread over the wall and then the colouring painted on. A water-based paint added to wet plaster is partially absorbed by the plaster as it dries. Paints that are suitable for wet plaster are **temperas, caseins, watercolours, water inks and dyes used for fabrics**. When the paint is applied to hard, dry plaster the colour quality will be heavier and truer. Any paint can be used. **Porous plasters should be sealed before they are painted.** Use a clear plastic spray, **clear shellac**, or brush on a solution of **glue and water**. Black paint will give the plaster a metallic-looking quality. Silver and bronze patinas may be simulated, the powders should be mixed with a **solution of clear lacquer and alcohol in equal parts**. A mixture of **ochre and linseed oil** will produce an antique finish. For a marbled effect, add small balls of powder colour to the dry plaster. A sealer coating will help to keep the plaster in its original white state. Sometimes **shellac** will turn slightly yellow: **do not use orange shellac**. If a plaster sculpture becomes dirty, immerse it in water and let it soak. After a while rub the loosened dirt with a sponge while the sculpture is still under the water. The dust that floats on the water must be removed. When no water remains on the water surface, lift out the sculpture and let it dry in a dustproof place. [...]

CHANEY, C. (1973)

## PLASTER MOLD AND MODEL MAKING

This is a brief guide on the use of plaster.

Soaping, or applying the separator. **Liquid soap.** A jelly-like product called English Crown Soap (dissolved in warm water and kept available in cool liquid condition). The mould is soaped enough when the surface looks glossy. Before soaping be sure the plaster is damp. **Stearic acid and kerosene.**  $\frac{1}{4}$  lb. of stearic acid in 1 pint of kerosene, melted by warming, removed from the heat, kerosene gradually stirred. Petroleum jelly. Carefully heat and blend 2 parts of kerosene one part of jelly. **Automotive oil.** 30WT. paint the oil with a small brush.

Types of Moulds. Piece mould, Multi-piece mould.

Types of Plaster. Industrial molding plaster is soft plaster or plaster of Paris. Softest, most porous, has no surface hardening additives, easily carved and best fitted for models and waste molds. Consistency 60-80 sets in 20+35 minutes. Casting plaster mixes easily is slightly harder, and develops a hard surface upon drying. Good for the cast to be painted. Consistency 67-80 sets in 20-35 minutes. Art plaster is similar to casting plaster, but not as hard. Hydrocal A-11\*: low coefficient of expansion, smooth, hard-surfaced, used for pattern-making industry. A short period of plasticity stiffens rapidly. Sets in 20 minutes, consistency 45-55. Hydrocal B-11\*: low coefficient of expansion, a high degree of plasticity, gradual setting action. Sets in 25-30 minutes, consistency 50. Hydrostone\*: one of the very hardest cements, consistency 32-40. Cannot be worked in a plastic state. Sets in 15-25 minutes. Ultracal 30\*: harder and stronger of hydrocal. At consistency 37 sets gradually (about 30 minutes).

DE JONGE, L. (1985)

## THE ART OF DOING: PLASTER TECHNIQUES

De Jonge describes the properties and the preparation of plaster, the tools used by the plasterers and some techniques to work with plaster.

Plaster is a very versatile, extremely useful and easy-to-work material. It has many uses: modelling, carving, making moulds, reliefs and sculptures. Plaster is extremely easy to use, but it also has the peculiar quality of penetrating every nook and cranny of a shape, and of drying very quickly. Nevertheless, it is not one of the 'noble' materials that have to be used for centuries to create great works of art; the material is too fragile and impermanent. It has always been used as an aid for many branches of art, due to the possibility of reproducing quickly, an infinite number of times. Casting in plaster, making the model and constructing the moulds. Plaster of Paris comes as a powder and goes hard when water is added. There are many different sorts of plaster.

Modelling plaster. This is relatively cheap and is more suitable for coarse work such as experimenting with casting moulds, studies in forms and for sculpture or modelling.

Casting plaster. This material has a finer structure, goes hard faster and is mainly used for casting. It is a more expensive plaster, but the results are also better. It should always be stored in a bucket.

A fast setting material. Plaster has to be mixed with water to go hard. The correct mixing technique depends on having the correct proportion and on experience. Plaster always goes hard very quick; therefore, you must work quickly and effectively.

The correct order. Always mix the plaster in a clean plaster container, a tray or a bucket and use old tap water. Use the proportion of 1 part of water to 1 ½ to 2 parts plaster. The best quality is achieved by measuring the quantities as accurately as possible. Always start with the water and add the plaster, never the other way around. Sprinkle the plaster evenly into the water with your hand until there is a mound of plaster on the surface of the water. Leave this to stand for about a minute and then stir in with your hand. There must be no lumps or air bubbles. You should also tap on the side a few times at the end of the process. All the air bubbles in the plaster will come up as a result of the vibrations and they can be scooped away. The plaster mixture should have roughly the consistency of yoghurt.

Working quickly and effectively. The plaster should be used quickly and effectively, for after about 6 to 8 minutes the plaster is barely liquid and after about 15 minutes it can no longer be spread. The hardening of the plaster, which releases the heat, follows this. From this point onwards you can no longer alter your work, which usually will take another 1 ½ to 2 hours.

Separating agents. Plaster is a material which easily adheres to any other material, although this is not usually the intention.

*[...] There are several ways in which we can prevent this, in some cases it may be necessary to use two agents: 1) A diluted **soap solution** made dissolving liquid (green) soap or a bar of soap in hot water and leaving this to stand for about a day. The proportions are usually one part of soap to two parts of water. 2) **Oil or Vaseline** can also be used as a separating agent (household oil, such as salad oil). 3) Another possible separating agent is a solution of **shellac in methylated spirits**. Fill a bottle with finely ribbed shellac, heat this up au bain Marie without the cork on the bottle. Shake thoroughly and use when is cooled down. [...]*

Tools. Chisel, rasp, gouge, wooden hammer, saw blades and others.

Techniques. Making a flat tile. Determining roughly the quantity:  $20 \times 15 \times 5 \text{cm} = 1500 \text{cm}^3$  correspondent to 1.5 litres of Plaster. Water:  $0.5 \times 1500 = 750 \text{cm}^3$ . Making and painting a plaster relief. Plaster relief with birds of paradise. Plaster casting with a 'lost' mould: there are two methods of making a mould. The 'lost' and 'not lost'. In the first case, the mould is destroyed and only one cast is made. In the second case, the mould is kept, and more than one identical reproduction can be made. A mould for a bowl or a dish made in one part. A mould-made into two parts. A mould-made in three parts. Plaster cast consisting of several sections. Reproducing a relief. Plaster casts consisting of several parts. Modelling with plaster.

*[...] An imitation leads elephant using **graphite powder, asphalt lacquer, wax, black vinyl emulsion paint, turpentine-based oil**. To make a model look like wood, varnish the plaster with **wax** or **wood stain**. **Gold, silver** or **bronze paint** can be bought in either liquid or solid form. To make the plaster look like ivory, heat the plaster in the oven, melt a large quantity of **stearic acid** in a container and lie the heated figure in this for about 5 minutes. Polish. [...] If the plaster is not coloured it will eventually become very dusty. If you spray it once or twice with **hair lacquer**, this will make it easier to clean as the dust is unable to penetrate the plaster. [...]*

PIVA, G. (2010)

## MANUALE PRATICO DI TECNICA PITTORICA

The author of this book collects information from many sources on definitions and practical recipes. Some of these, relevant to this research topic, are quoted here.

### Acqua di calce (limewater)

*[...] quell liquido limpido e trasparente che viene a galleggiare nelle vasche ove la calce è stata spenta con molta acqua. In soluzione con altri elementi (p. 1 colla di caseina, p. 1 vernice copale, p. 1 acqua di calce, un bianco d'uovo, ½ fiele) si usava nell'antichità per mescolarla ai colori e dipingervi su intonaci di calce e anche di gesso. [...]*

### Biacca (white lead)

*[...] Chiamasi con questo nome il bianco d'argento o cerussa o bianco di piombo o di Krems, che hanno la medesima combinazione chimica e si identificano tra loro. [...] rispetto al bianco di zinco ha particolare e maggiore potenza e resistenza ed è più coprente ed essicca più rapidamente. Circa la sua resistenza è provato che impastato con olio siccativo, come l'olio di lino, forma una sostanza che solidificandosi raggiunge una durezza non raggiunta da nessun altro bianco. [...] Come tutti i colori a base di piombo si altera e fa annerire se mescolato con solfuri (quali il vermiglione e i composti di cadmio che devono perciò essere usati col bianco di zinco). [...] Per ottenere o eliminare i difetti del bianco d'argento è consigliabile mescolarlo con del bianco di zinco, però non bisogna sorpassare la dose di 1 parte di bianco di zinco su 3 di bianco d'argento. [...] Una buona imprimitura si ottiene unendo del bianco d'argento con dell'olio di lino. [...]*

### Bianco di Barite (solfato di bario) (barium sulphate)

*[...] Può sostituire il bianco d'argento. Non è velenoso. È insolubile. [...]*

### Bianco di Champagne (carbonato di calcio) (calcium carbonate)

*[...] Tanto il bianco di Champagne che di Spagna, di Meudon, di Bougival o Biancone, sono delle crete bianche costituite da carbonato di calcio proveniente da giacimenti di conchiglie marine e che, macinate, decantate ed essiccate, formano una polvere bianca particolarmente utile per la pittura a tempera. [...]*

### Bianco Misto (mixed white)

*[...] Bianco di zinco misto a bianco d'argento. [...]*

### Bianco S. Giovanni (S. Giovanni white)

*[...] calce spenta seccata e ridotta in polvere, messa in un catino per otto giorni immersa nell'acqua che va cambiata rimescolando ogni giorno. Dopo questo periodo si toglie dal bagno e si fa asciugare al sole ridotta in piccolo pani. [...]*

### Bianco di Titanio (ossido di titanio) (titanium white)

*[...] Possiede una particolare potenza d'impasto, può sostituire la biacca temendone l'annerimento. [...]*

### Bianco di zinco (ossido di zinco) (zinc white)

*[...] Non altera I colori ma copre pochissimo. Lento ad essiccare. Resiste molto meno del bianco d'argento al contatto dell'aria. Non dà luogo ad annerimento per effetto della luce. [...]*

#### Calcari (limestone)

*[...] rocce costituite da carbonato di calcio e che sottoposte a speciale cottura si trasformano in calce (o calce viva). [...]*

#### Calce (calce viva, ossido di calcio) (quicklime)

*[...] È una materia ottenuta sottoponendo a speciale cottura le rocce contenenti carbonato di calcio (calcari). La calce viva serve a diversi usi industriali quali la preparazione della soda caustica e dell'ammoniaca, la raffinazione dello zucchero, la concia delle pelli, ecc., ma soprattutto serve, come cementante, per collegare fra loro pietre e mattoni, per formare le murature e nel campo pittorico per preparare l'intonaco per l'affresco. Per tali scopi la calce viva deve essere prima spenta e poi impastata con sabbia. [...] Calce spenta – Chiamasi così la calce dopo il fenomeno del suo spegnimento con l'acqua. Aggiungendo alla calce spenta dell'altra acqua si ottiene una poltiglia untuosa al tatto chiamata grassello, aggiungendo altra acqua si ottiene una poltiglia assai meno densa detta latte di calce, aggiungendo ancora acqua si ottiene infine l'acqua di calce. Dello spegnimento della calce. [...] per innaffiamento e per immersione. G. B. Alberti a questo proposito dice : < non dare alla calce viva gran copia di acqua a un tratto, poichèbisogna che si spenga poco a poco [...] Un altro modo di spegnere la calce consiste nel ridurre la calce viva in tanti pezzi e di metterli in un paniere che si immerge nell'acqua per mezzo minuto. Indi si versa il contenuto del paniere su di un piatto e si lascia cosifino a tanto che la calce, per effetto dell'acqua imbevuta, si è ridotta in polvere. In seguito si pesta fino a renderla impalpabile e la si conserva così secca. Calce grassa: quella che si spegne rapidamente e forma un grassello consistente, quasi untuoso ed è generalmente quello che serve per l'affresco perchè è di calcare più puro. Calce magra: calce che si spegne meno rapidamente, assorbe meno acqua, dà un grassello che lega poco, forma calcine che si essiccano troppo rapidamente. Calce idraulica: fa presa anche in presenza dell'acqua. Calce al latte: formata da una soluzione di 1 kg di calce spenta, sciolta poco per volta, in 5 litri di di latte scremato e non centrifugato. [...]*

#### Calcite (calcite)

*[...] Minerale composto di carbonato di calcio e cristalli. [...]*

#### Carbonatazione (carbonation)

*[...] processo per il quale la calce spenta, combinandosi con l'anidride carbonica contenuta nell'aria si pietrifica sempre più e si trasforma in carbonato di calcio. [...]*

#### Cera (wax)

*[...] Cera d'api, cera vegetale e cera montana. La cera d'api si ottiene togliendo dai favi il miele con diversi metodi e fondendola con acqua calda e si ottiene la cera grezza colorata in giallo-bruno. Per purificarla si fa bollire con acqua e per imbiancarla si sottopone in strati sottili all'azione della luce aggiungeno o no trementina. [...]*

#### Cerussa (cerussa)

*[...] Miscela di vari carbonati di piombo. Sotto l'azione dell'acido solfidrico si annerisce. [...]*

#### Colla (glue)

*[...] Sostanza viscosa e tenace che si ricava dall'ebollizione di alcune parti di animali [...] colla d'ossa, colla di pelle, colla di pesce, colle vegetali e colla di caseina. [...]*

#### Destrina (dextrin)

[...] *Gomma d'amido. Polvere leggera, bianca, insipida, di colore caratteristico che ricorda la materia amidacea da cui proviene. Si usa come surrogato economico della gomma arabica negli adesivi. [...]*

#### Essenze ed olii essenziali (essences and essential oils)

[...] *Alcune sostanze volatili, dotate di forte odore aromatico che sono contenute generalmente in alcune parti di piante o anche in certi oli minerali (petrolio). Possono volatizzarsi ed essere distillate con il concorso dell'acqua bollente oppure da sole alla temperatura di 150 o 170 °C, s'infiammano a temperature meno alta di quella necessaria alla combustion degli olii fissi. Sono presso a poco insolubili nell'acqua e in generale solubilissime nell'alcool e più ancora nell'etere. Essenza di trementina, essenza di petrolio ed altre essenze. Danno ai colori ad olio grande fluidità. Hanno il difetto di resinificarsi a contatto dell'aria (si inspessiscono e ingialliscono) e non sono più volatile. Essenza di trementina: olio etereo ottenuto distillando le parti resinose di alcuni alberi resiniferi. Essenza di petrolio: prodotto della distillazione del petrolio. [...]*

#### Farina (flour)

[...] *La polvere che si raccoglie dalla macinazione dei cereali utilizzata per la preparazione della colla di farina, particolarmente indicata per attaccare la carta sulle tavole per la pittura ad acquerello o a tempera, utilizzata anche nella preparazione delle tele e tavole. [...]*

#### Fiele di bue (ox bile)

[...] *Prodotto della secrezione del fegato e delle ghiandole mucose della vescica biliare. Conferisce solidità, corpo, adesione e vivacità alle tinte, ha la proprietà di sgrassare le superfici come fosse un sapone. Ricetta: 1 pinta di fiele bollito e schiumato, aggiungere 28gr, di allume in polvere fine e tenere il liquido al fuoco fino a che si combinino. Oppure bollire 1 litro fiele e dopo averlo schiumato aggiungervi 15 gr. Di sale e mescolarli sul fuoco, lasciar freddare e riposare per tre mesi. [...]*

#### Gesso (gypsum)

[...] *Minerale costituito da solfato di calcio idrato. Quando la calce é unita all'acido solforico forma la pietra da gesso che esiste nei terreni di sedimento cristallizzato, spesso in lamine più o meno cristallizzate. Cotto, ridotto in polvere e stemperato con acqua si adopera per cementare, stuccare, formare statue etc. a seconda delle diverse manipolazioni assume vari nomi ed è adoperato per diversi scopi. Gesso da falegname o a legno: va unito solo alla colla con la quale forma uno stucco tenacissimo. Unito da solo ai colori ad olio (olio di lino) forma una pasta che non asciuga mai. Esiste in polvere ed in pezzi e serve principalmente per fare Stucchi. Particolarmente indicato per le intelaiature delle tele e delle tavole. Caolino: silicato idrato di alluminio bianco, ossia argilla molto bianca e pura proveniente dalle decomposizioni di rocce granitiche, dalle quali l'acqua piovana asporta i silicate alcalini. Se ben macinato possiede una elevata plasticità, ossia può impastarsi con acqua, formando una pasta tenace. Viene utilizzato come argilla o nella pittura a tempera su muro. Il gesso a scagliola: (gesso da presa) gesso che da bagnato con semplice acqua, secca quasi istantaneamente, acquistando una durezza considerevole. La colla, eventualmente unita a questo gesso, si rapprende rapidamente e inutilizza il gesso medesimo. Per poterlo trattare con docilità bisogna diluirlo nell'aceto e non nell'acqua. [...]*

#### Glicerina (glycerine)

[...] *Sostanza oleosa leggermente zuccherina, estratta dalle materie grasse per mezzo della saponificazione. La glicerina si utilizza nelle verniciature col bianco d'uovo per togliere le verniciature, nelle imprimiture delle tele a gesso e colla e nella pittura a tempera con colla di caseina per rendere più flessibili le tele, nella pittura a tempera all'uovo per ritardare la rapida essiccabilità dell'uovo, per rendere miscibile la cera con l'acqua. [...]*

#### Gomme (gums)

*[...] La gomma è una mucillagine vegetale originata nella corteccia dei vari alberi, sotto forma di liquido viscoso che si raccoglie e si coagula in forma di gocce oppure in pezzetti trasparenti. Si scioglie completamente nell'acqua calda come nell'acqua fredda. La gomma miscelata con l'olio nelle pitture ad olio ha il vantaggio di ridurre l'ingiallimento. Gomme di ciliegio, pero, pruno, albicocca, etc. Gomma arabica. Gomma del Senegal. Gomma adragante o dragante. Gomma lacca. [...]*

Grassello (pure limestone)

*[...] Residuo calcinoso che si ottiene spegnendo la calce. Calcare puro, si adopera per formare l'intonaco nella pittura ad affresco. Per l'affresco richiede l'aggiunta di sabbia o pozzolana. [...]*

Itrato di alluminio (aluminium hydrate)

*[...] Nella pittura ad olio serve per ritardare il processo di ossidazione dei colori, ossia a ritardare l'essiccamento. Questo prodotto, preparato con materie pure, può fornire una pasta incolore della stessa consistenza dei colori ad olio. [...]*

Itrato di calce (hydrate of lime)

*[...] Combinazione di un ossido metallico con acqua. Nella pittura ad affresco l'idrato, contenuto nella calcina (idrato di calce), combinandosi con l'acido carbonico nell'atmosfera ritorna gradualmente ad essere pietra fissando e rendendo insolubili i colori precedentemente applicati. [...]*

Latte di calce (diluted limestone)

*[...] Se alla calce spenta si aggiunge dell'acqua si ottiene una poltiglia untuosa al tatto, chiamata grassello. Aggiungendo altra acqua si ottiene una poltiglia assai meno densa detta latte di calce. [...]*

Marmo, polvere di. (marble dust)

*[...] Polvere ricavata dalla pietra calcarea assai dura. Si utilizza per ingessare le tele, nell'affresco mischiata al gesso e nell'encausto. [...]*

Olii siccativi o fissi (drying oils)

*[...] Della famiglia delle materie grasse. Esposti all'aria hanno la proprietà di assorbire l'ossigeno ed applicati sopra una superficie si trasformano in uno strato solido elastico. Per rendere gli olii più puri, chiari ed essiccanti, ci sono metodi naturali ed artificiali. Olio di lino: I semi di lino contengono circa il 22% di olio. L'olio di lino crudo (o vergine) è il più indicato per la macinazione dei colori. È giallo. Chiarificato e purificato deve essere limpidissimo ed avere un colore giallo chiaro. Solidificando offre la maggiore resistenza a tutti gli agenti atmosferici. Olio di lino cotto è assai scuro ed ha un potere siccativo assai accentuato. Olio di papavero: estratto dai semi di papavero, è meno grasso e siccativo, bianchissimo. Olio di noce: dal frutto. Può essere chiarificato e reso siccativo. [...]*

Olii essenziali o volatili (essential oils)

*[...] Per rendere più siccativi gli olii si riscaldano, ma se cotti si scuriscono. Essenza di trementina, di petrolio ed altre essenze. [...]*

Resine (resins)

*[...] Gomma Lacca, sandracca, mastice, dammara, elemi, coppale, ambra o succino. [...]*

Sabbia (sand)

*[...] Si usa per dare più consistenza agli intonaci. [...]*

Sapone (soap)

[...] *Composto di olio e di alkali. [...]*

Seccativi (driers)

[...] *Sostanze che concorrono a rendere più rapida l'essiccazione della pittura. Alterano la natura delle sostanze. [...]*

Stucchi (plasters)

[...] *Calce e polvere di marmo o calce e sabbia, eventualmente colla. [...]*

Vernici (varnishes)

[...] *Proteggere e dare brillantezza. Vernici all'acqua: asciugano presto. A gomma (1/6 gomma arabica e resto acqua pura) e all'uovo (un chiaro d'uovo, 1/3 acqua distillata, poco zucchero). Vernici a spirito: generalmente gomma lacca bianca (sandracca sciolta nell'alcool). [...]*

## TURCO, T. (1990)

## IL GESSO. LAVORAZIONE, TRASFORMAZIONE, IMPIEGHI

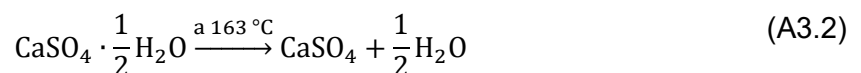
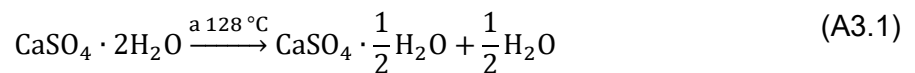
This book collects a wide range of information related to gesso: history, definitions and practical recipes. Some of these, relevant to this research topic, are quoted here.

Plaster across the centuries. [...] *La pietra di gesso è usata nell'edilizia da oltre cinquemila anni. La piramide di Cheope contiene 83% di gesso. I Romani utilizzarono il gesso in architettura e decorazione; è citato nelle opere di Giove, Vitruvio e Plinio. Dal 1200 si trova in Italia il tentativo dell'impiego del gesso come materiale per stucco e da costruzione. In Germania si trova sin dal VII secolo d.C. [...]*

Definition. [...] *col termine generico gesso (Greco γύψος, latino gypsum) si indica sia il materiale che il prodotto industriale che ne deriva e a volte anche il prodotto chimico. [...]*

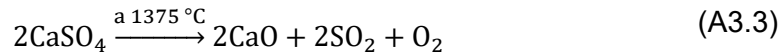
Natural gypsum. [...] *il gesso naturale è il minerale essenzialmente costituito da solfato di calcio con due molecole di acqua di cristallizzazione (solfato di calcio biidrato)  $\text{CaSO}_4 \cdot 2\text{H}_2\text{O}$ . Cristallizza nel Sistema monoclinico, comunemente una combinazione di un prisma verticale con un prisma obliquo e con il pinacoide (varietà selenite). Si hanno anche varietà in masse lamellari vetrose, in masse saccaroidi (alabastro gessoso o alabastrite), in masse fibrose (sericolite), in masse compatte. La montrmatrite è una varietà di gesso naturale che contiene anche il carbonato di calcio. L'anidride, minerale costituito da solfato di calcio anidro  $\text{CaSO}_4$ , cristallizza nel Sistema rombico. Ha un peso specifico di 28.45-29.28  $\text{N/dm}^3$  e una durezza 3-3.5 della scala di Mohs. Il gesso naturale o l'anidride contengono sempre salgemma o minerali a base di solfati solubili in acqua. Se il minerale è costituito da solfato di calcio biidrato chimicamente puro o quasi, il suo colore è bianco, con cristalli perfettamente incolori e trasparenti, se lo accompagnano delle impurezza (ossido ferrico, argilla e sostanze organiche) il colore varia molto. Buon gesso naturale: peso specifico 22.70-22.83  $\text{N/dm}^3$ , durezza 1.5-2 della scala di Mohs, solubilità in acqua 0.241% a 0 °C, più o meno solubile in acidi (tiosolfato di sodio, Sali d'ammonio e glicerina), insolubile in alcol etilico. [...]*

Heated gypsum. [...] *riscaldando il gesso naturale a 128 °C, il solfato di gesso biidrato perde una molecola e mezzo di acqua di cristallizzazione trasformandosi in gesso da presa (gesso da modellatori) costituito da solfato di calcio semiidrato  $\text{CaSO}_4 \cdot 1/2\text{H}_2\text{O}$  con peso specifico di 24.52-26.49  $\text{N/dm}^3$  e contiene 5-7.5% d'acqua. Polverizzato ed impastato con acqua fa prese e riforma un agglomerato cristallino compatto, con leggero aumento di volume. Due varietà allotropiche:  $\alpha$  a presa rapida e  $\beta$  a presa lenta entrambe estremamente solubili nell'acqua. Con ulteriore riscaldamento a 163 °C il solfato di calcio semiidrato perde tutta l'acqua di cristallizzazione e diventa solfato di calcio anidro solubile (anidride solubile o anidride  $\alpha$ , gesso da costruzione o Plaster of Paris).*

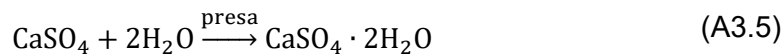
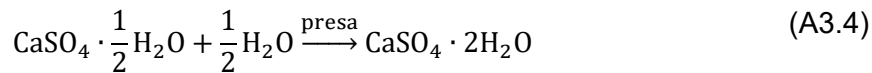


*Sui 500-600 °C si ha gesso morto, stracotto o bruciato non reagisce più con l'acqua e non fa presa. A 1000 °C circa si ha una parziale liberazione sino al 3% di ossido di calcio o calce*

viva CaO (gesso idraulico o gesso a lunga presa). A 1360 °C il prodotto fonde e a 1375 °C si ha praticamente una dissociazione completa. [...]



Setting. [...] indurimento, studiato per la prima volta nel 1765 dal chimico francese Antoine-Laurent Lavoisier e più razionalmente dal 1900 al 1903 dal chimico olandese Jacobus Henricus van't Hoff. I costituenti essenziali del gesso cotto sono capaci di riidratarsi riprendendo acqua di cristallizzazione perduta durante la cottura. Si ottiene il gesso biidrato.



La solidità della massa indurita dipende dalla feltratura dei cristalli (minore o maggiore secondo la quantità d'acqua impiegata per l'impasto). L'acqua in eccesso evaporando lascia dei vuoti o pori e la porosità nella massa vuol dire debole resistenza. Tempo di gemito: tempo che passa dall'inizio dell'impasto a quello in cui la pasta cessa di essere malleabile. Tempo di presa: tra la fine del tempo di gemito e l'indurimento completo. Impurità o particelle mal cotte nuocciono sensibilmente alla presa del gesso causando parziale cristallizzazione o rallentando o prolungando il tempo normale o la riducono molto meno dura. La presenza di impurità e particelle mal cotte nuocciono alla presa del gesso, il quale assorbe meno acqua. A volte le impurità prolungano o riducono il tempo di presa. La quantità di acqua necessaria per trasformare il semiidrato in biidrato s'aggira sul 25% in massa (peso) della polvere; ma tale quantità deve essere molto aumentata per avere una presa meno rapida ed un impasto più lavorabile. L'acqua che si adopera si aggira sul 65% in massa (peso) per i gessi macinati grossi e sul 75% per quelli macinati fini. [...]

Classification of heated or calcined gypsum. [...] Dalla natura della pietra del gesso e dalla sua purezza dipende la qualità del prodotto finale. [...] See tables 2, 3 and 4 in Turco (1990).

Alum plaster. [...] Miscela di anidrite a lenta presa e di allume, ottenuta con un processo di doppia cottura. Dopo la cottura, il gesso viene spento in una soluzione di allume al 10-12% e dopo 2-3 giorni di immersione si lascia asciugare e si ricuoce di nuovo sino a 900-1200 °C. Il prodotto è meno sensibile all'umidità. [...]

Parian plaster. [...] La stessa procedura che si utilizza per il gesso allumato, ma si utilizza una soluzione di borace. Ciò rallenta la presa e conferisce una durezza paragonabile a quella del marmo. [...]

'Sand' plaster. [...] Gesso calcinato e macinato con sabbia in opportune proporzioni. [...]

Lime plaster. [...] Miscela di semiidrato e calce idrata in polvere, che insieme alla sabbia si usa per la preparazione di buonemalte bastarde. [...]

Plaster with wood fibres. [...] Semiidrato con aggregati di fibre di legno (1-15%). [...]

Reinforced plaster. [...] Tutte miscele contenenti fibre vegetali e animali (2-3 Kg ogni 100 Kg di gesso). [...]

Colloidal plaster. [...] Gesso estremamente macinato, molto più solubile all'acqua, quindi origina una cristallizzazione più fitta e maggior durezza e compattezza dei manufatti. [...]

Perlite and Vermiculite plaster. [...] Miscela con gesso con perlite e vermiculite espanse. [...]

Plastic plaster. Gesso commerciale contenente resine sintetiche. [...]

Artificial plaster. [...] Solfato di calcio artificiale, composto da solfato di calcio biidrato più o meno puro. Si può ottenere mediante precipitazione, decomponendo una soluzione di cloruro di calcio con la soluzione di un solfato (comunemente di sodio o di potassio). [...]

How to change the setting of plaster. [...] I fattori che influenzano la presa del gesso sono: la qualità della pietra, la temperatura atmosferica e quella di cottura del forno, la macinazione, la conservazione nei depositi, l'acqua di impasto, il grado di idratazione. Gli acceleratori o ritardanti della presa del gesso influenzano soprattutto il tempo di gemito del gesso. Qualunque ingrediente deve essere dosato e ben disciolto nell'acqua di impasto o d'idratazione del gesso, affinché la sua azione sia perfetta ed uniforme nell'intera massa. Per il ritardo della presa è consigliato utilizzare una sostanza che abbia anche adesività, conferendo solidità e resistenza. Le soluzioni saline devono essere impiegate a temperature 35÷40 °C. Tutti i Sali che accelerano la presa del gesso determinano anche un'aumento della solubilità del gesso stesso ed un maggior sviluppo di calore. [...] See table 6 in (Turco, 1990) [...] I Sali che ritardano la presa diminuiscono anche la solubilità del gesso permettendo di ridurre l'acqua di impasto cosicché ne migliorano la resistenza all'umidità. Ritardatori: 1) sostanze organiche di peso molecolare elevato che agiscono come colloidali protettori: colle, caseine, cheratine, pectine, albumina d'uovo, gomma arabica, gelatina, proteine idrolizzate, melassa, prodotti di decomposizione degli albuminoidi, prodotti d'idrolisi da residui di natura animale, prodotti di reazioni di acidi amminici con aldeide formica, polvere e radice di altea, tannino. 2) Sostanze che diminuiscono la solubilità del gesso: glicerina, alcole, acetone, etere, zucchero, acido nitrico, acetico, fosforico, borico, lattico e loro Sali, fra cui i Sali alcalini e quelli di calcio, carbonato di sodio. 3) sostanze modificanti la struttura cristallografica del gesso: acetato di calcio, carbonato di magnesio e di calcio. Per variare la presa del gesso senza additivi di può agire sul rapporto gesso/acqua, sulla durata della miscelazione, sulle temperatura ambientale. Alcuni additivi agiscono come colloidali protettori: emulsioni cerose e resinose, gli alginati, la carbossimetilcellulosa e il silicato di sodio. Inconvenienti dell'aggiunta di additivi possono essere: la decomposizione delle pitture per azione chimica, l'apparizione di efflorescenze, la formazione di screpolature e vesciche e la perdita di aderenza. [...]

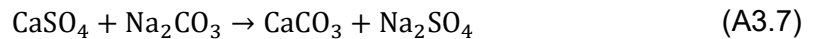
Hardening plaster during the mixing phase. [...] Incorporando agli impasti di gesso sostanze capaci di combinarsi fra loro o col solfato di calcio formando composti con durezza superiore a quella del gesso (trattamenti con silicati, fluati, carbonati, solfati, etc.). aggiungendo al gesso, prima o durante l'impasto, sostanze che non reagiscono, ma riempiono le porosità (soluzioni di gelatina, caseina, gomma arabica, albumina, metilcellulosa, alginati di sodio, emulsioni e soluzioni di resine sintetiche, soluzioni saponose). [...] Treatment with sulphates. [...] miscela di gesso con un sesto di calce grassa spenta e setacciata e s'impasta con una soluzione acquosa di solfato di ferro, di zinco o di magnesio. Il carbonato di calcio reagisce con i solfati formando carbonati metallici duri (conferendo maggiore durezza e impermeabilizzazione). [...] Treatment with fluates. [...] impastare la miscela di gesso e calce sopraddetta con una soluzione acquosa di fluati o fluorosilicati. I fuorosilicati sono Sali metallici dell'acido fluorosilicico (fluati di magnesio, zinco, alluminio e piombo, 10-20g per ogni litro d'acqua). I fuati reagiscono col carbonato di calcio insolubile formando fluorosilicato di calcio insolubile o ossidi metallici insolubili e duri. ). [...] Treatment with barite. [...] impastando il gesso con una soluzione di idrossido di bario, reagisce col solfato di calcio formando solfato di bario insolubile ed idrato di calcio (calce spenta). La barite libera e la calce formatasi si trasformano in carbonati insolubili che induriscono il gesso. ). [...] Treatment with lime. [...] aggiungendo calce grassa spenta si ottiene un ottimo indurimento dovuto alla formazione di carbonato di calcio insolubile. Calce p. 1 e gesso p. 6. Al posto della calce si può usare il carbonato di sodio. [...] Treatment with silicates. [...] impastando il gesso con una soluzione diluita di silicato di sodio o di potassio si migliora la

*durezza e resistenza meccanica e chimica ed un aspetto traslucido. 1 parte di silicato ogni 4-5 parti di acqua. Con una soluzione di 6 parti di gesso e 1 di calce spenta, con una soluzione al 10-15% di silicato di sodio si ottiene una massa che fa presa in poche ore ed acquista durezza ed impermeabilità. Il silicato reagisce col carbonato formando silicato monocalcico vetroso, duro ed impermeabile. Si può impiegare alluminato di sodio, col quale il silicato forma un silico-alluminato di sodio. Il silicato di sodio legato al fluosilicato di magnesio e di alluminio, conferisce resistenza agli agenti chimici. Col solfuro di antimonio, si può conferire una bella colorazione grigio-scura. Con carbonato di rame il gesso diventa verde-chiaro. [...] Treatment with alumen. [...] si discioglie l'allume in acqua calda (20-30%) e con tale soluzione si impasta il gesso e si può aggiungere una piccola quantità di calce spenta. Gesso p. 150-180, soluzione di allume al 30% p. 100, calce spenta p. 10-20. Ha presa lenta ma assume elevata durezza. L'acido solforico (combinato) di questo sale trasforma in gesso il carbonato di calcio, provocando una cristallizzazione più densa. Impastando il gesso da stucchi con la soluzione di allume si ottiene un prodotto a presa lenta, facilmente modellabile a cui si possono aggiungere fino a tre quarti di materiali inerti (sabbia, pietra polverizzata e marmo in polvere, pigmenti colorati, mica in scaglie etc.). [...] Treatment with altea gum. [...] Le radici di altea e di malva ridotte in polvere fine ed essiccate contengono fino al 20-3-% di mucillagine, amido, tannino e zucchero. Miscelando il 2-4% al gesso si ottiene indurimento. [...] Treatment with sodium bisulphite. [...] Gesso con bisolfito di sodio, la presa è più rapida e la durezza aumenta. p. 0.25 bisolfito per p. 100 di gesso. [...] Treatment with ammonium triborate. [...] Sale ottenuto sciogliendo l'acido borico nell'acqua calda e aggiungendo ammoniacca (p. 12 per p. 100 di acido borico). Si usa in soluzione al 6-8%. [...] Treatment with metallic oxides and phosphates and sulphates. [...] Si impasta il gesso con ossido di zinco o di magnesio o un loro miscuglio. Avvenuta la presa si imbevono i pezzi in una soluzione di acido fosforico e con fosfato acido di calcio solubile che combinandosi con gli ossidi, formano dei fosfati insolubili che rendono il gesso compatto e durissimo. Si possono anche impiegare solfati metallici, solfato di zinco e solfato di ferro. L'ossido di magnesio viene aggiunto al gesso nella proporzione del 15-30% e gli oggetti induriti vengono trattati con una soluzione contenente 20-30% di solfato metallico. [...]*

*Hardening plaster after it is dry. [...] Per facilitare l'assorbimento in profondità bisogna avere manufatti perfettamente asciutti. Riscaldamento: in stufe, forni, essiccatoi per una durata di 8-10 ore non superando la temperatura di 100-120 °C. **Successivamente si spruzzano con una soluzione di ammoniacca concentrata che aiuta l'azione successiva di bagni di indurimento a base di borati alcalini e di Sali capaci di formare Sali doppi con quelli di ammoniacca.** Trattamento con solventi: imbevono abbondantemente i manufatti in gesso con **acetone** che penetrando attraverso le cavità e i pori rimuove l'acqua occlusa. Per ottenere una buona disidratazione è necessario ripetere più volte il trattamento. Per ottenere una buona penetrazione in profondità delle **soluzioni indurenti a base di Sali, solfati, nitrati e cloruri** è necessario utilizzare soluzioni poco concentrate, ripetendo più volte l'applicazione e curando che la temperatura ambiente non scenda sotto i 20 °C. Trattamento con sostanze capaci di combinarsi fra loro o col **solfato di calcio** dando luogo alla formazione, entro le porosità del gesso, di composti più o meno complessi, aventi durezza superiore a quella del gesso. Trattamento con sostanze le quali non danno luogo ad alcuna reazione chimica ma promuovono l'indurimento del gesso per semplice formazione di prodottiche riempiono i pori del gesso. [...] Treatment with barite. [...] Gli oggetti essiccati in forno, si immergono mentre hanno ancora una temperatura di 70-80 °C, in una **soluzione di barite (ossido di bario) satura calda**, indi si rimettono a seccare ripetendo più volte il trattamento. La barite (BaO) assorbe avidamente acqua ed anidrite carbonica (CO<sub>2</sub>) dall'aria, trasformandosi in idrossido (barite caustica) e carbonato di bario il quale a sua volta reagisce col gesso trasformandolo in carbonato (molto più duro del solfato).*



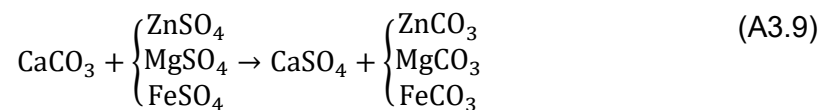
Trattando ulteriormente il manufatto con una soluzione al 10% di acido ossalico si migliora l'impermeabilizzazione. Sostituendo la barite con carbonato di sodio ottengono identici risultati.



Si ottiene un discreto indurimento anche per semplice immersione in una soluzione di triborato di ammonio che si ottiene saturando con ammoniaca una soluzione concentrata e calda di acido borico. [...] Treatment with lime. [...] **Immergendo in latte di calce (calce spenta) o spalmandolo.** [...]



Treatment with sulphates. [...] trattando i manufatti ben essiccati con **soluzioni concentrate di solfato di zinco, solfato ferrosio e solfato di magnesio.** Le soluzioni di questi reagiscono col carbonato di calcio dando luogo alla formazione di solfato di calcio e carbonati duri ed insolubili secondo le reazioni [...]:



Treatment with silicates. [...] per indurimento ed impermeabilizzazione. **Silicato di sodio con rapporto silice ed ossido 3.2-3.3.** Gli oggetti di piccola dimensione si fanno seccare in forno a 100 °C poi si immergono in una soluzione al 20-30% di silicato. Per i manufatti di grandi dimensioni si usano spugne o pennelli. Impegnando il silicato di sodio o l'alluminato di sodio i risultati sono ancora migliori. [...] Treatment with fluates. [...] **I fluosilicati di magnesio servono ad indurire, rendere resistente agli agenti chimici ed impermeabilizzare il gesso.** [...] Treatment with drying oils or varnishes. [...] Gli oggetti accuratamente seccati vengono immersi in un bagno mantenuto a 80-90 °C composto di **olio di lino cotto o di vernici grasse o sintetiche oppure di una loro miscela.** Si lascia la temperatura a 80-90 °C per un'ora o due e poi si fa raffreddare il bagno, si riporta a temperatura per un'altra ora e si raffredda. Si tolgono gli oggetti dal bagno e si portano in una stufa a 80-90 °C dove si lasciano sgocciolare e seccare per alcuni giorni. Gli oggetti possono essere spalmati con olio o vernice, mantenuti ad una temperatura 100-150 °C, ripetendo più volte le stratificazioni. [...] Treatment with resins. [...] Si prepara una **soluzione di sapone resinoso (p. 3 di colofonia in p. 5 di acqua e p. 1 di soda).** Se invece della soda si utilizza l'ammoniaca, questa se ne va con un riscaldamento prolungato (90-100 °C) e la resina resta liberata rendendo il gesso anche impermeabile. [...] Treatment with borax. Si prepara una **soluzione satura di borace in acqua (120g si sale in cristalli per ogni litro di acqua).** Applicato per immersione o per spalmatura. Limitato indurimento. [...] Treatment with casein. [...] **Soluzioni di caseina calcica conferiscono una buona resistenza all'acqua e all'umidità. p. 2 Calce spenta, p. 8 caseina, p. 90 Acqua.** Si discioglie la caseina in acqua e si aggiunge la calce spenta fino ad ottenere una soluzione omogenea. Si applica a spugna o a pennello, si ottiene buona durezza e impermeabilità (dovuta alla formazione di caseinato di calcio). Aggiungendo **silicato di sodio,** la caseina dissolve meglio e di ha più potere indurente. **p. 5 caseina, p. 5 calce spenta, p. 1 gomma arabica, p. 4 silicato di sodio, p. 70-100 Acqua.** [...] Treatment with synthetic resins. [...]

Conferisce elevata resistenza all'acqua. I migliori risultati si ottengono con **resine furaniche**. [...]

Waterproofing plaster. [...] 1) Impermeabilizzazione con sostanze impermeabilizzanti, 2) trattamento superficiale con sostanze capaci di reagire con il gesso stesso e formare un composto insolubile, 3) miscelazione del gesso prima dell'impasto con sostanze altamente impermeabili. 1) **Saponi (stearati, oleati, steropalmitati di calcio, stearati di iodio, ammonio, ecc), olidi origine animale o vegetale, cere (fuse o in soluzione con appropriati solventi), vernici grasse e sintetiche, resine sintetiche (in soluzione od emulsione), gomma elastica naturale e sintetica (disciolta in opportuni solventi), fluati e silicati.** 2) **cloruro di bario e sodio, fosfato ed ossalato d'ammonio, acetato di piombo e barite.** I migliori risultati si ottengono con la barite (ossido di bario) la quale reagisce con il solfato di calcio formando solfato di bario duro ed insolubile. **Quando i manufatti sono formati da gesso e calce idrata possono essere trattati con solfati e fluoruri di ferro, zinco e magnesio, con fluorosilicati di magnesio, alluminio, zinco e silicati di sodio e potassio.** I prodotti del gruppo 2) posso essere anche appartenenti al 3). [...] Waterproofing with drying oils and varnishes. [...] I manufatti in gesso devono essere sottoposti ad un preventiva e completa essiccazione in stufa (80-90 °C) e si immergono nell'olio o vernice (50-60 °C), il gesso deve essere totalmente impregnato e successivamente seccato in ambiente ben ventilato. Si immerge nuovamente per la metà del tempo e si secca nuovamente. Si può spalmare, molte volte. Il gesso acquista una colorazione giallo-bruna. Treatment with alumen soap. [...] **Soluzione diluita di sapone d'alluminio in essenza di trementina e benzina, applicata più volte a pennello.** Il sapone di alluminio si ottiene preparando una soluzione diluita e bollente di sapone e vi si aggiunge una soluzione di allume e solfato di alluminio che si raccoglie, si lava e si secca. Si può precipitare il sapone di alluminio nella massa del gesso applicando una soluzione al 10% di solfato di alluminio, seccando ed applicando poi una soluzione di sapone in acqua calda o meglio in alcole. [...] Treatment with lime casein. [...] Solubilizzando la **caseina con calce idrata o calce spenta** si ottiene un prodotto con notevole potere adesivo e di ottima resistenza all'acqua. Per accentuare ulteriormente tale proprietà si può aggiungere alla miscela una piccola quantità di perossido di bario. **p. 75 caseina, p. 17 calce spenta, p. 8 carbonato di sodio anidro, p. 1.5 perossido di bario, p. 280 acqua.** Il perossido si aggiunge alla fine. Il prodotto finale va utilizzato in massimo 20 minuti. [...] Treatment with fluates [...] Per l'efficacia dei **fluosilicati di magnesio e zinco** è necessario che nel gesso sia presente una discreta quantità di calce. [...] Treatment with soap solutions. [...] Le soluzioni saponose combinandosi con la calce formano composti insolubili che escludono i pori senza isolare le particelle che dovranno cementarsi. Basta mescolare queste sostanze all'acqua da utilizzare per l'idratazione del gesso. **p. 3 colofonia in p. 5 acqua e p. 1 soda.** Se invece della soda si usa l'ammoniaca è necessario un lungo riscaldamento 30-100 °C. Composizione mista: **p. 24 allume, p. 4 sapone bianco, p. 2 gomma arabica, p. 6 gelatina (soluzione al 12%), p. 24 acqua.** Altra composizione: **p. 25 vernice grassa, p. 35 solvente nafta, p. 40 tetracloruro di carbonio, p. 150 alcole denaturato, p. 50 sapone, p. 700 Acqua.** (applicare tenendo il prodotto a bagnomaria) Altra preparazione: a) **p. 1 colla di pesce, p. 420 acqua, p. 30 solforicinato di sodio, p. 49 acido stearico.** b) **p. 432 acido oleico, p. 122 ammoniaca a 28 °Bé, p. 61 alcole denaturato 95% in volume, p. 43 cloruro di alluminio, p. 37 cloruro di calcio, p. 305 acqua.** [...] Treatment with wax. [...] L'efficacia delle cere per l'impermeabilizzazione è superiore ai metodi precedenti. Aspetto traslucido di pregevole effetto estetico (imitazione marmo e avorio). Basso costo ed elevata efficacia: **paraffina, stearina ed ozocerite (fuse o dissolte in solventi).** Per pezzi di grandi dimensioni, cera in polvere sulla superficie e ferro caldo e l'oggetto assorbe meglio se precedentemente scaldato. Si può lavorare a freddo se in soluzione di cera in solfuro o tetracloruro di carbonio anche benzina. **Paraffina p. 20, ozocerite p. 30, white-spirit p. 20, toluolo p. 150.** Cere liquide emulsionate danno buon risultato se successivamente trattate per rendere le pellicole cerose dopo essiccazione insensibili all'acqua e all'umidità. Questo risultato si ottiene aggiungendo morfolina (ossido di dietilimina). **Ozocerite p. 2.4, Paraffina (50-52 °C) p. 8.9, oleina p. 2.5, morfolina p. 2.2, acqua p. 84.** [...] Treatment with gums. [...] Aderiscono tenacemente al gesso formando uno strato isolante e perfettamente insensibile all'acqua ed all'umidità. Il trattamento ha una durata limitata e lo strato perde le proprietà isolanti a causa della luce

e del calore. [...] Treatment with silicones. [...] I siliconi sono composti organici di silicio con struttura alternata di atomi di silicio e ossigeno. Liquidi o fluidi, resine, grassi, sostanze idrorepellenti, gomme, ect. Stabilità al freddo, caldo, all'ossidazione e idrorepellenza. Particolarmente idrorepellenti quando il radicale organico fissato sull'atomo di silicio è del tipo paraffinico o alifatico. I siliconi non sono dei veri e propri agenti impermeabilizzanti, ma più propriamente degli idrofughi. L'idrorepellenza presenta i seguenti vantaggi: maggiore resistenza alla penetrazione dell'umidità e agli agenti atmosferici, grande idrorepellenza, non alterano il colore delle superfici, ottima penetrazione perché bassa viscosità. [...] Treatment with wax liquid emulsions. [...] Aggiungendo una piccola quantità di siliconi al solvente, nelle soluzioni di cere si ottengono delle miscele di elevatissimo potere impermeabilizzante; ugualmente addizionando le emulsioni liquide di cera al 5-10% ad un'emulsione acquosa di silicone. **Paraffina p. 120, acido stearico p. 12, ammoniaca a 26 °Bé p. 6, emulsione di silicone al 30% p. 40, acqua p. 180.** Si scalda la paraffina a 55 °C, si aggiunge l'ammoniaca e poi l'acqua. A raffreddamento ottenuto si aggiunge il silicone. **Per l'applicazione si diluisce con l'acqua: ozocerite p. 90, linoleato di ammonio p. 14, acqua p. 400, emulsione di silicone al 30% p. 30.** [...] Admixture of silicones with potassium and sodium silicates. [...] I silicati addizionati ai siliconi acquistano plasticità e resistenza meccanica. **Soluzione di silicone in acqua al 40-50% p. 5, silicato di potassio p. 15, acqua p. 80.** [...] Admixture of plaster and gelatine. [...] Stemperando il gesso con una soluzione diluita di gelatina animale si ottiene un impasto che fa presa lenta e si può facilmente lavorare dopo il periodo di presa. Per preparare una buona soluzione di gelatina bisogna prima farla gonfiare per 12-24 ore in 2-4 volte la sua massa in acqua. Si allontana l'acqua non assorbita e si scalda a temperatura non superiore ai 70 °C. [...] Liquid glue with lime. [...] **colla forte p. 35, calce viva p. 65, acqua p. 65.** si aggiungono sostanze antisettiche come **bisolfiti, acido borico, borace, acido salicilico, fenolo, eugenolo, betanaftolo** etc. L'aldeide formica può essere utilizzata su gesso e gelatina come impermeabilizzante (sostituibile dai suoi derivati esametilenitetramina, urea-formaldeide etc). Anche l'allume rende la gelatina meno sensibile all'umidità e conferisce indurimento al gesso. Unendo le soluzioni di gelatina con cere, oli siccativi o vernici resinose ed impastando il gesso con queste miscele, si ottengono manufatti estremamente duri. Impastando il gesso con una soluzione di colla liquida calce, contenente poco solfato di zinco, acquista durezza ed impermeabilità. [...]

Rubberised plaster. [...] impastando il gesso con una soluzione di gomma arabica al 25% si ottiene un prodotto con buon indurimento, maggiore compattezza e minore porosità. p. 100 gesso, p. 25 gomma arabica. p. 50 gesso, p. 15 gomma arabica, p. 40 vetro polverizzato. p. 60 gesso, p. 15 gomma, p. 15 limatura di ferro, p. 2 cloruro di ammonio. [...]

Albuminate plaster. [...] impastando il gesso con una soluzione di albumina. Dopo indurimento, i manufatti possono essere trattati in forno alla temperatura di 70 °C per provocare la coagulazione dell'albumina, con cui il gesso diviene insolubile all'acqua. All'impasto di gesso ed albumina si possono aggiungere grassi, cere, saponi metallici, polveri inerti, pigmenti ed ocre, fibre. Il gesso albuminato misto a farina di legno, di sughero, mica in scagliette, vermiculite e simili è plastico e leggero. Con talco e mica diventa setaceo. [...]

Plaster with modern synthetic resins. [...] ci sono numerosissimi tipi di resine sintetiche o materie plastiche utilizzabili col gesso per conferire caratteristiche. I precondensati di urea e formaldeide solubili in acqua, per esempio, attribuiscono proprietà ignifughe (come anche l'aggiunta di vermiculite, perlite e mica). Le emulsioni di acetato di polivinile costituiscono uno dei più importanti prodotti capaci di migliorare le proprietà naturali del gesso trasformandolo in un materiale di elevata resistenza, elasticità, durata, impermeabilità e di spiccato potere isolante termico ed acustico. Alle emulsioni polivinilacetiche possono essere anche aggiunte: gomma arabica, colle animali, destrine, alginati, amido, carbossimetilcellulosa, emulsioni cerose, etc. [...]

Colouring plaster. [...] si differenzia dalla colorazione per il fatto che interessa la sola superficie dei manufatti e non l'intera massa. La tintura inoltre si differenzia in tintura superficiale e tintura profonda. Per ottenere una buona tintura in profondità è necessario che i manufatti si presentino con alquanto porosità e abbiano superfici non levigate e pulite, senza macchie di sostanze grasse od untuose. Gli impasti di gesso con colla, gomme,

resine, emulsioni cerose, resine acetoviniliche ed altre sostanze collanti od impermeabilizzanti, impediscono la penetrazione delle sostanze coloranti, per cui, in tali casi, ci si deve accontentare della semplice tintura superficiale. Gli acetati basici di Sali metallici forniscono le tinte più stabili e gradevoli ed anche le più adatte per le imitazioni del marmo. Impegnando solfati metallici **si imbevono gli oggetti di gesso con soluzioni diluite di questi Sali, si lasciano seccare e poi si trattano con acqua di barite, solfuro od altro sale di bario o calcio.** Con gli stessi acetati o solfati metallici si può tingere il gesso facendo seguire la loro applicazione da un trattamento con coloranti fenolici in mezzo alcalino ammoniacale o di altri idrati alcalino-terrosi. I colori ad ossidazione come il pirogallolo, la parafenildiamina, ecc. Si possono utilmente applicare facendone soluzioni alcaline o neutre con la presenza di sostanze catalizzanti e poi esponendo alla luce. Le materie coloranti solubili che non danno tinte chimiche hanno una tinta viva ed intensa quando si trovano in soluzione e forniscono tinte smorte e deboli depositandosi sul gesso per essiccamento. Queste rimangono più vive se addizionate alla massa del gesso con gomma, resine, silicati, grassi, caseina sodica, colla, ecc. Queste sostanze concorrono inoltre a migliorare la resistenza superficiale dei manufatti di gesso. Fra le sostanze organiche artificiali ne esiste un gran numero di solubili in sostanze volatili, oli e grassi e per questa via applicabili sulle superfici dei manufatti di gesso. Anche **i grassi penetrano in gesso abbastanza profondamente per cui possono essere impiegati per ottenere buone tinture trasparenti di effetto gradevolissimo, vivace, molto brillante e resistenti al lavaggio.** Un colorante ai grassi si scioglie a caldo in un miscuglio di paraffina, stearina, spermaceti e simili sostanze, nei quali si immergono i pezzi di gesso mantenendo la temperatura sui 100 °C per mezz'ora. Si lascia raffreddare di 30-40 °C e si torna a scaldare sui 100 °C ripetendo tale operazione per tre o quattro volte. Con i coloranti a grassi e a solvente si ottengono contemporaneamente la tintura e la impermeabilizzazione. I coloranti acidi e sostantivi in soluzione diluita di silicati, gomma, colla, zucchero, destrina, si prestano ottimamente per lavori superficiali. Una buona penetrazione in profondità delle soluzioni coloranti si ottiene anche scaldando dapprima i pezzi in forno per 7-9 ore e poi immergendo i pezzi per alcuni minuti in una soluzione satura di solfato di potassio e poi in una soluzione di: allume di cromo, solfato ferroso, solfato di zinco, solfato di manganese. Dopo circa 24 ore si ritirano e si lasciano seccare all'aria. La colorazione del gesso si distingue dalla tintura perchè la colorazione viene eseguita durante l'impasto. **Gesso imitazione avorio:** indispensabile avere il gesso scagliola o gesso da forma bianchissimo, gli oggetti devono essere scaldati al forno a 100-120 °C per renderli anidri e favorire la penetrazione delle **sostanze cerose.** Si immergono in un bagno di paraffina o stearina a spermaceti. La tonalità giallastra si ottiene tingendo le cere con tracce di **bitume o coloranti d'anilina ai grassi o Bitume di Giudea disciolto in essenza di trementina.** **Gesso imitazione porcellana:** si impasta il gesso bianco con **ossido di magnesio (o di zinco)** e dopo completo indurimento si imbevono i pezzi formati con **soluzione di acido fosforico o con fosfato acido di calcio.** Ottimi risultati si ottengono anche con l'ossido di alluminio o con l'allumina. **Gesso imitazione terracotta:** si miscela il gesso con calce grassa spenta in piccole quantità e si impasta con una **soluzione diluita di solfato di ferro.** Sfumature particolari si possono ottenere con ulteriori trattamenti superficiali. **Gesso imitazione bronzo:** ad una soluzione di **sapone (50 g di sapone bianco in 500 g di acqua)** si unisce una **soluzione di solfato rame al 10%** ed il precipitato verde formatosi (**sapone di rame**), dopo filtrazione si fa seccare completamente. Si prepara la miscela: **p. 15 sapone di rame, p. 15 cera bianca e p. 30 olio di lino per la quale si trattano i pezzi preventivamente scaldati in stufa a 100-150 °C.** Se si aggiunge **5-20% di solfato di ferro**, da bruno-bluastro diventa bruno-verdastro. Il gesso con questo diventa duro ed impermeabile. Per l'imitazione del bronzo antico: **p. 56 terra ombra bruciata, p. 15 verde, p. 5 bleu di Prussia, p. 15 ocra gialla, p. 5 giallo di cromo, p. 4 terra di siena bruciata.** Tali polveri si stemperano con **p. 60 essenza di trementina, p. 25-30 vernice copale, p. 10 essiccativo.** Gli oggetti si trattano dapprima con **vernice di gommalacca** e poi con la suddetta miscela. Per enfatizzare zone più lucide si aggiunge una cera disciolta in acqua. **Pietra artificiale:** in **500 litri di acqua, 7 kg di allume, 6 kg di calce spenta, 1 kg di ocra gialla.** A tale miscela si aggiunge **1 kg dicolla forte disciolta in 5 l di acqua calda e vi si stemperano 900 kg di gesso e 450 kg di sabbia fine, esente da argilla.** Levigatura dei manufatti in gesso, a secco, ad acqua ed ad olio. Con pomice in pezzi, con pomice ed abrasivi in polvere e con carte abrasive. Lucidatura, lustratura e patinatura dei

*manufatti in gesso: per oggetti di scarsa importanza tale operazione si effettua cospargendo la superficie levigata ed ancora umida con talco. Patinatura e lucidatura perfette vengono ottenute con paraffina o cera bianca o spermaceti in acquaragia, benzina o petrolio. Si possono utilizzare encaustici cerosi od emulsioni acquose di cere (da sole o con emulsioni di gommalacca bianca e di resine). Tali emulsioni devono essere molto concentrate o addensate con gomma arabica, alginati, metilcellulosa, carbossimetilcellulosa, colle animali, etc. La pitturazione del gesso: materiale ideale per l'applicazione dei materiali vernicianti, ma bisogna fare attenzione all'interazione tra il gesso e la vernice. Oltre ad un accurato studio ed elaborazione degli impasti, si deve sempre provvedere ad un'adeguata preparazione delle superfici di gesso, tenendo presente l'effetto di finitura che si intende raggiungere, il tipo di pittura da impiegare e le condizioni ambientali. [...]*

*Cleaning of plaster. [...] i gessi e gli stucchi in gesso hanno limitata resistenza all'azione dell'acqua, delle soluzioni acide ed alcaline per cui necessitano di attenzione e rapidità. La pulitura generale si effettua dopo aver rimosso eventuali macchie. Le seguenti tecniche sono in ordine di intensità: strofinamento con poltiglia di acqua fredda ed amido; strofinamento con poltiglia di segatura ed acqua; strofinamento come sopra con ammoniacca 5% seguito da rapido trattamento con acqua; strofinamento con poltiglia solvente costituita da impasto di talco, gesso, bianco meudon e solvente; lavatura a spazzola a freddo con bagno di acido acetico 10%; immersione in una soluzione al 4% di fosfato di sodio e successiva lavatura con poltiglia di segatura. Eliminate le macchie si esegue una pulitura generale strofinando gli oggetti con poltiglia di segatura semplice od ammoniacale, oppure a solventi. A tale trattamento si fa seguire l'asciugatura con polveri assorbenti come ad esempio segatura fine ed asciutta, farina di legno, amido in polvere, talco, caolino, bianco di zinco, gesso in polvere impalpabile e simili. [...]*

*Admixures with plaster. [...] qualsiasi miscela intima di gesso, acqua ed una sostanza particolare capace di rallentare il tempo di presa (soluzioni di gelatina animale, mucillagini di gomma arabica, soluzioni di alginati, di carbossimetilcellulosa e di metilcellulosa, alcuni tipi speciali di resine sintetiche idrosolubili, le emulsioni cerosi, l'acetato di polivinile in emulsione, gli alcoli polivinilici, l'olio di lino cotto, le vernici oleoresinose. Stucco da modellare: 50 l d'acqua, 700 g di allume, 600 g di idrato di calce in polvere 500 g di doluzione di colla forte al 12%. Con tale liquido si impastano 90 Kg di gesso da forma o da stucchi e 40 Kg di sabbia fine lavata. Stucco da decorare: gesso da stucchi o da forma con soluzione di colla contenente 1% di acido solforico. Con aggiunta di olio di lino diventa resistente all'umidità. Pasta da cornici o da stucchi: tutte le composizioni aventi come base preponderante il miscuglio gesso-colla. Stucco per quadri e cornici: colla di coniglio (500/500 g) biacca di piombo (250/125 g) carbonato di calcio (-/300 g) gesso da ornati (525/425 g) [...]*

Stucchi vari:

gesso	p. 500	350	100	1000
talco	p. 250	-	-	-
caolino	p. 250	-	-	-
colofonia in polvere	p. -	100	-	-
marmo in polvere	p. -	-	25	-
gelatina	p. -	-	30	20
destrina	p. 150	50	-	-
gomma arabica	p. -	-	-	20
acqua	p. 1200	-	200	1500

*[...] Stucco durissimo: a caldo, p. 30 colofonia, p. 35 colla forte, p. 30 acqua e p. 200 gesso da forma [...]*

*[...] Mastice o stucco bianco inglese: gesso con soluzione di allume di potassa in proporzioni tali che per p. 10 di gesso l'acqua di impasto contenga p. 1 di allume. [...]*

*Stucchi plastici moderni:*

<i>gesso</i>	<i>p. 35</i>	<i>40</i>	<i>50</i>	<i>35</i>	<i>55</i>	<i>48</i>
<i>talco</i>	<i>p. -</i>	<i>5</i>	<i>-</i>	<i>5</i>	<i>-</i>	<i>-</i>
<i>litopone</i>	<i>p. -</i>	<i>5</i>	<i>10</i>	<i>-</i>	<i>-</i>	<i>5</i>
<i>cadmio</i>	<i>p. 10</i>	<i>-</i>	<i>-</i>	<i>5</i>	<i>-</i>	<i>5</i>
<i>marmo in polvere</i>	<i>p. 15</i>	<i>15</i>	<i>-</i>	<i>15</i>	<i>-</i>	<i>-</i>
<i>metilcellulosa</i>	<i>p. 2</i>	<i>1</i>	<i>-</i>	<i>1</i>	<i>1</i>	<i>1</i>
<i>carbrossimetilcellulosa</i>	<i>p. -</i>	<i>2</i>	<i>-</i>	<i>1</i>	<i>1</i>	<i>1</i>
<i>alginato di sodio</i>	<i>p. -</i>	<i>-</i>	<i>3</i>	<i>1</i>	<i>-</i>	<i>-</i>
<i>gomma arabica</i>	<i>p. 1</i>	<i>-</i>	<i>-</i>	<i>-</i>	<i>-</i>	<i>-</i>
<i>alcole polivinilico</i>	<i>p. -</i>	<i>-</i>	<i>-</i>	<i>-</i>	<i>2</i>	<i>1</i>
<i>acqua</i>	<i>p. 37</i>	<i>32</i>	<i>37</i>	<i>37</i>	<i>41</i>	<i>38</i>

*uno stucco plastico perfetto per la lucidature può essere preparato con p. 43 di gesso, p. 2 di carbrossimetilcellulosa, p. 20 di emulsione di paraffina al 10-12%, p. 1 di alcole polivinilico e p. 34 di acqua. [...]*

*[...] Si prepara una soluzione di resina urea-formo; o al 10% e si aggiunge alla medesima quantità necessaria di induritore e con la miscela si impasta il gesso. [...]*

*[...] Le riproduzioni o copie posso essere di gesso oppure di altro materiale da usare per colata come ad esempio cera, gelatina, materie plastiche. Forma matta o perduta: destinata a servire una volta sola; forma semplice: fatta di un sol pezzo; forma a tasselli o composta: per la riproduzione di soggetti a sbalzo ed è composta di più pezzi preventivamente e giudiziosamente calcolati sul modello, prima di crearli, e completata di una custodia, pure in gesso, in modo da tenerla unita con tutti i suoi componenti; forma di colla o gelatina: elastica e allo stesso tempo tenace; forma di materia plastica: resine sintetiche o materie plastiche che consentono di raggiungere un alto grado di accuratezza. [...]*

*[...] Il gesso più adeguato per formare è quello detto da formare ma anche il cemento-gesso, il gesso Parian, l'Alabastrina. Adoperando il gesso da presa o da stuccatore è necessario sottoporre le forme ad opportuni trattamenti di indurimento ed impermeabilizzazione in modo da prolungare la durata o migliorarne l'efficienza. Il gesso idraulico raramente si usa da solo a causa della sua presa alquanto lenta. [...]*

*[...] Antiadesivi od isolanti per forme e modelli. Sostanze adesive od isolanti con le quali si ricopre, in sottile pellicola, l'intera superficie del modello o della forma. In genere gli isolanti sono costituiti da sostanze oleose o grasse come l'olio d'oliva, il tallolio, l'olio di cocco, il grasso animale, l'oleina, il sego, la vasellina, ecc. Anche le soluzioni saponose e la paraffina e la stearina disciolte in opportuni solventi od applicate a caldo, costituiscono degli ottimi antiadesivi particolarmente indicati per superfici molto porose ed assorbenti. In questi casi però è consigliabile isolare precedentemente la superficie con uno strato di esilissimo di una soluzione di gommalacca in alcole. La vernice di gommalacca può essere vantaggiosamente sostituita dalle emulsioni acetoviniliche. Un ottimo antiadesivo e lubrificante indicato per tutti i lavori di formatura: olio di cocco p. 2, acido stearico p. 5-10, petrolio p. 100. Il petrolio può essere sostituito dalla ragia minerale oppure dalla benzina. Altro isolante a base di sapone è: sapone p. 1, grasso animale p. 6, acqua p. 8. [...]*

### Appendix 4 List of Contents:

United States Patent No. 1361, 9 October 1839, by J. D. Greenwood and R. W. Keene. <i>Improvement in cements for forming artificial stone, &amp;c.</i>	70
United States Patent No. 59154, 23 October 1866, by D. E. Somes. <i>Improved composition for forming useful and ornamental articles</i>	71
United States Patent No. 192112, 19 June 1877, by W. B. Closson. <i>Improvement in the art of making molds and their counterparts</i>	72
United States Patent No. 308111, 18 November 1884, by J. H. Trickey. <i>Art or process of and composition for making artificial stone</i>	74
United States Patent No. 371550, 18 October 1887, by E. T. Laxton. <i>Process of hardening and preserving plaster-of-Paris casts and molds and making them impervious to water, &amp;c.</i>	75
United Kingdom Patent No. 16840, 28 October 1893, by A. Cléry. <i>A preservative composition, applicable also for the manufacture of artificial stone, statuary and the like</i>	76
United Kingdom Patent No. 10658, 22 April 1899, by W. R. Johnson and G. Nichols. <i>Improvements relating to Gypsum or Plaster of Paris</i>	77
United Kingdom Patent No. 15204, 16 November 1901, by A. Wolf. <i>Improvement in Composition for Coating Surfaces</i>	78
United States Patent No. 968505, 23 August 1910, by G. J. Zolnay. <i>Process of Making art models, &amp;c.</i>	79
United Kingdom Patent No. 143768, 3 June 1920, by W. J. de Bas. <i>Improvement in Plastic composition</i>	81
Canada Patent No. 446844, 24 February 1948, by M. C. Dailey and E. W. Duffy. <i>Gypsum Product</i>	82
United States Patent No. 2660776, 1 December 1953, by J. H. Miller. <i>Flexible mold for forming statues with spaced legs</i>	83
United Kingdom Patent No. 1461812, 19 January 1977, by F. F. Koblitz. <i>Modified Gypsum Composition</i>	85
United Kingdom Patent No. 2053184A, 4 February 1981, by L. W. Stockton. <i>Improvements in or related to gypsum plaster</i>	86

UNITED STATES

PATENT No. 1361, 9 OCTOBER 1839

BY J. D. GREENWOOD AND R. W. KEENE

IMPROVEMENT IN CEMENTS FOR FORMING ARTIFICIAL STONE, &C.

*[...] Our invention relates to a mode of producing cements from gypsum or sulphate of lime and alum. To make a white cement., we take any quantity of gypsum or sulphate of lime as quarried, which is to be deprived of its waters of crystallization by heat in a similar manner to that employed in the manufacture of plaster-of-Paris of commerce, as is well understood. Into a large tank, according to the quantity of gypsum, place a number of gallons of water, having dissolved therein one pound of alum of commerce for each gallon of water, into which the gypsum above mentioned is placed and allowed to remain until it has taken up as much as possible of the liquid. The stone thus saturated is then to be removed from the said liquid and suffered to dry in the air and is afterwards calcined in an oven-furnace or kiln at low red heat, visible by daylight, to permanently fix the alum. The product is next to be ground to a powder, and, if necessary, sifted for use. [...] For a colored cement we dissolve half a pound of alum of commerce with one-quarter of a pound of copperas or sulphate of iron in each gallon of water, and at this rate for any number of gallons of liquid that may be required, and, excepting the components of this liquid mixture, the process of manufacturing the colored cement is to be the same as previously described for the white cement, and the result will be a pale-red cement. [...]*

## UNITED STATES

PATENT NO. 59154, 23 OCTOBER 1866

BY D. E. SOMES

## IMPROVED COMPOSITION FOR FORMING USEFUL AND ORNAMENTAL ARTICLES

*[...] The nature of my invention consists in mixing or combining in various proportions the following substances for the manufacture of busts, statues, molds, vases, wares, chessmen, and other articles. My invention also consists in mixing and using substances for plastering, hard-finish, stucco, and the like. I mix, first, soap-stone dust with gypsum or plaster-of-Paris; second, soap-stone dust with plaster-of-Paris and brimstone or sulphur; third, soap-stone dust, lime, and plaster-of-Paris, pipe-clay, blue clay, or other clays, brimstone, marble-dust, or other stone-dust, black lead, red lead, white lead, sand, litharge, zinc, or their equivalents; fourth, soap-stone dust with cartilaginous or glutinous substances, varnishes, or their equivalents; soap-stone dust, gum-shellac, copal or other gums, brimstone, and the like; soap-stone dust and India-rubber subjected to heat, with or without brimstone or sulphur, to be used as a substitute for vulcanized rubber. In preparing compounds for dressing or covering the surface of leather, cloth, paper, and the like, I use soap-stone dust, paraffine, oils, or glycerine or varnish, or all these together. In dressing the above-named articles in imitation of patent-leather, enamelled leather, paper, or cloth, or oil-cloth, or oil-silk, proper driers are added, and heat applied to give to the composition tenacity. Coloring properties are also added when desirable. Soap-stone dust when sprinkled over the surface of India-rubber goods, oil-cloth, oil-silk, enamelled leather, or cloth, or any other article having an adhesive surface, will prevent such surfaces from adhering to other articles. Paper, silk, cloth, and the like moistened or saturated with oil, varnish, glue, cement, or any adhesive substance, and sprinkled or covered with soap-stone dust, and dried by heat or otherwise, forms a good and cheap article to interpose between government and other adhesive stamps, to prevent them from adhering to one another and other articles. I claim any two or more of the foregoing ingredients or substances, or their equivalents when mixed with water, alcohol, spirits of turpentine, steam, or their equivalents. [...]*

UNITED STATES

PATENT NO. 192112, 19 JUNE 1877

BY W. B. CLOSSON

IMPROVEMENT IN THE ART OF MAKING MOLDS AND THEIR COUNTERPARTS

*Figure A4.1: [...] Figure 1 is a side view, Figs. 2 and 3 edge views, and Fig. 4 a transverse section of an object or medal, as prepared in accordance with my invention, for being electroplated or electrotyped for producing a mold from it, for the casting of fac-similes -of such object or medal. In carrying out my invention I extend from the medal or object A, and at an angle or angles to its surface, wherever such may be necessary, two or other suitable number of thin plates, B, of metal, or of some suitable material susceptible of being covered with powdered graphite. in the drawing, the plates are shown as encompassing the medal at and around the middle of its circumference, and fitting together and thereto, or into a groove made therein. In this instance, the two plates abut together at their inner edges. Furthermore, I arrange and fix on the plates, and to extend from the medal in a manner as shown, one or more masses, a, of wax, whose outer surface I cover with powdered graphite, such being to form in the electrotype what is usually termed a sprue" or passage or duct," for conveying the metal into the mold. [...] The method, substantially as described, of producing a fac-simile from such mold, such consisting in covering the surface of the matrix with a very thin .coating of wax, and filling such coating with a re-enforce of plaster, or other suitable material, and subsequently applying powdered graphite to the waxen coating, and depositing thereon, by the electroplating or electrotyping process, a thin coating of metal. [...]*

W. B. CLOSSON.

ART OF MAKING MOLDS AND THEIR COUNTERPARTS.

No. 192,112.

Patented June 19, 1877.

Fig. 1.



Fig. 2.

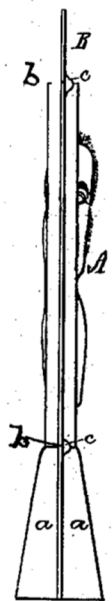


Fig. 4.



Fig. 3.



*Inventor*

William B. Closson

*Witnesses*

S. W. Piper

L. W. Miller

*by his attorney*

R. H. Eddy

Figure A4.1. Figures attached to Patent No. 192112, 19 June 1877, by W. B. Closson. Source: <https://worldwide.espacenet.com/>

UNITED STATES

PATENT NO. 308111, 18 NOVEMBER 1884

BY J. H. TRICKEY

ART OR PROCESS OF AND COMPOSITION FOR MAKING ARTIFICIAL STONE

*[...] The invention relates to a certain composition and process for making artificial stone and hardening it, which, when completed, is so firm and close in the grain as to be capable of receiving a very high polish, and suitable for being carved in relief. The composition can be run in a plastic state into gelatine molds in any desired form for ornamental work, such as centrepieces, mantel-pieces, statues, table-tops, wash-stand tops, grave-stones, &c., and all kinds of ornaments which are usually made of plaster of- Paris. The first part of my invention consists in mixing plaster-of-Paris, marble or stone dust, glycerine, and water, coloring it in imitation of marble or stone, as desired, then molding the composition into any desired form by hand or casting it in molds for the different purposes intended. When a sufficient number of articles are molded at any one time, they are piled up in a dry-kiln with air-spaces between and subjected to the action of drafts of atmospheric air and the solar rays, remaining thus exposed for about thirty days. The articles could be forced to dry quicker in a heated oven; but I prefer to allow them to dry slowly, as above stated. The second part of my invention consists in preparing a heated bath composed of a solution of brimstone and boiled linseed-oil or equivalent oil, (in some cases the oils might be omitted,) and placing therein the molded articles, as above stated, and boiling them until they sink to the bottom of the bath, which would vary according to the size of the article.*

*[...] When the articles remain a sufficient time in the heated bath, they are taken out and put into an oven heated to about from 125° to 150° and allowed to remain there two or three days, and gradually cooled off; or they may be put in a paper when taken out of the bath and allowed to stand for about a week in an airy room. After this the articles are polished by the same process as marble is polished, they taking a very high and smooth polish similar to it. It may be observed that when to wish to make the composition harder than usual I heat and cool alternately the brimstone bath before immersing the prepared composition therein. This has the effect of making the composition so hard as to admit of the same smooth and high polish as marble, and just as capable of being carved in relief. Plaster-of-Paris itself, boiled in the above-mentioned solution, is capable of taking a high polish, and becomes very hard, and will have a fine appearance if flowed with varnish. It may further be observed that soft kinds of stone—such as sand-stone, potter's clay, Portland cement, and similar substances—as well as wood—can be hardened very much by boiling them in my prepared bath, as hereinbefore mentioned. I may add that in experimenting I have added litharge, glue, soda-ash, or potash to the brimstone for boiling the composition in; but I prefer the brimstone alone, or it and boiled linseed or equivalent oils or varnish. [...]*

## UNITED STATES

PATENT No. 371550, 18 OCTOBER 1887

BY E. T. LAXTON

PROCESS OF HARDENING AND PRESERVING PLASTER-OF-PARIS CASTS AND  
MOLDS AND MAKING THEM IMPERVIOUS TO WATER, &C.

*[...] My invention relates to ornamental casts or ornaments used for architectural and building purposes, such as ceiling enrichments of the most elaborate character, statues, statuettes, and busts. Molds made solely of plaster-of-Paris (sulphate of lime) can by my invention be so strengthened that 'casts' can be taken from them. Casts to which my improved processes are to be applied must be made solely of plaster-of-Paris, without any other admixture, and preferably free from dirt or stain. By my invention such casts are made hard, strong, and durable, their original beauty is retained and added to, and when made of fine plaster-of-Paris they are capable of receiving a very high polish. They then have the appearance of statuary marble, but are more impervious to water, and will therefore last longer without discoloration. Casts treated according to my processes are not so liable to injury by dirt and atmospheric changes as most of the natural or artificial stones now in use, for they can be easily cleaned by washing with soap, hot or cold water, and sponge or brush, rendering unnecessary the ordinary method of whitewashing or painting as now practised for ceiling enrichments, statues, statuettes, and busts and objects of the like-kind, thus enabling them to retain their original beauty. [...] I use a novel hardening process, which consists in immersing the casts or molds, made solely of plaster-of-Paris, in a bath containing a solution of borax, (baborate of soda.) This I apply in the proportion of about one pound to every gallon of boiling water. All the articles to be treated should be quite dry at the time of immersion. When it is required that casts should be made extra hard—as, for instance, for external use—the aforesaid solution should be used while still hot; but when a slighter induration or hardness is sufficient the casts should be immersed in the same solution when cold. This will be saving both time and material, as the cold bath will suffice for those objects intended for internal use or decoration. The length of time of the immersion must vary according to the porosity and thickness of the articles to be treated [...] After the casts are taken from the bath, it is necessary that they should be immediately dried, which is best accomplished by placing them in a room heated by artificial heat, the range of temperature being from about 90° to 140° Fahrenheit. [...] This second process consists of placing the casts in a bath of melted pure white wax, paraffine by preference, as this keeps its whiteness better than any other. This wax I place in an ordinary bath, this bath being placed or standing within larger water -bath, which must be filled with hot or boiling water and kept up to boiling heat. The wax placed in the inner bath is melted by the action of the boiling water contained in the outer bath. During the whole time that any casts are immersed the water must be kept up to boiling heat and the wax in a molten state, or else the wax would get too cold, in which case the casts could not be effectually acted on. [...] The length of time for immersion must vary according to the porosity and thickness of the articles to be treated. [...] After the second process is completed and the casts are quite cold, those requiring to be polished are polished by the application of ordinary soft soap and water rubbed on with a sponge or soft brush, and then well rinsed and rubbed dry. This polish is renewed every time the casts or other articles are thus washed. [...]*

UNITED KINGDOM

PATENT No. 16840, 28 OCTOBER 1893

BY A. CLÉRY

A PRESERVATIVE COMPOSITION, APPLICABLE ALSO FOR THE MANUFACTURE  
OF ARTIFICIAL STONE, STATUARY AND THE LIKE

*[...] consists of a liquid and of a powder which are mixed together to be applied to any surface requiring to be provided with a protective damp-proof coating, a covering or layer imitating stonework. The same substance is likewise utilizable for casting and moulding statues, vases, ornaments and: other articles or objects and for repairing stone and marble works, pieces, parts or objects of every description. [...] I prepare a liquid containing the following; ingredients mixed in the proportions indicated viz.: (1) Muriatic acid 40 parts, Tin 30 parts, Sal ammoniac 30 parts. The tin is first dissolved in-the acid, after which the sal ammoniac is incorporated in small pieces in the mixture. I further prepare a powder containing the following ingredients mixed in the proportions indicated viz.: (2) Pulverised freestone 50 parts, Zinc oxide 20 parts, Pounded glass 15 parts, Powdered marble 10 parts, Calcined magnesia 5 parts. The above ingredients are intimately mixed and passed through a fine sieve so as to form a powder which is reduced to a pasty consistency with the above liquid (1), this paste is applied with a trowel to the surface (building front, inner or outer wall) which is to receive a damp proof covering, layer or coating. After a very short space of time this paste becomes very hard and assumes the appearance of stone and after being well set it is as hard as flint and has a smooth polished surface which can be rapidly painted if required the ordinary way. Or I may mix any suitable coloring material, dye or pigment with the above powder (2) so as to impart to the hardened coating either a plain color or a marbled, veined or motley surface. [...] This covering material is particularly applicable for walls in basements, cellars and other similar places which are liable to be damp as well as for lining cisterns, pits and the like, in short, it can be used as a damp-proof coating under any circumstances for covering wood, metal &c. as well as stonework, brickwork, masonry and the like. I also use the said material for' covering-the front, sides, rear or other parts of buildings so as to imitate stone, while obtaining a damp proof, hard and practically impenetrable surface. [...] generally, for all casting and moulding purposes for which plaster of- Paris is generally used, my improved paste being manipulated in exactly the same manner as the latter and producing ornaments of fine appearance having a hard surface and' being made to assume when required by the judicious addition of suitable colors the appearance of marble, granite or other ornamental stone. [...]*

This patent is also registered at the United States Patent Office, Patent No. 568239, dated September 22, 1896.

## UNITED KINGDOM

PATENT NO. 10658, 22 APRIL 1899

BY W. R. JOHNSON AND G. NICHOLS

## IMPROVEMENTS RELATING TO GYPSUM OR PLASTER OF PARIS

*[...] To carry out this invention the aforesaid moulds or goods made of gypsum or plaster of Paris are first burnt at a moderate temperature in a "kiln, potter's oven or other suitable places, the said moulds previous to, burning being broken up into small lumps to accelerate the burning. The mass is then removed from the oven and allowed to become partially cool, after which it is wetted or sprinkled with a solution of water and sulphuric acid, about 8% or thereabouts of the latter being employed. This should be done while the reburned plaster retains so much of its heat derived from the reburning that a large proportion of the water as. promptly evaporated. After the water has evaporated as described, the lumps may then be dried either by returning them to the oven for a short time or spreading them out upon the ground so as to allow free access to air thereto. This acidulated plaster is then ground to a powder in a mortar mill or other grinding machine and then if any moisture remains it may then be exposed to moderate heat in shallow pans. If the lumps are around before they have become thoroughly dry there will bow a certain amount of ebullition due to the escape of the water of crystallisation when the powder is again submitted to heat in the shallow pans and this is allowed to continue until such escape has practically ceased. The powder may then be allowed to cool and stored for use. This plaster may be worked in the same manner as ordinary plaster of Paris and is similar in its general qualities but is slower to set and harder. It is also somewhat darker in colour but although this is an objection for some uses it is not for moulds. [...] Instead of a solution of water and sulphuric acid (which we prefer) we may use a corresponding solution of alum the free acid in the alum being relied upon mainly as the useful element, or a corresponding solution of sulphate of potash. [...]*

UNITED KINGDOM

PATENT No. 15204, 16 NOVEMBER 1901

BY A. WOLF

IMPROVEMENT IN COMPOSITION FOR COATING SURFACES

*[...] The object of this invention is a new product for manufacture, to be used for hardening, agglomerating, coating or decorating different porous materials and manufactured articles. This industrial product or composition consists of a mixture composed of equal parts of stearine and resin and containing per each kilogramme, 0.20 grammes of bitumen, preferably jew's pitch, 0.50 grammes of benzoin, preferably from Sumatra, 0.05 grammes of creosote, preferably from beech and also if it is desirable any colouring matter. For preparing the product the said substances are taken in above-indicated proportions and heated in a proper recipient to a complete solution and suitably stirred to produce a homogeneous mixing of composition. The solution thus prepared is poured into and cooled in any mould. The composition may be used in melted or liquid form as a bath or a coating; the articles to be treated being previously heated, as gradual cooling is very desirable for good work and result. The hardening is obtained by immersing or dipping the articles in the bath for a time, generally 5 to 30 minutes, depending on nature, thickness etc. of the article as well as the degree of hardening desired. The articles are then wiped with an absorbent cloth and, dried in the air. If the article is not of convenient size, it may be operated fractionally to bring it into handy dimensions or proceeding by spraying or coating with a brush, sponge or the like. [...] This composition may be employed for decorating purposes being capable of being made in various colours by the addition of suitable colours. For instance, it may be advantageously used to coat statues and ornaments formed of plaster [...]*

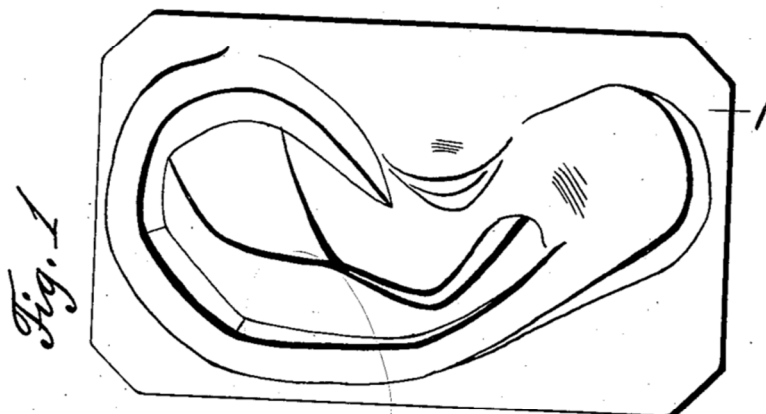
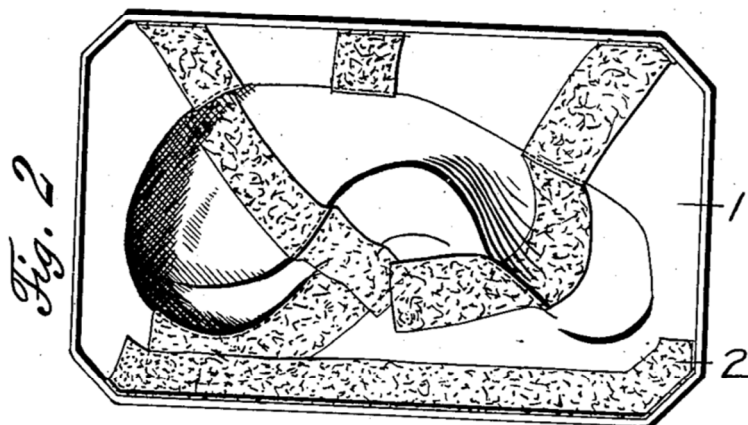
UNITED STATES  
PATENT NO. 968505, 23 AUGUST 1910  
BY G. J. ZOLNAY  
PROCESS OF MAKING ART MODELS, &C.

*Figure A4.2: [...] Figure 1 is a front view of a reproduction made in accordance with the invention, and Fig. 2 is a rear view thereof showing most clearly the manner of application of the reinforcing strips of asbestos. [...] For reproducing- simple art models it is contemplated to moisten several sheets of asbestos which are then pasted together by any suitable adhesive. A composite layer or body of material 1 is thus constituted and is of a pliable or flexible nature. This moistened layer or leather-like sheet of substance is shaped over the original model, and of which a reproduction is being made, suitable modelling tools being employed to press the layer into all of the recesses of the original model. The above layer of-asbestos is then permitted to dry while upon the model after which it is removed therefrom and saturated with a compound made gum, bees-wax, and gasolene, the latter rendering the molded article impervious, washable, and extraordinarily hard. In practising the invention with respect to more complicated models, the process consists in pressing about the article, the reproduction of which is being made, a thin layer of a plastic substance obtained by mixing raw asbestos pulp, kaolin, whiting, or plaster of Paris with dissolved glue, flour paste, and linseed oil, all in such proportions as .to yield a paste of about the consistency of dough. The above plastic layer is then backed by strips 2 of sheet asbestos, adhesively applied thereto. The above product is then permitted to dry, and when dry it is saturated with heated paraffin, oxide of lead, and a suitable pigment by which it is rendered impervious, washable, and of the desired color. The strips 2 of asbestos, as will be noted in Fig. 2 of the drawings, serve to reinforce and rigidify the body of the reproduction after it becomes hardened. [...]*

G. J. ZOLNAY.  
PROCESS OF MAKING ART MODELS, &c.  
APPLICATION FILED DEC. 24, 1909.

968,505.

Patented Aug. 23, 1910.



Witnesses  
*E. Larson*  
*S. E. Dodge*

Inventor  
*G. J. Zolnay*  
By *Beulah Cook*  
Attorney

Figure A4.2. Figures attached to Patent No. 968505, 23 August 1910, by G. J. Zolnay. Source: <https://worldwide.espacenet.com/>

## UNITED KINGDOM

PATENT No. 143768, 3 JUNE 1920

BY W. J. DE BAS

## IMPROVEMENT IN PLASTIC COMPOSITION

*[...] It is known for the purpose of producing moulded objects having the appearance of marble to mix mica and other ingredients with plaster of Paris and for the purpose of replacing slate as a backing for enamelled slabs to use powdered hematite mixed with slag from iron or copper works and with cement. [...] Iron ores or other material has also been added to broken granite or cement to form a coloured surface for concrete floors or pavements. [...] It is also known to mix the plaster with a metallic powder, for example with iron filings or finely divided zinc, and to treat objects cast or moulded of this material with a solution of metallic salt, in order to obtain a metallic, more particularly copper, external coating. [...] It is also known to apply a similar process to objects, casings and plastering, containing cement and hydraulic lime, the external coating formed by treatment with a solution of metallic salt, however, in this case being of plaster. To impart a pleasant appearance to the surface itself formed of the cement, lime or plaster. [...] a powdered micaceous iron ore is mixed with cement, lime or plaster in a pasty or moist condition to which colouring matters may be added. A sample of the micaceous iron ore used (in the dry conditions consisted of: silicic acid and small stones (7.24%), iron oxide ( $\text{Fe}_2\text{O}_3$ , 80.17%), Aluminum oxide (5.16%), Calcium Oxide (0.40%), sulphur in the form of sulphide (4.30%), Magnesia (1.33%), loss in calcining (1.28%), the remainder (not determined, 0.12%). Objects made of this composition possess a metallic lustre and a peculiar brilliancy under sunlight; such composition when cast and pressed in moulds do not adhere to the walls of the moulds. Objects made of this composition may be worked, just as stone, with a chisel without losing their metallic lustre. It may vary within the limits of 1 part of ore to 1 part of cement, lime or plaster and 1 part of ore to 10 parts of cement, lime or plaster. [...]*

CANADA

PATENT NO. 446844, 24 FEBRUARY 1948

BY M. C. DAILEY AND E. W. DUFFY

GYPSUM PRODUCT

*[...] This invention relates to compositions of matter comprising a major quantity of calcium sulfate hemihydrate and a minor quantity of a water-soluble aminotriazine-aldehyde condensation product capable of hardening to a water-insoluble resin, and more particularly formed articles made therefrom containing about from 95 to 55% by weight of set calcium sulphate dihydrate and from about 5 to 45% by weight of a cured aminotriazine-aldehyde condensation product, hereinafter for brevity referred to simply as a triazine-aldehyde condensation. [...] It is an object of the present invention to provide a composition of matter embodying in one product many of the advantages of both plaster of Paris and synthetic resins. [...] The resin found most satisfactory for our use is the water-soluble, heat-hardenable condensation product obtain by partially condensing formaldehyde and 2.4.6-triamino-1.3.5-triazine, ordinarily known as melamine. [...] Our preferred composition comprises dry mixtures of the powdered water-soluble, heat-hardenable resin and plaster of Paris, plus small amounts of a suitable catalyst to aid in curing the resin at moderate temperatures. [...] resin plasticizers may also be employed, as well as fillers and fibres reinforcements (paper fibres, asbestos, glass-wool, wood-flour, silica, clay, starch, talc, mica, etc. resin proportion are preferably maintained at below about 45% of the total composition weight. [...] a condensation product produced by reacting one mol of melamine with about three or more mol of formaldehyde is suitable, but the invention is not limited to that particular form of triazine-aldehyde resin. [...] ammonium chloride has been found to be an effective catalyst. Other acid salts, and weak acids, such as zinc sulfate, zinc chloride, aluminium sulfate, boric acid, etc., may be employed. [...] 126 parts of melamine (1 mol) are mixed with 300 parts of 37% formalin (4 mols). The formaldehyde is preferably first brought to an alkalinity corresponding to a pH of 8.84 by the addition of 2.7 parts of a 3% aqueous solution of sodium hydroxide. The mixture of melamine and alkalinized formaldehyde are preferably heated under a reflux condenser for about 15 minutes, whereafter the condenser is changed so as to operate as a distillation condenser. [...] thereafter the operation is interrupted, and the batch cooled to about 60°C as rapidly as possible. [...] using the above-mentioned resin: [...] water (32 parts by weight), syrup as above obtained (75 parts by weight), calcined gypsum (plaster of Paris) (150 parts by weight), ammonium chloride (1 part by weight), potassium sulfate (0.5 part by weight), Terra Alba ( $\text{CaSO}_4 \cdot 2\text{H}_2\text{O}$ ) (0.5 part by weight), sodium citrate (0.02 part by weight). [...]*

UNITED STATES

PATENT NO. 2660776, 1 DECEMBER 1953

BY J. H. MILLER

FLEXIBLE MOLD FOR FORMING STATUES WITH SPACED LEGS

*Figure A4.3: [...] Figure 1 is a perspective view of a mold formed of flexible material and embodying my invention; Fig. 2, a transverse sectional view, the section being taken at line 2—2 of Fig. 1; Fig. 3, an enlarged broken vertical sectional view; Fig. 4, a vertical sectional view of the mold shown in supported position for pouring; Fig. 5, a view similar to Fig. 4 but illustrating a method step for the forming of a coating on the inner side of the mold to stiffen the mold; Fig. 6, a view similar to Fig. 5 showing the mold provided with the stiffening lining; and Fig. 7, a view similar to Fig. 1 but showing the mold as finally filled. [...]*

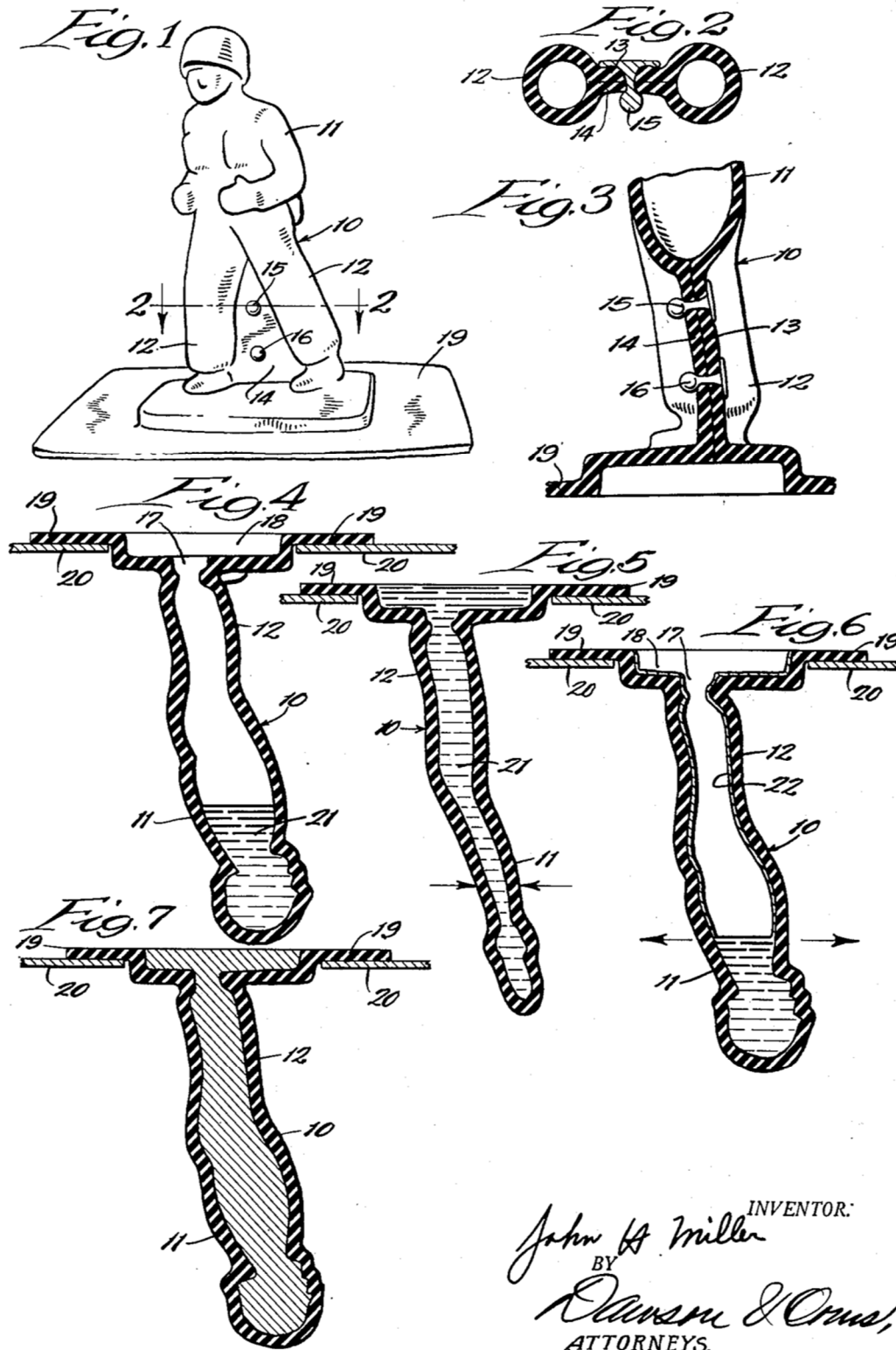
Dec. 1, 1953

J. H. MILLER

2,660,776

FLEXIBLE MOLD FOR FORMING STATUES WITH SPACED LEGS

Filed Dec. 1, 1950



INVENTOR:  
*John H. Miller*  
BY  
*Danson & Oms,*  
ATTORNEYS.

Figure A4.3. Figures attached to Patent No. 2660776, 1 December 1953, by J. H. Miller. Source: <https://worldwide.espacenet.com/>

## UNITED KINGDOM

PATENT NO. 1461812, 19 JANUARY 1977

BY F. F. KOBLITZ

## MODIFIED GYPSUM COMPOSITION

*[...] This invention relates to a novel gypsum-based mould making and moulding composition and more particularly to a composition which is suitable for use in applications where form retention and low fracture strength under compression are important. Gypsum plaster, as described in various Patent Specifications, is generally modified to provide specific desirable characteristics. For example, U.S. Patent No. 3,223,082 discloses the addition of carboxymethyl cellulose as a set inhibitor; U.S. Patent No. 2,753,608 discloses the addition of extenders such as talc, asbestos and silica, the addition of wetting agents and the addition of sodium chloride. [...] U.S. Patent No. 3,369,915 conventional gypsums, water and an anionic surfactant were used to produce a plaster having an especially high compressive strength which is desirable in the plasterboard industry. [...] U.S. Patents Nos. 3,393,116; 2,639,478; 2,494,403 and others describe the calcium sulphate hemihydrate which forms the basis for gypsum products because of its structure as well as its particularly useful composition. [...] It was thought that a more desirable approach to gypsum used as a mould making material would be to develop a composition which retained the desirable surface characteristics and form defining characteristics of gypsums generally with a material which was less brittle, more easily workable and which generally exhibited a lower fracture strength under compression than the relatively hard, brittle gypsum product of the art. The present invention provides a modified gypsum composition comprising from 60% to 85% by weight of calcium sulphate hemihydrate which is curable by hydration, from 5 to 20% by weight of an extender which is capable of holding in the composition after curing with water a volume of chemically uncombined water at least equal to the volume of the added extender, and from 3 to 15% by weight of a water-swellaible and water-dispersible compatible organic binder which is capable of enhancing the adherence of the added extender to the randomly oriented crystals of the substantially completely hydrated gypsum in the composition after curing with water, whereby the cured composition has a fracture strength under compression of less than 500 psi. The proportion of extender is preferably 7 to 14% and the proportion of binder is preferably 5 to 15%. When this composition is cured by the addition of water to hydrate the calcium sulphate hemihydrate, then all of these constituents uniquely combine to promote the formation of a rigid, dimensionally stable product having a crystal structure modified in a manner which produces a controlled reduction in the fracture strength of the final set composition under compression. In addition, the function of the binder in the composition of the present invention in serving to enhance the adhesion of the extender to the propagating crystal structure of the gypsum does so without significantly retarding the set or setting time of the material. [...] Model Plaster (calcium sulphate hemihydrate plaster of Paris) 60-85%, Corn-starch 5-15%, Celite (Trade Mark) 499 (diatomaceous earth) 7-14%, Carbowax (Trade Mark) 6000 (polyethylene oxide) 1-2%, Sodium Chloride 1%, Anionic Surfactant 0.3 %, Colourant (optional) 0.3 %, Flavourant (optional) 0.01%. [...]*

UNITED KINGDOM

PATENT No. 2053184A, 4 FEBRUARY 1981

BY L. W. STOCKTON

IMPROVEMENTS IN OR RELATED TO GYPSUM PLASTER

*[...] a novel composition employing gypsum plaster in combination with other organic and inorganic materials which would result in products which, in comparison with existing products, are either lighter or more flexible, or less brittle, or more water-resistant, or easier to cut or nail, or having properties which are a combination of two or more of the above properties. [...] According to the present invention, the novel composition suitable for the manufacture therefrom of the improved product which may be highly patterned, decorated or could become part of an overall design, comprises: (i) a water-settable inorganic binder which is one or more of a calcium sulphate binder, Plaster of Paris, Retarded Hemihydrate plaster, Anhydrous Calcium Sulphate, Anhydrate or any of the proprietary brands of plaster; (ii) water; (iii) Polymers, and Copolymers which may be water-dispersible e.g. polyvinyl acetates, styrene butadienes, acrylics, polyesters, epoxies, and other resinous or rubber-based materials; (iv) fibrous reinforcing materials, comprising inorganic or organic fibres or combinations of both. The composition preferably includes an aerating agent in the form of a lightweight filler - e.g. expanded so vermiculite, expanded perlite, sawdust, p.f.a. floaters, polystyrene beads and such other light-weight materials or any combination of the above materials. [...]*

Appendix 5 List of Contents:

**Küsthardt group**

Presbyter Bruno (REPRO.1873-380)	88
Choir screen (REPRO.1873-561)	89
Brass font (REPRO.1874-29)	90
Christ, St. Godehard and St. Epiphanius (REPRO.1874-45)	92
Count Ekkehard (REPRO.1875-16)	93
Regilindis, wife of Hermann (REPRO.1875-17)	94

**Notre-Dame Group**

Assumption of the Virgin (REPRO.1890-80)	95
Coronation of the Virgin (REPRO.1890-81)	97
Death of the Virgin (REPRO.A.1916-3152)	98
Entombment of the Virgin (REPRO.A.1916-3153)	99

**Franchi Group**

Raising of Lazarus (REPRO.1864-56)	100
Christ at Bethany (REPRO.1864-57)	101

## PRESBYTER BRUNO

*Küsthardt group*

**Accession no.** REPRO.1873-380  
**Location** Gallery 46A (NE side)  
**Dimensions** 218.5X77.0 cm  
**Material** Plaster



Figure A5.1. Presbyter Bruno (REPRO.1873-380), ca. 1873. Photographic record: 2006BK4555. © Victoria and Albert Museum, London/as specified by the rights holder. Source: V&A's Collection Management System.

Plaster cast of the tombstone of the Presbyter Bruno (d. 1194), in the Cathedral of Hildesheim, cast by F. Küsthardt, ca. 1873. The cast was purchased from F. Küsthardt in 1873 for £6. In 1873, the Museum acquired several plaster casts of key sculptural decorations in the cathedral of Hildesheim by F. Küsthardt. This slab reproduces an elaborate tomb memorial. **Conservation.** No records of previous treatments.

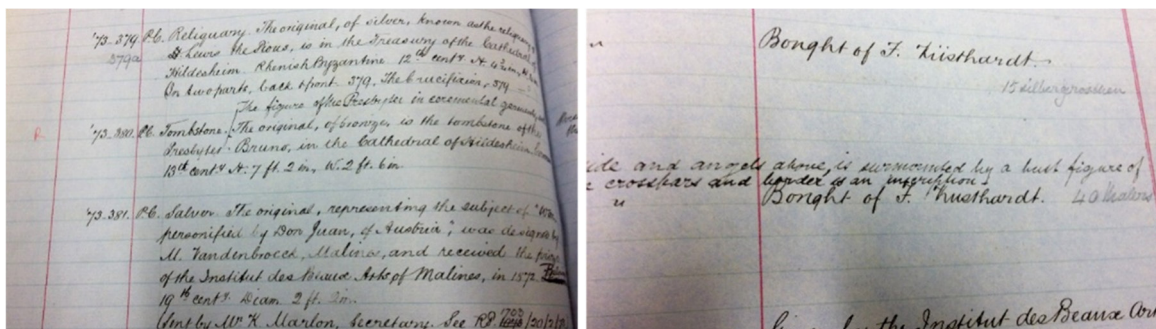


Figure A5.2. Record of the Presbyter Bruno (REPRO.1873-380) acquisition retrieved from the Registry of Reproductions of the V&A Museum (1873). The Registry reports the description of the cast, notes on the purchase, and the price paid. © Victoria and Albert Museum, London/as specified by the rights holder.

## CHOIR SCREEN

Küsthardt Group

**Accession no.** REPRO.1873-561  
**Location** Gallery 46A  
 (NE side)  
**Dimensions** 320.5X793.0 cm  
**Material** Plaster



Figure A5.3. Choir screen stucco (REPRO.1873-561), ca. 1873. © Victoria and Albert Museum, London/as specified by the rights holder. Source: V&A's Collection Management System.

Plaster cast of the stucco choir screen, in the Church of St. Michael, Hildesheim (Germany), ca. 1197, cast by F. Küsthardt, ca. 1873. The choir screen is decorated with scenes showing figures of (from the left) St. Benedict, St. James the Greater, St. Peter, the Virgin and Child, St. Paul, St. John the Evangelist and Bernard Bishop of the Church. The cast was purchased from F. Küsthardt in 1873 for £162 10s. Unlike most of the other objects in the Museum's plaster collection, this cast replicates an object which itself was made from *stucco*. In the years around 1200, several stucco choir screens were erected inside churches in Saxony (known for the skill of its metalworkers). The original screen would have been brightly painted. **Conservation.** Treated by Charlotte Hubbard (former Head of Sculpture Conservation at the V&A) in 2018. The surface was very well sealed for most areas so Blitz fix® sponges were used in combination with some water. The darker areas, mainly the bigger overpaints and handling marks were removed with latex poultice. The latex removed or softened the dirt, it softened also most overpaints. It was applied thinly to the localised areas, peeled off when set (in less than one minute) with chemical sponges. For the overpaints, the surface was wiped with acetone so the overpaint could be removed. Localised retouching with Acrylic colours.

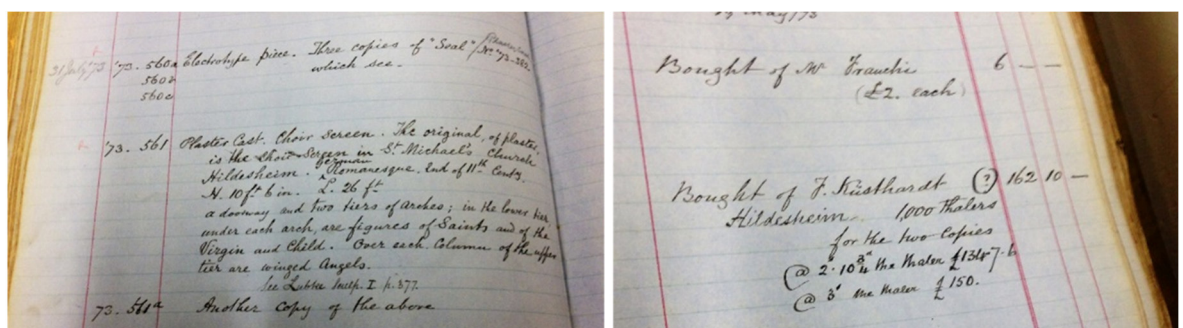


Figure A5.4. Record of the Choir screen stucco (REPRO.1873-561) acquisition retrieved from the Registry of Reproductions of the V&A Museum (1873). The Registry reports the description of the cast, notes on the purchase, and the price paid for the object. © Victoria and Albert Museum, London/as specified by the rights holder.

## BRASS FONT

*Küsthardt Group*

<b>Accession no.</b>	REPRO.1874-29
<b>Location</b>	Gallery 46A (N side)
<b>Dimensions</b>	183.0 cm (h), 990.0 cm (d)
<b>Material</b>	Plaster



*Figure A5.5. Font cast brass (REPRO.1874-29), ca. 1874. © Victoria and Albert Museum, London/as specified by the rights holder. Source: V&A's Collection Management System.*

Plaster cast of a font in the Cathedral of Hildesheim, Germany, about 1220. The font was cast by F. Küsthardt, ca. 1874. The font is decorated with representations on the cover of Moses and Aaron on either side of an altar, an Allegory of Pity, the Anointing of Christ by St. Mary Magdalen, and the Judgment of Solomon. On the bowl are represented: The Passage through the Red Sea of the Israelites and the Ark of the Covenant, the Baptism of Christ, and the Virgin and Child between two bishops and the Provost Wilbernus at her feet. The figures supporting the font represent the Rivers of Paradise. The font was given to the Cathedral of Hildesheim by Wilbernus, Provost of Hildesheim (1216-1220). The cast was purchased from F. Küsthardt in 1874 for £19. **Conservation.** Record Apr 2011. Sarah Healey-Dilkes (Senior Conservator at the V&A) suggested the removal and replacement of the figures at the bottom of the font. The sculpture studio was asked to remove the four figures temporarily to use a 3D scanning technique to produce images of the base of the font. Three of the four figures were dismantled easily by removing the screws holding the bars in place. Before its removal, Figure No.3's proper left foot was faced up using isinglass and tissues. Whilst dismantling, the foot broke along the old breaking line. Interfaces of the break were sealed using Paraloid® B72 10% in IMS and Acetone (50:50). The foot was re-adhered using Primal® 60A (46-47% solid) and the tissue was removed using warm water and swab. The crack was filled using Flugger. All figures were reinstated using their original fixings. Figure No.1 had a wooden spacer under the metal bar. This was reduced by 2mm to allow the back of the shoulders of the figures not to be abraded by the metal of the font. Similarly, as the alignment of Fig.4 to the metal plate caused some abrasion of the back, two thin pieces of card were placed over the wooden spacer to alter the position of the figure slightly. Treatment by Sayuri Morio, Contract Conservator at the V&A.

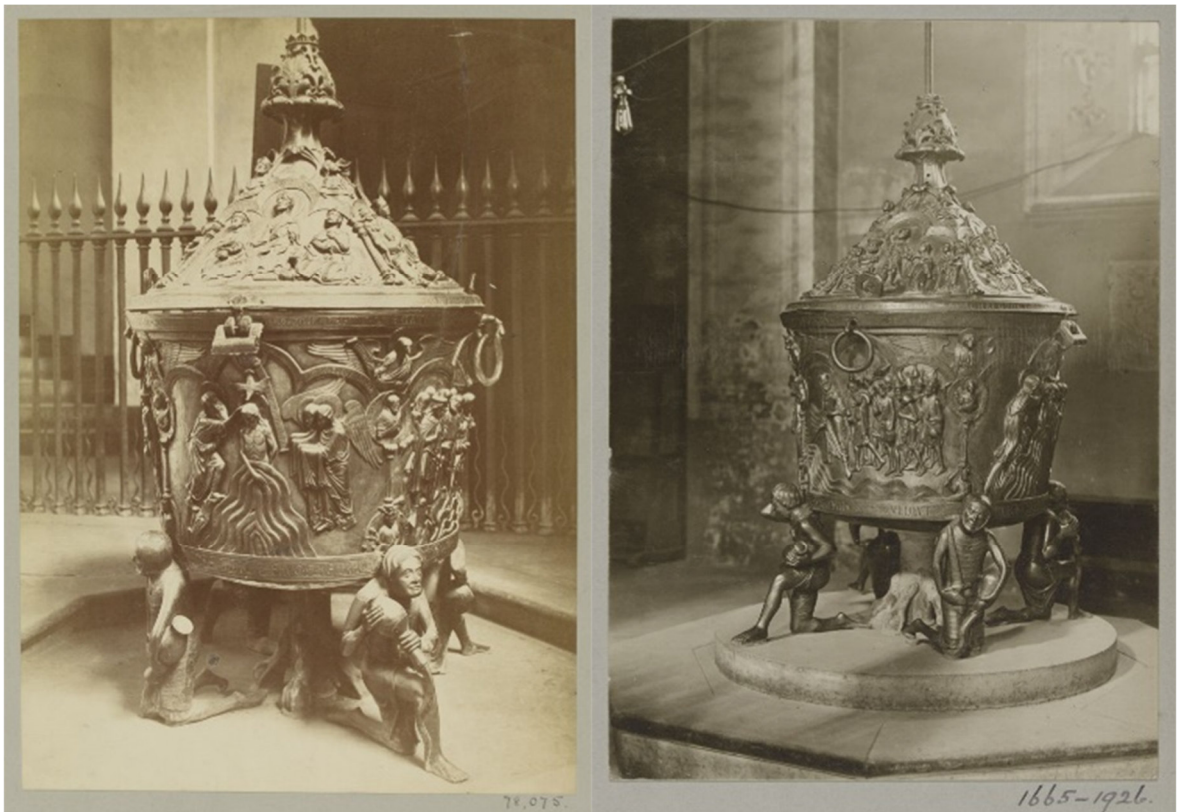


Figure A5.6. Left: V&A's objects number 78075. Right: V&A's objects number 1665-1926. Photograph, the font in the Cathedral of Hildesheim, Germany, gelatine silver print, late nineteenth to the early twentieth century. © Victoria and Albert Museum, London/as specified by the rights holder. Source: V&A's Collection Management System.

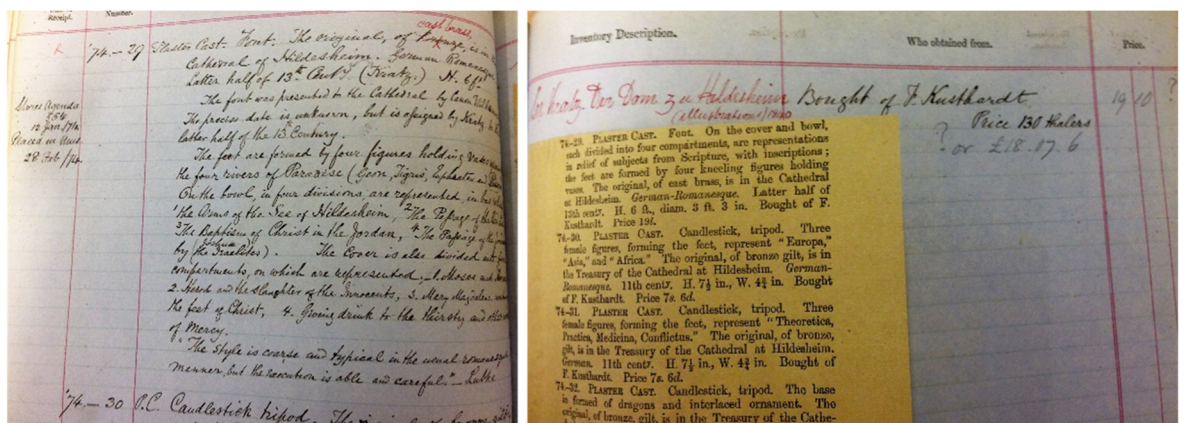


Figure A5.7. Record of the Font cast brass (REPRO.1874-29) acquisition retrieved from the Registry of Reproductions of the V&A Museum (1874). The Registry reports the description of the cast, notes on the purchase, and the price paid for the object. © Victoria and Albert Museum, London/as specified by the rights holder.

# CHRIST, ST. GODEHARD AND ST. EPIPHANIUS

Küsthardt Group

**Accession no.** REPRO.1874-45  
**Location** Gallery 46A  
 (S side)  
**Dimensions** 107.0X213.5 cm  
**Material** Plaster



Figure A5.8. Christ, St. Godehard and St. Epiphanius (REPRO.1874-45), ca. 1874. © Victoria and Albert Museum, London/as specified by the rights holder. Source: V&A's Collection Management System.

Plaster cast of the tympanum in stucco over the north door of the Church of St. Godehard, Hildesheim (Germany), about 1200, and cast by F. Küsthardt ca. 1874. Purchased from F. Küsthardt in 1874 for £9. Tough and durable plaster *stucco* was used for the original sculpture as it was positioned on the exterior of the Church, in the semi-circular space positioned over one of the main doors into the church. Christ appears between two saints: Godehard, the patron saint of the church and another bishop, probably Epiphanius of Pavia. **Conservation.** Record Oct-Nov 2017. The object was structurally sound. The surface was covered in accumulated layers of dust and dirt. There were minor losses near the base, on the PR side. The surface was dusted and hoovered. More stubborn dirt was removed with Blitz-Fix® suction blocks. The treatment was carried on by Johanna Puisto, Sculpture Conservator at the V&A.

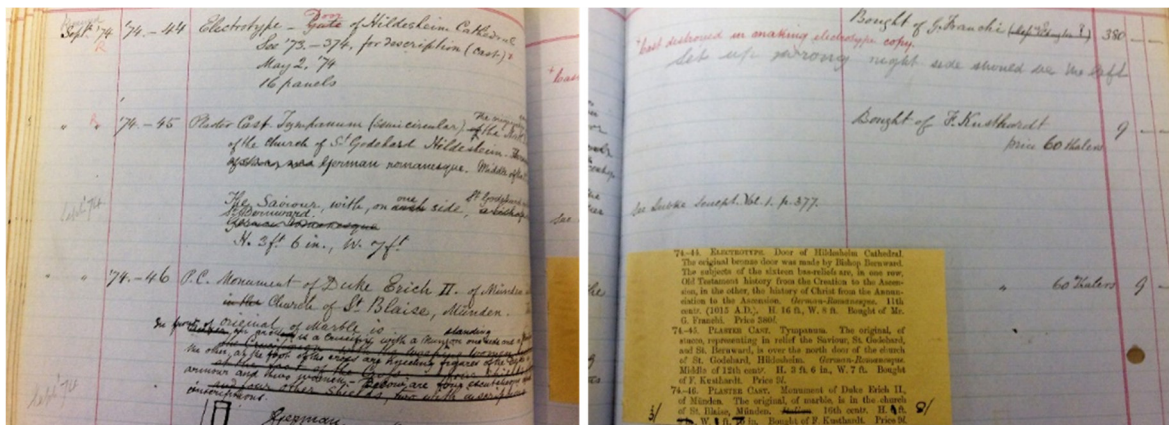


Figure A5.9. Record of the Christ, St. Godehard and St. Epiphanius (REPRO.1874-45) acquisition retrieved from the Registry of Reproductions of the V&A Museum (1874). © Victoria and Albert Museum, London/as specified by the rights holder.

# COUNT EKKEHARD

**Küsthardt Group**

**Accession no.** REPRO.1875-16  
**Location** Gallery 46A (S side)  
**Dimensions** 198.5X61.5 cm  
**Material** Plaster

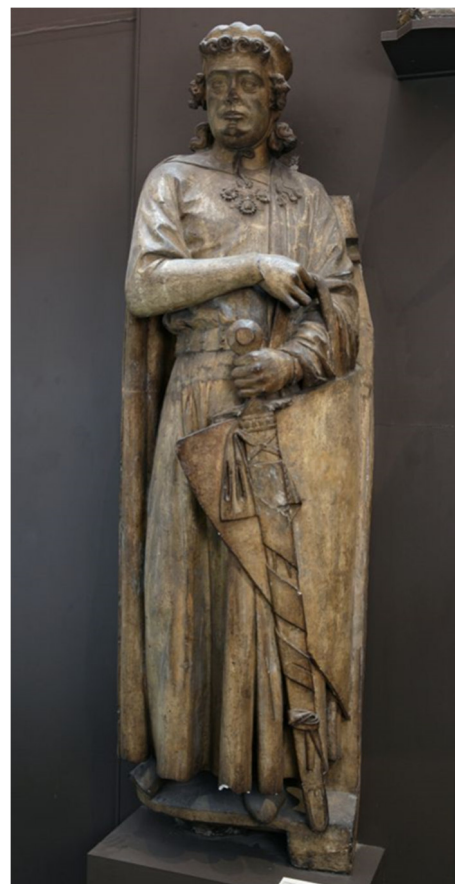


Figure A5.10. Count Ekkehard (REPRO.1875-16), ca. 1875. © Victoria and Albert Museum, London/as specified by the rights holder. Source: V&A's Collection Management System.

Plaster cast of a sandstone statue of Count Ekkehard, cast by F. Küsthardt in ca. 1875. Count Ekkehard (about 985-1046) was the Margrave of Lusatia (1034 onwards) and subsequently Margrave of Meissen (1038 until his death) and defended the eastern frontiers of Germany against Poland and Bohemia. This commemorative sculpture was a pendant to that of his wife, Uta von Ballenstedt and made two centuries after his death (1250-60). The coloured sandstone original stands in the choir of Naumburg Cathedral, founded by Ekkehard and his wife. The cast was purchased from F. Küsthardt in 1875 for £7 10s. **Conservation.** No records of previous treatments. Awaiting conservation.

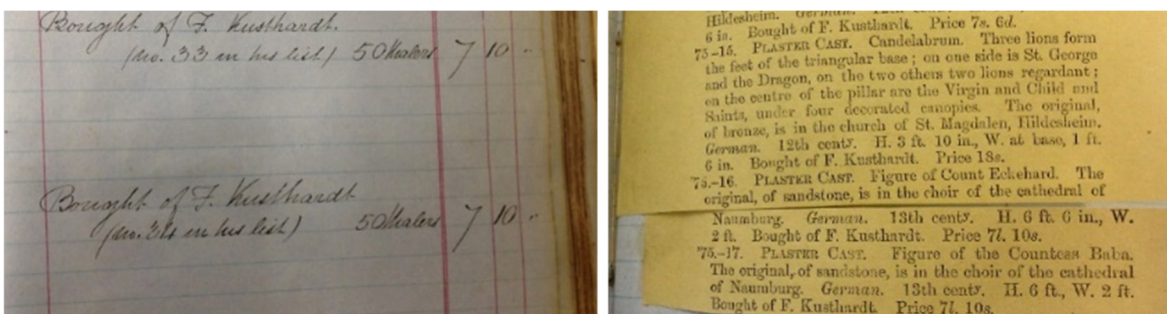
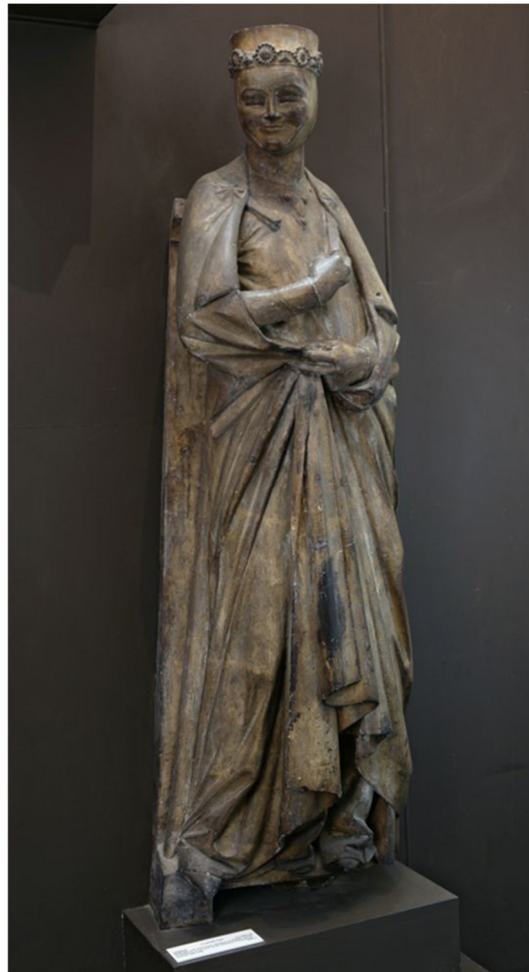


Figure A5.11. Records of Regilindis, wife of Hermann, Margrave of Meissen (REPRO.1875-17) and count Ekkehard (REPRO.1875-16) acquisition retrieved from the Registry of reproductions of the V&A museum (1875). © Victoria and Albert Museum, London/as specified by the rights holder.

## REGILINDIS, WIFE OF HERMANN

*Küsthardt Group*

<b>Accession no.</b>	REPRO.1875-17
<b>Location</b>	Gallery 46A (S side)
<b>Dimensions</b>	198.5X61.5 cm
<b>Material</b>	Plaster



*Figure A5.12. Regilindis, wife of Hermann, Margrave of Meissen (REPRO.1875-17), ca. 1875. © Victoria and Albert Museum, London/as specified by the rights holder. Source: V&A's Collection Management System.*

Plaster cast of a sandstone statue of Regilinda made in ca. 1250-60 for the choir of the Cathedral of Naumburg, attributed to Naumburg master. Plaster cast made by F. Küsthardt, Hildesheim (Germany), ca. 1875. This object was purchased from F. Küsthardt in 1875 for £7 10s. Regilinda (about 989-after 1014) was the wife of Hermann, Margrave of Meissen. The figure, made two centuries after her death, was one of 12 donor portraits commissioned for the west choir of the cathedral. A cast of the statue depicting Regilinda's brother-in-law, Ekkehard, also from the Naumburg cathedral choir, is likewise in the V&A's cast collection. **Conservation.** No records of previous treatments. Awaiting conservation.

## ASSUMPTION OF THE VIRGIN

*Notre-Dame Group*

<b>Accession no.</b>	REPRO.1890-80
<b>Location</b>	Gallery 46A (W side)
<b>Dimensions</b>	152.5X160.0 cm
<b>Material</b>	Plaster



Figure A5.13. Relief Assumption of the Virgin stone (REPRO.1890-80). Plaster cast made by Messrs Jean Pouzadoux, ca. 1890. © Victoria and Albert Museum, London/as specified by the rights holder. Source: V&A's Collection Management System.

Plaster cast of a relief after The Assumption of the Virgin (originally carved in stone) executed under Pierre de Chelles (active about 1287; d. 1320), on the north side of the exterior of the apse of Notre Dame, Paris, after 1296 but before 1316, cast by Messrs Jean Pouzadoux, ca. 1890. Purchased from Messrs Jean Pouzadoux in 1890 for £12 (300 francs). The Virgin is shown ascending to Heaven, in a *mandorla* surrounded by angels. **Conservation.** The treatment was undertaken by Adriana Francescutto Miro, Senior Conservator at the V&A. The panel was in fair condition and structurally stable. There were minor stable hairline cracks due to compression and uneven distribution of weight, some superficial losses and a collapsed area (air pocket) on the back of one of the bowing angels (possibly due to the casting method and the reinforcement fibres used on the plaster are visible in this area). All figures around the Virgin showed cracks/separation between their hands and the *mandorla*, where the Virgin is, some of these have plaster losses. This was possibly due to the casting method, where all parts were cast individually and then joined, and possibly triggered by the movements of the wooden armature. One of the arms of the angels around the *mandorla* showed major movement and it is held by its internal armature. There were tool-marks around the lower edge and several abrasions on protruding areas. The lower edge showed a retouched area of the same colour as the surface. There were numerous red paint splashes on the upper edge of the object and some sparingly distributed. There were some dark grey inpaintings (older treatments to cover abraded or lost areas) and a thick layer of dust and ingrained dirt distributed on all surfaces, especially on protruding areas. There was debris from previous gallery maintenance activities such as dusting feathers but also small time-capsules in form of a newspaper embedded in fresh plaster on the proper right inner corner and two matches. There were two major cracked areas on the plaster. The top side crack is on a wooden reinforcement baton that joins the plaster relief, perpendicular to the external wooden structure. The bottom cracks run along with the plaster lower bottom edge, between the two wooden batons, possibly caused by the movement of the wood due to hygrometric changes, as well as an uneven distribution of weight and the handling process. The majority of the

cracked area run along the edge of the bottom part but also affected the bottom layer of the proper right side. The different colour, texture and filling of the plaster around this cracked area suggested that this had been repaired in the past (whiter, grainier and less dense instead of the vegetable fibre or horsehair used on the relief). Treatment performed on 02/05/2019 (after the sampling). Superficial dust removed with a vacuum cleaner and soft brushes. Surfaces cleaned with a smoke sponge. Front: ingrained dirt removed with localised use of Anjusil® latex and Blitzfix® with deionised water. Flaking plaster consolidated with Paraloid® B44, paint splashes inpainted with acrylic paint after. The loose arm was consolidated using Paraloid® B44 20% in 50:50 IMS- Acetone. Areas of plaster loss were consolidated using 25%Primal® B60A and retouched using acrylic paint. The crack on the underside was reinforced with carbon fibre matting and Paraloid® B44 30%.



Figure A5.14. V&A's objects number 76395. Photograph, a plaster cast of a relief depicting *The Assumption of the Virgin* (REPRO.1890-80), executed under Pierre de Chelles, Notre Dame, Paris, albumen print, late nineteenth century. Albumen print. © Victoria and Albert Museum, London/as specified by the rights holder. Source: V&A's Collection Management System.

## CORONATION OF THE VIRGIN

*Notre-Dame Group*

**Accession no.** REPRO.1890-81  
**Location** Gallery 46A (W side)  
**Dimensions** 155.0X135.0 cm  
**Material** Plaster



*Figure A5.15. Relief Coronation of the Virgin stone (REPRO.1890-81). Plaster cast made by Messrs Jean Pouzadoux, ca. 1890. © Victoria and Albert Museum, London/as specified by the rights holder. Source: V&A's Collection Management System.*

Plaster cast of a relief after The Coronation of the Virgin (originally carved in stone) executed under Pierre de Chelles (active about 1287; d. 1320), on the north side of the exterior of the apse of Notre Dame, Paris, after 1296 but before 1316, cast by Messrs Jean Pouzadoux, ca. 1890. Purchased from Messrs Jean Pouzadoux in 1890 for £12 (300 francs). **Conservation.** Record May 2019. Two samples of paint from the front and a sample of plaster with horsehair at the back were taken to identify lead or arsenic or any other hazardous materials present, or anything else that will be useful to identify before treatment. XRF analysis of samples showed no hazardous materials. Treated by conservator Sarah Healey-Dilkes (Senior Conservator at the V&A). Treatment was similar to the one undertaken on REPRO.1890-80.

## DEATH OF THE VIRGIN

*Notre-Dame Group*

**Accession no.** REPRO.A.1916-3152  
**Location** Gallery 46A (W side)  
**Dimensions** 90.0X86.0 cm  
**Material** Plaster



*Figure A5.16. Relief death of the Virgin stone (REPRO.A.1916-3152). Plaster cast made ca. 1850-1900. © Victoria and Albert Museum, London/as specified by the rights holder. Source: V&A's Collection Management System.*

Nineteenth-century relief plaster cast after the death of the Virgin executed under Pierre de Chelles (active about 1287; d. 1320). The original was carved in stone between 1296 and 1316, on the north side of the exterior of the apse of Notre Dame, Paris. The cast was made ca. 1850-1900. Given by the Architectural Association in 1916. **Conservation.** Record May 2019 (after sampling) by the conservator Sayuri Morio. The object is structurally sound. Straight joint lines are visible, especially on a frame area; some cracks and opening can be observed along the contour of the Virgin and some areas on the frame. There is a brown uneven paint layer on the surface; flat vertical surfaces are lighter brown and sky facing surfaces are darker brown due to grim and dirt. Salt efflorescent can be seen on the recessed areas; after the removal of the salt with a soft brush, the areas of salt left small white spots. There is some water damage on the lower quarter of the left-hand side; the water would have washed the paint and dissolved some gypsum, resulted in a very porous surface that collected dust and dirt. Some splash of red paint can be seen on the surface of the object. The object is very dusty. The object was examined under UV light. The surface fluoresces in mid-tone purple; small areas of overpaints and adhesive drips fluoresced in dull orange and greenish-white respectively. Another cast object with a similar kind of brown paint (REPRO.1893-2 Portal Cathedral Bordeaux) was also reported to have had some salt crystals, which was analysed with Quantofix® salt strips. Sulfates were detected from the sample, which could be from the gypsum (plaster) itself. The object was dusted with a brush and vacuum. The vertical surface with lighter brown was cleaned with a smoke sponge to remove surface dirt, and sky-facing surfaces in dark brown were cleaned with Britzfix® sponge lightly dampened with deionised water. To remove the dark grim on the pronounced area, the latex poultice method was used. The red museum paint was removed with acetone on cotton swabs. Paint losses and chipped areas were retouched with acrylic paint.

## ENTOMBMENT OF THE VIRGIN

*Notre-Dame Group*

**Accession no.** REPRO.A.1916-3153  
**Location** Gallery 46A (W side)  
**Dimensions** 61.5X53.5 cm  
**Material** Plaster



*Figure A5.17. Relief entombment of the Virgin stone (REPRO.A.1916-3153). Plaster cast made ca. 1850-1900. © Victoria and Albert Museum, London/as specified by the rights holder. Source: V&A's Collection Management System.*

Nineteenth-century relief plaster cast after the Entombment of the Virgin executed under Pierre de Chelles (active about 1287; d. 1320). The original was carved in stone between 1296 and 1316, on the north side of the exterior of the apse of Notre Dame, Paris. The cast was made ca. 1850-1900. Given by the Architectural Association in 1916. **Conservation.** Record May 2019 (after sampling) by the conservator Sayuri Morio. The object is structurally sound. Straight joint lines are visible. Some cracks can be observed on the coffin and the proper top left along with the frame. The entire surface of the object is brown. There is a small area of the flaky surface where there is a fill. Salt efflorescence can be seen in the recessed areas. After the removal of the salt with a soft brush, the areas of salt left small white spots. There is a small area of water damage in the middle. A small amount of red paint can be seen on the surface of the object. The bottom of the object has a shiny waxy texture. The object is very dusty. There is a museum number written on the proper bottom left, and a start mark on the proper top right. The object was examined under UV light. The surface fluoresced in mid-tone purple; small areas of overpaints are visible on the proper top left corner, where there is a fill. Samples from the reliefs were analysed by XRF to check if any hazardous materials were present. None were detected. The dark colouration of the surface can be related to the presence of iron oxides. The object was dusted with a brush and vacuum. The vertical surface with lighter brown was cleaned with a smoke sponge to remove surface dirt, and sky-facing surfaces in dark brown were cleaned with Britzfix® sponge lightly dampened with deionised water. To remove the dark grim on the pronounced area, the latex poultice method was used, applied by a nylon brush. This was followed by cleaning with a dampened Britzfix® sponge with deionised water. The red museum paint was removed with acetone on cotton swabs. Paint losses and chipped areas were sealed with Paraloid® B44 5% in acetone and IMS, then were retouched with acrylic paint.

## RAISING OF LAZARUS

**Franchi Group**

**Accession no.** REPRO.1864-56  
**Location** Gallery 46A  
(N side)  
**Dimensions** 122.0X117.0 cm  
**Material** Plaster



*Figure A5.18. Relief raising of Lazarus stone (REPRO.1864-56). Plaster cast made ca. 1864. © Victoria and Albert Museum, London/as specified by the rights holder. Source: V&A's Collection Management System.*

Plaster cast of a stone relief depicting the Raising of Lazarus, the second quarter of the twelfth century, in Chichester Cathedral, West Sussex, cast by Messrs Franchi & Son, ca. 1864. Purchased from Messrs Franchi & Son in 1864 together with V&A's museum object no. 1864-57 for £30.  
**Conservation.** No records of previous treatments. Awaiting conservation.



*Figure A5.19. Left: V&A's objects number PH.2462-1904. Photograph of the plaster cast (REPRO.1864-56) of the relief showing the raising of Lazarus, from Chichester cathedral, possibly a print from a publication, late nineteenth century. Right: V&A's objects number PH.191-1902. Photograph of a relief showing the raising of Lazarus, in Chichester cathedral, possibly a print from a publication, late nineteenth century. © Victoria and Albert Museum, London/as specified by the rights holder. Source: V&A's collection management system.*

## CHRIST AT BETHANY

**Franchi Group**

<b>Accession no.</b>	REPRO.1864-57
<b>Location</b>	Gallery 46A (N side)
<b>Dimensions</b>	135.0X112.0 cm
<b>Material</b>	Plaster

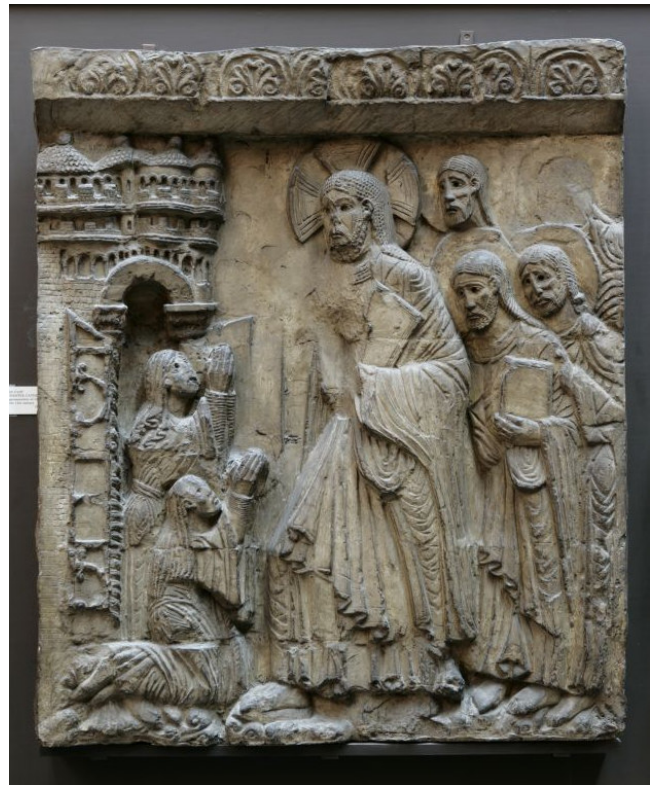


*Figure A5.20. Relief Christ at Bethany stone (REPRO.1864-57). Plaster cast made ca. 1864. © Victoria and Albert Museum, London/as specified by the rights holder. Source: V&A's Collection Management System.*

Plaster cast of a relief, in stone, with a representation of Christ at Bethany, Chichester Cathedral (UK), the second quarter of the twelfth century, cast made by Giovanni Franchi and Son in London possibly in 1851. Bought from Messrs Franchi & Son in 1864 together with museum no. 1864-56 for £30. **Conservation.** No records of previous treatments. Awaiting conservation.



### Appendix 6 List of Contents:

#### **Küsthardt Group**

Copy of the tombstone of Presbyter Bruno (REPRO.1873-380)	105
Copy of Part of a Choir Screen (REPRO.1873-561)	161
Copy of a Font (REPRO.1874-29)	187
Copy of a tympanum (REPRO.1874-45)	215
Copy of a Statue - Count Ekkehard (REPRO.1875-16)	233
Copy of a Statue - Regilindis, wife of Hermann (REPRO.1875-17)	255

#### **Notre-Dame Group**

Copy of a relief - The Assumption of the Virgin (REPRO.1890-80)	277
Copy of a relief - The Coronation of the Virgin (REPRO.1890-81)	297
Copy of a relief - The Death of the Virgin (REPRO.A.1916-3152)	317
Copy of a relief - The Entombment of the Virgin (REPRO.A.1916-3153)	337

#### **Franchi Group**

Copy of a relief - The Raising of Lazarus (REPRO.1864-56)	357
Copy of a relief - Christ at Bethany (REPRO.1864-57)	383

The images in the reports are not numbered following the thesis' images numbering.





**Northumbria  
University**  
NEWCASTLE

Analysis Report - Valentina Risdonne

Copy of the tombstone of Presbyter Bruno

(REPRO.1873-380)

Initiator: Charlotte Hubbard; Conservation Department

10 November 2020

© Victoria and Albert Museum



## Analysis Report

### Copy of the tombstone of Presbyter Bruno (REPRO.1873-380)

## Contents

Contents.....	106
List of abbreviations.....	107
Summary.....	108
Sample 1.....	114
Sample 2.....	116
Sample 3.....	119
Sample 4.....	123
Sample 5.....	127
Sample 6.....	131
Sample 7.....	134
Sample 8.....	137
Sample 9.....	141
Sample 10.....	145
Sample 11.....	148
Sample 12.....	151
Sample 13.....	154
Experimental.....	158
Notes.....	159
References.....	160

## List of abbreviations

BSE	Back Scattered Electron
EDS	Energy Dispersive Spectrometry
FT-IR	Fourier-Transform Infra-Red
FPA	Focal Plane Array
GC/MS	Gas Chromatography-Mass Spectrometry
OM	Optical Microscopy
PL	Proper Left
PR	Proper Right
py	pyrolysis
SEM	Scanning Electron Microscopy
TMAH	tetramethylammonium hydroxide
UVf	Ultraviolet Fluorescence
VLR	Visible Light Reflectance
XRD	X-ray Diffraction

## Summary

The stratigraphy of the samples is quite consistent, featuring a **'substrate'** layer, an **'interface'** layer and a **coating** 'dark' layer, likely a combination of aged coating and dust. On top of these, some samples feature additional layers, having been overpainted or having been sampled from an area of repair. The bulk of the object is made of gypsum plaster, which contains several types of inclusions (naturally present or purposely added, including silicates and carbonates). By looking at the results, it is possible to hypothesise that in the surface layer, containing **silicon** and **aluminium**, but also traces of other elements, the medium is a **diterpenic resin**. **Areas of repairs** consist of **overpaints made of alkyd paint** and inpaints containing silicon or barium. Areas showing an additional varnish layer might have locally highlighted or the additional layer might be due to a local difference in the surface absorbance or to an accidental spillage (as for example in sample 12, see Figure 3). A summary of the results can be seen in Table 1.



Figure 1. The copy of the tombstone.

The object, **'Copy of the Tombstone of Presbyter Bruno' (REPRO.1873-380)** (Figure 1), is a plaster cast made in ca. 1873 in Hildesheim (Germany) by the sculptor and plasterer Friedrich Küsthardt (1830-1900). The original tombstone is dated 1194 and is located in the Cathedral of Hildesheim. The cast was acquired in 1873 (purchased from F. Küsthardt for £6, see 1873 V&A's registry and Collection Management System) when the Museum acquired several plaster casts of key sculptural decorations in the cathedral of Hildesheim, all produced by the workshop of F. Küsthardt. This slab reproduces an elaborate tomb memorial, which commemorates a priest who is praised in the inscriptions for having given to the poor. It is unclear whether this slab would originally have been displayed horizontally. The cast is now located in Gallery 46A (The Ruddock Family Cast Court), displayed upright as framed in a wooden support and pedestal. Its dimensions are 218.5X77.0 cm.

Samples from the plaster cast were taken from pre-existing areas of loss to investigate the stratigraphy and the method of manufacture (Figure 2). The samples were analyzed to provide data for the study of the objects of the Cast Courts collection within the PhD project 'Materials and techniques for coating of the nineteenth-century plaster casts'. Details on the experimental procedure are available in the Experimental section of this report. A selection of significant results is shown in the following pages and the relevant database of analysis (<https://doi.org/10.25398/rd.northumbria.13469925>).

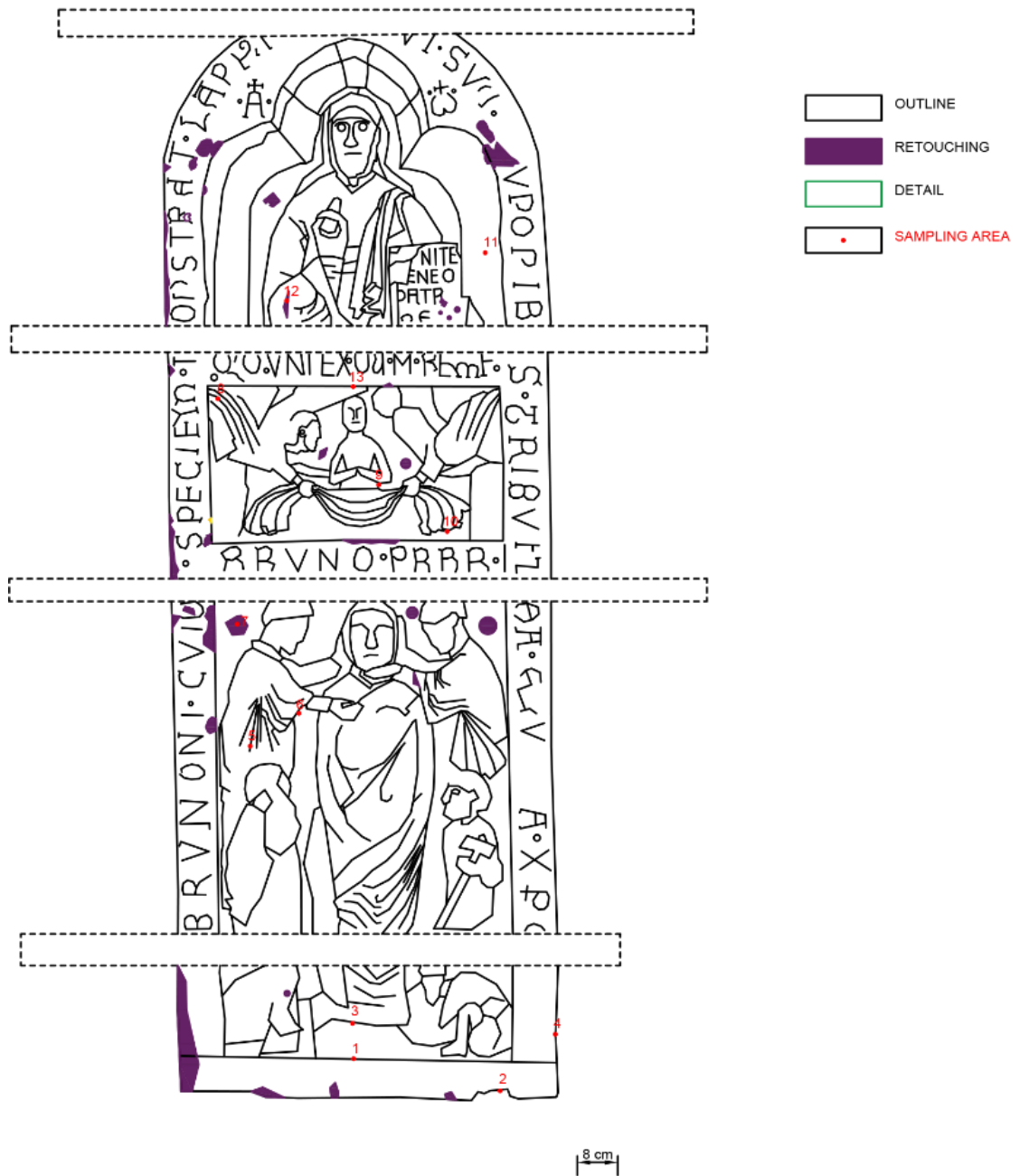


Figure 2. The tombstone outline with marked sampling sites.

**Sample 1:** loose dust deposited on the lower platform at the lowest part of the tombstone.

**Sample 2:** consists of plaster taken from the inner bulk, exposed on a broken area, below the base.

**Sample 3:** dark fragment taken from the hidden area below the vest of the presbyter.

**Sample 4:** fragment taken from the PL edge of the lowest section of the tombstone, from a darkened area.

**Sample 5:** fragment taken from an area of loss on the fold of the dress of the monk on the PR of the presbyter.

**Sample 6:** fragment taken from a hidden area underneath the arm of the monk on the PR of the presbyter.

**Sample 7:** fragment taken from an area of loss on an area of repair next to the monk on the PR of the presbyter.

**Sample 8:** fragment taken from an area of loss on the wing of the PR angel.

**Sample 9:** fragment taken from the hidden area below the PL arm of the resurrected Christ.

**Sample 10:** fragment taken from the hidden area below the PL of the brim of the cloth held by the angels.

**Sample 11:** fragment taken from an area of loss on the PL outer arc of the top section of the tombstone.

**Sample 12:** fragment taken from a fluorescent area on the PR sleeve of the main top figure.

**Sample 13:** fragment taken from the undercut just above the head of the figure carried by the angels.

**Dust** deposited on the tombstone was sampled and analysed to have a better understanding of the contaminants present in Gallery 46A. Under the microscope, the sample seems to be mostly made of fibres of various colours (red, green, blue). FT-IR analysis highlighted that the dust is made mostly of **sulfates (gypsum)**, **carbonates (calcite)**, **silicates** and unidentified organic materials possibly deriving from **fibres** and residues of human interaction (skin, oils and as such) (Derrick et al., 2000; Kumar & Rajkumar, 2014; Price et al., 2009).

The **substrate** (layer 0 in samples 3 to 13) is made of **gypsum plaster (calcium sulfate, CaSO<sub>4</sub>)**, confirmed by EDS, XRD and by the peaks at about 1005, 1105, 1600, 1680 cm<sup>-1</sup> in the FT-IR spectra, which also show the sulfate overtones centred on 2220 cm<sup>-1</sup> area) (Manfredi et al., 2015; Melita et al., 2020; Miliani et al., 2012; Toniolo et al., 2009). Sample 2 was taken from the inner plaster bulk (about 5 cm from the surface), exposed on a deep crack of the tombstone, to understand whether the organic medium detected in the surface layers was also used as an additive in the plaster mixture (Barash, 1985; Meilach, 1966; Turco, 1990). No organic materials were detected in this sample by FT-IR (Beran, 2002; Price et al., 2009). However, py-TMAH-GC/MS analysis suggests the presence of a Pine resin (markers: 7-Oxodehydroabiatic acid, methyl ester and Methyl dehydroabietate) (Colombini & Modugno, 2009; Mills & White, 2012). Fatty Acids were also detected, suggesting that the resin has been mixed with a non-drying oil, or are either from other sources of lipids or naturally present in the resin (Colombini & Modugno, 2009). The inconsistency of the FT-IR and py-TMAH-GC/MS results in this sample suggests that a very small quantity of resin was added to the plaster or that such small amount had penetrated deep in the plaster from the surface. **Aluminium (Al)** is overall present as used as a

polishing agent, but could also, together with **potassium** (K) and **silicon** (Si) be present as part of silicate inclusions. FT-IR spectra suggest vibrations in the 950-1100  $\text{cm}^{-1}$  region, characteristic of **clay minerals** (Si-O containing minerals, such as kaolin). FT-IR peaks at 1440 and 1770  $\text{cm}^{-1}$  and overtone centred at 2400  $\text{cm}^{-1}$  suggest the presence of **calcite** (**calcium carbonate**,  $\text{CaCO}_3$ ). **Magnesium** (Mg) was also detected by EDS and it is possibly an exchangeable element of the sulphate variety  $\text{MgSO}_4$  (more or less hydrated, chalcantite  $\text{CuSO}_4 \cdot 5\text{H}_2\text{O}$ , kieserite  $\text{MgSO}_4 \cdot \text{H}_2\text{O}$ , starkeyite  $\text{MgSO}_4 \cdot 4\text{H}_2\text{O}$ , hexahydrate  $\text{MgSO}_4 \cdot 6\text{H}_2\text{O}$ , epsomite  $\text{MgSO}_4 \cdot 7\text{H}_2\text{O}$  and meridianiite  $\text{MgSO}_4 \cdot 11\text{H}_2\text{O}$ ). Minor variations of the position of the FT-IR peaks related to the inorganic components can be observed for several reasons, one of which is the local substitution of elements such as Mg and Pb in the gypsum and other minerals' structure (Cox et al., 1974; Manfredi et al., 2015; Melita et al., 2020). Small quantities of sulfate varieties such as barite ( $\text{BaSO}_4$ ), celestite ( $\text{SrSO}_4$ ), anglesite ( $\text{PbSO}_4$ ) and the Mg varieties mentioned above can be naturally present in the gypsum quarries or form after the rehydration of the gypsum plaster (Cox et al., 1974; Turco, 1990). This composition of the plaster was consistently found in layer 0 of samples 3 to 8 and 10 to 13. Sample 5 shows small inclusions of titanium (Ti) in the plaster bulk. Sample 9 additionally shows inclusions made of silicon (Si), aluminium (Al), iron (Fe) strontium (Sr) throughout the stratigraphy. EDS mapping and XRD analysis confirmed that despite inclusions of calcium carbonate are present in the bulk, the object is made of gypsum plaster rather than lime plaster as was demonstrated in other case studies (Melita et al., 2020).

An **interface layer**, yellow under visible illumination and possibly consisting of a portion of lower layer soaked with the surface coating(s), showing characteristics of both layers, is visible in samples 3 to 6 and 8 to 13. The **tabular crystalline** structure typical of gypsum plaster can be seen in the substrate layer and the interface layer in the BSE image (Cox et al., 1974). In samples 10 and 11, the casting resin homogeneously penetrated the stratigraphy and in samples 3, 4, 5, 6, 8, 12 and 13 layer 1 appears 'denser' than layer 0, suggesting that the coating layer had penetrated the plaster, impeding the casting resin from filling the pores and possibly preserving the mineral structure of the gypsum plaster.

Samples 3 to 5 and 8 to 13 show a **coating layer**, dark under visible illumination (layer 2 in these samples). EDS mapping shows that this dark layer contains **calcium sulfate** but consists mostly of **Si** and **Al**. The presence of an **organic medium**, likely a wax or resin is suggested in all the FT-R spectra; however, the crowded appearance of the spectra and the broadness of the peaks impede the unique assignment of such contributions. **Calcium oxalate** might be also present in layer 2, but it was not possible to uniquely assign its peaks, as usually close to the vibrations characteristic of calcium sulfate (Toniolo et al., 2009). Traces of other elements were detected and vary across the samples, due to local surface contamination or locally distribution of trace elements in the plaster or coating. Sample 3 shows traces of Na, Cl, K, Fe and Ti; sample 4 shows traces of K, Ba, Zn, Cl and P; sample 8 shows traces of K, Fe and Na; sample 5 shows traces of Mg, Ti, Na, Fe and K; sample 10 shows traces of K and Cl; sample 11 shows traces of Fe; sample 12 shows traces of p, Cl and Fe; sample 13 shows traces of Fe, Cl, Ti and Na.

The presence of the contributions of vibrations of the **organic material** in the FT-IR spectra of all the layers indicates that either the material was added to the gypsum plaster wet mixture or that the coating has also penetrated in layer 0. The latter seems also possible as the average depth of the samples is about 0.5 mm. py-TMAH-GC/MS of samples 3, 4, 5, 8, 9 shows markers characteristic of a **diterpenic resin**, such as rosin or pine resin, possibly mixed with a non-drying oil or another source of lipids (Colombini & Modugno, 2009). py-TMAH-GC/MS of samples 8 and 9 also shows a **triterpene** marker, suggesting that, as rarely diterpene and triterpene molecules are found together in a plant resin, a birch, dammar o mastic is additionally present in the stratigraphy. The markers characteristic of dammar and mastic were not detected, but it cannot be excluded that their absence in the chromatogram is due to the natural degradation of the molecule or the derivatization processes applied on the already degraded organic material. The small quantity of the organic material, when compared to the inorganic portion, surely also contributed to the small relative abundance of the di- and tri- terpene molecules in the chromatogram. As pointed out by Colombini & Modugno (2009), the characterization of unknown organic materials in aged samples is the most challenging application of GC/MS techniques.

Moreover, in sample 8 and additional layer (layer 3) fluoresces white under UV illumination, suggesting that these could be an additional layer or that layer 2 has not been absorbed evenly, as seen in the other samples. The same was also observed in samples 11, 12 and 13.

Sample 4 is characterised by the same stratigraphy described above, but additionally presents an additional layer (layer 3), purple under visible illumination. EDS mapping suggested that this layer is mostly made of **iron** (Fe), **silicon** (Si) and **titanium** (Ti). py-TMAH-GC/MS of this sample highlighted that a **drying oil modified alkyd paint** is the medium in this layer (Singer & McGuigan, 2007). Samples 6 and 7 broadly present the same stratigraphy of the other samples, however, the coating layer is made of K, Fe, Si and Al and traces of Na, Pb and Cl in sample 6 and Fe and Ba and traces of Mg, K and Cl in sample 7. In samples 8, 11, 12 and 13 an additional surface layer (layer 3 in these samples) fluoresces milky-white under UV illumination. No differences can be seen in the FT-IR spectra of these samples nor the GC/MS chromatograms, suggesting that either layer 3 is an additional layer of varnish made of the same material of the medium of layer 2 (diterpene resin) or layer 3 is an unabsorbed portion of the medium of layer 2 visible on the surface.



Figure 3. An accidental spillage was highlighted under UV illumination. Sample 12 was taken from this area.

**NOTE:** casting in resin the fragments of plaster resulted in the fragments absorbing the resin when in the liquid state. This was visible in the BSE image as well as through the EDS mapping (Tiranti resin and catalyst are mainly made of organic compounds C, H and O). The presence of the **casting resin** (Tiranti polyester resin) was also detected in all the layers by FT-IR spectra ( $\delta$  OH phenol at about  $1312\text{ cm}^{-1}$  and  $\delta$  CH aromatic at about  $1760\text{ cm}^{-1}$ ). Aluminium (Al) traces are present in all the samples, due to the polishing chemical.

Table 1. Summary of findings in the samples' layers.

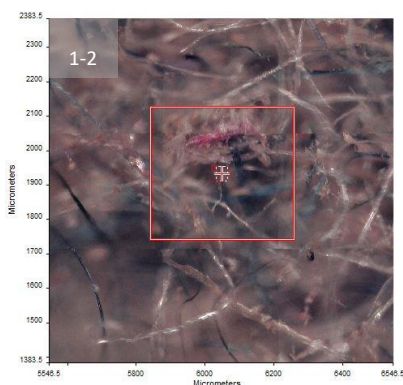
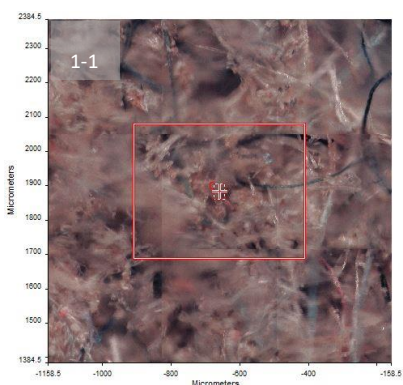
SAMPLE	TYPE	NOTES	no. of LAYERS	LAYERS	PLASTER	INTERFACE	COATING	OVERPAINT
1	dust	fibres and mixture of organic and inorganic material	-	-	-	-	-	-
2	plaster from the inner bulk		-	-	calcium sulfate, calcium carbonate, clay minerals, Al, Mg, Si, diterpenic resin	-	-	-
3	cross-section		3	2. Dark layer 1. Yellowish and undefined layer 0. Plaster bulk	calcium sulfate, calcium carbonate, clay minerals, Mg, diterpenic resin	Intermediate of plaster and dark layer	Mostly Si and Al; Fe, Ti and traces of Na, Cl and K, diterpenic resin	-
4	cross-section	edge area of sampling	4	3. Purple layer 2. Dark layer 1. Yellowish and undefined layer 0. Plaster bulk	calcium sulfate, calcium carbonate, clay minerals, Mg, diterpenic resin	Intermediate of plaster and dark layer	Mostly Si and Al, traces of K, Ba, Zn, Cl and P, diterpenic resin	Fe, Si and Ti, traces of K, Ba, Zn, Cl and P, drying oil modified alkyd paint
5	cross-section		3	2. Dark layer 1. Yellowish and undefined layer 0. Plaster bulk	calcium sulfate, calcium carbonate, clay minerals, Mg, Ti, diterpenic resin	Intermediate of plaster and dark layer	Mostly Si and Al, traces of Mg, Ti, Na, Fe and K, diterpenic resin	-
6	cross-section	area of repair	3	2. Dark layer 1. Yellowish and undefined layer 0. Plaster bulk	calcium sulfate, calcium carbonate, clay minerals, Mg, Ti, traces of K and Fe, organic medium	Intermediate of plaster and dark layer	Mostly K, Fe, Si and Al, traces of Na, Pb and Cl, organic medium	-
7	cross-section	area of repair	2	1. Yellowish and undefined layer with large orange and black particles 0. Plaster bulk	calcium sulfate, calcium carbonate, clay minerals, organic medium	-	Mostly Fe and Ba, traces of Mg, K and Cl, organic medium	-
8	cross-section	fluorencent varnish	4	3. Varnish 2. Dark layer 1. Yellowish and undefined layer 0. Plaster bulk	calcium sulfate, calcium carbonate, clay minerals, Mg, Cl, diterpenic resin, possibly additional triterpenic resin or birch	Intermediate of plaster and dark layer	Mostly Si and Al, traces of K, Fe and Na, diterpenic resin, possibly additional triterpenic resin or birch	-
9	cross-section		3	2. Dark layer 1. Yellowish and undefined layer 0. Plaster bulk	calcium sulfate, calcium carbonate, clay minerals, Mg, Al, Sr and Fe, diterpenic resin, possibly additional	Intermediate of plaster and dark layer	Mostly Si, Al, Mg, Sr and Fe, traces of K and Ti, diterpenic resin, possibly additional triterpenic resin or birch	-
10	cross-section		3	2. Dark layer 1. Yellowish and undefined layer 0. Plaster bulk	calcium sulfate, calcium carbonate, clay minerals, Mg, organic medium	Intermediate of plaster and dark layer	Mostly Si and Al, traces of K and Cl, organic medium	-
11	cross-section		4	3. Varnish 2. Dark layer 1. Yellowish and undefined layer 0. Plaster bulk	calcium sulfate, calcium carbonate, clay minerals, Mg, organic medium	Intermediate of plaster and dark layer	Mostly Si and Al, traces of Fe and Mg, organic medium	-
12	cross-section	fluorencent varnish	4	3. Varnish 2. Dark layer 1. Yellowish and undefined layer 0. Plaster bulk	calcium sulfate, calcium carbonate, clay minerals, Mg	Intermediate of plaster and dark layer	Mostly Si and Al, traces of P, Cl and Fe, organic medium	-
13	cross-section	fluorencent varnish	4	3. Varnish 2. Dark layer 1. Yellowish and undefined layer 0. Plaster bulk	calcium sulfate, calcium carbonate, clay minerals, Mg, diterpenic resin	Intermediate of plaster and dark layer	Mostly Si and Al, traces of Fe, Mg, Cl, Ti and Na, diterpenic resin	-

# Sample 1

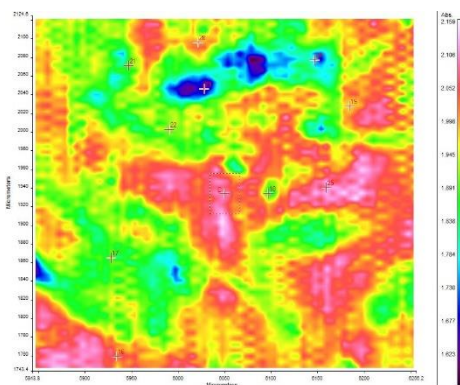
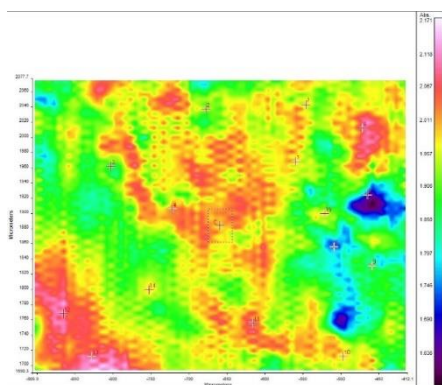


**Sampling.** Loose dust deposited on the lower platform at the lowest part of the tombstone was sampled.

**Summary.** The dust was taken with the aid of a painting brush. Under the microscope, the sample seems to be mostly made of fibres of various colours (red, green, blue) (see [Survey Images](#)). The dust is made mostly of sulfates (gypsum), carbonates (calcite), silicates and unidentified organic materials possibly deriving from fibres and residues of human skin and as such (Derrick et al., 2000; Price et al., 2009).



Spotlight 400  
FT-IR  
microscope  
**Survey Images**  
(left) of the dust  
showing dust  
and fibres



**FT-IR (FPA)**  
image (left).

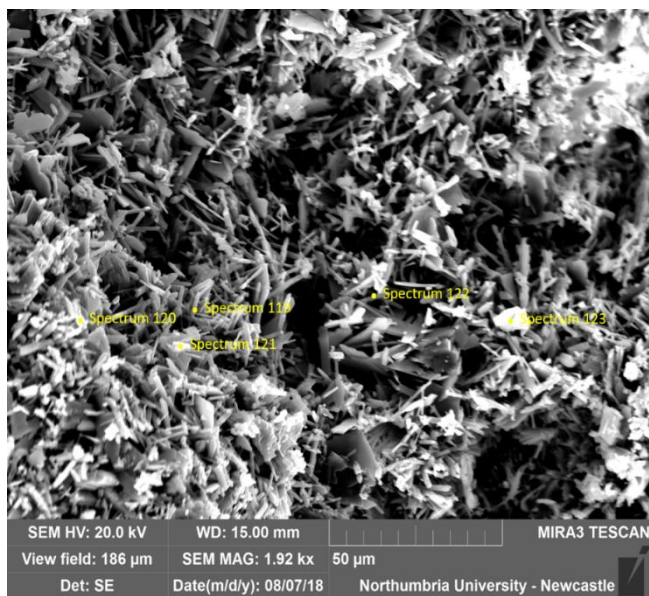
**Spectra 1-15** (area 1-1, FT-IR imaging), **Spectra 16-25** (area 1-2, FT-IR imaging).



## Sample 2

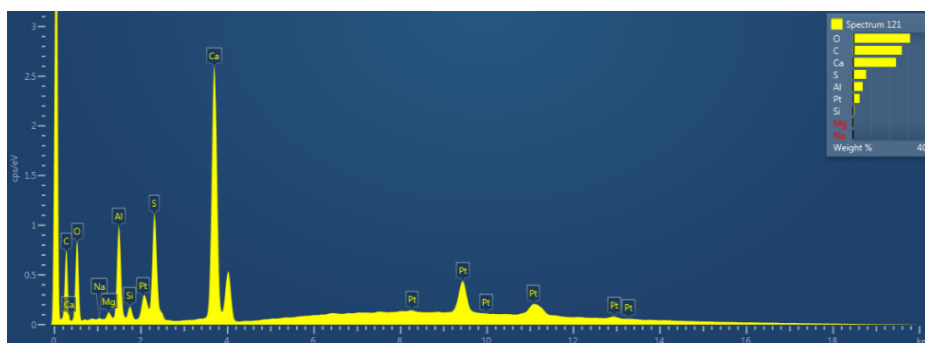


**Sampling.** This sample consists of plaster taken from the inner bulk, exposed on a broken area, below the base.

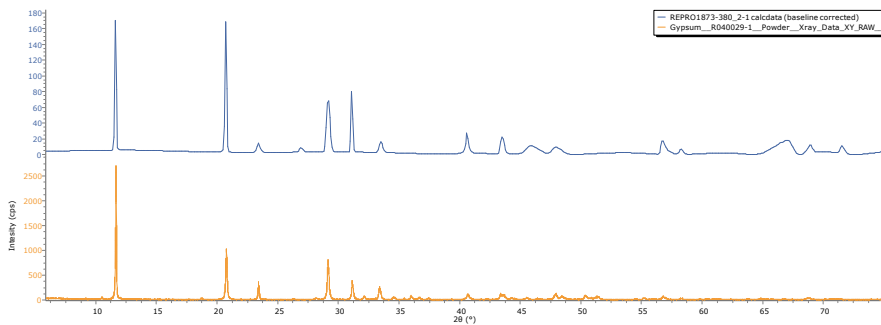


**BSE image (above)** shows the *tabular* structure of the crystals of gypsum. **Analysis spots.** EDS analysis (yellow): Spectra 119-123.

**Summary.** XRD, EDS and FT-IR analysis confirmed that the sample consists of **calcium sulfate**,  $\text{CaSO}_4$  (gypsum/plaster of Paris), but also **carbonates** and **Al-silicates**. No organic materials were detected in this sample by FT-IR (Beran, 2002; Price et al., 2009). py-TMAH-GC/MS analysis suggests the presence of a **Pine resin** (markers: 7-Oxodehydroabietic acid, methyl ester and Methyl dehydroabietate) (Colombini & Modugno, 2009; Mills & White, 2012). Fatty Acids were also detected, suggesting that the resin has been mixed with a non-drying oil, or are either from other sources of lipids or naturally present in the resin (Colombini & Modugno, 2009). The presence of the pine resin was not uniquely detected in the FT-IR spectra, but this can be due to the small concentration of the resin in the plaster or related to the particular location of the FT-IR analysis.

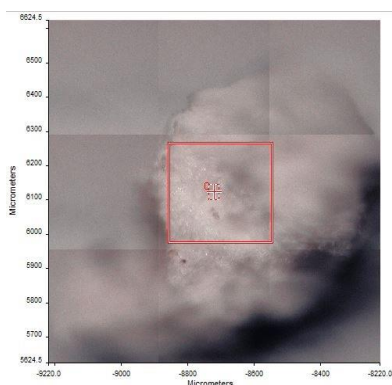


**EDS spectrum 121 (left)** shows Ca, S, O and C. Al, Mg and Si were also detected. Pt derived from the paint applied to the sample to increase the conductivity.

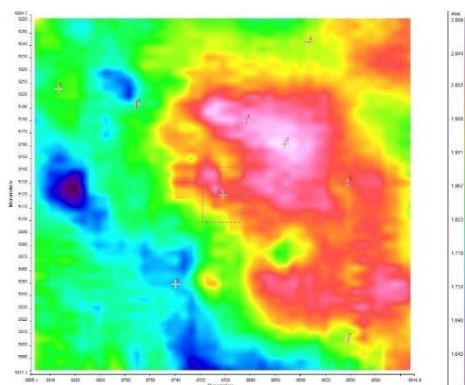


2θ (°) = 11.63, 20.69, 23.38, 26.87, 29.12, 31.10, 33.46, 40.57, 43.47, 45.83, 47.87, 56.68, 58.21, 67.02, 68.95, 71.47.

A fragment of this sample was pulverised and analysed by **XRD**. It was possible to identify the profile of gypsum (calcium sulfate). **XRD diffractograms** (left): sample 2 (blue), RRUFF Database (orange) (Lafuente et al., 2016).



Spotlight 400 microscope Survey Image (above)

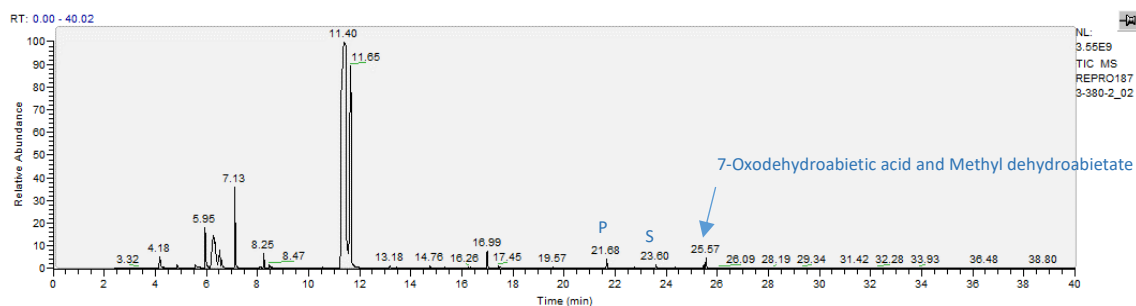


FT-IR (FPA) image (above)

**Spectra 1-8** were taken from the fragment shown on the left.

The spectra were not very distinct, which suggest a mixture of components. Several peaks suggest the presence of **calcium sulfate**, CaSO<sub>4</sub>, but also **carbonates** and **Al-silicates**. No organic materials were detected in this sample by FT-IR. The table below summarises the results.

Peaks (cm-1)	Spectrum								Assignment	
	1	2	3	4	5	6	7	8		
							752		v AlOAl	
						768			v SiOSi	v CH
			784	784						δ CH
832	832						816		v AlO	
		864				864		832	v COC	
							880	864	v CCO	δ CH
			896	896					δ CO	
	928					944	944		v SiO	
1008									vs SO4	
		1024	1024				1024	1024	v CO	v SiO
		1088			1088	1088	1088	1088	v1s CO3	v SiOSi
1104			1104						vs SO4	
	1120								SiCH2	
			1246			1260			v CO	δ CH
	1280	1272	1280	1278, 1296		1296	1284	1273	v CO	
	1616								v2 H2O	v CC
1632	1632	1632	1632	1632		1632	1632	1632	v2 H2O	v CC
1660									v2 H2O	v C=O
	1680	1680	1680	1680		1680	1680	1680	v2 H2O	v C=O
2128	2128				2128	2144	2128	2128	v OH HSO4	
2224	2208	2224	2224	2224		2240	2240	2240	v OH HSO4	
	2256								v OH HSO4	
					2352			2320	v OH HSO4	
	3088					3056				
3168	3168	3152								
3216	3200	3200	3216			3232				
3248	3248	3289	3280		3296		3248, 3296	3248		
3312	3328	3344	3344		3328	3344				
	3360	3392			3360	3392		3360		
3408	3424		3440	3424			3408, 3456	3408, 3440	v OH	
3472	3488	3488	3488	3483		3486		3493		
3583	3572	3536	3590	3568		3568	3518, 3536			
3664	3632	3648		3648		3616, 3664		3600		
	3696									
	3792									



RT	m/z	Assignment	Formula
4.18	45(100), 59(7), 75(74)	Ethyl ether	C4H10O
5.95	42(13), 58(100), 117(18)	1,2-Ethanediamine, N'-ethyl-N,N-dimethyl-	C6H16N2
6.29	58(3), 83(8), 113(21), 145(35), 157(14), 176(100)	m-TFPTAH related fragment	
7.13	44(7), 72(100)	1,2-Ethanediamine, N'-ethyl-N,N-dimethyl-	C6H16N2
8.25	58(7), 83(8), 113(21), 145(35), 157(15), 176(100)	m-TFPTAH related fragment	
11.4	145(14), 172(15), 188(100)	1H,5H-Benzo[ij]quinolizin-8-ol, 2,3,6,7-tetrahydro-	C12H15NO
11.65	145(15), 172(14), 188(100)	1H,5H-Benzo[ij]quinolizin-8-ol, 2,3,6,7-tetrahydro-	C12H15NO
16.99	76(8), 103(5), 135(16), 163(100), 194(26)	1,4-Benzenedicarboxylic acid, dimethyl ester	C10H10O4
17.45	44(8), 5(9), 59(8), 74(15), 120(10), 147(10), 162(100), 179(68)	m-TFPTAH related fragment	
21.68	55(14), 74(100), 87(57), 101(5), 129(6), 145(21), 185(7), 227(15), 270(6)	methyl palmitate	C17H34O2
23.6	74(100), 87(57), 129(6), 143(25), 199(13), 255(18), 298(9)	methyl stearate	C19H38O2
25.47	187(5), 207(7), 253(100), 313(10), 328(7)	7-Oxodehydroabiatic acid, methyl ester	
25.57	141(7), 155(7), 197(8), 239(100), 253(34), 314(8)	Methyl dehydroabietate	

RT = retention time, m/z = mass/charge ratio

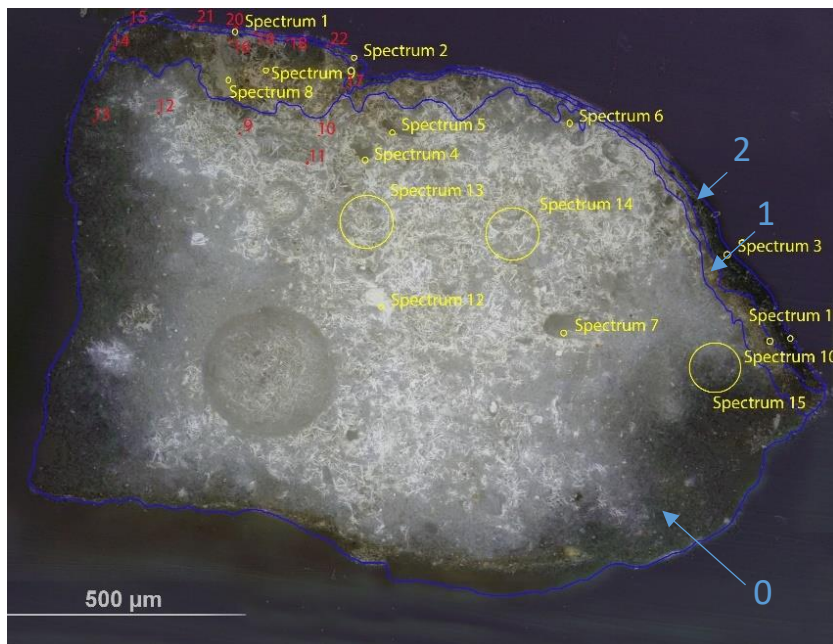
**py-TMAH-GC/MS.** 2  $\mu$ l Meth Prep II (2) solution, 1  $\mu$ l TMAH. Thermal Programme (1). **py-TMAH-GC/MS chromatogram** (top and described in the table [above](#)) shows small fragments due to derivatization (from  $t = 3.03$  to  $16.99$  min) and markers characteristic of a **Pine resin** ( $t = 25.47$  and  $25.57$ ) (Colombini & Modugno, 2009; Mills & White, 2012). The presence of, **methyl palmitate** ( $t = 21.68$ ) and **stearate** ( $t = 23.60$ ) might suggest that the resin has been mixed with an **oil** ( $P/S = 2.15$ ), but the absence of **methyl azelate** suggests that the FA are either from a non-drying oil, another source of lipids or naturally present in the resin (Colombini & Modugno, 2009).

The presence of the pine resin was not uniquely detected in the FT-IR spectra, especially as no peaks in the  $2800\text{--}3000\text{ cm}^{-1}$  (CH stretching bands) were observed. However, this can be due to the small concentration of the resin in the plaster or related to the particular location of the FT-IR analysis.

## Sample 3



**Sampling.** This sample consists of a dark fragment taken from the hidden area below the vest of the presbyter.



Left: Overlapped (OM and BSE) cross-section image showing the stratigraphy (blue indicators).

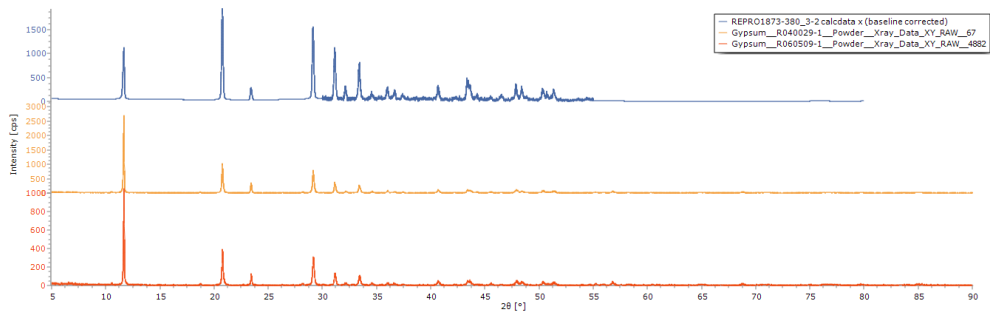
- 2. Dark layer
- 1. Yellowish and undefined layer
- 0. Plaster bulk

**Analysis spots.** EDS analysis (yellow): Spectra 1-15; FT-IR analysis (red): nos. 9-22

**Summary.** The sample is mostly made of C, O, S and Ca (**calcium sulfate**,  $\text{CaSO}_4$ , confirmed by EDS, XRD and by FT-IR). **Al** is overall present as used as a polishing agent, but could also, together with **Si** and **Mg**, be present as part of silicate inclusions, which are present in all the layers (FT-IR confirmed the presence of **clay minerals**, such as kaolin). Traces of **Na**, **Cl**, **K**, **Fe** and **Ti** were also detected. **Calcite** or other carbonate minerals were also suggested by FT-IR. The mineral structure typical of gypsum plaster can be seen in layers 0 and 1. Layer 1 appears yellowish under visible illumination and consists of the plaster substrate soaked with the outmost layer. Layer 2 appears dark under visible illumination and is mostly made of Si and Al. A **wax or resin** is suggested by FT-IR and detected in all the layers. py-TMAH-GC/MS shows markers characteristic of a **diterpenic resin**, such as rosin or pine resin, possibly mixed with a non-drying oil or another source of lipids (Colombini & Modugno, 2009).

Right: XRD diffractogram of gypsum.

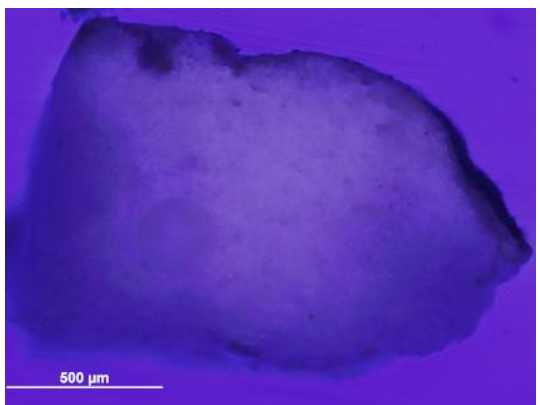
Sample 3 (blue); RRUFF Database (yellow and orange) (Lafuente et al., 2016).



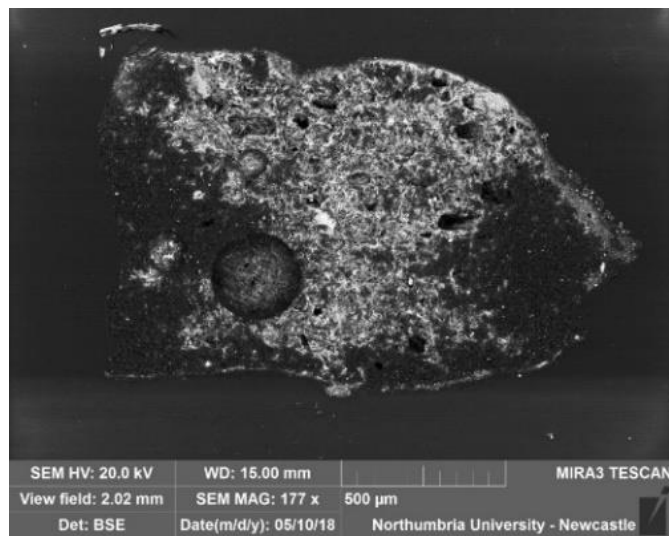
2θ (°) = 11.67, 20.74, 23.37, 29.10, 31.12, 33.35, 40.63, 43.38, 45.51, 47.85, 56.73, 58.19, 68.67, 71.22



VLR OM (above)



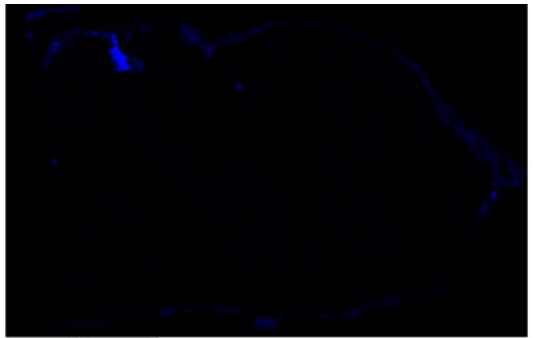
UVfOM (above)



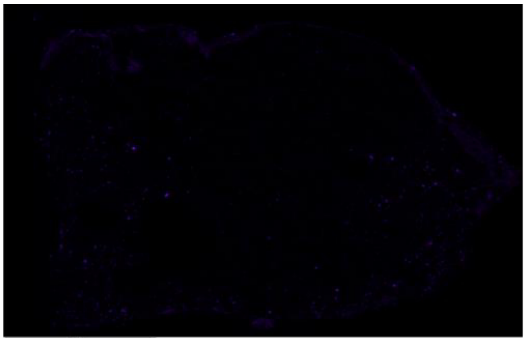
The tabular structure of calcium sulfate ( $\text{CaSO}_4$ ) can be seen in layers 0 and 1 (BSE image, left).

Below: EDS mapping showed that layer 2 is mostly made of Si (left) and Al (right).

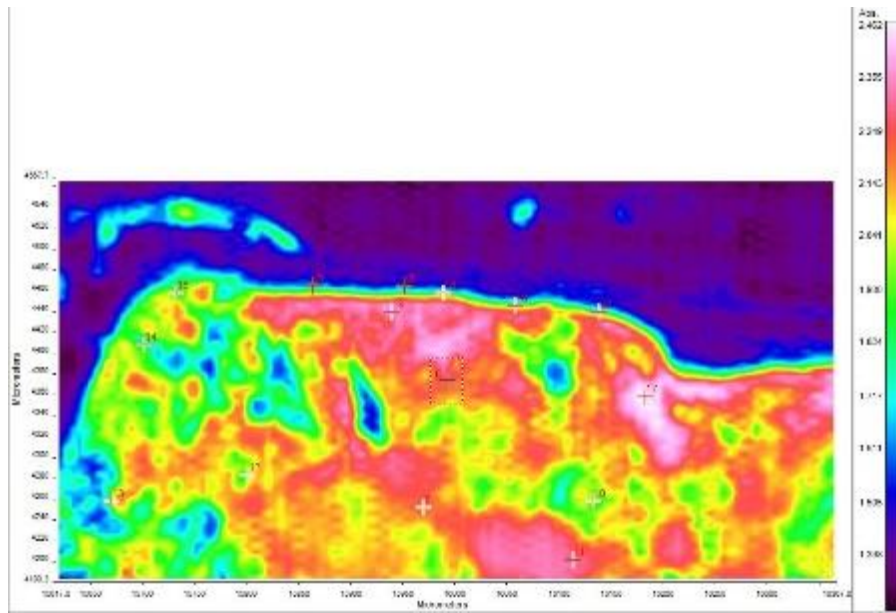
EDS spectra suggest that calcium sulfate and traces of Mg and Al are present in all the layers. Layer 2 is mostly made of calcium sulfate, Si and Al, but traces of Na, Cl, K and Fe were also detected.



Silicon (Si)



Aluminium (Al)

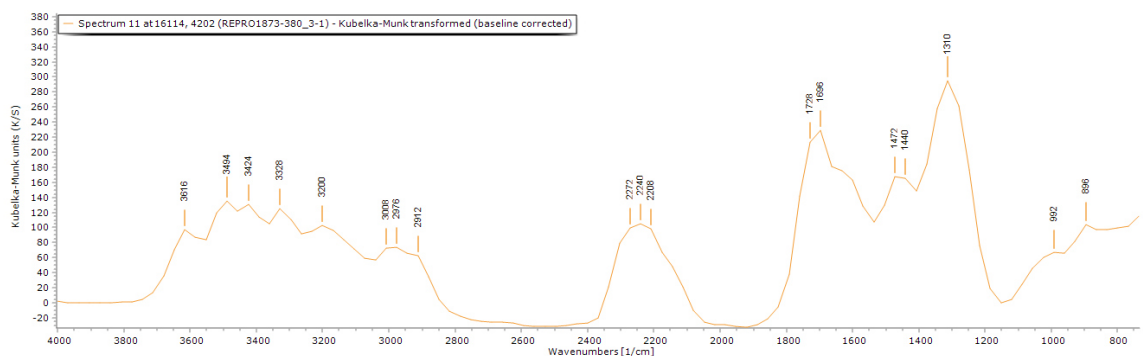


**FT-IR (FPA) image (left).** No clear indication of different reflectance of the layers can be observed in the FPA image.

**Spectra 9-22** (see for example **spectrum 11** below) show a similar pattern with broad bands rather than sharp and defined peaks, which is expected for mixtures containing several components. Overall, no significant difference within the layers can be noticed by FT-IR analysis (see table on the right).

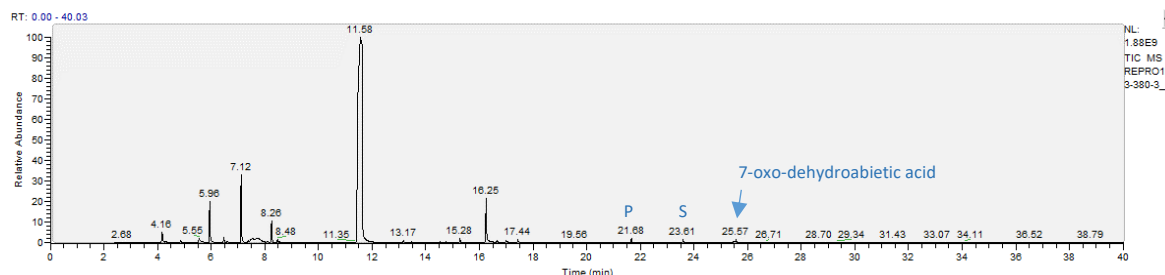
Spectrum	Layer	Material					
		Casting resin	Gypsum plaster	Calcite	Clay minerals	Organic material	Calcium oxalate
9	0	x	x			x	
10	0	x	x			x	
11	0	x	x	x	x	x	
12	0	x	x	x		x	
13	0	x	x		x	x	
14	2	x	x	x		x	
15	2	x	x		x	x	
16	1	x	x			x	
17	1	x	x	x	x	x	
18	2	x	x		x	x	
19	2	x	x		x	x	
20	2	x	x			x	
21	2	x	x			x	
22	2	x	x		x	x	

The presence of the **casting resin** (Tiranti polyester resin) and **gypsum plaster** ( $\text{CaSO}_4 \cdot 0.5\text{H}_2\text{O}$ ) was detected in all the layers. **Calcite** (calcium carbonate,  $\text{CaCO}_3$ ) and **clay minerals** (Si-O containing minerals) were also identified in several spectra. A minor variation of the position of the peaks can be observed for several reasons, one of which is the local substitution of elements such as Mg and Pb in the gypsum and other minerals' structure (Melita et al., 2020). As reported in other publications (Manfredi et al., 2015; Miliani et al., 2012), the strong and broad band at  $2000\text{-}2500\text{ cm}^{-1}$  is due to the combination of bending and vibration modes of  $\text{H}_2\text{O}$  ( $\nu_1 + \nu_3$  and  $2\nu_3$ ) related to the presence of gypsum (centred at  $2200\text{ cm}^{-1}$ ) and other minerals. The presence of **organic material**, likely a **wax** or **resin** is suggested in all the spectra; however, the crowded appearance of the spectra and the broadness of the peaks impede the unique assignment of such contributions. The several peaks that can be identified in the area over  $3000\text{ cm}^{-1}$  cannot be considered diagnostic, as the OH and NH stretches occur in this region and once again due to the complexity of the mixture, the water present in the crystals and the pores of the plaster, as well as in the organic components will add up in this area. **Calcium oxalate** might be also present, but it was not possible to uniquely assign its peaks (Toniolo et al., 2009).



Sample	Sample prep method	Thermal programme
REPRO.1873-380_3-01	Py-TMAH-GCMS 1 µl TMAH	(1)
REPRO.1873-380_3-02	Py-TMAH-GCMS 1 µl TMAH	(1)
REPRO.1873-380_3-03	Py-TMAH-GCMS 5 µl Meth Prep II (2) solution, 1 µl TMAH	(1)
REPRO.1873-380_3-04	Py-TMAH-GCMS 10 µl Meth Prep II (2) solution, 1 µl TMAH	(1)
REPRO.1873-380_3-05	Py-TMAH-GCMS 10 µl Meth Prep II (2) solution, 1 µl TMAH	(1)

Despite the different prep methods used on **samples 3-01 to 3-05** (see table on the left, and description in the *Experimental* section), the results were consistent and shown, for example in the chromatogram and table below (**sample 3-05**).



**py-TMAH-GC/MS chromatogram** (top and described in the table on the right) shows small fragments due to derivatization (from  $t = 4.18$  to  $13.17$  min) and markers characteristic of a **natural terpenoid resin** ( $t = 23.39$ ,  $25.56$  and  $26.56$ ) (Colombini & Modugno, 2009; Mills & White, 2012). The presence of **methyl palmitate** (P,  $t = 21.68$ ) and **stearate** (S,  $t = 23.60$ ) might suggest that the resin has been mixed with an **oil** (P/S = 1.03) suggests that the FA are either from a non-drying oil, another source of lipids or naturally present in the resin (Colombini & Modugno, 2009).

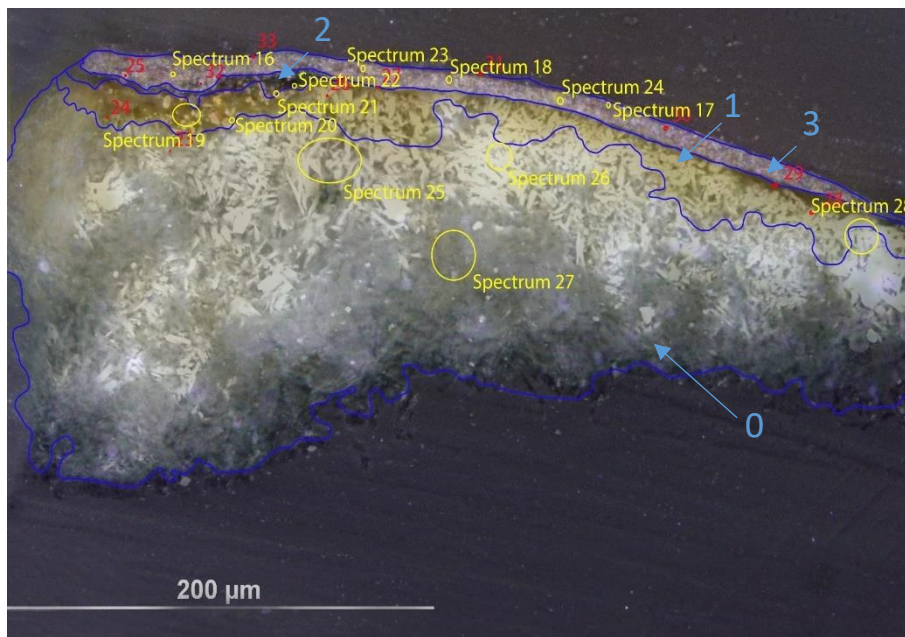
RT	m/z	Assignment	Formula
4.18	45(100), 58(8), 74(93)	Ethyl Ether	C <sub>4</sub> H <sub>10</sub> O
5.53	42(14), 58(100), 72(10), 88(4), 116(7)	1,2-Ethanediamine, N'-ethyl-N,N-dimethyl-	C <sub>6</sub> H <sub>16</sub> N <sub>2</sub>
5.96	42(14), 58(100), 117(18)	1,2-Ethanediamine, N'-ethyl-N,N-dimethyl-	C <sub>6</sub> H <sub>16</sub> N <sub>2</sub>
6.48	58(20), 66(23), 79(21), 95(100), 125(11)	Sulfuric acid, dimethyl ester	C <sub>2</sub> H <sub>6</sub> O <sub>4</sub> S
7.13	42(5), 72(100), 131(2)	Amine fragment	
8.25	58(7), 83(7), 96(5), 113(17), 133(23), 145(17), 157(8), 176(100)	Unidentified fragment	
11.58	118(3), 145(12), 172(9), 188(100)	Unidentified fragment, MetPrep related	
13.17	58(26), 74(5), 88(14), 98(21), 116(31), 130(100), 141(8), 188(7)	Unidentified fragment, MetPrep related	
15.28	58(56), 75(5), 85(5), 127(5), 145(25), 159(28), 172(28), 186(21), 200(62), 216(51), 232(100), 247(43)	Sesquiterpene fragment	C <sub>15</sub> H <sub>20</sub> O <sub>2</sub>
16.25	55(30), 69(62), 74(78), 83(43), 87(36), 111(21), 129(100), 138(82), 171(72), 188(5)	Dimethyl suberate	C <sub>10</sub> H <sub>18</sub> O <sub>4</sub>
17.44	58(43), 74(23), 83(10), 129(13), 148(5), 178(100)	Three benzene ring fragment	
21.68	74(100), 87(58), 129(15), 143(14), 171(12), 185(7), 227(16), 239(5), 270(5)	Methyl palmitate	C <sub>17</sub> H <sub>34</sub> O <sub>2</sub>
23.39	58(100), 74(22), 79(34), 97(11), 171(14), 207(5), 253(5), 281(5), 355(5), 401(5), 549(5)	Unidentified Terpenoid fragment	
23.6	58(78), 74(100), 87(58), 128(21), 143(16), 171(12), 199(5), 255(5), 298(5)	Methyl stearate	C <sub>19</sub> H <sub>38</sub> O <sub>2</sub>
25.56	44(49), 58(100), 74(21), 79(44), 97(5), 129(24), 171(25), 207(22), 239(73), 253(45), 281(5), 299(5), 314(5), 328(5)	7-oxo-dehydroabiatic acid	
26.56	44(51), 58(100), 74(17), 129(17), 171(14), 207(23), 267(5), 281(10), 327(5), 342(8), 355(5)	Dehydroabiatic acid fragment	

RT = retention time, m/z = mass/charge ratio

## Sample 4



**Sampling.** This sample was taken from the PL edge of the lowest section of the tombstone, from a darkened area.



Left: Overlapped (OM and BSE) cross-section image showing the stratigraphy (blue indicators).

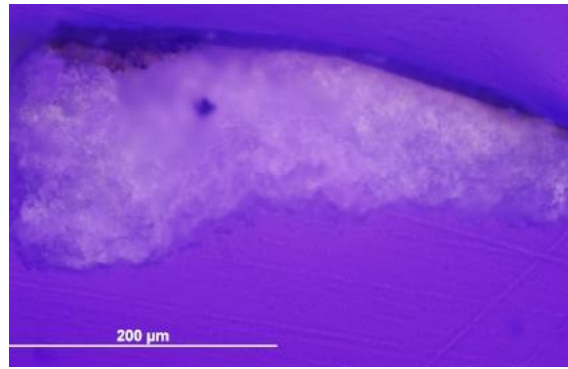
- 3. Purple layer
- 2. Dark layer
- 1. Yellowish and undefined layer
- 0. Plaster bulk

**Analysis spots.**  
EDS analysis (yellow): Spectra 16-28; FT-IR analysis (red): nos.23-33

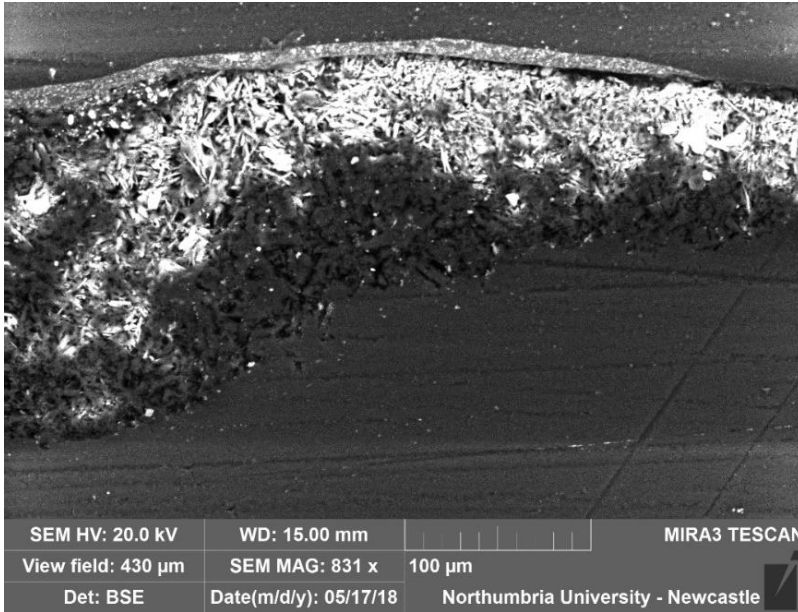
**Summary.** The sample is mostly made of C, O, S and Ca (**calcium sulfate**,  $\text{CaSO}_4$ , confirmed by EDS and by FT-IR). **Al** is overall present as used as a polishing agent, but could also, together with **Si** and **Mg**, be present as part of silicate inclusions, which are present in all the layers (FT-IR confirmed the presence of **clay minerals**, such as kaolin). Traces of **K**, **Ba**, **Zn**, **Cl** and **P** were also detected. **Calcite** or other carbonate minerals were also suggested by FT-IR. The mineral structure typical of gypsum plaster can be seen in layers 0 and 1. Layer 1 appears yellowish under visible illumination and consists of the plaster substrate soaked with the outmost layer. Layer 2 appears dark under visible illumination. Layer 3 appears purple under visible illumination and is mostly made of iron (Fe), silicon (Si) and titanium (Ti). A **wax or resin** is suggested by FT-IR and detected in all the layers. py-TMAH-GC/MS shows markers characteristic of a **diterpenic resin**, such as rosin or pine resin, possibly mixed with a non-drying oil or another source of lipids (Colombini & Modugno, 2009). A marker for **alkyd paint (dimethyl phthalate)** was also identified in the chromatogram, possibly suggesting that layer 3 is a repaint.



VLR OM (above)

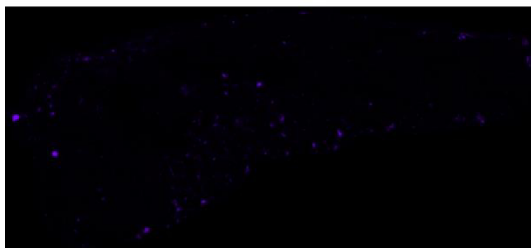


UVfOM (above)

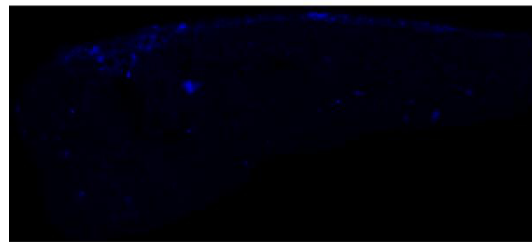


**BSE image** (left). The tabular crystalline structure typical of gypsum plaster can be seen in layers 0 and 1. The BSE image suggests that layer 1 was permeated by the utmost layer.

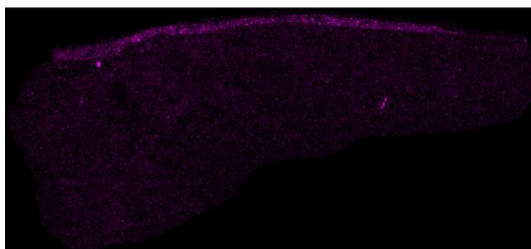
**EDS spectra and mapping** suggest that **calcium sulfate (CaSO<sub>4</sub>)** and **Al-Si inclusions** were detected in all the layers. Layer 2 is mostly made of **Si, Ti** and **Fe**. Additional traces of **K, Mg, Ba, Zn, Cl** and **P** were detected in all the layers.



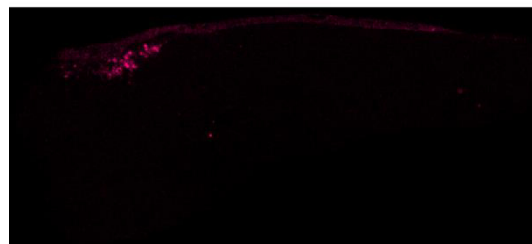
Aluminium (Al)



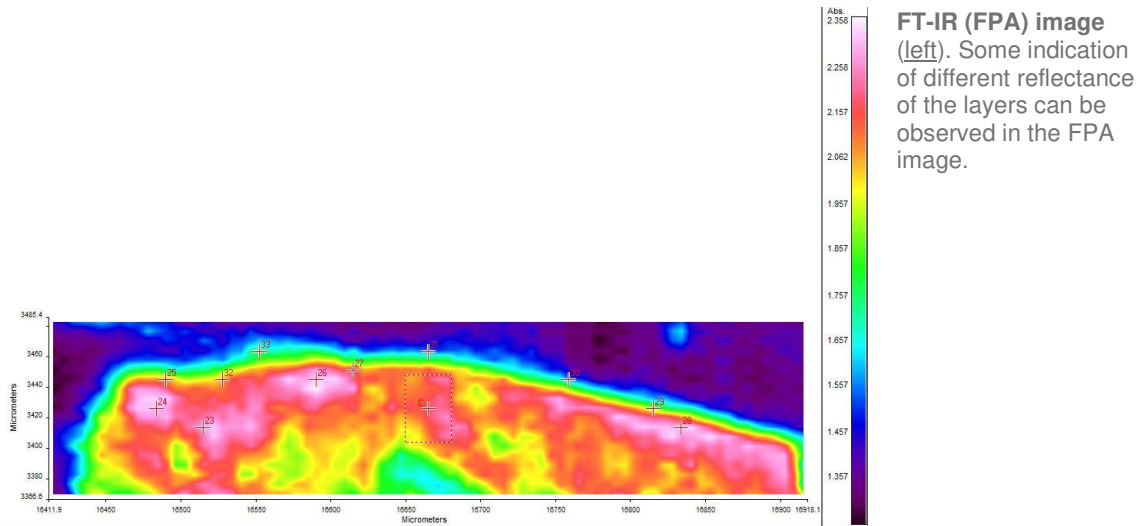
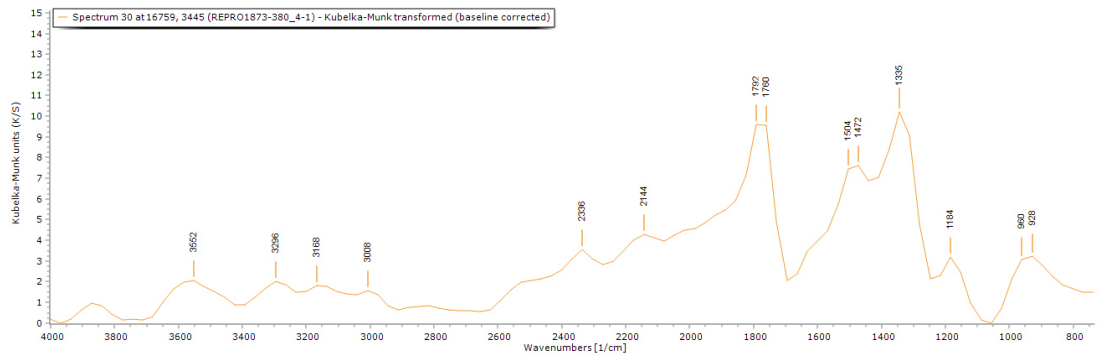
Silicon (Si)



Titanium (Ti)



Iron (Fe)



**FT-IR (FPA) image (left).** Some indication of different reflectance of the layers can be observed in the FPA image.

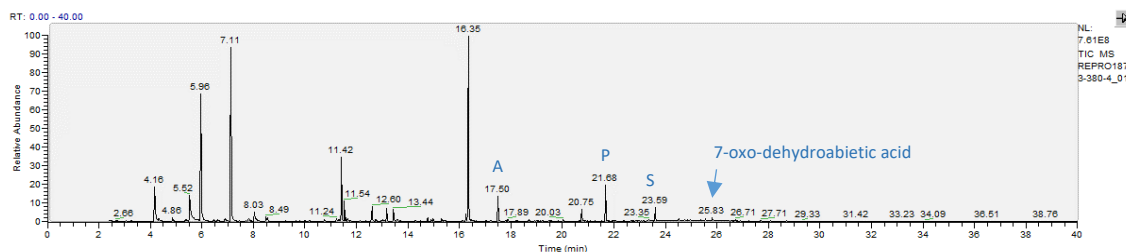
**Spectra 23-33** (see for example **spectrum 30** of layers 2-3 above) show a similar pattern with broad bands rather than sharp and defined peaks, which is expected for mixtures containing several components. Overall, no significant difference within the layers can be noticed by FT-IR analysis (see table below).

Spectrum	Layer	Material					
		Casting resin	Gypsum plaster	Calcite	Clay minerals	Organic material	Calcium oxalate
23	0	x		x	x	x	
24	1	x	x	x		x	
25	2-3	x		x		x	
26	2-3	x	x	x		x	
27	2-3	x		x		x	
28	2-3			x		x	
29	2-3	x		x	x	x	
30	2-3	x		x	x		
31	2-3	x		x	x		
32	2-3	x	x	x	x	x	
33	2-3			x		x	

The **casting resin** (Tiranti polyester resin) and **gypsum plaster** ( $\text{CaSO}_4 \cdot 0.5\text{H}_2\text{O}$ ) are present in all the layers, although the relevant peaks in the FT-IR spectra are not always clearly visible. **Calcite** (calcium carbonate,  $\text{CaCO}_3$ ) was identified in all the layers and **clay minerals** (Si-O containing minerals) were also identified in several spectra. A minor variation of the position of the peaks can be observed for several reasons, one of which is the local substitution of elements such as Mg in the gypsum and other minerals' structure (Melita et al., 2020). As reported in other publications (Manfredi et al., 2015; Miliani et al., 2012), the strong and broad band at  $2000\text{-}2500\text{ cm}^{-1}$  is due to the combination of bending and vibration modes of  $\text{H}_2\text{O}$  ( $\nu_1 + \nu_3$  and  $2\nu_3$ ) related to the presence of gypsum (centred at  $2200\text{ cm}^{-1}$ ) and other minerals. The presence of **organic material**, likely a **wax** or **resin** is suggested in most of the spectra; however, the crowded appearance of the spectra and the broadness of the peaks impede the unique assignment of such contributions. The several peaks that can be identified in the area over  $3000\text{ cm}^{-1}$  cannot be considered diagnostic, as the OH and NH stretches occur in this region and once again due to the complexity of the mixture, the water present in the crystals and the pores of the plaster, as well as in the organic components will add up in this area. **Calcium oxalate** might be also present, but it was not possible to uniquely assign its peaks (Toniolo et al., 2009).

Sample	Sample prep method	Thermal programme
REPRO.1873-380_4-01	Py-TMAH-GCMS 1 µl TMAH	(1)
REPRO.1873-380_4-02	GCMS 1 µl PFPA solution	(3)
REPRO.1873-380_4-03	GCMS 1 µl PFPA solution	(3)
REPRO.1873-380_4-04	GCMS 1 µl PFPA solution	(3)

The prep method used on **samples 4-02 to 4-04** (see table on the [left](#) and description in the *Experimental* section) did not provide meaningful results. However, the analysis of **sample 4-01** provided a good set of results (chromatogram and table [below](#)).



### py-TMAH-GC/MS chromatogram

([top](#) and described in the table on the [right](#)) shows small fragments due to derivatization (from  $t = 4.16$  to  $13.44$  min) and markers characteristic of a **pine resin** ( $t = 25.57$  and  $26.71$ ) (Colombini & Modugno, 2009; Mills & White, 2012). The peak at  $t = 16.25$  (**dimethyl phthalate**) is a marker for **alkyd paint**. The presence of **methyl azelate** (A,  $t = 17.50$ ), **methyl palmitate** (P,  $t = 21.68$ ) and **stearate** (S,  $t = 23.60$ ) might suggest that the resin or the alkyd paints have been mixed with an **oil** (A/P = 0.87, P/S = 2.60) (Colombini & Modugno, 2009).

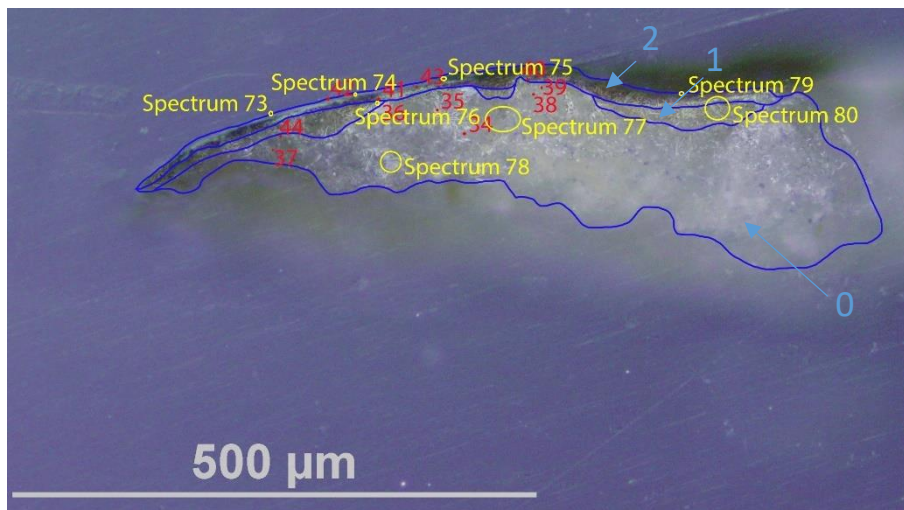
RT	m/z	Assignment	Formula
4.16	45(100), 58(3), 74(96)	Ethyl Ether	C4H10O
5.52	42(14), 58(100), 72(9), 116(8)	1,2-Ethanediamine, N'-ethyl-N,N-dimethyl-	C6H16N2
5.96	42(13), 58(100), 117(28)	1,2-Ethanediamine, N'-ethyl-N,N-dimethyl-	C6H16N2
7.11	42(4), 72(100), 116(1), 131(2)	Amine fragment	
11.42	42(9), 58(100), 70(21), 116(12)	1,2-Ethanediamine, N'-ethyl-N,N-dimethyl-	C6H16N2
11.54	45(25), 71(29), 75(100), 85(18), 128(16)	Amine fragment	
12.6	45(42), 71(59), 75(100), 85(22), 101(13), 114(12), 130(4)	Amine fragment	
13.18	71(13), 88(16), 98(25), 116(45), 130(100), 157(5), 189(5)	Amine fragment	
13.44	72(100), 130(6)	Amine fragment	
16.25	55(30), 69(62), 74(78), 83(43), 87(36), 111(21), 129(100), 138(82), 171(72), 188(5)	Dimethyl phthalate	C10H10O4
17.5	74(100), 83(60), 87(24), 111(86), 124(45), 143(26), 152(92), 185(47)	Monomethyl azelate	C10H18O4
20.75	75(6), 103(4), 119(5), 135(2), 162(5), 193(4), 221(100)	Phenol fragment	
21.68	74(100), 87(38), 143(12), 171(7), 199(6), 227(19), 239(6), 270(5)	Methyl palmitate	C17H34O2
23.6	74(100), 87(38), 129(7), 143(14), 199(12), 255(15), 298(8)	Methyl stearate	C19H38O2
24.54	44(100), 71(39), 115(25), 169(5), 191(5), 207(49), 237(18), 281(5), 305(5), 320(19), 341(5)	Terpenic resin fragment	
25.57	44(100), 69(68), 83(34), 109(38), 119(28), 137(41), 169(35), 201(66), 207(68), 239(31), 281(5), 299(5), 314(5), 327(5)	7-oxo-dehydroabiatic acid	
25.83	44(83), 71(100), 95(60), 109(34), 119(23), 137(34), 159(35), 201(51), 207(58), 239(5), 281(17), 327(5), 341(5), 355(5)	Terpenic resin fragment	
26.71	44(100), 79(22), 115(14), 165(13), 191(5), 207(68), 267(25), 281(21), 327(5), 342(19)	Dehydroabiatic acid fragment	

RT = retention time, m/z = mass/charge ratio

## Sample 5



**Sampling.** This sample was taken from an area of loss on the fold of the dress of the monk on the PR of the presbyter.



Left: Overlapped (OM and BSE) cross-section image showing the stratigraphy (blue indicators).

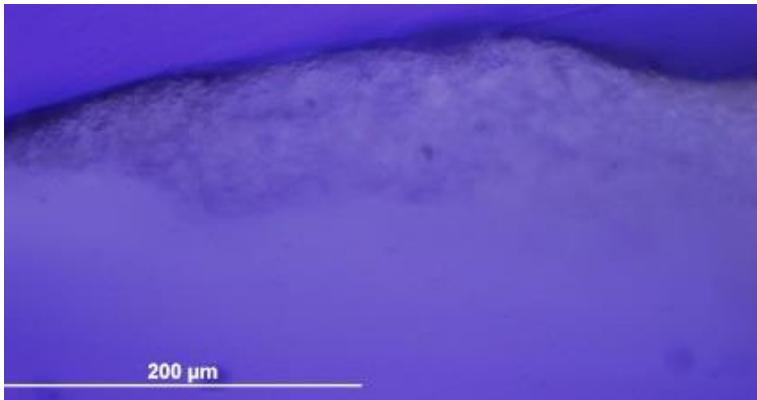
- 2. Dark layer
- 1. Yellowish and undefined layer
- 0. Plaster bulk

**Analysis spots.** EDS analysis (yellow): Spectra 73-80; FT-IR analysis (red): nos. 73-80.

**Summary.** The sample is mostly made of C, O, S and Ca (**calcium sulfate**,  $\text{CaSO}_4$ , confirmed by EDS and by FT-IR). **Al** is overall present as used as a polishing agent, but could also, together with **Si**, be present as part of **silicate** inclusions, which are present in all the layers (FT-IR confirmed the presence of **clay minerals**, such as kaolin). Spare **titanium** (Ti) inclusion can be also seen by EDS mapping. Traces of **Mg**, **Ti**, **Na**, **Fe** and **K** were also detected in the utmost layers. The mineral structure typical of gypsum plaster can be seen in layers 0 and 1. Layer 1 appears yellowish under the visible illumination and consists of the plaster substrate soaked with the outmost layer. Layer 2 appears dark under visible illumination. A **wax or resin** is suggested by FT-IR and detected in all the layers. py-TMAH-GC/MS shows markers characteristic of a **tree resin** and several **fatty acids**, but it was not clear whether the resin or have been mixed with an oil or the FA are naturally present in the resin (Colombini & Modugno, 2009).



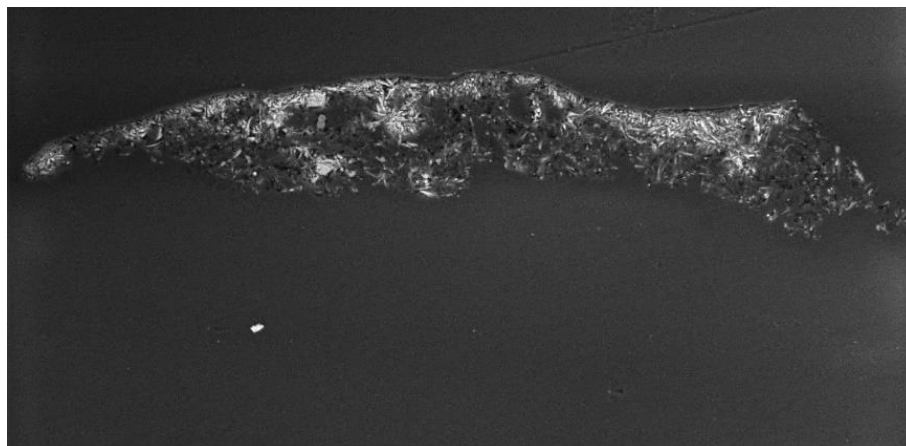
VLR OM (left)



UVfOM (left)

**BSE image (below).** The tabular crystalline structure typical of gypsum plaster can be seen in layers 0 and 1.

**EDS mapping (below)** shows the presence of **Al-containing inclusions** as well as **Ti** but does not suggest any particular element distribution in a layer fashion.



**EDS spectra** indicate that all the layers consist of **C, O, Ca, S, Al** and **Si**. Traces of **Mg, Ti, Na, Fe** and **K** were additionally detected in the surface layer.

SEM HV: 20.0 kV	WD: 15.00 mm	MIRA3 TESCAN
View field: 681 µm	SEM MAG: 524 x	200 µm
Det: BSE	Date(m/d/y): 06/14/18	Northumbria University - Newcastle



Aluminium (Al)

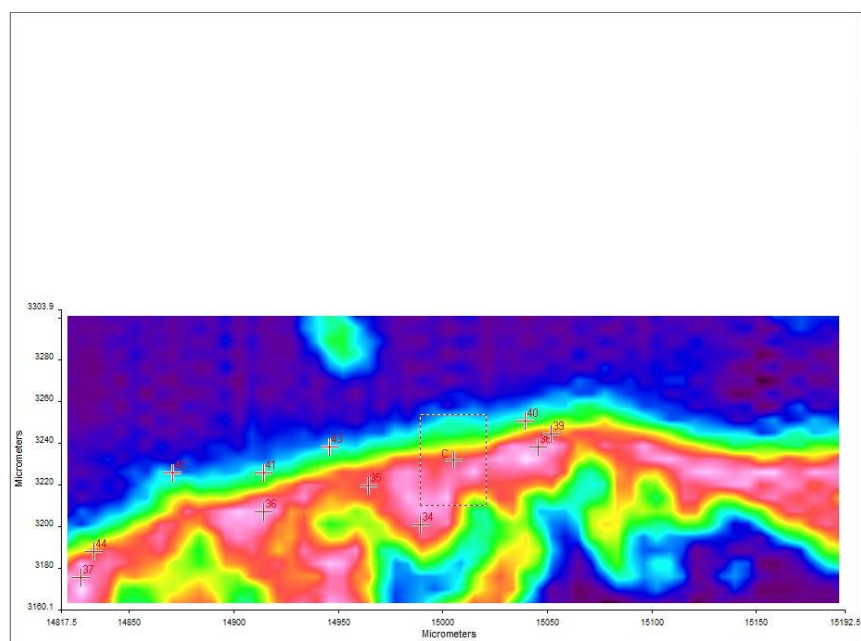
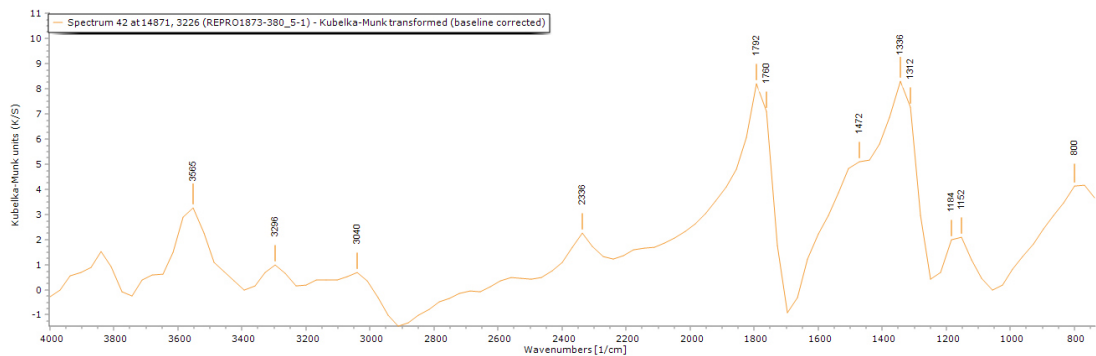


Titanium (Ti)

**Spectra 34-44** (see for example **spectrum 42** of layer 2 below) show a similar pattern with broad bands rather than sharp and defined peaks, which is expected for mixtures containing several components. Overall, no significant difference within the layers can be noticed by FT-IR analysis (see table below).

Spectrum	Layer	Material					
		Casting resin	Gypsum plaster	Calcite	Clay minerals	Organic material	Calcium oxalate
34	0	x	x			x	
35	0	x	x			x	
36	0	x	x			x	
37	0	x					
38	0	x	x		x	x	
39	0	x			x	x	
40	2	x	x		x		
41	2	x			x	x	
42	2	x			x		
43	2	x				x	
44	1	x	x			x	

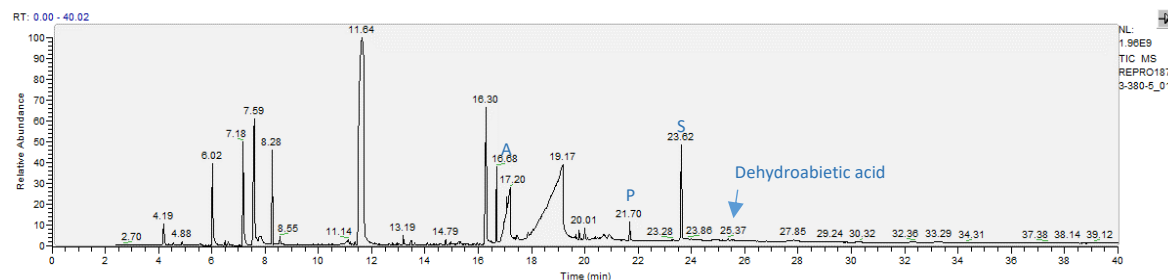
The **casting resin** and **gypsum plaster** ( $\text{CaSO}_4 \cdot 0.5\text{H}_2\text{O}$ ) are present in all the layers, although the relevant peaks in the FT-IR spectra are not always clearly visible. **Calcite** (calcium carbonate,  $\text{CaCO}_3$ ) was not identified by FT-IR and **clay minerals** (Si-O containing minerals) were identified in several spectra. A minor variation of the position of the peaks can be observed for several reasons, one of which is the local substitution of elements such as Mg in the gypsum and other minerals' structure (Melita et al., 2020). As reported in other publications (Manfredi et al., 2015; Miliiani et al., 2012), the strong and broad band at  $2000\text{--}2500\text{ cm}^{-1}$  is due to the combination of bending and vibration modes of  $\text{H}_2\text{O}$  ( $\nu_1 + \nu_3$  and  $2\nu_3$ ) related to the presence of gypsum (centred at  $2200\text{ cm}^{-1}$ ) and other minerals. The presence of **organic material**, likely a **wax** or **resin** is suggested in most of the spectra; however, the crowded appearance of the spectra and the broadness of the peaks impede the unique assignment of such contributions. The several peaks that can be identified in the area over  $3000\text{ cm}^{-1}$  cannot be considered diagnostic, as the OH and NH stretches occur in this region and once again due to the complexity of the mixture, the water present in the crystals and the pores of the plaster, as well as in the organic components will add up in this area. **Calcium oxalate** might be also present, but it was not possible to uniquely assign its peaks (Toniolo et al., 2009).



**FT-IR (FPA) image (left).** An indication of different reflectance of the layers can be observed in the FPA image.

Sample	Sample prep method	Thermal programme
REPRO.1873-380_5-01	Py-TMAH-GCMS	(1)
	1 µl Meth Prep II (1) solution, 1 µl TMAH	
REPRO.1873-380_5-02	Py-TMAH-GCMS	(1)
	2 µl Meth Prep II (2) solution, 1 µl TMAH	

The prep methods used on **samples 5-01** and **5-02** (see table [above](#) and described in the *Experimental* section) provided the same set of results. As an example, **sample 5-01** are shown in the chromatogram and the table [below](#).

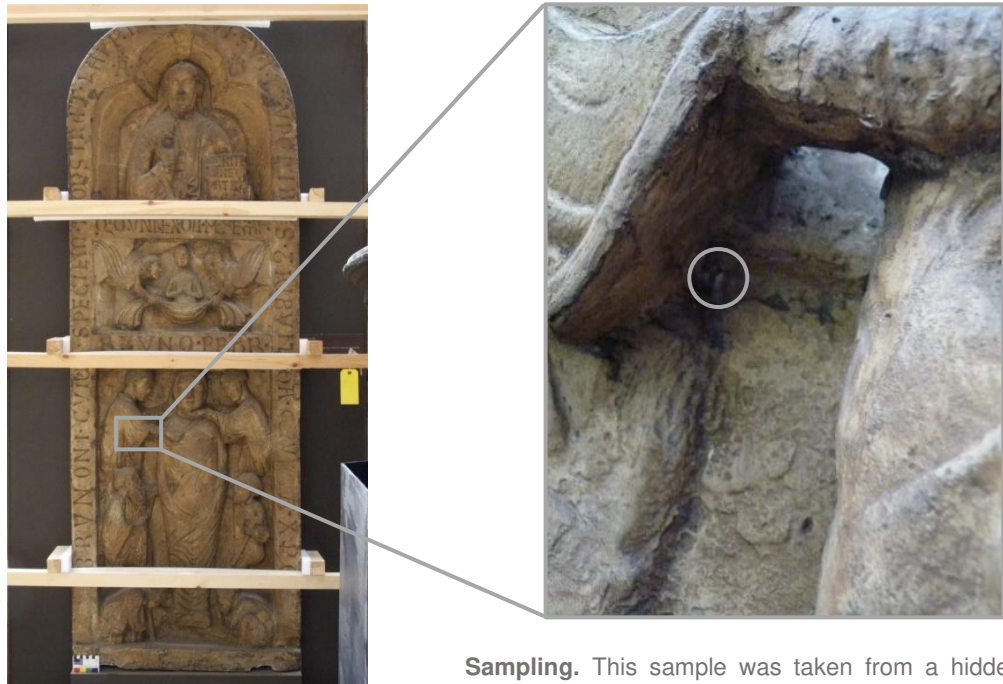


**py-TMAH-GC/MS chromatogram** ([top](#) and described in the table [below](#)) shows small fragments due to derivatization (from  $t = 4.16$  to  $13.19$  min) and a marker characteristic of a **tree resin** ( $t = 25.37$ ) (Colombini & Modugno, 2009; Mills & White, 2012). Between  $t = 16.30$  and  $t = 23.62$  several Fatty Acids (FA, see table [below](#)) were identified, but it was not clear whether the resin or have been mixed with an oil or the FA are naturally present in the resin (A/P = 3.02, P/S = 0.19) (Colombini & Modugno, 2009).

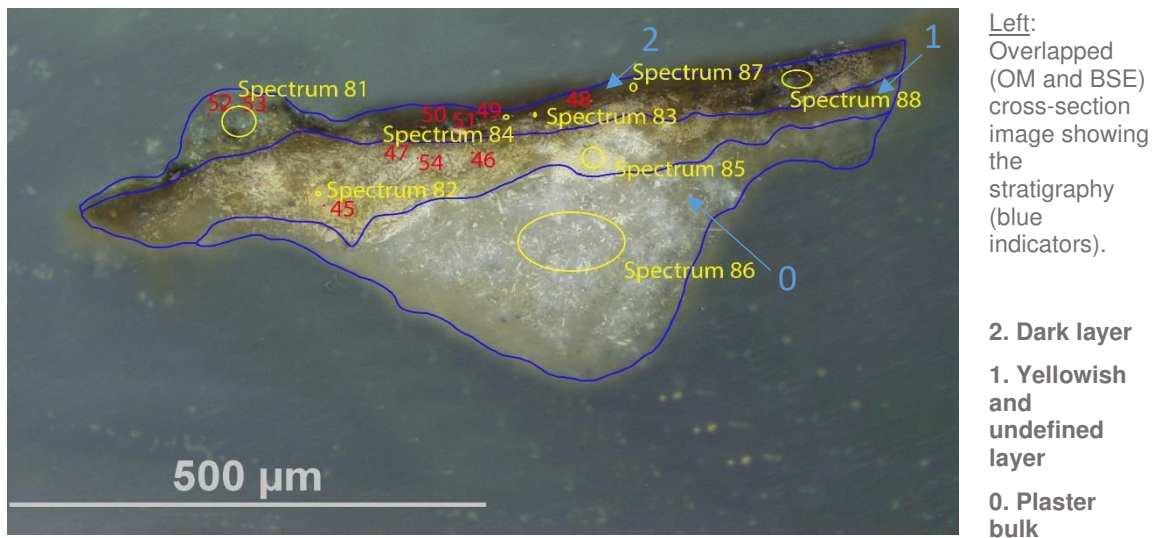
RT	m/z	Assignment	Formula
4.16	45(100), 59(7), 74(78)	Ethyl Ether	C <sub>4</sub> H <sub>10</sub> O
6.02	42(14), 58(100), 117(15)	1,2-Ethanediamine, N'-ethyl-N,N-	C <sub>6</sub> H <sub>16</sub> N <sub>2</sub>
7.11	42(5), 72(100), 116(1), 131(2)	Amine fragment	
7.59	75(5), 83(11), 96(6), 133(28), 145(20), 157(8), 176(100)	2,5-Dichlorophenylhydrazine hydrochloride	
8.28	75(5), 83(11), 113(18), 133(27), 145(19), 157(8), 176(100)	2,5-Dichlorophenylhydrazine hydrochloride	
11.64	127(5), 145(13), 172(10), 188(100)	Unidentified fragment, MetPrep related	
13.19	58(59), 74(17), 98(25), 116(33), 130(100), 170(5), 188(5)	Unidentified fragment, MetPrep related	
16.3	74(74), 83(43), 87(43), 97(58), 111(22), 129(100), 138(94), 171(58)	Myristic acid	C <sub>14</sub> H <sub>28</sub> O <sub>2</sub>
16.68	74(34), 83(47), 87(31), 97(37), 129(37), 152(36), 171(5), 185(5)	Azelaic acid, monomethyl ester	C <sub>10</sub> H <sub>18</sub> O <sub>4</sub>
17.2	74(100), 87(31), 97(35), 138(85), 157(25), 171(5), 213(5)	Pentadecanoic acid	C <sub>15</sub> H <sub>30</sub> O <sub>2</sub>
19.17	73(71), 82(26), 97(78), 138(100), 157(5)	FA fragment	
21.7	74(100), 87(38), 143(12), 171(7), 199(6), 227(19), 239(6), 270(5)	Methyl palmitate	C <sub>17</sub> H <sub>34</sub> O <sub>2</sub>
23.62	74(100), 87(38), 129(7), 143(14), 199(12), 255(15), 298(8)	Methyl stearate	C <sub>19</sub> H <sub>38</sub> O <sub>2</sub>
25.37	44(100), 69(68), 83(34), 109(38), 119(28), 137(41), 169(35), 201(66), 207(68), 239(31), 281(5), 299(5), 313(5)	Dehydroabiatic acid	

RT = retention time, m/z = mass/charge ratio

## Sample 6

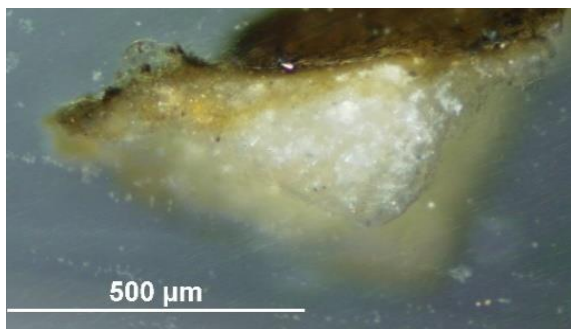


**Sampling.** This sample was taken from a hidden area underneath the arm of the monk on the PR of the presbyter.

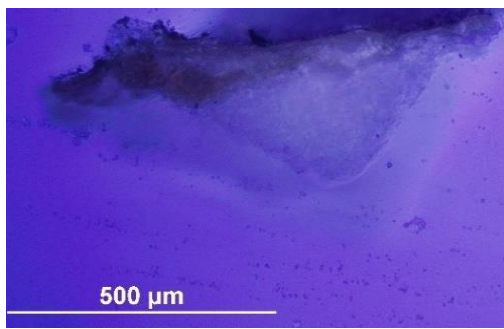


**Analysis spots.** EDS analysis (yellow): Spectra 81-88; FT-IR analysis (red): nos. 45-54.

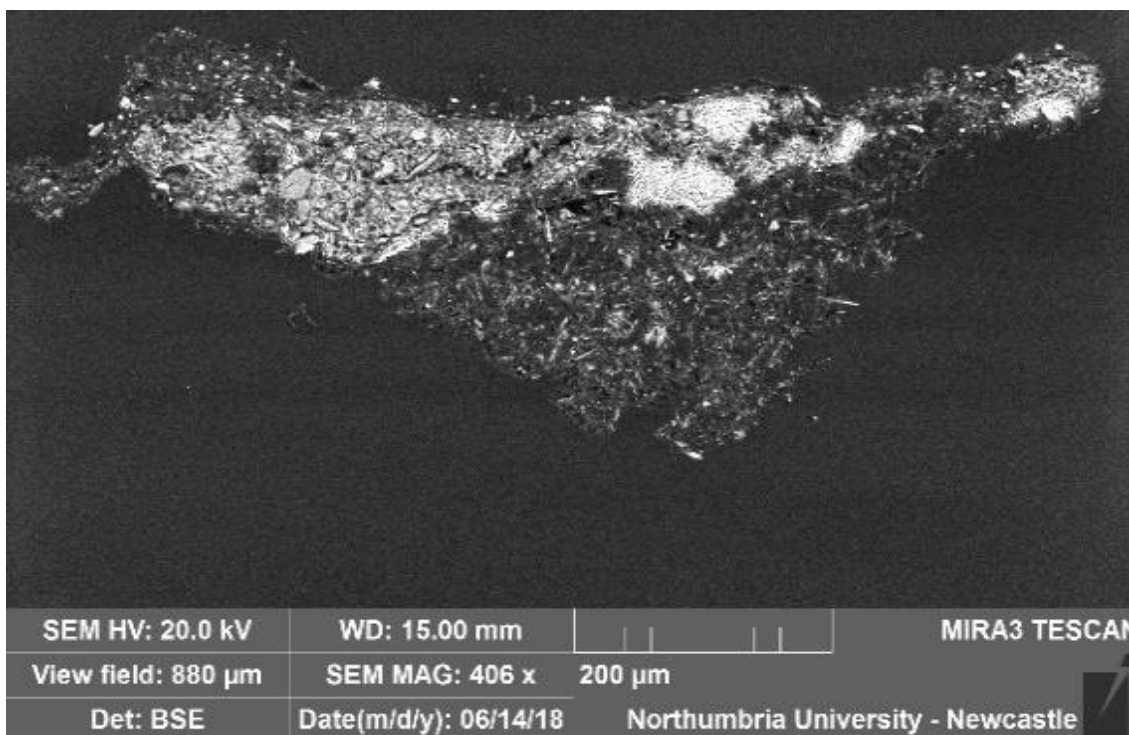
**Summary.** The sample is mostly made of C, O, S and Ca (**calcium sulfate**,  $\text{CaSO}_4$ , confirmed by EDS). **Al** is overall present as used as a polishing agent, but could also, together with **Si**, be present as part of **silicate** inclusions, which are present in all the layers (FT-IR confirmed the presence of **clay minerals**, such as kaolin). Spare **titanium** (Ti) inclusion can be also seen by EDS mapping. **Potassium** (K) and **Iron** (Fe) were also detected in all the layers, but **K**, **Fe**, **Si** and **Al** are the main components of layers 1 and 2. Additionally, **Na**, **Fe**, **Pb** and **Cl** were also detected in the utmost layers. The mineral structure typical of gypsum plaster can be seen in layers 0 and 1. Layer 1 appears yellowish under visible illumination and consists of the plaster substrate soaked with the outmost layer. Layer 2 appears dark under visible illumination. A **wax or resin** is suggested by FT-IR and detected in all the layers.



VLR OM (above)

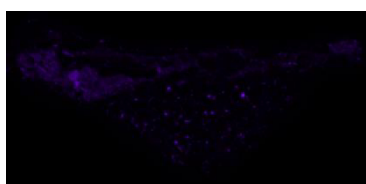


UVfOM (above)

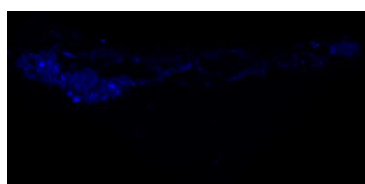


BSE image (above). The tabular crystalline structure typical of gypsum plaster can be seen in layers 0 and 1.

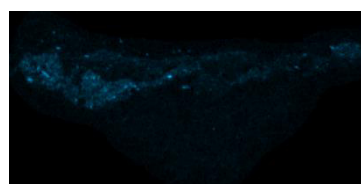
Calcium sulfate ( $\text{CaSO}_4$ ), Al-Si inclusions and traces of Na, Mg and K were detected in all the layers. Additionally, Fe, Pb and Cl were detected in the utmost layers.



Aluminium (Al)



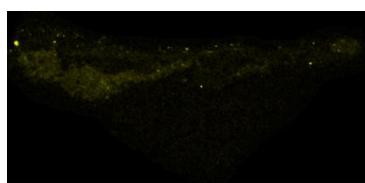
Silicon (Si)



Potassium (K)

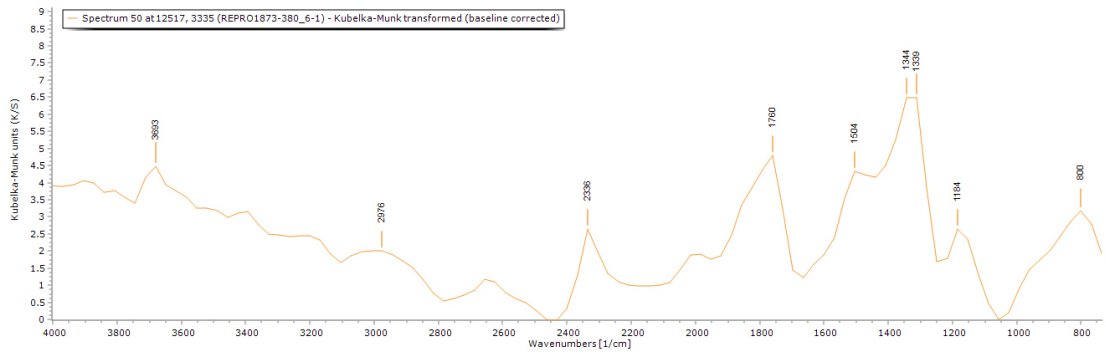


Titanium (Ti)

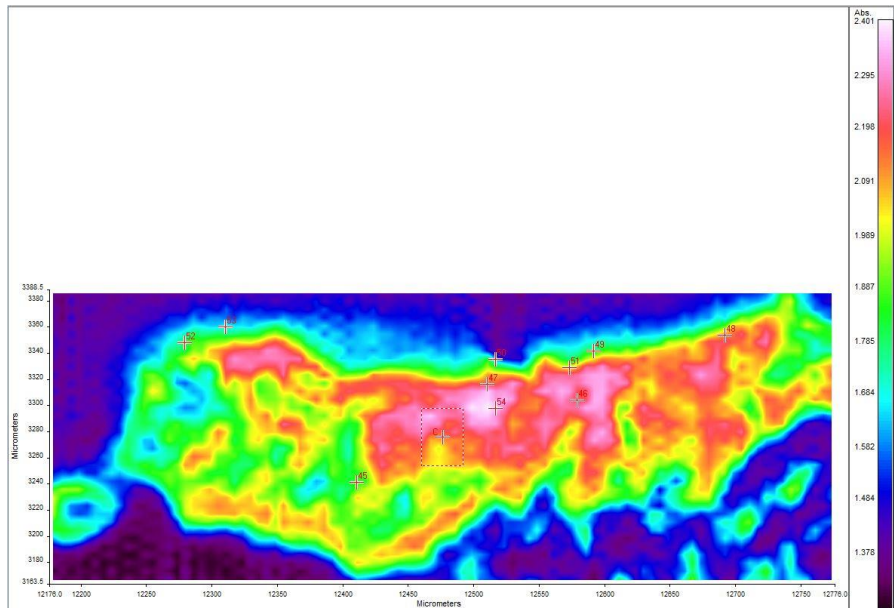


Iron (Fe)

EDS mapping shows that layer 1 is mostly made of Al, Si, K and Fe. Al, K and Fe are also present in layers 0 and 2. Ti inclusions were also observed.



**FT-IR (FPA) image (right).** The different reflectance of the layers can be observed in the FPA image.



**Spectra 45-54** (see for example **spectrum 50** of layer 2 above) show a similar pattern with broad bands rather than sharp and defined peaks, which is expected for mixtures containing several components. Overall, no significant difference within the layers can be noticed by FT-IR analysis (see table below).

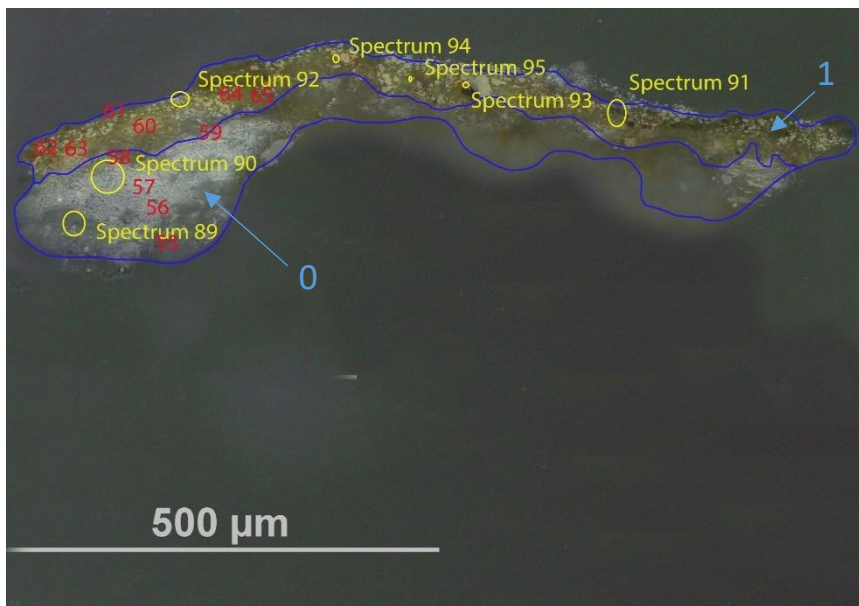
Spectrum	Layer	Material					
		Casting resin	Gypsum plaster	Calcite	Clay minerals	Organic material	Calcium oxalate
45	1	x	x		x		
46	1	x	x	x		x	
47	1	x				x	
48	2	x				x	
49	2	x				x	
50	2	x				x	
51	2	x			x	x	
52	2	x	x		x	x	
53	2	x			x	x	
54	1	x	x	x	x	x	

The **casting resin** (Tiranti polyester resin) and **gypsum plaster** ( $\text{CaSO}_4 \cdot 0.5\text{H}_2\text{O}$ ) are present in all the layers, although the relevant peaks in the FT-IR spectra are not always clearly visible. **Calcite** (calcium carbonate,  $\text{CaCO}_3$ ) and **clay minerals** (Si-O containing minerals) were identified in several spectra. A minor variation of the position of the peaks can be observed for several reasons, one of which is the local substitution of elements such as Mg in the gypsum and other minerals' structure (Melita et al., 2020). As reported in other publications (Manfredi et al., 2015; Miliani et al., 2012), the strong and broad band at  $2000\text{-}2500\text{ cm}^{-1}$  is due to the combination of bending and vibration modes of  $\text{H}_2\text{O}$  ( $\nu_1 + \nu_3$  and  $2\nu_3$ ) related to the presence of gypsum (centred at  $2200\text{ cm}^{-1}$ ) and other minerals. The presence of **organic material**, likely a **wax** or **resin** is suggested in most of the spectra; however, the crowded appearance of the spectra and the broadness of the peaks impede the unique assignment of such contributions. The several peaks that can be identified in the area over  $3000\text{ cm}^{-1}$  cannot be considered diagnostic, as the OH and NH stretches occur in this region and once again due to the complexity of the mixture, the water present in the crystals and the pores of the plaster, as well as in the organic components will add up in this area. **Calcium oxalate** might be also present, but it was not possible to uniquely assign its peaks (Toniolo et al., 2009).

## Sample 7



**Sampling.** This sample was taken from an area of loss on an area of repair next to the monk on the PR of the presbyter.



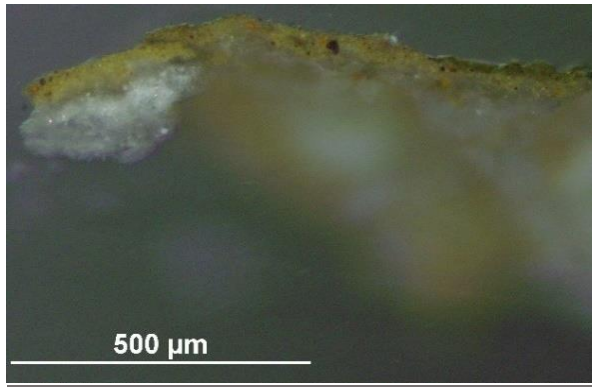
Left: Overlapped (OM and BSE) cross-section image showing the stratigraphy (blue indicators).

**1. Yellowish and undefined layer with large orange and black particles**

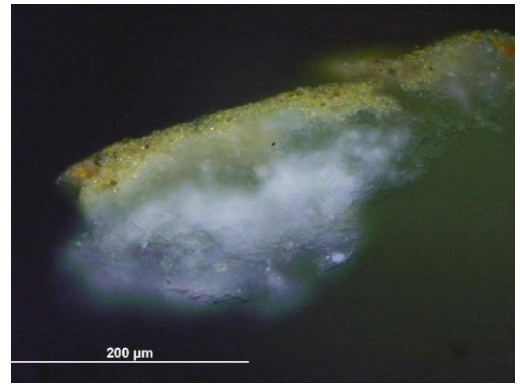
**0. Plaster bulk**

**Analysis spots.** EDS analysis (yellow): Spectra 89-95; FT-IR analysis (red): nos. 55-65.

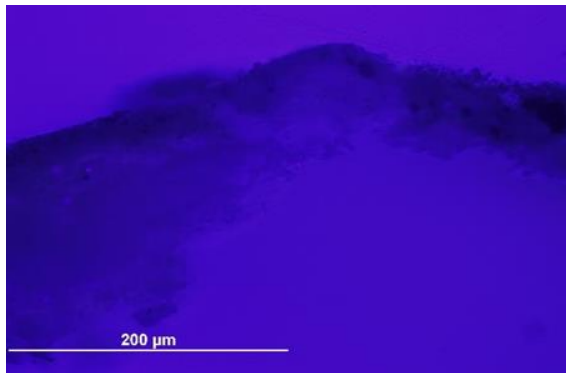
**Summary.** The sample is mostly made of C, O, S and Ca (**calcium sulfate**,  $\text{CaSO}_4$ , confirmed by EDS). **Al** is overall present as used as a polishing agent, but could also, together with **Si**, be present as part of **silicate** inclusions, which are present in all the layers (FT-IR confirmed the presence of **clay minerals**, such as kaolin). The mineral structure typical of gypsum plaster can be seen in layer 0. Layer 1 appears yellow under visible illumination and orange and black inclusions can also be seen. EDS mapping suggests that this layer is mostly made of **barium** and **iron**. Mg, K and Cl were also detected in both the layers. A **wax or resin** is suggested by FT-IR and detected in all the layers.



VLR OM (above)

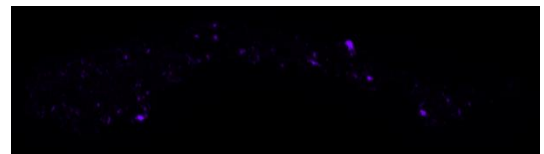


VLR OM, detail (above)



UVfOM, detail (above)

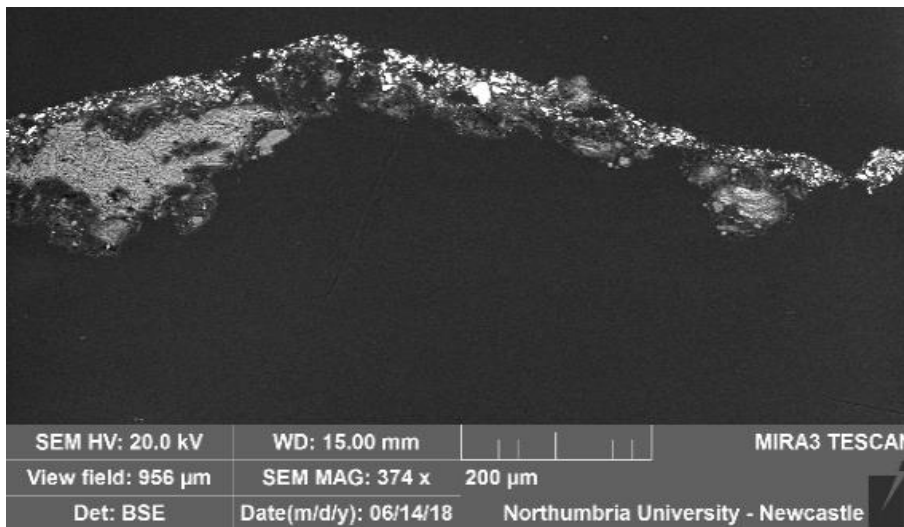
Aluminium (Al)



Silicon (Si)



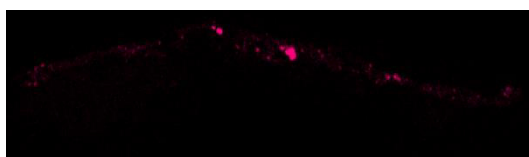
**BSE image** (below). The tabular crystalline structure typical of gypsum plaster can be seen in layer 0 and heavier elements inclusions can be seen in layer 2.



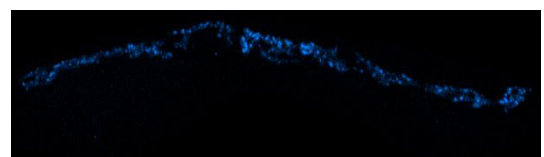
**Layers 0 and 1** consists of **calcium sulfate (CaSO<sub>4</sub>)**. **Silicon (Si)** and **Aluminium (Al)** inclusions are present in all the layers (see **EDS mapping** above). Mg, K and Cl were also detected.

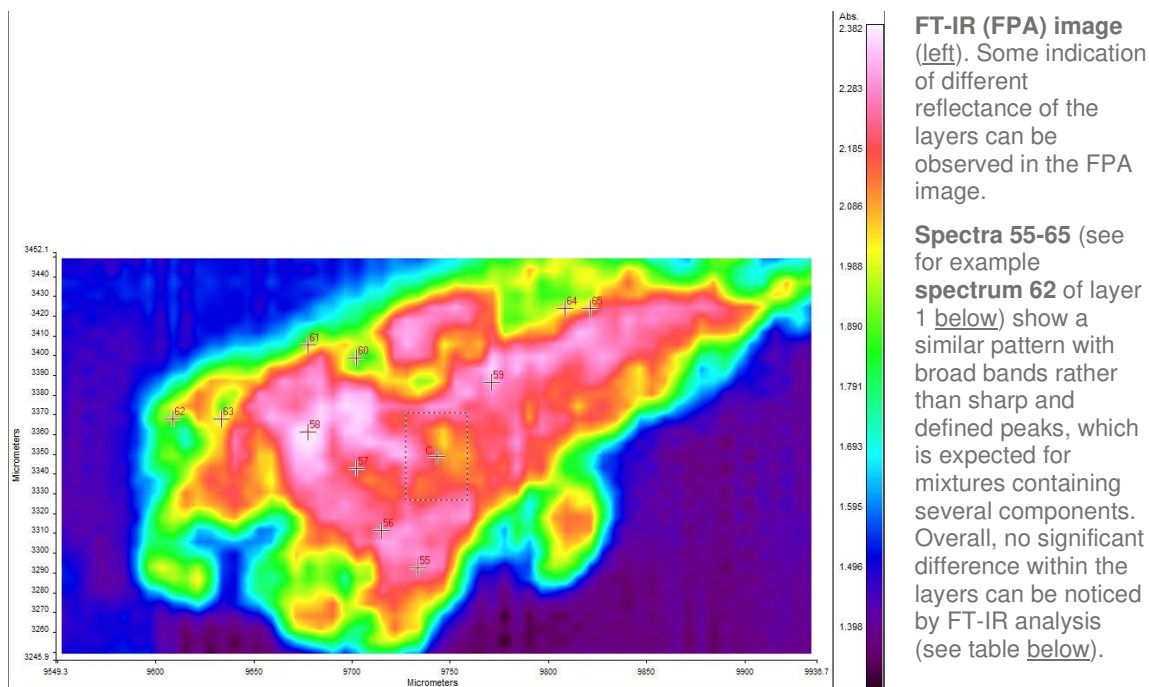
**Layer 1** is made of **Fe** and **Ba** (see **EDS mapping** below).

Iron (Fe)



Barium (Ba)



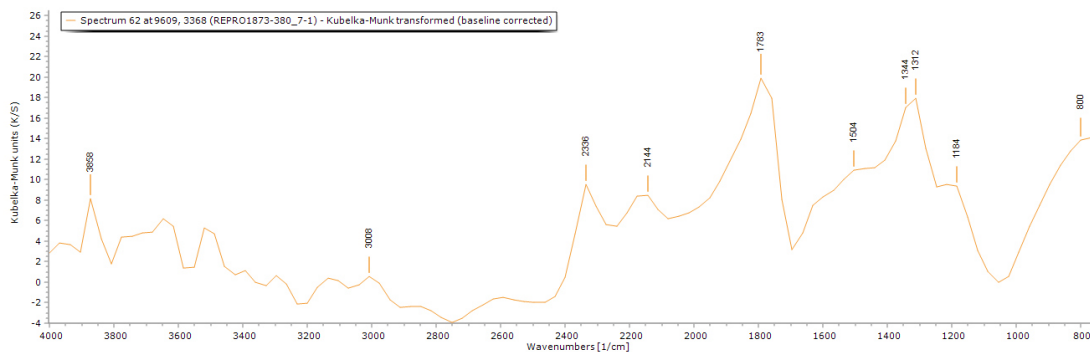


**FT-IR (FPA) image (left).** Some indication of different reflectance of the layers can be observed in the FPA image.

**Spectra 55-65** (see for example **spectrum 62** of layer 1 below) show a similar pattern with broad bands rather than sharp and defined peaks, which is expected for mixtures containing several components. Overall, no significant difference within the layers can be noticed by FT-IR analysis (see table below).

Spectrum	Layer	Material					
		Casting resin	Gypsum plaster	Calcite	Clay minerals	Organic material	Calcium oxalate
55	0	x	x	x		x	
56	0	x	x		x	x	
57	0	x	x				
58	0	x	x	x			
59	0	x		x		x	
60	1	x	x	x			
61	1	x		x		x	
62	1	x		x			
63	1	x		x			
64	1	x		x	x	x	
65	1	x		x			

The **casting resin** (Tiranti polyester resin), **gypsum plaster** ( $\text{CaSO}_4 \cdot 0.5\text{H}_2\text{O}$ ) and **calcite** (calcium carbonate,  $\text{CaCO}_3$ ) are present in all the layers, although the relevant peaks in the FT-IR spectra are not always clearly visible. **Clay minerals** (Si-O containing minerals) were identified in several spectra. A minor variation of the position of the peaks can be observed for several reasons, one of which is the local substitution of elements such as Mg in the gypsum and other minerals' structure (Kumar & Rajkumar, 2014; Melita et al., 2020). As reported in other publications (Manfredi et al., 2015; Miliani et al., 2012), the strong and broad band at  $2000\text{--}2500\text{ cm}^{-1}$  is due to the combination of bending and vibration modes of  $\text{H}_2\text{O}$  ( $\nu_1 + \nu_3$  and  $2\nu_3$ ) related to the presence of gypsum (centred at  $2200\text{ cm}^{-1}$ ) and other minerals. The presence of **organic material**, likely a **wax** or **resin** is suggested in most of the spectra; however, the crowded appearance of the spectra and the broadness of the peaks impede the unique assignment of such contributions. The several peaks that can be identified in the area over  $3000\text{ cm}^{-1}$  cannot be considered diagnostic, as the OH and NH stretches occur in this region and once again due to the complexity of the mixture, the water present in the crystals and the pores of the plaster, as well as in the organic components will add up in this area.



## Sample 8



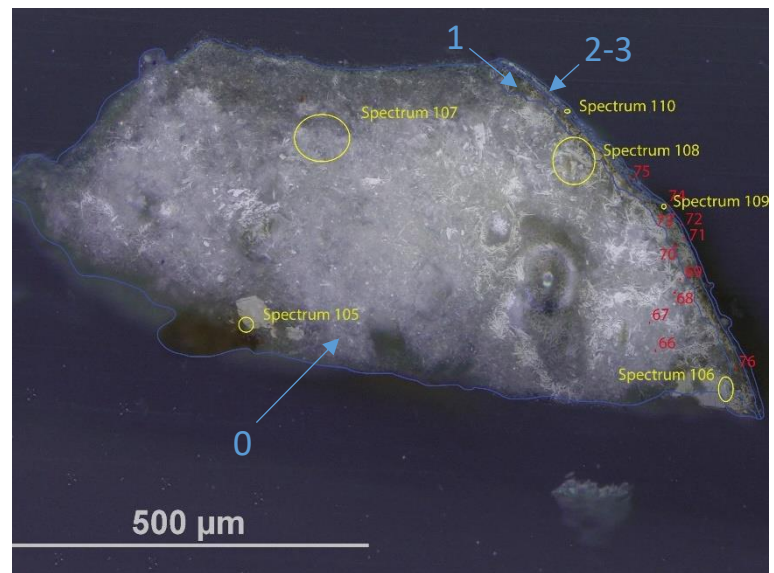
**Sampling.** This sample was taken from an area of loss on the wing of the PR angel.

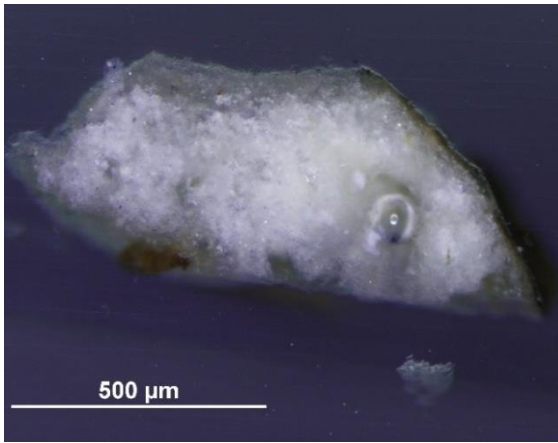
Below: Overlapped (OM and BSE) cross-section image showing the stratigraphy (blue indicators).

3. Varnish
2. Dark layer
1. Yellowish and undefined layer
0. Plaster bulk

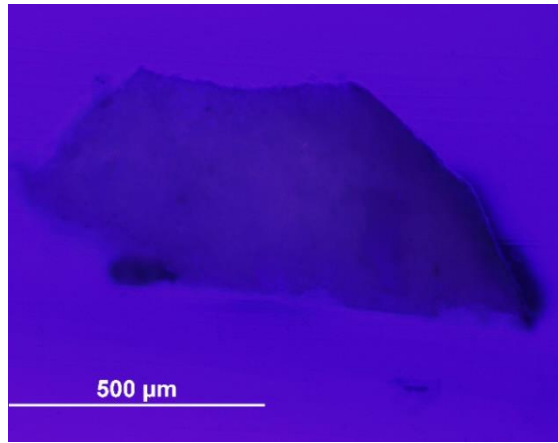
**Summary.** The sample is mostly made of C, O, S and Ca (**calcium sulfate**,  $\text{CaSO}_4$ , confirmed by EDS). **Al** is overall present as used as a polishing agent, but could also, together with **Si**, be present as part of **silicate** inclusions, which are present in all the layers (FT-IR confirmed the presence of **clay minerals**, such as kaolin). **Chlorine (Cl)** is also present in all the layers. The utmost layers are mostly made of Si and Al, and K, Fe and Na were also detected. The mineral structure typical of gypsum plaster can be seen in layers 0 and 1. Layer 1 appears yellowish under visible illumination and consists of the plaster substrate soaked with the outmost layer. Layer 2 appears dark under visible illumination and layer 3 fluoresces white under UV illumination. A **wax or resin** is suggested by FT-IR and detected in all the layers. py-TMAH-GC/MS shows markers characteristic of a **triterpene resin** and several **fatty acids**, but it was not clear whether the resin or have been mixed with an oil or the FA are naturally present in the resin (Colombini & Modugno, 2009).

**Analysis spots.** EDS analysis (yellow): Spectra 105-110; FT-IR analysis (red): nos. 45-54.

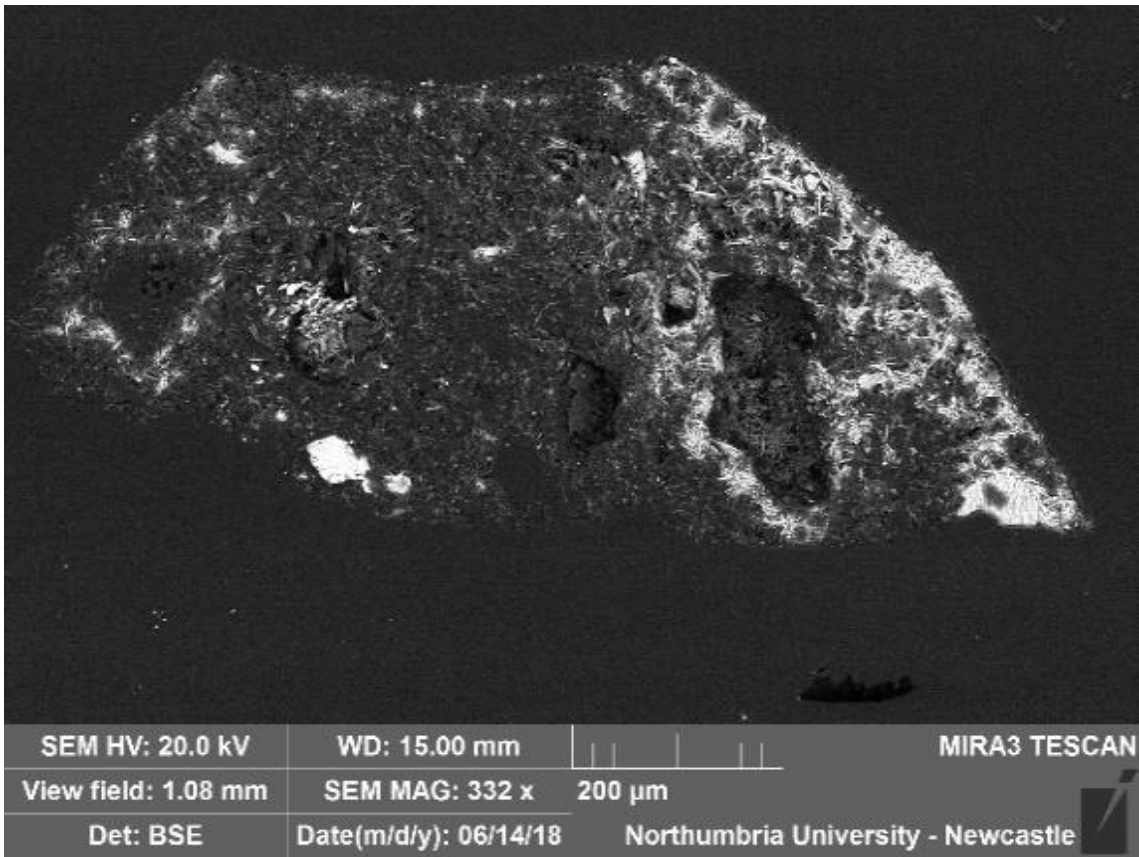




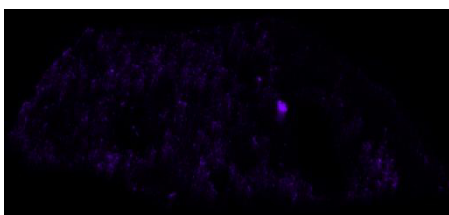
VLR OM (above)



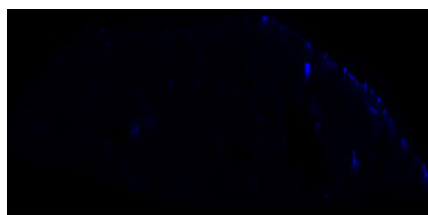
UVf OM (above)



**BSE image** (above). The tabular crystalline structure typical of gypsum plaster can be seen in layers 0 and 1. **Calcium sulfate (CaSO<sub>4</sub>)** was detected in all the layers. Additionally, K, Fe and Na were detected in the utmost layers.



Aluminium (Al)



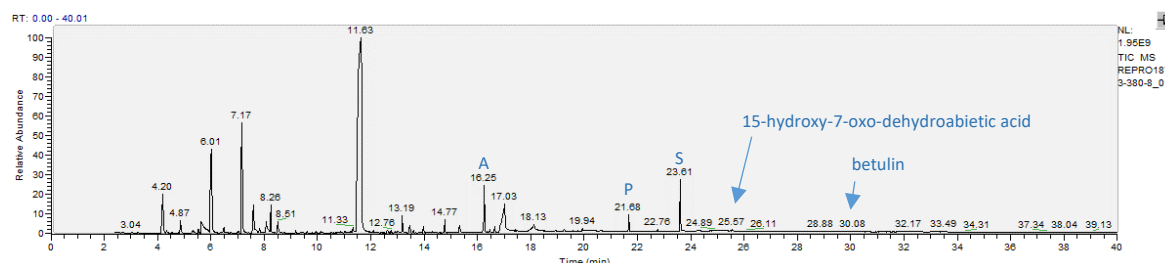
Silicon (Si)

**EDS mapping** shows that the utmost layers are mostly made of **Al** and **Si**, which are also present in the bulk, together with **Cl**.



Sample	Sample prep method	Thermal programme
REPRO.1873-380_8-01	Py-TMAH-GCMS 1 µl Meth Prep II (1) solution, 1 µl TMAH	(1)
REPRO.1873-380_8-02	Py-TMAH-GCMS 2 µl Meth Prep II (2) solution, 1 µl TMAH	(1)

The prep methods used on **samples 8-01** and **8-02** (see table [above](#) and described in the *Experimental* section) provided the same set of results. As an example, **sample 8-01** are shown in the chromatogram and the table [below](#).



**py-TMAH-GC/MS chromatogram** ([top](#) and described in the table [below](#)) shows small fragments due to derivatization (from  $t = 4.16$  to  $13.19$  min) and a marker characteristic of a **triterpene resin** ( $t = 25.37$ ,  $25.57$ ,  $30.08$ ,  $33.13$  and  $33.49$ ) (Colombini & Modugno, 2009; Mills & White, 2012). Between  $t = 16.25$  and  $t = 23.61$  several Fatty Acids (FA, see table [below](#)) were identified, but it was not clear whether the resin or have been mixed with an oil or the FA are naturally present in the resin (A/P = 0.41, P/S = 0.32) (Colombini & Modugno, 2009).

RT	m/z	Assignment	Formula
4.16	45(100), 59(4), 74(78)	Ethyl Ether	C4H10O
4.87	43(9), 59(100), 75(4), 88(6)	Dimethylacetylcarbinol	C5H10O2
6.01	42(14), 58(100), 117(13)	1,2-Ethanediamine, N'-ethyl-N,N-dimethyl-	C6H16N2
7.17	44(6), 56(5), 72(100), 131(3)	Amine fragment	
7.6	58(4), 83(10), 113(18), 133(26), 145(19), 157(8), 176(100)	2,5-Dichlorophenylhydrazine hydrochloride	
8.26	42(12), 58(100), 83(7), 113(12), 133(18), 145(13), 176(67)	2,5-Dichlorophenylhydrazine hydrochloride	
11.63	58(8), 127(5), 173(6), 188(100)	Unidentified fragment, MetPrep related	
13.19	71(9), 87(3), 98(20), 116(31), 130(100), 170(2), 189(2)	Unidentified amine fragment	
14.77	58(7), 84(7), 116(100), 128(8), 138(4), 173(6)	Unidentified amine fragment	
16.25	55(40), 74(83), 83(47), 87(38), 97(49), 111(23), 129(100), 138(93), 171(70)	Myristic acid	C14H28O2
16.65	74(34), 83(47), 87(31), 97(37), 129(37), 152(36), 171(5), 185(5)	Azelaic acid, monomethyl ester	C10H18O4
17.03	55(40), 69(68), 74(83), 83(47), 87(38), 97(49), 111(23), 129(100), 138(93), 171(70)	Methyl undecenate	C12H22O2
18.13	73(62), 97(60), 138(100), 157(5)	FA fragment	
19.94	73(54), 87(100), 97(48), 138(87), 157(5), 184(5)	FA fragment	
21.68	55(24), 69(29), 74(100), 87(63), 97(16), 138(23), 227(16)	Methyl palmitate	C17H34O2
23.61	69(21), 74(100), 87(64), 97(11), 129(12), 143(18), 199(10), 255(16), 299(8)	Methyl stearate	C19H38O2
25.57	44(31), 69(60), 79(100), 87(31), 129(29), 138(53), 171(18), 239(82), 281(5), 299(5), 313(5), 341(5)	15-hydroxy-7-oxo-dehydroabiatic acid	
30.08	79(100), 121(29), 138(39), 163(5), 189(27), 205(23), 442(5)	betulin	
33.13	79(74), 121(21), 138(30), 163(100), 189(19), 205(23), 427(5), 442(5)	betulin-like fragment	
33.49	79(80), 121(30), 138(32), 163(5), 189(5), 205(5), 442(5)	betulin-like fragment	

RT = retention time, m/z = mass/charge ratio

## Sample 9



**Sampling.** This sample was taken from the hidden area below the PL arm of the resurrected Christ.

Below: Overlapped (OM and BSE) cross-section image showing the stratigraphy (blue indicators).

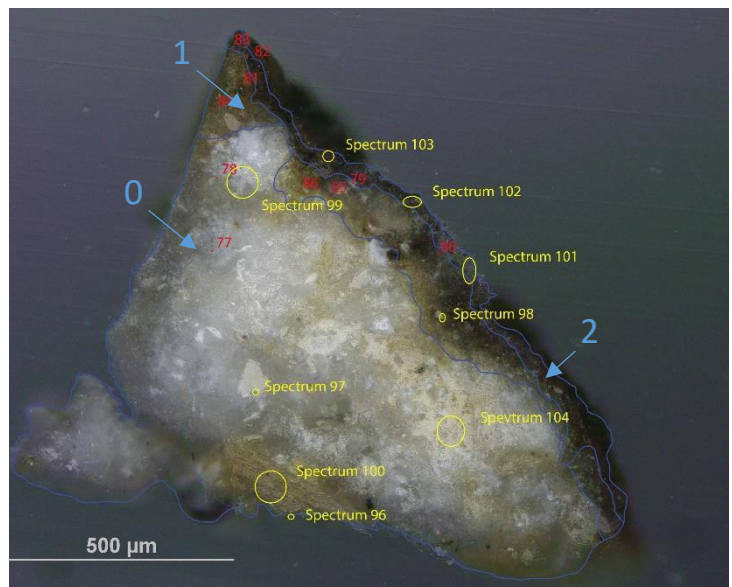
**Summary.** The sample is mostly made of C, O, S and Ca (**calcium sulfate**,  $\text{CaSO}_4$ , confirmed by EDS). **Al** is overall present as used as a polishing agent, but could also, together with **Si**, **Sr** and **Fe** be present as part of **silicate** inclusions, which are present in all the layers (FT-IR confirmed the presence of **clay minerals**, such as kaolin). **Magnesium (Mg)** is also present in all the layers. Additionally, traces of K and Ti were also detected. The mineral structure typical of gypsum plaster can be seen in layers 0 and 1. Layer 1 appears yellowish under visible illumination and consists of the plaster substrate soaked with the outmost layer. Layer 2 appears dark under visible illumination. A **wax or resin** is suggested by FT-IR and detected in all the layers. py-TMAH-GC/MS shows markers characteristic of a **triterpene resin** and several **fatty acids**, but it was not clear whether the resin or have been mixed with an oil or the FA are naturally present in the resin (Colombini & Modugno, 2009).

### 2. Dark layer

#### 1. Yellowish and undefined layer

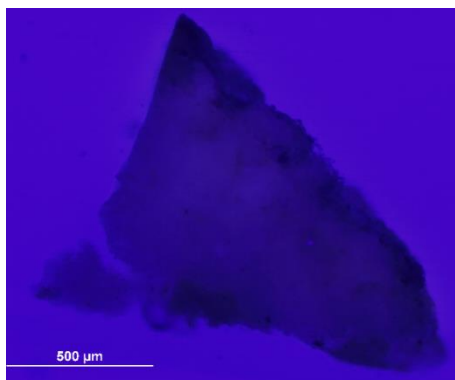
#### 0. Plaster bulk

**Analysis spots.** EDS analysis (yellow): Spectra 96-104; FT-IR analysis (red): nos. 77-86.

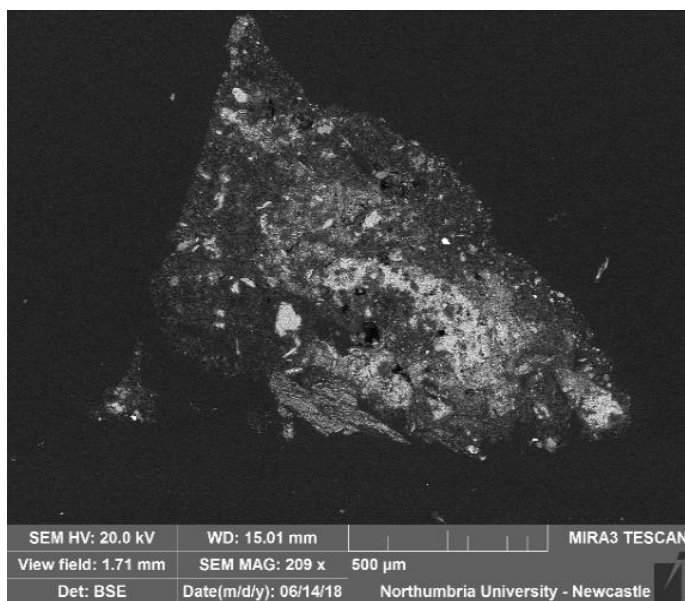




VLR OM (above)

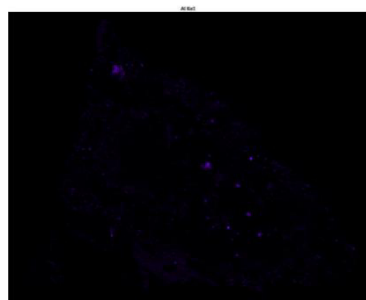


UVf OM (above)

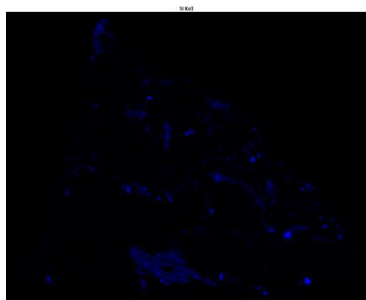


**BSE image (left).** The tabular crystalline structure typical of gypsum plaster can be seen in layers 0 and 1. Large mineral inclusions can also be seen.

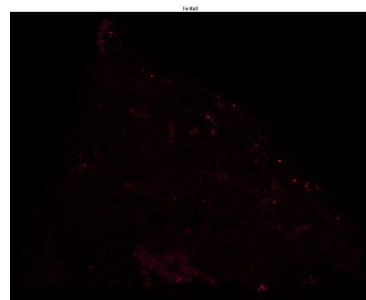
**Calcium sulfate (CaSO<sub>4</sub>)** was detected in all the layers. Additionally, K, Fe, Mg and Ti were also detected.



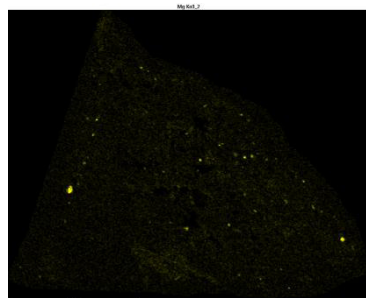
Aluminium (Al)



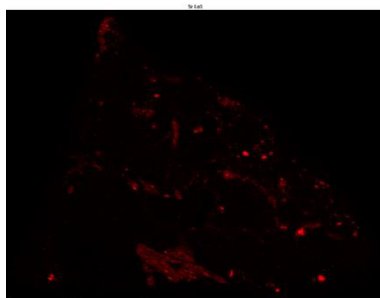
Silicon (Si)



Iron (Fe)

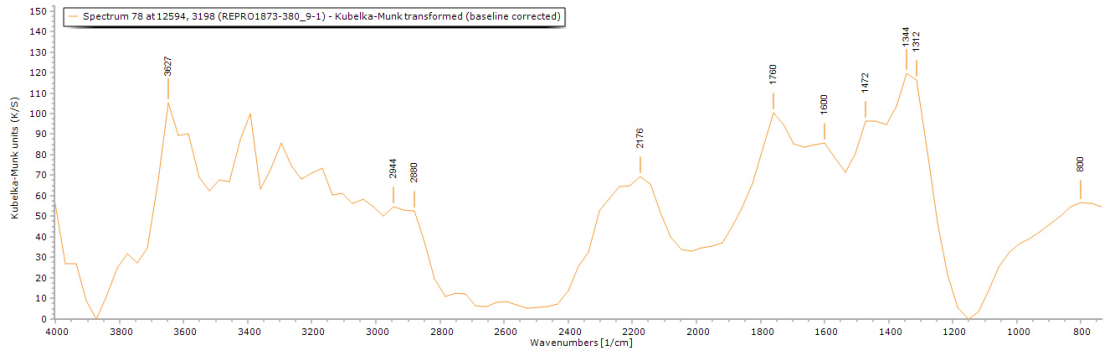


Magnesium (Mg)



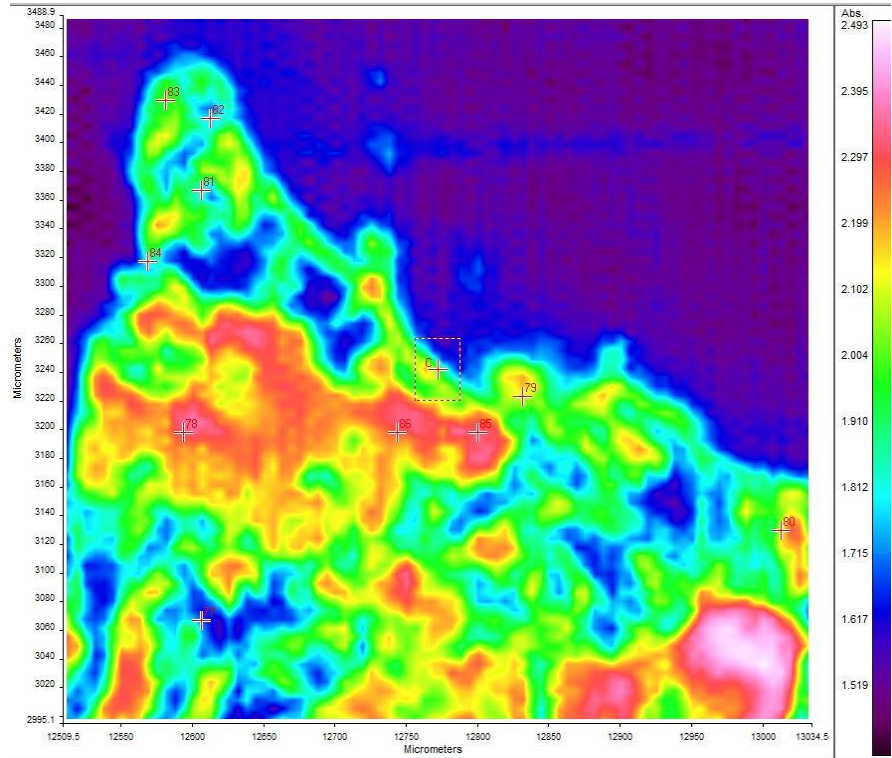
Strontium (Sr)

**EDS mapping** does not show any difference in a layer fashion but highlights that the large mineral inclusions are made of **Al, Si, Fe** and **Sr**. Mg inclusions are also present.



**FT-IR (FPA) image (right).** No clear indication of different reflectance of the layers can be observed in the FPA image.

**Spectra 77-86** (see for example **spectrum 78** of layer 0 above) show a similar pattern with broad bands rather than sharp and defined peaks, which is expected for mixtures containing several components. Overall, no significant difference within the layers can be noticed by FT-IR analysis (see table below).

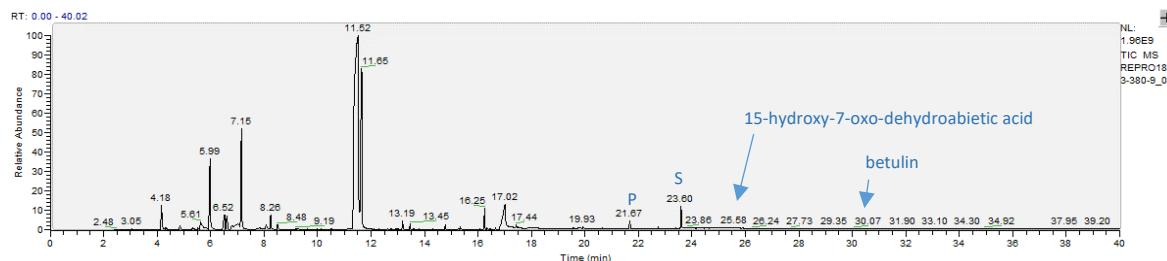


Spectrum	Layer	Material					
		Casting resin	Gypsum plaster	Calcite	Clay minerals	Organic material	Calcium oxalate
77	0	x					
78	0	x	x			x	
79	1	x				x	
80	1	x	x			x	
81	1	x				x	
82	1	x			x		
83	2	x			x	x	
84	2	x				x	
85	1	x				x	
86	1	x	x	x	x	x	

The **casting resin** (Tiranti polyester resin), **gypsum plaster** ( $\text{CaSO}_4 \cdot 0.5\text{H}_2\text{O}$ ) and organic material (likely a **resin** or a **wax**) are present in most of the layers, although the relevant peaks in the FT-IR spectra are not always clearly visible. **Calcite** (calcium carbonate,  $\text{CaCO}_3$ ) and **clay minerals** (Si-O containing minerals) are also suggested by some of the spectra. A minor variation of the position of the peaks can be observed for several reasons, one of which is the local substitution of elements such as Mg in the gypsum and other minerals' structure (Kumar & Rajkumar, 2014; Melita et al., 2020). The crowded appearance of the spectra and the broadness of the peaks impede the unique assignment of the materials in the sample.

Sample	Sample prep method	Thermal programme
REPRO.1873-380_9-01	Py-TMAH-GCMS 1 µl Meth Prep II (1) solution, 1 µl TMAH	(1)
REPRO.1873-380_9-02	Py-TMAH-GCMS 2 µl Meth Prep II (2) solution, 1 µl TMAH	(1)

The prep methods used on **samples 9-01** and **9-02** (see table [above](#) and described in the *Experimental* section) provided the same set of results. As an example, **sample 9-01** are shown in the chromatogram and the table [below](#).



**py-TMAH-GC/MS chromatogram** ([top](#) and described in the table [below](#)) shows small fragments due to derivatization (from  $t = 4.18$  to  $13.19$  min) and a marker characteristic of a **triterpene resin** ( $t = 25.36$ ,  $25.57$  and  $30.07$ ) (Colombini & Modugno, 2009; Mills & White, 2012). Between  $t = 16.25$  and  $t = 23.61$  several Fatty Acids (FA, see table [below](#)) were identified, but it was not clear whether the resin or have been mixed with an oil or the FA are naturally present in the resin (A/P = 0.15, P/S = 0.34) (Colombini & Modugno, 2009).

RT	m/z	Assignment	Formula
4.18	45(100), 74(78)	Ethyl Ether	C4H10O
5.61	42(10), 58(100)	1,2-Ethanediamine, N'-ethyl-N,N-dimethyl-	C6H16N2
5.99	42(13), 58(100), 117(15)	1,2-Ethanediamine, N'-ethyl-N,N-dimethyl-	C6H16N2
6.52	45(16), 66(24), 79(20), 95(100), 126(4)	Sulfuric acid, dimethyl ester	C2H6O4S
7.15	72(100)	Amine fragment	
8.26	58(13), 83(10), 113(18), 127(12), 133(26), 145(19), 157(8), 176(100)	2,5-Dichlorophenylhydrazine hydrochloride	
11.52	127(5), 173(6), 188(100)	Unidentified fragment, MetPrep related	
13.19	71(9), 88(15), 98(29), 116(30), 130(100)	Unidentified amine fragment	
13.45	72(100), 130(9)	Unidentified amine fragment	
16.25	55(38), 69(66), 74(83), 87(36), 97(46), 111(23), 129(100), 138(91), 171(69)	Myristic acid	
16.66	74(34), 83(47), 87(31), 97(37), 129(37), 152(36), 171(5), 185(5)	Azelaic acid, monomethyl ester	C10H18O4
17.02	69(49), 74(100), 87(29), 110(18), 129(19), 138(85), 157(26)	Methyl undecenate	C10H18O4
21.67	74(100), 87(60), 97(8), 129(11), 138(10), 143(14), 171(7), 185(7), 227(15), 239(6)	Methyl palmitate	C17H34O2
23.6	74(100), 87(64), 129(10), 143(18), 199(10), 255(17), 299(8)	Methyl stearate	C19H38O2
25.36	44(35), 69(62), 79(100), 87(39), 129(32), 138(55), 171(19), 281(5), 327(5), 341(5), 401(5), 429(5)	Triterpene resin fragment	
25.57	44(35), 69(54), 79(100), 87(31), 129(28), 138(52), 239(78), 281(5), 299(5), 313(5), 341(5)	15-hydroxy-7-oxo-dehydroabiatic acid	
30.07	79(100), 129(28), 138(52), 163(5), 189(27), 205(23), 442(5)	betulin	

RT = retention time, m/z = mass/charge ratio

## Sample 10



**Sampling.** This sample was taken from the hidden area below the PL of the brim of the cloth held by the angels.

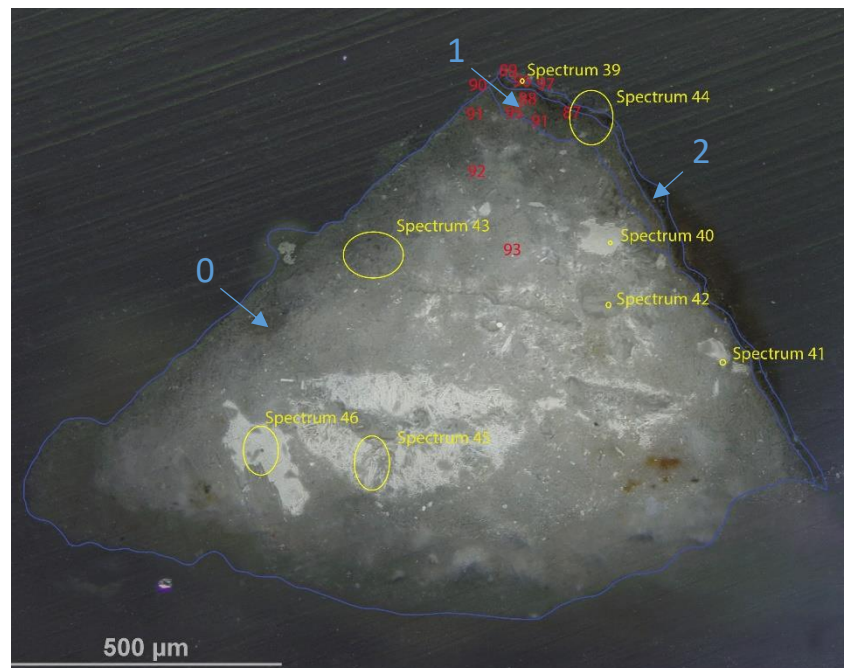
Right: Overlapped (OM and BSE) cross-section image showing the stratigraphy (blue indicators).

**2. Dark layer**

**1. Yellowish and undefined layer**

**0. Plaster bulk**

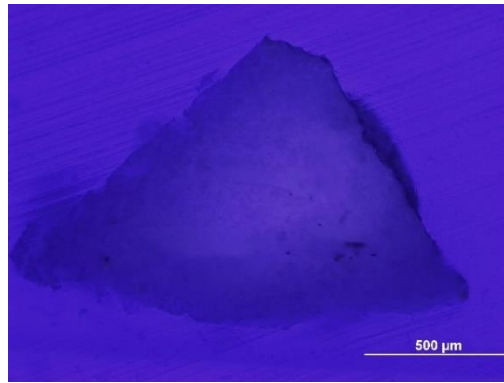
**Analysis spots.** EDS analysis (yellow): Spectra 39-46; FT-IR analysis (red): nos. 87-97.



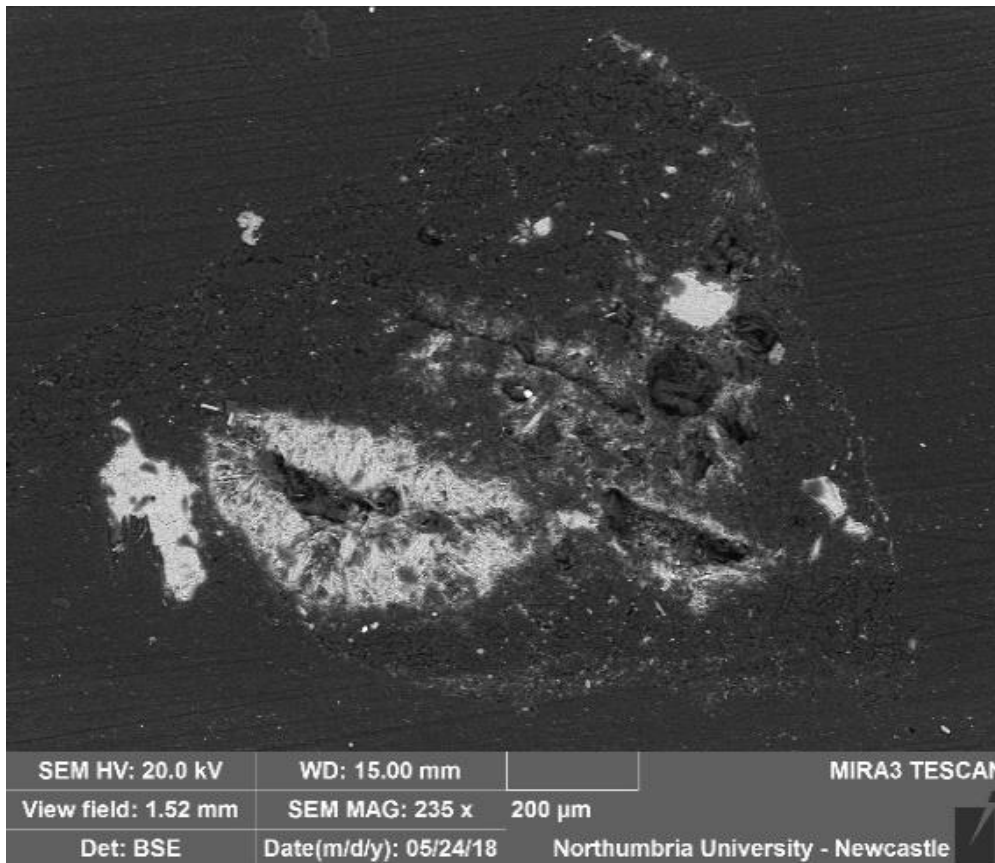
**Summary.** The sample is mostly made of C, O, S and Ca (**calcium sulfate**,  $\text{CaSO}_4$ , confirmed by EDS). **Al** is overall present as used as a polishing agent, but could also, together with **Si**, be present as part of **silicate** inclusions, which are present in all the layers (FT-IR confirmed the presence of **clay minerals**, such as kaolin). **Magnesium (Mg)** is also present in all the layers. Additionally, traces of K and Cl were also detected. Large mineral inclusions can be observed in the BSE image. The casting resin appears to have been absorbed evenly by the plaster sample. Layer 2 appears dark under visible illumination and is mostly made of **Si** and **Al**. A **wax or resin** is suggested by FT-IR and detected in all the layers.



VLR OM (above)



UVf OM (above)



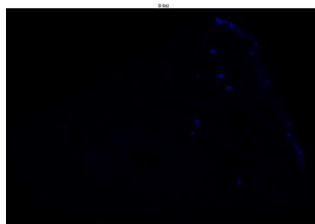
**BSE image (left).** Large mineral inclusions can be observed in the sample. The casting resin appears to have been absorbed evenly by the plaster sample.

**Calcium sulfate (CaSO<sub>4</sub>)** was detected in all the layers. Additionally, **Si, Al, K** and **Cl** were also detected in the utmost layer.

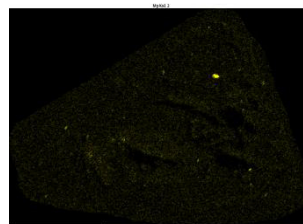
**EDS mapping** shows that layer 2 is mostly made of **Si**. **Si-Al inclusions** are present in all the layers. Mg inclusions are also present.



Aluminium (Al)



Silicon (Si)

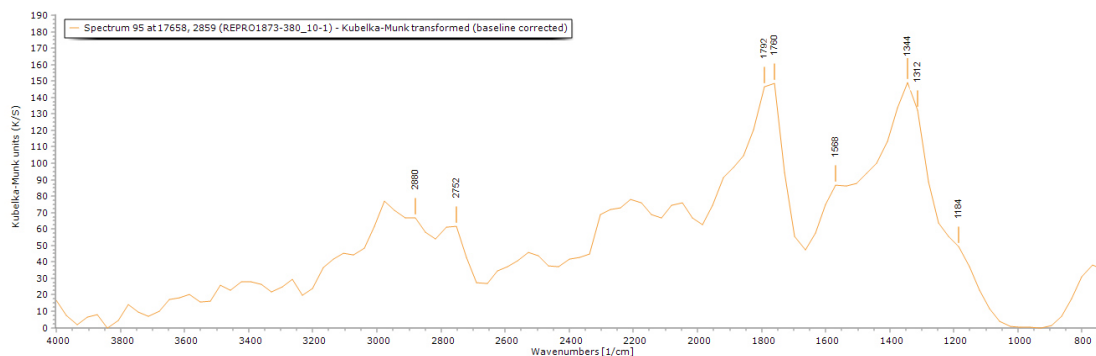
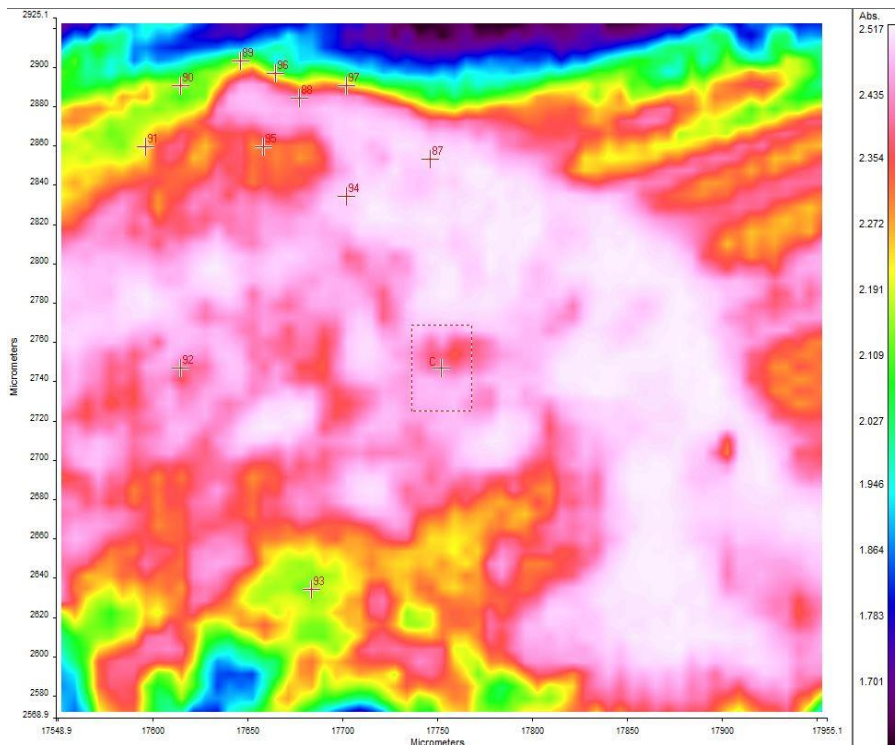


Magnesium (Mg)

Spectrum	Layer	Material					
		Casting resin	Gypsum plaster	Calcite	Clay minerals	Organic material	Calcium oxalate
87	1	x					
88	1	x	x			x	
89	2	x				x	
90	0	x				x	
91	0	x				x	
92	0	x	x			x	
93	0	x				x	
94	0	x	x			x	
95	1	x				x	
96	2	x				x	
97	2	x				x	

**FT-IR (FPA) image (right).** No clear indication of different reflectance of the layers can be observed in the FPA image.

**Spectra 87-97** (see for example **spectrum 95** of layer 1 below) show a similar pattern with broad bands rather than sharp and defined peaks, which is expected for mixtures containing several components. Overall, no significant difference within the layers can be noticed by FT-IR analysis (see table above).



The **casting resin** (Tiranti polyester resin) and an **organic material** (likely a **resin** or a **wax**) are present in all the layers. **Gypsum plaster** ( $\text{CaSO}_4 \cdot 0.5\text{H}_2\text{O}$ ), **calcite** (calcium carbonate,  $\text{CaCO}_3$ ) and **clay minerals** (Si-O containing minerals) are suggested by EDS analysis and likely contributes to the FT-IR spectra, although their relevant peaks are not visible. The crowded appearance of the spectra and the broadness of the peaks impede the unique assignment of the materials in the sample.

The prep methods used on **samples 10-01** and **10-02** (see table below and description in the *Experimental* section) and **GC/MS analysis** did not provide meaningful data.

<i>Sample</i>	<i>Sample prep method</i>	<i>Thermal programme</i>
REPRO.1873-380_10-01	GCMS 1 µl PFFA solution	(3)
REPRO.1873-380_10-02	GCMS 1 µl PFFA solution	(3)

## Sample 11



**Sampling.** This sample was taken from an area of loss on the PL outer arc of the top section of the tombstone.

Right: Overlapped (OM and BSE) cross-section image showing the stratigraphy (blue indicators).

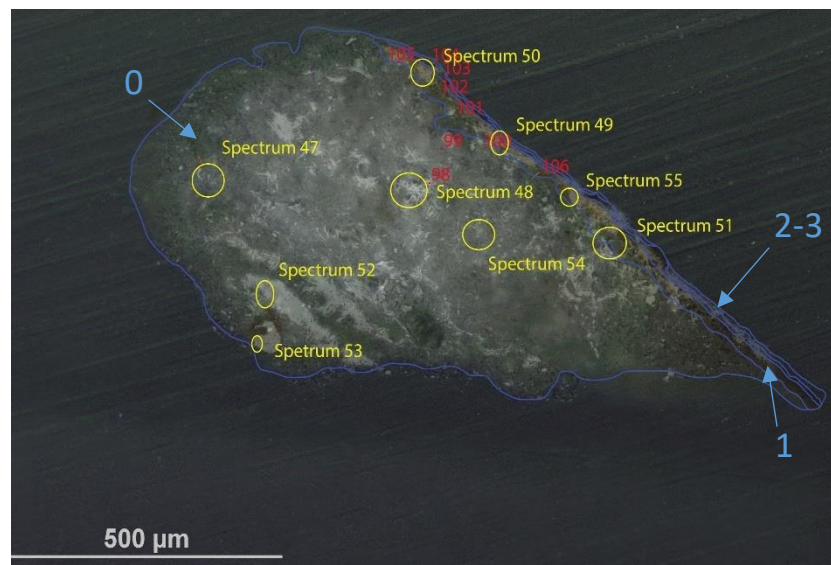
### 3. Varnish

### 2. Dark layer

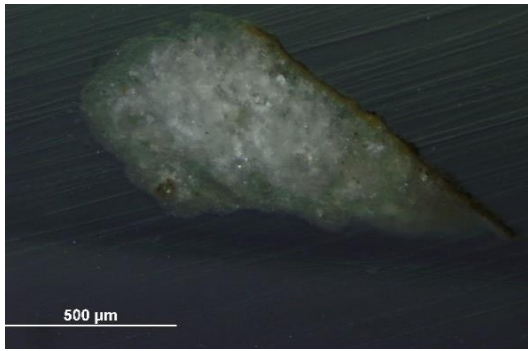
### 1. Yellowish and undefined layer

### 0. Plaster bulk

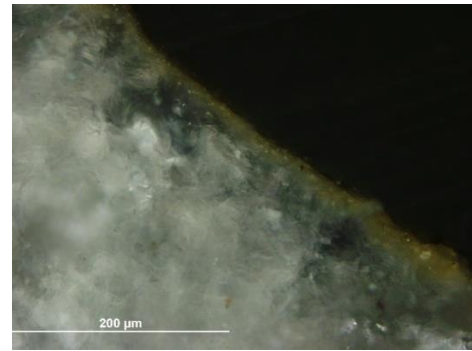
**Analysis spots.** EDS analysis (yellow): Spectra 47-55; FT-IR analysis (red): nos. 98-106.



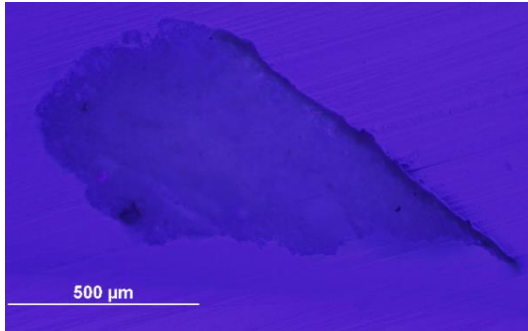
**Summary.** The sample is mostly made of C, O, S and Ca (**calcium sulfate**,  $\text{CaSO}_4$ , confirmed by EDS). **Al** is overall present as used as a polishing agent, but could also, together with **Si** and **K**, be present as part of **silicate** inclusions, which are present in all the layers (FT-IR confirmed the presence of **clay minerals**, such as kaolin). Additionally, traces of **Fe** and **Mg** were also detected. Large mineral inclusions can be observed in the BSE image. The casting resin appears to have been absorbed evenly by the plaster sample. Layer 2 appears dark under visible illumination and is mostly made of **Si** and **Al**. Layer 3 fluoresces milky-white under UV illumination. A **wax or resin** is suggested by FT-IR and detected in all the layers.



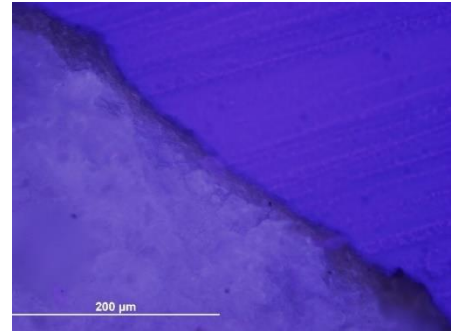
VLR OM (above)



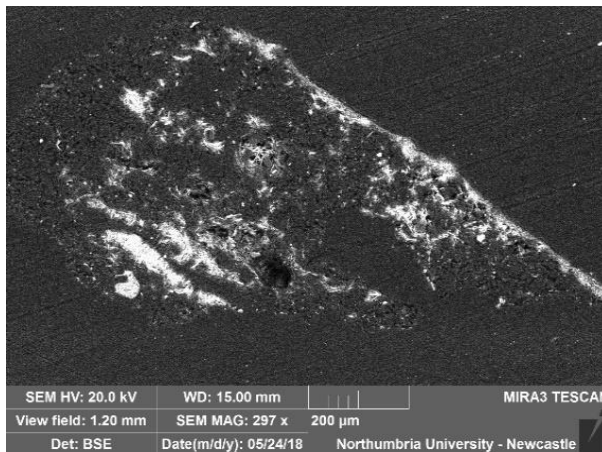
VLR OM, detail (above)



UVfOM (above)



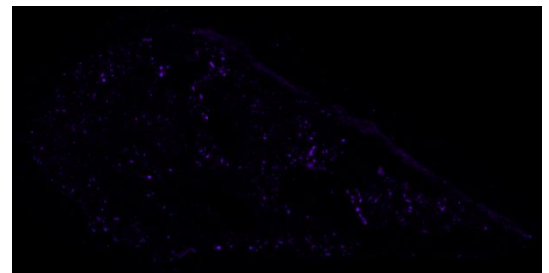
UVfOM, detail (above)



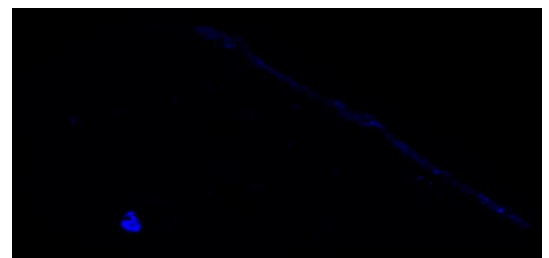
**BSE image** (above). Large mineral inclusions can be observed in the sample. The casting resin appears to have been absorbed evenly by the plaster sample. The utmost layers contain heavier elements.

**Calcium sulfate (CaSO<sub>4</sub>)** was detected in all the layers. Additionally, **Al**, **K**, **Fe** and **Mg** were also detected.

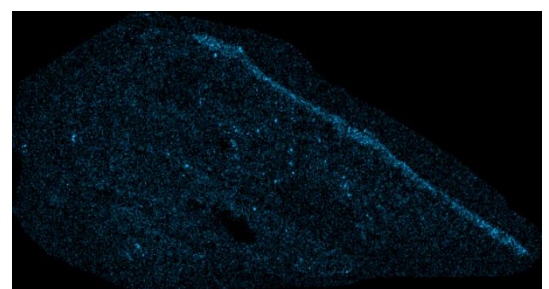
**EDS mapping** (right) shows that layers 2-3 are mostly made of **Si**, **Al** and **K**. **Si-Al inclusions** are present in all the layers.



Aluminium (Al)



Silicon (Si)

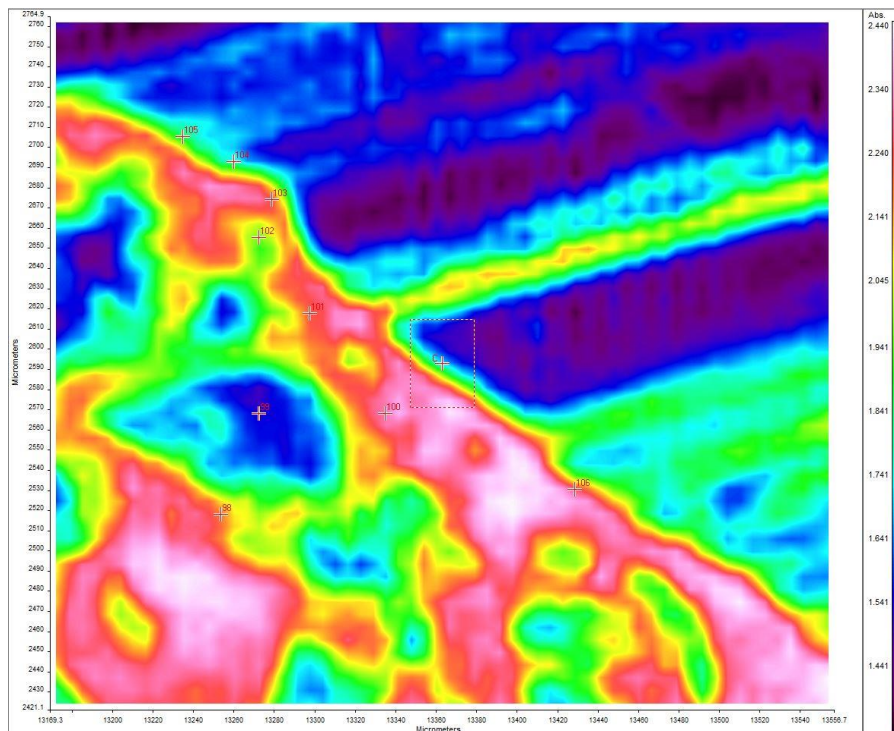


Potassium (K)

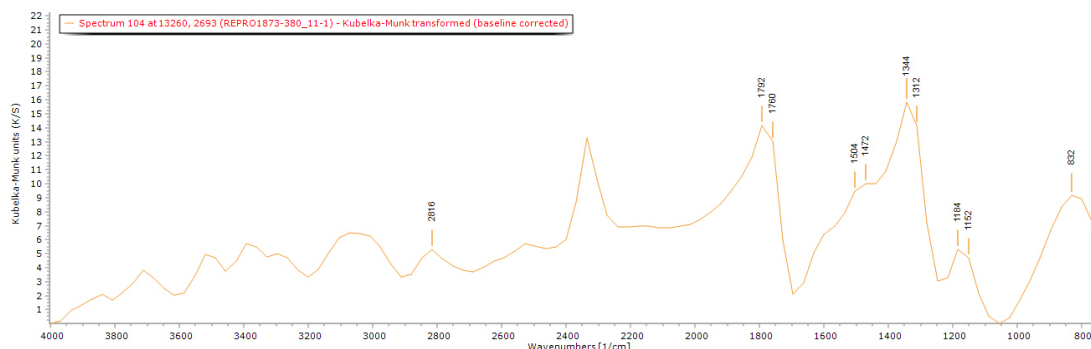
Spectrum	Layer	Material					
		Casting resin	Gypsum plaster	Calcite	Clay minerals	Organic material	Calcium oxalate
98	0	x	x			x	
99	0	x	x	x		x	
100	0	x		x		x	
101	1	x	x		x	x	
102	1	x	x		x	x	
103	3	x		x		x	
104	3	x		x		x	
105	2	x		x		x	
106	1	x	x	x		x	

**FT-IR (FPA) image (right).** No clear indication of different reflectance of the layers can be observed in the FPA image.

**Spectra 98-106** (see for example **spectrum 104** of layer 3 below) show a similar pattern with broad bands rather than sharp and defined peaks, which is expected for mixtures containing several components. Overall, no significant difference within the layers can be noticed by FT-IR analysis (see table above).



The **casting resin** (Tiranti polyester resin) and an **organic material** (likely a resin or a wax) are present in all the layers. **Gypsum plaster** ( $\text{CaSO}_4 \cdot 0.5\text{H}_2\text{O}$ ), **calcite** (calcium carbonate,  $\text{CaCO}_3$ ) and **clay minerals** (Si-O containing minerals) are suggested by EDS analysis and likely contributes to the FT-IR spectra, although their relevant peaks are not visible. The crowded appearance of the spectra and the broadness of the peaks impede the unique assignment of the materials in the sample.



The prep methods used on **samples 11-01** and **11-02** (see table below and description in the *Experimental* section) and **GC/MS analysis** did not provide meaningful data.

Sample	Sample prep method	Thermal programme
REPRO.1873-380_11-01	GCMS 1µl PFFA solution	(3)
REPRO.1873-380_11-01	GCMS 1µl PFFA solution	(3)

## Sample 12

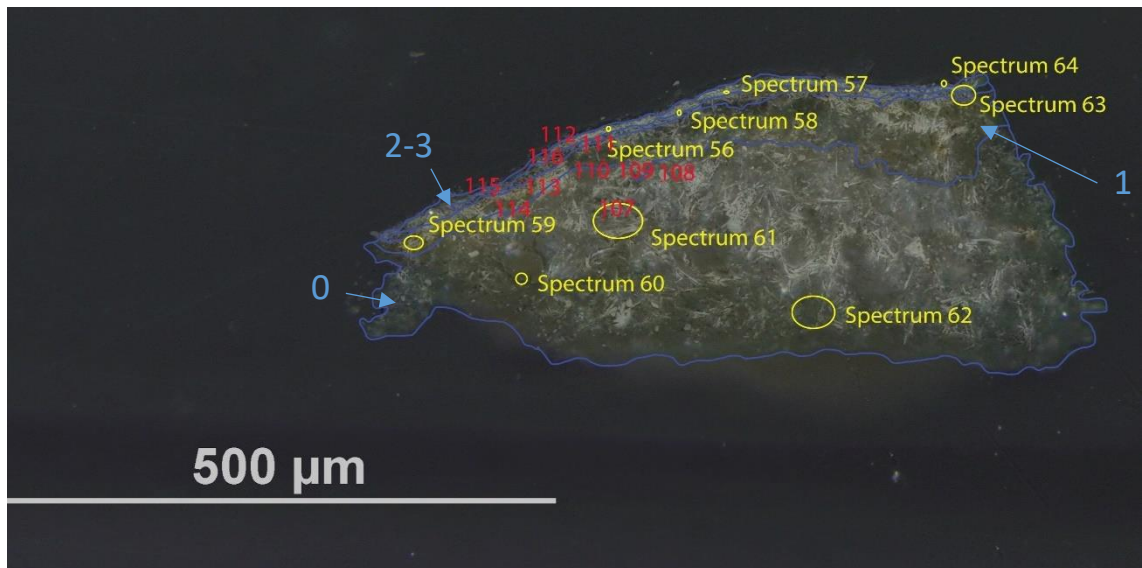


**Sampling.** This sample was taken from a fluorescent area on the PR sleeve of the main top figure.

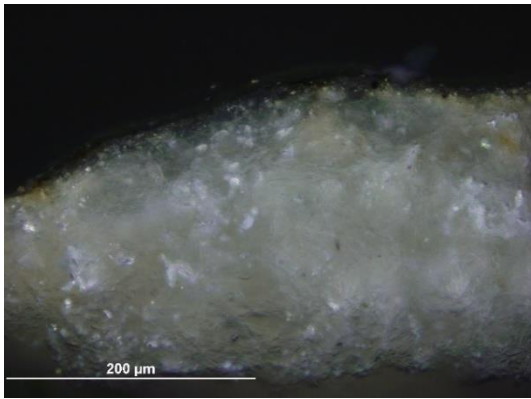
Below: Overlapped (OM and BSE) cross-section image showing the stratigraphy (blue indicators).

**Analysis spots.** EDS analysis (yellow): Spectra 56-64; FT-IR analysis (red): nos. 107-116.

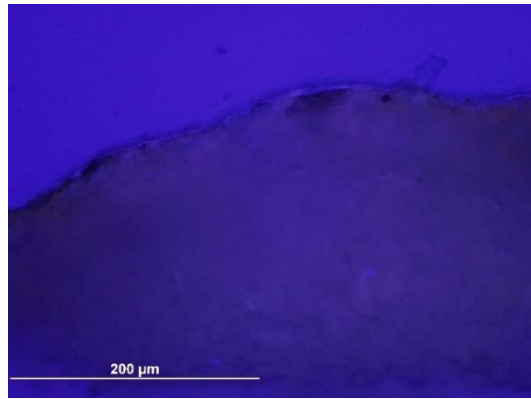
- 3. Varnish
- 2. Dark layer
- 1. Yellowish and undefined layer
- 0. Plaster bulk



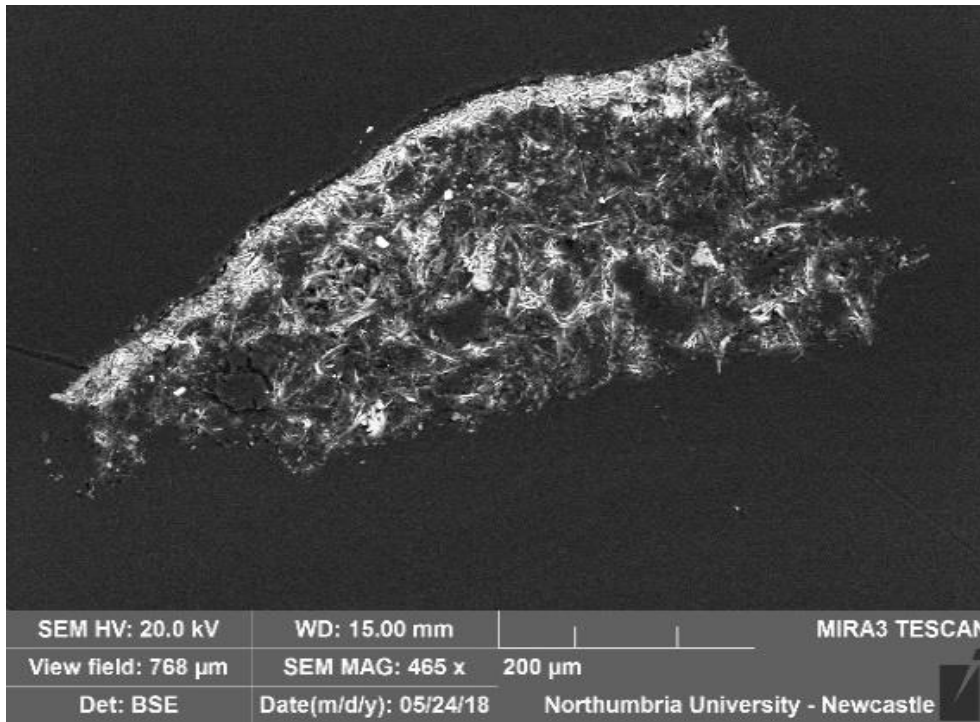
**Summary.** The sample is mostly made of C, O, S and Ca (**calcium sulfate**,  $\text{CaSO}_4$ , confirmed by EDS). **Al** is overall present as used as a polishing agent, but could also, together with **Si** and **K**, be present as part of **silicate** inclusions, which are present in all the layers (FT-IR confirmed the presence of **clay minerals**, such as kaolin). Additionally, traces of **Mg** were also detected in all the layers and **P**, **Cl** and **Fe** in the utmost layers. The tabular mineral structure typical of gypsum can be seen in layers 0 and 1. Layer 1 appears denser than layer 0. Layer 2 appears dark under visible illumination and is mostly made of **Si** and **Al**. Layer 3 fluoresces milky-white under UV illumination. A **wax or resin** is suggested by FT-IR and detected in all the layers.



VLR OM (above)



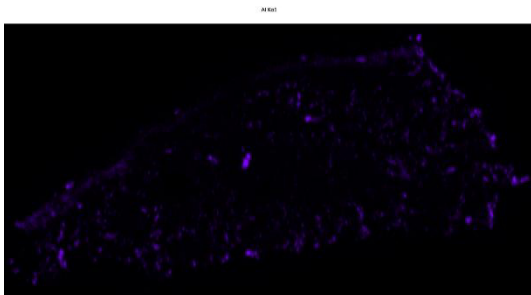
UVf OM (above)



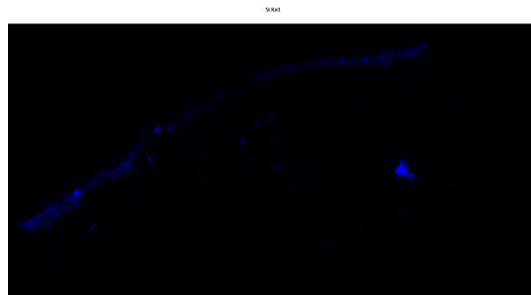
**BSE image (left).** The *tabular* mineral structure typical of gypsum can be seen in layers 0 and 1. Layer 1 appears denser than layer 0.

Calcium sulfate ( $\text{CaSO}_4$ ), Mg, Si and Al were detected in all the layers. Additionally, P, Cl, K and Fe were detected in the utmost layer.

EDS mapping (below) shows that layer 2 is mostly made of Si and Al. Si-Al inclusions are present in all the layers.



Aluminium (Al)

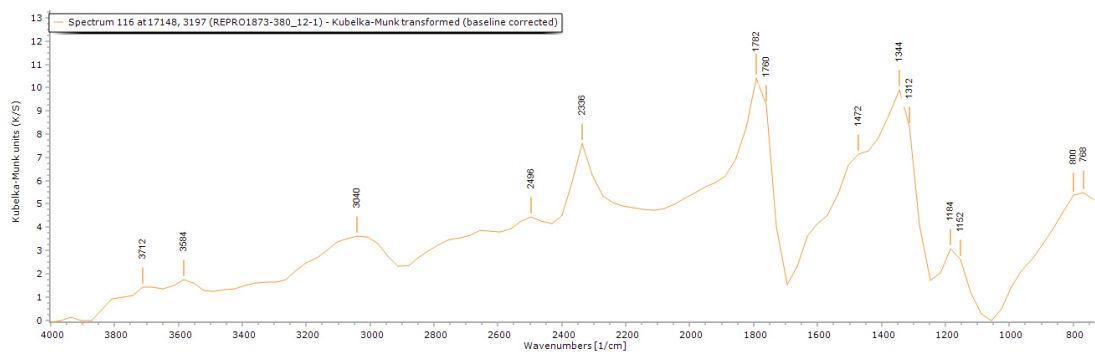
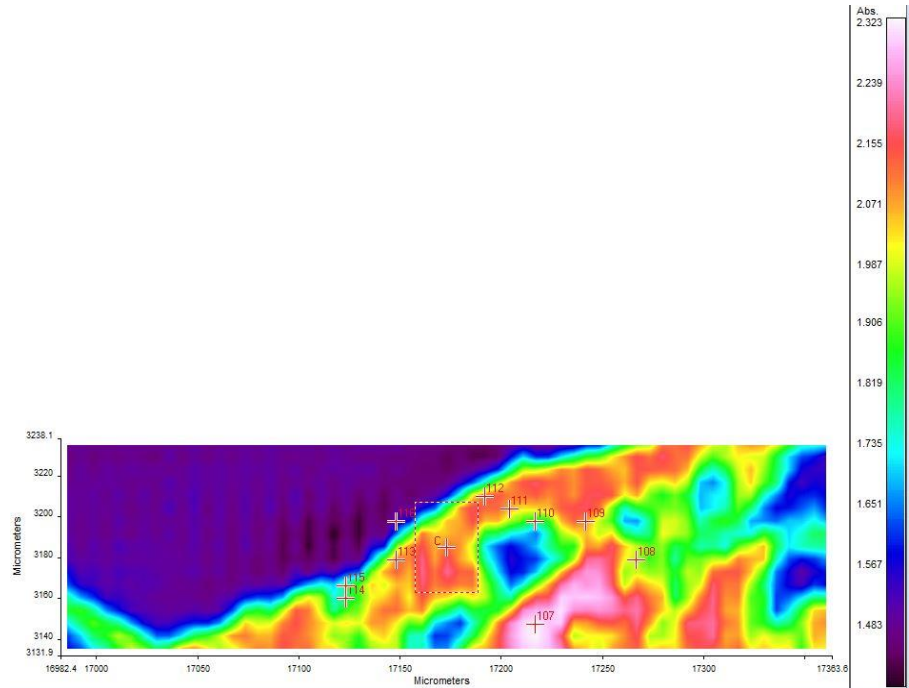


Silicon (Si)

Spectrum	Layer	Material					
		Casting resin	Gypsum plaster	Calcite	Clay minerals	Organic material	Calcium ox
107	0	x				x	
108	0	x		x			
109	1	x	x	x	x		
110	1	x	x	x			
111	1	x	x	x		x	
112	2		x	x		x	
113	2	x		x			
114	1	x	x	x			
115	2	x		x	x		
116	3	x	x	x			

**FT-IR (FPA) image** (right). Some indication of different reflectance of the layers can be observed in the FPA image.

**Spectra 107-116** (see for example **spectrum 116** of layer 3 below) show a similar pattern with broad bands rather than sharp and defined peaks, which is expected for mixtures containing several components. Overall, no significant difference within the layers can be noticed by FT-IR analysis (see table above).



The **casting resin** (Tiranti polyester resin), **gypsum plaster** ( $\text{CaSO}_4 \cdot 0.5\text{H}_2\text{O}$ ) and **calcite** (calcium carbonate,  $\text{CaCO}_3$ ) are present in most of the layers, although the relevant peaks in the FT-IR spectra are not always clearly visible. An organic material (likely a **resin** or a **wax**) and **clay minerals** (Si-O containing minerals) are also suggested by some of the spectra. A minor variation of the position of the peaks can be observed for several reasons, one of which is the local substitution of elements such as Mg in the gypsum and other minerals' structure (Kumar & Rajkumar, 2014; Melita et al., 2020). The crowded appearance of the spectra and the broadness of the peaks impede the unique assignment of the materials in the sample.

## Sample 13



**Sampling.** This sample was taken from the undercut just above the head of the figure carried by the angels.

Right: Overlapped (OM and BSE) cross-section image showing the stratigraphy (blue indicators).

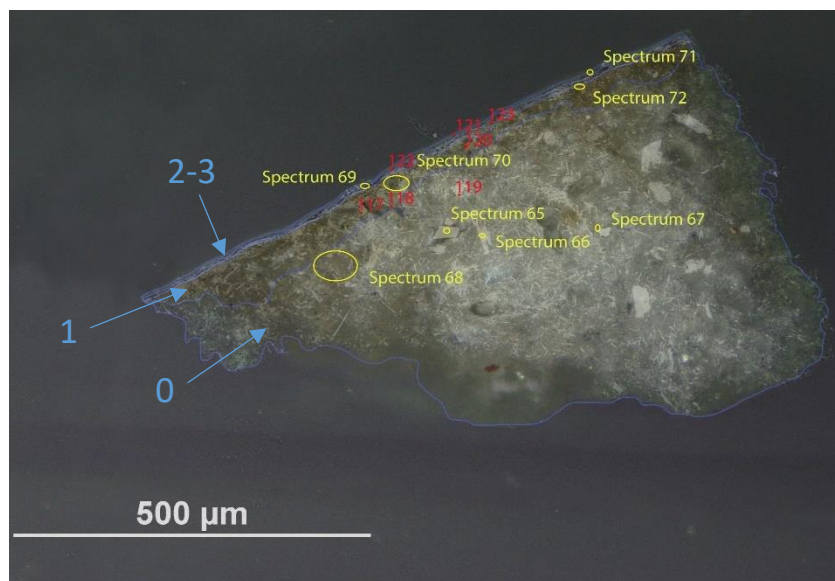
### 3. Varnish

### 2. Dark layer

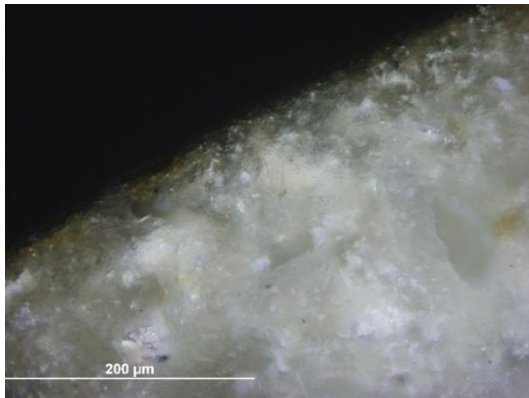
### 1. Yellowish and undefined layer

### 0. Plaster bulk

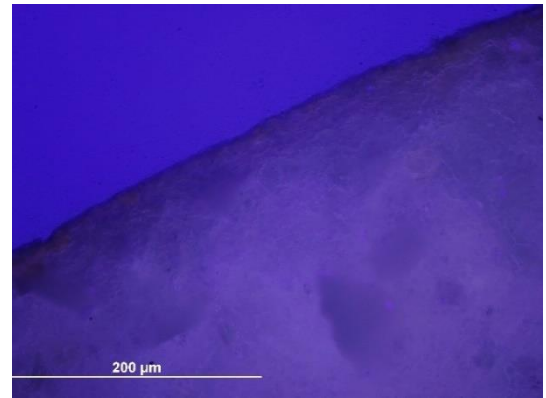
**Analysis spots.** EDS analysis (yellow): Spectra 65-72; FT-IR analysis (red): nos. 117-123.



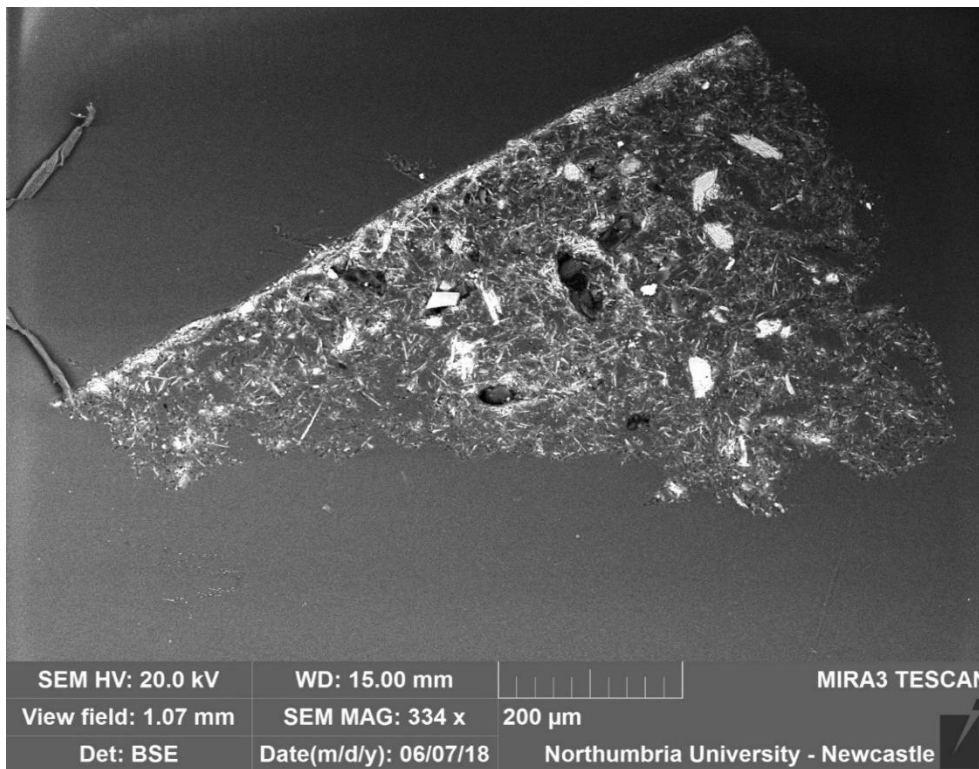
**Summary.** The sample is mostly made of C, O, S and Ca (**calcium sulfate**,  $\text{CaSO}_4$ , confirmed by EDS). **Al** is overall present as used as a polishing agent, but could also, together with **Si** and **K**, be present as part of **silicate** inclusions, which are present in all the layers (FT-IR confirmed the presence of **clay minerals**, such as kaolin). Additionally, **Fe**, **Mg**, **Cl**, **Ti** and **Na** were detected in the utmost layers. The tabular mineral structure typical of gypsum can be seen in layers 0 and 1. Layer 1 appears denser than layer 0. Layer 2 appears dark under visible illumination and is mostly made of **Si** and **Al**. Layer 3 fluoresces milky-white under UV illumination. A **wax or resin** is suggested by FT-IR and detected in all the layers. A **wax or resin** is suggested by FT-IR and detected in all the layers. py-TMAH-GC/MS shows markers characteristic of a **terpenic resin**, such as rosin or pine resin, possibly mixed with a non-drying oil or another source of lipids (Colombini & Modugno, 2009).



VLR OM (above)



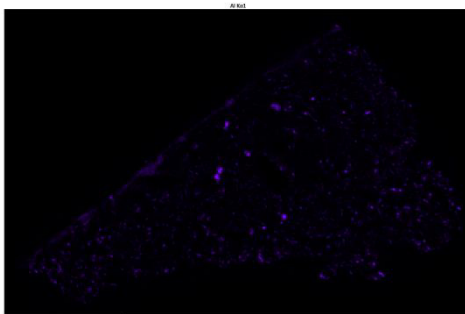
UVfOM (above)



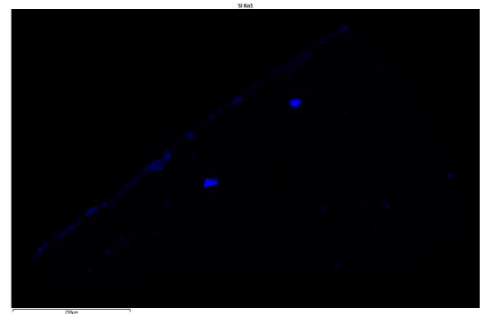
**BSE image (left).** The *tabular* mineral structure typical of gypsum can be seen in layers 0 and 1. Layer 1 appears denser than layer 0.

**Calcium sulfate ( $\text{CaSO}_4$ ), Si and Al** were detected in all the layers. Additionally, **Fe, Mg, K, Cl, Ti and Na** were detected in the utmost layers.

**EDS mapping (below)** shows that layer 2 is mostly made of **Si** and **Al**. **Si-Al inclusions** are present in all the layers.



Aluminium (Al)



Silicon (Si)

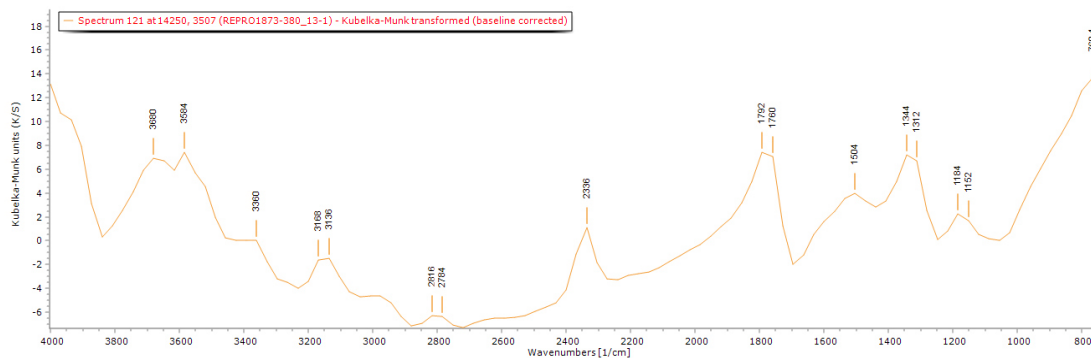
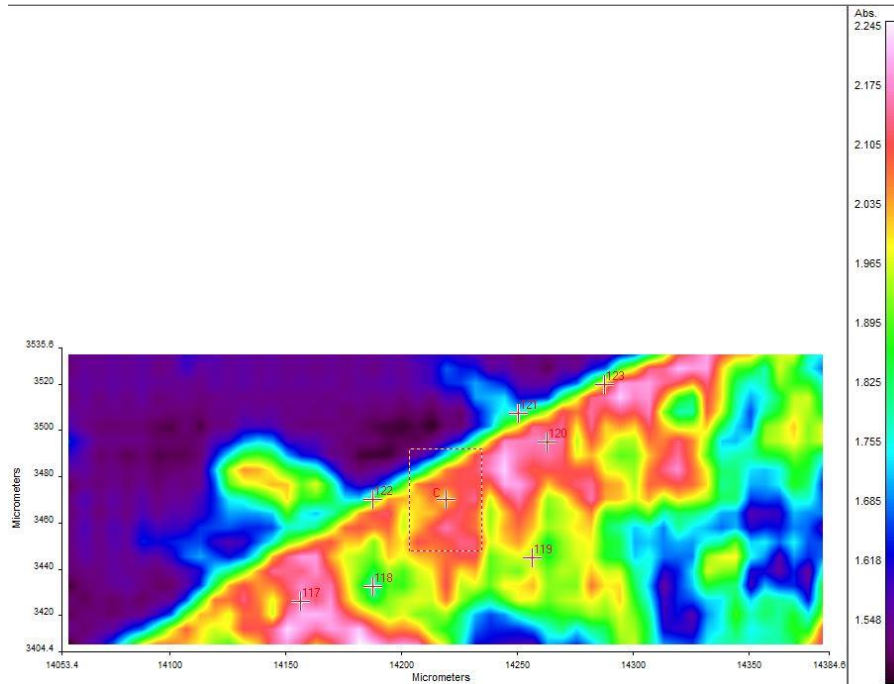
Spectrum	Layer	Material					
		Casting resin	Gypsum plaster	Calcite	Clay minerals	Organic material	Calcium oxalate
117	1	x	x	x			
118	1	x	x	x			
119	0	x		x		x	
120	1	x	x		x	x	
121	3	x	x	x	x	x	
122	3	x		x		x	
123	2	x	x	x		x	

**FT-IR (FPA) image**

(right). Some indication of different reflectance of the layers can be observed in the FPA image.

**Spectra 117-123**

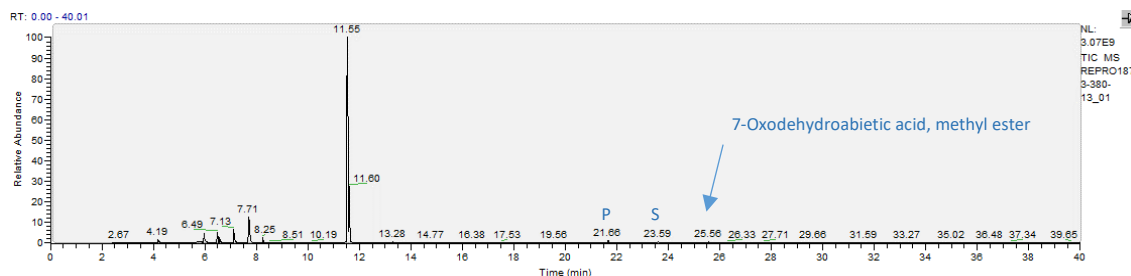
(see for example **spectrum 121** of layer 3 below) show a similar pattern with broad bands rather than sharp and defined peaks, which is expected for mixtures containing several components. Overall, no significant difference within the layers can be noticed by FT-IR analysis (see table below).



The **casting resin** (Tiranti polyester resin), **gypsum plaster** ( $\text{CaSO}_4 \cdot 0.5\text{H}_2\text{O}$ ), **calcite** (calcium carbonate,  $\text{CaCO}_3$ ) and an **organic material** (likely a **resin** or a **wax**) are present in most of the layers, although the relevant peaks in the FT-IR spectra are not always clearly visible. **Clay minerals** (Si-O containing minerals) are also suggested by some of the spectra. A minor variation of the position of the peaks can be observed for several reasons, one of which is the local substitution of elements such as Mg in the gypsum and other minerals' structure (Kumar & Rajkumar, 2014; Melita et al., 2020). The crowded appearance of the spectra and the broadness of the peaks impede the unique assignment of the materials in the sample.

Sample	Sample prep method	Thermal programme
REPRO.1873-380_13-01	Py-TMAH-GCMS	(1)
	2 µl Meth Prep II (2) solution, 1 µl TMAH	
REPRO.1873-380_13-03	Py-TMAH-GCMS	(1)
	2 µl Meth Prep II (2) solution, 1 µl TMAH	

The prep methods used on **samples 13-01** and **13-03** (see table [above](#) and described in the *Experimental* section) provided the same set of results. As an example, **sample 13-01** are shown in the chromatogram and the table [below](#).



**py-TMAH-GC/MS chromatogram** ([top](#) and described in the table [below](#)) shows small fragments due to derivatization (from  $t = 4.19$  to  $11.55$  min) and a marker characteristic of a **terpene resin** ( $t = 25.46$  and  $25.56$ ) (Colombini & Modugno, 2009; Mills & White, 2012). The presence of **methyl azelate** (A,  $t = 17.52$ ), **methyl palmitate** (P,  $t = 21.66$ ) and **stearate** (S,  $t = 23.59$ ) might suggest that the resin has mixed with an **oil** or that these FA are naturally present in the resin (A/P = 0.30, P/S = 1.16) (Colombini & Modugno, 2009).

RT	m/z	Assignment	Formula
4.19	45(100), 74(75)	Ethyl Ether	C <sub>4</sub> H <sub>10</sub> O
5.96	42(11), 58(100), 117(15)	1,2-Ethanediamine, N'-ethyl-N,N-dimethyl-	C <sub>6</sub> H <sub>16</sub> N <sub>2</sub>
6.49	45(23), 58(13), 66(22), 79(57), 95(100), 125 (7)	Sulfuric acid, dimethyl ester	C <sub>2</sub> H <sub>6</sub> O <sub>4</sub> S
7.13	72(100)	Amine fragment	
8.25	58(12), 113(22), 133(25), 145(35), 157(14), 176(100)	2,5-Dichlorophenylhydrazine hydrochloride	
11.55	145(14), 172(13), 188(100)	Unidentified fragment, MetPrep related	
17.52	74(34), 83(47), 87(31), 97(37), 129(37), 152(36), 171(5), 185(5)	Azelaic acid, monomethyl ester	C <sub>10</sub> H <sub>18</sub> O <sub>4</sub>
21.66	74 (100), 87(52), 239 (6), 270 (3)	Methyl palmitate	C <sub>17</sub> H <sub>34</sub> O <sub>2</sub>
23.59	74 (100), 87(55), 129(9), 143(27), 255(9), 298(3)	Methyl stearate	C <sub>19</sub> H <sub>38</sub> O <sub>2</sub>
25.46	207(61), 253(100), 313 (5), 328 (10)	7-Oxodehydroabiatic acid, methyl ester	
25.56	155(17), 239(100), 253(44), 281 (30), 314(5)	Methyl dehydroabietate	

RT = retention time, m/z = mass/charge ratio

## Experimental

The object was observed, and its conditions were documented. Samples from selected areas were taken by Valentina Risdonne. When possible, each sample was split into two parts: one fragment was embedded in polyester resin (Tiranti clear casting resin), polished and analysed under optical microscope and the other was put aside for (py)-GC/MS and XRD analysis.

The optical microscopy was performed with an Olympus BX51 Metallurgical Microscope equipped with four objectives (magnification of x5, x20, x50 and x100), and an x10 eyepiece. In many instances, a small amount of white spirit was applied to the surface of the cross-section to improve the saturation under the microscope. The microscope is equipped with a 6-cube filter turret which allows to operate the system in reflected visible light (brightfield and darkfield mode) and reflected UV light (365 nm) using a 100 W mercury burner.

The SEM-EDS analysis was performed with a field emission TESCAN MIRA 3 with gigantic chamber. The SEM is equipped with: secondary electron detector (SE), secondary electron in-beam detector (In-beam SE), back-scatter detector (BSE), back-scatter in-beam detector (In-beam BSE), cathodoluminescence detector (without wavelength detection) (CL), plasma chamber/sample cleaner and software Alicona 3D imaging. For the EDS analytical part, it has an Oxford Instruments setup: Software: AztecEnergy, X-ray detector X-Max 150 mm<sup>2</sup> and X-ray detector X-Max Extreme, low energy detector for thin films, high resolution and low voltage. The samples were analysed by SEM-EDS Low Vacuum Mode (10-15 Pa). EDS Mapping and data processing were performed with Aztec Oxford software. A fragment of sample 2 was mounted on appropriate support, adhered with silver paint and coated with a layer of platinum (5 nm thick). This sample preparation is required when high vacuum SEM-EDS (1.5x10<sup>-2</sup> Pa) is performed. This mode allows a higher magnification with a better definition.

A Perkin Elmer Frontier FT-IR spectrometer (350 cm<sup>-1</sup> at the best resolution of 0.4 cm<sup>-1</sup>) was used, equipped with a germanium crystal for ATR measurements and combined with a Spectrum Spotlight 400 FT-IR microscope equipped with a 16x1 pixel linear mercury cadmium telluride (MCT) array detector standard with InGaAs array option for optimised NIR imaging. Spectral images from sample areas are possible at pixel resolutions of 6.25, 25, or 50 microns. The Perkin Elmer ATR imaging accessory consists of a germanium crystal for ATR imaging. These run with Perkin Elmer Spectrum 10™ software and with SpectrumIMAGE™ software. Baseline and Kubelka-Munk corrections were applied to the raw data acquired in diffuse reflectance. Samples 1 to 13 were analysed by FT-IR, using the imaging mode. Sample 1 was also analysed by ATR and sample 2 was analysed as a loose fragment.

The XRD analysis was performed with a Rigaku SmartLab SE equipped with a HyPix-400, a semiconductor hybrid pixel array detector and Cu source. The analyses were performed in Bragg-Brentano geometry mode, with 40 kV tube voltage and 50 mA tube current. The diffractograms were processed with a SmartLab II software. The data was compared to the RUFF database (Lafuente et al., 2016) COD Database (Gražulis et al., 2009).

The instrument used for GC/MS is a Thermo Focus Gas Chromatographer with DSQ II single quadrupole mass spec. The column currently installed is an Agilent DB5-MS UI column (ID: 0.25 mm, length: 30 m, df: 0.25 μm, Agilent, Santa Clara, CA, USA). Carrier gas: helium. Detector temperature: 280 °C, Injector temperature: 250 °C. It can be used with the PyroLab 2000 Platinum filament pyrolyser (PyroLab, Sweden) attachment or in split/splitless mode. Detection: Total Ion monitoring (TIC). Three different types of samples preparation were coupled with different GC thermal programmes.

Sample preparation for GC/MS: Derivatization with *n*-propanol followed by pentafluoropropionic anhydride (PFPA). 1 mg of sample, grinded between two glass slides, was pulverised and placed in Reacti-Vial. 150 μL of Hydrochloric acid (HCl) were added to hydrolyse the sample (Reactival cap on during this step). Nitrogen was used to remove the excess Oxygen in the vial. The vial was left in a heating block at 90°C for 3 days, the vial was put in a glass vacuum desiccator for 24 hours to remove the acid. 180 μL of propan-1-ol : acetyl chloride (3:1) were added in the Reacti-Vial, the sample was heated at 110 °C for 45 minutes (cap on), the temperature was lowered to 50°C for about 30 min, the cap was removed and the vial was filled with nitrogen to vaporise the reagent excess and dry out the sample. The residue was dissolved in 50 μL 0.2% pyridine. 150 μL of dichloromethane (DCM) and 150 μL perfluoropropionic anhydride (PFPA) were added and the sample was heated at 110°C for 15 minutes (cap on).

Sample preparation for py-GC/MS: Methylation with Tetramethylammonium hydroxide (TMAH). The sample was grinded between two glass slides and about 0.5 mg were positioned onto the Pt filament

and directly derivatised in an aliquot of 1 µl of 25 % (wt) in methanol tetramethylammonium hydroxide; Methylation with 3-trifluoromethylphenyltrimethylammonium hydroxide (5% wt in Methanol) CAS number 68254-41-1, C<sub>10</sub>H<sub>14</sub>F<sub>3</sub>NO m-TFPTAH (commercially known as MetPrep II) Method (1). 1-3 drops of MetPrep II, depending on sample size, is added to the sample in a Reacti-Vial. The solution is heated gently in a heating block set at 60°C for 24 hours; Method (2). 0.3 mg of sample in 30 µl of MetPrep II is heated gently in a heating block set at 60°C for 24 hours in a Reacti-Vial.

Thermal Programme (1). (PaintpyrolysisTMAH30m.meth) Seg1 start 2.40 Scan events MS, Heated zones Ion Source 250 °C, Detector Gain 1.21·10<sup>5</sup> (Multiplier Voltage 1025 V). Oven: Initial temp 40 °C hold 4 minutes Ramp 1 10.0 °C/min (rate), until 250 °C, hold 15 min. Mode: splitless.

Thermal Programme (2). (PaintpyrolysisTMAH30m.meth) Seg1 start 2.40 Scan events MS, Heated zones Ion Source 250 °C, Detector Gain 1.21·10<sup>5</sup> (Multiplier Voltage 1025 V). Oven: Initial temp 40 °C hold 4 minutes Ramp 1 10.0 °C/min (rate), 250 °C, hold 45 min.

Thermal Programme (3). (ProteinBM\_Valentina.meth) Seg1 start 13.00 Scan events MS, Heated zones Ion Source 250 °C, Detector Gain 1.21·10<sup>5</sup> (Multiplier Voltage 1025 V). Oven: Initial temp 60 °C hold 2 minutes Ramp 1 6.0 °C/min (rate), 250 °C, hold 0 min. Ramp 2 25 °C/min, 300 °C, 20 min hold. Mode: split

The inlet temperature to the GC was kept at 250 °C. The helium carrier gas flow rate was 1.5 ml/min with a split flow of 41 ml/min and split ratio of 27. The MS transfer line was held at 260 °C and the ion source at 250 °C. The pyrolysis chamber was heated to 175 °C, and pyrolysis was carried out at 600 °C for 2 s. This run with Xcalibur™ and PyroLab™ software. The library browser supported NIST MS Version 2.0 (Linstrom & Mallard, 2014).

Valentina Risdonne, PhD student

[v.risdonne@vam.ac.uk](mailto:v.risdonne@vam.ac.uk) / [valentina.risdonne@northumbria.ac.uk](mailto:valentina.risdonne@northumbria.ac.uk)

Victoria and Albert Museum – Northumbria University

PhD project 'Materials and techniques for coating of the nineteenth-century plaster casts'

©V&A Museum

10 November 2020

## Notes

23 March 2018	Sampling	Valentina's PhD Lab book 1, page 59
16 April 2018	Casting	Valentina's PhD Lab book 1, page 70
2-3 May 2018	Microscopy	Valentina's PhD Lab book 1, page 81
10-24 May 2018	SEM-EDS	Valentina's PhD Lab book 1, page 86
2 October 2018	FT-IR	Valentina's PhD Lab book 1, page 126
3 December 2019	XRD	Valentina's PhD Lab book 2, page 4
18 March 2020	GC/MS	Valentina's PhD Lab book 2, page 50

A full record of analyses is available at <https://doi.org/10.25398/rd.northumbria.13469925>

## References

- Barash, M. (1985). *Theories of Art: From Plato to Winckelmann*. New York: New York University Press.
- Beran, A. (2002). Infrared spectroscopy of micas. *Reviews in Mineralogy and Geochemistry*, 46(1), 351–369.
- Colombini, M. P., & Modugno, F. (2009). *Organic mass spectrometry in art and archaeology*. John Wiley & Sons.
- Cox, K. G., Price, N. B., & Harte, B. (1974). *An introduction to the practical study of crystals, minerals, and rocks*. Halsted Press.
- Derrick, M. R., Stulik, D., & Landry, J. M. (2000). *Infrared spectroscopy in conservation science*. Getty Publications.
- Gražulis, S., Chateigner, D., Downs, R. T., Yokochi, A. F. T., Quirós, M., Lutterotti, L., Manakova, E., Butkus, J., Moeck, P., & Le Bail, A. (2009). Crystallography Open Database—an open-access collection of crystal structures. *Journal of Applied Crystallography*, 42(4), 726–729.
- Kumar, R. S., & Rajkumar, P. (2014). Characterization of minerals in air dust particles in the state of Tamilnadu, India through FT-IR, XRD and SEM analyses. *Infrared Physics & Technology*, 67, 30–41.
- Lafuente, B., Downs, R. T., Yang, H., & Stone, N. (2016). The power of databases: the RRUFF project. In *Highlights in mineralogical crystallography* (pp. 1–29). Walter de Gruyter GmbH.
- Linstrom, P. J., & Mallard, W. G. (2014). *NIST Chemistry WebBook, NIST standard reference database number 69, National Institute of Standards and Technology, Gaithersburg MD, 20899*.
- Manfredi, M., Barberis, E., Rava, A., Robotti, E., Gosetti, F., & Marengo, E. (2015). Portable diffuse reflectance infrared Fourier transform (DRIFT) technique for the non-invasive identification of canvas ground: IR spectra reference collection. *Analytical Methods*, 7(6), 2313–2322.
- Meilach, D. Z. (1966). *Creating with plaster*.
- Melita, L., Węglowska, K., & Tamburini, D. (2020). Investigating the Potential of the Er:YAG Laser for the Removal of Cemented Dust from Limestone and Painted Plaster. *Coatings*, 10, 1099. <https://doi.org/10.3390/coatings10111099>
- Miliani, C., Rosi, F., Daveri, A., & Brunetti, B. G. (2012). Reflection infrared spectroscopy for the non-invasive in situ study of artists' pigments. *Applied Physics A*, 106(2), 295–307.
- Mills, J., & White, R. (2012). *Organic chemistry of museum objects*. Routledge.
- Price, B. A., Pretzel, B., & Lomax, S. Q. (2009). Infrared and Raman Users Group Spectral Database; 2007 ed. *IRUG: Philadelphia, PA, USA*.
- Singer, B., & McGuigan, R. (2007). The simultaneous analysis of proteins, lipids, and diterpenoid resins found in cultural objects. *Annali Di Chimica: Journal of Analytical, Environmental and Cultural Heritage Chemistry*, 97(7), 405–417.
- Toniolo, L., Zerbi, C. M., & Bugini, R. (2009). Black layers on historical architecture. *Environmental Science and Pollution Research*, 16(2), 218–226. <https://doi.org/10.1007/s11356-008-0046-8>
- Turco, A. (1990). *Il gesso*. HOEPLI Editore.



**Northumbria  
University**  
NEWCASTLE

Analysis Report - Valentina Risdonne

Copy of Part of a Choir Screen

(REPRO.1873-561)

Initiator: Charlotte Hubbard; Conservation Department

30 October 2020

© Victoria and Albert Museum



## Analysis Report - Copy of Part of a Choir Screen (REPRO.1873-561)

### Contents

Contents.....	162
List of abbreviations.....	162
Summary.....	163
Sample 1.....	166
Sample 2.....	169
Sample 3.....	172
Sample 4.....	175
Sample 5.....	178
Sample 6.....	181
Experimental.....	185
Notes.....	186
References.....	186

### List of abbreviations

BSE	Back Scattered Electron
EDS	Energy Dispersive Spectrometry
FT-IR	Fourier-Transform Infra-Red
FPA	Focal Plane Array
GC/MS	Gas Chromatography-Mass Spectrometry
OM	Optical Microscopy
PL	Proper Left
PR	Proper Right
py	pyrolysis
SEM	Scanning Electron Microscopy
TMAH	tetramethylammonium hydroxide
UVf	Ultraviolet Fluorescence
VLR	Visible Light Reflectance
XRD	X-ray Diffraction

## Summary

In summary, the bulk of the object is made of gypsum plaster, which contains several types of inclusions (including silicates and carbonates). By looking at the results, it is possible to hypothesise that in the surface layer, containing **silicon** and **aluminium**, but also traces of other elements, the medium is a **diterpenic resin**. **Sample 6** might have been taken from an area of overpaint.



Figure 1. The copy of part of a choir screen.

The object, '**Copy of Part of a Choir Screen (REPRO.1873-561)**' (Figure 1), is a plaster cast of part of a choir screen that depicts Saints (St. Benedict, St. James, St. Peter, St. Paul, St. John) and the Virgin and Child alongside Bishop Bernward made by Friedrich Küsthardt in Hildesheim (Germany) about 1873. The original was made from stucco by an unknown artist in Germany probably in 1194-97 for the west choir in the church of St Michael, Hildesheim. The cast was purchased from F. Küsthardt in 1873 for £162 10s and is now located in Room 46A (The Ruddock Family Cast Court). Its dimensions are 320.5X793.0 cm.

Samples from the plaster cast were taken from pre-existing areas of loss to investigate the stratigraphy and the method of manufacture (Figure 2). The samples were analyzed to provide data for the study of the objects of the Cast Courts collection within the PhD project 'Materials and techniques for coating of the nineteenth-century plaster casts'. Details on the experimental procedure are available in the Experimental section of this report. A selection of significant results is shown in the following pages and the relevant database of analysis (<https://doi.org/10.25398/rd.northumbria.13811594>).

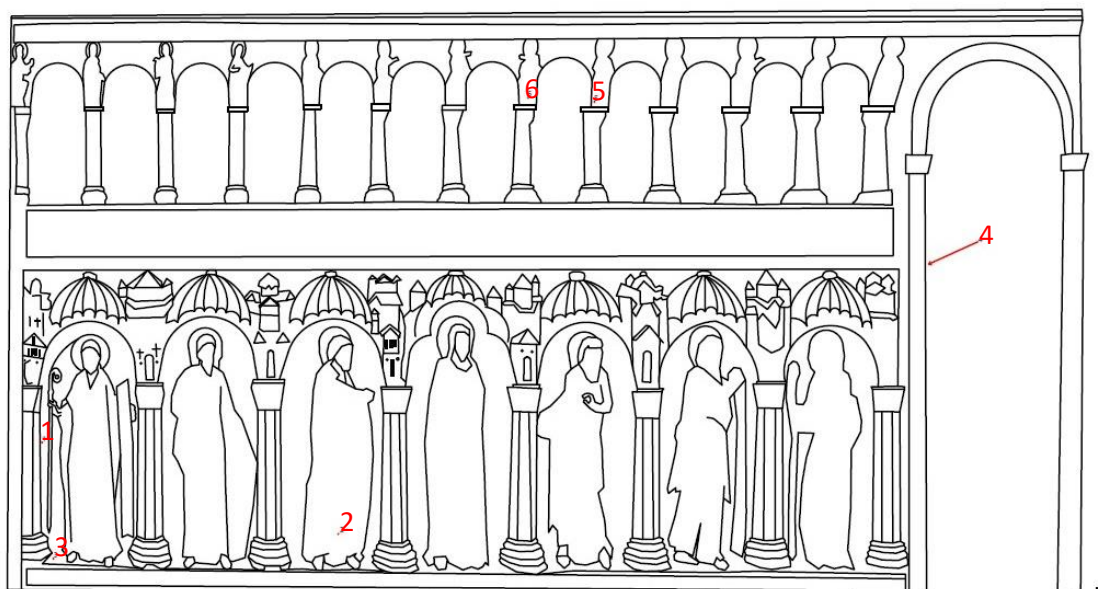


Figure 2. The screen outline with marked sampling sites.

**Sample 1:** fragment taken from an area of loss along a crack. The sample was taken from the background on the PR of the figure in the first frame from the PR.

**Sample 2:** fragment taken from an area of loss on the vest of the figure in the third frame from the PR.

**Sample 3:** loose fragment, taken from the base below the first frame.

**Sample 4:** fragment from the greasy dark area, the fragment was almost detached. Taken from the edge of the PR column of the arc, backside.

**Sample 5:** dark fragment taken from the vest of the ninth figure from the PR on the second level of columns.

**Sample 6:** fragment from an area of loss from the foot of the eighth figure from the PR on the second level of columns.

The **substrate** (layer 0 in all the samples) is made of gypsum plaster (**calcium sulfate**,  $\text{CaSO}_4$ , confirmed by EDS, XRD and by the peak at  $1600\text{-}1648\text{ cm}^{-1}$  in the FT-IR spectra, which also show the sulfate overtones in the  $2100\text{-}2300\text{ cm}^{-1}$  area). An **interface layer**, yellow under visible illumination and possibly consisting of a portion of lower layer soaked with the surface coating(s), showing characteristics of both layers, is visible in all the samples. The tabular crystalline structure typical of gypsum plaster can be seen in the substrate layer and the interface layer. Inclusions made of **aluminium (Al)**, **silicon (Si)** are present in all the layers of all the samples; traces of **magnesium (Mg)** were detected in all the layers of samples 1 and 4 and **iron (Fe)** was also detected in all the layers of sample 2.

All the samples show a layer, **dark** under visible illumination (layer 2 in all the samples). EDS mapping shows that this dark layer contains **calcium sulfate** but consists also of **Si** in sample 2. In sample 6 this layer 2 mainly consists of **Si**, **Ba** and **Ti**. Samples 1, 2 and 4 shows an additional **finishing layer** that fluoresces white under UV illumination. This can suggest either that a varnish was applied only on the selected areas or that the varnish was applied on all the surface, but it was differently adsorbed depending on the local variation of porosity. Additional traces of, Na, Cl and K were also detected in the utmost layer of all the samples. Traces of Zn and Pb were detected in the utmost layers of sample 1, Fe and

P in sample 2, Mg, Fe and Ba in sample 3, Mg, Fe and Pb in sample 5 and Fe, Mg and Mn in sample 6. **Sample 6** shows a stratigraphy similar to the rest of the samples however, the presence of Ba and Pb on the surface layer suggest that this area might have been **repainted** or **highlighted**.

A **wax** or **resin** (FT-IR peaks at 1200-1500 and 2800-3000  $\text{cm}^{-1}$ ) was detected in all the layers of all the samples. This indicates that either the material was added to the gypsum plaster wet admixture or that the coating has also penetrated in layer 0. The latter seems also possible as the average depth of the samples is about 0.5 mm. py-TMAH-GC/MS of sample 6 shows markers characteristic of a **diterpenic resin** (Colombini & Modugno, 2009).

**NOTE:** casting in resin the fragments of plaster resulted in the fragments absorbing the resin when in the liquid state. This was visible in the BSE image as well as through the EDS mapping (Tiranti resin and catalyst are mainly made of organic compounds C, H and O). Aluminium (Al) traces are present in all the samples, due to the polishing chemical.

## Sample 1

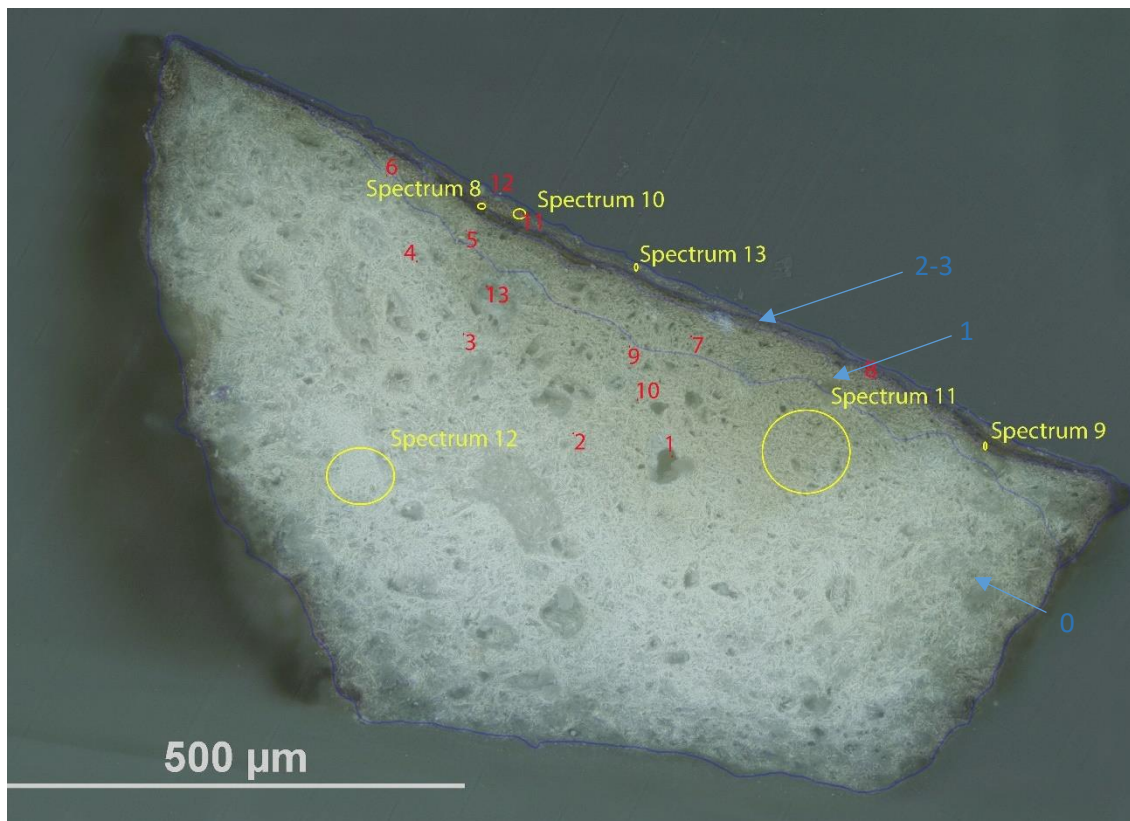


Below: Overlapped (OM and BSE) cross-section image showing the stratigraphy (blue indicators).

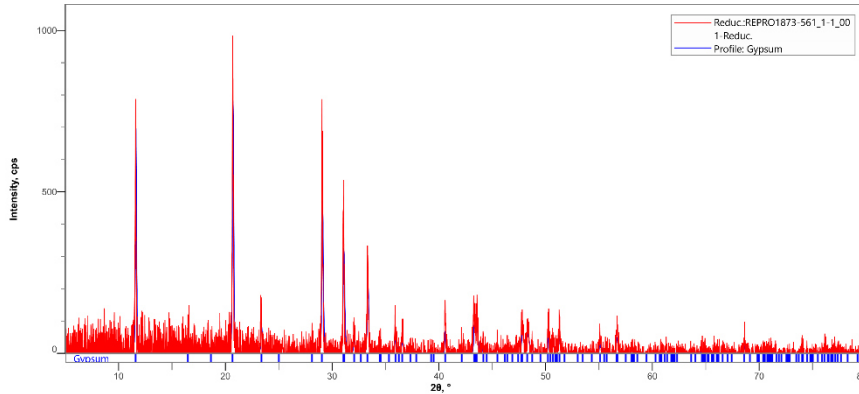
- 3. Varnish
- 2. Dark layer
- 1. Yellowish and undefined layer
- 0. Plaster bulk

**Sampling.** This fragment taken from an area of loss along a crack. The sample was taken from the background on the PR of the figure in the first frame from the PR.

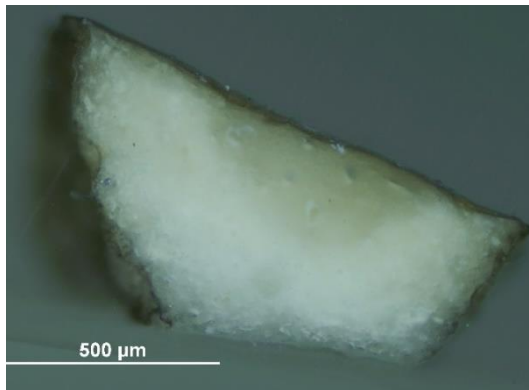
**Analysis spots.** EDS analysis (yellow): Spectra 8-13; FT-IR analysis (red): nos. 1-13.



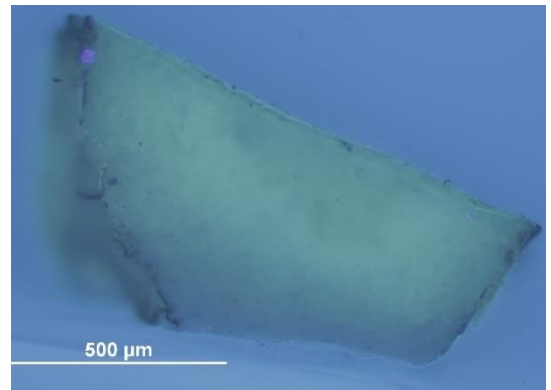
**Summary.** The substrate (layer 0) is made of plaster (**calcium sulfate**,  $\text{CaSO}_4$ , confirmed by EDS, XRD and by the peak at  $1600\text{-}48\text{ cm}^{-1}$  and overtones in the FT-IR spectra). The tabular crystalline structure typical of gypsum plaster can be seen in layers 0 and 1. Layer 1 appears yellow under visible illumination and it is consistent with the ground layer soaked with a **wax** or **resin** (FT-IR peaks at  $100\text{-}1200$  and  $2800\text{-}3000\text{ cm}^{-1}$ ) which was detected in all the layers. Layer 2 is dark under visible and UV illumination and layer 3 fluoresces white under UV illumination. Inclusions made of Al and Si are present in all the layers and traces of Mg were also detected. Traces of Pb, Na, Zn, Cl and K were also detected in the utmost layer.



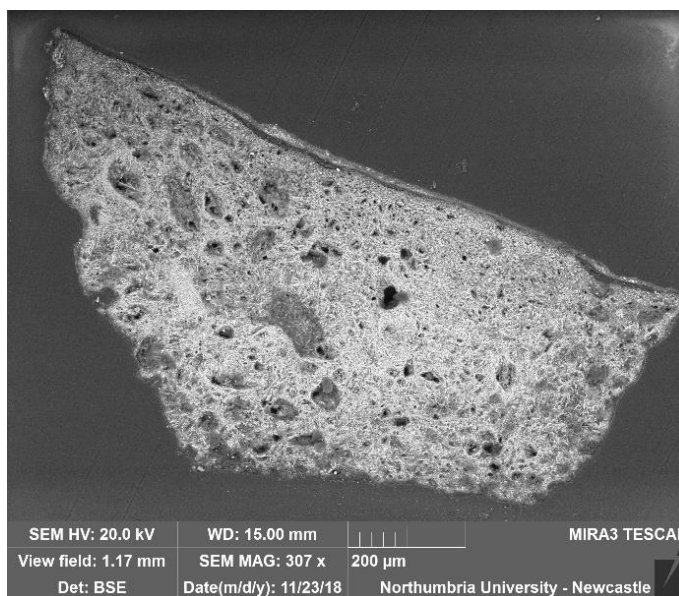
A fragment of this sample was pulverised and analysed by **XRD**. It was possible to identify the profile of gypsum (calcium sulfate) and the diffractogram was compared to references from the Rigaku SmartLab Database and the most significant peaks were at  $2\theta = 11.59, 20.69, 23.36, 29.05, 31.06, 33.31, 47.81$ .



VLR OM (above)



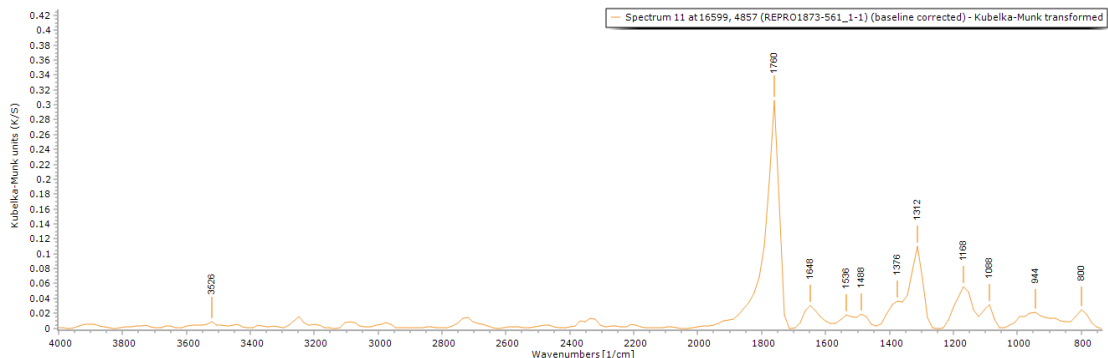
UVf OM (above)



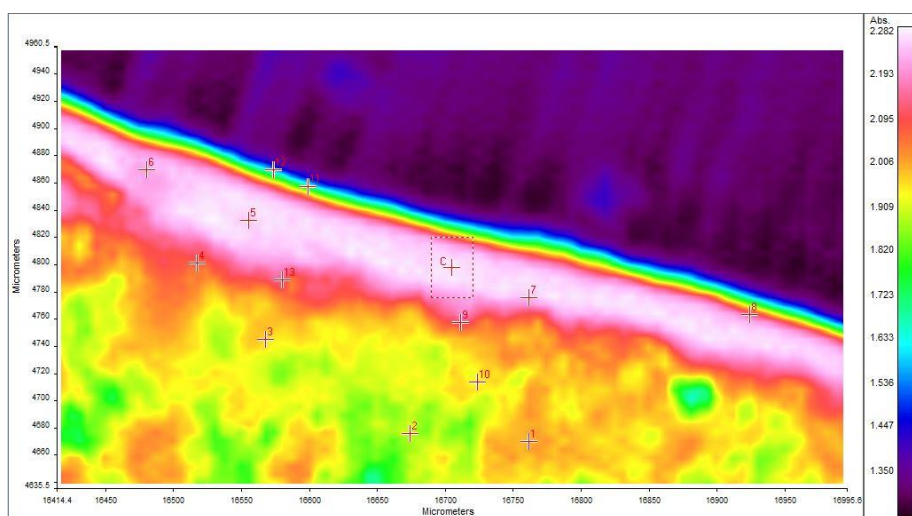
**BSE image (left).** The tabular crystalline structure typical of gypsum plaster can be seen in layers 0 and 1, which are made of **calcium sulfate**,  $\text{CaSO}_4$ . Large pores and large inclusions can be also seen.

Inclusions made of **Al** and **Si** are present in all the layers and traces of **Mg** were also detected.

Traces of **Pb**, **Na**, **Zn**, **Cl** and **K** were also detected in the utmost layer.



**FT-IR spectrum 11** (above) of layer 3. Peaks for the casting resin (1312, 1760  $\text{cm}^{-1}$ ), gypsum (1648  $\text{cm}^{-1}$ ) and a wax/resin (1000-1200, 1488 and 2800-3000  $\text{cm}^{-1}$ ). A summary of the peaks observed in the spectra 1-13 can be seen in the table below.



**FT-IR (FPA) image** (left). The different reflectance of the utmost layer can be observed in the FPA image.

Spectrum	Layer	peaks (cm-1)						
		Casting Resin	Gypsum	Carbonate	Wax/resin	C=O ester carbonyl	SO overtone	Unknown
1	0	1312, 1760	1616		768, 880, 928, 976, 1056, 1088, 1248, 1392, 1488, 1648, 2864, 2928		2224, 2288	
2	0	1328, 1760			816, 944, 1024, 1072, 1248, 1408, 1472, 1664, 2864, 2928		2224	
3	0	1312	1632		896, 1008, 1072, 1248, 1472, 1504, 2928	1712, 1744	2224	
4	0	1312	1600		816, 896, 992, 1088, 1232, 1408, 1664, 2864, 2928		2190	1792
5	1	1312	1600	800	896, 1008, 1056, 1184, 1360, 1440, 1664		2272, 2400	1808
6	1	1760	1648		848, 896, 944, 1088, 1168, 1248, 1296, 1344, 1424, 1488, 1584, 2816			1808
7	1	1328	1648		896, 1056, 1216, 1376, 1472, 1584, 2832, 2912		2224, 2435	1792
8	2	1328, 1760	1648		848, 912, 1008, 1088, 1136, 1200, 1424, 1456, 1568, 2832, 2928		2304	
9	0		1632		896, 976, 1072, 1248, 1280, 1392, 1424, 1456, 1552, 1664, 2912	1744	2231	
10	0	1328	1600		848, 912, 1024, 1232, 1376, 1680, 2864, 2928	1744	2240	
11	3	1312, 1760	1648	800	944, 1088, 1168, 1376, 1488, 1536			
12	3	1312, 1760	1649		777, 928, 1008, 1088, 1152, 1184, 1488		2336	
13	0	1312	1600	1776	768, 848, 944, 1024, 1072, 1216, 1264, 1360, 1408, 1488, 1680, 2880		2256	

## Sample 2

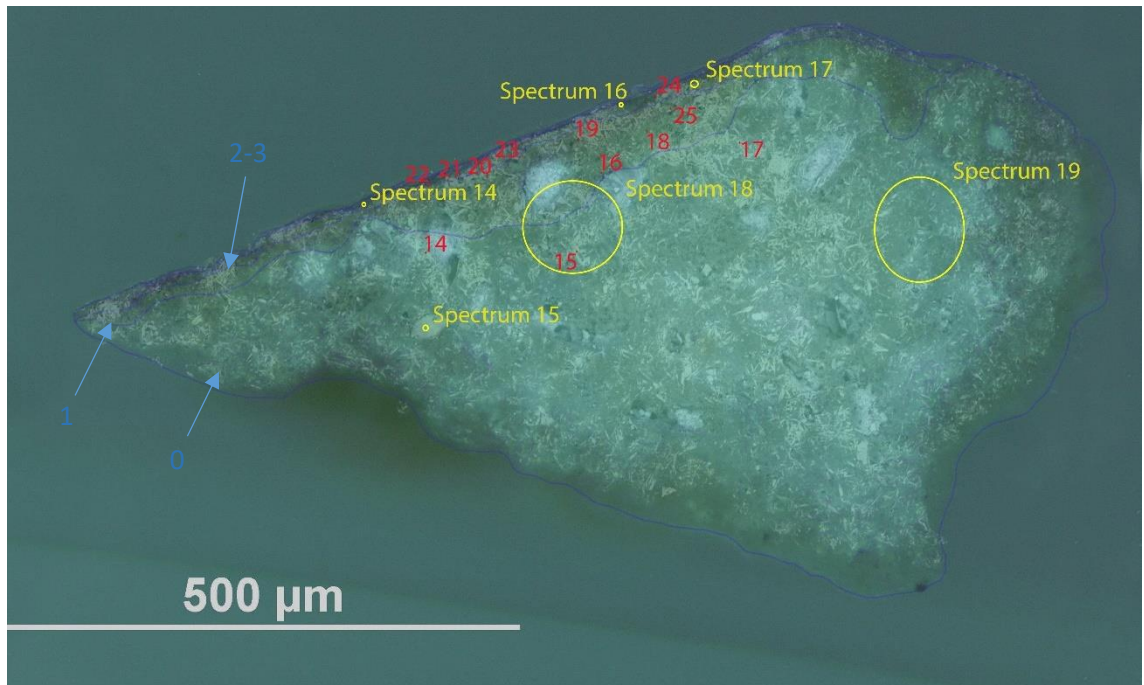


Below: Overlapped (OM and BSE) cross-section image showing the stratigraphy (blue indicators).

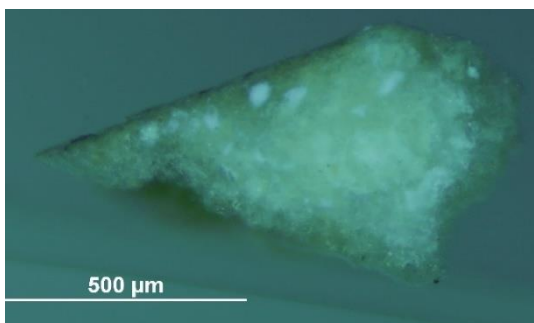
- 3. Varnish
- 2. Dark layer
- 1. Yellowish and undefined layer
- 0. Plaster bulk

**Analysis spots.** EDS analysis (yellow): Spectra 14-19; FT-IR analysis (red): nos. 14-25.

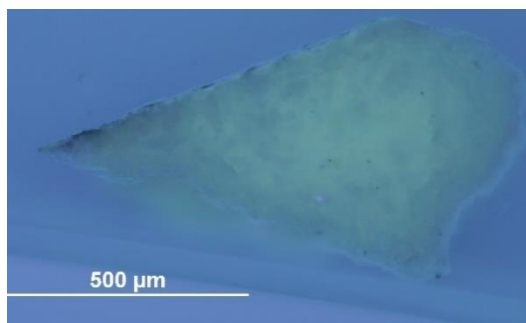
**Sampling.** This sample consists of a fragment taken from an area of loss on the vest of the figure in the third frame from the PR.



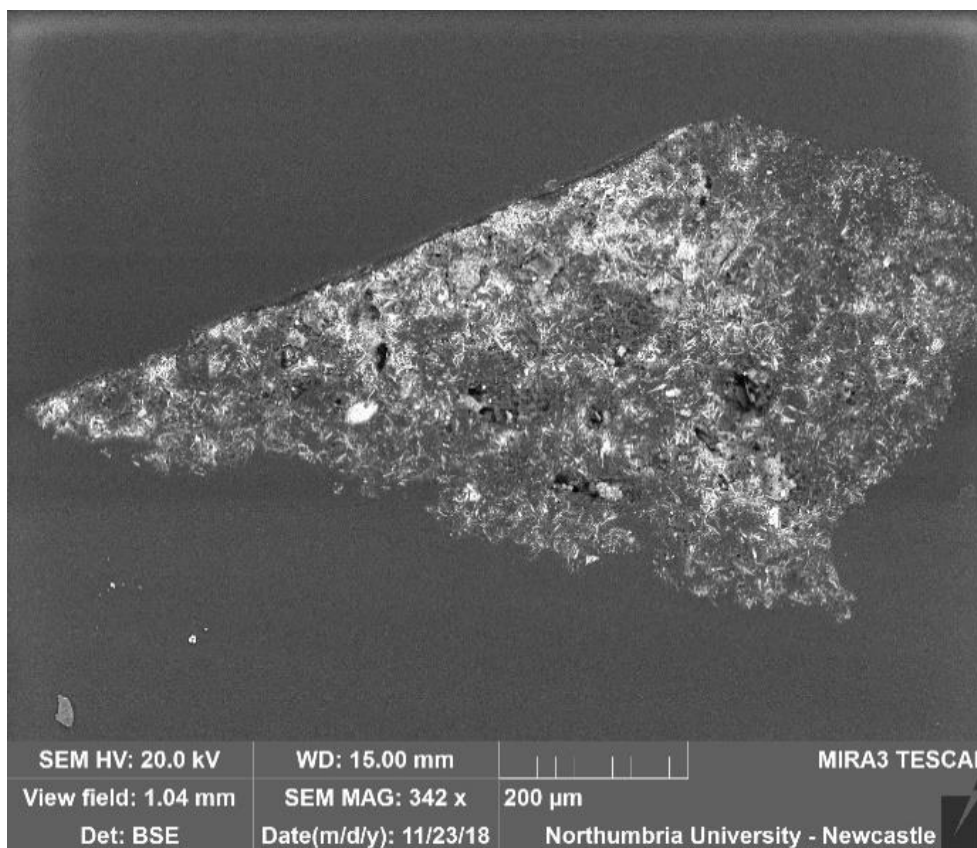
**Summary.** The substrate (layer 0) is made of plaster (**calcium sulfate**,  $\text{CaSO}_4$ , confirmed by EDS and by the peak at  $1600\text{ cm}^{-1}$  and overtones in the FT-IR spectra) and Si-Al inclusions and Fe are present in all the layers. The tabular crystalline structure typical of gypsum plaster can be seen in layers 0 and 1. Layer 1 is an intermediate layer, where the plaster is soaked with layer 2. Layer 2, dark under visible illumination, consists mostly of **silicon (Si)**. Traces of **Na, K, Cl, Fe** and **P** were detected in the utmost layers. Layer 3 fluoresces white under UV illumination. A **wax or resin** (FT-IR peaks at  $1200\text{-}1500$  and  $2800\text{-}3000\text{ cm}^{-1}$ ) was detected in all the layers.



VLR OM (above)



UVfOM (above)

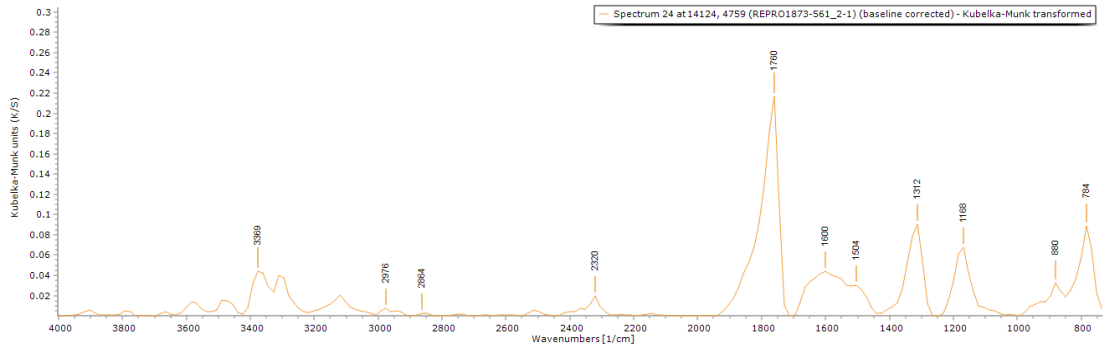


**EDS spectra and EDS mapping** suggest that the sample is mostly made of calcium sulfate (C, O, Ca, S), Al-Si inclusions are present in all the layers.

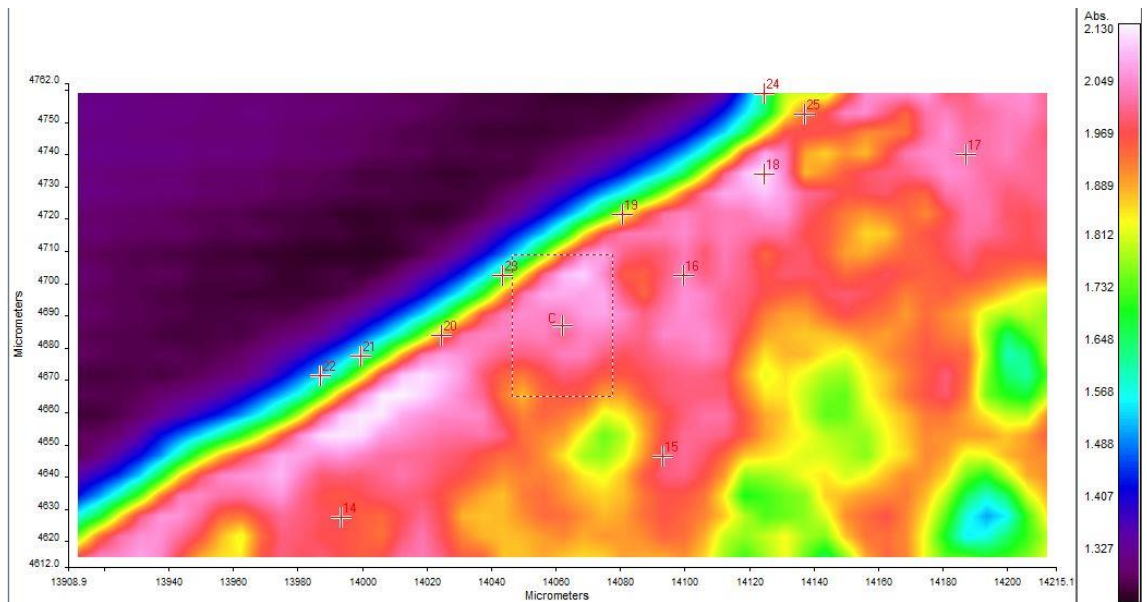
Layer 2 consists mostly of **silicon (Si)**.

Traces of **Na, K, Cl, Fe** and **P** were detected in the utmost layers.

The **BSE image (above)** shows that the tabular structure characteristic of gypsum is present in layer 0. The dark (lighter) inclusions are made of **potassium (K)**.



FT-IR spectrum 24 (above) of layers 2 and 3. Peaks for the casting resin (1312, 1760 cm<sup>-1</sup>), gypsum (1600 cm<sup>-1</sup>, overtone 2200-2300 cm<sup>-1</sup>) and a wax/resin (1000-1200, 1504, 2800-3000 cm<sup>-1</sup>). A summary of the peaks observed in the spectra 14-25 can be seen in the table below.



FT-IR (FPA) image (above). Some indication of different reflectance of the layers can be observed in the FPA image.

Spectrum	Layer	peaks (cm <sup>-1</sup> )							
		Casting Resin	Gypsum	Carbonate	Wax/resin	C=O ester carbonyl	SO overtone	Unknown	
14	0	1312	1600	800	832, 912, 992, 1072, 1216, 1440, 1648, 2880, 2992	1744		2208	
15	0	1328			784, 864, 896, 928, 976, 1056, 1200, 1264, 1456, 1568, 1664, 2880, 2960, 2992	1744		2251	
16	1	1760			816, 896, 960, 1024, 1104, 1216, 1296, 1392, 1504, 1584, 1680, 2848, 2960			2300	
17	0	1328	1600	800	912, 960, 1056, 1088, 1232, 1392, 1472, 2848, 2928	1744		2176, 1792	
18	1		1600	800, 1776	928, 1008, 1088, 1216, 1296, 1360, 1408, 1536, 2848, 2944			2289	
19	1	1312, 1760	1632		768, 880, 1168, 2800, 2912			2336	
20	1	1312, 1760	1632		768, 880, 1088, 1168, 1472, 1552, 2880			2384	
21	2-3	1312, 1760	1616		816, 1104, 1152, 1552			2336	
22	2-3	1312, 1760	1616	800	864, 1088, 1152			2352	
23	1	1312, 1760	1600	800	1088, 1168, 1520			2336	
24	2-3	1312, 1760	1600		784, 880, 1168, 1504, 2864, 2976			2320	
25	1	1312, 1760		800	848, 960, 1008, 1104, 1184, 1584, 2880			2336	

## Sample 3



Below: Overlapped (OM and BSE) cross-section image showing the stratigraphy (blue indicators).

**Sampling.** This is a loose fragment, taken from the base below the first frame.

2. Dark layer

1. Intermediate yellowish layer

0. Plaster bulk

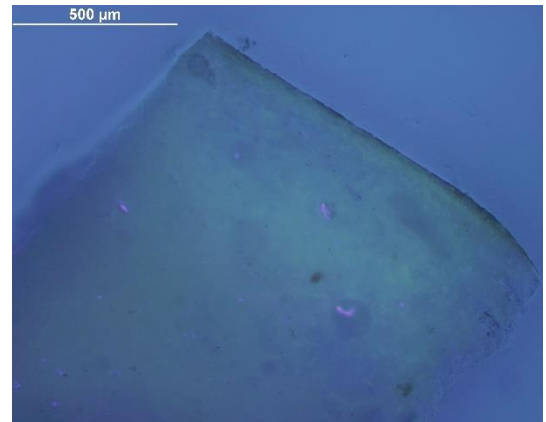
**Analysis spots.** EDS analysis (yellow): Spectra 20-25; FT-IR analysis (red): nos. 26-38.



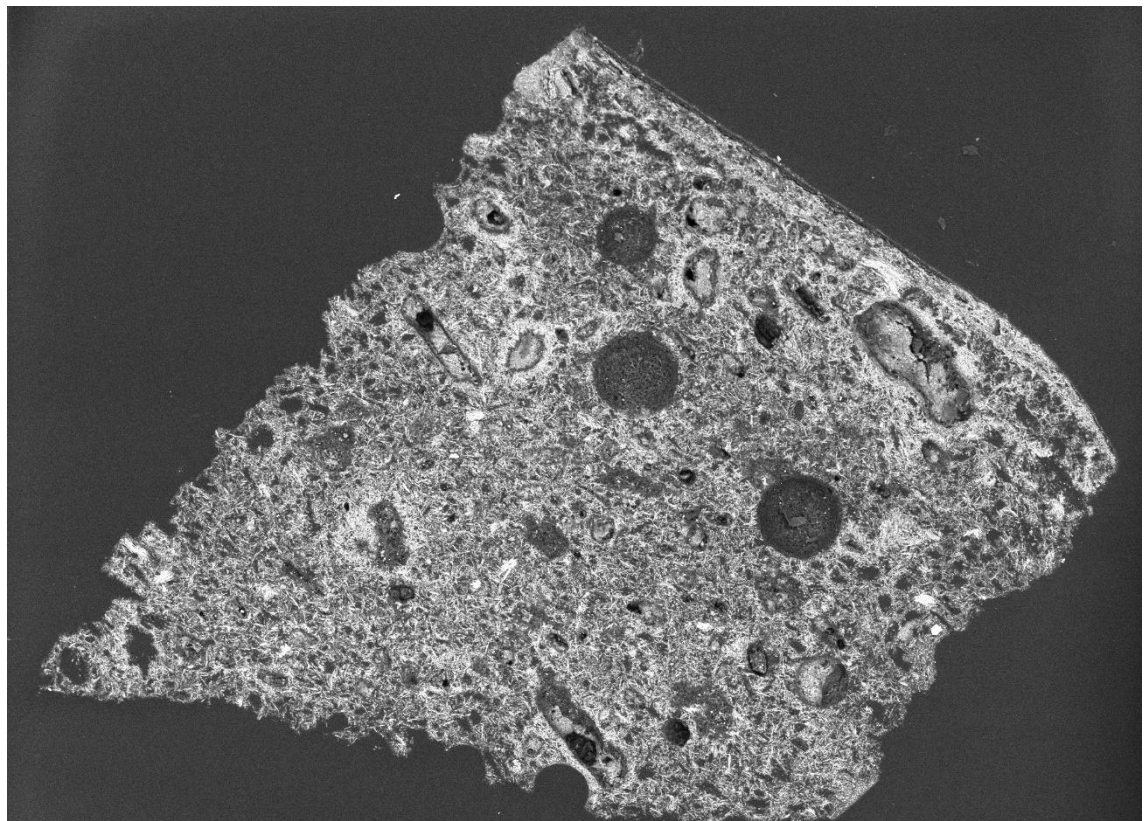
**Summary.** The sample is mostly made of C, O, S and Ca (**calcium sulfate**,  $\text{CaSO}_4$ , confirmed by EDS and by the peak at  $1600\text{-}1616\text{ cm}^{-1}$  in the FT-IR spectra). The tabular crystalline structure typical of gypsum plaster can be seen in layers 0 and 1. **Al-Si inclusions** were detected in all the layers and additional traces of **Na, Cl, Mg, K, Fe** and **Ba** were detected in the utmost layers. Layer 1 is yellow under visible illumination and consists of the plaster substrate soaked with the outmost layer. Layer 2 appears dark under visible illumination. A **wax or resin** is suggested by FT-IR (peaks at  $1000\text{-}1200$  and  $2800\text{-}3000\text{ cm}^{-1}$ ) and was detected in all the layers.



VLR OM (above)



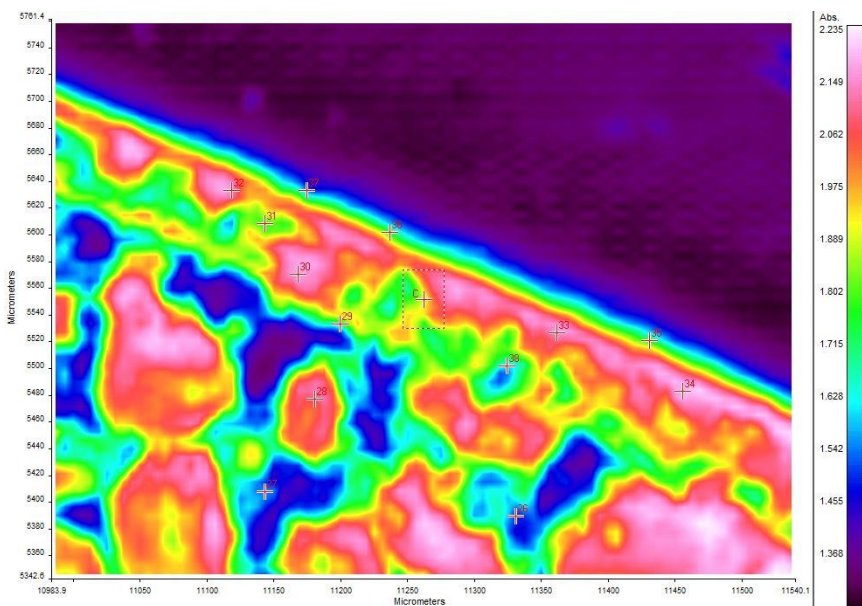
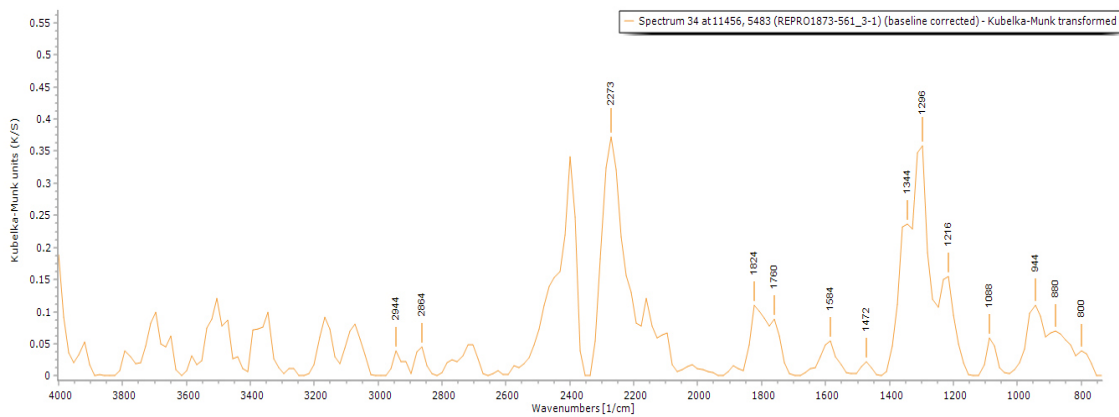
UVf OM (above)



SEM HV: 20.0 kV	WD: 16.16 mm	MIRA3 TESCAN
View field: 2.13 mm	SEM MAG: 168 x	500 µm
Det: BSE	Date(m/d/y): 11/26/18	Northumbria University - Newcastle

**BSE image** (above). The tabular crystalline structure typical of gypsum plaster can be seen in layers 0 and 1. Large pores are also visible.

**EDS spectra and mapping** suggest that **calcium sulfate** ( $\text{CaSO}_4$ ) and **Al-Si inclusions** were detected in all the layers. Additional traces of **Na, Cl, Mg, K, Fe** and **Ba** were detected in the utmost layers.



**FT-IR spectrum 34** (above) of layer 2. Peaks for the casting resin (1312, 1760  $\text{cm}^{-1}$ ) and a wax/resin (1472  $\text{cm}^{-1}$  and 2800-3000  $\text{cm}^{-1}$ ). A summary of the peaks observed in the spectra 26-38 can be seen in the table below.

**FT-IR (FPA) image** (left). Some indication of different reflectance of the layers can be observed in the FPA image.

Spectrum	Layer	peaks ( $\text{cm}^{-1}$ )						
		Casting Resin	Gypsum	Carbonate	Wax/resin	C=O ester carbonyl	SO overtone	Unknown
26	0	1312, 1760	1616		816, 864, 944, 1168, 1520			2336
27	0	1312, 1760	1616		896, 1008, 1088, 1168, 1504, 2960			2336
28	0	1312, 1760	1632		912, 1040, 1120, 1200, 1472, 1536, 1664, 2832, 2880, 2960		2208, 2400	1792
29	1	1312, 1760			832, 928, 1088, 1152, 1504, 1584, 2864			2336
30	1	1312, 1760	1632		784, 864, 928, 1008, 1088, 1232, 1376, 1472, 2848, 2944			2334
31	1	1312, 1760	1616		776, 832, 944, 1024, 1184, 1504, 2848, 2992			2336, 1888
32	1		1600	1776	784, 832, 896, 1008, 1136, 1168, 1296, 1344, 1392, 2880, 2976			2272
33	1	1328, 1760			832, 896, 992, 1040, 1200, 1472, 1520, 1568, 1696, 2816, 2880, 2992		2281	1808
34	2	1760		800	880, 944, 1088, 1216, 1296, 1344, 1472, 1584, 2864, 2944		2273	1824
35	2	1312, 1760			784, 912, 960, 1088, 1184, 1408, 1472, 1568, 2864			
36	2	1312, 1760	1600		784, 832, 1008, 1152, 1408, 1472, 2832		2352	
37	2	1312, 1760			784, 848, 896, 960, 1024, 1088, 1168, 1552			
38	1	1760	1632		752, 848, 960, 1072, 1200, 1296, 1472, 2864			

## Sample 4

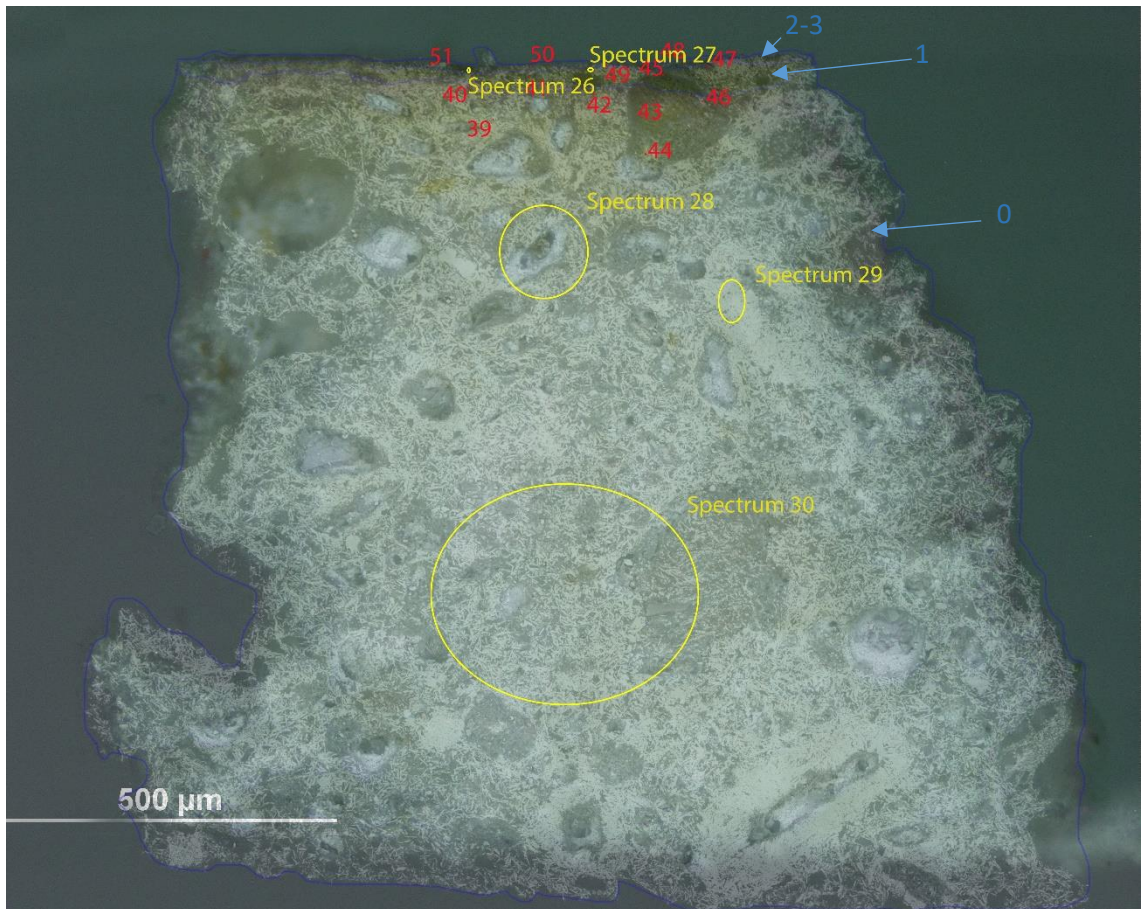


Below: Overlapped (OM and BSE) cross-section image showing the stratigraphy (blue indicators).

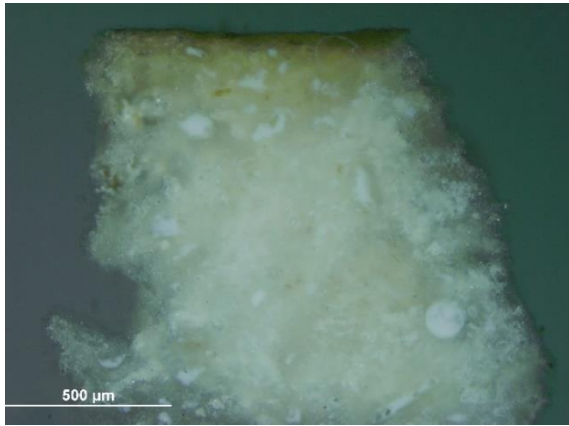
- 3. Varnish
- 2. Dark layer
- 1. Yellowish layer
- 0. Plaster bulk

**Sampling.** This fragment was taken from the greasy dark area; the fragment was almost detached. Taken from the edge of the PR column of the arc, backside.

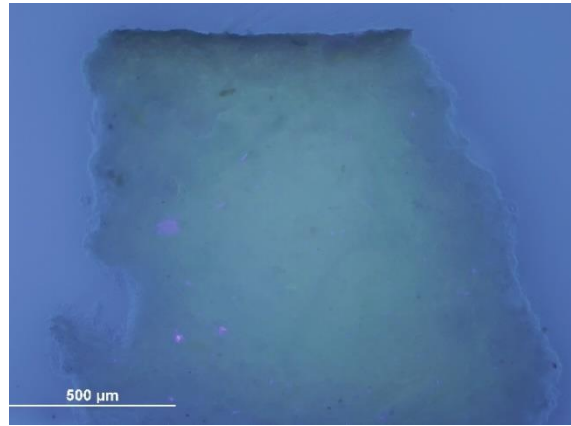
**Analysis spots.** EDS analysis (yellow): Spectra 26-29; FT-IR analysis (red): nos. 39-51.



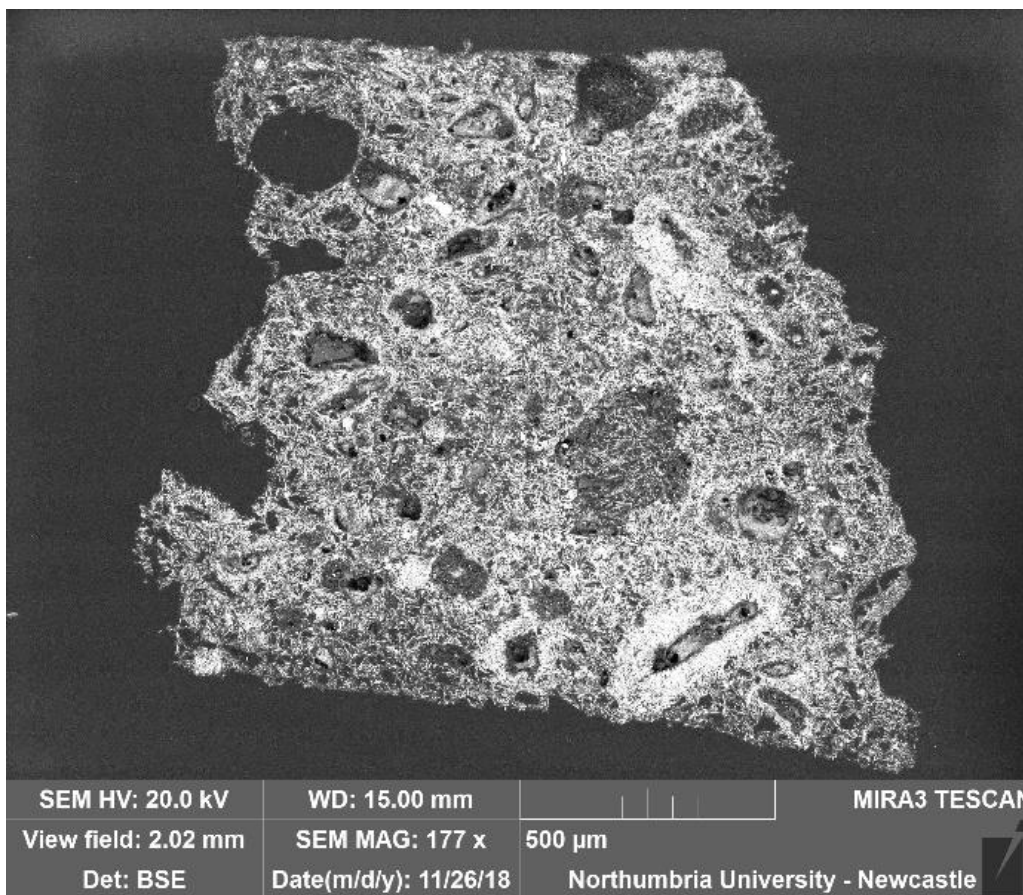
**Summary.** The sample is mostly made of C, O, S and Ca (**calcium sulfate**,  $\text{CaSO}_4$ , confirmed by EDS and by the peak at  $1600\text{-}1632\text{ cm}^{-1}$  in the FT-IR spectra). Al is overall present as used as a polishing agent, but could also, together with Si and Mg, be present as part of silicate inclusions, which are present in all the layers, but no particular element distribution in a layer fashion can be seen. Traces of **Cl**, **Na**, **K** and **Fe** were additionally detected in the surface layers. A **wax or resin** is suggested by FT-IR (peaks at  $1000\text{-}1200$  and  $2800\text{-}3000\text{ cm}^{-1}$ ) and was detected in all the layers.



VLR OM (above)



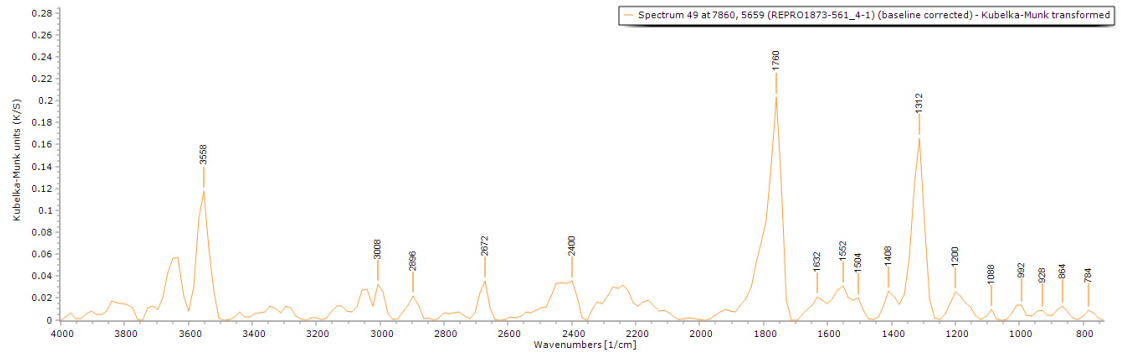
UVfOM (above)



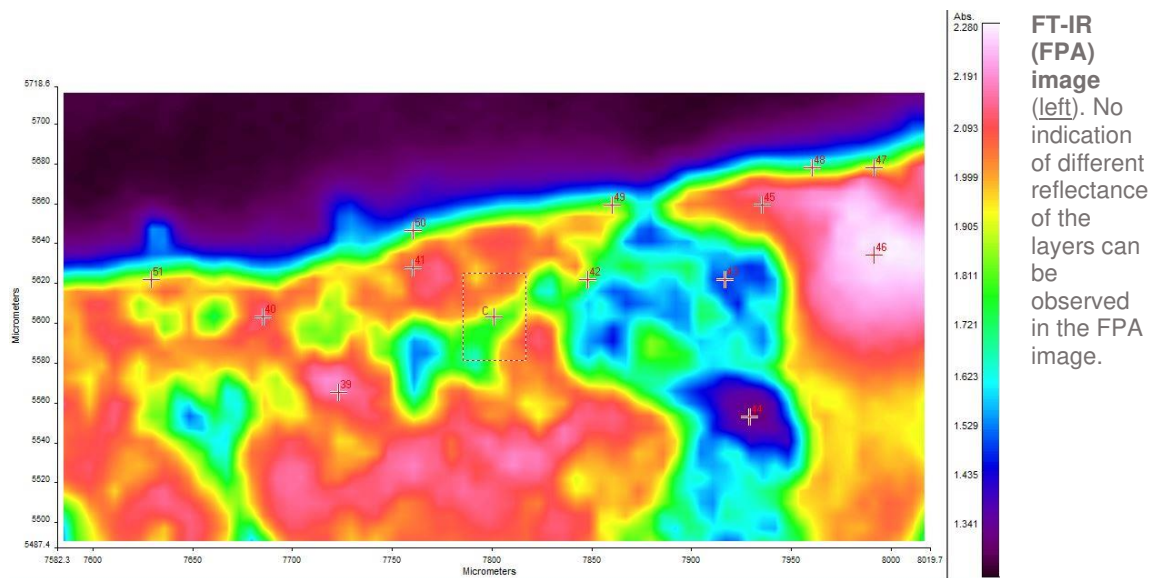
**BSE image (left).** The tabular crystalline structure typical of gypsum plaster can be seen in layers 0 and 1.

**EDS mapping** shows the presence of **Al-Si inclusions** but does not suggest any particular element distribution in a layer fashion.

**EDS spectra** indicate that all the layers consist of **C, O, Ca, S, Al, Si and Mg**. Traces of **Cl, Na, K and Fe** were additionally detected in the surface layer.



**FT-IR spectrum 49** (above) of layers 2-3. Peaks for the casting resin (1312, 1760  $\text{cm}^{-1}$ ), gypsum (1632  $\text{cm}^{-1}$ , overtone 2200-2300  $\text{cm}^{-1}$ ) and a wax/resin (1100-1500, 2800-3000  $\text{cm}^{-1}$ ). A summary of the peaks observed in the spectra 39-51 can be seen in the table below.



**FT-IR (FPA) image (left)**. No indication of different reflectance of the layers can be observed in the FPA image.

Spectrum	Layer	peaks ( $\text{cm}^{-1}$ )						
		Casting Resin	Gypsum	Carbonate	Wax/resin	C=O ester carbonyl	SO overtone	Unknown
39	0	1328	1632		768, 816, 864, 896, 1056, 1232, 1280, 1376, 1520, 2784, 2864	1744	2235	1792
40	0	1760			768, 896, 976, 1056, 1216, 1248, 1296, 1392, 1488, 1584, 2832, 2912		2260	
41	1		1600	800	880, 944, 976, 1072, 1136, 1232, 1296, 1472, 1552, 2816		2272	1777
42	0	1312, 1760	1616		848, 896, 992, 1072, 1152, 1216, 1472, 2960		2368	2688
43	0	1312, 1760	1616	800	896, 960, 1152, 1520, 2992			
44	0	1312, 1760	1616	800	880, 960, 1168, 1472			2224
45	1	1760	1632		784, 832, 928, 1024, 1088, 1216, 1296, 1472, 1520, 1584, 2800, 2992		2272	
46	0	1760			768, 848, 896, 928, 1040, 1088, 1152, 1216, 1344, 1408, 1456, 1584, 2800, 2912		2263	1824
47	1	1312, 1760	1616		784, 1072, 1168, 1472, 1552, 2848		2240	
48	2-3	1312, 1760	1600	800	944, 1088, 1168, 1504, 2828		2320	
49	2-3	1312, 1760	1632		784, 864, 928, 992, 1088, 1200, 1408, 1504, 1552, 2896		2400	2672
50	2-3	1312, 1760	1616		784, 1072, 1152, 1520, 2800			
51	2-3	1312, 1760		800	880, 1088, 1152, 1536, 1568, 2816, 2864			

## Sample 5

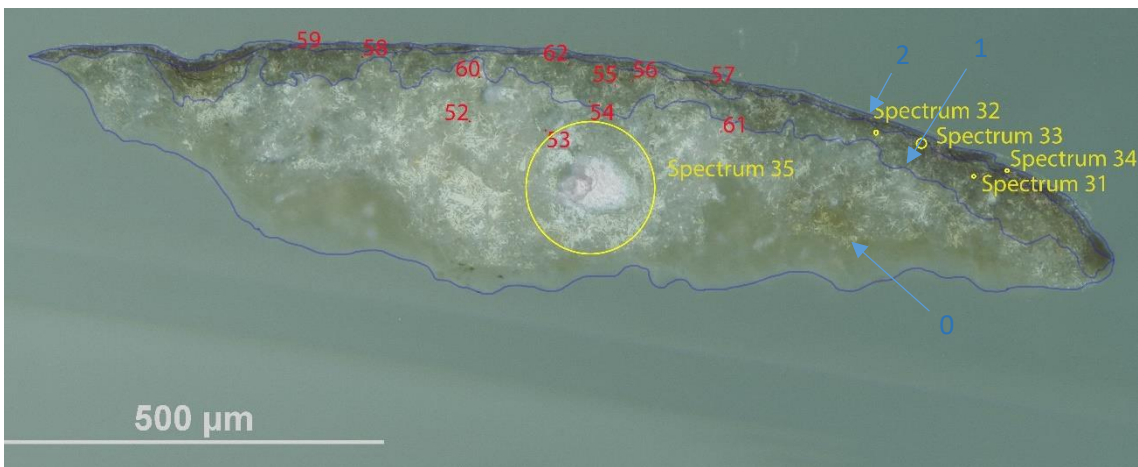


**Sampling.** This is a dark fragment taken from the vest of the ninth figure from the PR on the second level of columns.

Below: Overlapped (OM and BSE) cross-section image showing the stratigraphy (blue indicators).

- 2. Dark layer
- 1. Yellow layer
- 0. Plaster bulk

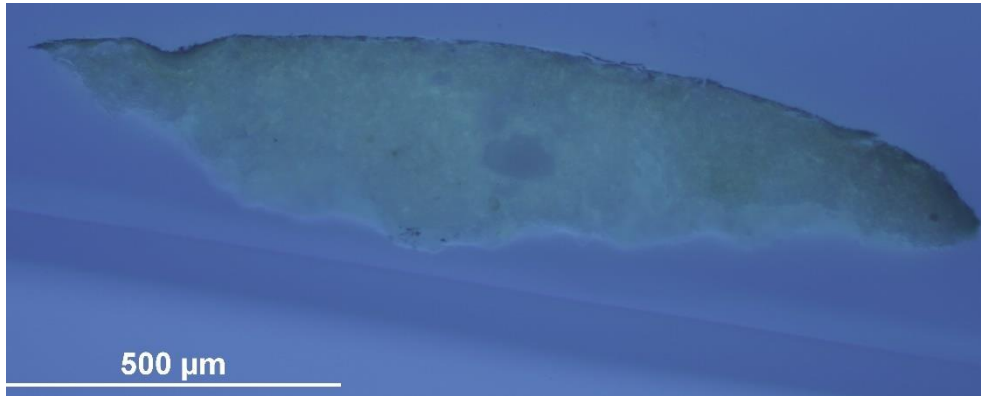
**Analysis spots.** EDS analysis (yellow): Spectra 31-35; FT-IR analysis (red): nos. 52-62.



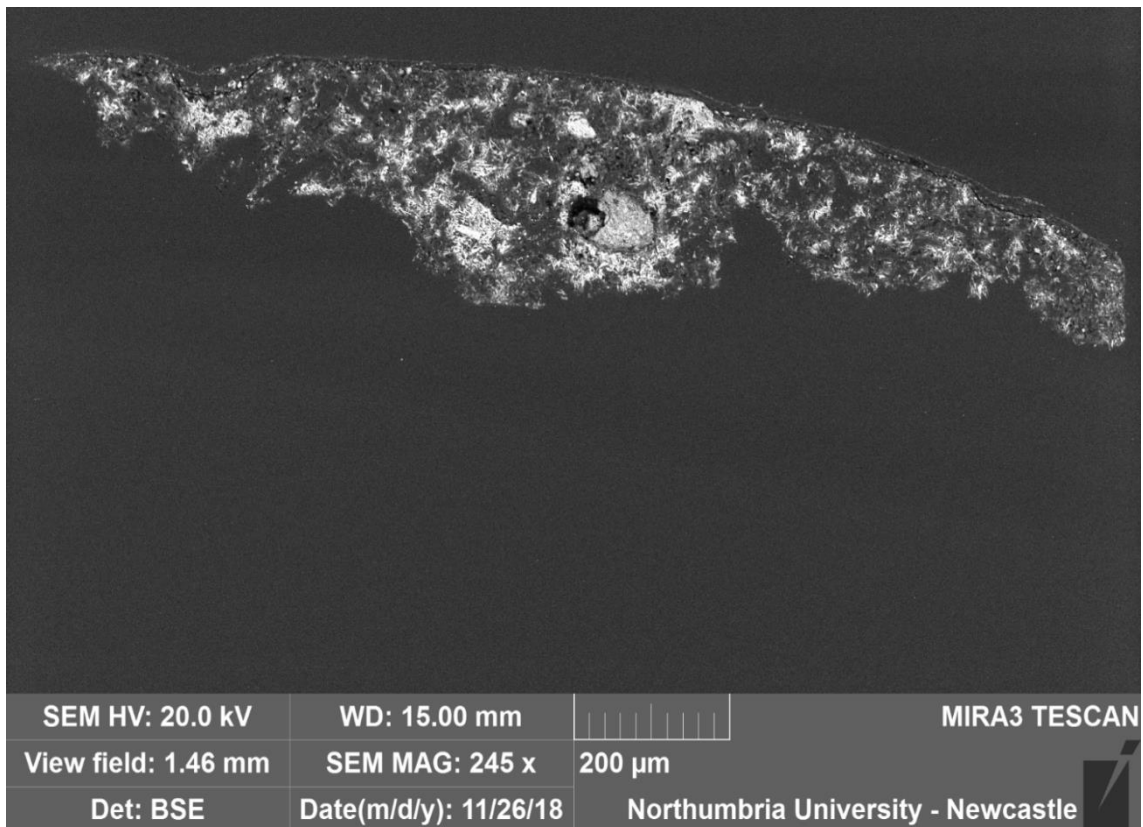
**Summary.** The sample is mostly made of C, O, S and Ca (**calcium sulfate**,  $\text{CaSO}_4$ , confirmed by EDS and by the peak at  $1600\text{-}1632\text{ cm}^{-1}$  in the FT-IR spectra). **Si-Al inclusions** are present in all the layers and additional traces of **Mg, K, Fe, Pb, Cl** and **Na** were detected in the utmost layers. The structure typical of gypsum plaster can be seen in layers 0 and 1. A **wax or resin** is suggested by FT-IR (peaks at  $1000\text{-}1500$  and  $2800\text{-}3000\text{ cm}^{-1}$ ) and was detected in all the layers.



VLR OM  
(left)

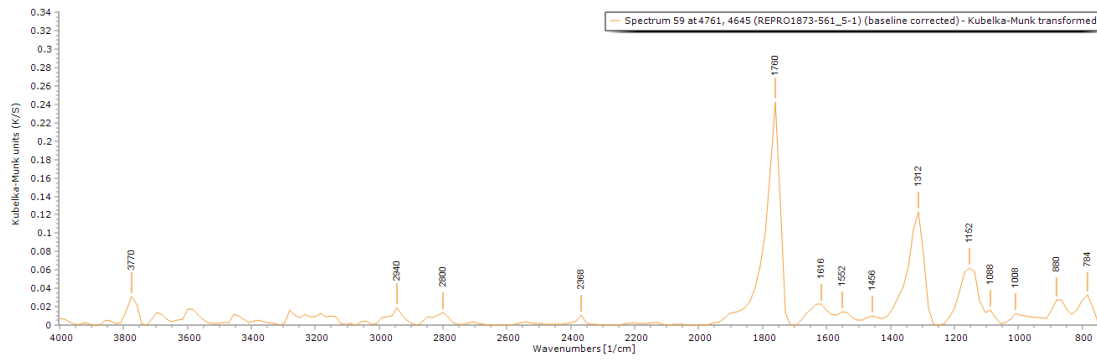


UVfOM  
(left)



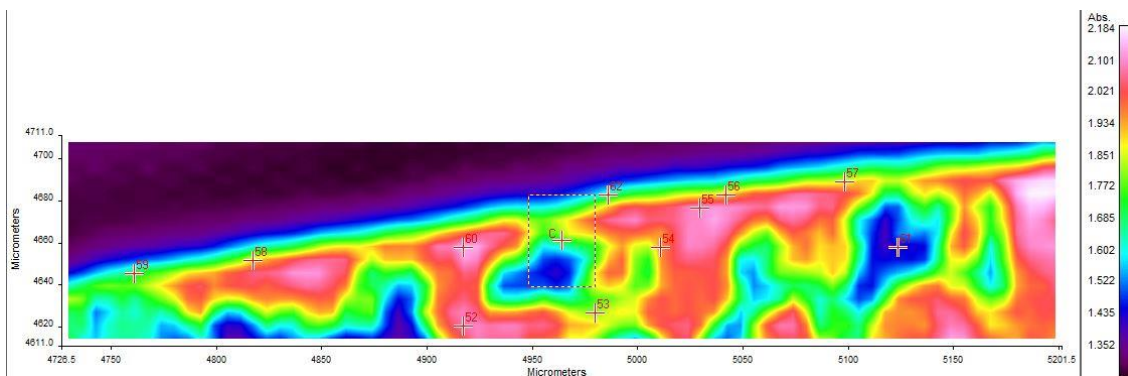
**BSE image** (above). The tabular crystalline structure typical of gypsum plaster can be seen in layers 0 and 1.

**Calcium sulfate (CaSO<sub>4</sub>)** and **Al-Si inclusions** were detected in all the layers. Additional traces of **Mg, K, Fe, Pb, Cl** and **Na** were detected in the utmost layers.



**FT-IR spectrum 59** (above) of layer 2. Peaks for the casting resin (1312, 1760  $\text{cm}^{-1}$ ), gypsum (1632  $\text{cm}^{-1}$ , overtone 2200-2300  $\text{cm}^{-1}$ ) and a wax/resin (1456  $\text{cm}^{-1}$  and 2800-3000  $\text{cm}^{-1}$ ). A summary of the peaks observed in the spectra 52-62 can be seen in the table below.

**FT-IR (FPA) image** (below). No indication of different reflectance of the layers can be observed in the FPA image.



Spectrum	Layer	peaks ( $\text{cm}^{-1}$ )						
		Casting Resin	Gypsum	Carbonate	Wax/resin	C=O ester carbonyl	SO overtone	Unknown
52	0	1760	1600		816, 896, 944, 1008, 1120, 1296, 1376, 1456, 1536, 2848, 2976		2272	
53	0	1312, 1760			784, 1072, 1392, 1456, 1584, 1680, 2816		2288, 2416	
54	1	1312, 1760			770, 928, 1088, 1136, 1408, 1488, 1680, 2880, 2944		2240	
55	1	1328, 1760	1600		880, 944, 1024, 1200, 1392, 1472, 1664, 2776, 2848, 2960		2384	
56	1	1312, 1760	1632		784, 880, 976, 1088, 1152, 1488, 2848, 2960			
57	2	1312, 1760	1616		784, 864, 1024, 1152, 1392, 1488, 2841, 2912		2304	
58	1	1312, 1760			960, 1072, 1184, 1488, 1584, 2912		2384	
59	2	1312, 1760	1616		784, 880, 1008, 1088, 1152, 1456, 1552, 2800, 2940		2368	
60	0	1328, 1760	1632	800	928, 992, 1072, 1168, 1472, 1568, 2816, 2928		2272, 2420	
61	0	1312, 1760	1600		832, 1152, 1488			
62	1	1312, 1760	1616		864, 928, 1088, 1152, 1200, 1520, 2944			

## Sample 6



Below: Overlapped (OM and BSE) cross-section image showing the stratigraphy (blue indicators).

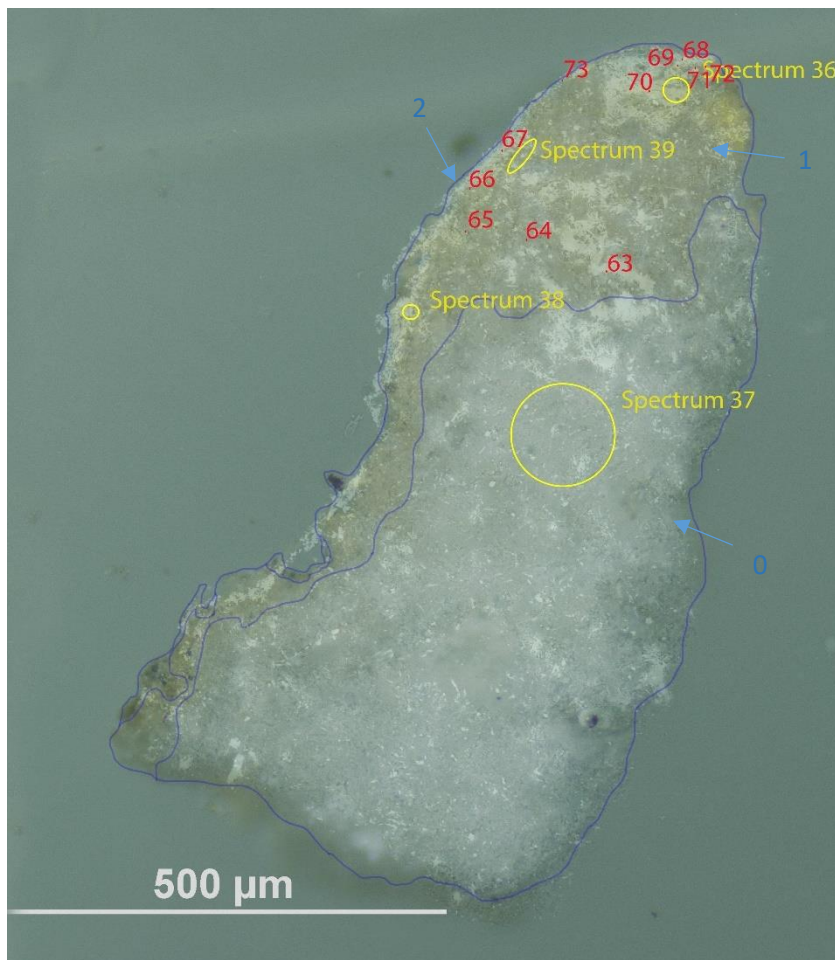
### 2. Dark layer

### 1. Yellowish and undefined layer

### 0. Plaster bulk

**Sampling.** This fragment was taken from an area of loss from the foot of the eighth figure from the PR on the second level of columns.

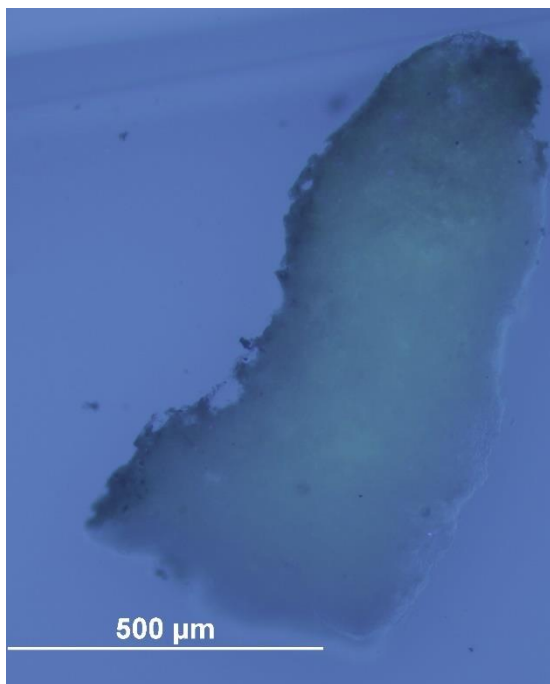
**Analysis spots.** EDS analysis (yellow): Spectra 36-39; FT-IR analysis (red): nos. 63-73.



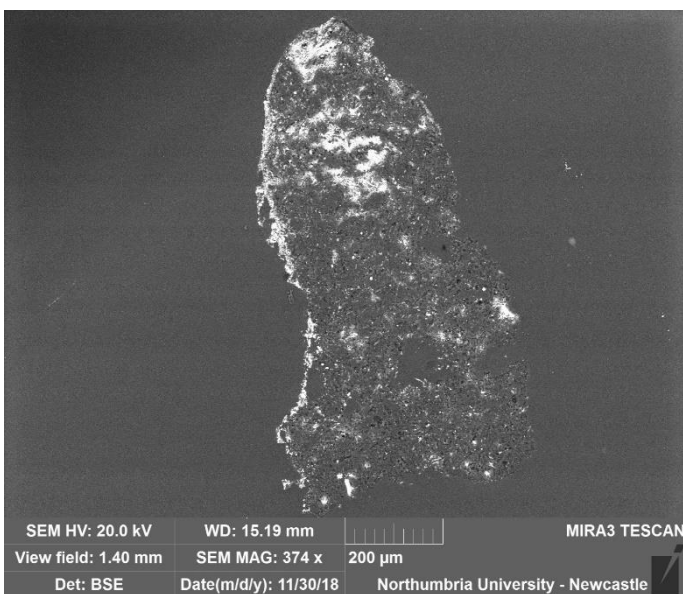
**Summary.** The sample is mostly made of C, O, S and Ca (**calcium sulfate**,  $\text{CaSO}_4$ , confirmed by EDS and by the peak at  $1600\text{-}1632\text{ cm}^{-1}$  in the FT-IR spectra). The structure typical of gypsum plaster can be seen in layers 0 and 1. **Si-Al inclusions** are present in all the layers. Layer 2 mainly consists of **Si**, **Ba** and **Ti**. Additional traces of **Fe**, **Na**, **K**, **Mg**, **Mn** and **Cl** were detected in the utmost layers. A **wax or resin** is suggested by FT-IR (peaks at  $1000\text{-}1500$  and  $2800\text{-}3000\text{ cm}^{-1}$ ) and was detected in all the layers. py-TMAH-GC/MS shows markers characteristic of a **diterpenic resin** (Colombini & Modugno, 2009).



VLR OM (above)



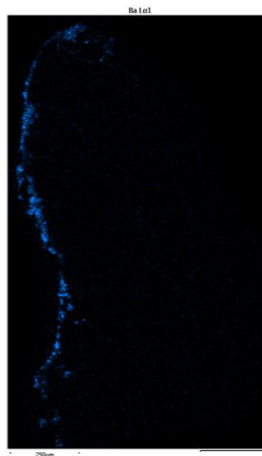
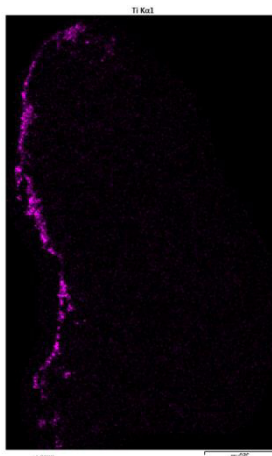
UVfOM (above)

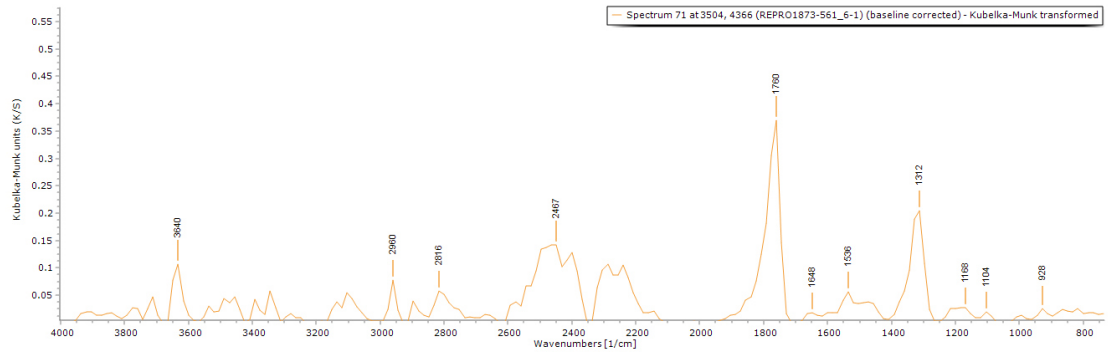


**BSE image (left).** The tabular crystalline structure typical of gypsum plaster can be seen in layers 0 and 1.

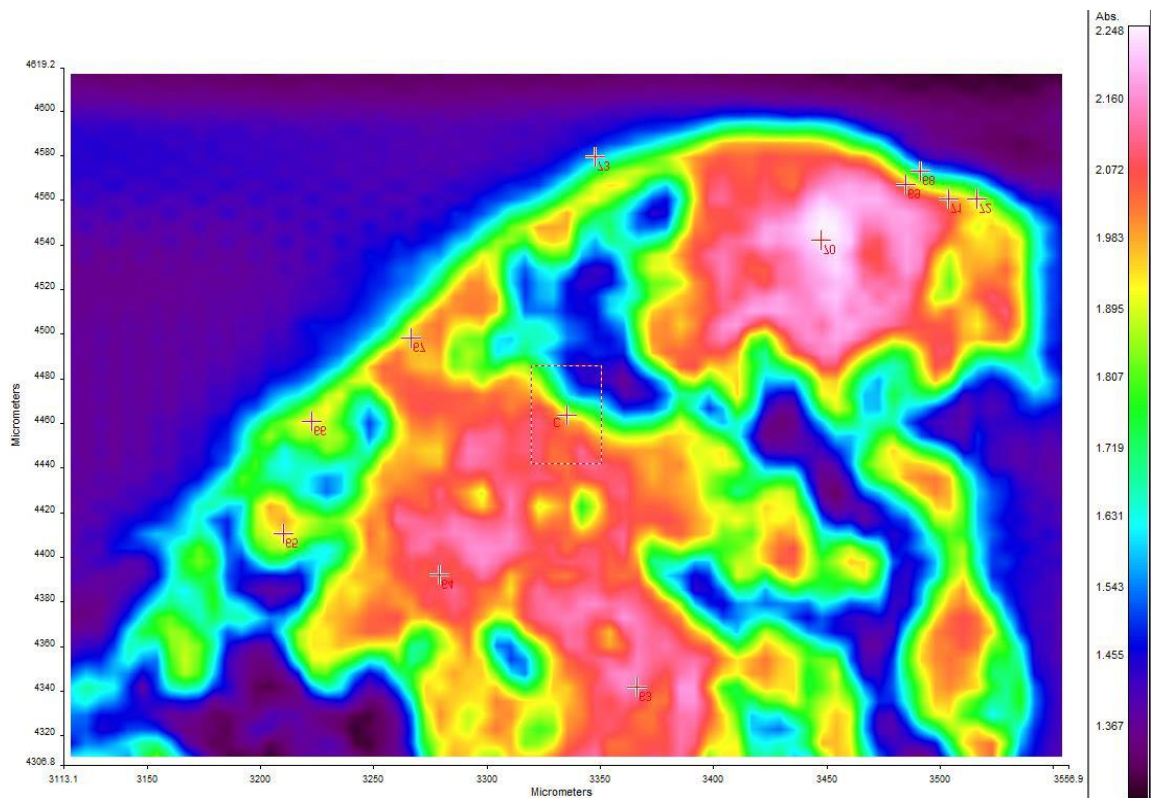
**Layers 0 and 1** consists of **calcium sulfate (CaSO<sub>4</sub>)**. **Silicon (Si)** and **Aluminium (Al)** inclusions are present in all the layers.

**Layer 2** shows a higher concentration of **Si, Ba** and **Ti** (see **EDS mapping** below). **Barium** and **Titanium** could be mixed in the spectra, but it was clear that they were both present in the sample. Traces of **Fe, Na, K, Mg, Mn** and **Cl** were also detected in layer 2.



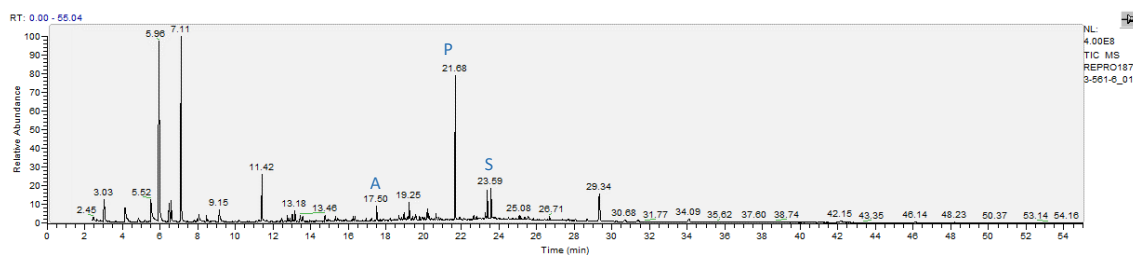


**FT-IR spectrum 71** (above) of layer 2. Peaks for the casting resin (1312, 1760  $\text{cm}^{-1}$ ) and a wax/resin (1536  $\text{cm}^{-1}$  and 2800-3000  $\text{cm}^{-1}$ ). A summary of the peaks observed in the spectra 63-73 can be seen in the table below.



**FT-IR (FPA) image** (above). Some indication of different reflectance of the layers can be observed in the FPA image.

Spectrum	Layer	peaks ( $\text{cm}^{-1}$ )						
		Casting Resin	Gypsum	Carbonate	Wax/resin	C=O ester carbonyl	SO overtone	Unknown
63	1	1312	1600		768, 832, 880, 960, 1072, 1408, 1696, 2864, 2944		2256	1792
64	1	1312	1616	1776	880, 960, 992, 1120, 1456, 2720, 2816, 2912	1728	2224, 2384	1824
65	1	1328	1632		768, 848, 960, 1104, 1136, 1200, 1408, 1472, 2912		2368	
66	2	1312, 1760	1600		768, 1088, 1216, 1376, 1504, 1664, 2912		2384	1872
67	2	1312, 1760	1632		752, 880, 1168, 1488, 2880		2304	
68	2	1312, 1760	1616		832, 896, 1168, 1408, 1504, 2960		2368	
69	2	1312, 1760	1616		784, 848, 912, 976, 1024, 1072, 1168, 1456, 2896, 2944		2320	
70	1				768, 880, 928, 1008, 1072, 1280, 1376, 1504, 1584, 2832	1744	2144, 2272, 2400	1808, 1856, 1952, 2016
71	2	1312, 1760	1648		928, 1104, 1168, 1536, 2816, 2960		2467	
72	2	1328, 1760	1600, 1632	800	928, 1184, 1392, 1488, 1536, 2832, 2960		2368	
73	2	1312, 1760	1648		832, 896, 1088, 1168, 1584, 2864			



RT	m/z	Assignment	Formula
3.03	41(68), 44(14), 58(47), 69(100), 85(16), 100(33)	2-Propenoic acid, 2-methyl-, methyl ester	C5H8O2
4.16	45(100), 74(57), 91(1)	Acetaldehyde, methoxy-	C3H6O2
5.52	42(11), 58(100), 88(3), 116(3)	1,2-Ethanediamine, N'-ethyl-N,N-dimethyl-	C6H16N2
5.96	42(11), 58(100), 117(14)	1,2-Ethanediamine, N'-ethyl-N,N-dimethyl-	C6H16N2
6.5	45(18), 58(32), 66(21), 95(100), 125(7)	Sulfuric acid, dimethyl ester	C2H6O4S
7.11	56(7), 72(100), 116(2), 131(3)	1,2-Ethanediamine, N'-ethyl-N,N-dimethyl-	C6H16N2
9.15	44(100), 58(37), 86(61), 105(4), 128(53)	Unidentified amine fragment	
11.42	42(7), 58(100), 70(10), 115(5), 146(2)	1,2-Ethanediamine, N'-ethyl-N,N-dimethyl	C6H16N2
13.18	58(36), 74(100), 88(25), 98(37), 116(39), 130(100), 140(9), 189(1)	Unidentified amine fragment	
17.5	43(16), 55(62), 74(63), 83(59), 87(27), 97(21), 111(54), 124(27), 143(31), 152(100), 185(39)	Nonanedioic acid, monomethyl ester	C10H18O4
18.97	44(25), 58(65), 71(27), 91(37), 105(29), 121(24), 135(49), 147(29), 163(100), 179(5), 195(36), 208(5), 239(5)	Unidentified terpenoid fragment	
19.25	45(74), 59(57), 71(47), 75(77), 85(77), 101(64), 109(90), 115(30), 156(41), 169(100), 183(5), 197(5), 215(5), 229(5), 257(5)	Unidentified terpenoid fragment	
20.2	45(93), 58(77), 71(68), 85(87), 101(100), 115(38), 123(5), 139(35), 161(29), 183(5), 207(5), 231(5), 250(5)	Unidentified terpenoid fragment	
20.68	45(81), 58(100), 69(67), 83(93), 97(57), 111(43), 125(5), 139(34), 153(5), 167(5), 179(5), 199(5), 227(5), 264(5)	Unidentified terpenoid fragment	
21.68	55(17), 74(100), 87(71), 143(23), 199(7), 227(16), 239(6), 270(5)	methyl palmitate	C17H34O2
23.35	59(100), 74(7), 87(5), 97(3), 165(5), 253(4), 285(3)	Unidentified FA fragment	
23.59	55(22), 74(100), 87(75), 97(7), 129(8), 143(28), 185(6), 199(14), 255(18), 298(6)	methyl stearate	C19H38O2
29.34	45(48), 55(58), 69(61), 83(100), 97(70), 111(52), 125(23), 139(5), 153(5), 167(5), 207(5), 223(5), 237(5), 265(5), 308(5), 336(5)	Unidentified terpenoid fragment	
30.68	44(59), 58(100), 73(32), 79(21), 91(5), 121(5), 155(5), 191(5), 207(48), 281(12), 311(16), 339(5), 371(5), 386(5)	Unidentified terpenoid fragment	
34.09	44(63), 58(100), 83(62), 97(46), 111(33), 191(5), 207(49), 281(5), 355(5)	Dihydroxydehydroabiatic acid fragment	
42.19	58(100), 69(55), 83(85), 97(63), 111(45), 207(59), 281(5), 355(5)	Dihydroxydehydroabiatic acid fragment	

RT = retention time, m/z = mass/charge ratio

**py-TMAH-GC/MS chromatogram** (top and described in the table above) shows small fragments due to derivatization (from  $t = 3.03$  to  $11.42$  min) and markers characteristic of a **diterpenic resin** ( $t = 20.68$ ,  $29.34$ ,  $30.68$ ,  $34.09$  and  $42.19$ ) (Colombini & Modugno, 2009; Mills & White, 2012). The presence of **methyl azelate** ( $t = 17.50$ ), **methyl palmitate** ( $t = 21.67$ ) and **stearate** ( $t = 23.60$ ) might suggest that the resin has been mixed with an **oil** ( $P/S = 2.81$ ), but the low **A/P ratio** ( $A/P = 0.17$ ) suggests that the FA are either from a non-drying oil, another source of lipids or naturally present in the resin (Colombini & Modugno, 2009).

## Experimental

The object was observed, and its conditions were documented. Samples from selected areas were taken by Valentina Risdonne. When possible, each sample was split into two parts: one fragment was embedded in polyester resin (Tiranti clear casting resin), polished and analysed under optical microscope and the other was put aside for py-TMAH-GC/MS and XRD analysis.

The optical microscopy was performed with an Olympus BX51 Metallurgical Microscope equipped with four objectives (magnification of x5, x20, x50 and x100), and an x10 eyepiece. In many instances, a small amount of white spirit was applied on the surface of the cross-section to improve the saturation under the microscope. The microscope is equipped with a 6-cube filter turret which allows to operate the system in reflected visible light (brightfield and darkfield mode) and reflected UV light (365 nm) using a 100 W mercury burner.

The SEM-EDS analyses were performed with a field emission TESCAN MIRA 3 with gigantic chamber. The SEM is equipped with: secondary electron detector (SE), secondary electron in-beam detector (In-beam SE), back-scatter detector (BSE), back-scatter in-beam detector (In-beam BSE), cathodoluminescence detector (without wavelength detection) (CL), plasma chamber/sample cleaner and software Alicona 3D imaging. For the EDS analytical part, it has an Oxford Instruments setup: Software: AztecEnergy, X-ray detector X-Max 150 mm<sup>2</sup> and X-ray detector X-Max Extreme, low energy detector for thin films, high resolution and low voltage. The samples were analysed by SEM-EDS Low Vacuum Mode (10-15 Pa). EDS Mapping and data processing were performed with Aztec Oxford software.

A Perkin Elmer Frontier FT-IR spectrometer (350 cm<sup>-1</sup> at the best resolution of 0.4 cm<sup>-1</sup>) was used, equipped with a germanium crystal for ATR measurements and combined with a Spectrum Spotlight 400 FT-IR microscope equipped with a 16×1 pixel linear mercury cadmium telluride (MCT) array detector standard with InGaAs array option for optimised NIR imaging. Spectral images from sample areas are possible at pixel resolutions of 6.25, 25, or 50 microns. The Perkin Elmer ATR imaging accessory consists of a germanium crystal for ATR imaging. These run with Perkin Elmer Spectrum 10™ software and with SpectrumIMAGE™ software. Baseline and Kubelka-Munk corrections were applied to the raw data acquired in diffuse reflectance.

The XRD analyses were performed with a Rigaku SmartLab SE equipped with a HyPix-400, a semiconductor hybrid pixel array detector and Cu source. The analyses were performed in Bragg-Brentano geometry mode, with 40 kV tube voltage and 50 mA tube current. The diffractograms were processed with a SmartLab II software. The data was compared to the RUFF database (Lafuente et al., 2016) COD Database (Gražulis et al., 2009).

The instrument used for GC/MS is a Thermo Focus Gas Chromatographer with DSQ II single quadrupole mass spec. The column currently installed is an Agilent DB5-MS UI column (ID: 0.25 mm, length: 30 m, df: 0.25 µm, Agilent, Santa Clara, CA, USA). Carrier gas: helium. Detector temperature: 280 °C, Injector temperature: 250 °C. It can be used with the PyroLab 2000 Platinum filament pyrolyser (PyroLab, Sweden) attachment or in split/splitless mode. Detection: Total Ion monitoring (TIC). 1 µl of the sample with 1 µl of TMAH was placed on the Pt filament for the py-GC/MS. The inlet temperature to the GC was kept at 250 °C. The helium carrier gas flow rate was 1.5 ml/min with a split flow of 41 ml/min and split ratio of 27. The MS transfer line was held at 260 °C and the ion source at 250 °C. The pyrolysis chamber was heated to 175 °C, and pyrolysis was carried out at 600 °C for 2 s. This run with Xcalibur™ and PyroLab™ software. The library browser supported NIST MS Version 2.0 (Linstrom & Mallard, 2014).

Valentina Risdonne, PhD student

[v.risdonne@vam.ac.uk](mailto:v.risdonne@vam.ac.uk) / [valentina.risdonne@northumbria.ac.uk](mailto:valentina.risdonne@northumbria.ac.uk)

Victoria and Albert Museum – Northumbria University

PhD project 'Materials and techniques for coating of the nineteenth-century plaster casts'

©V&A Museum

30 October 2020

## Notes

10 September 2018	Sampling	Valentina's PhD Lab book 1, page 112
24 October 2018	Casting	Valentina's PhD Lab book 1, page 133
6 November 2018	Microscopy	Valentina's PhD Lab book 1, page 137
14 October 2019	FT-IR	Valentina's PhD Lab book 1, page 175
3 December 2019	XRD	Valentina's PhD Lab book 2, page 4
18 March 2020	GC/MS	Valentina's PhD Lab book 2, page 50

A full record of analyses is available at <https://doi.org/10.25398/rd.northumbria.13811594>

## References

- Colombini, M. P., & Modugno, F. (2009). *Organic mass spectrometry in art and archaeology*. John Wiley & Sons.
- Gražulis, S., Chateigner, D., Downs, R. T., Yokochi, A. F. T., Quirós, M., Lutterotti, L., Manakova, E., Butkus, J., Moeck, P., & Le Bail, A. (2009). Crystallography Open Database—an open-access collection of crystal structures. *Journal of Applied Crystallography*, 42(4), 726–729.
- Lafuente, B., Downs, R. T., Yang, H., & Stone, N. (2016). The power of databases: the RRUFF project. In *Highlights in mineralogical crystallography* (pp. 1–29). Walter de Gruyter GmbH.
- Linstrom, P. J., & Mallard, W. G. (2014). *NIST chemistry WebBook, NIST standard reference database number 69, National Institute of Standards and Technology, Gaithersburg MD, 20899*.
- Mills, J., & White, R. (2012). *Organic chemistry of museum objects*. Routledge.



**Northumbria  
University**  
NEWCASTLE

Analysis Report - Valentina Risdonne

Copy of a Font

(REPRO.1874-29)

Initiator: Charlotte Hubbard; Conservation Department

23 October 2020

© Victoria and Albert Museum

V&A

## Analysis Report - Copy of a Font (REPRO.1874-29)

### Contents

Contents.....	188
List of abbreviations.....	188
Summary.....	189
Sample 1.....	192
Sample 2.....	196
Sample 3.....	199
Sample 4.....	202
Sample 5.....	206
Sample 6.....	209
Experimental.....	213
Notes.....	214
References.....	214

### List of abbreviations

BSE	Back Scattered Electron
EDS	Energy Dispersive Spectrometry
FT-IR	Fourier-Transform Infra-Red
FPA	Focal Plane Array
GC/MS	Gas Chromatography-Mass Spectrometry
OM	Optical Microscopy
PL	Proper Left
PR	Proper Right
py	pyrolysis
SEM	Scanning Electron Microscopy
TMAH	tetramethylammonium hydroxide
UVf	Ultraviolet Fluorescence
VLR	Visible Light Reflectance
XRD	X-ray Diffraction

## Summary

In summary, the bulk of the object is made of gypsum plaster, which contains several types of inclusions (including silicates and carbonates). By looking at the results, it is possible to hypothesise that in the surface layer, containing **Si** and **Al**, but also Cu, Cl, Zn, Fe, P, Mg and K the organic medium is **shellac** and that the additionally a **drying oil** was either mixed with the organic medium or applied onto the surface. **Sample 6** appears different from the rest of the samples, presenting extra layers, and it is possible that this area was repaired.



Figure 1. The copy of a font.

The object, '**Copy of a Font (REPRO.1874-29)**' (Figure 1), is a plaster cast, made by Friedrich Küsthardt in about 1874, reproducing a bronze baptismal font (about 1220-25) from Hildesheim Cathedral, Germany. The font represents on the cover Moses and Aaron on either side of an altar, an Allegory of Pity, the Anointing of Christ by St. Mary Magdalen, and the Judgment of Solomon; on the bowl, the Passage through the Red Sea of the Israelites and the Ark of the Covenant, the Baptism of Christ, and the Virgin and Child between two bishops and the Provost Wilbernus at her feet; the figures supporting the font represent the Rivers of Paradise, which flowed from the Garden of Eden. The kneeling figure in front of the Virgin and Child is probably the man who commissioned the font, Wilbrandus of Oldenburg. The cast was purchased from F. Küsthardt in 1874 for £19 and is now located in Room 46A (The Ruddock Family Cast Court). Its dimensions are 183.0 cm (h), 99.0 cm (d).

In April 2011 the conservator **Sarah Healey-Dilkes** suggested the removal and replacement of figures. The sculpture studio was also asked to remove the four figures temporarily to use a 3D scanning technique to produce images of the base of the font. Three of the four figures were dismantled easily by removing the screws holding the bars in place.

Before its removal, Figure No.3's proper left foot was faced up using isinglass and tissues. Whilst dismantling the foot broke along the old breaking line. Interfaces of the break were sealed using Paraloid B72 10% in IMS and Acetone (50:50). The foot was re-adhered using Primal 60A (46-47% solid) and the tissue was removed using warm water and swab. The crack was filled using a white poly(butyl methacrylate) and calcium carbonate paste (Flügger). All figures were reinstated using their original fixings. Figure No. 1 had a wooden spacer under the metal bar. This was reduced by 2 mm to allow the back of the figures' shoulders not to be abraded by the metal of the font. Similarly, as the alignment of Part 4 to the metal plate caused some abrasion of the back, two thin pieces of card were placed over the wooden spacer to alter figures position slightly. Areas around the fixings were toned in using acrylic paints.

Samples from the plaster cast were taken from pre-existing areas of loss (Figure 2) to investigate the stratigraphy and the method of manufacture. The samples were analyzed to provide data for the study of the objects of the Cast Courts collection within the PhD project 'Materials and techniques for coating of the nineteenth-century plaster casts'. Details on the experimental procedure are available in the Experimental section of this report. A selection of significant results is shown in the following pages and the relevant database of analysis (<https://doi.org/10.25398/rd.northumbria.13902737>).

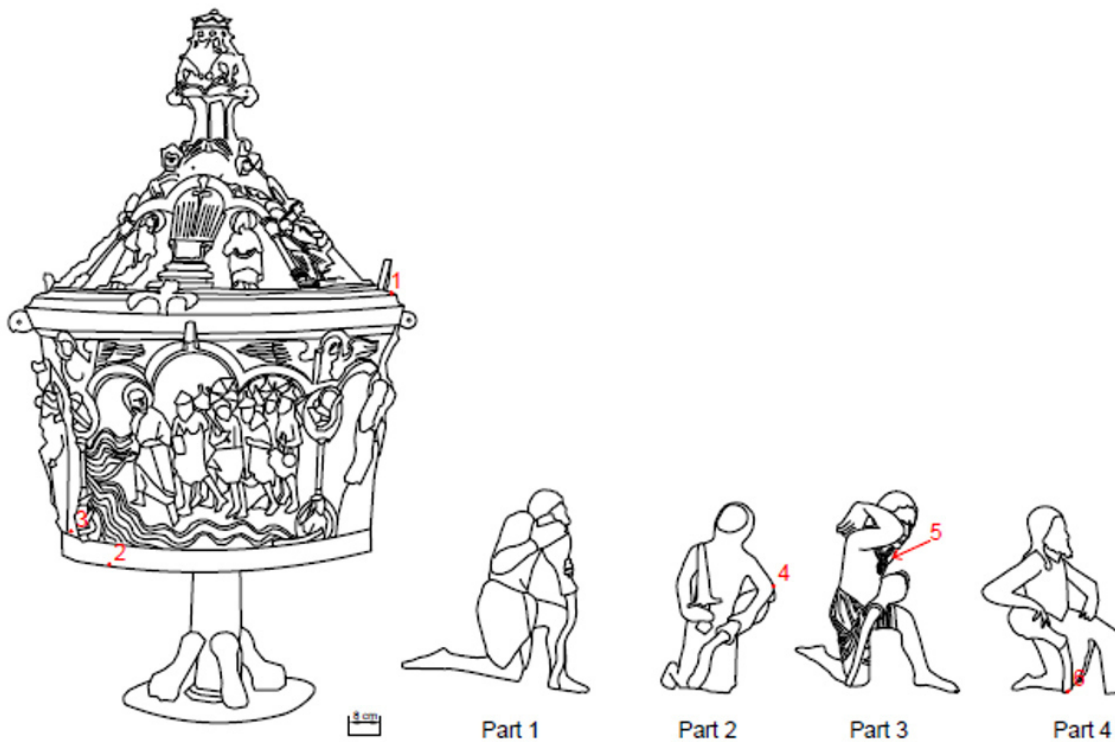


Figure 2. The font outline with marked sampling sites.

**Sample 1:** fragment taken from an area of loss along a crack, just below one of the lid's handles.

**Sample 2:** fragment taken from an area of loss on the font's bottom rim.

**Sample 3:** fragment taken from an area of loss on the top part of the bottom rim of the font.

**Sample 4:** fragment from an area of loss on the elbow of one of the base's figures (Part 2).

**Sample 5:** fragment from an area of loss on the chest of one of the base's figures (Part 3).

**Sample 6:** fragment from an area of loss on the water flow held by one of the base's figures (Part 4).

The **substrate** (layer 0 in all the samples) is made of gypsum plaster (**calcium sulfate**,  $\text{CaSO}_4$ , confirmed by EDS, XRD and by the peak at  $1600\text{-}1648\text{ cm}^{-1}$  in the FT-IR spectra, which also show the sulfate overtones in the  $2100\text{-}2300\text{ cm}^{-1}$  area). An **interface layer**, yellow under visible illumination and possibly consisting of a portion of lower layer soaked with the surface coating(s), showing characteristics of both layers, is visible in samples 1, 3, 4 and 5. The tabular crystalline structure typical of gypsum plaster can be seen in the substrate layer and the interface layer. Inclusions made of **aluminium (Al)**, **silicon (Si)** and **magnesium (Mg)** are present in all the layers of all the samples; **potassium (K)** and **iron (Fe)** were also detected in all the layers of samples 1 and 2. **Sodium (Na)** and **chlorine (Cl)** were also detected in sample 2 and sample 6 **lead (Pb)** and traces of **barium (Ba)** and **titanium (Ti)** were detected in all the layers.

All the samples show either only a layer, **dark** under visible illumination (layer 2 in samples 1, 4 and 5, layer 2 in samples 2 and 6 and layer 3 in sample 3) or this layer preceded by a defined layer, yellow under visible illumination and pink-orange under UV illumination (layer 2 in sample 3). EDS mapping shows that the dark layer contains **CaSO<sub>4</sub>** but also **Cu**, Cl, Si, Al, Zn, Fe, P, Mg and K. In sample 4 a higher Si and Ba content in the utmost layers was also observed.

The pink-orange fluorescence of several layers in the samples indicates the presence of **shellac**, also consistent with the FT-IR peaks at  $100\text{-}1200$  and  $2800\text{-}3000\text{ cm}^{-1}$ ) which were detected in all the layers. This indicates that either the material was added to the gypsum plaster wet admixture or that the coating has also penetrated in layer 0. The latter seems also possible as the average depth of the samples is about 0.5 mm. py-TMAH-GC/MS of sample 4 shows markers characteristic of **shellac**, possibly mixed with **drying oil**. Oil is consistent with the fluorescence, in this sample, of layer 3 under UV illumination (Colombini & Modugno, 2009).

Samples 2 and 4 shows this same **finishing layer** that fluoresces white under UV illumination. This can suggest either that varnish was applied only on the selected areas or that the varnish was applied on all the surface, but it was differently adsorbed depending on the local variation of porosity.

Sample 6 shows a stratigraphy different from all the rest of the samples, suggesting that it is either a repair or that the area was built differently due to its supporting position at the base of the casts. This sample is mostly made of C, O, S and Ca ( $\text{CaSO}_4$ , confirmed by EDS and by the peak at  $1600\text{-}1616\text{ cm}^{-1}$  in the FT-IR spectra). Layer 0 consists of  $\text{CaSO}_4$ , Pb and traces of Ba, Ti and Al. Traces of Si are present in all the layers. Layer 1 does not show any significant elements' distribution. Layer 2 contains brass fillings (Zn and Cu were detected) and traces of Cl. Layer 3 consists of  $\text{CaSO}_4$ , lead and traces of Fe, Ba, Ti and Cl. Layer 4 consists of  $\text{CaSO}_4$  and Pb and layer 5 does not show any significant elements distribution. A wax or resin is suggested by FT-IR (peaks at  $1000\text{-}1500$  and  $2800\text{-}3000\text{ cm}^{-1}$ ) and was detected in all the layers.

**NOTE:** casting in resin the fragments of plaster resulted in the fragments absorbing the resin when in the liquid state. This was visible in the BSE image as well as through the EDS mapping (Tiranti resin and catalyst are mainly made of organic compounds C, H and O). Al traces are present in all the samples, due to the polishing chemical.

## Sample 1

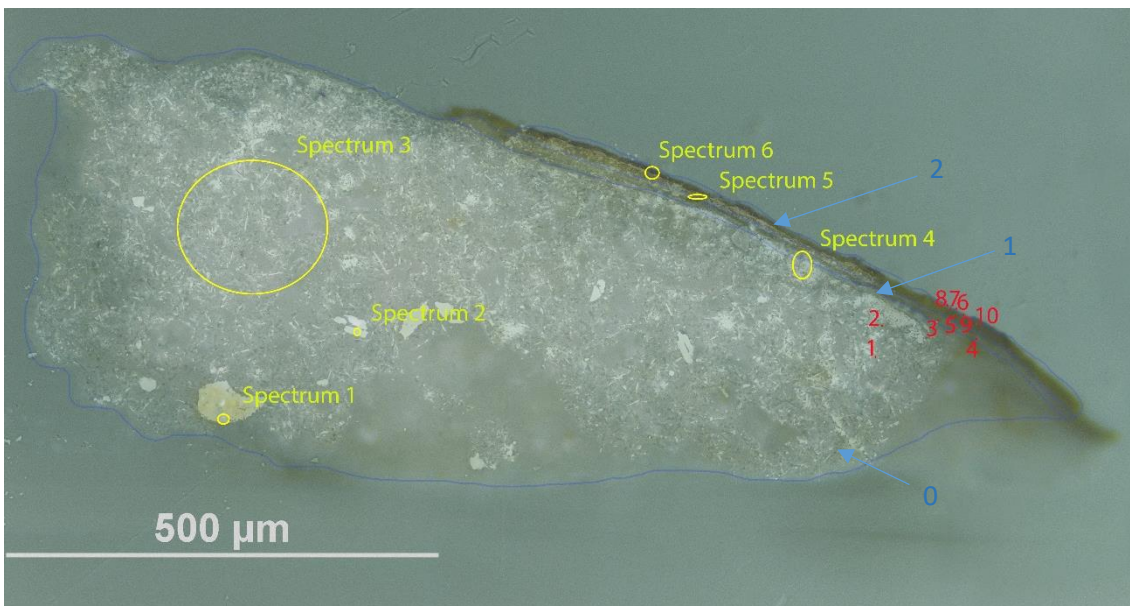


**Sampling.** This fragment taken from an area of loss along a crack, just below one of the lid's handles.

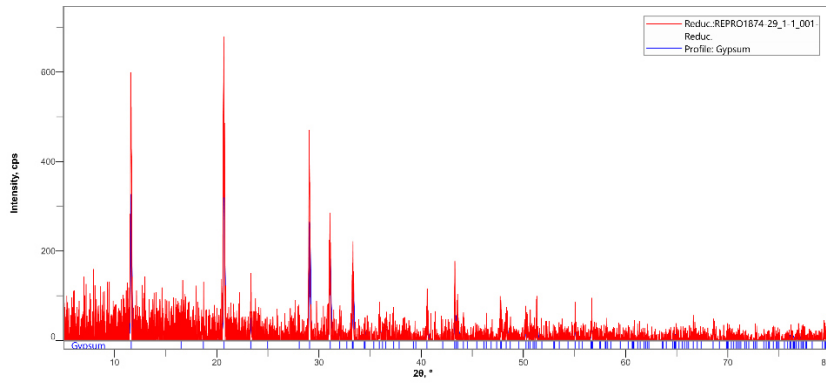
Below: Overlapped (OM and BSE) cross-section image showing the stratigraphy (blue indicators).

- 2. Dark-yellow layer
- 1. Yellowish layer
- 0. Plaster bulk

**Analysis spots.** EDS analysis (yellow): Spectra 1-6; FT-IR analysis (red): nos. 1-10



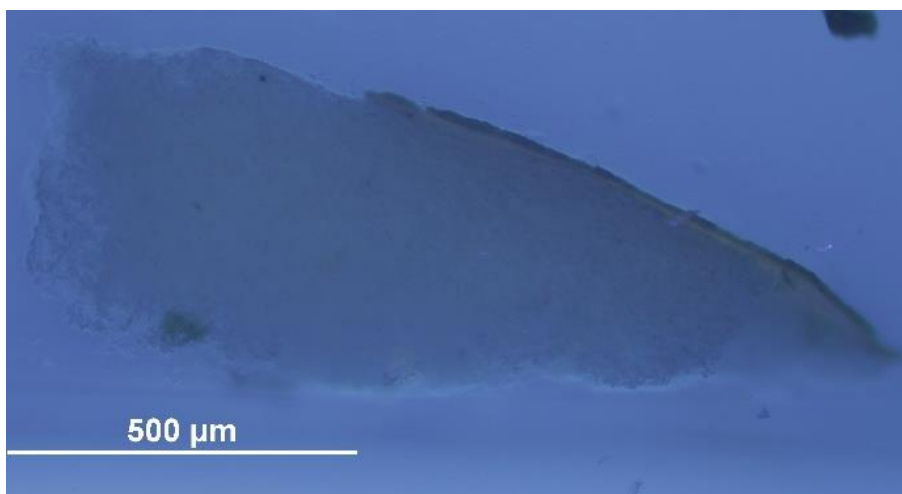
**Summary.** The substrate (layer 0) is made of plaster ( $\text{CaSO}_4$ , confirmed by EDS, XRD and by the peak at  $1600\text{-}32\text{ cm}^{-1}$  and overtones in the FT-IR spectra). The tabular crystalline structure typical of gypsum plaster can be seen in layers 0 and 1. Layer 1 appears yellow under visible illumination and it is consistent with the ground layer soaked with a wax or resin (FT-IR peaks at  $100\text{-}1200$  and  $2800\text{-}3000\text{ cm}^{-1}$ ) which was detected in all the layers. The fluorescing orange colour of layer 1 under UV illumination suggests that the resin is **shellac**. Traces of Si, Al, K, Mg and Fe were also detected in layers 0 and 1. Layer 2 contains calcium sulfate but also **Cu**, Cl, Si, Al, Zn, P, Mg and K.



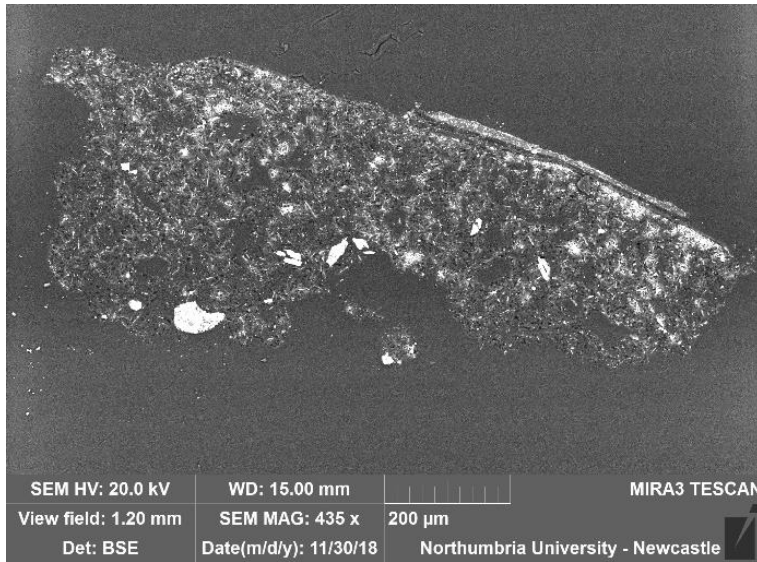
A fragment of this sample was pulverised and analysed by **XRD**. It was possible to identify the profile of gypsum (calcium sulfate) and the diffractogram was compared to references from the Rigaku SmartLab Database and the most significant peaks were at  $2\theta = 11.59, 20.67, 29.04, 31.05, 33.30, 47.79$ .



VLR OM (left)

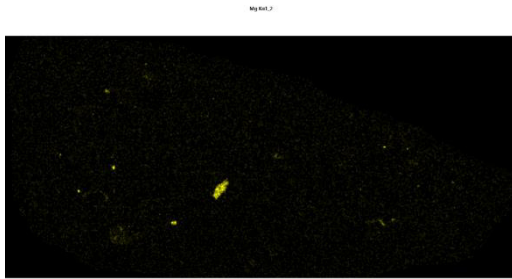


UVf OM (left)

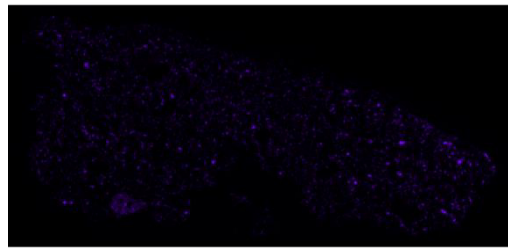


**BSE image (left).** The tabular crystalline structure typical of gypsum plaster can be seen in layers 0 and 1, which are made of  $\text{CaSO}_4$ . Traces of Si, Al, K, Mg and Fe were also detected in these layers (see also **EDS mapping below**). Layer 2 contains calcium sulfate but also Cu, Cl, Si, Al, Zn, P, Mg and K (see for example **spectrum 5 below**).

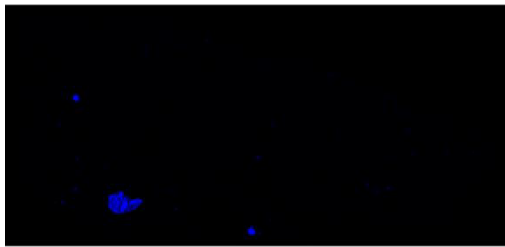
**Magnesium (Mg)**



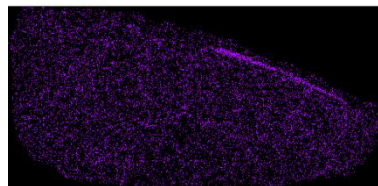
**Aluminium (Al)**

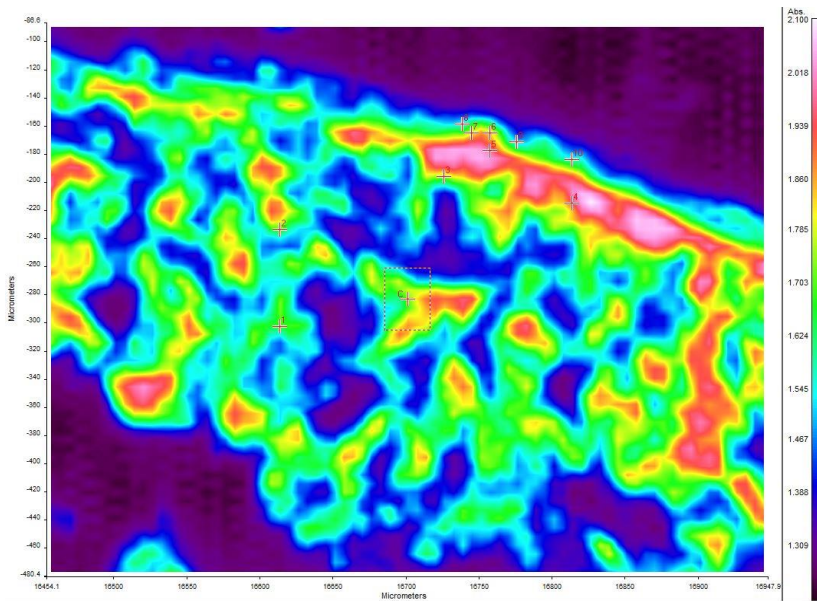
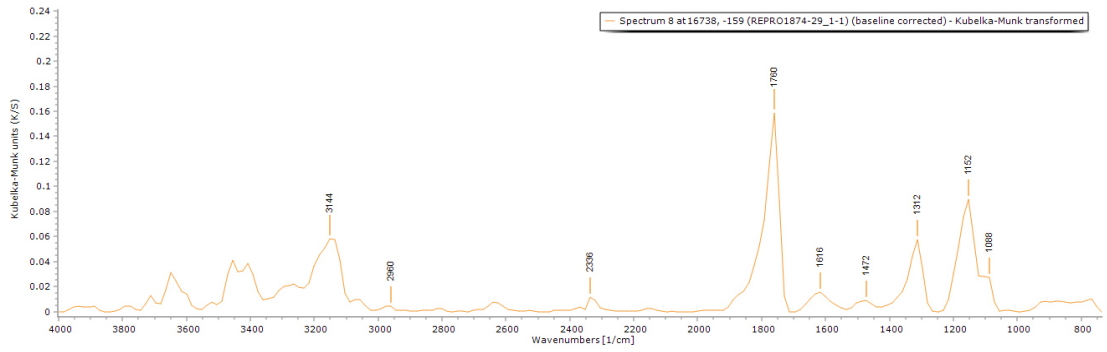


**Silicon (Si)**



**Copper (Cu)** was observed as one of the main components of **layer 2**, but EDS mapping ([below](#)) shows a distribution which might mislead the interpretation due to the distribution algorithm. **Cu was not detected in layers 0 and 1.**





**FT-IR spectrum 8** (above) of layer 2. Peaks for the casting resin (1312, 1760  $\text{cm}^{-1}$ ), gypsum (1616  $\text{cm}^{-1}$ , overtone 2200-2300  $\text{cm}^{-1}$ ) and a wax/resin (1000-1200, 1472 and 2800-3000  $\text{cm}^{-1}$ ). A summary of the peaks observed in the spectra 1-10 can be seen in the table below.

**FT-IR (FPA) image** (left). The different reflectance of the utmost layer can be observed in the Focal FPA image.

Spectrum	Layer	peaks (cm-1)						
		Casting Resin	Gypsum	Carbonate	Wax/resin	C=O ester carbonyl	SO overtone	Unknown
1	0	1312, 1760			960, 1072, 1232, 1392, 1472, 2848, 2960		2240, 2352	
2	0	1312, 1760			784, 1104, 1152, 1504, 1584, 1664, 2848			
3	1	1312, 1760		800	848, 1088, 1216, 1392, 1536, 2944		2304, 2416	
4	1	1312, 1760	1600		768, 832, 1088, 1216, 2768		2240, 2416	
5	2	1312, 1760	1632	800	960, 1040, 1088, 1168, 1424, 1552, 2864		2160, 2256	
6	2	1312, 1760	1616		832, 1088, 1184, 3008		2304, 2400	
7	2	1312, 1760	1632	800	992, 1088, 1184, 1488, 2928		2320, 2480	
8	2	1312, 1760	1616		1088, 1152, 1472, 2960		2336	
9	2	1328, 1760	1616	800	864, 1168, 1456, 2784		2352	
10	2	1312, 170	1632		784, 1088, 1152, 1472, 2960		2384	

## Sample 2

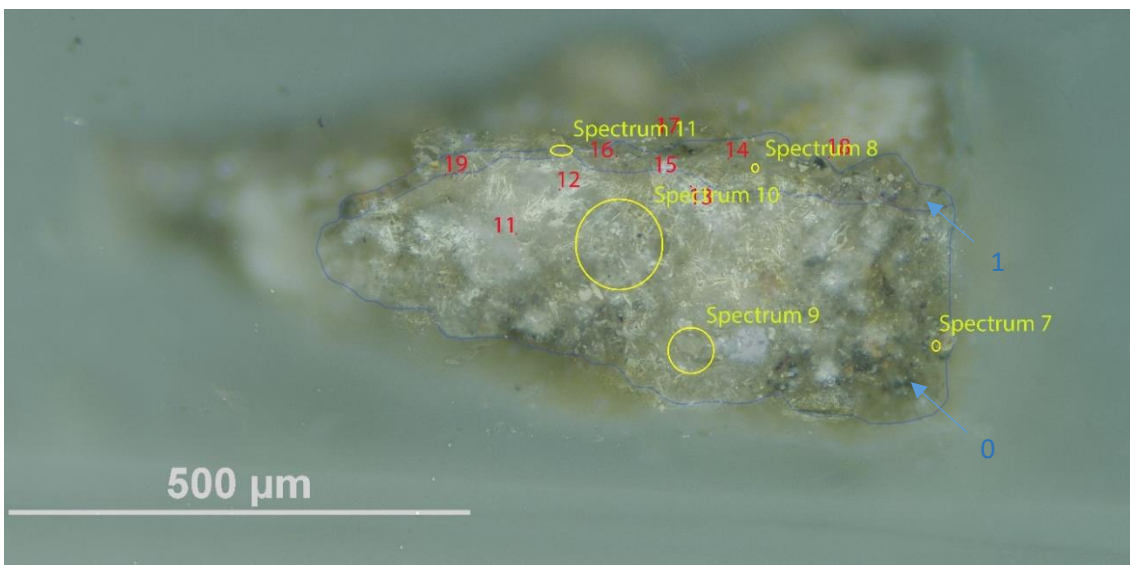


**Sampling.** This sample consists of a fragment taken from an area of loss on the font's bottom rim.

Below: Overlapped (OM and BSE) cross-section image showing the stratigraphy (blue indicators).

- 1. Dark layer with dark inclusions**
- 0. Plaster bulk with dark inclusions**

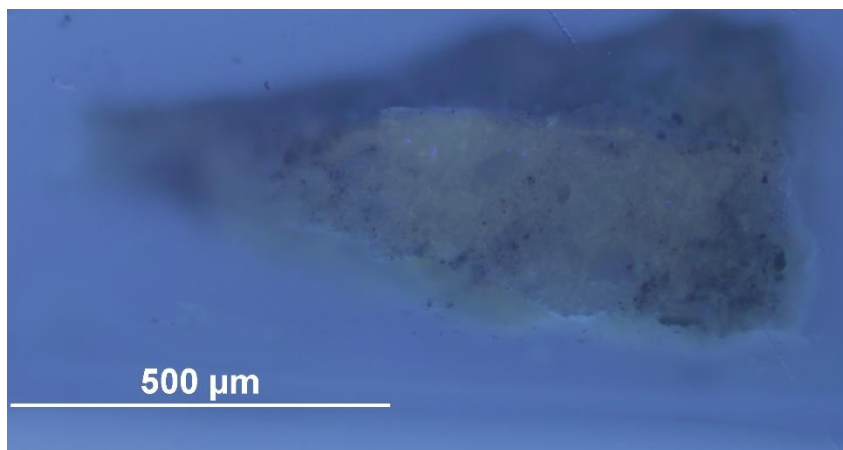
**Analysis spots.** EDS analysis (yellow): Spectra 7-11; FT-IR analysis (red): nos. 11-19.



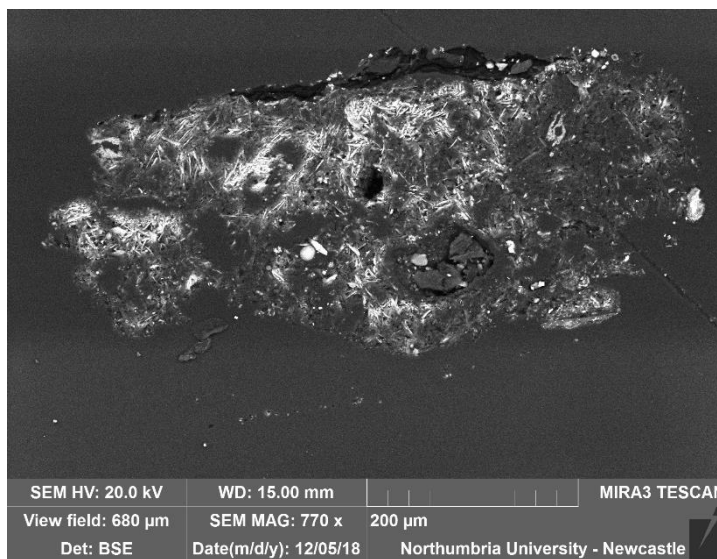
**Summary.** The substrate (layer 0) is made of plaster ( $\text{CaSO}_4$ , confirmed by EDS and by the peak at  $1600\text{ cm}^{-1}$  and overtones in the FT-IR spectra) and Si-Al inclusions and Fe are present in all the layers. The tabular crystalline structure typical of gypsum plaster can be seen in layer 0. Traces of K, Na, Cl and Mg were also detected. Layer 0 shows a pink-orange tone under UV illumination, suggesting the presence of **shellac**, whereas layer 1 fluoresces white under UV illumination, suggesting a different coating material. A **wax or resin** (FT-IR peaks at  $1200\text{-}1500$  and  $2800\text{-}3000\text{ cm}^{-1}$ ) was detected in all the layers.



VLR OM (left)



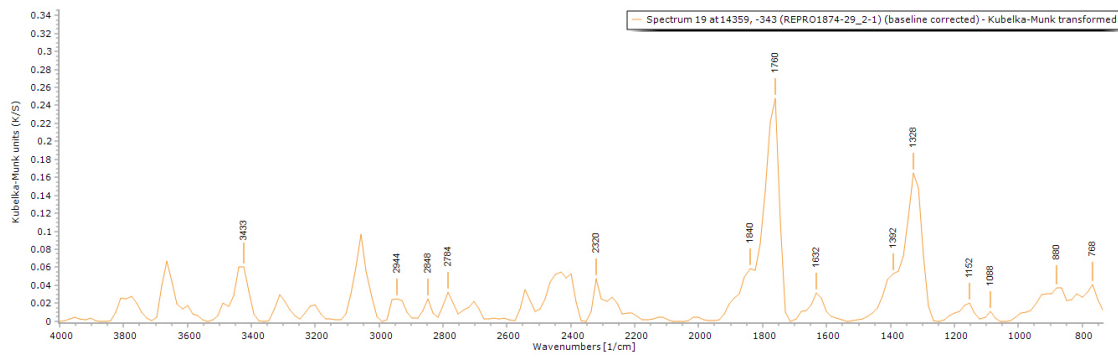
UVfOM (left)



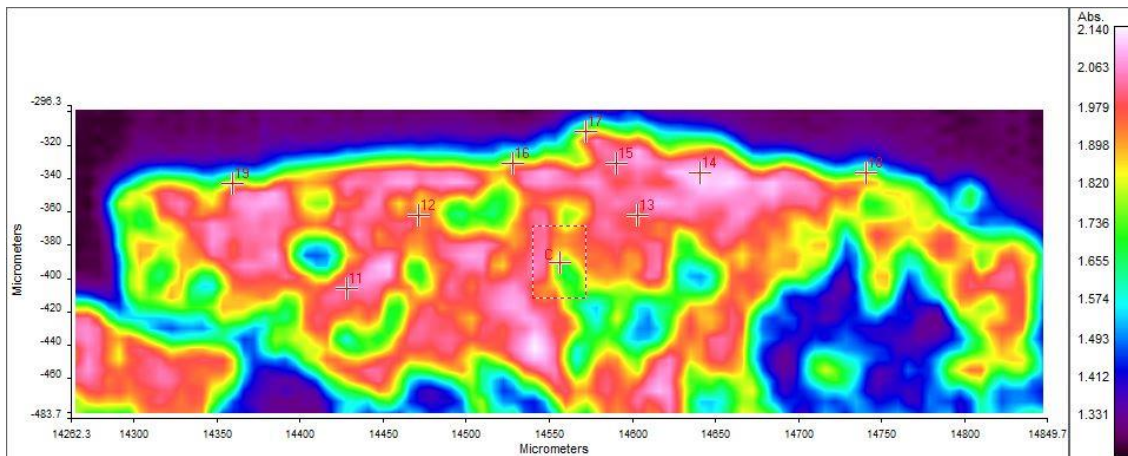
The **BSE image** (left) shows that the tabular structure characteristic of gypsum is present in layer 0.

**EDS spectra** suggest that the sample is mostly made of  $\text{CaSO}_4$  (C, O, Ca, S), Al, Si and Fe. Traces of K, Na, Cl and Mg were also detected.

**EDS mapping** does not show elements distribution in a layer fashion but suggests that inclusions made of **Si** and **Al** are present and the dark inclusions visible under visible illumination contain **Fe**.



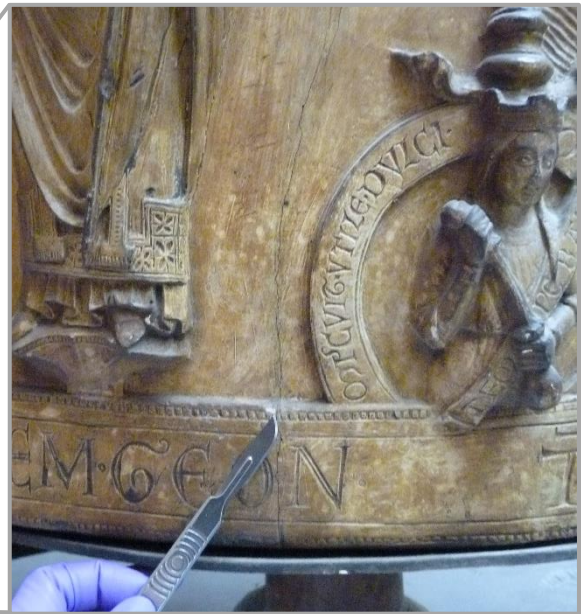
**FT-IR spectrum 19** (above) of layer 1. Peaks for the casting resin (1328, 1760  $\text{cm}^{-1}$ ), gypsum (1632  $\text{cm}^{-1}$ , overtone 2200-2300  $\text{cm}^{-1}$ ) and a wax/resin (1000-1200, 1392, 2800-3000  $\text{cm}^{-1}$ ). A summary of the peaks observed in the spectra 11-19 can be seen in the table below.



**FT-IR (FPA) image** (above). Some indication of different reflectance of the layers can be observed in the FPA image.

Spectrum	Layer	peaks ( $\text{cm}^{-1}$ )						
		Casting Resin	Gypsum	Carbonate	Wax/resin	C=O ester carbonyl	SO overtone	Unknown
11	0	1312, 1760		800	912, 976, 1072, 1232, 1408		2416	
12	0	1312, 1760			779, 880, 976, 1088, 1232, 1456, 1568, 2848, 2944		2504	
13	0	1312			784, 848, 896, 1008, 1072, 1120, 1296, 1376, 1456, 1552, 2752, 2800, 2880	1744	2212	
14	1	1312, 1760	1600, 1648	800	848, 896, 960, 1040, 1104, 1424, 1472, 2848, 2928		2288, 2400	
15	1	1760	1616	1792	768, 848, 880, 976, 1136, 1296, 1488, 2800, 2944		2304	
16	1	1328, 1760			816, 1088, 1200, 1408, 1520, 2944		2208, 2400	
17	1	1312, 1760		800	1024, 1088, 1184, 1440, 1504, 2896, 2944		2368	
18	1	1312, 1760	1616		784, 912, 1088, 1184, 1520		2336	1824
19	1	1328, 1760	1632		768, 880, 1088, 1152, 1392, 2784, 2848, 2944		2320	1840

## Sample 3

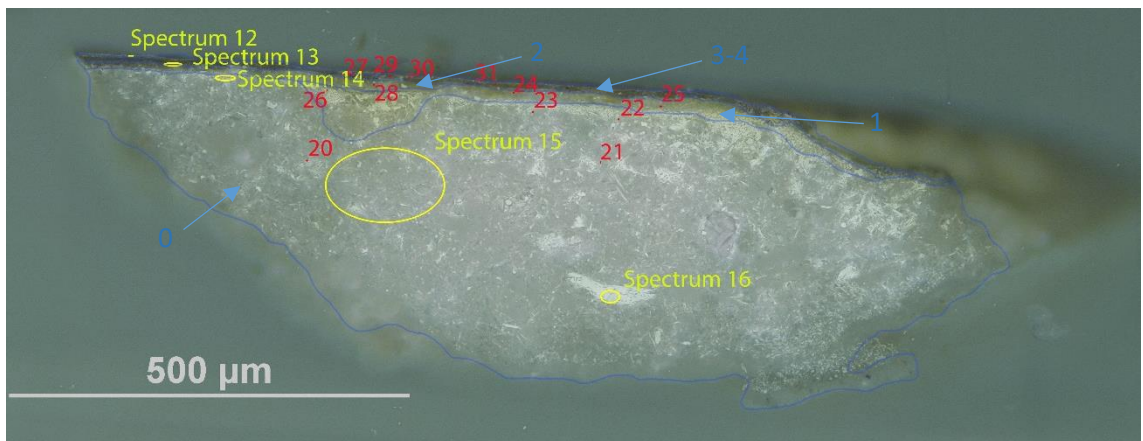


**Sampling.** This fragment taken from an area of loss on the top part of the bottom rim of the font.

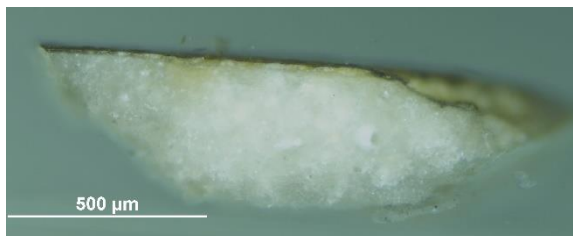
Below: Overlapped (OM and BSE) cross-section image showing the stratigraphy (blue indicators).

- 4. Varnish
- 3. Dark layer
- 2. Yellow layer
- 1. Intermediate yellowish layer
- 0. Plaster bulk

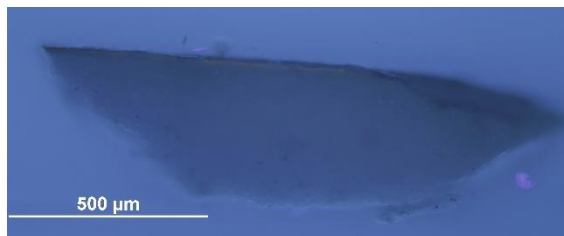
**Analysis spots.** EDS analysis (yellow): Spectra 12-16; FT-IR analysis (red): nos. 20-31.



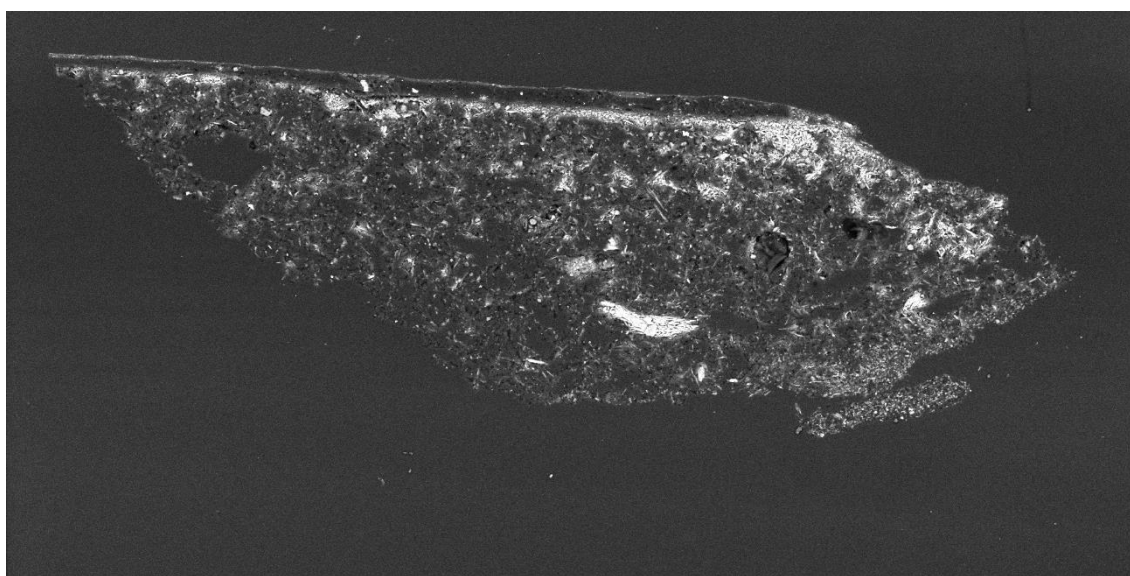
**Summary.** The sample is mostly made of C, O, S and Ca (**calcium sulfate**,  $\text{CaSO}_4$ , confirmed by EDS and by the peak at  $1600\text{-}1616\text{ cm}^{-1}$  in the FT-IR spectra). **Si-Al inclusions** are present in all the layers and additional traces of **Cl, P, Cu, Fe, K** and **Zn** were detected in the utmost layers. The structure typical of gypsum plaster can be seen in layers 0 and 1. A **wax or resin** is suggested by FT-IR (peaks at  $1000\text{-}1200$  and  $2800\text{-}3000\text{ cm}^{-1}$ ) and was detected in all the layers.



VLR OM (above)



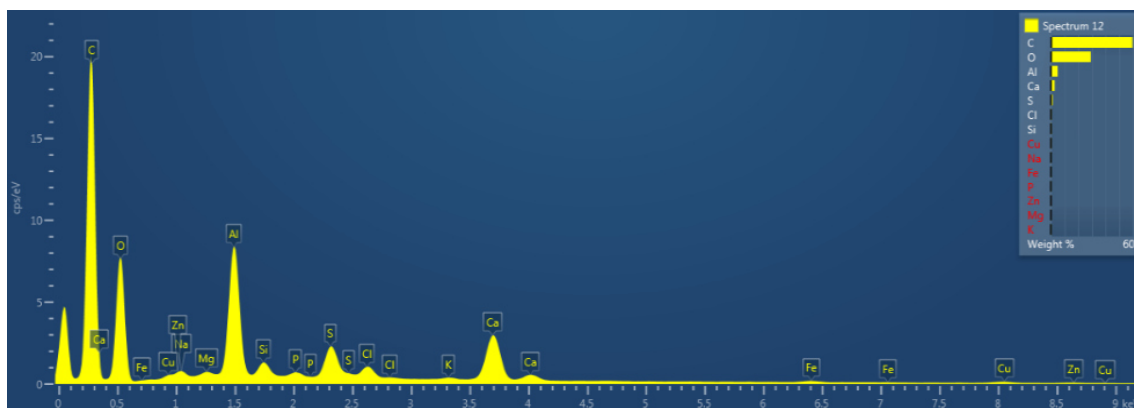
UVfOM (above)

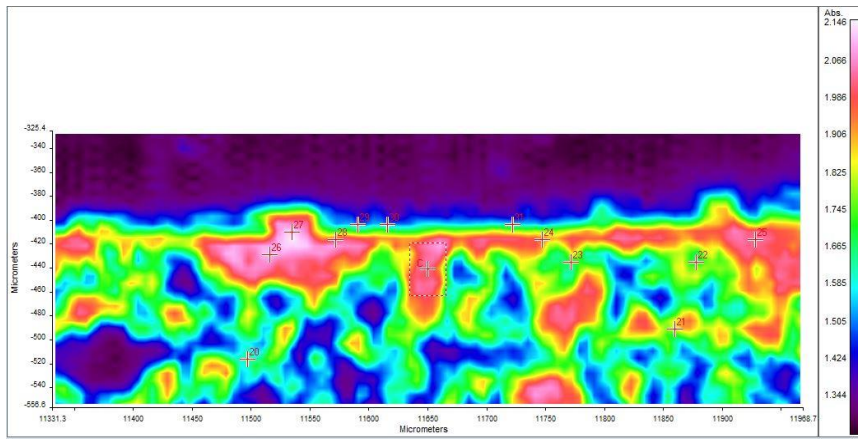
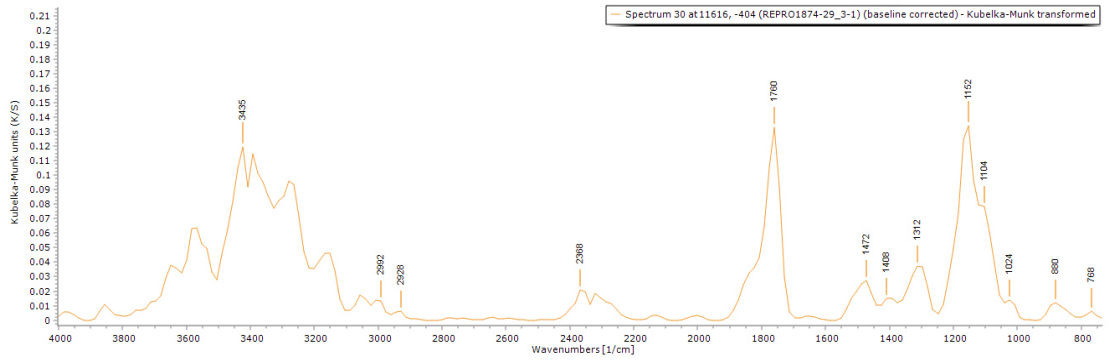


SEM HV: 20.0 kV	WD: 15.00 mm	MIRA3 TESCAN
View field: 1.33 mm	SEM MAG: 395 x	200 µm
Det: BSE	Date(m/d/y): 12/05/18	Northumbria University - Newcastle

**BSE image** (above). The tabular crystalline structure typical of gypsum plaster can be seen in layers 0 and 1.

**Calcium sulfate ( $\text{CaSO}_4$ )** and **Al-Si inclusions** and traces of Mg and Na were detected in all the layers. Additional traces of **Cl, P, Cu, Fe, K** and **Zn** were detected in the utmost layers (see **spectrum 12** below).





**FT-IR spectrum 30** (above) of layers 3-4. Peaks for the casting resin (1312, 1760  $\text{cm}^{-1}$ ) and a wax/resin (1472  $\text{cm}^{-1}$  and 2800-3000  $\text{cm}^{-1}$ ). A summary of the peaks observed in the spectra 20-31 can be seen in the table below.

**FT-IR (FPA) image** (left). Some indication of different reflectance of the layers can be observed in the FPA image.

Spectrum	Layer	peaks (cm-1)						
		Casting Resin	Gypsum	Carbonate	Wax/resin	C=O ester carbonyl	SO overtone	Unknown
20	0	1312, 1760	1616		780, 1088, 1136, 2736, 2800			
21	0	1328, 1760			784, 848, 976, 1088, 1216, 1440, 1584, 1664, 2864, 2960		2224	
22	0	1312, 1760	1632		762, 896, 1008, 1072, 1200, 1392, 1504			
23	0	1312, 1760	1600		794, 848, 1104, 1488, 1664, 2832, 2944		2224	
24	1	1312, 1760	1632		752, 832, 944, 1008, 1088, 1216, 1552, 2864, 2960		2288	
25	1	1760	1616		832, 944, 1024, 1088, 1248, 1294, 1360, 1424, 1472, 2928		2304	
26	1	1328, 1760	1632		784, 880, 992, 1168, 1296, 1472, 1584, 2864, 2912	1744	2208	1808
27	2	1312, 1760	1600		784, 864, 912, 1072, 1168, 1216, 1344, 1440, 1520, 2848, 2896		2384	1824
28	2	1328, 1760	1632		768, 880, 1088, 1136, 1200, 1376, 1488, 2816, 2912, 2960		2288	1872
29	3-4	1312, 1760	1632		768, 816, 1088, 1184, 1488, 2960		2352	
30	3-4	1312, 1760			768, 880, 1024, 1104, 1152, 1408, 1472, 2928, 2992		2368	
31	3-4	1312, 1760	1616		784, 1088, 1552, 2944		2336, 2587	

## Sample 4

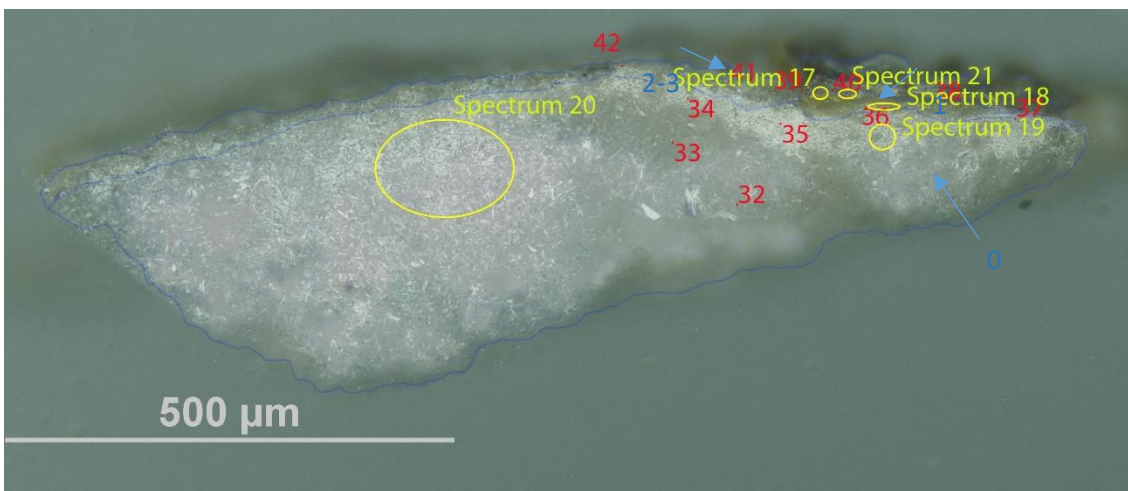


**Sampling.** This fragment was taken from an area of loss on the elbow of one of the base's figures (Part 2).

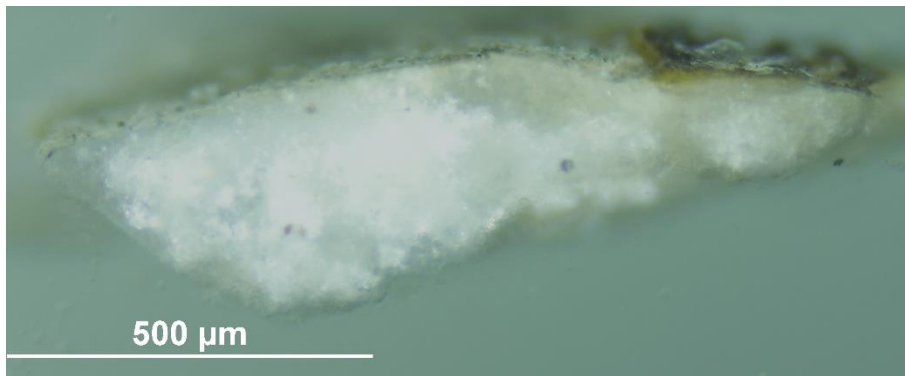
Below: Overlapped (OM and BSE) cross-section image showing the stratigraphy (blue indicators).

3. Varnish
2. Dark layer
1. Yellowish layer
0. Plaster bulk

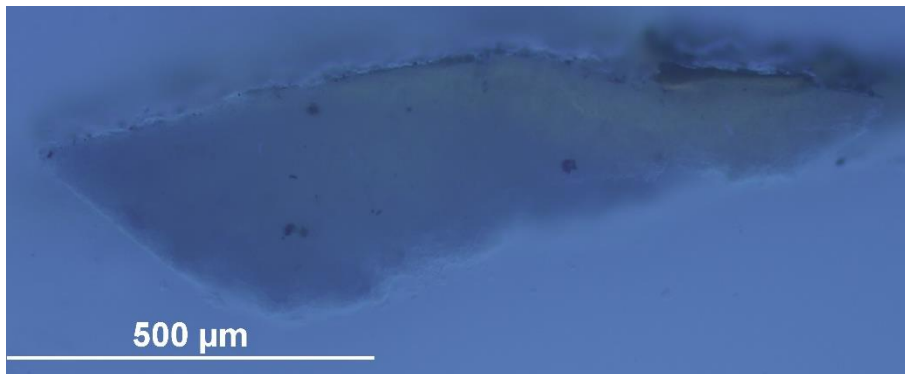
**Analysis spots.** EDS analysis (yellow): Spectra 17-21; FT-IR analysis (red): nos. 32-42.



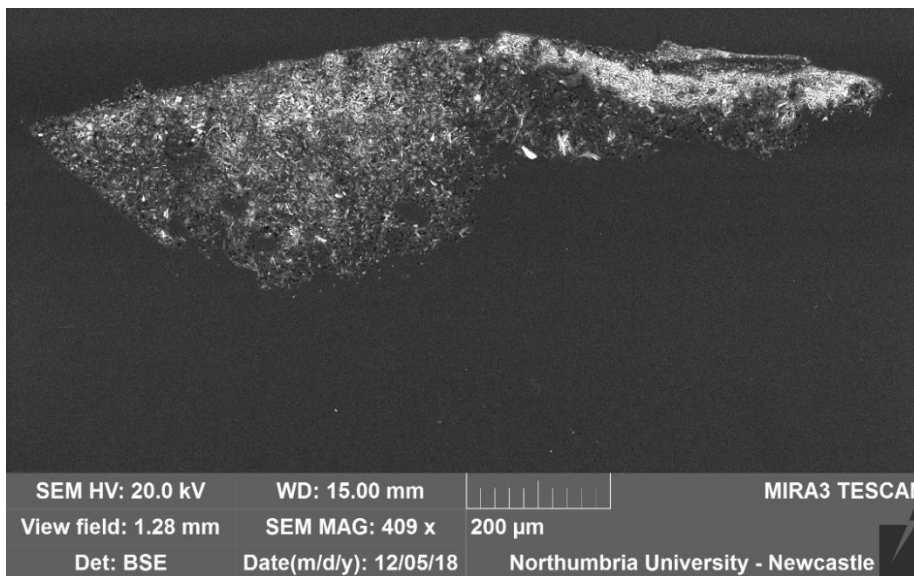
**Summary.** The sample is mostly made of C, O, S and Ca (**calcium sulfate**,  $\text{CaSO}_4$ , confirmed by EDS and by the peak at  $1600\text{-}1632\text{ cm}^{-1}$  in the FT-IR spectra). Al is overall present as used as a polishing agent, but could also, together with Si, be present as part of silicate inclusions, which are present in all the layers, but no particular element distribution in a layer fashion can be seen, apart from a higher Si and Ba content in the utmost layers (see EDS mapping). All the layers consist of C, O, Ca, S, Al, Si and Mg; traces of Cl, Pb, Cu, Na, Cr, Zn, Fe, K and Ba were additionally detected in the surface layers. py-TMAH-GC/MS shows markers characteristic of **shellac**, possibly mixed with **drying oil**. Oil is consistent with the fluorescence of layer 3 under UV illumination (Colombini & Modugno, 2009).



VLROM (left)



UVfOM (left)

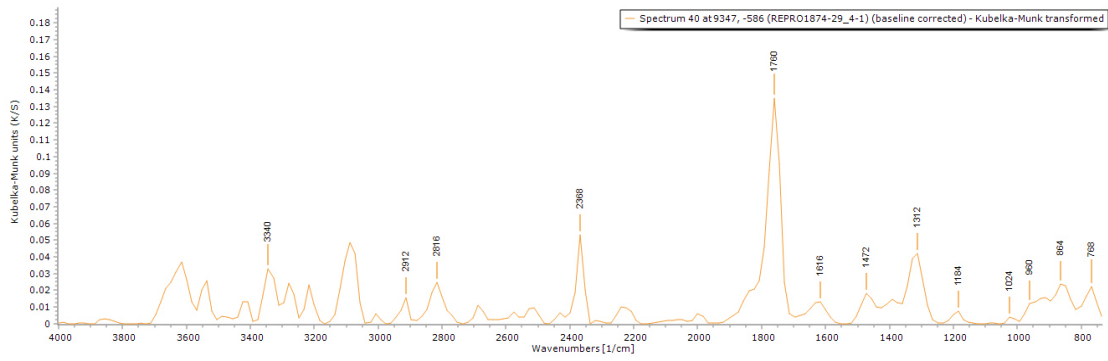


**BSE image (left).** The tabular crystalline structure typical of gypsum plaster can be seen in layers 0 and 1. Layer 1 appears denser than layer 0.

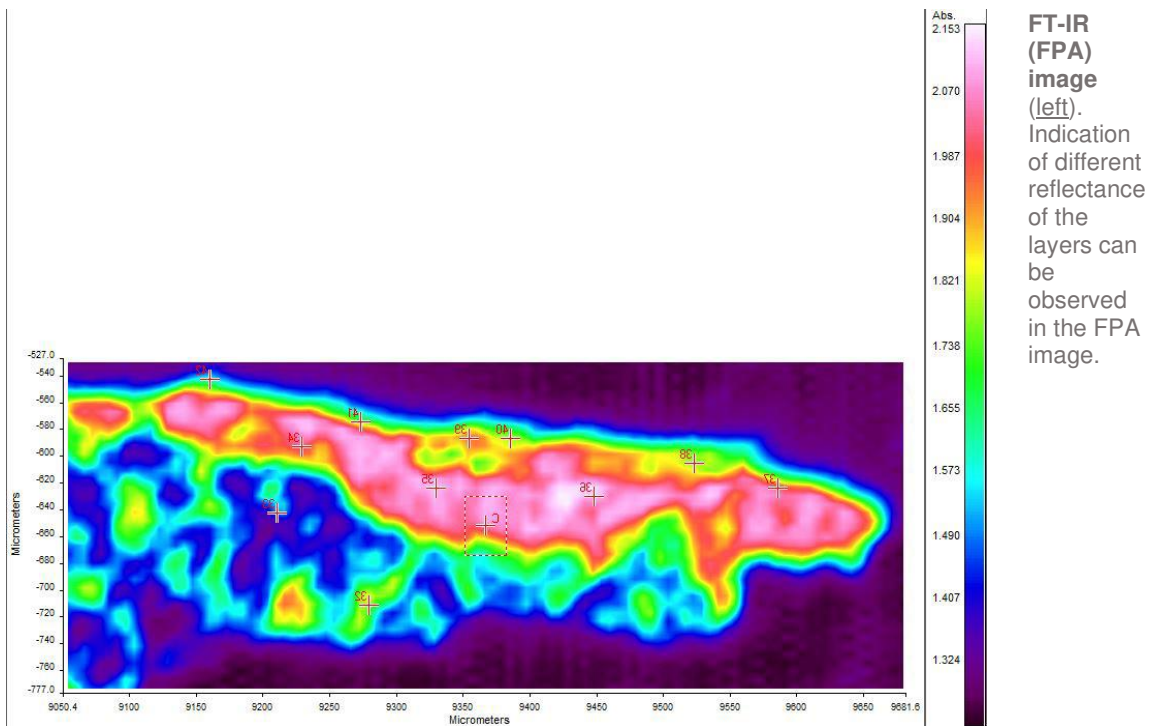
**EDS mapping** shows the presence of **Al-Si inclusions** but does not suggest any particular element distribution in a layer fashion, apart from a higher **Si** and **Ba** content in the utmost layers.

**EDS spectra** indicate that all the layers consist of C, O, Ca, S, Al, Si and Mg. Traces of Cl, Pb, Cu, Na, Cr, Zn, Fe, K and Ba were additionally detected in the surface layers (spectrum 17 below).

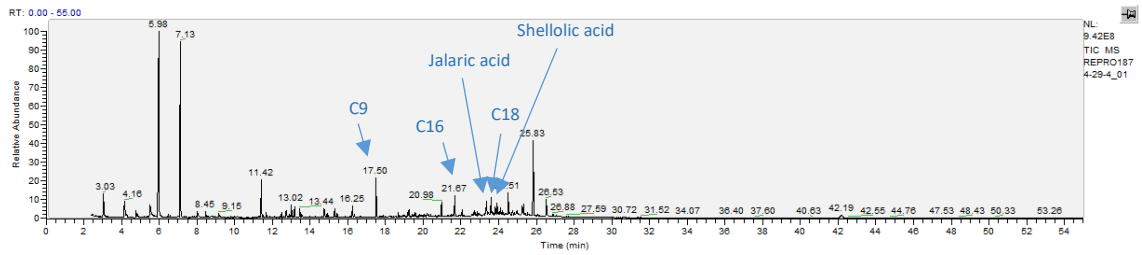




FT-IR spectrum 40 (above) of layers 2-3. Peaks for the casting resin (1312, 1760  $\text{cm}^{-1}$ ), gypsum (1616  $\text{cm}^{-1}$ , overtone 2200-2300  $\text{cm}^{-1}$ ) and a wax/resin (1100-1500, 2800-3000  $\text{cm}^{-1}$ ). A summary of the peaks observed in the spectra 32-42 can be seen in the table below.



Spectrum	Layer	peaks ( $\text{cm}^{-1}$ )						
		Casting Resin	Gypsum	Carbonate	Wax/resin	C=O ester carbonyl	SO overtone	Unknown
32	0	1312, 1760	1600		784, 864, 1088, 1184, 1456, 2896, 2944		2240	1872
33	0	1328, 1760	1616	800	880, 960, 1008, 1104, 1168, 1488, 2960			2352
34	0	1312	1648	1776	768, 816, 944, 1040, 1088, 1456, 1584, 2848			2320, 2498
35	0	1312, 1760	1600		1040, 1088, 1232, 2880, 2960		2277, 2400	1824
36	1	1312, 1760	1632		768, 896, 1008, 1072, 1216, 1424, 1568, 2848, 2960			2256, 2384
37	1	1312, 1760	1600		784, 880, 1008, 1088, 1232, 1472, 2816, 2944			2272, 2432
38	1	1312, 1760	1616		784, 880, 1104, 1168, 1392, 1488, 1568, 2864, 2944			2352
39	2-3	1312, 1760			832, 880, 944, 1216, 1664, 2848, 2912			2304
40	2-3	1312, 1760	1616		768, 864, 960, 1024, 1184, 1472, 2816, 2912			2368
41	2-3	1312, 1760	1648	800	864, 912, 1088, 1136, 1200, 1456, 2848			2368
42	2-3	1312, 1760	1600		784, 976, 1088, 1136, 1536, 2832, 2960			2346



RT	m/z	Assignment	Formula
3.03	41(72), 58(41), 82(8), 85(16), 100(33), 207(5)	2-Propenoic acid, 2-methyl-, methyl ester	C5H8O2
4.16	45(100), 58(12), 74(63)	Ethyl ether	C4H10O
4.78	44(14), 58(41), 69(100), 86(22), 99(26), 114(6)	2-Propenoic acid, 2-methyl-, ethyl ester	C6H10O2
5.53	42(11), 58(100), 72(9), 88(7), 103(4), 116(3)	1,2-Ethanediamine, N'-ethyl-N,N-dimethyl-	C6H16N2
5.98	42(12), 58(100), 117(17)	1,2-Ethanediamine, N'-ethyl-N,N-dimethyl-	C6H16N2
7.13	44(7), 56(7), 72(100), 116(2), 131(3)	1,2-Ethanediamine, N'-ethyl-N,N-dimethyl-	C6H16N2
8.04	42(11), 58(100), 74(9), 99(4), 115(6), 131(4)	1,2-Ethanediamine, N,N,N'-trimethyl-	C5H14N2
8.45	44(11), 58(37), 86(100), 110(2), 128(2)	1,2-Ethanediamine, N,N-diethyl-N'-methyl-	C7H18N2
9.15	44(100), 58(41), 86(64), 118(5), 128(53)	Unidentified amine fragment	
11.42	42(6), 58(100), 70(9), 88(1), 116(6)	1,2-Ethanediamine, N'-ethyl-N,N-dimethyl	C6H16N2
11.66	41(25), 55(36), 58(86), 74(92), 87(41), 98(85), 115(14), 127(100), 149(5)	FA fragment	
12.48	41(26), 56(37), 59(87), 69(79), 73(53), 88(49), 101(28), 113(52), 128(100), 152(5), 157(34)	Unidentified fragment	
12.74	42(8), 58(100), 85(2), 112(2), 128(2), 144(2), 175(2)	Unidentified amine fragment	
13.02	41(12), 58(75), 67(41), 95(28), 126(100), 154(20)	Unidentified amine fragment	
13.18	56(14), 71(13), 88(23), 98(31), 116(36), 130(100), 150(5), 189(5)	Unidentified amine fragment	
13.44	59(9), 72(100), 114(5), 130(7), 143(3)	Unidentified amine fragment	
14.75	58(10), 71(3), 84(6), 99(4), 116(100), 139(7), 173(4)	Unidentified amine fragment	
15.31	58(11), 71(2), 84(5), 99(4), 116(100), 128(7), 139(5), 173(5)	Unidentified amine fragment	
16.23	41(29), 55(77), 69(78), 74(92), 83(51), 87(45), 111(30), 129(80), 138(100), 171(59)	FA fragment	
17.5	43(16), 55(62), 74(63), 83(59), 87(27), 97(21), 111(54), 124(27), 143(31), 152(100), 185(39)	Nonanedioic acid, monomethyl ester	C10H18O4
18.69	41(41), 55(100), 74(84), 83(53), 87(41), 98(49), 115(36), 125(71), 138(49), 157(38), 189(10), 199(46), 208(5), 241(5)	Unidentified FA fragment	
19.25	45(74), 59(57), 71(47), 75(77), 85(77), 101(64), 109(90), 115(30), 156(41), 169(100), 183(5), 197(5), 215(5), 229(5), 257(5)	Unidentified terpenoid fragment	
20.98	45(22), 55(36), 69(59), 82(46), 95(20), 107(14), 127(100), 159(65), 167(5), 191(5), 209(5), 227(5), 241(5), 268(5)	Unidentified terpenoid fragment	
21.67	55(21), 74(100), 87(70), 143(20), 199(6), 227(13), 239(5), 270(5)	methyl palmitate	C17H34O2
22.06	45(49), 58(45), 69(71), 95(30), 101(72), 109(41), 119(28), 137(66), 153(5), 169(35), 201(100), 274(5)	Unidentified terpenoid fragment	
22.71	45(62), 55(70), 58(85), 69(73), 79(65), 91(78), 115(55), 121(65), 135(47), 165(49), 179(58), 201(49), 217(5), 233(5), 261(100), 276(5), 293(5), 308(5), 59(66), 69(50), 83(43), 87(52), 105(55), 121(39), 135(5), 145(5), 167(64), 179(40), 191(50), 203(32), 208(5), 231(5), 247(35), 262(100), 275(68), 307(5), 322(5)	shellac marker (Mills & White, 2012)	
23.35		jalaric acid	
23.6	55(34), 74(100), 87(74), 95(13), 109(5), 129(5), 143(26), 157(5), 185(5), 199(14), 255(15), 275(5), 298(5)	methyl stearate	C19H38O2
23.82	55(84), 71(63), 97(56), 109(41), 137(57), 169(37), 201(100), 231(5), 261(5), 291(5), 304(5), 336(5)	shellolic acid	
23.92	59(69), 79(56), 91(74), 115(53), 129(44), 145(45), 159(51), 187(54), 215(5), 229(5), 247(100), 291(5), 306(5), 323(5)	Unidentified terpenoid fragment	
24.51	59(60), 79(47), 91(55), 129(46), 169(55), 206(59), 229(48), 238(62), 260(5), 288(5), 305(5), 320(100), 337(5)	shellolic acid	
25.83	55(18), 71(97), 95(90), 109(30), 137(45), 159(59), 169(27), 201(100), 258(5), 291(5), 329(5)	Unidentified terpenoid fragment	
26.53	71(100), 81(26), 95(93), 109(33), 145(45), 155(55), 169(18), 187(33), 201(47), 207(5), 281(5)	Unidentified terpenoid fragment	
42.19	57(86), 69(64), 83(100), 97(72), 111(54), 207(33), 281(5)	Unidentified terpenoid fragment	

RT = retention time, m/z = mass/charge ratio

**Py-TMAH-GC/MS chromatogram** (top and described in the table on the left) shows small fragments due to derivatization (from t = 3.03 to 11.42 min) and markers characteristic of **shellac** (jalaric and shellolic acids) (Colombini & Modugno, 2009; Mills & White, 2012). The presence of **methyl azelate** (t = 17.50), **methyl palmitate** (t = 21.67) and **stearate** (t = 23.60) might suggest that the resin has been mixed with an **oil** (A/S = 1.15 and P/S = 1.22), possibly **linseed oil** (Colombini & Modugno, 2009).

## Sample 5

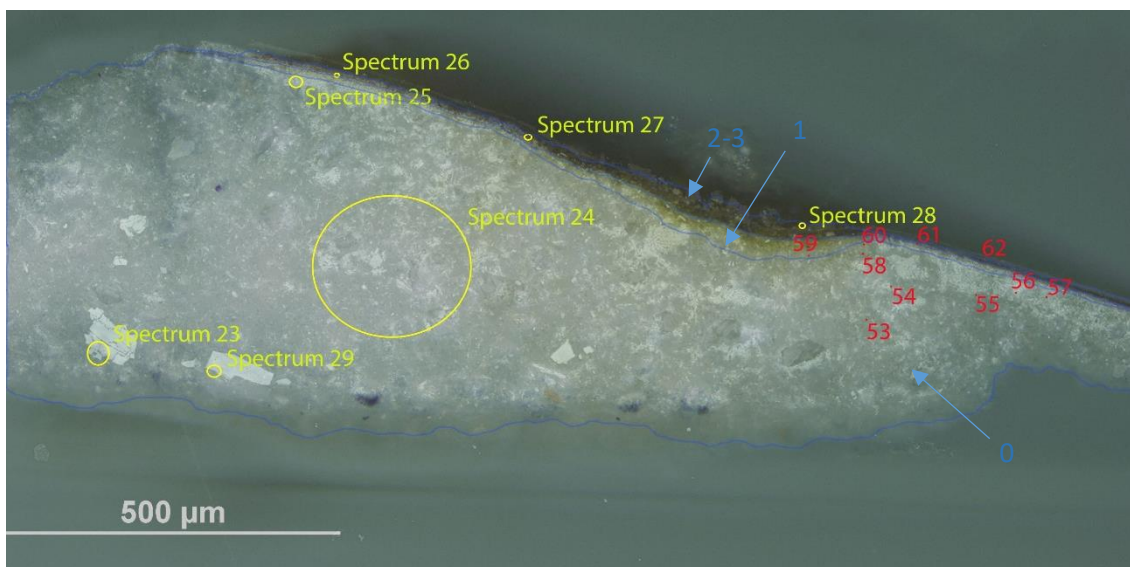


**Sampling.** This fragment was taken from an area of loss on the chest of one of the base's figures (Part 3).

Below: Overlapped (OM and BSE) cross-section image showing the stratigraphy (blue indicators).

- 3. Varnish
- 2. Dark layer
- 1. Yellow layer
- 0. Plaster bulk

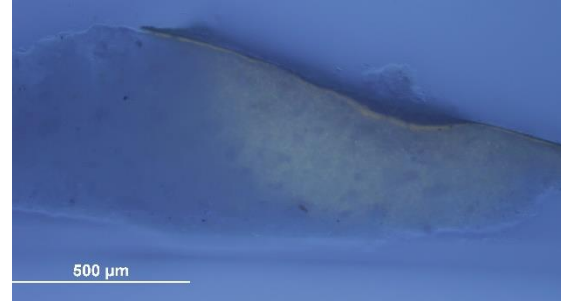
**Analysis spots.** EDS analysis (yellow): Spectra 23-29; FT-IR analysis (red): nos. 53-62.



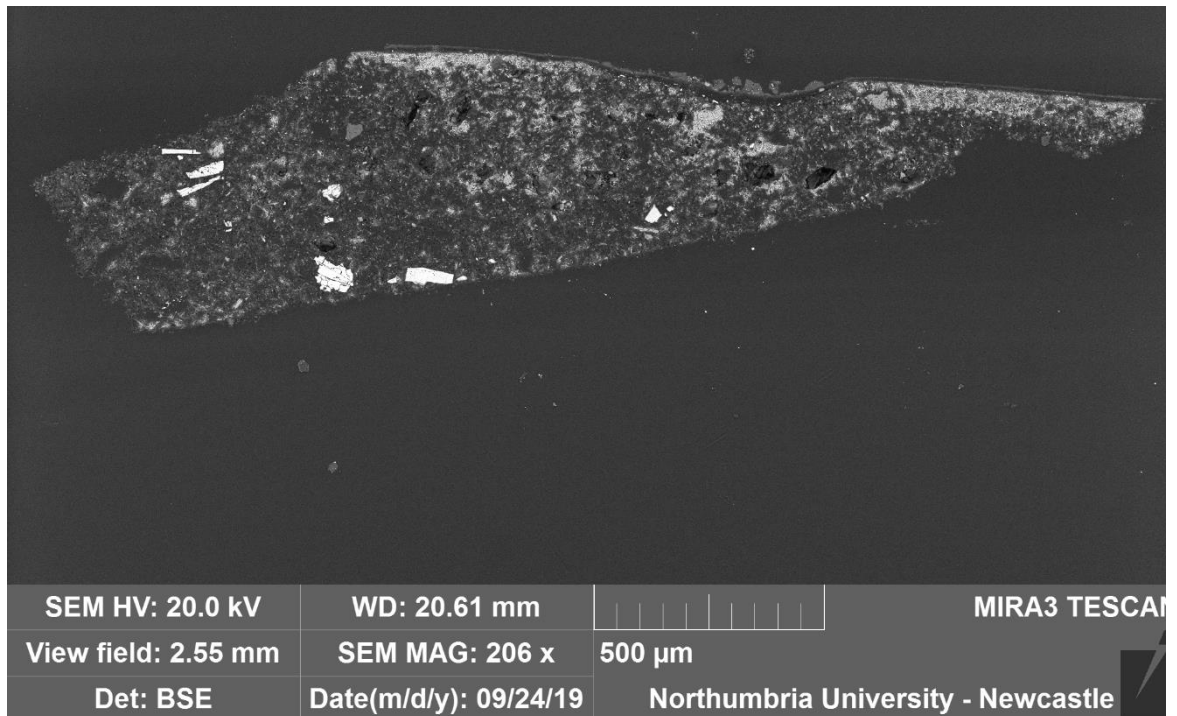
**Summary.** The sample is mostly made of C, O, S and Ca (**calcium sulfate**,  $\text{CaSO}_4$ , confirmed by EDS and by the peak at  $1600\text{-}1632\text{ cm}^{-1}$  in the FT-IR spectra). **Si-Al inclusions** and traces of **Mg** are present in all the layers and additional traces of **Cl, Cu, Si and Zn** were detected in the utmost layers. The structure typical of gypsum plaster can be seen in layer 0. A **wax or resin** is suggested by FT-IR (peaks at  $1000\text{-}1500$  and  $2800\text{-}3000\text{ cm}^{-1}$ ) and was detected in all the layers.



VLR OM (above)

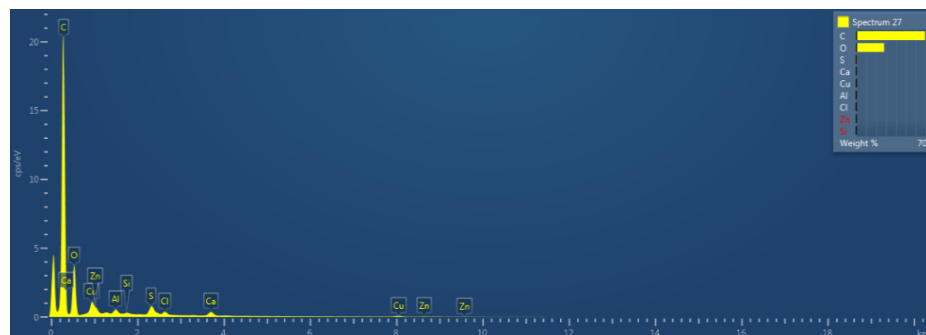


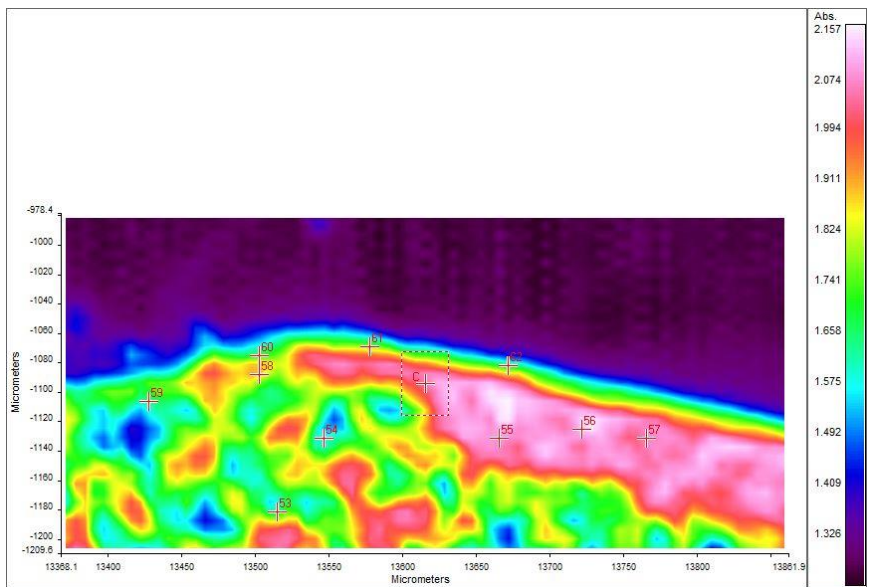
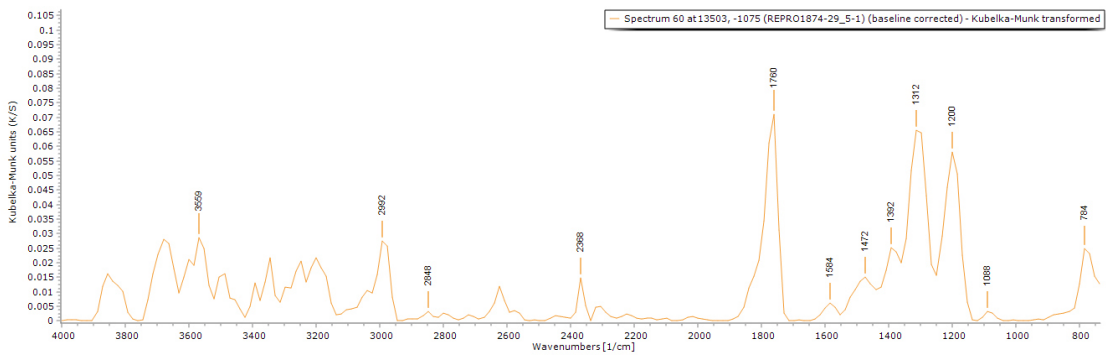
UVf OM (above)



**BSE image** (above). The tabular crystalline structure typical of gypsum plaster can be seen in layer 0.

**Calcium sulfate ( $\text{CaSO}_4$ )** and **Al-Si inclusions** and traces of **Mg** were detected in all the layers. Additional traces of **Cl, Cu, Si and Zn** were detected in the utmost layers (see **spectrum 27** below).





**FT-IR spectrum 60** (above) of layer 1. Peaks for the casting resin (1312, 1760  $\text{cm}^{-1}$ ) and a wax/resin (1472  $\text{cm}^{-1}$  and 2800-3000  $\text{cm}^{-1}$ ). A summary of the peaks observed in the spectra 53-62 can be seen in the table below.

**FT-IR (FPA) image** (left). Some indication of different reflectance of the layers can be observed in the FPA image.

Spectrum	Layer	peaks (cm-1)						
		Casting Resin	Gypsum	Carbonate	Wax/resin	C=O ester carbonyl	SO overtone	Unknown
53	0	1312, 1760			764, 864, 1088, 1472, 2800, 2864			2320
54	0	1312, 1760	1600		784, 848, 1088, 1136, 1216, 1392, 1472, 1664, 2848, 2960			2320
55	0	1312, 1760			880, 992, 1072, 1264, 1456, 1584, 1648, 2880			2208
56	0	1312, 1760	1600		928, 960, 1072, 1248, 1504, 2832, 2928			2277
57	0		1600		928, 1024, 1072, 1296, 2848			2272
58	0	1760	1600		784, 896, 960, 1088, 1216, 1296, 2912			2368
59	1	1312, 1760	1632	800	896, 1008, 1088, 1200, 1408, 1584, 2992			2336
60	1	1312, 1760			784, 1088, 1200, 1392, 1472, 1584, 2848, 2992			2368
61	2-3	1312, 1760	1632		784, 896, 1152, 1408, 2816, 2896			
62	2-3	1312, 1760	1632		832, 1088, 1200, 2992			2320

## Sample 6

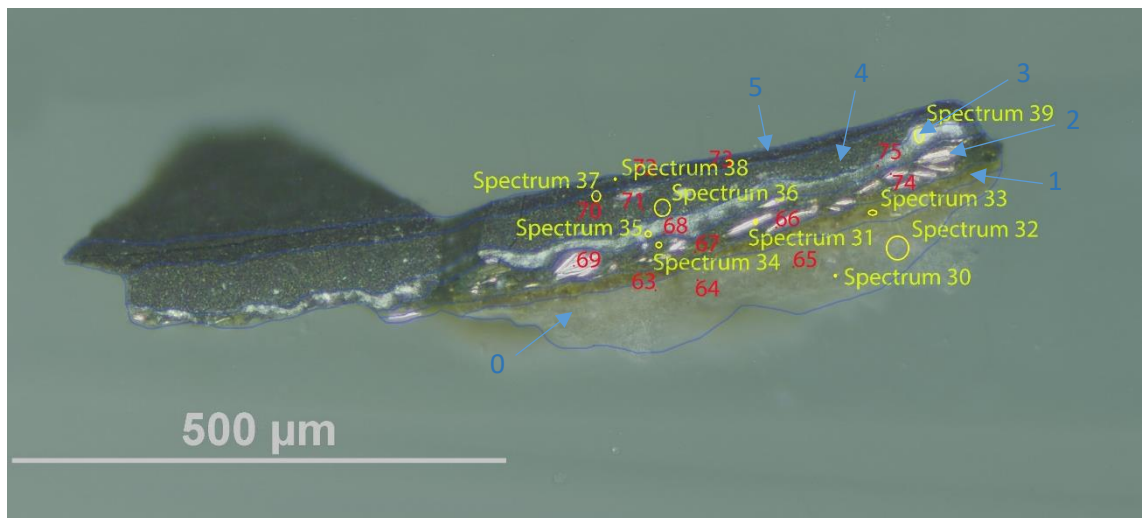


**Sampling.** This fragment was taken from an area of loss on the water flow held by one of the base's figures (Part 4).

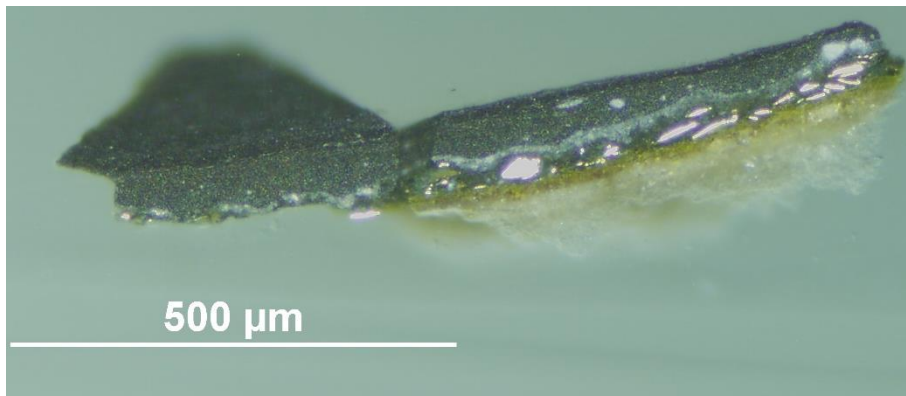
Below: Overlapped (OM and BSE) cross-section image showing the stratigraphy (blue indicators).

5. Dark layer with shellac
4. Dark layer
3. Grey layer
2. Dark layer with metal inclusions
1. Dark-Yellow layer
0. Plaster bulk

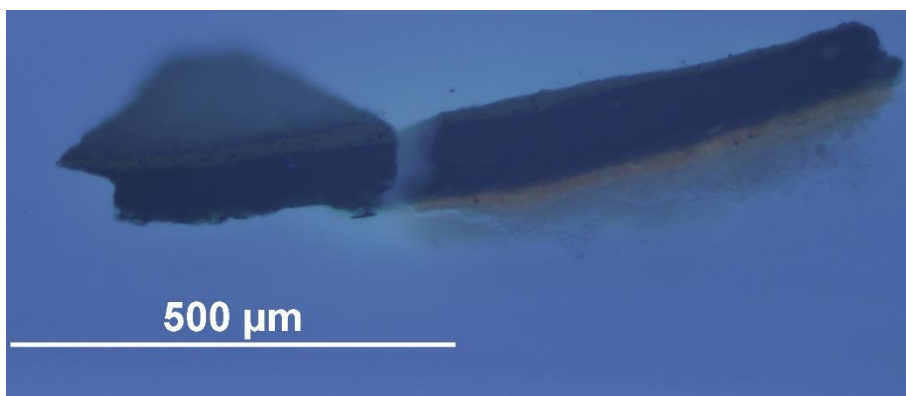
**Analysis spots.** EDS analysis (yellow): Spectra 30-39; FT-IR analysis (red): nos. 63-75.



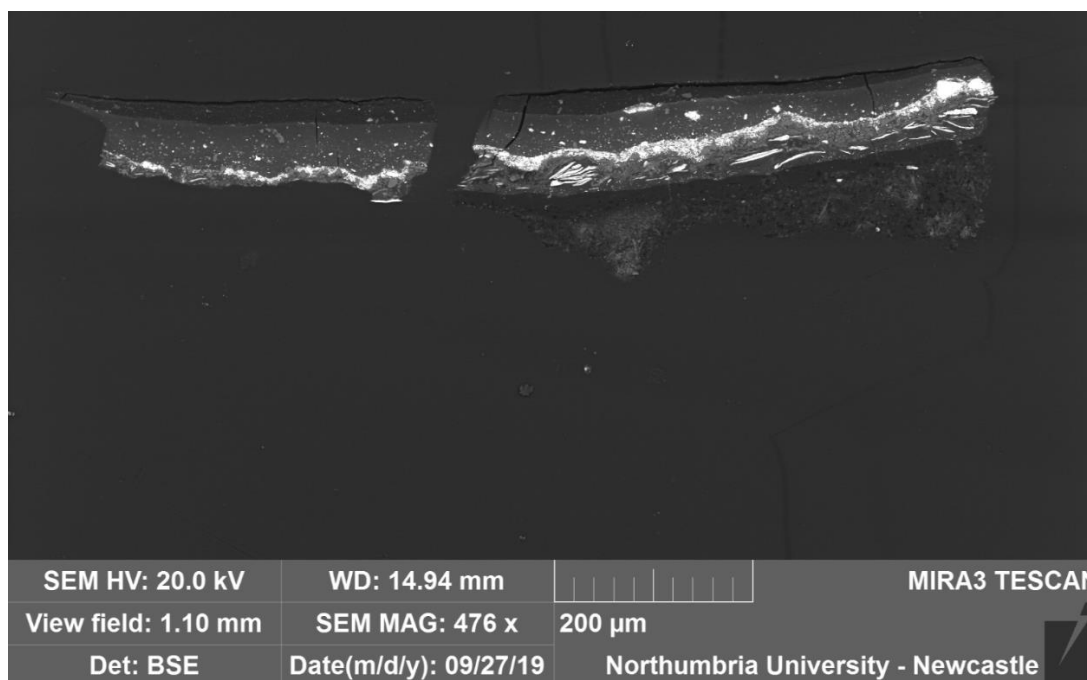
**Summary.** The sample is mostly made of C, O, S and Ca (**calcium sulfate**,  $\text{CaSO}_4$ , confirmed by EDS and by the peak at  $1600\text{-}1616\text{ cm}^{-1}$  in the FT-IR spectra). **Layer 0** consists of **calcium sulfate ( $\text{CaSO}_4$ )**, **lead (Pb)** and traces of **Ba, Ti** and **Al**. Traces of **Silicon** are present in all the layers. **Layer 1** does not show any significant elements' distribution. **Layer 2** contains **brass fillings (Zn and Cu)** were detected) and traces of **chlorine (Cl)**. **Layer 3** consists of **calcium sulfate ( $\text{CaSO}_4$ )**, **lead** and traces of **Fe, Ba, Ti** and **Cl**. Layer 4 consists of **calcium sulfate ( $\text{CaSO}_4$ )** and **lead** and **layer 5** does not show any significant elements distribution. A **wax or resin** is suggested by FT-IR (peaks at  $1000\text{-}1500$  and  $2800\text{-}3000\text{ cm}^{-1}$ ) and was detected in all the layers.



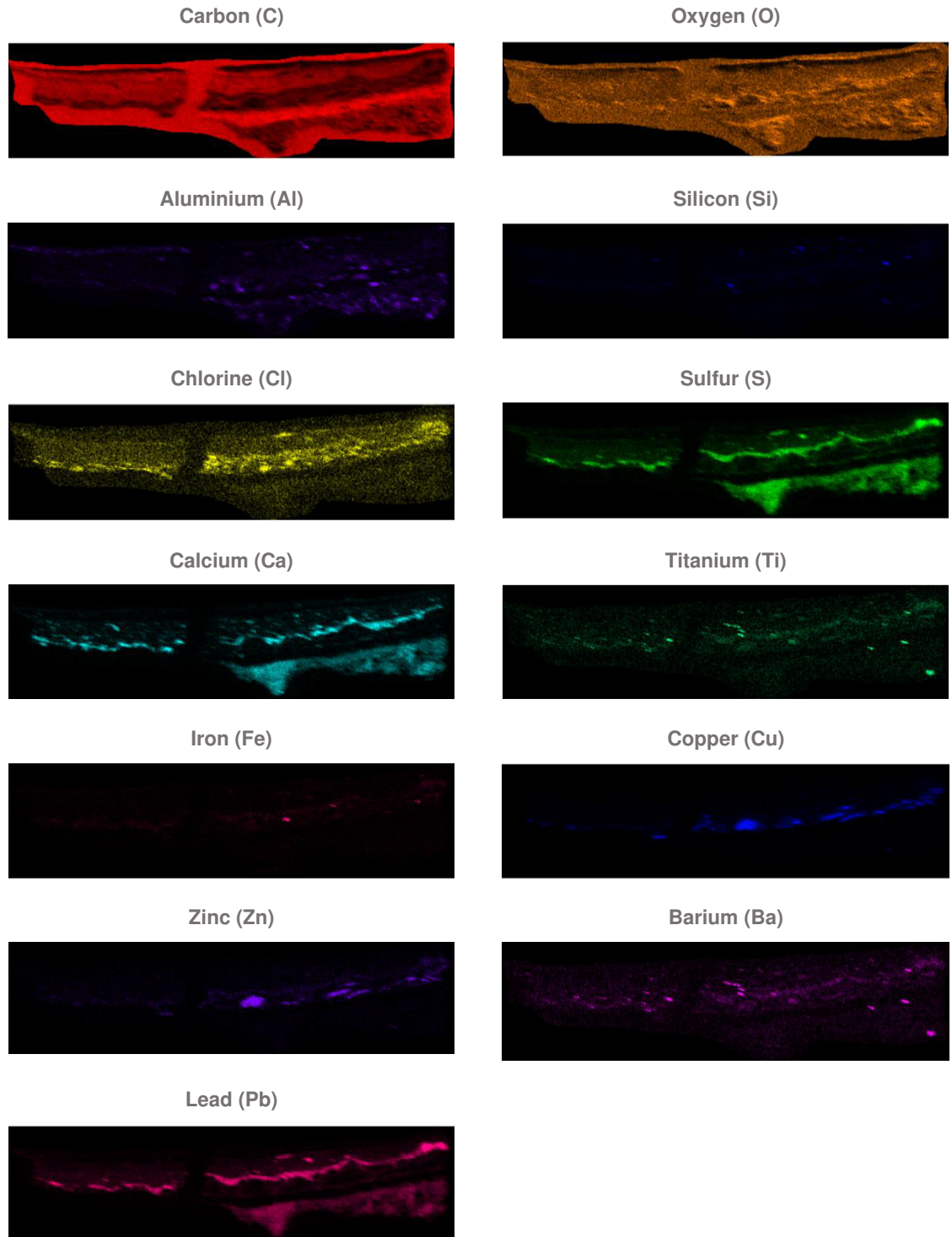
VLR OM (left)



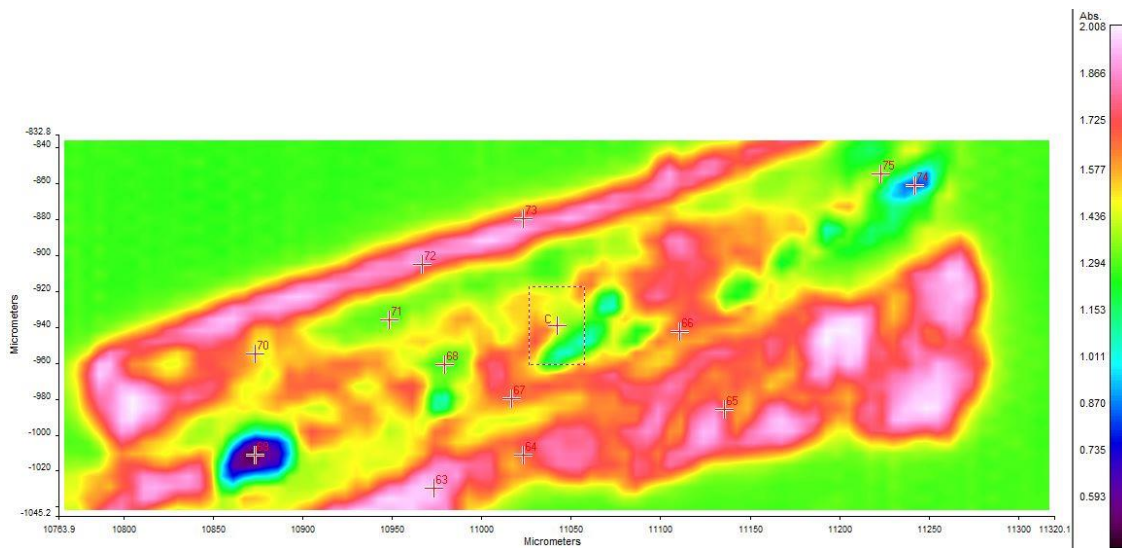
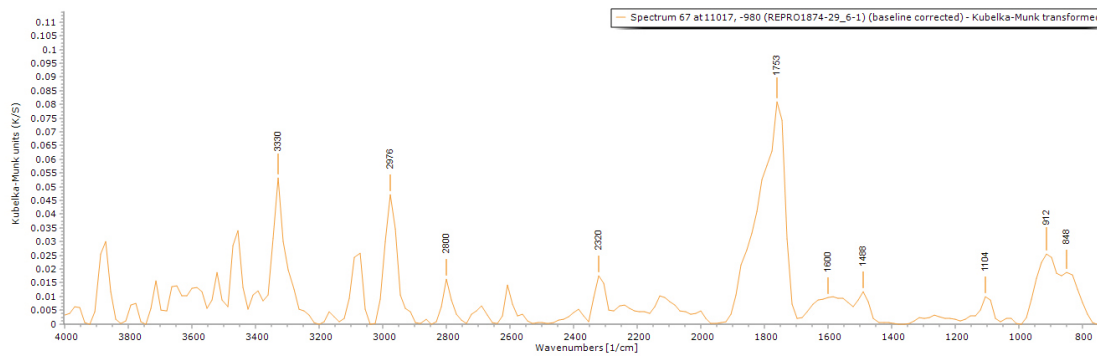
UVfOM (left)



**BSE image (above).** The tabular crystalline structure typical of gypsum plaster can be seen in layer 0 and metal fillings can be seen in layer 2. Layer 3 is made of heavier elements.



Layer 0 consists of **calcium sulfate (CaSO<sub>4</sub>)**, **lead (Pb)** and traces of **Ba**, **Ti** and **Al**. Traces of **Silicon** are present in all the layers. **Layer 1** does not show any significant elements' distribution. **Layer 2** contains **brass fillings (Zn and Cu were detected)** and traces of **chlorine (Cl)**. **Layer 3** consists of **calcium sulfate (CaSO<sub>4</sub>)**, **lead** and traces of **Fe**, **Ba**, **Ti** and **Cl**. **Layer 4** consists of **calcium sulfate (CaSO<sub>4</sub>)** and **lead** and **layer 5** does not show any significant elements distribution.



FT-IR spectrum 30 ([above](#)) of layer 1. Peaks for the casting resin ( $1312, 1760\text{ cm}^{-1}$ ) and a wax/resin ( $1488\text{ cm}^{-1}$  and  $2800\text{-}3000\text{ cm}^{-1}$ ). A summary of the peaks observed in the spectra 63-75 can be seen in the table [below](#).

FT-IR (FPA) image ([above](#)). Some indication of different reflectance of the layers can be observed in the FPA image.

Spectrum	Layer	peaks (cm-1)							
		Casting Resin	Gypsum	Carbonate	Wax/resin	C=O ester carbonyl	SO overtone	Unknown	
63	0	1312, 1760	1616		839, 944, 992, 1024, 1104, 1232, 1424, 1552, 2736, 2816, 2896			2304	
64	0	1312, 1760	1616		848, 1104, 1184, 1376, 1472, 1520, 2848, 2992			2320	
65	0	1312, 1760	1600		832, 1024, 1088, 1200, 1376, 1456, 2816, 2960			2368	
66	2		1600		864, 960, 1056, 1120, 1216, 1296, 1504, 1648, 2864, 2992	1744		2352	
67	1	1760	1600		848, 912, 1104, 1488, 2800, 2976			2320	
68	3	1760			944, 1040, 1104, 1184, 1488			2345	
69	2							2352	1120
70	4			800	848, 896, 1088, 1152, 1456, 1568, 1696			2336	
71	4	1312, 1760	1616	800	1088, 1136, 1184, 1488			2342	
72	5	1312, 1760			848, 928, 1088, 1168, 1488, 1552, 2896, 2960			2320	
73	5	1328, 1760	1600		784, 1088, 1200, 1392, 1456, 1536, 2832		2320, 2368		
74	2		1616		832, 1136, 1488, 2816	1744		2344	
75	3	1760	1600		1136, 1280, 1552, 2960			2342	

## Experimental

The object was observed, and its conditions were documented. Samples from selected areas were taken by Valentina Risdonne. When possible, each sample was split into two parts: one fragment was embedded in polyester resin (Tiranti clear casting resin), polished and analysed under optical microscope and the other was put aside for py-TMAH-GC/MS and XRD analysis.

The optical microscopy was performed with an Olympus BX51 Metallurgical Microscope equipped with four objectives (magnification of x5, x20, x50 and x100), and an x10 eyepiece. In many instances, a small amount of white spirit was applied on the surface of the cross-section to improve the saturation under the microscope. The microscope is equipped with a 6-cube filter turret which allows to operate the system in reflected visible light (brightfield and darkfield mode) and reflected UV light (365 nm) using a 100 W mercury burner.

The SEM-EDS analysis was performed with a field emission TESCAN MIRA 3 with gigantic chamber. The SEM is equipped with: secondary electron detector (SE), secondary electron in-beam detector (In-beam SE), back-scatter detector (BSE), back-scatter in-beam detector (In-beam BSE), cathodoluminescence detector (without wavelength detection) (CL), plasma chamber/sample cleaner and software Alicona 3D imaging. For the EDS analytical part, it has an Oxford Instruments setup: Software: AztecEnergy, X-ray detector X-Max 150 mm<sup>2</sup> and X-ray detector X-Max Extreme, low energy detector for thin films, high resolution and low voltage. The samples were analysed by SEM-EDS Low Vacuum Mode (10-15 Pa). EDS Mapping and data processing were performed with Aztec Oxford software.

A Perkin Elmer Frontier FT-IR spectrometer (350 cm<sup>-1</sup> at the best resolution of 0.4 cm<sup>-1</sup>) was used, equipped with a germanium crystal for ATR measurements and combined with a Spectrum Spotlight 400 FT-IR microscope equipped with a 16×1 pixel linear mercury cadmium telluride (MCT) array detector standard with InGaAs array option for optimised NIR imaging. Spectral images from sample areas are possible at pixel resolutions of 6.25, 25, or 50 microns. The Perkin Elmer ATR imaging accessory consists of a germanium crystal for ATR imaging. These run with Perkin Elmer Spectrum 10™ software and with SpectrumIMAGE™ software. Baseline and Kubelka-Munk corrections were applied to the raw data acquired in diffuse reflectance.

The XRD analysis was performed with a Rigaku SmartLab SE equipped with a HyPix-400, a semiconductor hybrid pixel array detector and Cu source. The analyses were performed in Bragg-Brentano geometry mode, with 40 kV tube voltage and 50 mA tube current. The diffractograms were processed with a SmartLab II software. The data was compared to the RUFF database (Lafuente et al., 2016) and COD Database (Gražulis et al., 2009).

The instrument used for GC/MS is a Thermo Focus Gas Chromatographer with DSQ II single quadrupole mass spec. The column currently installed is an Agilent DB5-MS UI column (ID: 0.25 mm, length: 30 m, df: 0.25 µm, Agilent, Santa Clara, CA, USA). Carrier gas: helium. Detector temperature: 280 °C, Injector temperature: 250 °C. It can be used with the PyroLab 2000 Platinum filament pyrolyser (PyroLab, Sweden) attachment or in split/splitless mode. Detection: Total Ion monitoring (TIC). 1 µl of the sample with 1 µl of TMAH was placed on the Pt filament for the py-GC/MS. The inlet temperature to the GC was kept at 250 °C. The helium carrier gas flow rate was 1.5 ml/min with a split flow of 41 ml/min and split ratio of 27. The MS transfer line was held at 260 °C and the ion source at 250 °C. The pyrolysis chamber was heated to 175 °C, and pyrolysis was carried out at 600 °C for 2 s. This run with Xcalibur™ and PyroLab™ software. The library browser supported NIST MS Version 2.0 (Linstrom & Mallard, 2014).

Valentina Risdonne, PhD student

[v.risdonne@vam.ac.uk](mailto:v.risdonne@vam.ac.uk) / [valentina.risdonne@northumbria.ac.uk](mailto:valentina.risdonne@northumbria.ac.uk)

Victoria and Albert Museum – Northumbria University

PhD project 'Materials and techniques for coating of the nineteenth-century plaster casts'

©V&A Museum

23 October 2020

## Notes

10 September 2018	Sampling	Valentina's PhD Lab book 1, page 113
24 October 2018	Casting	Valentina's PhD Lab book 1, page 133
6 November 2018	Microscopy	Valentina's PhD Lab book 1, page 137
14 October 2019	FT-IR	Valentina's PhD Lab book 1, page 175
3 December 2019	XRD	Valentina's PhD Lab book 2, page 4
18 March 2020	GC/MS	Valentina's PhD Lab book 2, page 50

A full record of analyses is available at <https://doi.org/10.25398/rd.northumbria.13902737>

## References

- Colombini, M. P., & Modugno, F. (2009). *Organic mass spectrometry in art and archaeology*. John Wiley & Sons.
- Gražulis, S., Chateigner, D., Downs, R. T., Yokochi, A. F. T., Quirós, M., Lutterotti, L., Manakova, E., Butkus, J., Moeck, P., & Le Bail, A. (2009). Crystallography Open Database—an open-access collection of crystal structures. *Journal of Applied Crystallography*, 42(4), 726–729.
- Lafuente, B., Downs, R. T., Yang, H., & Stone, N. (2016). The power of databases: the RRUFF project. In *Highlights in mineralogical crystallography* (pp. 1–29). Walter de Gruyter GmbH.
- Linstrom, P. J., & Mallard, W. G. (2014). *NIST Chemistry WebBook, NIST standard reference database number 69, National Institute of Standards and Technology, Gaithersburg MD, 20899*.
- Mills, J., & White, R. (2012). *Organic chemistry of museum objects*. Routledge.



**Northumbria  
University**  
NEWCASTLE

Analysis Report - Valentina Risdonne

Copy of a Tympanum - Christ, St. Godehard and St. Epiphanius

(REPRO.1874-45)

Initiator: Charlotte Hubbard; Conservation Department

11 February 2021

© Victoria and Albert Museum



## Analysis Report - Copy of a tympanum (REPRO.1874-45)

### Contents

Contents.....	216
List of abbreviations.....	216
Summary.....	217
Sample 1.....	219
Sample 2.....	221
Sample 3.....	224
Sample 4.....	226
Experimental.....	230
Notes.....	231
References.....	231

### List of abbreviations

BSE	Back Scattered Electron
EDS	Energy Dispersive Spectrometry
FT-IR	Fourier-Transform Infra-Red
FPA	Focal Plane Array
GC/MS	Gas Chromatography-Mass Spectrometry
OM	Optical Microscopy
PL	Proper Left
PR	Proper Right
py	pyrolysis
SEM	Scanning Electron Microscopy
TMAH	tetramethylammonium hydroxide
UVf	Ultraviolet Fluorescence
VLR	Visible Light Reflectance
XRD	X-ray Diffraction

## Summary

In summary, the bulk of the object is made of gypsum plaster, which contains several types of inclusions (including silicates and carbonates). By looking at the results, it is possible to hypothesise that the surface layer is mostly made of **silicon** and **aluminium** and the organic medium is **shellac**.



Figure 1. The copy of a tympanum.

The object, '**Copy of a tympanum - Christ, St. Godehard and St. Epiphanius (REPRO.1874-45)**' (Figure 1), is a plaster cast of a Tympanum made by Friedrich Küsthardt about 1874 and depicting the figures of Christ, Saint Godehard and probably Epiphanius of Pavia. The original was sculpted by an unknown artist about 1200-10 and it was positioned on the exterior of a church in Hildesheim, Germany (above the north nave door). The cast was purchased from F. Küsthardt in 1874 for £9 and is now located in Gallery 46A (The Ruddock Family Cast Court). Its dimensions are 107.0X213.5 cm.

Samples from the plaster cast were taken from pre-existing areas of loss to investigate the stratigraphy and the method of manufacture. The samples were analyzed to provide data for the study of the objects of the Cast Courts collection within the PhD project 'Materials and techniques for coating of the nineteenth-century plaster casts'. Details on the experimental procedure are available in the Experimental section of this report. A selection of significant results is shown in the following pages and the relevant database of analysis (<https://doi.org/10.25398/rd.northumbria.14034986>). The samples were taken by Charlotte Hubbard and images and samples' locations are not available for this object, due to the object accessibility and other difficulties.

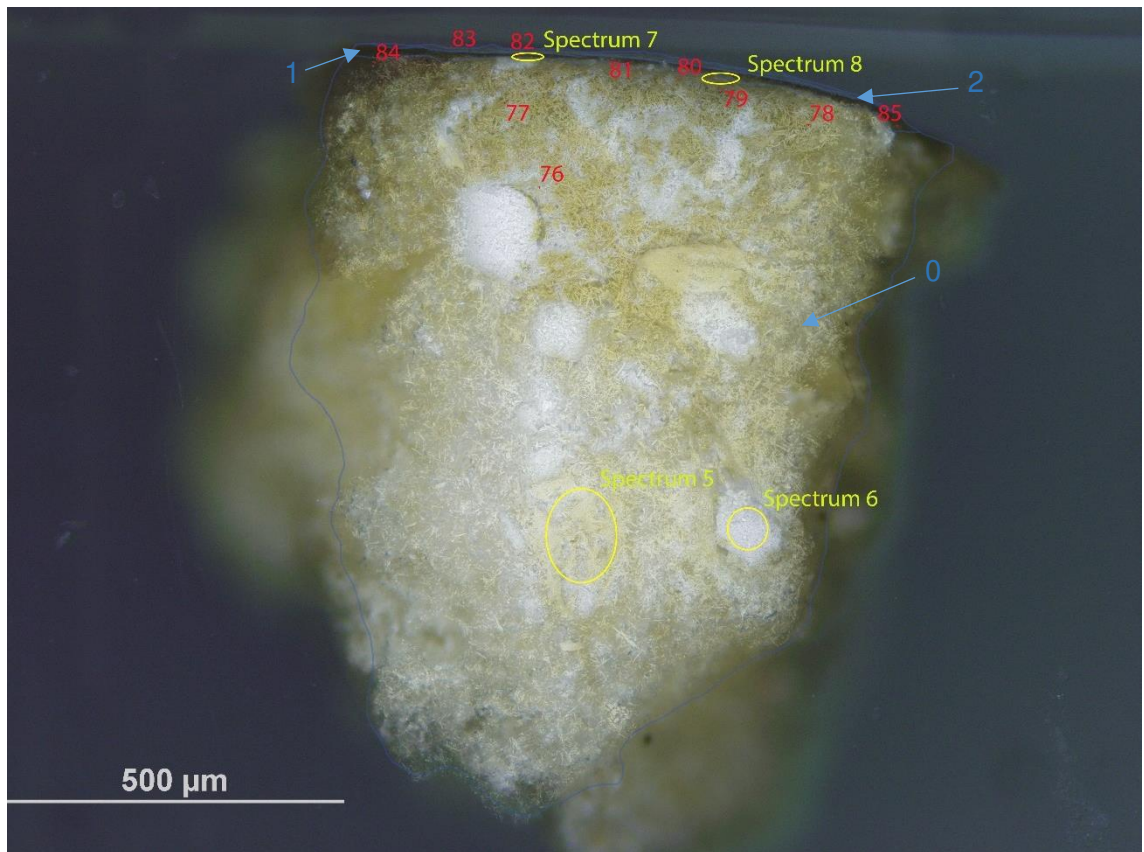
The **substrate** (layer 0 in all the samples) is made of gypsum plaster (**calcium sulfate**,  $\text{CaSO}_4$ , confirmed by EDS, XRD and by the peak at  $1600\text{-}1648\text{ cm}^{-1}$  in the FT-IR spectra, which also show the sulfate overtones in the  $2100\text{-}2300\text{ cm}^{-1}$  area). Inclusions made of **aluminium (Al)** and **silicon (Si)** are present in all the layers of all the samples and **magnesium (Mg)** was also detected in sample 5. The tabular crystalline structure typical of gypsum plaster can be seen in layer 0. In sample 2 and 5, the BSE images show that the crystalline structure of calcium sulfate is denser. An **interface layer**, yellow under visible illumination and possibly consisting of a portion of lower layer soaked with the surface coating(s), showing characteristics of both layers, can be only seen in samples 4 and 5. All

the samples show a layer, **dark** under visible illumination and mapping suggests that this layer is mainly made of **silicon (Si)** and **aluminium (Al)** (particularly visible in samples 2, 4 and 5) and traces of Na, Fe, Mg, K, Cl and Ti. Sample 1, 4 and 5 show an additional layer, which fluoresces under UV illumination and can be consistent with a **finishing layer**. This can suggest either that varnish was applied only on the selected areas or that the varnish was applied on all the surface, but it was differently adsorbed depending on the local variation of porosity.

A **wax** or **resin** (FT-IR peaks at 1000-1200 and 2800-3000  $\text{cm}^{-1}$ ) was detected in all the layers of all the samples, which indicates that either the material was added to the gypsum plaster wet mixture or that the coating has also penetrated in layer 0. The latter seems also possible as the average depth of the samples is about 0.5 mm. The additional presence of a **protein** cannot be excluded by interpreting the FT-IR spectra, due to the complexity of the admixture and also to the crowded pattern of the resins' FT-IR spectra (Price et al., 2009). Py-TMAH-GC/MS analysis of sample 4 suggests that the organic medium in this sample consists of **shellac**, possibly mixed with **an oil** (Colombini & Modugno, 2009).

**NOTE:** casting in resin the fragments of plaster resulted in the fragments absorbing the resin when in the liquid state. This was visible in the BSE image as well as through the EDS mapping (Tiranti resin and catalyst are mainly made of organic compounds C, H and O). Aluminium (Al) traces are present in all the samples, due to the polishing chemical.

## Sample 1



Above: Overlapped (OM and BSE) cross-section image showing the stratigraphy (blue indicators).

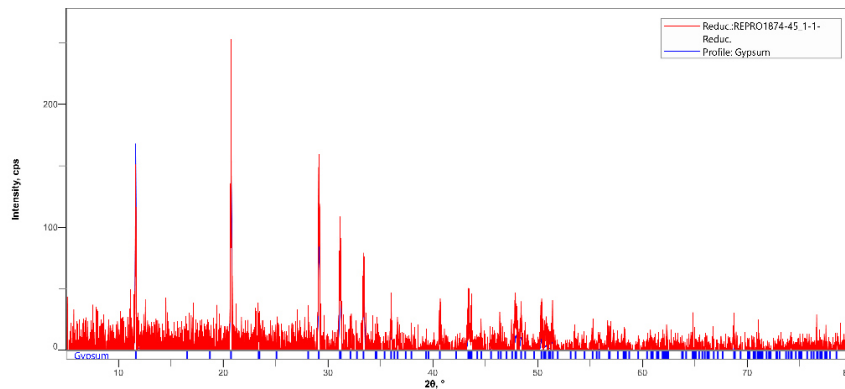
### 2. Varnish

#### 1. Dark layer

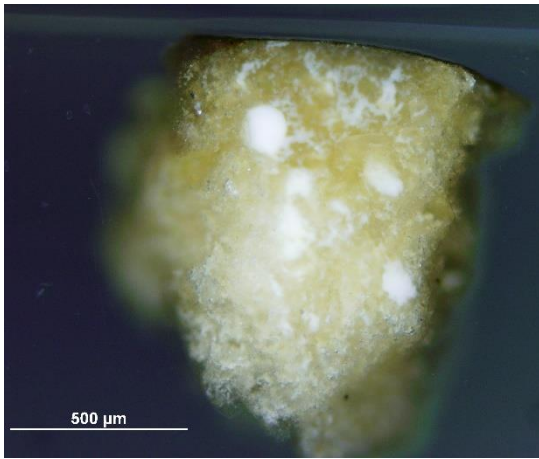
#### 0. Plaster bulk, yellowish with large white clusters

**Analysis spots.** EDS analysis (yellow): Spectra 5-8; FT-IR analysis (red): nos. 76-85

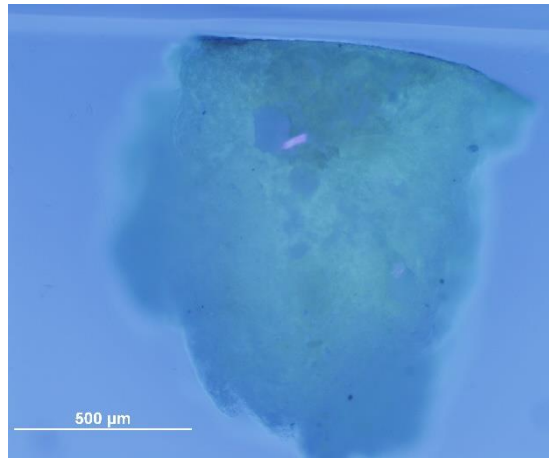
**Summary.** The substrate (layer 0) is made of plaster (**calcium sulfate**,  $\text{CaSO}_4$ , confirmed by EDS, XRD and by the peak at  $1600\text{ cm}^{-1}$  and overtones in the FT-IR spectra). The tabular crystalline structure typical of gypsum plaster can be seen in layer 0. Al is possibly due to the polishing agent and traces of **Si**, **Mg** and **Na** were detected. Layer 1 is black under visible illumination and seems consistent with layers of dirt. Layer 2 is white under visible illumination and is likely to consist of a **wax or resin** (FT-IR peaks at  $100\text{-}1200$  and  $2800\text{-}3000\text{ cm}^{-1}$  were detected in all the layers).



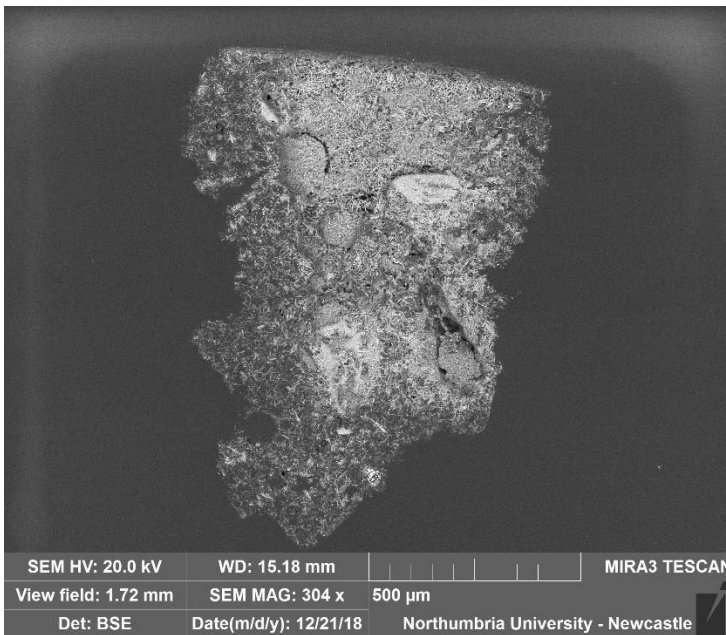
A fragment of this sample was pulverised and analysed by **XRD**. It was possible to identify the profile of gypsum (calcium sulfate) and the diffractogram was compared to references from the Rigaku SmartLab Database and the most significant peaks were at  $2\theta = 11.63, 20.77, 29.13, 31.16, 33.47, 36.04, 47.94$ .



VLR OM (above)

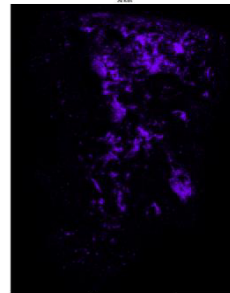


UVfOM (above)



**BSE image (left).** The tabular crystalline structure typical of gypsum plaster can be seen in layer 0, which is made of **calcium sulfate**,  $\text{CaSO}_4$ . Large white inclusions can be seen and **EDS mapping (below)** suggests that they might have been caused by the polishing agent. Traces of **Si**, **Mg** and **Na** were also detected.

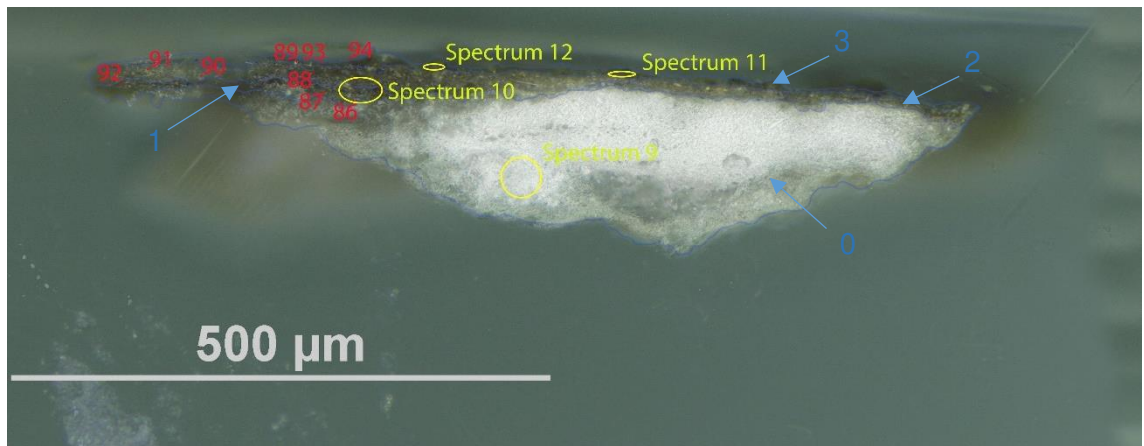
Aluminium (Al)



Peaks for the casting resin ( $1312, 1760 \text{ cm}^{-1}$ ), gypsum ( $1632 \text{ cm}^{-1}$ , overtone  $2200-2300 \text{ cm}^{-1}$ ) and a wax/resin ( $1000-1200-1500$  and  $2800-3000 \text{ cm}^{-1}$ ). A summary of the peaks observed in the spectra 76-85 can be seen in the table below.

Spectrum	Layer	peaks ( $\text{cm}^{-1}$ )					
		Casting Resin	Gypsum	Carbonate	Wax/resin	C=O ester carbonyl	SO overtone
76	0	1312	1680		784, 848, 896, 960, 1024, 1248, 1360, 2864, 2928, 3248, 3328, 3488, 3576	1728	2128, 2224
77	0	1344, 1760	1632		896, 928, 1056, 1088, 1232, 1296, 1456, 2880, 2944, 3312, 3488, 3613	1728	2216, 2272, 2384
78	0	1312		1776	768, 816, 880, 1072, 1200, 1376, 1408, 1584, 2832, 3024, 3168, 3381, 3568		2292, 2400
79	0	1344		1776	816, 896, 1008, 1088, 1168, 1296, 1392, 1504, 1584, 2816, 2864, 2976, 3104, 3184, 3440, 3568		2224, 2272, 2384
80	1	1312, 1760	1616		768, 832, 960, 1168, 1376, 1472, 2880, 3072, 3296, 3552, 3700		2240, 2432, 2512
81	1	1312, 1760	1600		800, 1136, 1664, 2880, 3040, 3284, 3405, 3648		2288, 2384
82	1	1312, 1760	1616		784, 896, 976, 1088, 1168, 1472, 3280, 3408, 3822		2304, 2400
83	2	1312, 1760	1616		784, 896, 1008, 1168, 1392, 1504, 2736, 3008, 3360, 3488		2368
84	0	1312, 1767	1616		800, 864, 1152, 1392, 1520, 2880, 2960, 3156, 3296, 3568, 3664		2320
85	1	1312, 1760			784, 928, 992, 1184, 3136, 3383		2320, 2384

## Sample 2



Above: Overlapped (OM and BSE) cross-section image showing the stratigraphy (blue indicators).

**3. Dark layer**

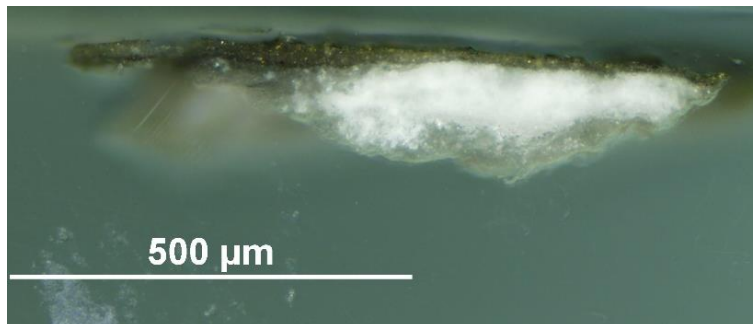
**2. Dark yellowish layer**

**1. Dark line**

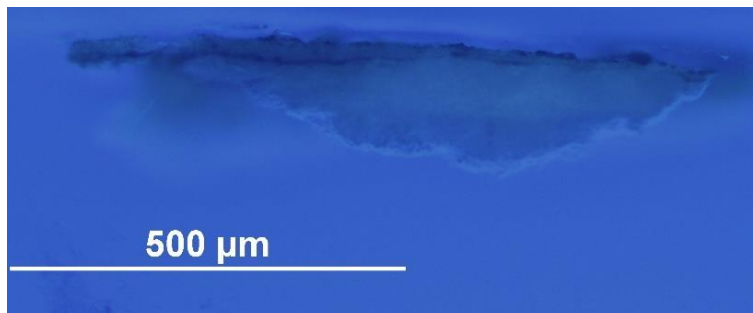
**0. Plaster bulk**

**Analysis spots.** EDS analysis (yellow): Spectra 9-12; FT-IR analysis (red): nos. 86-94.

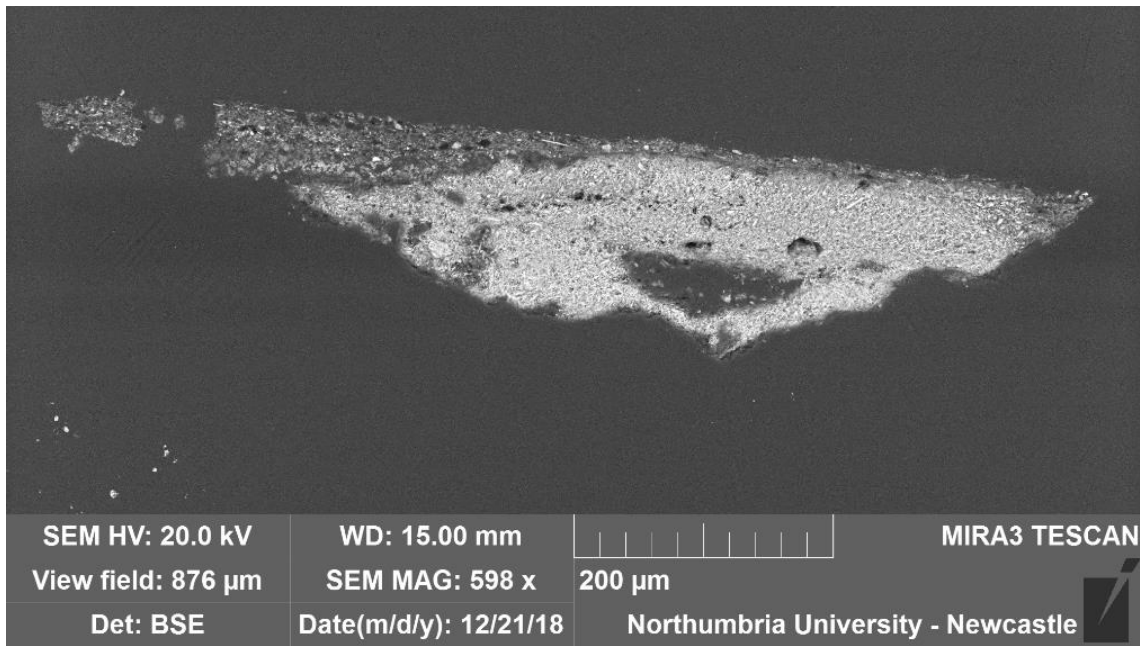
**Summary.** The substrate (layer 0) is made of plaster (**calcium sulfate**,  $\text{CaSO}_4$ , confirmed by EDS and by the peak at  $1600\text{ cm}^{-1}$  and overtones in the FT-IR spectra) and Si-Al inclusions and Mg are present in all the layers. The tabular crystalline structure typical of gypsum plaster can be seen in layer 0. Layers 1 to 3 structure appears very different from the substrate. Layers 1 and 3 are dark under the VLR OM, seemingly consistent with layers of dirt. Layer 2 is a coating layer made of Si and Al. In the outmost layers, traces of Cl, Na, K and Fe were also detected. A **wax or resin** (FT-IR peaks at  $1200\text{-}1500$  and  $2800\text{-}3000\text{ cm}^{-1}$ ) was detected in all the layers. **Py-TMAH-GC/MS** suggests that the organic medium is **shellac** (Colombini & Modugno, 2009; Mills & White, 2012).



VLR OM (left)

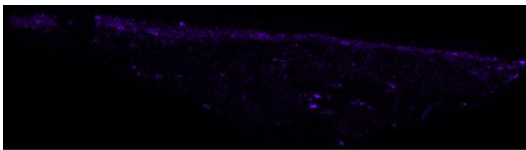


UVfOM (left)

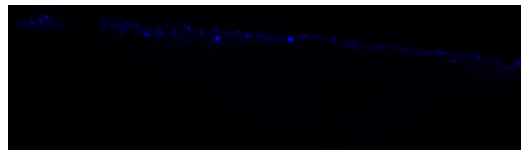


**BSE image** ([above](#)). The tabular crystalline structure typical of gypsum plaster can be seen in layer 0. The structure of layers 1 to 3 appears very different. Layers 2 and 3 appear consisting of **Si** and **Al** (**EDS mapping**, [below](#)). **EDS spectra** suggest that the sample is mostly made of calcium sulfate (C, O, Ca, S), Al, Si and Mg. Traces of Cl, Na, K and Fe were detected in the utmost layers.

Aluminium (Al)

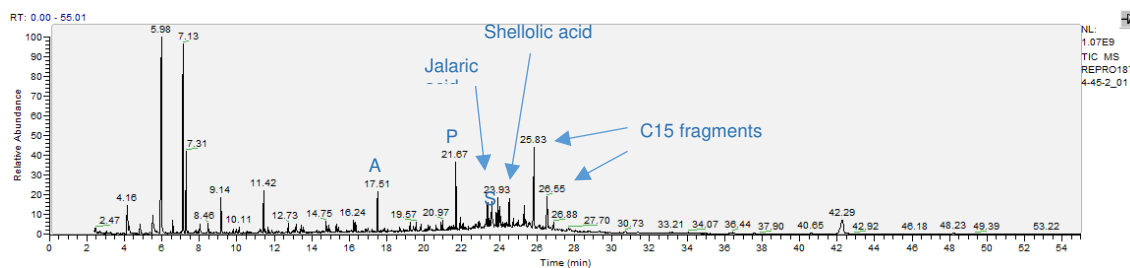


Silicon (Si)



**FT-IR spectra are consistent within the layers.** Peaks for the casting resin (1312, 1760  $\text{cm}^{-1}$ ), gypsum (1600  $\text{cm}^{-1}$ , overtone 2200-2300  $\text{cm}^{-1}$ ) and a wax/resin (1000-1200, 2800-3000  $\text{cm}^{-1}$ ). A summary of the peaks observed in the spectra 86-94 can be seen in the table [below](#).

Spectrum	Layer	peaks ( $\text{cm}^{-1}$ )					
		Casting Resin	Gypsum	Carbonate	Wax/resin	C=O ester carbonyl	overtones
86	0				1040, 1232, 1584, 3568		2240
87	1		1648		1056, 1232, 1456, 2960, 3088, 3440, 3610	1744	2246, 2400
88	2	1760	1648		960, 1040, 1088, 1216, 1296, 3200, 3380		2280, 2384
89	3	1312, 1760	1600		768, 816, 976, 1024, 1216, 1392, 1504, 1664, 2800, 2864, 2912, 3280, 3605, 3696		2304, 2384
90	2	1760			848, 992, 1056, 1088, 1200, 1296, 1424, 1472, 1552, 2976, 3088, 3342, 3664		2208, 2368, 2672
91	2	1328, 1760			880, 1184, 1528, 1552, 2720, 2992, 3072, 3206, 3472, 3536, 3744		2256, 2384
92	2	1312, 1760	1616		800, 896, 1072, 1168, 1504, 3008, 3136, 3264		2288, 2400
93	3	1344	1616	1776	832, 960, 1040, 1088, 1200, 1392, 1488, 2832, 3008, 3088, 3280, 3536, 3632		2240, 2384, 2464
94	3	1328, 1760	1600		816, 928, 1088, 1152, 1488, 2960, 3216, 3388, 3568		

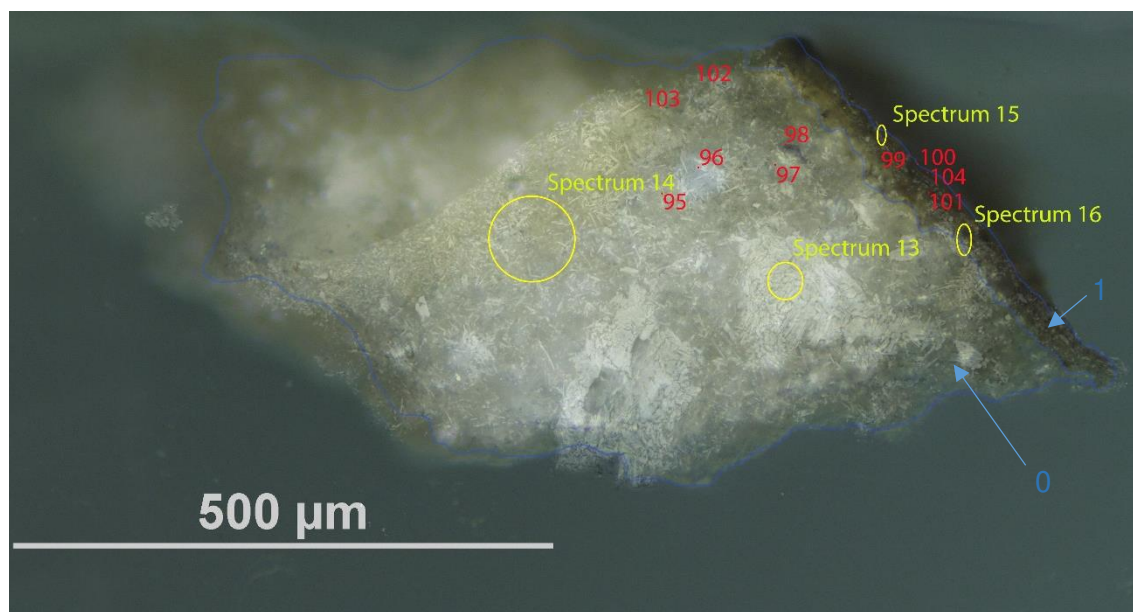


RT	m/z	Assignment	Formula
4.16	45(100), 59(6), 74(65), 91(15)	Acetaldehyde, methoxy-	C3H6O2
5.51	42(11), 58(100), 88(3), 116(3)	1,2-Ethanediamine, N'-ethyl-N,N-dimethyl-	C6H16N2
5.98	42(12), 58(100), 117(17)	1,2-Ethanediamine, N'-ethyl-N,N-dimethyl-	C6H16N2
6.59	58(20), 65(21), 79(100), 91(5), 106(5)	Methanesulfonic acid, methyl ester	C2H6O3S
7.13	56(7), 72(100), 116(2), 131(3)	1,2-Ethanediamine, N'-ethyl-N,N-dimethyl-	C6H16N2
9.14	44(100), 57(23), 86(74), 118(8), 128(58)	Unidentified amine fragment	
11.42	42(2), 58(100), 70(10), 116(6)	1,2-Ethanediamine, N'-ethyl-N,N-dimethyl-	C6H16N2
16.24	55(78), 69(78), 74(92), 87(44), 97(58), 111(30), 129(80), 138(100), 171(63), 198(5)	Unidentified FA fragment	
17.51	55(67), 74(72), 83(65), 87(30), 97(22), 111(57), 124(28), 143(33), 152(100), 185(40)	Nonanedioic acid, monomethyl ester	C10H18O4
19.23	45(82), 55(42), 71(51), 75(100), 85(85), 101(73), 115(31), 123(20), 139(28), 161(39), 183(24), 215(5), 260(5), 281(5)	Unidentified terpenoid fragment	
19.57	55(23), 74(100), 87(64), 115(11), 129(9), 143(23), 199(17), 211(5), 242(5)	Unidentified FA fragment	
21.67	55(18), 74(100), 87(65), 129(8), 143(21), 171(7), 185(7), 199(7), 227(14), 239(5), 270(5)	methyl palmitate	C17H34O2
21.9	55(84), 74(100), 84(68), 87(50), 98(97), 112(41), 149(43), 167(39), 199(33), 208(5), 241(40)	Tridecanedioic acid, dimethyl ester	C15H28O4
23.37	59(100), 69(47), 77(37), 87(57), 115(37), 129(31), 167(67), 179(37), 191(49), 247(34), 262(100), 275(74), 307(32), 322(5)	jalaric acid	
23.59	55(30), 74(100), 87(75), 87(75), 115(11), 143(26), 157(5), 185(5), 199(13), 213(5), 255(14), 275(5), 298(5)	methyl stearate	C19H38O2
23.93	55(18), 77(15), 91(25), 115(18), 145(20), 145(20), 159(23), 187(38), 215(14), 247(100), 306(5), 323(5)	C15 acid	
24.53	55(71), 75(67), 91(83), 115(69), 129(64), 169(63), 201(58), 206(66), 229(57), 238(65), 305(63), 320(100), 337(5)	shellolic acid	
25.83	45(36), 55(18), 71(100), 95(88), 109(29), 119(15), 137(43), 159(53), 169(23), 185(11), 201(85)	C15 acid	
26.55	55(30), 71(100), 95(93), 109(31), 155(57), 201(47), 237(5)	C15 acid	
42.19	57(84), 69(64), 83(100), 97(72), 111(45), 125(22), 139(5), 207(5), 222(5)	C20 acid	

RT = retention time, m/z = mass/charge ratio

**Py-TMAH-GC/MS chromatogram** (top and described in the table above) shows small fragments due to derivatization (from  $t = 4.16$  to  $11.42$  min) and markers characteristic of **shellac** (jalaric, shellolic and other C15 acids) (Colombini & Modugno, 2009; Mills & White, 2012). The intensity of the peaks of **methyl azelate** ( $t = 17.51$ ), **methyl palmitate** ( $t = 21.67$ ) and **stearate** ( $t = 23.59$ ) do not suggest an assignments of these FAs (**A/P = 0.54** and **P/S = 0.91**) (Colombini & Modugno, 2009).

## Sample 3



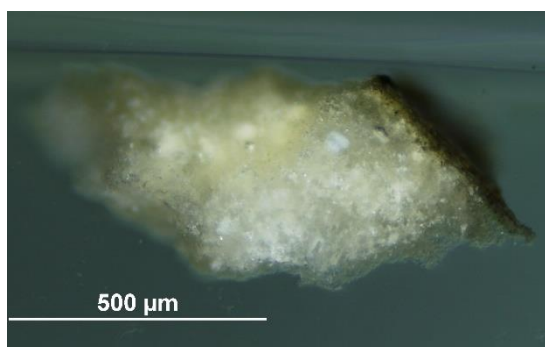
Above: Overlapped (OM and BSE) cross-section image showing the stratigraphy (blue indicators).

1. Dark yellowish layer

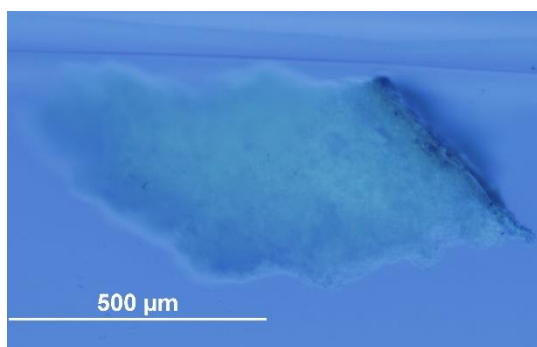
0. Plaster bulk

**Analysis spots.** EDS analysis (yellow): Spectra 13-16; FT-IR analysis (red): nos. 95-104.

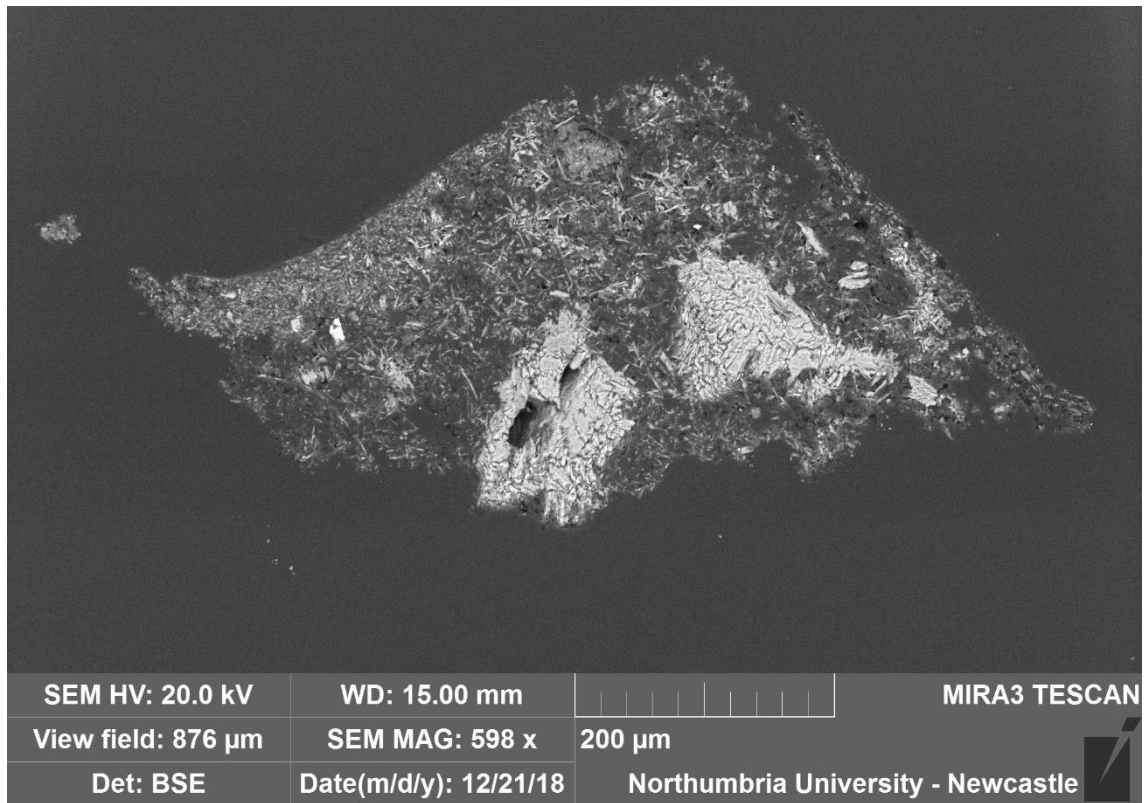
**Summary.** The sample is mostly made of C, O, S and Ca (**calcium sulfate**,  $\text{CaSO}_4$ , confirmed by EDS and by the peak at  $1600\text{-}1616\text{ cm}^{-1}$  in the FT-IR spectra). Si-Al inclusions are present in all the layers and additional traces K, Cl, Na, Mg, Fe and Ti were detected in the utmost layer. The structure typical of gypsum plaster can be seen in layer 0. A **wax or resin** is suggested by FT-IR (peaks at  $1000\text{-}1200$  and  $2800\text{-}3000\text{ cm}^{-1}$ ) and was detected in all the layers.



VLR OM (above)

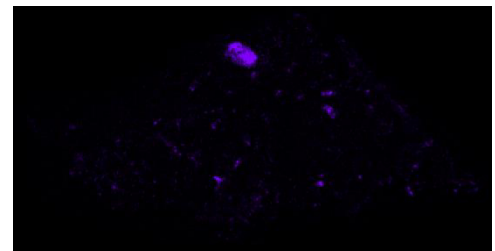


UVf OM (above)



**BSE image (above).** The tabular crystalline structure typical of gypsum plaster can be seen in layers 0 and 1. The brighter cluster is tighter crystallised gypsum plaster and Al inclusions can be seen in the **EDS mapping (right)**. **Calcium sulfate (CaSO<sub>4</sub>)** and **Al** and **Si** were detected in all the layers. Additional traces of K, Cl, Na, Mg, Fe and Ti were detected in the utmost layer.

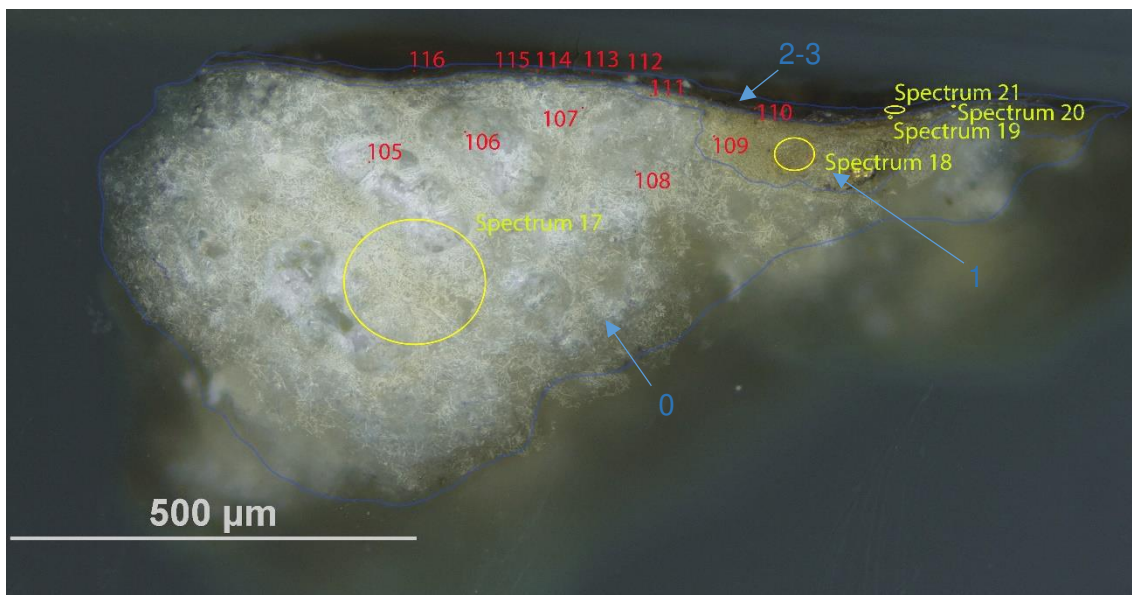
**Aluminium (Al)**



A summary of the **FT-IR** peaks observed in the spectra 95-104 can be seen in the table below. Peaks for the casting resin (1312, 1760 cm<sup>-1</sup>), gypsum (1616 cm<sup>-1</sup>), and a wax/resin (1200-1500 cm<sup>-1</sup> and 2800-3000 cm<sup>-1</sup>).

Spectrum	Layer	peaks (cm <sup>-1</sup> )					
		Casting Resin	Gypsum	Carbonate	Wax/resin	C=O ester carbonyl	overtones
95	0	1312, 1760			912, 1152, 1488, 2848, 3120, 3392, 3560		2240
96	0	1312, 1750	1008, 1632		864, 960, 1152, 1376, 1888, 2848, 2944, 3328, 2504, 3583		2208
97	0	1760	1008, 1616		832, 944, 1216, 1296, 1456, 2864, 2951, 3040, 3232, 3520, 3654		2144, 2256
98	0	1312	1600, 1680		784, 864, 976, 1088, 1440, 2848, 2959, 3088, 3328, 3472, 3641	1744	2224
99	1	1312, 1760	1008, 1648		800, 1088, 1184, 1488, 2800, 2960, 3296, 3424, 3578		
100	1	1312, 1760	1632		784, 960, 1200, 1392, 1472, 1552, 1840, 2800, 2864, 2976, 3152, 3360, 3784		2256, 2384
101	1	1312, 1760	1024, 1664		848, 896, 944, 1088, 1248, 1504, 1936, 2800, 3120, 3328, 3689		2240, 2395
102	0	1312, 1760	1600		784, 1088, 1136, 1520, 2992, 3392, 3513		2288
103	0	1312, 1760	1648		992, 1088, 1152, 1392, 1488, 2992, 3120		
104	1	1328, 1760	1008		800, 1088, 1392, 1584, 2848, 2960, 3296, 3541		2368

## Sample 4



Above: Overlapped (OM and BSE) cross-section image showing the stratigraphy (blue indicators).

3. Varnish

2. Dark layer

1. Yellowish layer

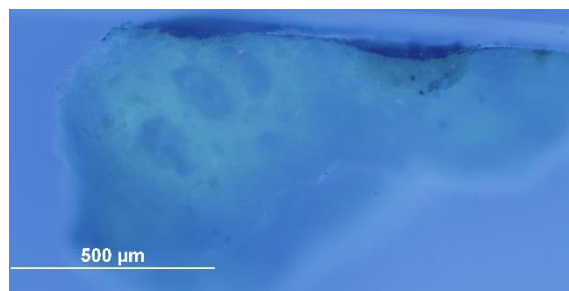
0. Plaster bulk

**Analysis spots.** EDS analysis (yellow): Spectra 17-21; FT-IR analysis (red): nos. 105-116.

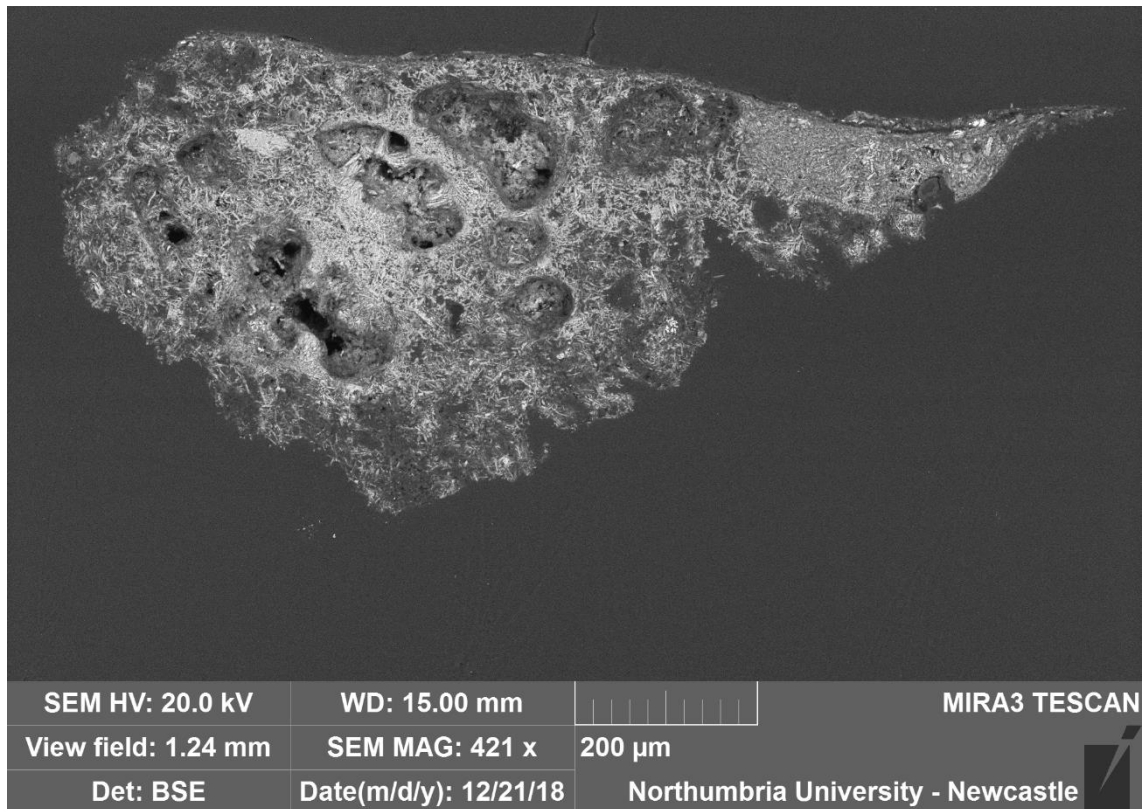
**Summary.** The sample is mostly made of C, O, S and Ca (**calcium sulfate**,  $\text{CaSO}_4$ , confirmed by EDS and by the peak at  $1600\text{-}1616\text{ cm}^{-1}$  in the FT-IR spectra). Al is overall present as used as a polishing agent, but could also, together with Si, be present as part of silicate inclusions, which are present in all the layers (see EDS mapping). The surface layers are mostly made of Si and Al, and traces of Na, Fe, Mg, K, Cl and Ti were also detected. A **wax or resin** is suggested by FT-IR (peaks at  $1000\text{-}1200$  and  $2800\text{-}3000\text{ cm}^{-1}$ ).



VLR OM (above)

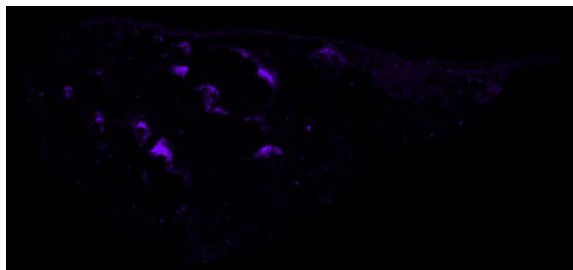


UVf OM (above)

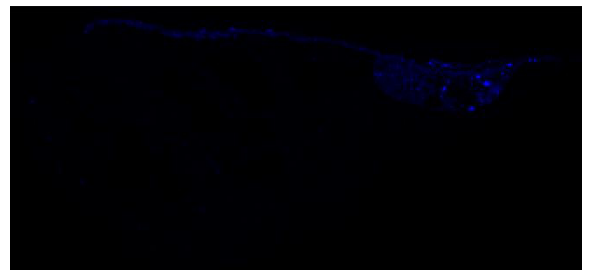


**BSE image (left).** The tabular crystalline structure typical of gypsum plaster can be seen in layer 0. **EDS mapping (below)** shows that layers 1 to 3 are mostly made of Si and Al. **EDS spectra** indicate that all the layers consist of C, O, Ca and S. Al traces are present in all the layers (polishing medium), but Al could also, together with Si be present as part of silicate inclusions. Traces of Na, Fe, Mg, K, Cl and Ti were also detected in the surface layers.

Aluminium (Al)



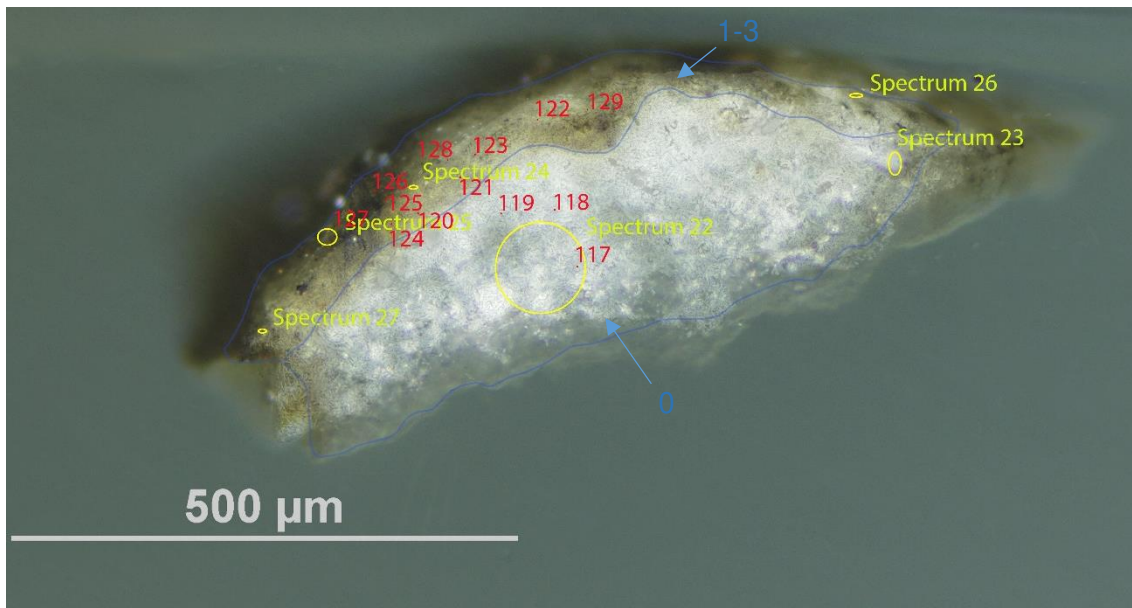
Silicon (Si)



Spectrum	Layer	peaks (cm-1)						
		Casting Resin	Gypsum	Carbonate	Wax/resin	C=O ester carbonyl	overtones	
105	0	1312, 1760	1616, 1680		752, 912, 992, 1248, 1472, 2928, 3280, 3656		2249, 2384	
106	0	1344	1024		848, 1296, 1584, 2864, 2944, 3334, 3552, 3648	1728	2304, 2400	
107	0	1312-44		1776	880, 1072, 1152, 1456, 1584, 2992, 3102, 3632		2248, 2384	
108	0	1312, 1760			992, 1184, 1504, 3408		2336	
109	1	1312, 1760	1600		864, 960, 1072, 1216, 1408, 1488, 2976, 3248, 3392, 3632		2304	
110	2-3	1312, 1760	1600		880, 944, 1072, 1216, 1472, 2800, 2944, 3120, 3364		2294, 2400	
111	1	1312, 1760	1648		1184, 1536, 1856, 2896, 3040, 2488, 3616		2304, 2416	
112	2-3	1312, 1760	1664		768, 1088, 1184, 1408, 3120, 3319, 3440		2320, 2384	
113	2-3	1312, 1760	1616		896, 1088, 1200, 1392, 1520, 1824, 2944, 3072, 3216, 3418, 3616		2288, 2384	
114	2-3	1312, 1760	1616		784, 944, 1088, 1168, 1520, 3184, 3338, 3488			
115	2-3	1312, 1760	1616		784, 1136, 1168, 1520, 2992, 3168, 3296, 3453, 3552		2288	
116	2-3	1312, 1760	1008, 1616		1088, 1184, 1472, 2848, 2960, 3109, 3440, 3648		2304, 2400	

**FT-IR peaks** for the casting resin (1312, 1760  $\text{cm}^{-1}$ ), gypsum (1616  $\text{cm}^{-1}$ , overtone 2200-2300  $\text{cm}^{-1}$ ) and a wax/resin (1100-1500, 2800-3000  $\text{cm}^{-1}$ ). A summary of the peaks observed in the spectra 105-116 can be seen in the table on the left.

## Sample 5



Above: Overlapped (OM and BSE) cross-section image showing the stratigraphy (blue indicators).

3. Varnish (layer 2 and 3 are distinguishable only in the BSE image)

2. Dark layer

1. Yellowish layer

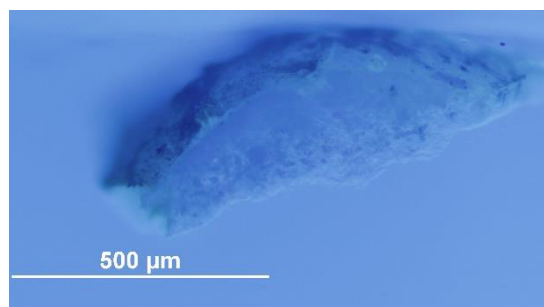
0. Plaster bulk

**Analysis spots.** EDS analysis (yellow): Spectra 22-27; FT-IR analysis (red): nos. 117-129.

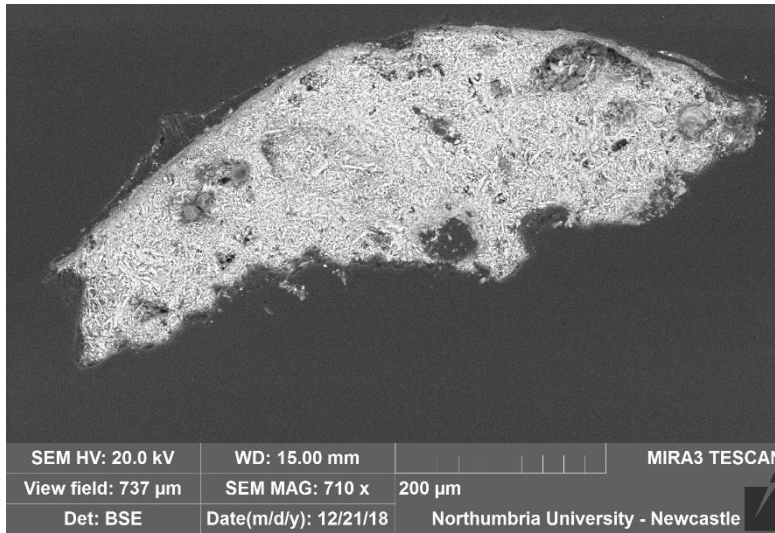
**Summary.** The sample is mostly made of C, O, S and Ca (**calcium sulfate**,  $\text{CaSO}_4$ , confirmed by EDS and by the peak at  $1600\text{-}1632\text{ cm}^{-1}$  in the FT-IR spectra). Al is overall present as used as a polishing agent, but could also, together with Si, be present as part of silicate inclusions, which are present in all the layers (see EDS mapping). Si is mostly located in the surface layers, where traces of Ti, Fe, Mg, Na, and Cl were also detected. A **wax or resin** is suggested by FT-IR (peaks at  $1000\text{-}1200$  and  $2800\text{-}3000\text{ cm}^{-1}$ ) and present in all the layers.



VLR OM (above)

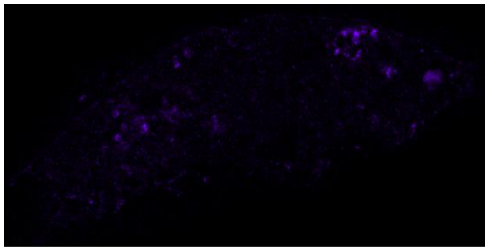


UVfOM (above)

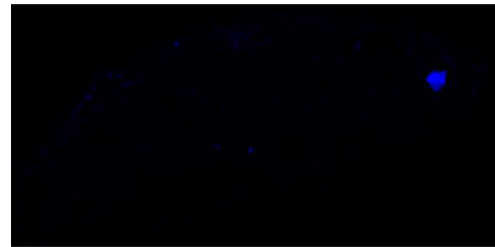


**BSE image (left).** The tabular crystalline structure typical of gypsum plaster can be seen in layer 0. Layer 1 consists of calcium sulfate. **EDS mapping (below)** shows that inclusions made of Si-Al are present in all the layers and the outmost layers are mostly made of Si and Al. Mg and Ti inclusions were also observed. **EDS spectra** indicate that all the layers consist of C, O, Ca, S, Al and Si. Al traces are present in all the layers (polishing medium), but Al could also, together with Si be present as part of silicate inclusions. Traces of Ti, Fe, Mg, Na, and Cl were also detected in the surface layers.

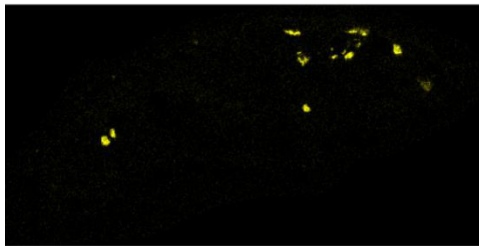
Aluminium (Al)



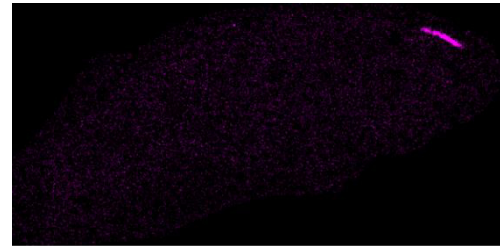
Silicon (Si)



Magnesium (Mg)



Titanium (Ti)



Spectrum	Layer	peaks (cm <sup>-1</sup> )					
		Casting Resin	Gypsum	Carbonate	Wax/resin	C=O ester carbonyl	overtones
117	0		1008		816, 928, 1040, 1248, 1408, 1472, 1808, 3072, 3184, 3569	1712	2249, 2400
118	0	1344	1616, 1696	1776	784, 928, 992, 1072, 1264, 1440, 1536, 1824, 2784, 2844, 3680, 3776		2233, 2400
119	0	1312, 1760	1024		944, 976, 1264, 1360, 1872, 2832, 2912, 3296, 3600, 3786		2208, 2284, 2400
120	1-3	1344	1008, 1632		784, 944, 1088, 1216, 1264, 1488, 2928, 3200, 3344, 3481, 3664	1744	2288, 2395
121	1-3	1312	1008, 1632, 1696	1776	960, 1232, 1440, 1472, 1584, 1952, 2832, 2944, 3056, 3312, 3571		2281, 2432
122	1-3	1312, 1760	1008, 1616		848, 896, 960, 1072, 1216, 1472, 1536, 2832, 2966, 3552, 3664		2288
123	1-3	1312, 1760	1008, 1616		848, 896, 960, 1072, 1216, 1472, 1536, 2832, 2966, 3552, 3665		2289
124	1-3	1757	1024		891, 960, 1088, 1296, 1440, 1552, 1872, 1952, 2736, 2928, 3024, 3104, 3312, 3568		2176, 2288, 2400
125	1-3	1344, 1760			768, 832, 976, 1088, 1136, 1216, 1296, 1456, 1536, 2800, 2912, 3296, 3464, 3664		2256, 2384
126	1-3	1312, 1766	1008, 1616		800, 912, 1078, 1152, 1408, 1488, 2984, 3088, 3200		2320
127	1-3	1312, 1767			801, 864, 944, 1056, 1184, 1504, 2944, 3296, 3421, 3744		2160, 2608
128	1-3	1312, 1769	1008, 1632		794, 912, 1088, 1152, 1200, 1392, 1488, 3356		2288, 2416
129	1-3	1328, 1760	1008		800, 928, 1088, 1216, 1440, 2848, 2944, 3072, 3152, 3331, 3456		2304, 2384

**FT-IR peaks for the casting resin (1312, 1760 cm<sup>-1</sup>), gypsum (1616 cm<sup>-1</sup>, overtone 2200-2300 cm<sup>-1</sup>) and a wax/resin (1100-1500, 2800-3000 cm<sup>-1</sup>).** A summary of the peaks observed in the spectra 117-129 can be seen in the table on the left.

## Experimental

The object was observed, and its conditions were documented. Samples from selected areas were taken by Charlotte Hubbard. Sampling images are not available for this object due to the object location and other difficulties. When possible, each sample was split into two parts: one fragment was embedded in polyester resin (Tiranti clear casting resin), polished and analysed under an optical microscope and the other was put aside for py-TMAH-GC/MS and XRD analysis.

The optical microscopy was performed with an Olympus BX51 Metallurgical Microscope equipped with four objectives (magnification of x5, x20, x50 and x100), and an x10 eyepiece. In many instances, a small amount of white spirit was applied on the surface of the cross-section to improve the saturation under the microscope. The microscope is equipped with a 6-cube filter turret which allows to operate of the system in reflected visible light (brightfield and darkfield mode) and reflected UV light (365 nm) using a 100 W mercury burner.

The SEM-EDS analysis was performed with a field emission TESCAN MIRA 3 with gigantic chamber. The SEM is equipped with: secondary electron detector (SE), secondary electron in-beam detector (In-beam SE), back-scatter detector (BSE), back-scatter in-beam detector (In-beam BSE), cathodoluminescence detector (without wavelength detection) (CL), plasma chamber/sample cleaner and software Alicona 3D imaging. For the EDS analytical part, it has an Oxford Instruments setup: Software: AztecEnergy, X-ray detector X-Max 150 mm<sup>2</sup> and X-ray detector X-Max Extreme, low energy detector for thin films, high resolution and low voltage. The samples were analysed by SEM-EDS Low Vacuum Mode (10-15 Pa). EDS Mapping and data processing were performed with Aztec Oxford software.

A Perkin Elmer Frontier FT-IR spectrometer (350 cm<sup>-1</sup> at the best resolution of 0.4 cm<sup>-1</sup>) was used, equipped with a germanium crystal for ATR measurements and combined with a Spectrum Spotlight 400 FT-IR microscope equipped with a 16×1 pixel linear mercury cadmium telluride (MCT) array detector standard with InGaAs array option for optimised NIR imaging. Spectral images from sample areas are possible at pixel resolutions of 6.25, 25, or 50 microns. The Perkin Elmer ATR imaging accessory consists of a germanium crystal for ATR imaging. These run with Perkin Elmer Spectrum 10™ software and with SpectrumIMAGE™ software. Baseline and Kubelka-Munk corrections were applied to the raw data acquired in diffuse reflectance.

The XRD analysis was performed with a Rigaku SmartLab SE equipped with a HyPix-400, a semiconductor hybrid pixel array detector and Cu source. The analyses were performed in Bragg-Brentano geometry mode, with 40 kV tube voltage and 50 mA tube current. The diffractograms were processed with a SmartLab II software. The data was compared to the RUFF database (Lafuente et al., 2016) and COD Database (Gražulis et al., 2009).

The instrument used for GC/MS is a Thermo Focus Gas Chromatographer with DSQ II single quadrupole mass spec. The column currently installed is an Agilent DB5-MS UI column (ID: 0.25 mm, length: 30 m, df: 0.25 μm, Agilent, Santa Clara, CA, USA). Carrier gas: helium. Detector temperature: 280 °C, Injector temperature: 250 °C. It can be used with the PyroLab 2000 Platinum filament pyrolyser (PyroLab, Sweden) attachment or in split/splitless mode. Detection: Total Ion monitoring (TIC). 1 μl of the sample with 1 μl of TMAH was placed on the Pt filament for the py-GC/MS. The inlet temperature to the GC was kept at 250 °C. The helium carrier gas flow rate was 1.5 ml/min with a split flow of 41 ml/min and split ratio of 27. The MS transfer line was held at 260 °C and the ion source at 250 °C. The pyrolysis chamber was heated to 175 °C, and pyrolysis was carried out at 600 °C for 2 s. This run with Xcalibur™ and PyroLab™ software. The library browser supported NIST MS Version 2.0 (Linstrom & Mallard, 2014).

Valentina Risdonne, PhD student

[v.risdonne@vam.ac.uk](mailto:v.risdonne@vam.ac.uk) / [valentina.risdonne@northumbria.ac.uk](mailto:valentina.risdonne@northumbria.ac.uk)

Victoria and Albert Museum – Northumbria University

PhD project 'Materials and techniques for coating of the nineteenth-century plaster casts'

©V&A Museum

11 February 2021

## Notes

12 December 2018	Casting	Valentina's PhD Lab book 1, page 144
4 February 2019	Microscopy	Valentina's PhD Lab book 1, page 162
14 October 2019	FT-IR	Valentina's PhD Lab book 1, page 175
3 December 2019	XRD	Valentina's PhD Lab book 2, page 4
18 March 2020	GC/MS	Valentina's PhD Lab book 2, page 50

A full record of analyses is available at <https://doi.org/10.25398/rd.northumbria.14034986>

## References

- Colombini, M. P., & Modugno, F. (2009). *Organic mass spectrometry in art and archaeology*. John Wiley & Sons.
- Gražulis, S., Chateigner, D., Downs, R. T., Yokochi, A. F. T., Quirós, M., Lutterotti, L., Manakova, E., Butkus, J., Moeck, P., & Le Bail, A. (2009). Crystallography Open Database—an open-access collection of crystal structures. *Journal of Applied Crystallography*, *42*(4), 726–729.
- Lafuente, B., Downs, R. T., Yang, H., & Stone, N. (2016). The power of databases: the RRUFF project. In *Highlights in mineralogical crystallography* (pp. 1–29). Walter de Gruyter GmbH.
- Linstrom, P. J., & Mallard, W. G. (2014). *NIST Chemistry WebBook, NIST standard reference database number 69, National Institute of Standards and Technology, Gaithersburg MD, 20899*.
- Mills, J., & White, R. (2012). *Organic chemistry of museum objects*. Routledge.
- Price, B. A., Pretzel, B., & Lomax, S. Q. (2009). *Infrared and Raman Users Group Spectral Database; 2007 ed. IRUG: Philadelphia, PA, USA*.





**Northumbria  
University**  
NEWCASTLE

Analysis Report - Valentina Risdonne

Copy of a Statue - Count Ekkehard

(REPRO.1875-16)

Initiator: Charlotte Hubbard; Conservation Department

15 October 2020

© Victoria and Albert Museum



## Analysis Report - Copy of a Statue - Count Ekkehard (REPRO.1875-16)

### Contents

Contents.....	234
List of abbreviations.....	234
Summary.....	235
Sample 1.....	238
Sample 2.....	242
Sample 3.....	245
Sample 4.....	248
Experimental.....	252
Notes.....	253
References.....	253

### List of abbreviations

BSE	Back Scattered Electron
EDS	Energy Dispersive Spectrometry
FT-IR	Fourier-Transform Infra-Red
FPA	Focal Plane Array
GC/MS	Gas Chromatography-Mass Spectrometry
OM	Optical Microscopy
PL	Proper Left
PR	Proper Right
py	pyrolysis
SEM	Scanning Electron Microscopy
TMAH	tetramethylammonium hydroxide
UVf	Ultraviolet Fluorescence
VLR	Visible Light Reflectance
XRD	X-ray Diffraction

## Summary

The bulk of the object is made of gypsum plaster, which contains several types of inclusions (including silicates and carbonates). By looking at the results, it is possible to hypothesise that in the surface layer, containing **silicon** and **aluminium**, the organic medium is **shellac** mixed with **drying oil** and that **dammar** was also applied onto the surface. **Sample 1** appears different from the rest of the samples, presenting two extra layers, and it is possible that this area was repaired and repainted.

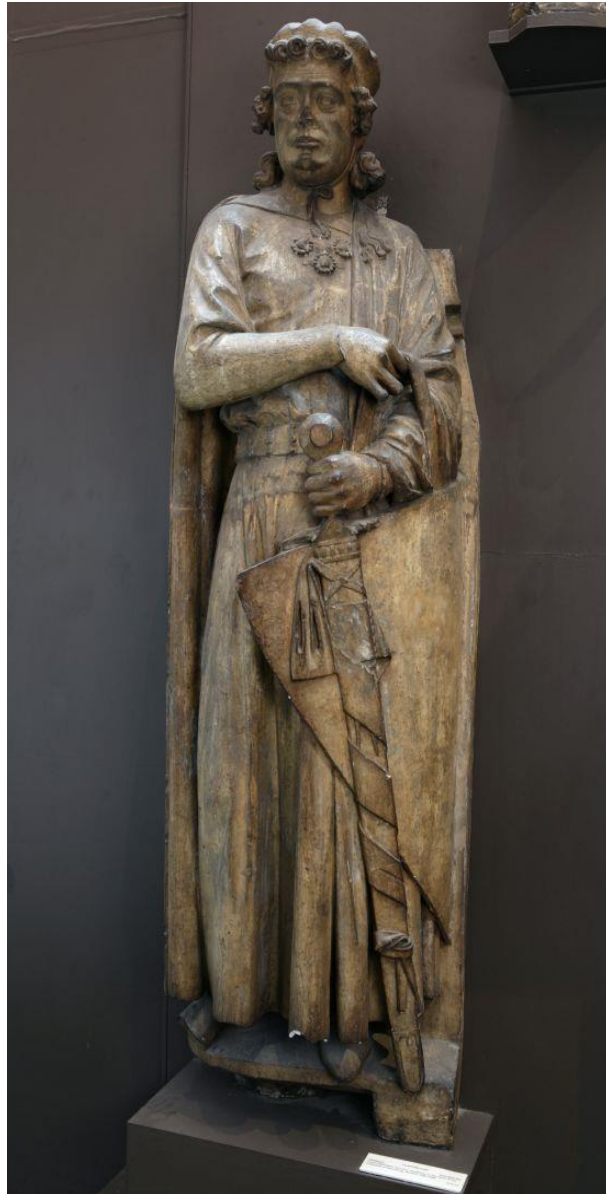


Figure 1. The copy of a statue.

The object, '**Copy of a Statue - Count Ekkehard (REPRO.1875-16)**' (Figure 1), is a plaster cast of a statue commemorating Count Ekkehard (about 985–1046). He was the Margrave (similar to a count or duke) of Lusatia and later of Meissen and defended the eastern frontiers of Germany against Poland and Bohemia. The original statue was made two centuries after his death and placed in Naumburg Cathedral, Germany. Both Ekkehard and his wife were among the founders of the cathedral. This cast, made by F. Küsthardt about 1875, does not replicate the bright painted decoration of the original sculpture, attributed to the Naumburg Master and made about 1250-60. The cast was purchased from F. Küsthardt

in 1875 for £7 10s and is now located in Gallery 46A (The Ruddock Family Cast Court). Its dimensions are 198.5x61.5 cm.

Samples from the plaster cast were taken from pre-existing areas of loss to investigate the stratigraphy and the method of manufacture (Figure 2). The samples were analyzed to provide data for the study of the objects of the Cast Courts collection within the PhD project 'Materials and techniques for coating of the nineteenth-century plaster casts'. Details on the experimental procedure are available in the Experimental section of this report. A selection of significant results is shown in the following pages and the relevant database of analysis (<https://doi.org/10.25398/rd.northumbria.14039279>).

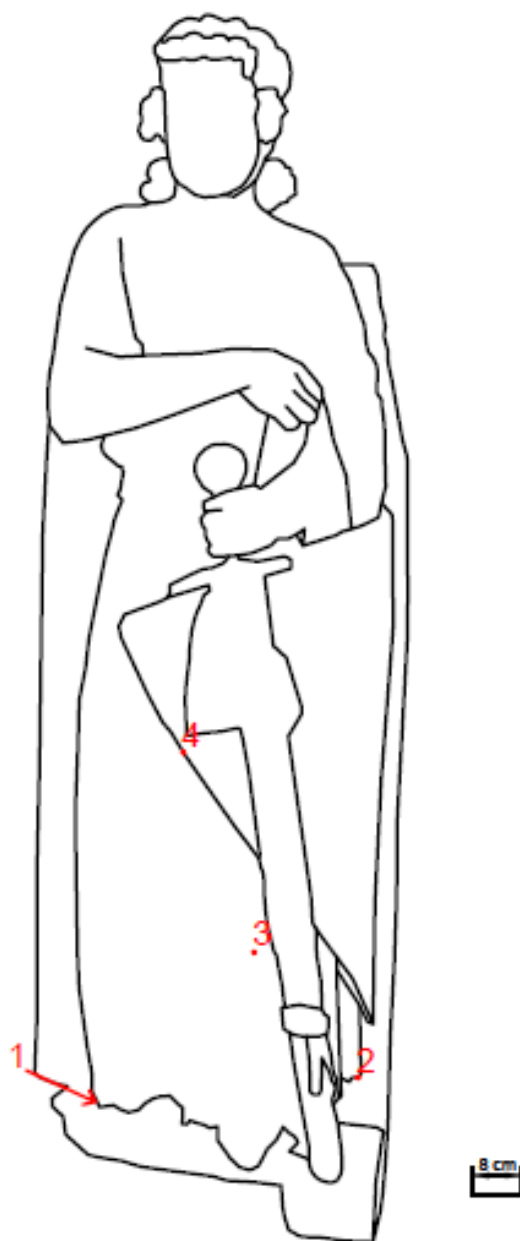


Figure 2. The statue outline with marked sampling sites.

**Sample 1:** fragment taken from an area of loss, close to one of the screws used to secure the statue to the support, PR side.

**Sample 2:** fragment taken from an area of loss on the bottom rim of the vest of the statue, PL side.

**Sample 3:** fragment taken from an area of loss on the vest of the statue, PR side.

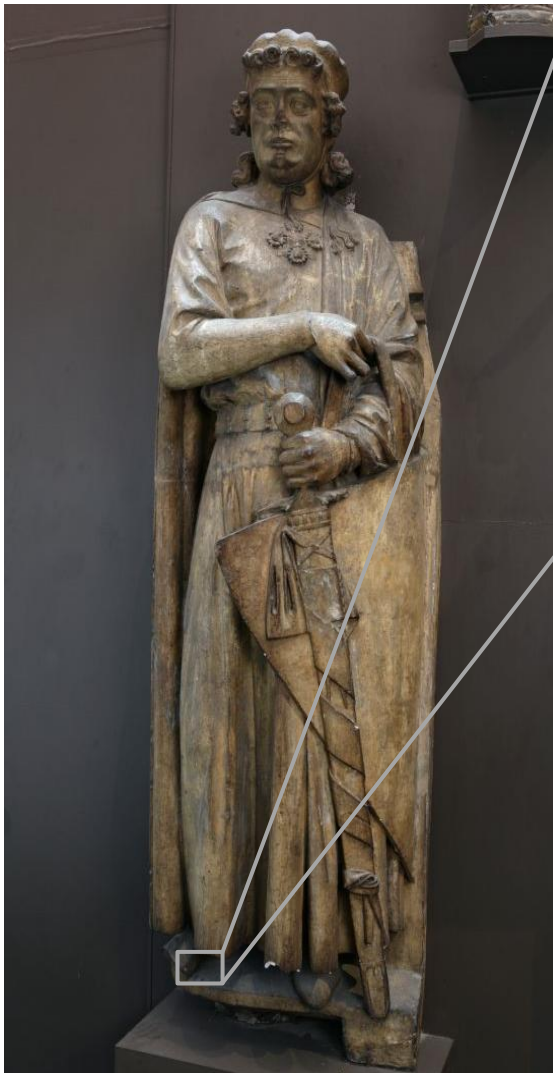
**Sample 4:** fragment from an area of loss on the darker rim of the shield held by the figure.

The **substrate** (layer 0 in samples 0 and 1 and missing in samples 2 and 3) is made of gypsum plaster (**calcium sulfate**,  $\text{CaSO}_4$ , confirmed by EDS, XRD and by the peak at  $1600\text{-}1648\text{ cm}^{-1}$  in the FT-IR spectra, which also show the sulfate overtones in the  $2100\text{-}2300\text{ cm}^{-1}$  area). Inclusions made of **aluminium (Al)** and **silicon (Si)** are present in all the layers of all the samples and **magnesium (Mg)** was also detected in samples 1 and 2. An **interface layer**, yellow under visible illumination and possibly consisting of a portion of lower layer soaked with the surface coating(s), showing characteristics of both layers, is visible in all the samples and samples 3 and 4 is the deepest layer sampled. The tabular crystalline structure typical of gypsum plaster can be seen in the plaster bulk layer and the interface layer. All the samples show a layer, **dark** under visible illumination (layer 2 in samples 1 and 2 and layer 1 in samples 3 and 4). EDS mapping shows that this layer contains **iron (Fe)** and **silicon (Si)** and traces of Na, P, K, Ba, Mn, Zn, Ti and Cl. Samples 1 shows two additional layers, layer 3, white under visible illumination, consists of a **barium-based paint** and layer 4, black under visible illumination is consistent with a layer of dirt (Na, Cl, Zn and Fe are the main component of this layer). Sample 4 shows an additional layer (layer 2), which fluoresces under UV illumination and can be consistent with a **finishing layer**. This can suggest either that varnish was applied only on the selected areas or that the varnish was applied on all the surface, but it was differently adsorbed depending on the local variation of porosity.

A **wax or resin** (FT-IR peaks at  $1000\text{-}1200$  and  $2800\text{-}3000\text{ cm}^{-1}$ ) was detected in all the layers of all the samples, which indicates that either the material was added to the gypsum plaster wet admixture or that the coating has also penetrated in layer 0. The latter seems also possible as the average depth of the samples is about 0.5 mm. The additional presence of a **protein** cannot be excluded by interpreting the FT-IR spectra, due to the complexity of the admixture and also to the crowded pattern of the resins' FT-IR spectra (Price et al., 2009). Py-TMAH-GC/MS analysis of sample 4 suggests that the organic medium in this sample consists of **shellac**, possibly mixed with **drying oil**. Indication of a small quantity of **dammar** is also suggested by py-GC/MS, which could be consistent with the fluorescence of layer 2 under UV illumination (Colombini & Modugno, 2009).

**NOTE:** casting in resin the fragments of plaster resulted in the fragments absorbing the resin when in the liquid state. This was visible in the BSE image as well as through the EDS mapping (Tiranti resin and catalyst are mainly made of organic compounds C, H and O). Aluminium (Al) traces are present in all the samples, due to the polishing chemical.

## Sample 1

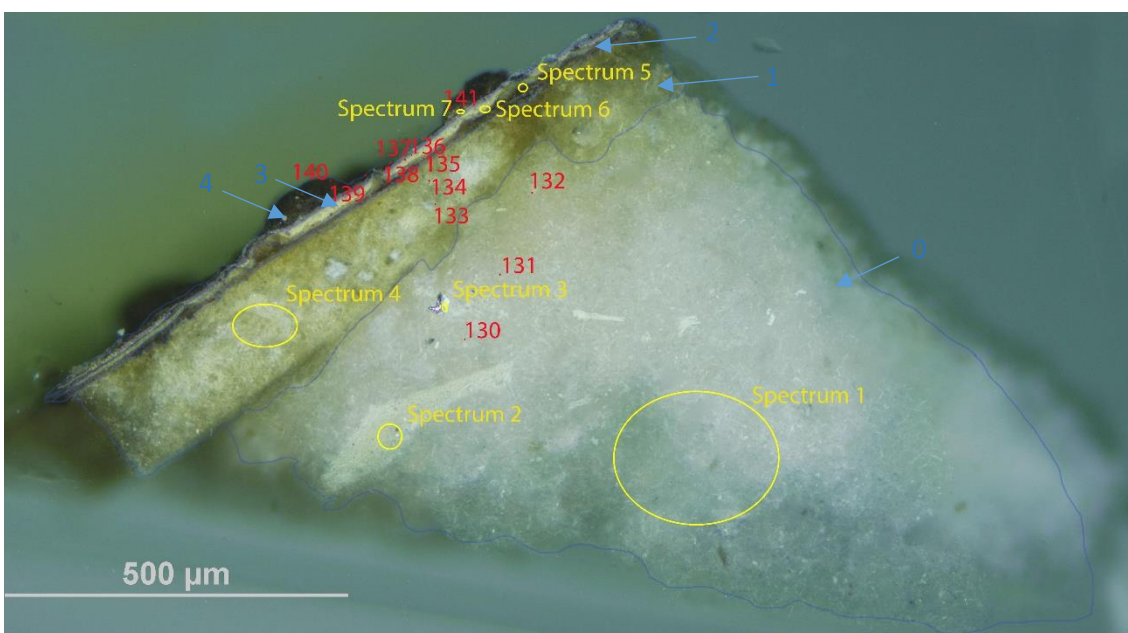


**Sampling.** This fragment taken from an area of loss, close to one of the screws used to secure the statue to the support, PR side.

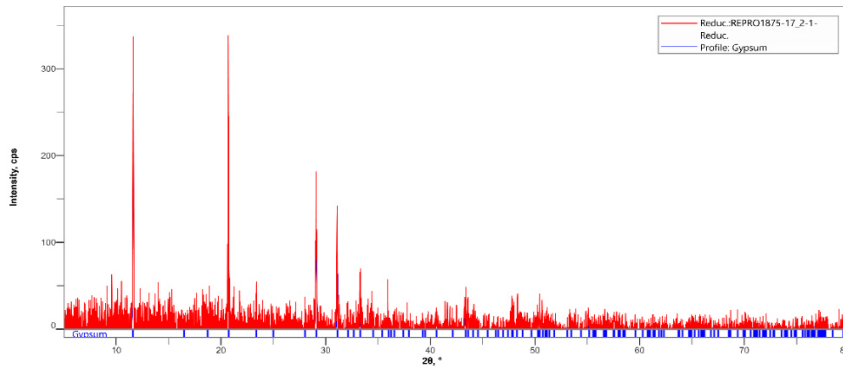
Below: Overlapped (OM and BSE) cross-section image showing the stratigraphy (blue indicators).

- 4. Dark layer
- 3. White-yellowish layer
- 2. Dark layer
- 1. Yellowish layer
- 0. Plaster bulk

**Analysis spots.** EDS analysis (yellow): Spectra 1-7; FT-IR analysis (red): nos. 130-141



**Summary.** The substrate (layer 0) is made of plaster (**calcium sulfate**,  $\text{CaSO}_4$ , confirmed by EDS, XRD and by the peak at  $1600\text{ cm}^{-1}$  and overtones in the FT-IR spectra). The tabular crystalline structure typical of gypsum plaster can be seen in layers 0 and 1. Layer 1 appears yellow under visible illumination and it is consistent with the ground layer soaked with the utmost layer (EDS mapping also shows that the element distribution in this layer is denser). Inclusions made of **Si**, **Mg** and **Al** were detected in all the layers. Layer 2 and 4 are black under visible illumination and seem consistent with layers of dirt. Layer 3 is white under visible illumination and is likely a barium-based paint (as suggested by EDS mapping). The utmost layers composition suggests that salt efflorescence (Na and Cl) is present on the surface. A **wax or resin** (FT-IR peaks at  $100\text{-}1200$  and  $2800\text{-}3000\text{ cm}^{-1}$ ) was detected in all the layers.

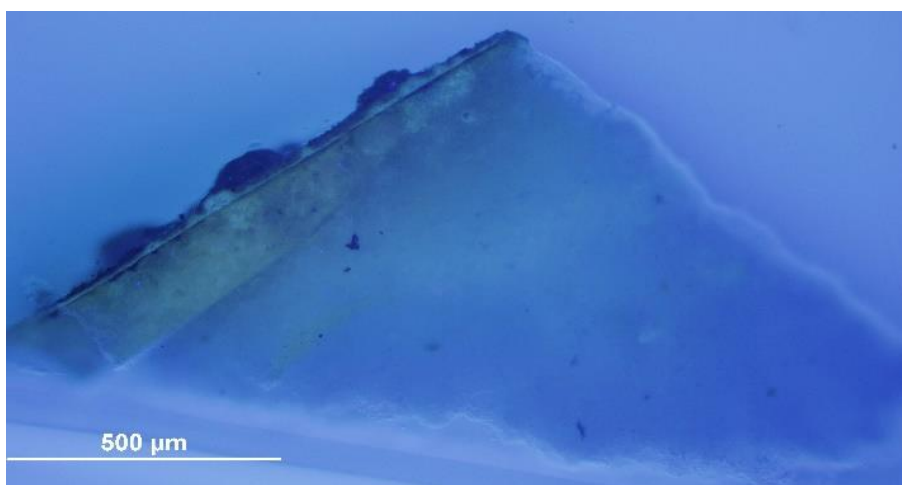


A fragment of this sample was pulverised and analysed by **XRD**.

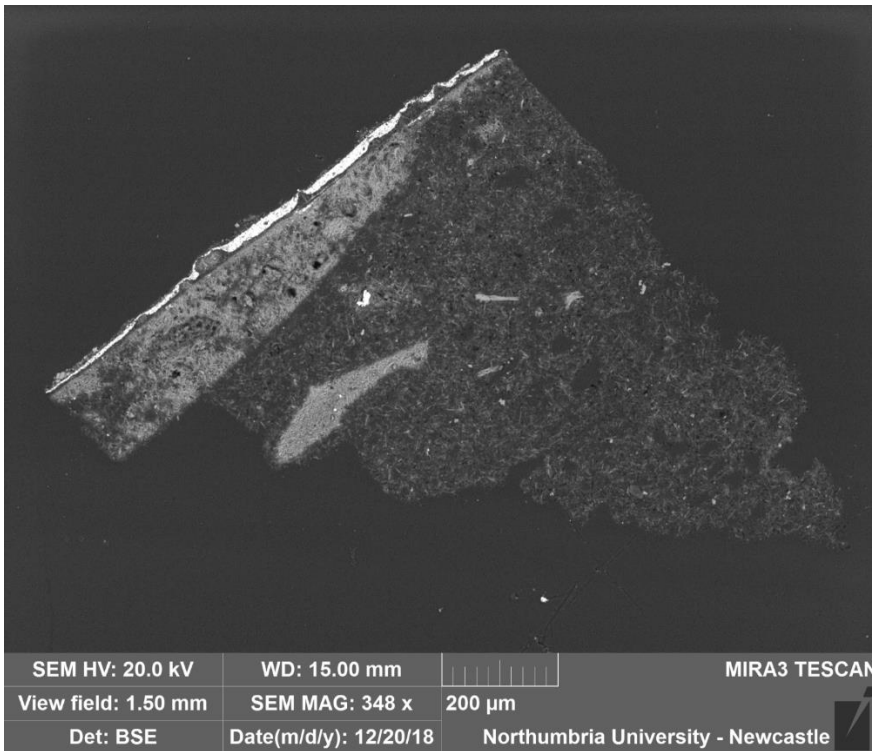
It was possible to identify the profile of gypsum (calcium sulfate) and the diffractogram was compared to references from the Rigaku SmartLab Database and the most significant peaks were at  $2\theta = 11.63, 20.81, 29.17, 31.21, 33.47, 47.95$ .



**VLR OM** (left)

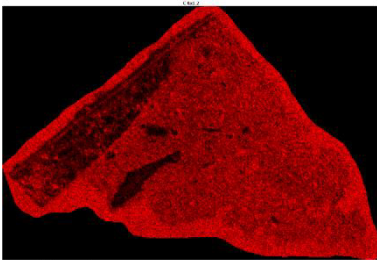


**UVf OM** (left)

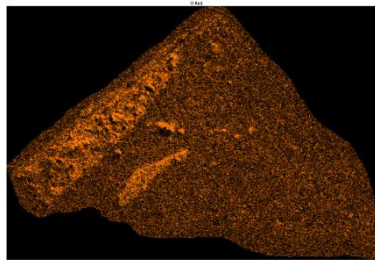


**BSE image (left).**  
 The tabular crystalline structure typical of gypsum plaster can be seen in layers 0 and 1, which are made of **calcium sulfate**,  $\text{CaSO}_4$ . The elemental distribution in layer 1 appears denser than in layer 0, as also shown by the **EDS mapping below**. **Si, Mg** and **Al** were detected in all the layers.

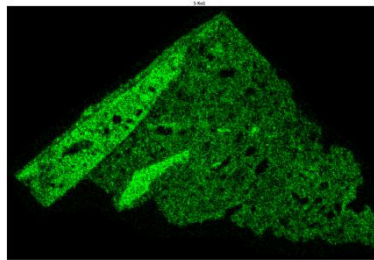
Carbon (C)



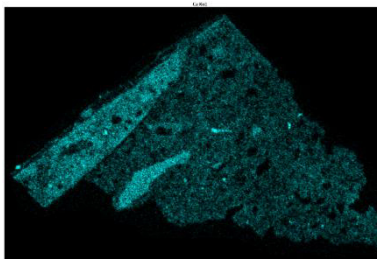
Oxygen (O)



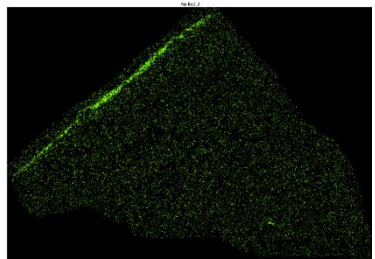
Sulfur (S)



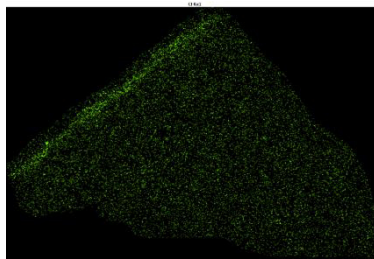
Calcium (Ca)



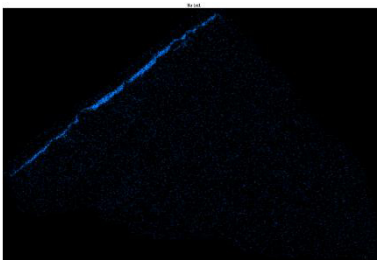
Sodium (Na)



Chlorine (Cl)



Barium (Ba)



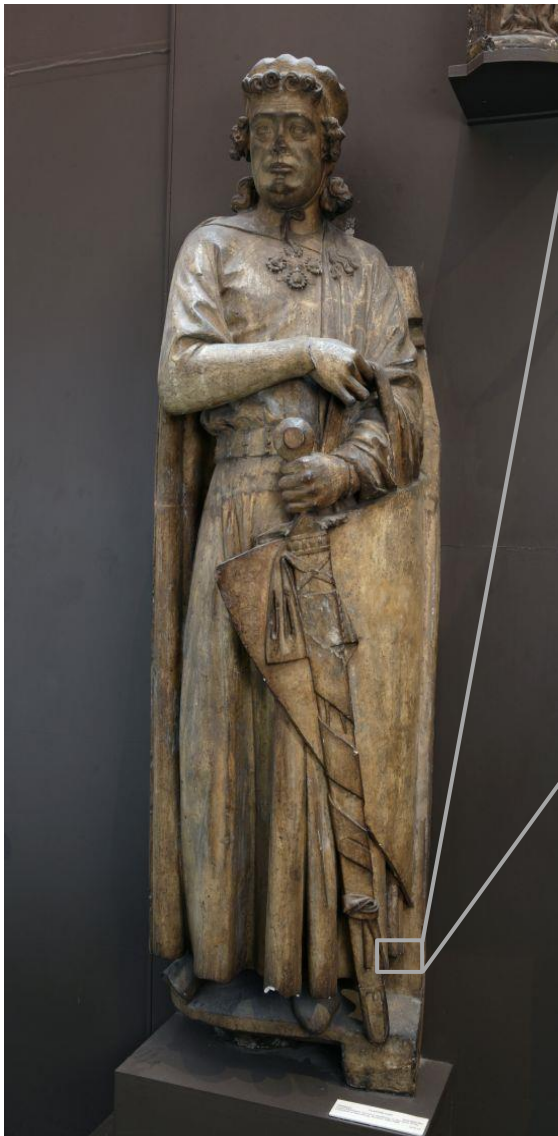
Iron (Fe)



The utmost layers (2, 3 and 4) all contain Na, Cl, Ba and Fe. Traces of Zn, Mn, K and P were also detected in layers 3 and 4 and Ti in layer 4.



## Sample 2



**Sampling.** This sample consists of a fragment taken from an area of loss on the bottom rim of the vest of the statue, PL side.

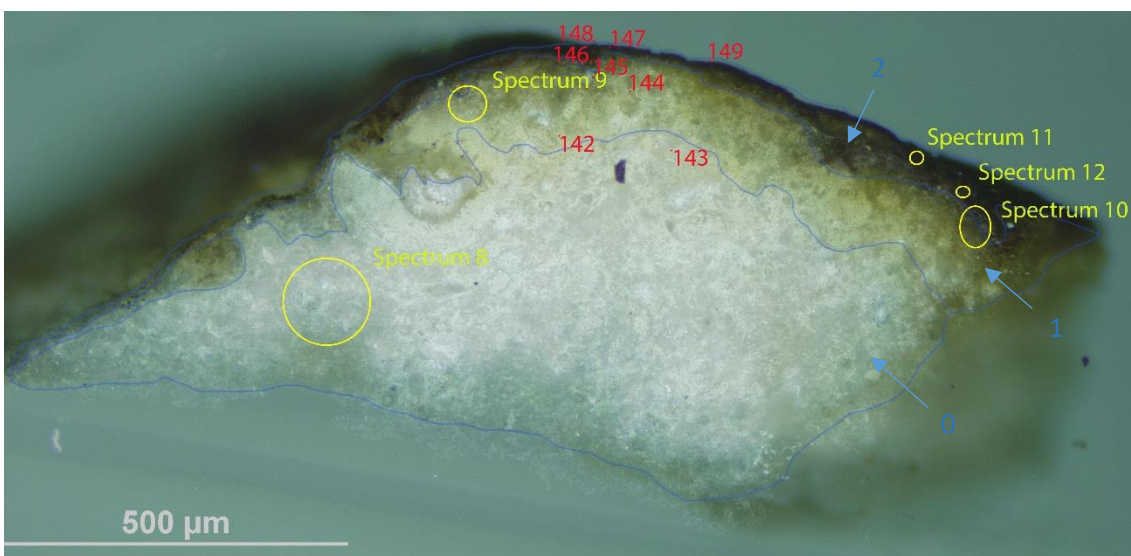
**Below:** Overlapped (OM and BSE) cross-section image showing the stratigraphy (blue indicators).

**2. Dark layer**

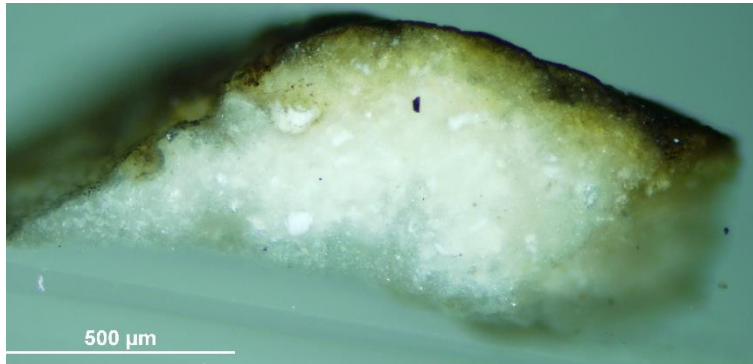
**1. Yellowish and undefined layer**

**0. Plaster bulk**

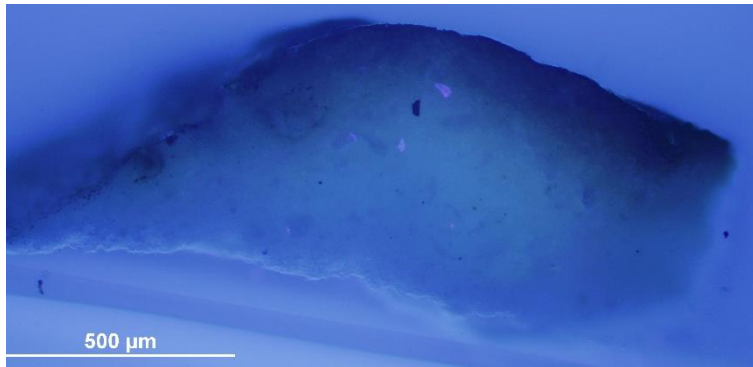
**Analysis spots.** EDS analysis (yellow): Spectra 8-12; FT-IR analysis (red): nos. 142-149.



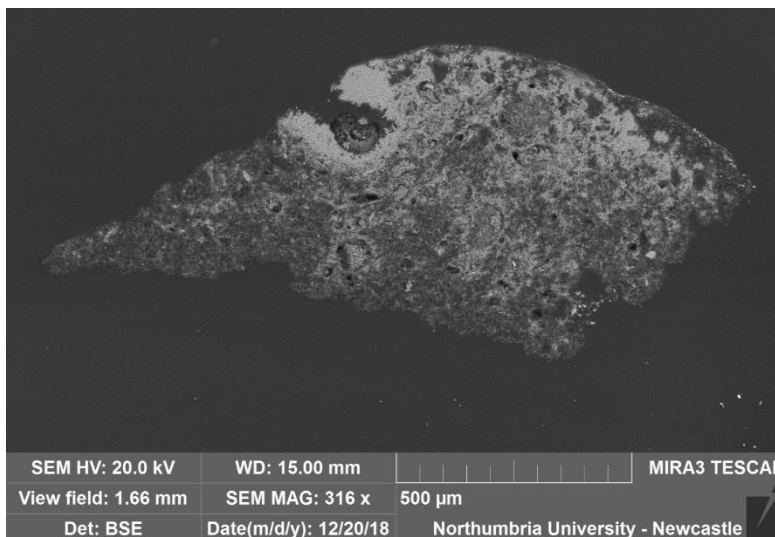
**Summary.** The substrate (layer 0) is made of plaster (**calcium sulfate**,  $\text{CaSO}_4$ , confirmed by EDS and by the peak at  $1600\text{ cm}^{-1}$  and overtones in the FT-IR spectra) and Si-Al inclusions and Mg are present in all the layers. The tabular crystalline structure typical of gypsum plaster can be seen in layers 0 and 1. Layer 1, which appears yellow under the microscope, consists of a portion of the lower layer soaked with the surface coating, showing characteristics of both layer 0 and layer 2. Layer 2, dark under visible illumination, is made of Fe (see EDS mapping) and traces of Na, P, K, Ba, Mn, Zn and Cl were also detected. A **wax or resin** (FT-IR peaks at  $1200\text{-}1500$  and  $2800\text{-}3000\text{ cm}^{-1}$ ) was detected in all the layers.



VLR OM (left)

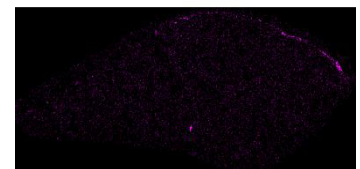


UVfOM (left)



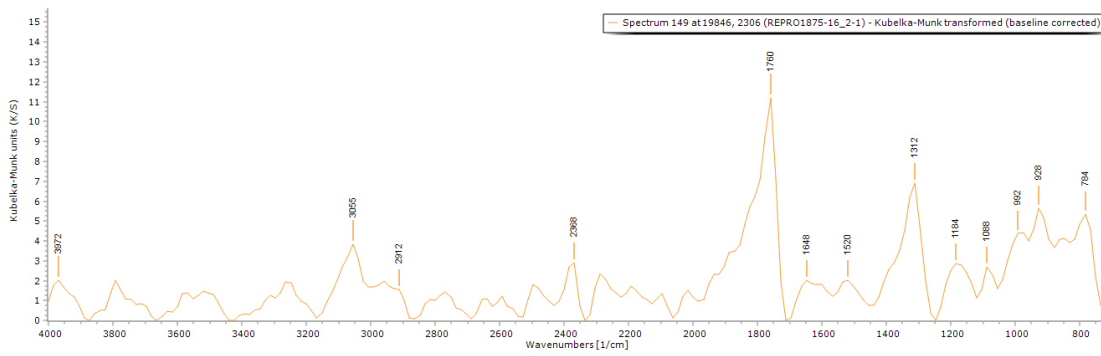
**BSE image (left).** The tabular crystalline structure typical of gypsum plaster can be seen in layers 0 and 1.

Iron (Fe)

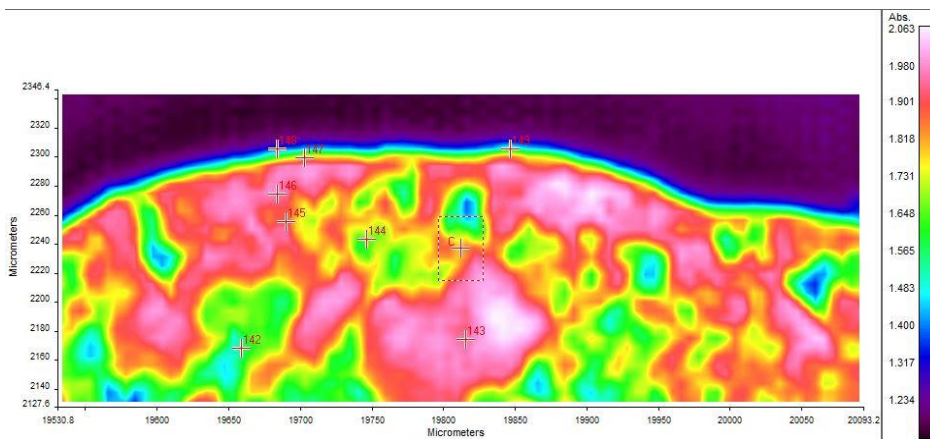


**EDS mapping (top right)** shows that Fe is present in layer 2 and that Si-Al inclusions are present in all the layers.

**EDS spectra** suggest that the sample is mostly made of calcium sulfate (C, O, Ca, S), Al, Si and Mg. Traces of Na, P, K, Ba, Mn, Zn and Cl were detected in the utmost layer.



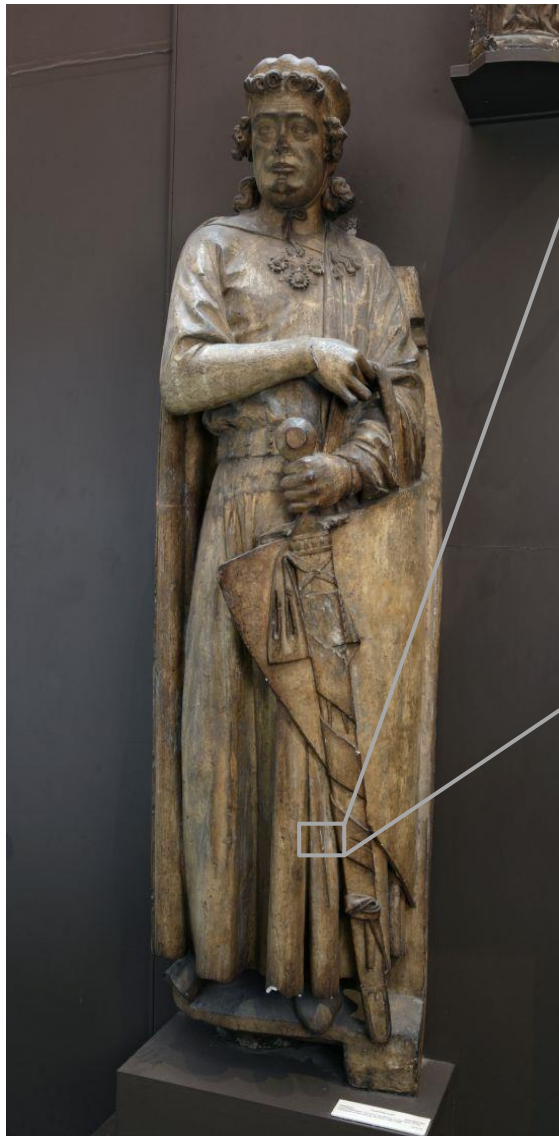
**FT-IR spectrum 149** (above) of layer 2. Peaks for the casting resin (1312, 1760  $\text{cm}^{-1}$ ), gypsum (1648  $\text{cm}^{-1}$ , overtone 2200-2300  $\text{cm}^{-1}$ ) and a wax/resin (1000-1200, 1520, 2800-3000  $\text{cm}^{-1}$ ). A summary of the peaks observed in the spectra 142-149 can be seen in the table below.



**FT-IR (FPA) image** (left). Some indication of different reflectance of the layers can be observed in the FPA image.

Spectrum	Layer	peaks (cm-1)						
		Casting Resin	Gypsum	Carbonate	Wax/resin	C=O ester carbonyl	SO overtone	Unknown
142	1	1312, 1760	1616		816, 896, 960, 1040, 1216, 1456, 1536, 2816, 2928			2304
143	0	1760	1600		784, 832, 912, 960, 1024, 1072, 1152, 1296, 1360, 1424, 1504, 2976			2240
144	1	1312, 1760	1616		784, 832, 960, 1152, 1216, 1376, 1552, 2880, 2944			
145	1	1312, 1760	1648		768, 912, 960, 1024, 1456, 1520, 2944			2384
146	2	1312, 1760	1616		960, 1024, 1472, 1520, 1696, 2832, 2864			2240
147	2	1312, 1760	1600		848, 992, 1088, 1216, 1472, 1536, 1664, 2800, 2928			2469
148	2	1312, 1760	1616		784, 880, 992, 1200, 1472, 3008			2336
149	2	1312, 1760	1648		784, 928, 992, 1088, 1184, 1520, 2912			2368

### Sample 3



**Sampling.** This fragment taken from an area of loss on the vest of the statue, PR side.

Below: Overlapped (OM and BSE) cross-section image showing the stratigraphy (blue indicators).

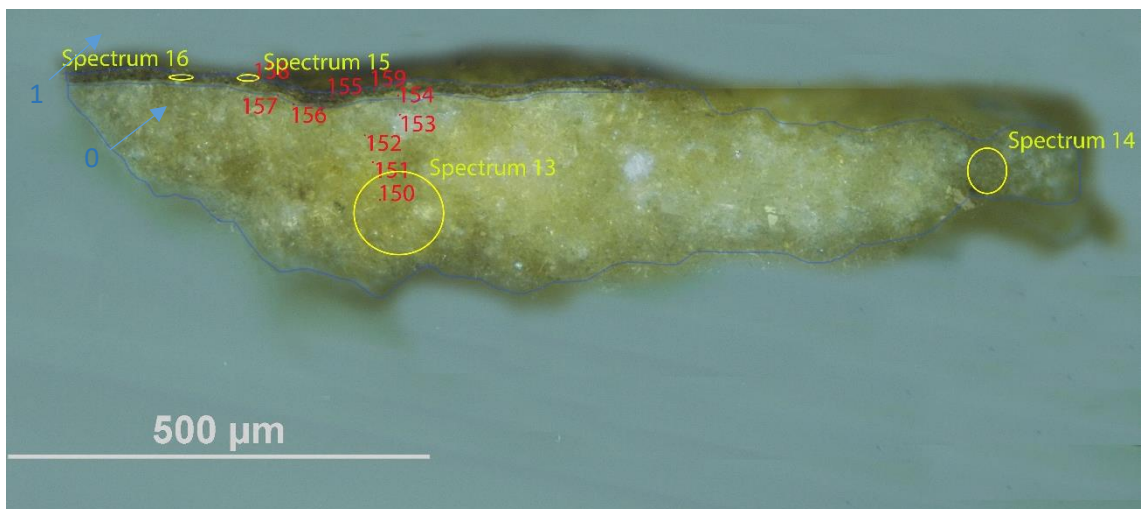
**1. Dark layer**

**0. Yellowish plaster bulk**

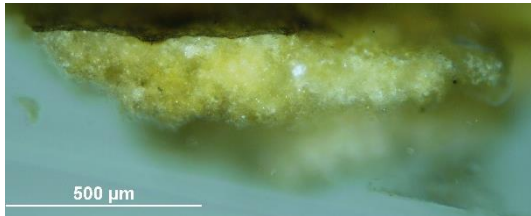
**Analysis spots.**

EDS analysis (yellow): Spectra 14-16

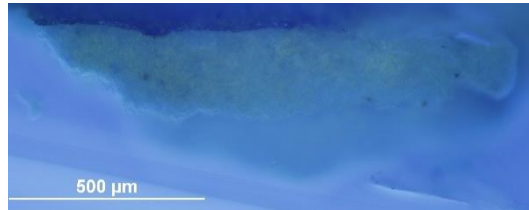
FT-IR analysis (red): nos. 150-159



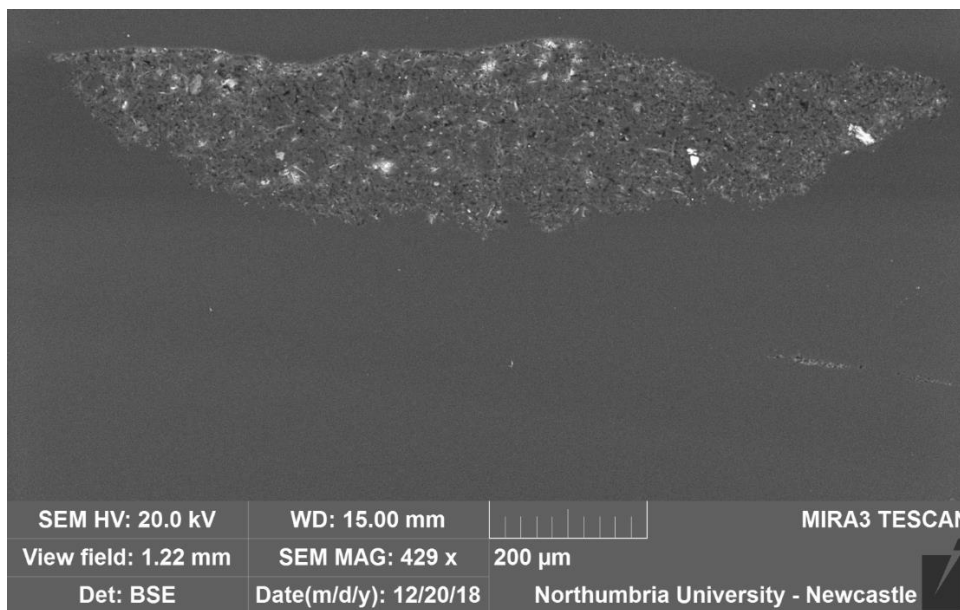
**Summary.** The sample is mostly made of C, O, S and Ca (**calcium sulfate**,  $\text{CaSO}_4$ , confirmed by EDS and by the peak at  $1600\text{-}1616\text{ cm}^{-1}$  in the FT-IR spectra). Si-Al inclusions are present in all the layers and additional traces of Ba, Na and Mg were detected in the utmost layer. The structure typical of gypsum plaster can be seen in layers 0 and 1. A **wax or resin** is suggested by FT-IR (peaks at  $1000\text{-}1200$  and  $2800\text{-}3000\text{ cm}^{-1}$ ) and was detected in all the layers.



VLR OM (above)



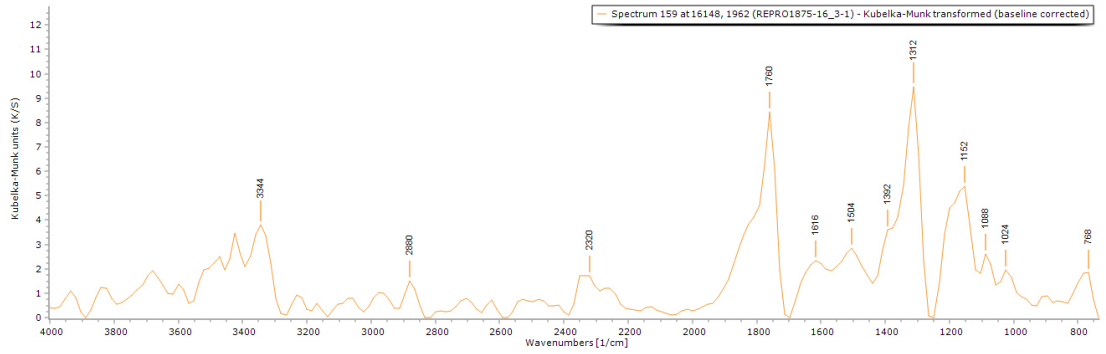
UVfOM (above)



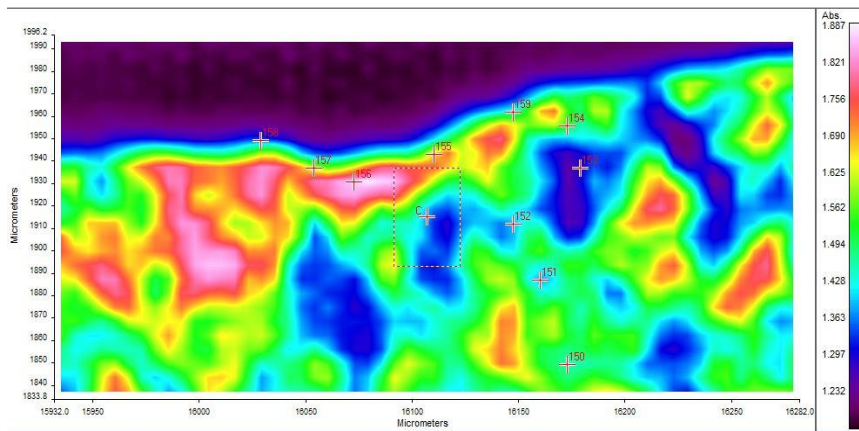
**BSE image (left).** The tabular crystalline structure typical of gypsum plaster can be seen in layers 0 and 1.

**Calcium sulfate ( $\text{CaSO}_4$ )** and **Al-Si inclusions** were detected in all the layers. Additional traces of **Ba, Na** and **Mg** were detected in the utmost layer (see **spectrum 15 below**). No element distribution in a layer fashion can be observed in the EDS mapping.





**FT-IR spectrum 159** (above) of layer 1. Peaks for the casting resin (1312, 1760  $\text{cm}^{-1}$ ), gypsum (1616  $\text{cm}^{-1}$ ), and a wax/resin (1504  $\text{cm}^{-1}$  and 2800-3000  $\text{cm}^{-1}$ ). A summary of the peaks observed in the spectra 150-159 can be seen in the table below.



**FT-IR (FPA) image** (left). No indication of different reflectance of the layers can be observed in the FPA image.

Spectrum	Layer	peaks (cm-1)						
		Casting Resin	Gypsum	Carbonate	Wax/resin	C=O ester carbonyl	SO overtone	Unknown
150	0	1312, 1760	1600		768, 864, 944, 1008, 1104, 1472, 2848, 2944			
151	0	1328, 1760	1616		784, 864, 992, 1088, 1200, 1408, 2896			2240
152	0	1328, 1760	1616		816, 876, 1088, 1088, 1184, 1488, 2992			2272
153	0	1312, 1760	1632		777, 864, 976, 1088, 1136, 1216, 1488, 2935			2320
154	1	1312, 1760			784, 1024, 1136, 1472, 1536, 2880, 2960			2240
155	1	1312, 1760	1616	800	880, 1152, 1488, 2832, 2944			2384
156	0	1312, 1760	1616		832, 992, 1072, 1136, 1216, 1456, 1504, 2816, 2976			2240
157	1	1328, 1760	1648		816, 880, 976, 1088, 1152, 1488, 2970			2320
158	1	1312, 1760	1616		816, 848, 912, 992, 1088, 1152, 1472, 1584, 2832, 2945			2368
159	1	1312, 1760	1616		768, 1024, 1088, 1152, 1504, 2880			2320

## Sample 4



**Sampling.** This fragment was taken from an area of loss on the darker rim of the shield held by the figure (blue indicators).

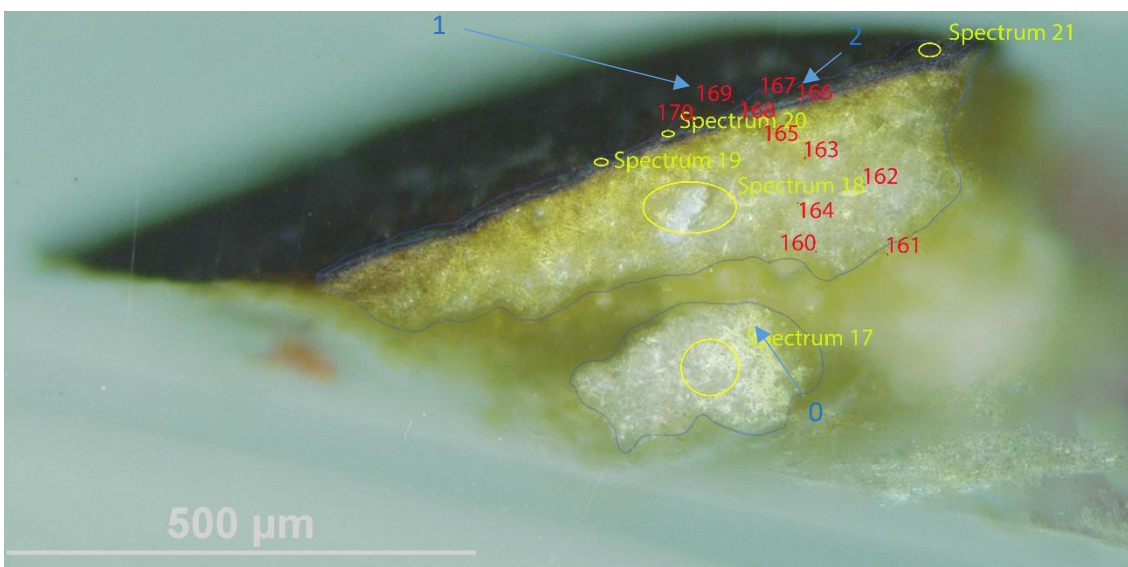
**Below:** Overlapped (OM and BSE) cross-section image showing the stratigraphy (blue indicators).

### 2. Varnish

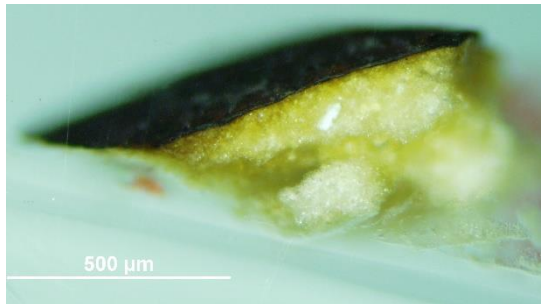
#### 1. Dark layer

#### 0. Yellow plaster bulk

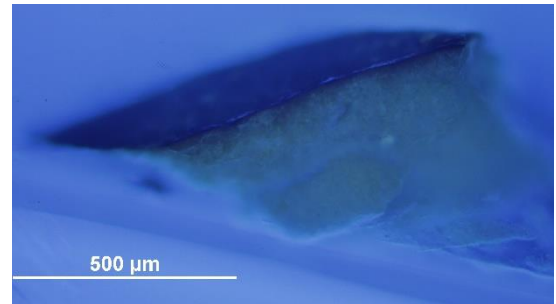
**Analysis spots.** EDS analysis (yellow): Spectra 17-21; FT-IR analysis (red): nos. 160-170.



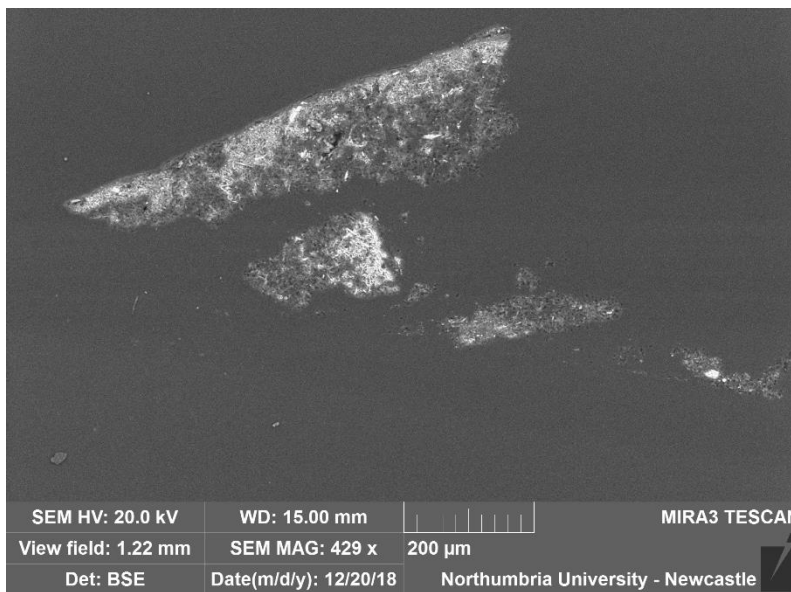
**Summary.** The sample is mostly made of C, O, S and Ca (**calcium sulfate**,  $\text{CaSO}_4$ , confirmed by EDS and by the peak at  $1600\text{-}1632\text{ cm}^{-1}$  in the FT-IR spectra). Al is overall present as used as a polishing agent, but could also, together with Si, be present as part of silicate inclusions, which are present in all the layers (see EDS mapping). Si is mostly located in the surface layers, where traces of Na, Fe, Cl, K and Ti were also detected. A **wax or resin** is suggested by FT-IR (peaks at  $1000\text{-}1200$  and  $2800\text{-}3000\text{ cm}^{-1}$ ) and present in all the layers. py-TMAH-GC/MS shows markers characteristic of **shellac**, possibly mixed with **drying oil**. Indication of a small quantity of **dammar** is also suggested by py-TMAH-GC/MS, which could be consistent with the fluorescence of layer 2 under UV illumination (Colombini & Modugno, 2009).



VLR OM (above)



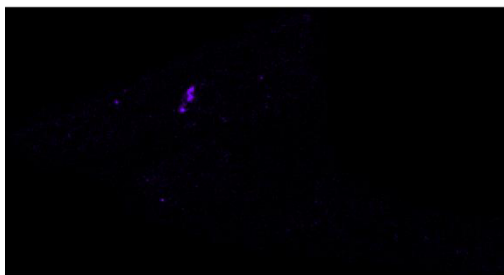
UVf OM (above)



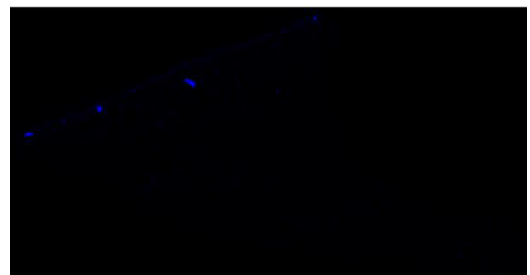
**BSE image (left).** The tabular crystalline structure typical of gypsum plaster can be seen in layer 0. **EDS mapping (below)** does not show any particular element distribution in a layer fashion, apart from a higher Si content in the utmost layers and shows the presence of Al-Si inclusions.

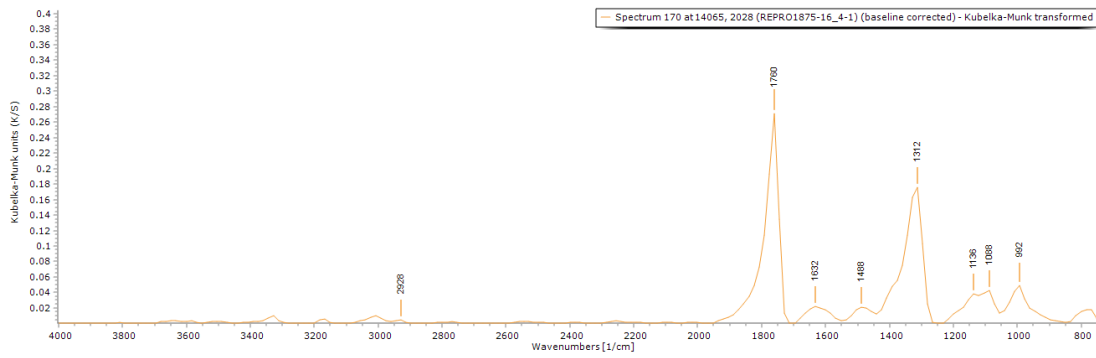
**EDS spectra** indicate that all the layers consist of C, O, Ca, S, Al and Si. Al traces are present in all the layers (polishing medium), but Al could also, together with Si be present as part of silicate inclusions. Traces of Na, Fe, Cl, K and Ti were also detected in the surface layers.

Aluminium (Al)



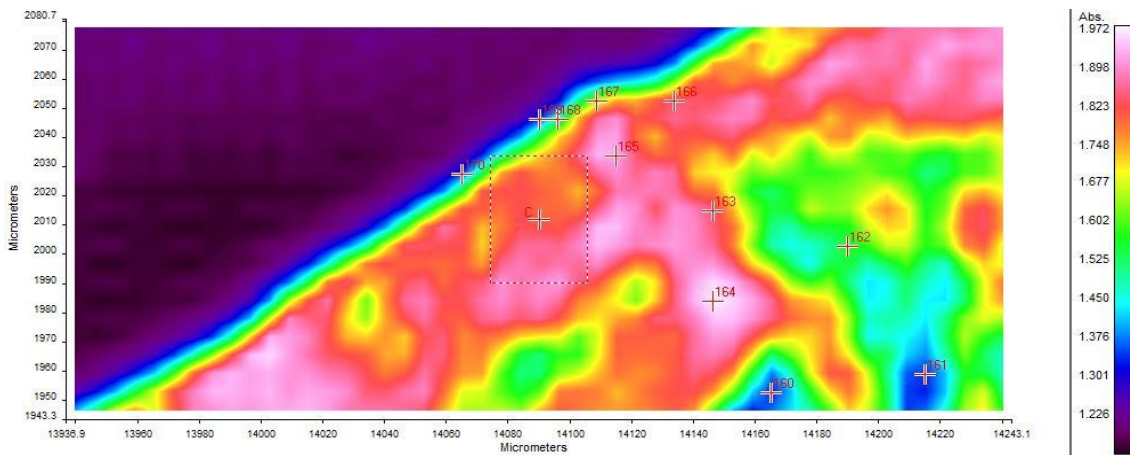
Silicon (Si)



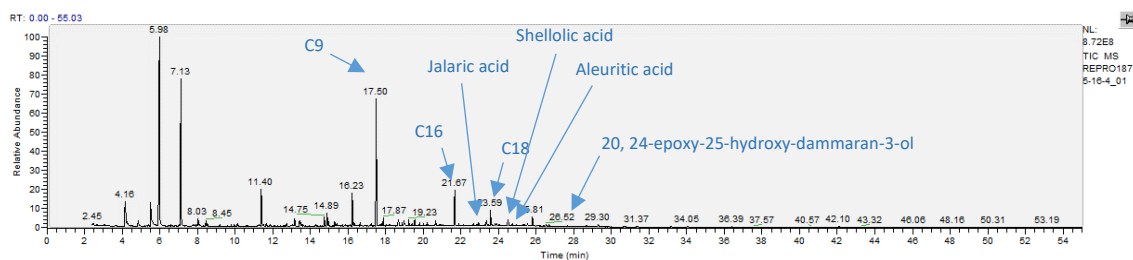


**FT-IR spectrum 170** (above) of layer 2. Peaks for the casting resin (1312, 1760  $\text{cm}^{-1}$ ), gypsum (1632  $\text{cm}^{-1}$ , overtone 2200-2300  $\text{cm}^{-1}$ ) and a wax/resin (1100-1500, 2800-3000  $\text{cm}^{-1}$ ). A summary of the peaks observed in the spectra 160-170 can be seen in the table below.

**FT-IR (FPA) image** (below). Indication of different reflectance of the layers can be observed in the FPA image.



Spectrum	Layer	peaks (cm-1)						
		Casting Resin	Gypsum	Carbonate	Wax/resin	C=O ester carbonyl	SO overtone	Unknown
160	0	1312, 1760	1616		754, 832, 880, 992, 1088, 1200, 1472, 2768, 2944		2352	
161	0	1312, 1760	1632		754, 880, 960, 1072, 1184, 1472, 2905		2304	
162	0	1312, 1760	1600		848, 928, 992, 1200, 2944		2240	
163	0	1312, 1760	1600		876, 960, 1088, 1408, 1472, 2896, 2960		2272	
164	0	1312, 1760	1616		768, 912, 1040, 1104, 1232, 1664, 2912, 2952		2272	
165	0	1312		1776	816, 960, 1072, 1216, 1360, 1440, 1504, 2928		2391	
166	1	1312, 1760	1632		784, 992, 1088, 1216, 1376, 1456, 1504, 2864		2304	
167	2	1312, 1760	1648		928, 1024, 1072, 1184, 1536, 2864, 2860		2320	
168	2	1312, 1760	1616		792, 848, 992, 1088, 1136, 1200, 2973		2288	
169	2	1312, 1760	1632		800, 864, 992, 1136, 1392			
170	2	1312, 1760	1632		768, 992, 1088, 1136, 1488, 2928			



RT	m/z	Assignment	Formula
4.16	45(100), 58(16), 74(62)	Ethyl ether	C4H10O
5.5	42(9), 58(100), 88(3), 116(4)	1,2-Ethanediamine, N'-ethyl-N,N-dimethyl-	C6H16N2
5.98	42(12), 58(100), 117(15)	1,2-Ethanediamine, N'-ethyl-N,N-dimethyl-	C6H16N2
7.13	44(7), 56(7), 72(100), 116(2), 131(3)	1,2-Ethanediamine, N'-ethyl-N,N-dimethyl-	C6H16N2
8.03	42(10), 58(100), 74(6), 87(3), 115(2), 131(4)	1,2-Ethanediamine, N,N,N'-trimethyl-	C5H14N2
8.45	44(18), 58(66), 70(8), 86(100), 110(2)	1,2-Ethanediamine, N,N-diethyl-N'-methyl-	C7H18N2
11.4	42(16), 58(100), 70(9), 116(5)	1,2-Ethanediamine, N'-ethyl-N,N-dimethyl	C6H16N2
13.16	42(13), 58(22), 71(13), 88(21), 98(30), 130(100), 141(7)	Unidentified amine fragment	
14.89	42(25), 55(65), 59(76), 74(73), 83(43), 97(22), 111(27), 115(100), 125(48), 128(33), 131(5), 157(32), 162(5)	Undecylenic Acid	C11H20O2
16.23	41(27), 55(69), 69(71), 74(90), 83(46), 87(42), 97(55), 111(28), 129(76), 138(100), 171(58)	Unidentified FA fragment	
17.5	43(17), 55(55), 59(33), 74(58), 83(57), 87(25), 111(57), 124(27), 143(30), 152(100), 185(39)	Nonanedioic acid, monomethyl ester	C10H18O4
17.87	41(25), 55(63), 59(52), 71(44), 83(30), 88(100), 111(32), 131(5), 139(27), 143(20), 163(5), 166(47), 171(22), 177(5), 199(5)	Unidentified FA fragment	
19.56	55(21), 58(30), 74(100), 87(63), 101(5), 129(7), 143(23), 157(5), 185(5), 199(17), 211(6), 242(5)	Heptadecanoic acid, methyl ester	C18H36O2
20.66	45(45), 58(100), 69(34), 83(45), 97(25), 111(21), 151(5), 178(5), 189(5), 199(5), 227(5), 243(5), 256(5)	Unidentified terpenoid fragment	
21.67	55(20), 74(100), 87(66), 115(5), 129(7), 143(20), 171(6), 185(6), 199(6), 227(12), 239(5), 270(5)	methyl palmitate	C17H34O2
23.35	59(100), 69(13), 87(11), 115(9), 135(5), 167(9), 191(5), 203(5), 219(5), 247(5), 262(11), 275(5), 307(5), 322(3)	jalaric acid	
23.59	43(19), 58(30), 74(100), 87(69), 97(8), 129(8), 143(25), 157(5), 185(5), 199(12), 213(3), 241(5), 255(13), 267(5), 298(5)	methyl stearate	C19H38O2
24.5	44(45), 58(100), 79(24), 91(23), 115(21), 129(18), 155(5), 167(21), 192(5), 206(19), 238(5), 260(5), 288(5), 305(5), 320(25), 337(5)	shellolic acid	
25.54	44(44), 58(100), 83(38), 95(20), 109(25), 119(5), 137(36), 157(26), 169(24), 201(70), 207(5), 239(54), 299(5), 312(5), 327(5)	aleuritic acid	
25.81	45(36), 58(65), 71(100), 81(19), 95(76), 109(27), 119(16), 137(40), 159(46), 169(22), 201(74), 227(5), 291(5), 329(5)	C20	
27.68	44(48), 58(100), 74(32), 87(22), 91(5), 115(5), 143(12), 207(18), 255(5), 281(5), 311(5), 354(5), 401(5)	20, 24-epoxy-25-hydroxy-dammaran-3-ol	
28.68	44(49), 58(100), 73(26), 79(11), 81(9), 121(5), 141(16), 165(5), 191(5), 207(21), 257(5), 281(10), 297(21), 313(10), 340(10), 372(9)	C22	

RT = retention time, m/z = mass/charge ratio

**Py-TMAH-GC/MS chromatogram** (top and described in the table above) shows small fragments due to derivatization (from  $t = 4.16$  to  $11.40$  min) and markers characteristic of **shellac** (jalaric, shellolic and aleuritic acids) (Colombini & Modugno, 2009; Mills & White, 2012). The presence of **methyl azelate** ( $t = 17.50$ ), **methyl palmitate** ( $t = 21.67$ ) and **stearate** ( $t = 23.59$ ) might suggest that the resin has been mixed with an **oil** ( $A/P = 2.89$  and  $P/S = 1.77$ ), possibly **linseed oil** (Colombini & Modugno, 2009). The small contribution at  $t = 27.68$  suggests that a small quantity of **dammar** could also be present.

## Experimental

The object was observed, and its conditions were documented. Samples from selected areas were taken by Valentina Risdonne. When possible, each sample was split into two parts: one fragment was embedded in polyester resin (Tiranti clear casting resin), polished and analysed under an optical microscope and the other was put aside for py-TMAH-GC/MS and XRD analysis.

The optical microscopy was performed with an Olympus BX51 Metallurgical Microscope equipped with four objectives (magnification of x5, x20, x50 and x100), and an x10 eyepiece. In many instances, a small amount of white spirit was applied on the surface of the cross-section to improve the saturation under the microscope. The microscope is equipped with a 6-cube filter turret which allows operating the system in reflected visible light (brightfield and darkfield mode) and reflected UV light (365 nm) using a 100 W mercury burner.

The SEM-EDS analysis was performed with a field emission TESCAN MIRA 3 with gigantic chamber. The SEM is equipped with: secondary electron detector (SE), secondary electron in-beam detector (In-beam SE), back-scatter detector (BSE), back-scatter in-beam detector (In-beam BSE), cathodoluminescence detector (without wavelength detection) (CL), plasma chamber/sample cleaner and software Alicona 3D imaging. For the EDS analytical part, it has an Oxford Instruments setup: Software: AztecEnergy, X-ray detector X-Max 150 mm<sup>2</sup> and X-ray detector X-Max Extreme, low energy detector for thin films, high resolution and low voltage. The samples were analysed by SEM-EDS Low Vacuum Mode (10-15 Pa). EDS Mapping and data processing were performed with Aztec Oxford software.

A Perkin Elmer Frontier FT-IR spectrometer (350 cm<sup>-1</sup> at the best resolution of 0.4 cm<sup>-1</sup>) was used, equipped with a germanium crystal for ATR measurements and combined with a Spectrum Spotlight 400 FT-IR microscope equipped with a 16×1 pixel linear mercury cadmium telluride (MCT) array detector standard with InGaAs array option for optimised NIR imaging. Spectral images from sample areas are possible at pixel resolutions of 6.25, 25, or 50 microns. The Perkin Elmer ATR imaging accessory consists of a germanium crystal for ATR imaging. These run with Perkin Elmer Spectrum 10™ software and with SpectrumIMAGE™ software. Baseline and Kubelka-Munk corrections were applied to the raw data acquired in diffuse reflectance.

The XRD analysis was performed with a Rigaku SmartLab SE equipped with a HyPix-400, a semiconductor hybrid pixel array detector and Cu source. The analyses were performed in Bragg-Brentano geometry mode, with 40 kV tube voltage and 50 mA tube current. The diffractograms were processed with a SmartLab II software. The data was compared to the RUFF database (Lafuente et al., 2016) and the COD Database (Gražulis et al., 2009).

The instrument used for GC/MS is a Thermo Focus Gas Chromatographer with DSQ II single quadrupole mass spec. The column currently installed is an Agilent DB5-MS UI column (ID: 0.25 mm, length: 30 m, df: 0.25 µm, Agilent, Santa Clara, CA, USA). Carrier gas: helium. Detector temperature: 280 °C, Injector temperature: 250 °C. It can be used with the PyroLab 2000 Platinum filament pyrolyser (PyroLab, Sweden) attachment or in split/splitless mode. Detection: Total Ion monitoring (TIC). 1 µl of the sample with 1 µl of TMAH was placed on the Pt filament for the py-GC/MS. The inlet temperature to the GC was kept at 250 °C. The helium carrier gas flow rate was 1.5 ml/min with a split flow of 41 ml/min and split ratio of 27. The MS transfer line was held at 260 °C and the ion source at 250 °C. The pyrolysis chamber was heated to 175 °C, and pyrolysis was carried out at 600 °C for 2 s. This run with Xcalibur™ and PyroLab™ software. The library browser supported NIST MS Version 2.0 (Linstrom & Mallard, 2014).

Valentina Risdonne, PhD student

[v.risdonne@vam.ac.uk](mailto:v.risdonne@vam.ac.uk) / [valentina.risdonne@northumbria.ac.uk](mailto:valentina.risdonne@northumbria.ac.uk)

Victoria and Albert Museum – Northumbria University

PhD project 'Materials and techniques for coating of the nineteenth-century plaster casts'

©V&A Museum

15 October 2020

## Notes

10 September 2018	Sampling	Valentina's PhD Lab book 1, page 114
24 October 2018	Casting	Valentina's PhD Lab book 1, page 133
6 November 2018	Microscopy	Valentina's PhD Lab book 1, page 137
14 October 2019	FT-IR	Valentina's PhD Lab book 1, page 175
3 December 2019	XRD	Valentina's PhD Lab book 2, page 4
18 March 2020	GC/MS	Valentina's PhD Lab book 2, page 50

A full record of analyses is available at <https://doi.org/10.25398/rd.northumbria.14039279>

## References

- Colombini, M. P., & Modugno, F. (2009). *Organic mass spectrometry in art and archaeology*. John Wiley & Sons.
- Gražulis, S., Chateigner, D., Downs, R. T., Yokochi, A. F. T., Quirós, M., Lutterotti, L., Manakova, E., Butkus, J., Moeck, P., & Le Bail, A. (2009). Crystallography Open Database—an open-access collection of crystal structures. *Journal of Applied Crystallography*, 42(4), 726–729.
- Lafuente, B., Downs, R. T., Yang, H., & Stone, N. (2016). The power of databases: the RRUFF project. In *Highlights in mineralogical crystallography* (pp. 1–29). Walter de Gruyter GmbH.
- Linstrom, P. J., & Mallard, W. G. (2014). *NIST Chemistry WebBook, NIST standard reference database number 69, National Institute of Standards and Technology, Gaithersburg MD, 20899*.
- Mills, J., & White, R. (2012). *Organic chemistry of museum objects*. Routledge.
- Price, B. A., Pretzel, B., & Lomax, S. Q. (2009). Infrared and Raman Users Group Spectral Database; 2007 ed. *IRUG: Philadelphia, PA, USA*.





**Northumbria  
University**  
NEWCASTLE

Analysis Report - Valentina Risdonne

Copy of a Statue - Regilindis, wife of Hermann, Margrave of Meissen

(REPRO.1875-17)

Initiator: Charlotte Hubbard; Conservation Department

30 September 2020

© Victoria and Albert Museum



## Analysis Report

Regilindis, wife of Hermann, Margrave of Meissen (REPRO.1875-17)

### Contents

Contents .....	256
List of abbreviations.....	256
Summary .....	257
Sample 1 .....	260
Sample 2 .....	263
Sample 3 .....	267
Sample 4 .....	271
Experimental.....	274
Notes.....	275
References.....	275

### List of abbreviations

BSE	Back Scattered Electron
EDS	Energy Dispersive Spectrometry
FT-IR	Fourier-Transform Infra-Red
FPA	Focal Plane Array
GC/MS	Gas Chromatography-Mass Spectrometry
OM	Optical Microscopy
PL	Proper Left
PR	Proper Right
py	pyrolysis
SEM	Scanning Electron Microscopy
TMAH	tetramethylammonium hydroxide
UVf	Ultraviolet Fluorescence
VLR	Visible Light Reflectance
XRD	X-ray Diffraction

## Summary

The bulk of the object is made of gypsum plaster, which contains several types of inclusions (including silicates and carbonates). By looking at the results, it is possible to hypothesise that in the surface layer, containing **silicon** and **aluminium**, the organic medium is **dammar** mixed with **drying oil** or just one of these; in the case in which just one of them was present in the medium, the other was then applied as finishing. It is not possible to discriminate, due to the penetration of the coating into the plaster. **Sample 2** appears different from the rest of the samples, containing lead in all the layers and iron and chlorine in the surface layer. There is therefore the possibility that the sample was taken from an area of repair.

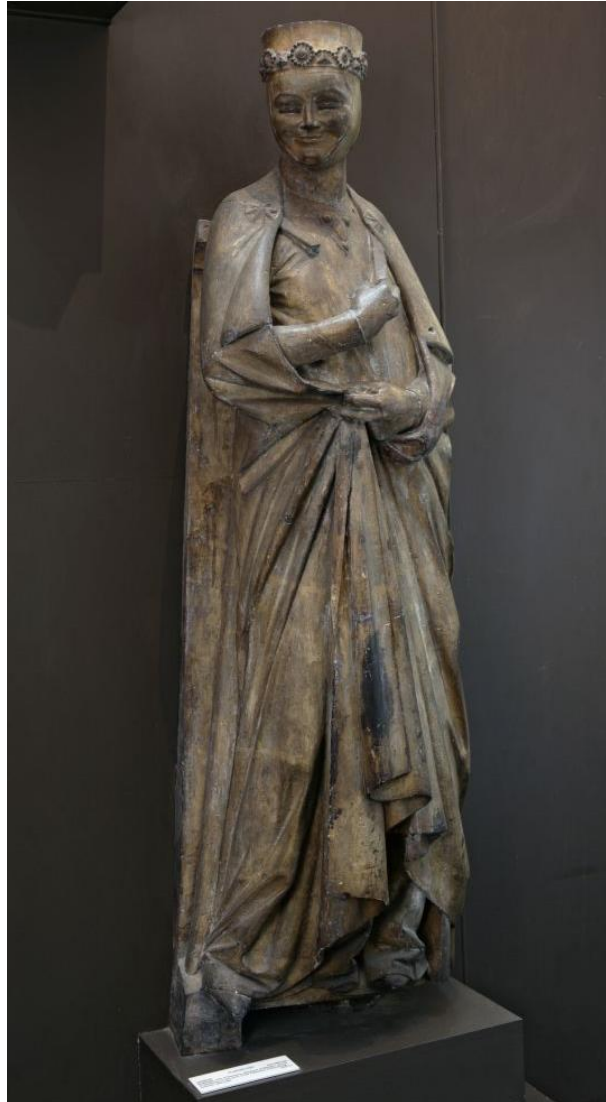


Figure 1. The copy of a statue.

The object, '**Copy of a Statue - Regilindis, wife of Hermann, Margrave of Meissen (REPRO.1875-17)**' (Figure 1), is a plaster cast of a statue of Regilinda, wife of Hermann, Margrave of Meissen, made in plaster by F. Küsthardt in Hildesheim about 1875 and purchased from F. Küsthardt in 1875 for £7 10s. The original was made in coloured sandstone in Germany and has been attributed to the Naumburg Master. The statue is from Naumburg Cathedral in Germany, it was made 200 years after Regilinda's death and copied here. This was one of 12 'founder' portraits commissioned for the cathedral. A cast of the statue depicting Regilinda's brother-in-law, Ekkehard, also from Naumburg Cathedral, is

displayed nearby. The cast is now located in Gallery 46A (The Ruddock Family Cast Court). Its dimensions are 198.5x61.5 cm.

Samples from the plaster cast were taken from pre-existing areas of loss to investigate the stratigraphy and the method of manufacture (Figure 2). The samples were analyzed to provide data for the study of the objects of the Cast Courts collection within the PhD project 'Materials and techniques for coating of the nineteenth-century plaster casts'. Details on the experimental procedure are available in the Experimental section of this report. A selection of significant results is shown in the following pages and the relevant database of analysis (<https://doi.org/10.25398/rd.northumbria.14039306>).

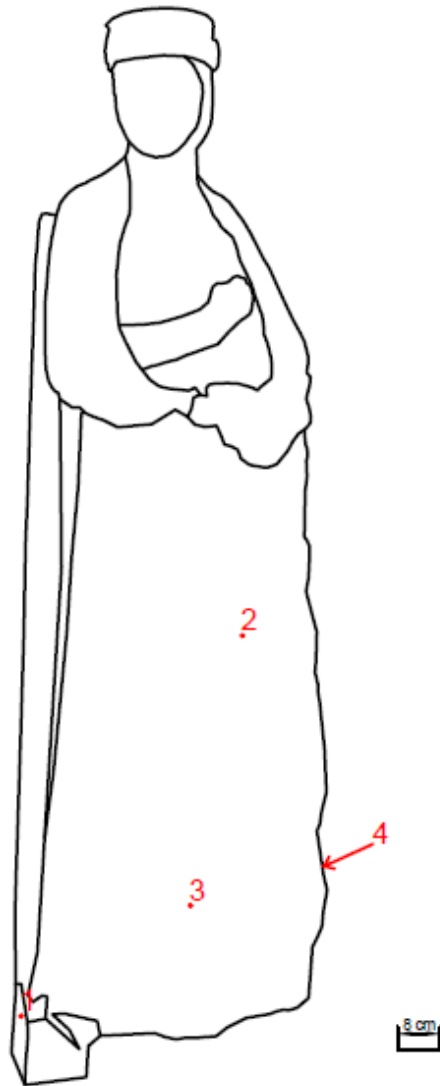


Figure 2. The statue outline with marked sampling sites.

**Sample 1:** fragment taken from an area of loss on the base of the statue, PR side.

**Sample 2:** fragment taken from a crack on a dark area on the vest of the statue.

**Sample 3:** fragment taken from an area of loss on the vest of the statue.

**Sample 4:** fragment from a large area of loss on the PL side.

The **substrate** (layer 0 in all the samples) is made of gypsum plaster (**calcium sulfate**,  $\text{CaSO}_4$ , confirmed by EDS, XRD and by the peak at  $1600\text{-}1648\text{ cm}^{-1}$  in the FT-IR spectra, which also show the sulfate overtones in the  $2100\text{-}2300\text{ cm}^{-1}$  area). Traces of **magnesium (Mg)** and **strontium (Sr)** were also detected in layer 0. Inclusions made of **aluminium (Al)** and **silicon (Si)** are present in all the samples. **Lead (Pb)** is present in all the layers of sample 2. The tabular crystalline structure typical of gypsum plaster can be seen in layer 0 of sample 1 and layers 0 and 1 of samples 2 to 4. Layer 1 of samples 2 to 4 is the **interface layer**, yellow under visible illumination and possibly consisting of a portion of lower layer soaked with the surface coating(s), showing characteristics of both layers. All the samples show a layer, **dark** under visible illumination, which contains **silicon (Si)** and **aluminium (Al)**. This dark layer contains traces of **titanium (Ti)** in sample 1 and **chlorine (Cl)**, **lead (Pb)** and **iron (Fe)** and traces of Ba, Na, Zn, Ti and P in sample 2. Traces of Na, Mg, K, Zn and P were also detected in the utmost layers of samples 1, 3 and 4. Samples 1 and 2 show an additional layer (layer 2 in sample 1 and layer 3 in sample 2), which fluoresces under UV illumination and can be consistent with a **finishing layer**. This can suggest either that varnish was applied only on the selected areas or that the varnish was applied on all the surface, but it was differently adsorbed depending on the local variation of porosity.

A **wax** or **resin** (FT-IR peaks at  $1000\text{-}1200$  and  $2800\text{-}3000\text{ cm}^{-1}$ ) was detected in all the layers of all the samples, which indicates that either the material was added to the gypsum plaster wet admixture or that the coating has also penetrated in layer 0. The latter seems also possible as the average depth of the samples is about 0.5 mm. The additional presence of a **protein** cannot be excluded by interpreting the FT-IR spectra, due to the complexity of the admixture and also to the crowded pattern of the resins' FT-IR spectra (Price et al., 2009). Py-TMAH-GC/MS analysis of sample 3 suggests that the organic medium in this sample consists of **dammar** mixed with **drying oil**. Amine fragments were also identified, as in the majority of natural 'non-protein binders' a minority of protein component is present too (Colombini & Modugno, 2009).

**NOTE:** casting in resin the fragments of plaster resulted in the fragments absorbing the resin when in the liquid state. This was visible in the BSE image as well as through the EDS mapping (Tiranti resin and catalyst are mainly made of organic compounds C, H and O). Aluminium (Al) traces are present in all the samples, due to the polishing chemical.

## Sample 1



**Sampling.** This fragment taken from an area of loss on the base of the statue, PR side.

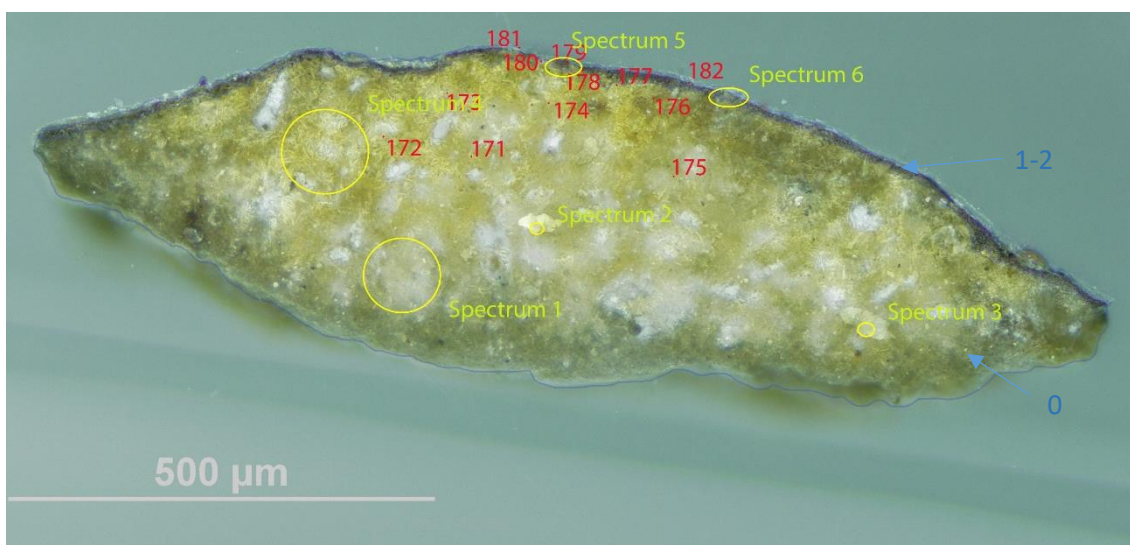
Below: Overlapped (OM and BSE) cross-section image showing the stratigraphy (blue indicators).

### 2. Varnish

#### 1. Dark layer

#### 0. Plaster bulk

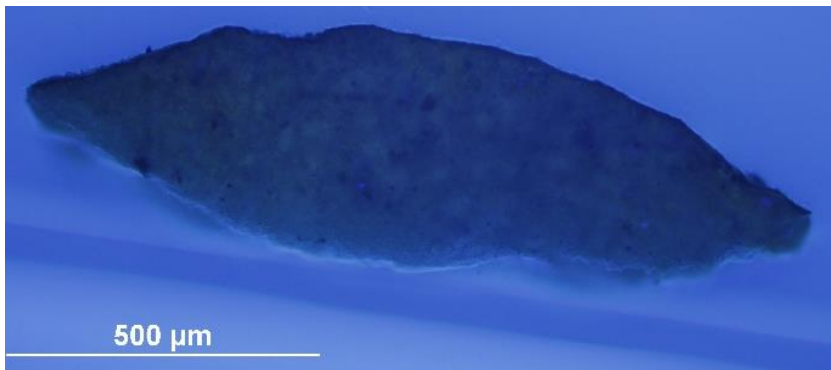
**Analysis spots.** EDS analysis (yellow): Spectra 1-6; FT-IR analysis (red): nos. 171-182



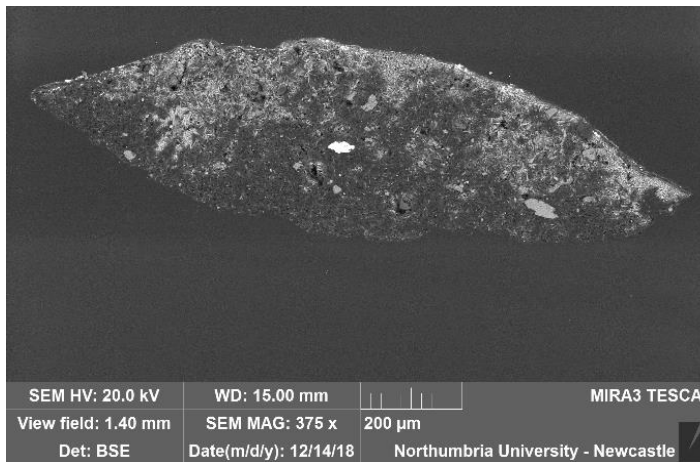
**Summary.** The substrate (layer 0) is made of plaster (**calcium sulfate**,  $\text{CaSO}_4$ , confirmed by EDS and by the peak at  $1600\text{ cm}^{-1}$  and overtones in the FT-IR spectra). The tabular crystalline structure typical of gypsum plaster can be seen in layer 0, which also shows large white inclusions made of **Al** and **Si**, as shown by the **EDS mapping**. **Cl** is also present in all the layers and traces of Sr in layer 0. Traces of Fe, Pb, Na, Mg, K, Zn and P were also detected in the utmost layers, which are mostly made of **Ti**. Traces of a fluorescing varnish can be seen on the surface (layer 2). A **wax or resin** (FT-IR peaks at  $100\text{-}1200$  and  $2800\text{-}3000\text{ cm}^{-1}$  was detected in all the layers.



VLR OM (left)

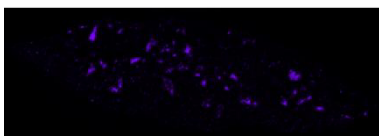


UVf OM (left)



**BSE image (left).** The tabular crystalline structure typical of gypsum plaster can be seen in layer 0, which is made of **calcium sulfate**,  $\text{CaSO}_4$ . **Cl** and **Al** were detected in all the layers, traces of Sr in layer 0 and traces of Fe, Pb, Na, Mg, K, Zn and P were detected in the utmost layers, which are mostly made of **Ti**. The large white inclusions visible in the VIS OM image above are made of **Al** and **Si**, as shown by the **EDS mapping below**.

Aluminium (Al)

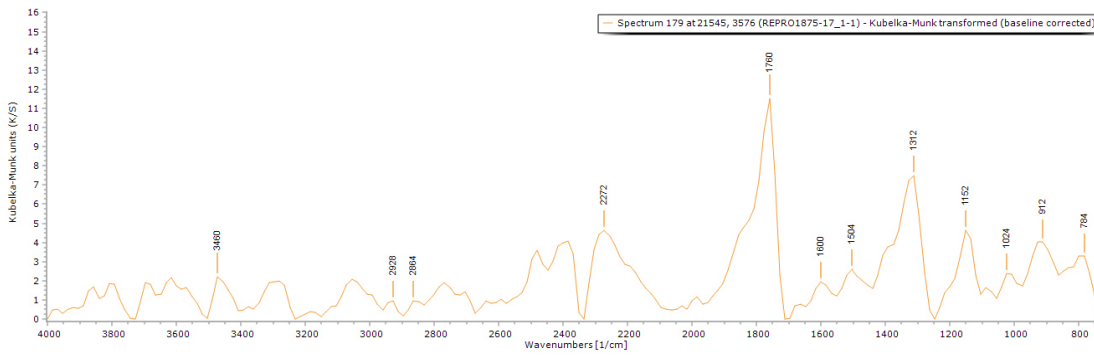


Silicon (Si)

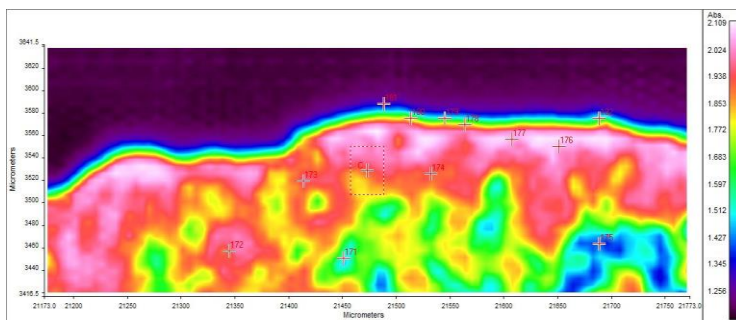


Titanium (Ti)





**FT-IR spectrum 179** (above) of layer 1. Peaks for the casting resin (1312, 1760  $\text{cm}^{-1}$ ), gypsum (1600  $\text{cm}^{-1}$ , overtone 2200-2300  $\text{cm}^{-1}$ ) and a wax/resin (1000-1200 and 2800-3000  $\text{cm}^{-1}$ ). A summary of the peaks observed in the spectra 171-182 can be seen in the table below.



**FT-IR (FPA) image** (left). The different reflectance of the layers can be observed in the FPA image.

Spectrum	Layer	peaks ( $\text{cm}^{-1}$ )						
		Casting Resin	Gypsum	Carbonate	Wax/resin	C=O ester carbonyl	SO overtone	Unknown
171	0	1312, 1760	1600		864, 960, 992, 1088, 1200, 1520, 2960		2240	
172	0	1328, 1760	1616	1776	832, 864, 944, 992, 1056, 1216, 1408, 2928		2240	
173	0	1312		1776	896, 992, 1088, 1136, 1408, 1584, 1680, 2928		2256	
174	0		1616		768, 880, 960, 1040, 1168, 1232, 1296, 1360, 1456, 2848, 2984	1744	2208	
175	0	1328, 1760	1616		816, 944, 1088, 1184, 1488, 1664, 2944		2240	
176	0	1328, 1768			784, 896, 992, 1168, 1216, 1408, 1520, 1584		2304, 2453	
177	0	1328	1600	1776	832, 896, 1024, 1088, 1280, 1392, 1568, 1680, 2816, 2976		2272	
178	1	1312, 1760	1616		784, 928, 976, 1072, 1152, 1200, 1472, 2912, 2984			
179	1	1312, 1760	1600		784, 912, 1024, 1152, 1504, 2864, 2928		2272	
180	1	1312, 1760	1600		784, 896, 944, 1088, 1184, 1520, 2880, 2944		2256	
181	2	1312, 1760	1616		784, 928, 1008, 1088, 1152, 1472			
182	2	1312, 1760		800	864, 928, 992, 1136, 1520, 2944		2288	

## Sample 2

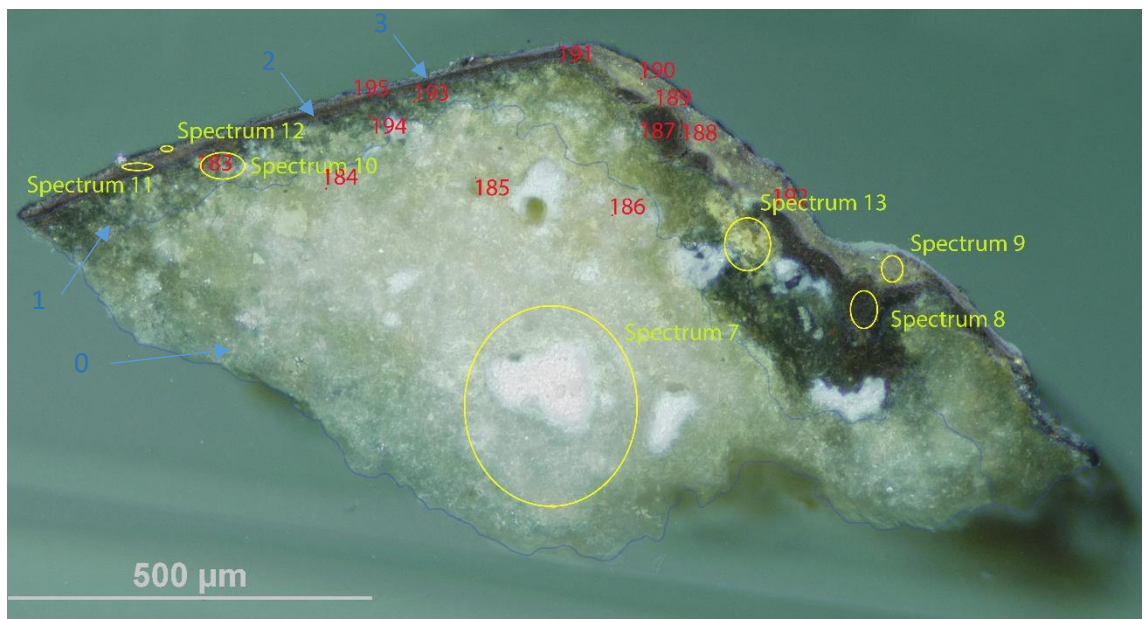


**Sampling.** This sample consists of a fragment taken from a crack on a dark area on the vest of the statue (blue indicators).

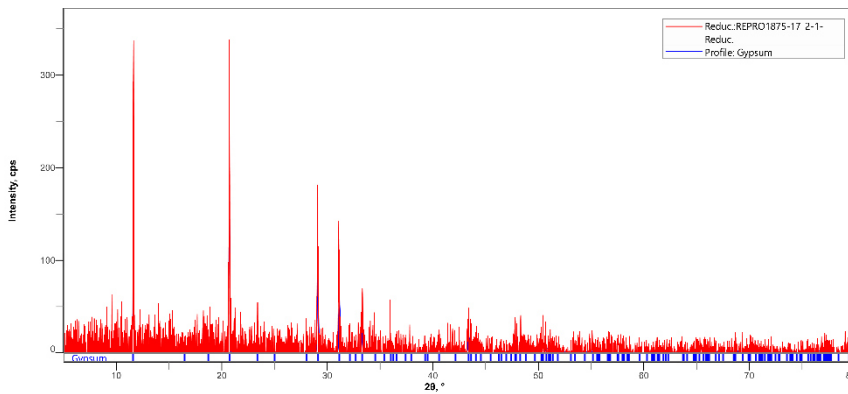
Below: Overlapped (OM and BSE) cross-section image showing the stratigraphy.

- 3. Varnish and dirt**
- 2. Dark layer**
- 1. Yellowish and undefined layer**
- 0. Plaster bulk**

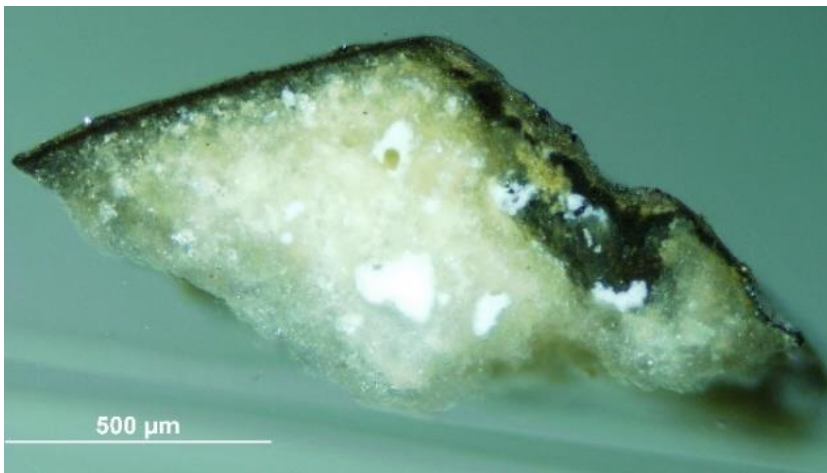
**Analysis spots.** EDS analysis (yellow): Spectra 7-13; FT-IR analysis (red): nos. 183-195



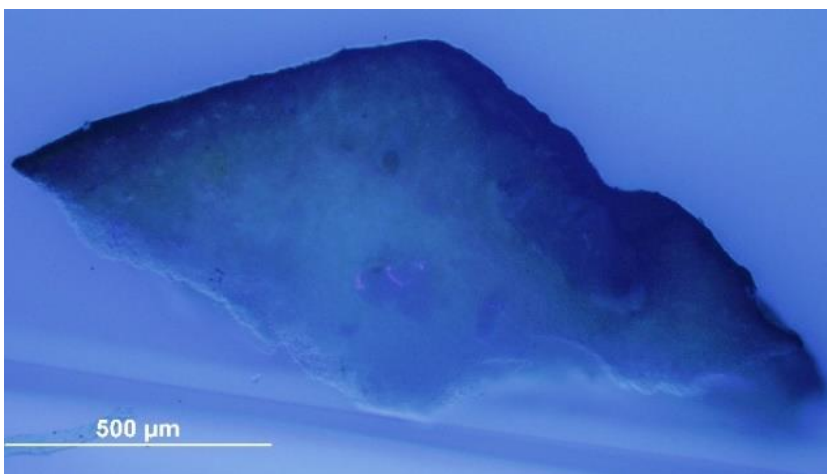
**Summary.** The substrate (layer 0) is made of plaster (**calcium sulfate**,  $\text{CaSO}_4$ , confirmed by EDS, XRD and by the peak at  $1600\text{ cm}^{-1}$  and overtones in the FT-IR spectra) and lead (Pb) is present in all the layers. The tabular crystalline structure typical of gypsum plaster can be seen in layers 0 and 1. Layer 1, which appears yellow under the microscope, consists of a portion of the lower layer soaked with the surface coating, showing characteristics of both layer 0 and layer 2. Layer 2, dark under visible illumination, is made of Si, Cl, Fe and Pb (see EDS mapping) and traces of Ba, Na, Zn, Ti and P were also detected. The BSE mapping shows that Al from the polishing solution has penetrated the larger pores. A **wax or resin** (FT-IR peaks at  $1200\text{-}1500$  and  $2800\text{-}3000\text{ cm}^{-1}$ ) was detected in all the layers. The utmost layer (layer 3) seems consistent with a layer of varnish/dirt.



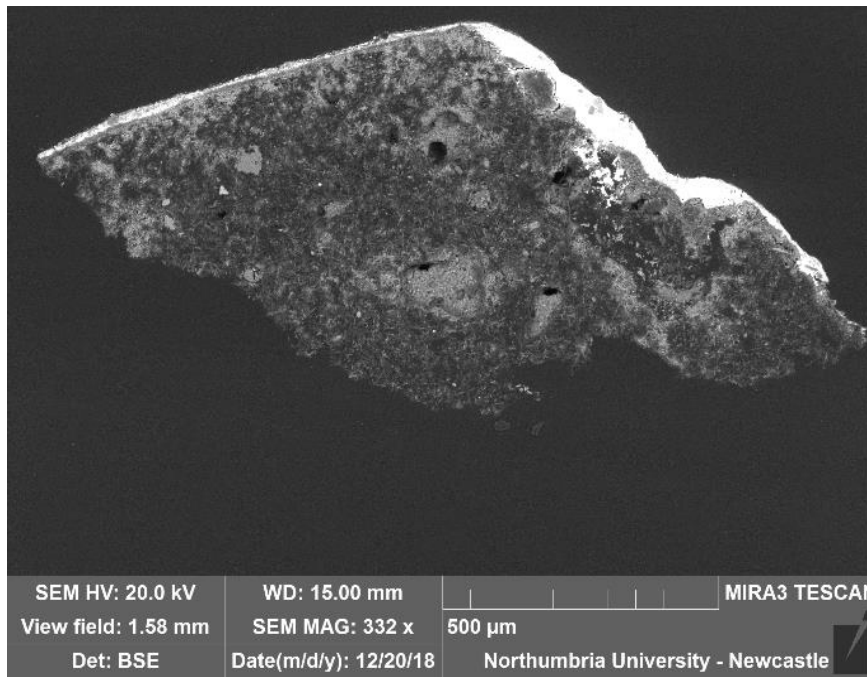
A fragment of this sample was pulverised and analysed by **XRD**. It was possible to identify the profile of gypsum (calcium sulfate) and the diffractogram was compared to references from the Rigaku SmartLab Database and the most significant peaks were at  $2\theta = 11.63, 20.70, 29.09, 31.09, 33.31, 43.58$ .



VLR OM (left)

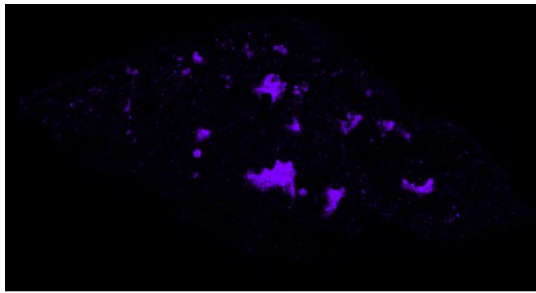


UVf OM (left)

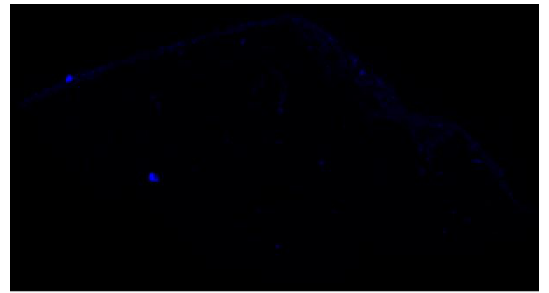


**BSE image (left).** The tabular crystalline structure typical of gypsum plaster can be seen in layers 0 and 1. Layer 2 appears solid and bright white, suggesting heavy elements, identified as Si, Cl, Fe and Pb by **EDS mapping (below)**. The mapping also shows that Pb is present in all the layers and that Al from the polishing solution penetrated the larger pores. **EDS spectra** suggest that the sample is mostly made of calcium sulfate (C, O, Ca, S) Si and Pb with traces of Ba, Na, Zn, Cl, Ti and P. The utmost layers are made of Si, Pb, Cl and Fe

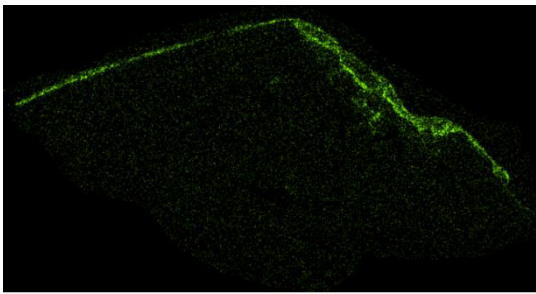
Aluminium (Al)



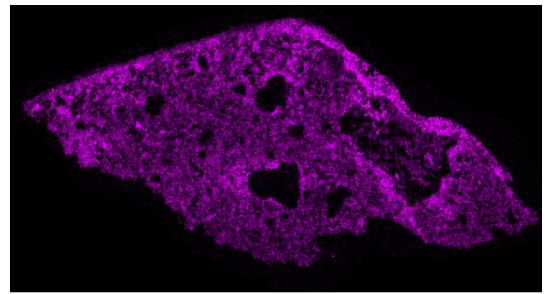
Silicon (Si)



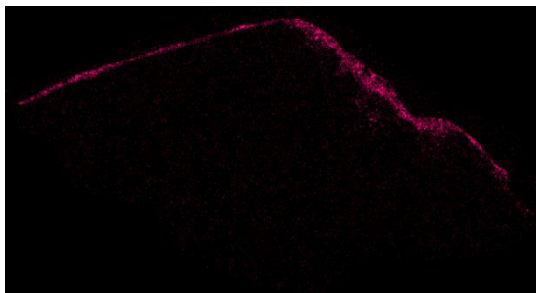
Chlorine (Cl)

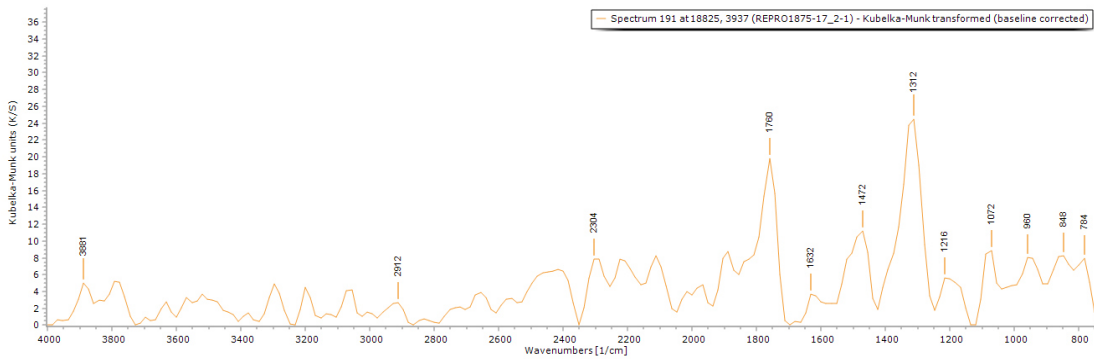


Lead (Pb)

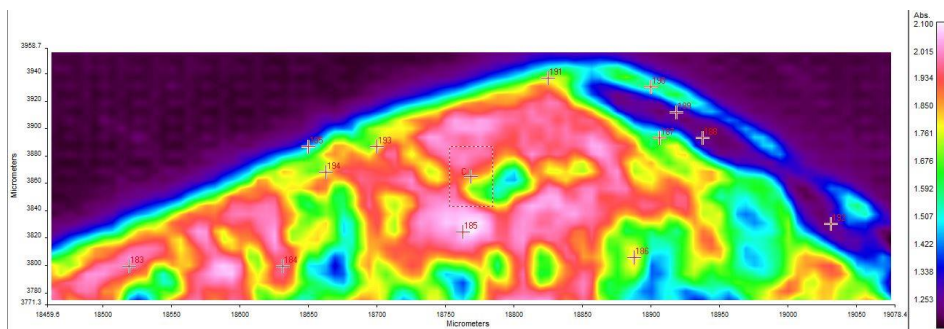


Iron (Fe)





**FT-IR spectrum 191** (above) of layer 2. Peaks for the casting resin (1312, 1760  $\text{cm}^{-1}$ ), gypsum (1632  $\text{cm}^{-1}$ , overtone 2200-2300  $\text{cm}^{-1}$ ) and a wax/resin (1216, 1472, 2800-3000  $\text{cm}^{-1}$ ). A summary of the peaks observed in the spectra 183-195 can be seen in the table below.



**FT-IR (FPA) image** (left). Some indication of different reflectance of the layers can be observed in the FPA image.

Spectrum	Layer	peaks ( $\text{cm}^{-1}$ )						
		Casting Resin	Gypsum	Carbonate	Wax/resin	C=O ester carbonyl	SO overtone	Unknown
183	1	1312	1648	1776	752, 880, 1056, 1376, 1472, 1584, 2960		2384	2624
184	0	1312, 1760	1648		832, 1008, 1056, 1360, 1456, 1504, 2976		2272	1792
185	0	1760	1600		768, 832, 960, 1040, 1088, 1296, 1392, 1536, 1664, 2848, 2912		2272	1824
186	0	1760	1616		778, 912, 992, 1072, 1296, 1456, 2848		2288	
187	2	1760			829, 912, 1136, 1296, 1552, 2848, 2928		2224	
188	2				800, 944, 1072, 1152, 1488, 2955			
189	2	1760			816, 912, 1120, 1296, 1488, 1664, 2970			
190	3	1328, 1760	1632		816, 944, 1088, 1152, 1472, 2800, 2938		2320	
191	2	1312, 1760	1632		784, 848, 960, 1072, 1216, 1472, 2912		2304	
192	2	1760			832, 960, 1120, 1296, 1472, 1536, 2944		2224	
193	1	1344, 1760			848, 912, 1088, 1216, 1296, 1488, 1568, 1664, 2832, 2960		2400	
194	1	1328, 1760			896, 1024, 1104, 1264, 1472, 1664, 2800, 2966		2288	
195	2	1312, 1760	1600	800	880, 992, 1088, 1184, 1488, 2864, 2989		2368	

## Sample 3



**Sampling.** This fragment taken from an area of loss on the vest of the statue.

Below: Overlapped (OM and BSE) cross-section image showing the stratigraphy (blue indicators).

**2. Dark layer**

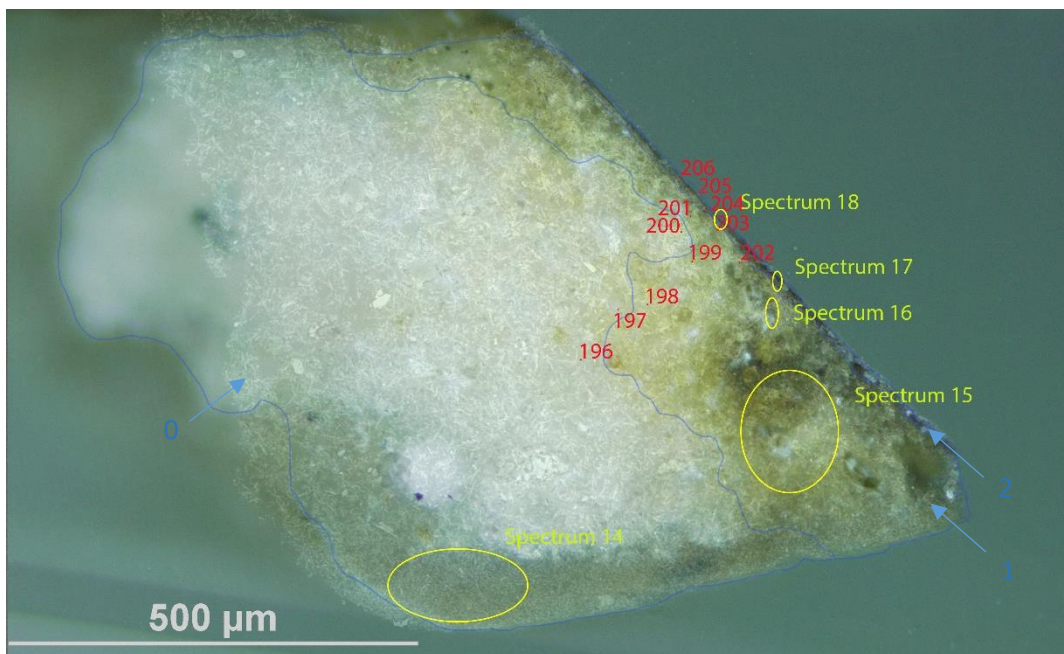
**1. Yellowish and undefined layer**

**0. Plaster bulk**

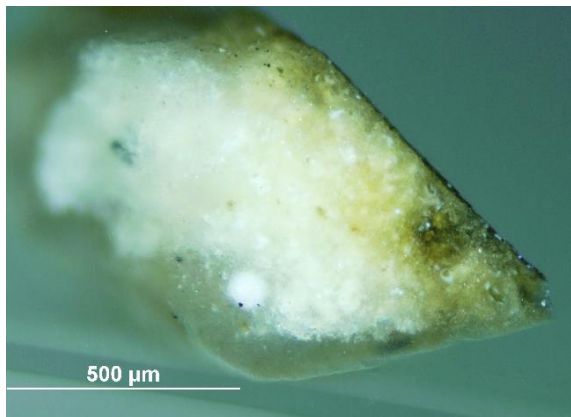
**Analysis spots.**

EDS analysis (yellow): Spectra 14-18

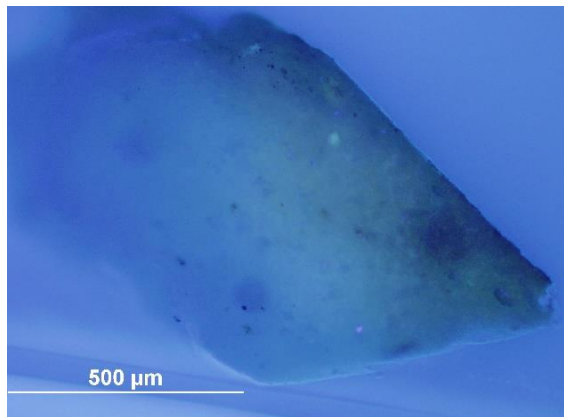
FT-IR analysis (red): nos. 196-206



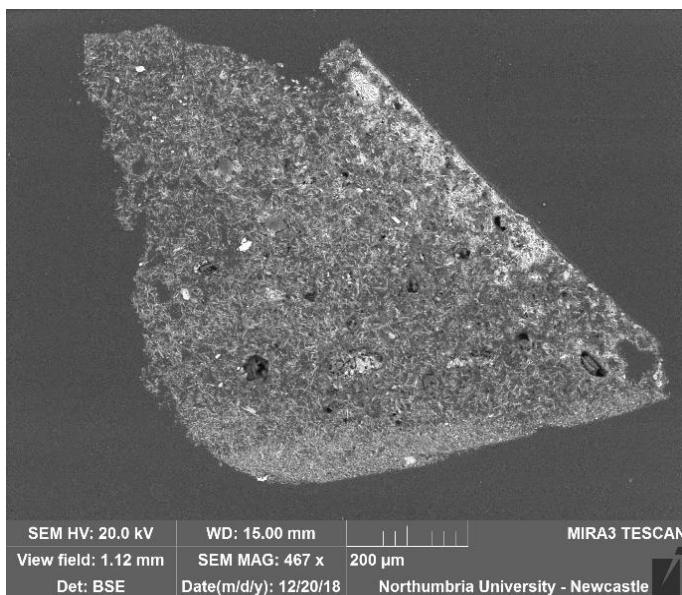
**Summary.** The sample is mostly made of C, O, S and Ca (**calcium sulfate**,  $\text{CaSO}_4$ , confirmed by EDS and by the peak at  $1600\text{-}1616\text{ cm}^{-1}$  in the FT-IR spectra). Al is overall present as used as a polishing agent, but could also, together with Si and Mg be present as part of silicate inclusions, which were observed in all the layers. The structure typical of gypsum plaster can be seen in layers 0 and 1. Layer 1 appears yellow under visible illumination and layer 2 is dark. A **wax or resin** is suggested by FT-IR (peaks at  $1000\text{-}1200$  and  $2800\text{-}3000\text{ cm}^{-1}$ ) and was detected in all the layers. py-TMAH-GC/MS shows markers characteristic of **dammar** mixed with **drying oil**. Amine fragments were also identified, as in the majority of natural 'non-protein binders' a minority of protein component is present too (Colombini & Modugno, 2009).



VLR OM (above)

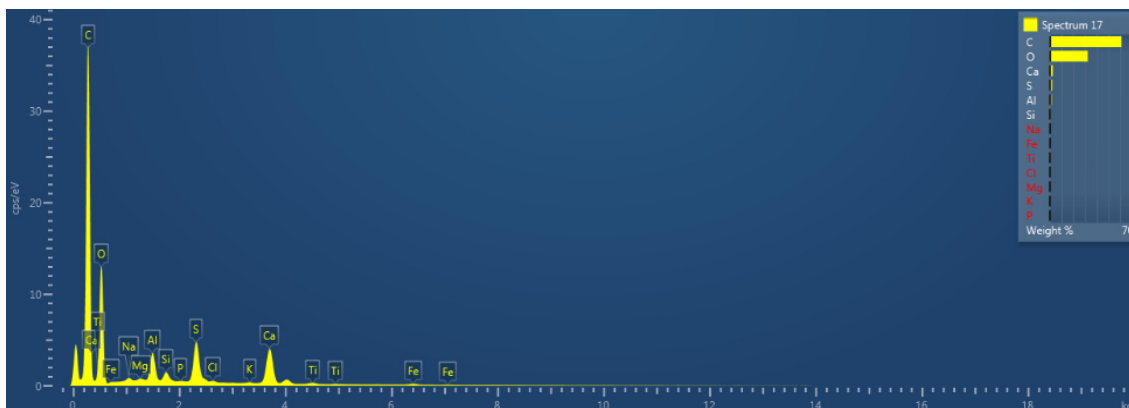


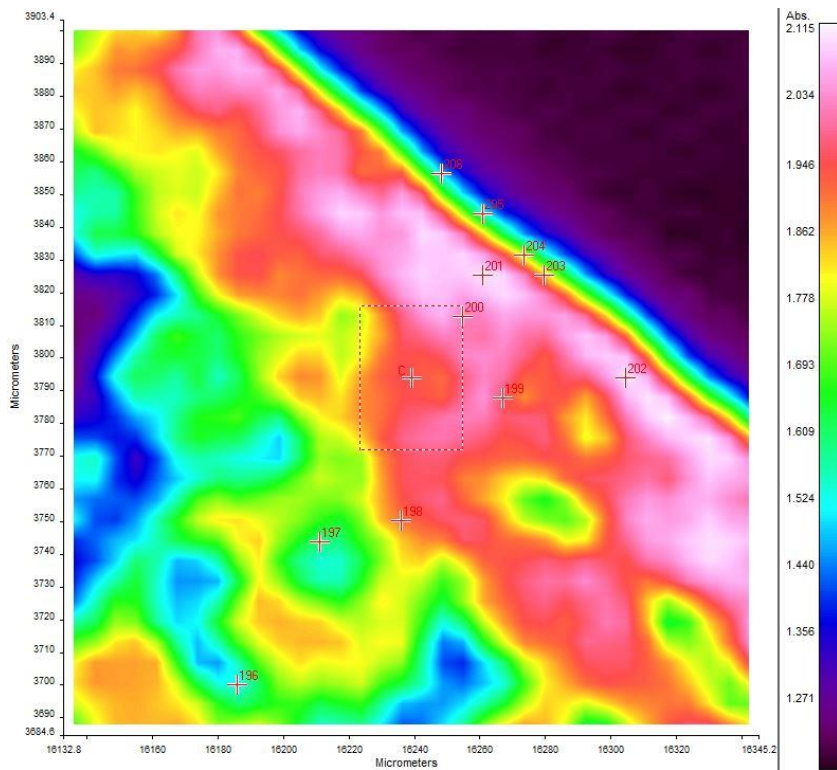
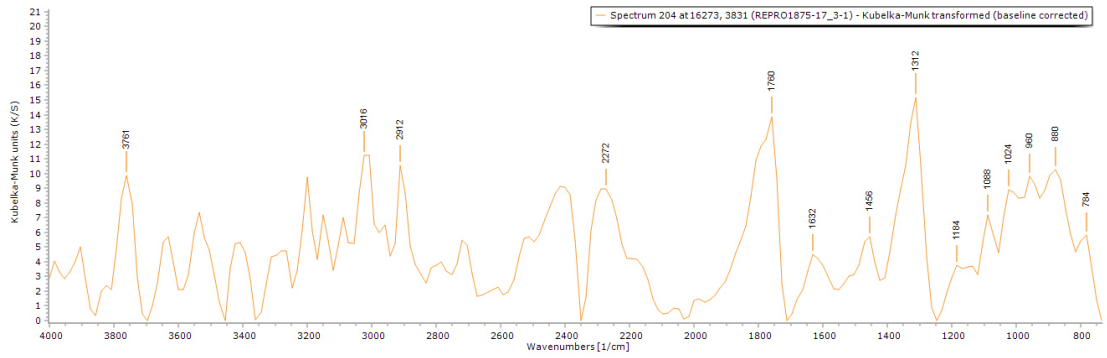
UVfOM (above)



**BSE image (left).** The tabular crystalline structure typical of gypsum plaster can be seen in layers 0 and 1.

Calcium sulfate ( $\text{CaSO}_4$ ) and Al, Si, Mg and traces of Na and Cl were detected in all the layers. Additional traces of Ti, Fe, K and P were detected in the utmost layers (see **spectrum 17 below**). **EDS mapping** shows inclusions made of **aluminium (Al)** and **silicon (Si)**, but no element distribution in a layer fashion can be observed.

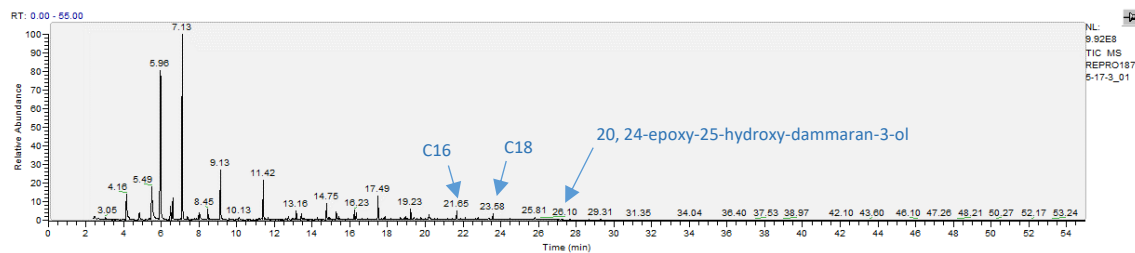




**FT-IR spectrum 204** (above) of layer 2. Peaks for the casting resin (1312, 1760  $\text{cm}^{-1}$ ), gypsum (1632  $\text{cm}^{-1}$ ), and a wax/resin (1456  $\text{cm}^{-1}$  and 2800-3000  $\text{cm}^{-1}$ ). A summary of the peaks observed in the spectra 196-206 can be seen in the table below.

**FT-IR (FPA) image** (left). Indication of different reflectance of the layers can be observed in the Focal Plane Array (FPA) image.

Spectrum	Layer	peaks (cm-1)						
		Casting Resin	Gypsum	Carbonate	Wax/resin	C=O ester carbonyl	SO overtone	Unknown
196	0	1312, 1760	1616	800	880, 1024, 1120, 1456, 2848, 2960			2272
197	0	1328, 1760	1616		784, 864, 928, 976, 1024, 1104, 1472, 2880, 2928			2256
198	1	1328	1616		752, 832, 928, 1024, 1072, 1392, 1472, 1680, 2848, 2896	1744		2240
199	1	1328, 1760	1600	800	848, 912, 960, 1008, 1104, 1408, 1680, 2848, 2928			2192, 1840
200	0	1328, 1760	1600, 1632		848, 928, 1040, 1104, 1264, 1376, 1472, 2800, 2864, 2939			2272, 1818
201	1	1312, 1760	1600		864, 912, 976, 1104, 1440, 1536, 2880, 2960			2272
202	1	1328		1792	832, 928, 992, 1040, 1104, 1232, 1440, 1520, 1584, 1648, 2896, 2992	1744		2254
203	2	1312, 1760	1600		816, 896, 976, 1088, 1152, 1216, 1376, 1472, 1536, 2784, 2960			2400
204	2	1312, 1760	1632		784, 880, 960, 1024, 1088, 1184, 1456, 2912			2272
205	2	1312, 1760	1616		768, 864, 1008, 1088, 1168, 1504, 2880			2240
206	2	1312, 1760	1616		784, 928, 1008, 1088, 1168, 1504, 2966			2304

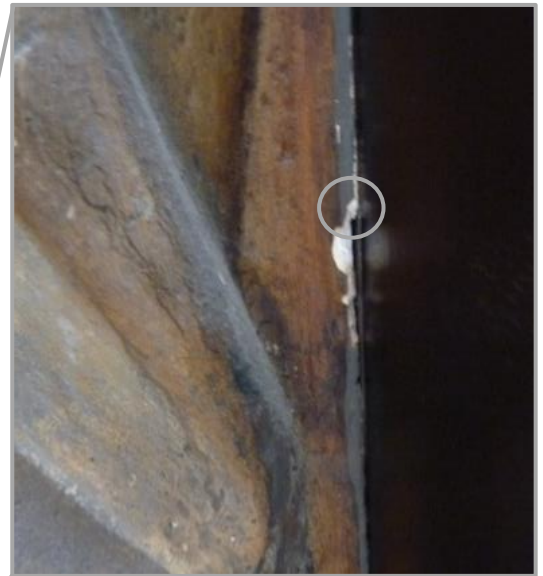
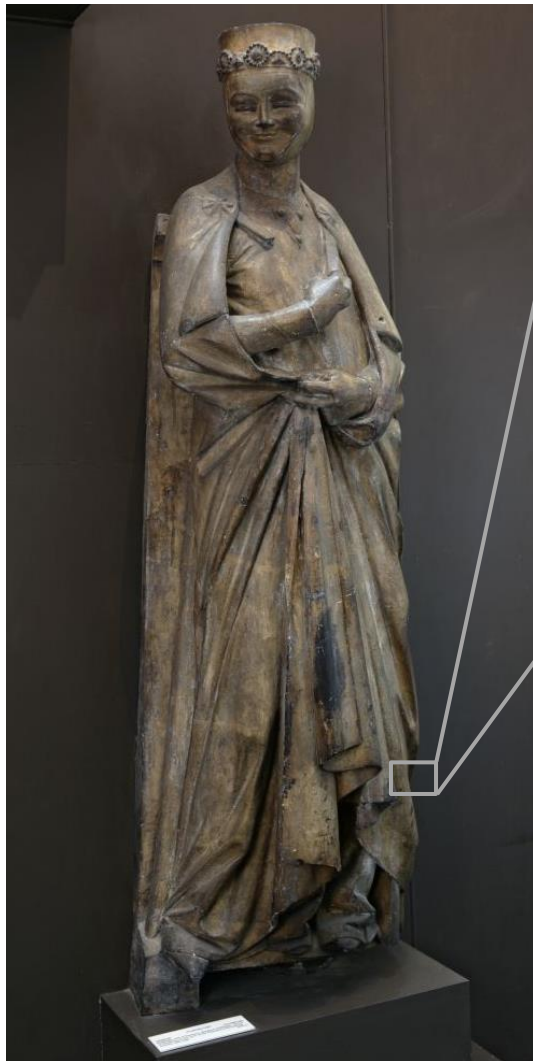


RT	m/z	Assignment	Formula
4.16	45(100), 59(7), 74(64)	Ethyl ether	C4H10O
4.84	59(100), 73(15), 88(5)	3-Pentanol, 2-methyl-	C6H14O
5.49	42(9), 58(100), 72(5), 88(3), 116(4)	1,2-Ethanediamine, N'-ethyl-N,N-dimethyl-	C6H16N2
5.96	42(12), 58(100), 117(15)	1,2-Ethanediamine, N'-ethyl-N,N-dimethyl-	C6H16N2
6.5	45(20), 58(13), 66(22), 79(18), 95(100), 125(7)	Sulfuric acid, dimethyl ester	C2H6O4S
6.62	45(8), 65(18), 79(100), 95(12), 109(6)	Methanesulfonic acid, methyl ester	C2H6O3S
7.13	44(7), 56(7), 72(100), 116(2), 131(3)	1,2-Ethanediamine, N'-ethyl-N,N-dimethyl-	C6H16N2
8.45	58(31), 70(8), 86(100), 110(2)	1,2-Ethanediamine, N,N-diethyl-N'-methyl-	C7H18N2
9.13	44(100), 57(22), 86(69), 128(55)	1-Butanamine, N-butyl-	C8H19N
11.42	58(100), 70(9), 116(5)	1,2-Ethanediamine, N'-ethyl-N,N-dimethyl	C6H16N2
13.16	58(19), 71(16), 75(7), 98(33), 116(41), 130(100), 142(9), 145(3)	Unidentified amine fragment	
14.75	58(7), 84(6), 99(4), 116(100), 128(6), 139(8), 173(4)	Unidentified amine fragment	
14.89	42(29), 55(72), 74(76), 83(45), 111(27), 115(100), 125(47), 128(33), 135(5), 139(5), 157(34), 166(5)	Undecylenic Acid	C11H20O2
15.29	45(38), 58(45), 75(37), 75(37), 85(52), 91(43), 115(32), 119(100), 149(83), 165(75), 180(60)	Unidentified terpenoid fragment	
15.43	58(19), 75(5), 77(28), 91(40), 105(25), 119(100), 133(25), 149(81), 165(70), 180(57)	Unidentified terpenoid fragment	
16.23	41(30), 55(74), 69(77), 74(97), 83(49), 87(44), 111(31), 129(74), 138(100), 171(52), 197(5)	Unidentified FA fragment	
16.34	58(5), 77(16), 92(5), 104(61), 133(6), 163(100), 194(4)	Dimethyl phthalate	C10H10O4
16.95	45(83), 58(100), 71(33), 85(54), 95(5), 111(24), 113(34), 125(30), 143(28), 171(29), 185(5), 217(5)	Unidentified terpenoid fragment	
17.49	43(18), 55(68), 59(40), 74(71), 83(59), 87(28), 97(21), 111(53), 124(27), 143(32), 152(100), 185(41)	Nonanedioic acid, monomethyl ester	C10H18O4
17.87	41(25), 55(63), 59(52), 71(44), 83(30), 88(100), 111(32), 131(5), 139(27), 143(20), 163(5), 166(47), 171(22), 177(5), 199(5)	Unidentified FA fragment	
18.69	45(52), 58(100), 74(81), 83(53), 98(44), 115(54), 125(61), 138(43), 161(45), 166(5), 190(60), 199(42), 207(5), 222(5)	Unidentified FA fragment	
19.23	45(82), 55(33), 71(52), 75(100), 85(83), 101(69), 115(25), 139(26), 152(17), 161(35), 170(5), 183(20), 215(5), 228(5), 260(5)	Unidentified terpenoid fragment	
19.41	45(73), 58(65), 85(46), 99(5), 109(38), 122(28), 137(55), 163(5), 182(38), 193(100), 207(5), 224(5), 236(5)	Unidentified terpenoid fragment	
20.19	45(100), 58(61), 71(80), 85(85), 101(92), 123(5), 139(32), 161(5), 169(5), 193(5), 207(5), 231(5), 246(5)	Unidentified terpenoid fragment	
21.65	55(21), 59(14), 74(100), 87(64), 143(20), 199(7), 227(12), 239(5), 270(5)	methyl palmitate	C17H34O2
22.79	58(100), 71(43), 85(36), 115(30), 149(5), 207(5), 219(5), 251(33), 270(5), 299(5), 331(5)	7-oxo-15-hydroxy-dehydroabietic acid	
23.58	43(21), 58(33), 74(100), 87(65), 115(5), 143(25), 199(13), 255(13), 279(5), 298(5)	methyl stearate	C19H38O2
25.81	58(100), 71(88), 95(63), 109(28), 119(22), 137(38), 159(41), 169(21), 201(63), 207(40), 281(5), 322(5)	Unidentified terpenoid fragment	
27.68	44(76), 58(100), 74(62), 115(5), 143(23), 191(5), 207(49), 255(5), 288(5), 311(5), 354(5), 401(5)	20, 24-epoxy-25-hydroxy-dammaran-3-ol	
28.67	44(80), 58(100), 79(33), 115(13), 141(17), 165(5), 191(5), 207(57), 225(5), 281(17), 297(21), 313(5), 340(5), 357(5), 372(5)	Dammar fragment	
29.31	58(100), 97(28), 139(5), 191(5), 207(56), 281(5), 355(5), 401(5), 429(5)	Dammar fragment	

RT = retention time, m/z = mass/charge ratio

**Py-TMAH-GC/MS chromatogram** (top and described in the table above) shows small fragments due to derivatization (from  $t = 4.16$  to  $11.42$  min) and markers characteristic of **dammar** (several terpenoid fragments and marker at  $t = 27.68$  min) (Colombini & Modugno, 2009; Mills & White, 2012). The presence of methyl azelate ( $t = 17.49$ ), **methyl palmitate** ( $t = 21.65$ ) and **stearate** ( $t = 23.58$ ) suggest that the resin has been mixed with a **drying oil** ( $A/P = 2.42$  and  $P/S = 1.79$ ), possibly **linseed oil**. Amine fragments were also identified, as in the majority of natural 'non-protein binders' a minority of protein component is present too (Colombini & Modugno, 2009).

## Sample 4



**Sampling.** This fragment taken from a large area of loss on the PL side.

Below: Overlapped (OM and BSE) cross-section image showing the stratigraphy (blue indicators).

**2. Dark layer**

**1. Yellowish and undefined layer**

**0. Plaster bulk**

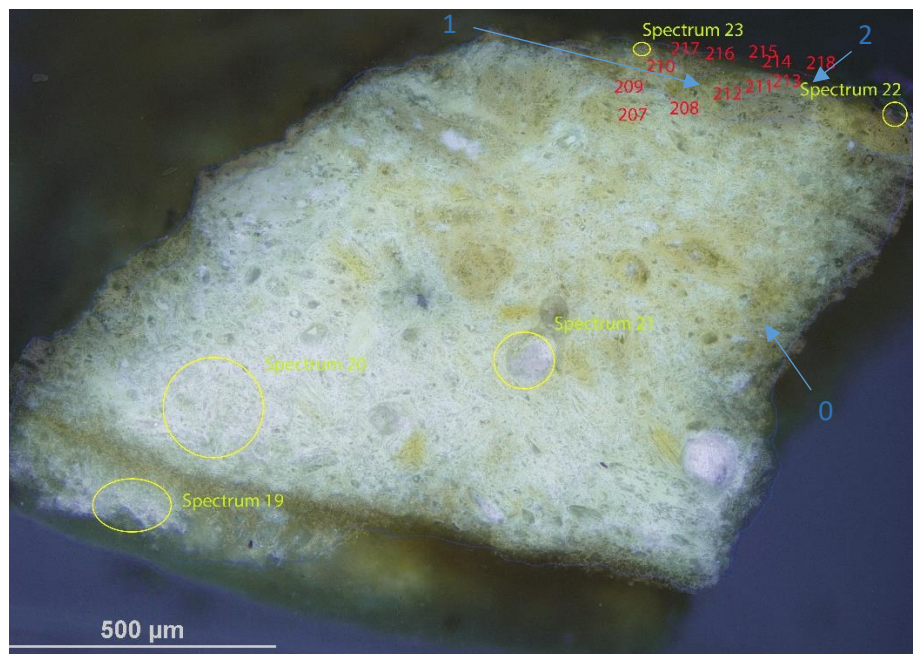
### Analysis spots.

EDS analysis  
(yellow):

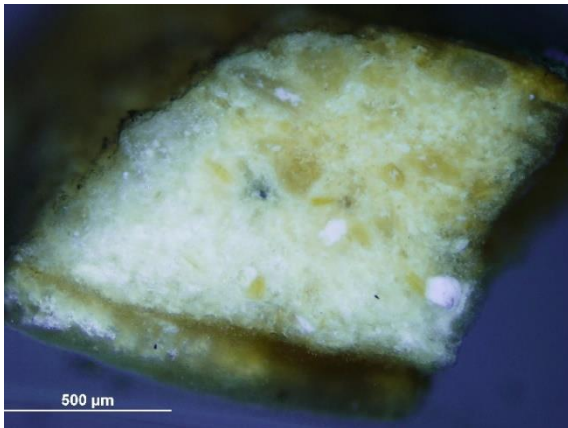
Spectra 19-23

FT-IR analysis  
(red):

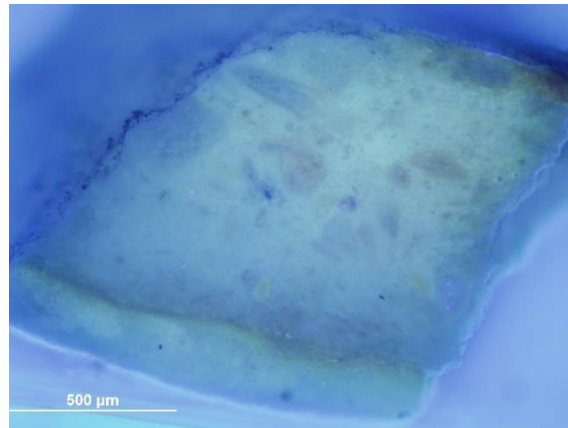
nos. 207-218



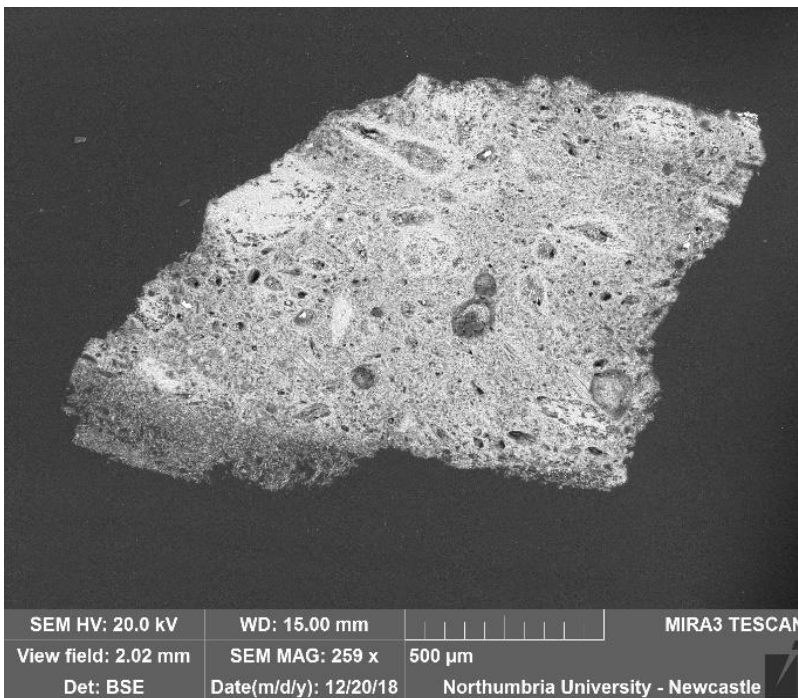
**Summary.** The sample is mostly made of C, O, S and Ca (**calcium sulfate**,  $\text{CaSO}_4$ , confirmed by EDS and by the peak at  $1600\text{-}1632\text{ cm}^{-1}$  in the FT-IR spectra). Al is overall present as used as a polishing agent, but could also, together with Si, K and Mg be present as part of silicate inclusions, which are present in all the layers (see EDS mapping). Layer 2 appears dark under visible illumination and traces of Ba, Cr, Zn, Fe, Pb and Cl were also detected in this layer. Layer 1 appear yellow under visible illumination and presents characteristics common at layer 0 and 1. A **wax or resin** is suggested by FT-IR (peaks at  $1000\text{-}1200$  and  $2800\text{-}3000\text{ cm}^{-1}$ ) and present in all the layers.



VLR OM (above)



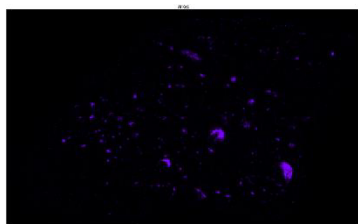
UVf OM (above)



**BSE image (left).** The tabular crystalline structure typical of gypsum plaster can be seen in layers 0 and 1. **EDS mapping (below)** does not show any particular element distribution in a layer fashion and shows the presence of Al-Si inclusions.

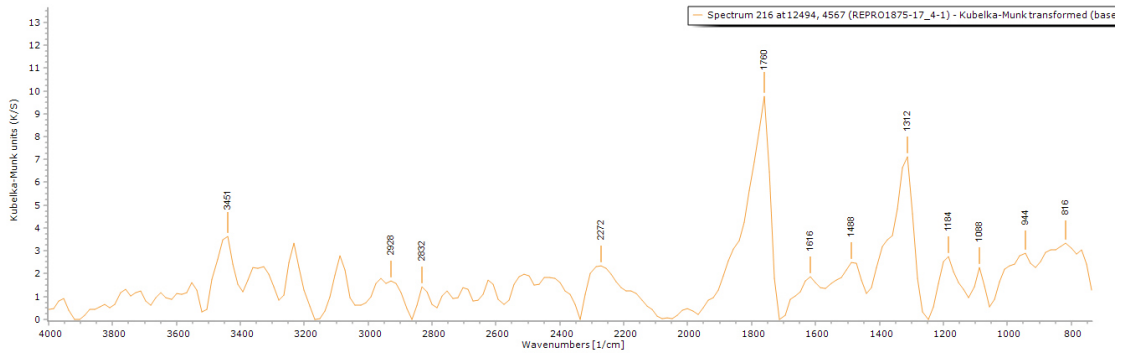
**EDS spectra** indicate that all the layers consist of C, O, Ca, S, Al and Si. Al traces are present in all the layers (polishing medium), but Al could also, together with K and Si be present as part of silicate inclusions. Ba, Cr, Zn, Fe, Pb and Cl were also detected in the surface layer.

Aluminium (Al)

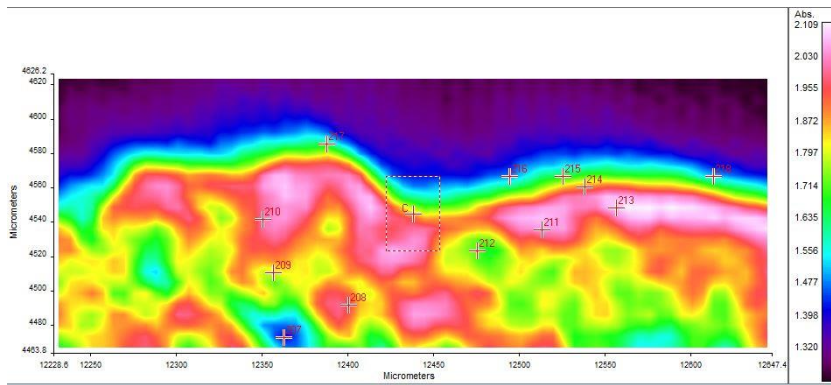


Silicon (Si)





**FT-IR spectrum 216** (above) of layer 2. Peaks for the casting resin (1312, 1760  $\text{cm}^{-1}$ ), gypsum (1616  $\text{cm}^{-1}$ , overtone 2200-2300  $\text{cm}^{-1}$ ) and a wax/resin (1100-1500, 2800-3000  $\text{cm}^{-1}$ ). A summary of the peaks observed in the spectra 207-218 can be seen in the table below.



**FT-IR (FPA) image** (left). Indication of different reflectance of the layers can be observed in the FPA image.

Spectrum	Layer	peaks ( $\text{cm}^{-1}$ )						
		Casting Resin	Gypsum	Carbonate	Wax/resin	C=O ester carbonyl	SO overtone	Unknown
207	0	1312, 1760	1632		992, 1216, 1520		2288	
208	0	1312, 1760	1632		784, 912, 1008, 1248, 1472, 1568, 1680, 2864, 2960		2192	1952
209	1	1312, 1760	1616		928, 1008, 1408, 1504, 2928		2272	
210	1	1328, 1760	1616	800	976, 1040, 1232, 1392, 1504, 1568, 1680, 2864, 2928		2232	
211	1	1344	1600	1776	768, 832, 1008, 1248, 1296, 1472, 1696, 2848, 2944		2216	
212	1	1760	1632		768, 864, 944, 1008, 1072, 1216, 1296, 1392, 2864, 2944			
213	1	1328, 1760	1600		880, 944, 1008, 1216, 1280, 1488, 1680, 2784, 2944		2245	1872
214	2	1312, 1760			896, 960, 1024, 1088, 1216, 1424, 1520, 1584, 1664, 2912			
215	2	1312, 1760	1616		768, 864, 944, 1072, 1168, 1216, 1392, 1504, 2960		2368	
216	2	1312, 1760	1616		816, 944, 1088, 1184, 1488, 2832, 2928		2272	
217	2	1312, 1760	1600		784, 864, 992, 1072, 1152, 1472, 2944			
218	2	1312, 1760	1600	800	912, 992, 1120, 1472, 2944			

## Experimental

The object was observed, and its conditions were documented. Samples from selected areas were taken by Valentina Risdonne. When possible, each sample was split into two parts: one fragment was embedded in polyester resin (Tiranti clear casting resin), polished and analysed under an optical microscope and the other was put aside for py-TMAH-GC/MS and XRD analysis.

The optical microscopy was performed with an Olympus BX51 Metallurgical Microscope equipped with four objectives (magnification of x5, x20, x50 and x100), and an x10 eyepiece. In many instances, a small amount of white spirit was applied on the surface of the cross-section to improve the saturation under the microscope. The microscope is equipped with a 6-cube filter turret which allows operating the system in reflected visible light (brightfield and darkfield mode) and reflected UV light (365 nm) using a 100 W mercury burner.

The SEM-EDS analysis was performed with a field emission TESCAN MIRA 3 with gigantic chamber. The SEM is equipped with: secondary electron detector (SE), secondary electron in-beam detector (In-beam SE), back-scatter detector (BSE), back-scatter in-beam detector (In-beam BSE), cathodoluminescence detector (without wavelength detection) (CL), plasma chamber/sample cleaner and software Alicona 3D imaging. For the EDS analytical part, it has an Oxford Instruments setup: Software: AztecEnergy, X-ray detector X-Max 150 mm<sup>2</sup> and X-ray detector X-Max Extreme, low energy detector for thin films, high resolution and low voltage. The samples were analysed by SEM-EDS Low Vacuum Mode (10-15 Pa). EDS Mapping and data processing were performed with Aztec Oxford software.

A Perkin Elmer Frontier FT-IR spectrometer (350 cm<sup>-1</sup> at the best resolution of 0.4 cm<sup>-1</sup>) was used, equipped with a germanium crystal for ATR measurements and combined with a Spectrum Spotlight 400 FT-IR microscope equipped with a 16×1 pixel linear mercury cadmium telluride (MCT) array detector standard with InGaAs array option for optimised NIR imaging. Spectral images from sample areas are possible at pixel resolutions of 6.25, 25, or 50 microns. The Perkin Elmer ATR imaging accessory consists of a germanium crystal for ATR imaging. These run with Perkin Elmer Spectrum 10™ software and with SpectrumIMAGE™ software. Baseline and Kubelka-Munk corrections were applied to the raw data acquired in diffuse reflectance.

The XRD analysis was performed with a Rigaku SmartLab SE equipped with a HyPix-400, a semiconductor hybrid pixel array detector and Cu source. The analyses were performed in Bragg-Brentano geometry mode, with 40 kV tube voltage and 50 mA tube current. The diffractograms were processed with a SmartLab II software. The data was compared to the RUFF database (Lafuente et al., 2016) and the COD Database (Gražulis et al., 2009).

The instrument used for GC/MS is a Thermo Focus Gas Chromatographer with DSQ II single quadrupole mass spec. The column currently installed is a Agilent DB5-MS UI column (ID: 0.25 mm, length: 30 m, df: 0.25 µm, Agilent, Santa Clara, CA, USA). Carrier gas: helium. Detector temperature: 280 °C, Injector temperature: 250 °C. It can be used with the PyroLab 2000 Platinum filament pyrolyser (PyroLab, Sweden) attachment or in split/splitless mode. Detection: Total Ion monitoring (TIC). 1 µl of the sample with 1 µl of TMAH was placed on the Pt filament for the py-GC/MS. The inlet temperature to the GC was kept at 250 °C. The helium carrier gas flow rate was 1.5 ml/min with a split flow of 41 ml/min and a split ratio of 27. The MS transfer line was held at 260 °C and the ion source at 250 °C. The pyrolysis chamber was heated to 175 °C, and pyrolysis was carried out at 600 °C for 2 s. This run with Xcalibur™ and PyroLab™ software. The library browser supported NIST MS Version 2.0 (Linstrom & Mallard, 2014).

Valentina Risdonne, PhD student

[v.risdonne@vam.ac.uk](mailto:v.risdonne@vam.ac.uk) / [valentina.risdonne@northumbria.ac.uk](mailto:valentina.risdonne@northumbria.ac.uk)

Victoria and Albert Museum – Northumbria University

PhD project 'Materials and techniques for coating of the nineteenth-century plaster casts'

©V&A Museum

30 September 2020

## Notes

10 September 2018	Sampling	Valentina's PhD Lab book 1, page 115
24 October 2018	Casting	Valentina's PhD Lab book 1, page 133
6 November 2018	Microscopy	Valentina's PhD Lab book 1, page 137
14 October 2019	FT-IR	Valentina's PhD Lab book 1, page 175
3 December 2019	XRD	Valentina's PhD Lab book 2, page 4
18 March 2020	GC/MS	Valentina's PhD Lab book 2, page 50

A full record of analyses is available at <https://doi.org/10.25398/rd.northumbria.14039306>

## References

- Colombini, M. P., & Modugno, F. (2009). *Organic mass spectrometry in art and archaeology*. John Wiley & Sons.
- Gražulis, S., Chateigner, D., Downs, R. T., Yokochi, A. F. T., Quirós, M., Lutterotti, L., Manakova, E., Butkus, J., Moeck, P., & Le Bail, A. (2009). Crystallography Open Database—an open-access collection of crystal structures. *Journal of Applied Crystallography*, 42(4), 726–729.
- Lafuente, B., Downs, R. T., Yang, H., & Stone, N. (2016). The power of databases: the RRUFF project. In *Highlights in mineralogical crystallography* (pp. 1–29). Walter de Gruyter GmbH.
- Linstrom, P. J., & Mallard, W. G. (2014). *NIST Chemistry WebBook, NIST standard reference database number 69, National Institute of Standards and Technology, Gaithersburg MD, 20899*.
- Mills, J., & White, R. (2012). *Organic chemistry of museum objects*. Routledge.
- Price, B. A., Pretzel, B., & Lomax, S. Q. (2009). Infrared and Raman Users Group Spectral Database; 2007 ed. *IRUG: Philadelphia, PA, USA*.





**Northumbria  
University**  
NEWCASTLE

Analysis Report - Valentina Risdonne

Copy of a relief - The Assumption of the Virgin

(REPRO.1890-80)

Initiator: Charlotte Hubbard; Conservation Department

22 September 2020

© Victoria and Albert Museum



## Analysis Report - The Assumption of the Virgin (REPRO.1890-80)

### Contents

Contents.....	278
List of abbreviations.....	278
Summary.....	279
Sample 1.....	282
Sample 2.....	285
Sample 3.....	288
Sample 4.....	291
Experimental.....	295
Notes.....	296
References.....	296

### List of abbreviations

BSE	Back Scattered Electron
EDS	Energy Dispersive Spectrometry
FT-IR	Fourier-Transform Infra-Red
FPA	Focal Plane Array
GC/MS	Gas Chromatography-Mass Spectrometry
OM	Optical Microscopy
PL	Proper Left
PR	Proper Right
py	pyrolysis
SEM	Scanning Electron Microscopy
TMAH	tetramethylammonium hydroxide
UVf	Ultraviolet Fluorescence
VLR	Visible Light Reflectance
XRD	X-ray Diffraction

## Summary

The bulk of the object is made of gypsum plaster, which contains several types of inclusions (including silicates and carbonates). By looking at the results, it is possible to hypothesise that in the surface layer, containing **magnesium, silicon** and **aluminium**, the organic medium is **oxidised colophony** mixed with **drying oil** or just one of these; in the case in which just one of them was present in the medium, the other was then applied as finishing. It is not possible to discriminate, due to the penetration of the coating into the plaster.



Figure 1. The copy of a relief.

The object, '**Copy of a relief - The Assumption of the Virgin (REPRO.1890-80)**' (Figure 1), is a plaster cast of a relief, with a representation of the Assumption of the Virgin (ascending to Heaven, in a mandorla surrounded by angels) executed under Pierre de Chelles (active about 1287; d. 1320). The original was carved in stone between 1296 and 1316, on the north side of the exterior of the apse of Notre Dame, Paris. The cast was made by Messrs Jean Pouzadoux, ca. 1890 and purchased for £12 (300 francs). The cast is now located in Gallery 46A (The Ruddock Family Cast Court), displayed upright. Its dimensions are 152.5x160.0 cm.

Conservation was carried out by the **conservator Sarah Healey** after the sampling procedure hereinafter discussed (**record from June 2019**). The panel appeared structurally

stable without major cracks or losses. There were minor hairline cracks due to compression and uneven distribution of weight, and some superficial losses and a collapsed area (air pocket) on the back of one of the bowing angels (possibly due to the casting method). All figures around the Virgin show cracks/separation between their hands and the mandorla, where the Virgin is, some of these have plaster losses, possibly due to the casting method, where all parts were cast individually and then joined together, and also possibly triggered by the movements of the wooden armature. There are tool-marks around the lower edge and several abrasions due to normal wear and tear on protruding areas. There was a thick layer of dust and ingrained dirt distributed on all surfaces but especially on protruding areas and debris from previous gallery maintenance activities. Superficial dust was removed with a vacuum cleaner and soft brushes. The surfaces were rubbed with a smoke sponge. Ingrained dirt was removed with Anjusil® latex and Blitzfix® with deionised water. Flaking plaster was consolidated with PB44®, paint splashes were inpainted with acrylic paint. The loose parts were consolidated using Paraloid® B44 20% in 50:50 IMS- Acetone. Areas of plaster loss were consolidated using 25%Primal® B60A and retouched using acrylic paint.

Samples from the plaster cast were taken from pre-existing areas of loss to investigate the stratigraphy and the method of manufacture. The samples were analyzed to provide data for the study of the objects of the Cast Courts collection within the PhD project 'Materials and techniques for coating of the nineteenth-century plaster casts'. Details on the experimental procedure are available in the Experimental section of this report. A selection of significant results is shown in the following pages and the full database of analysis is available upon request (<https://doi.org/10.25398/rd.northumbria.14040080>).

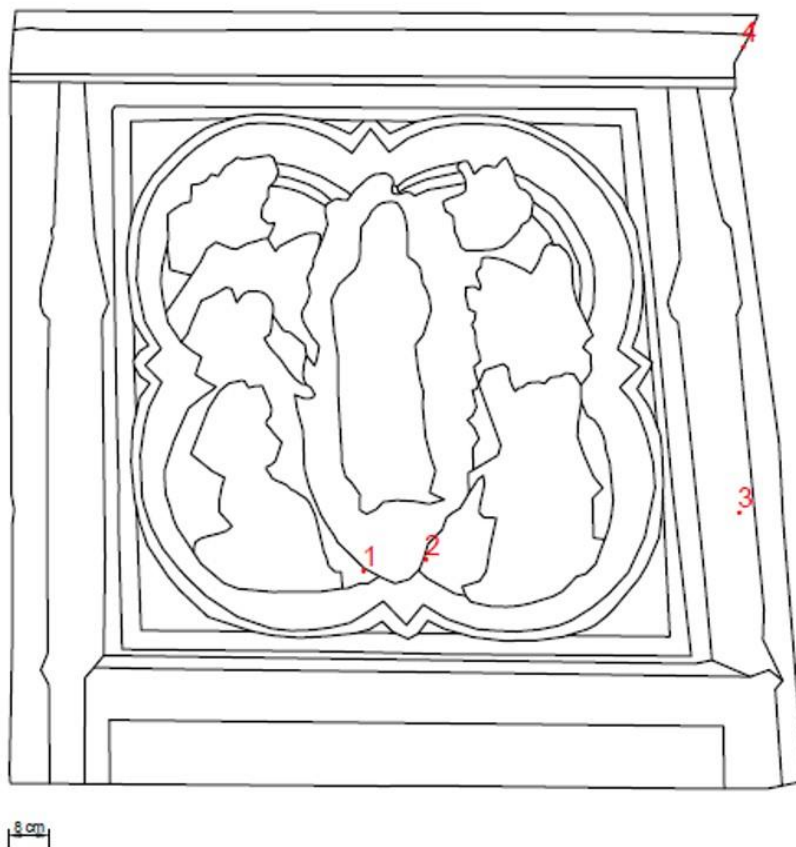


Figure 2. The relief outline with marked sampling sites.

**Sample 1:** fragment taken from an area of loss along a crack, PR side.

**Sample 2:** fragment taken from an area of loss along a crack, PL side.

**Sample 3:** fragment taken from an area of loss on the PL edge.

**Sample 4:** fragment taken from a large area of loss on the PL side, top rim.

The **substrate** (layer 0 in all the samples) is made of gypsum plaster (**calcium sulfate**,  $\text{CaSO}_4$ , confirmed by EDS, XRD and by the peak at  $1600\text{-}1648\text{ cm}^{-1}$  in the FT-IR spectra, which also show the sulfate overtones in the  $2100\text{-}2300\text{ cm}^{-1}$  area). The tabular crystalline structure typical of gypsum plaster can be seen in layer 0 of all the samples and layer 1 of samples 2 (**interface layer**, yellow under visible illumination and possibly consisting of a portion of lower layer soaked with the surface coating(s), showing characteristics of both layers). The BSE image of sample 2 shows that the interface layer appears thicker than layer 0, which resulted in less casting resin penetrated in this layer pores. All the samples show a dark layer (under visible illumination) which contains **silicon** (Si), **magnesium** (Mg) and **aluminium** (Al). **Si**, **Mg** and **Al** are the main elements of the inclusions present in all the layers in all the samples (see EDS mapping). In sample 1 these inclusions also contain **Sr** (**strontium**) and are present in the plaster bulk, but particularly located in layer 1. Samples 3 and 4 show an additional layer (layer 2 in both samples), which fluoresces under UV illumination and can be consistent with a **finishing layer**. This can suggest either that a varnish was applied only on the projection areas or that the varnish was applied on all the surface, but it was differently adsorbed depending on the local variation of porosity.

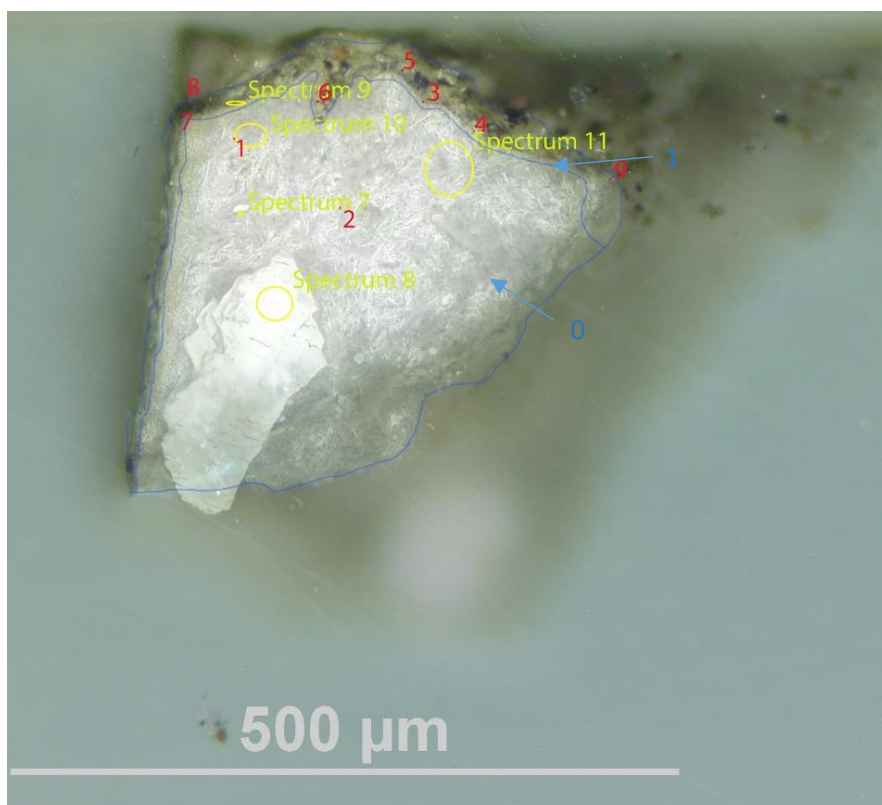
A **wax** or **resin** (FT-IR peaks at  $1000\text{-}1200$  and  $2800\text{-}3000\text{ cm}^{-1}$ ) was detected in all the layers of all the samples, which indicates that either the material was added to the gypsum plaster wet admixture or that the coating has also penetrated in layer 0. The latter seems also possible as the average depth of the samples is about 0.5 mm. The additional presence of a **protein** cannot be excluded by interpreting the FT-IR spectra, due to the complexity of the admixture and also to the crowded pattern of the resins' FT-IR spectra (Price et al., 2009). Py-TMAH-GC/MS analysis of sample 4 suggests that the organic medium in this sample consists of **oxidised colophony** mixed with **drying oil**. Amine fragments were also identified, as in the majority of natural 'non-protein binders' a minority of protein component is present too (Colombini & Modugno, 2009).

**NOTE:** casting in resin the fragments of plaster resulted in the fragments absorbing the resin when in the liquid state. This was visible in the BSE image as well as through the EDS mapping (Tiranti resin and catalyst are mainly made of organic compounds C, H and O). Aluminium (Al) traces are present in all the samples, due to the polishing chemical.

## Sample 1



**Sampling.** This fragment was taken from an area of loss along a crack, PR side.



Left: Overlapped (OM and BSE) cross-section image showing the stratigraphy (blue indicators).

**1. Layer with dark inclusions**

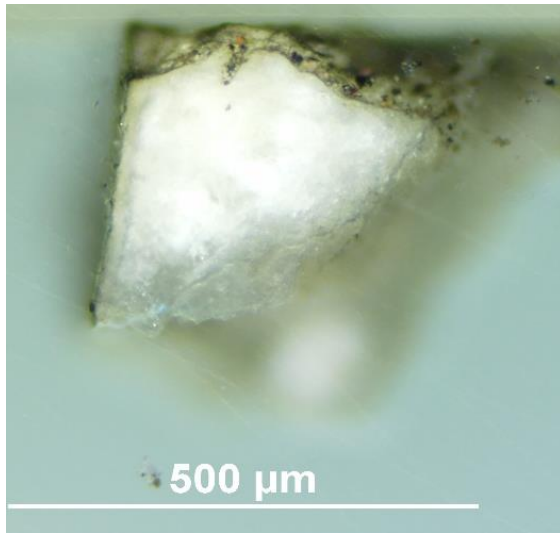
**0. Plaster bulk**

**Analysis spots.**

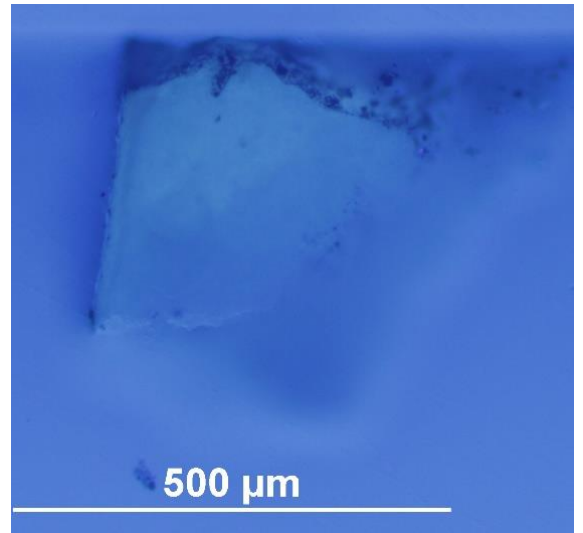
EDS analysis (yellow): Spectra 7-11

FT-IR analysis (red): nos. 1-9

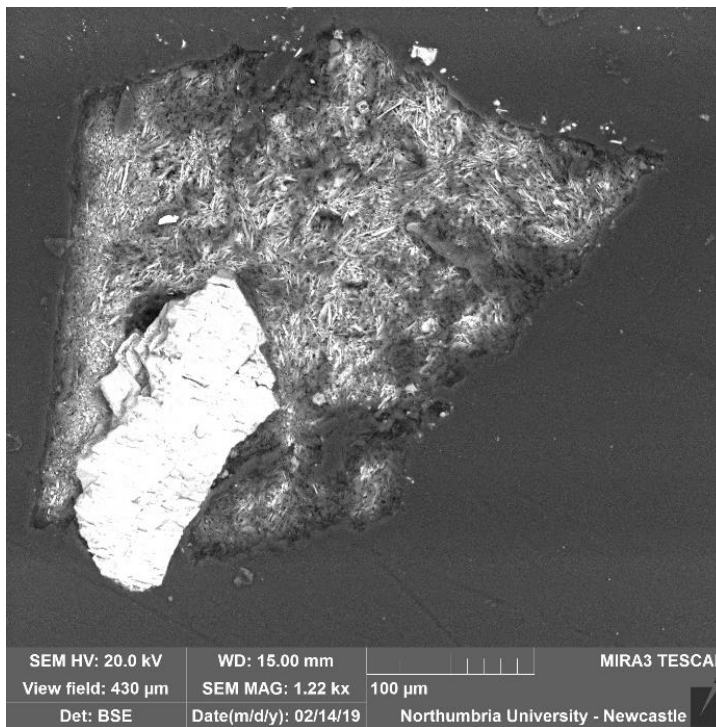
**Summary.** The substrate (layer 0) is made of plaster (**calcium sulfate**,  $\text{CaSO}_4$ , confirmed by EDS and by the peak at  $1600\text{ cm}^{-1}$  and overtones in the FT-IR spectra). Inclusions made of Mg, Sr, Si and Al are present in the plaster bulk but are particularly located in layer 1, which appears dark under visible illumination. The tabular crystalline structure typical of gypsum plaster can be seen in layer 0. A **wax or resin** (FT-IR peaks at  $100\text{-}1200$  and  $2800\text{-}3000\text{ cm}^{-1}$ ) was detected in all the layers.



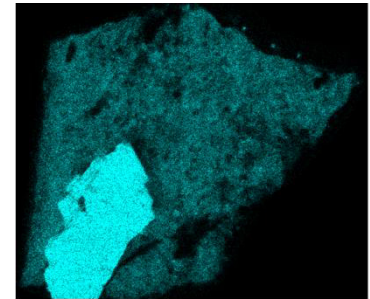
VLR OM (above)



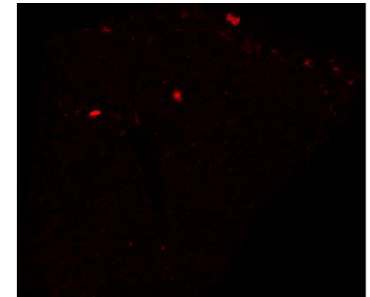
UVfOM (above)



Calcium (Ca)

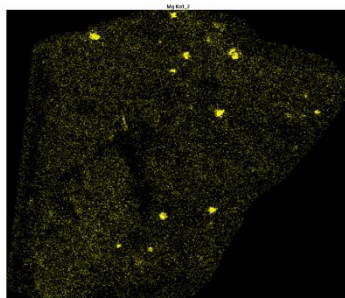


Strontium (Sr)

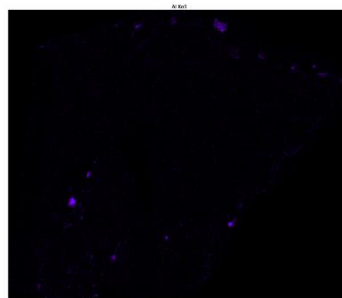


**BSE image (above).** The tabular crystalline structure typical of gypsum plaster can be seen in layer 0, which is made of **calcium sulfate**,  $\text{CaSO}_4$ . The fragment on the bottom PR of the sample is made of **calcium** (Ca, see **EDS mapping** on the top right). **EDS mapping** shows that inclusions made of Sr, Mg, Al and Si are present in all the layers.

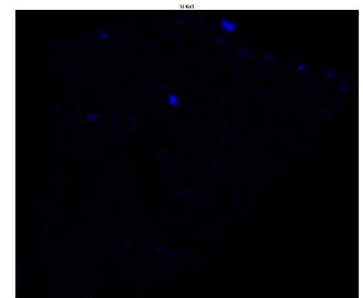
Magnesium (Mg)

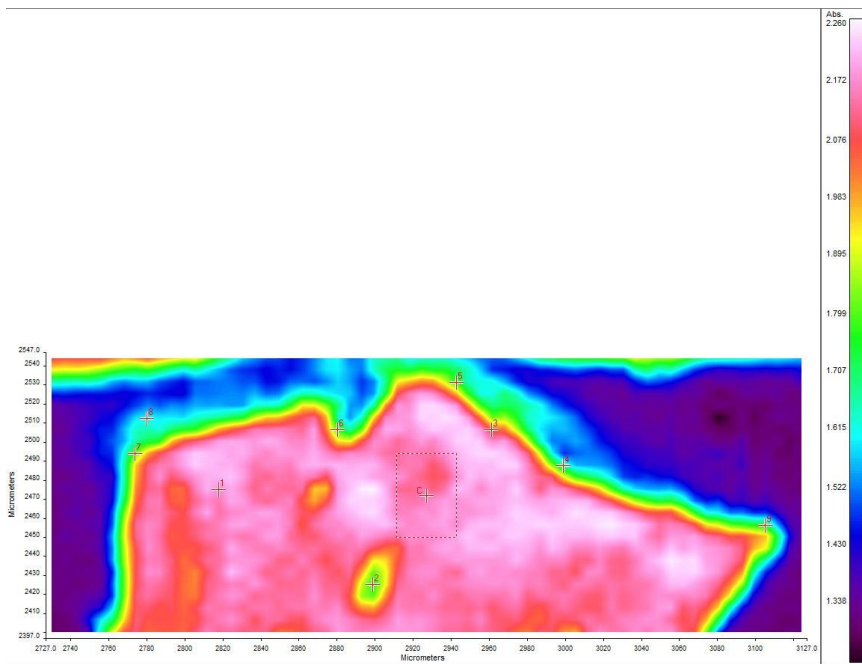
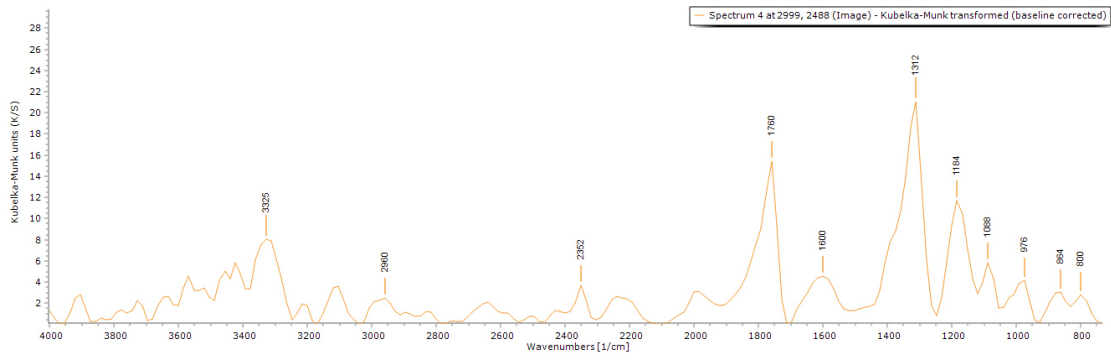


Aluminium (Al)



Silicon (Si)



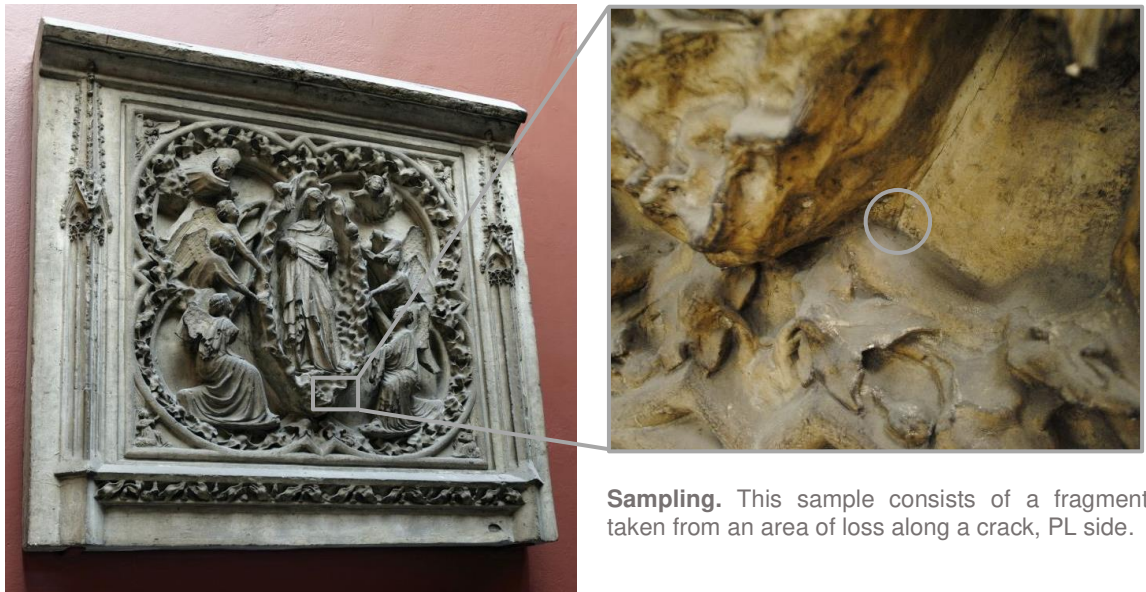


**FT-IR spectrum 4** (above) of layer 1. Peaks for the casting resin ( $1312, 1760\text{ cm}^{-1}$ ), gypsum ( $1600\text{ cm}^{-1}$ , overtone  $2200\text{-}2300\text{ cm}^{-1}$ ) and a wax/resin ( $1000\text{-}1200$  and  $2800\text{-}3000\text{ cm}^{-1}$ ). A summary of the peaks observed in the spectra 1-9 can be seen in the table below.

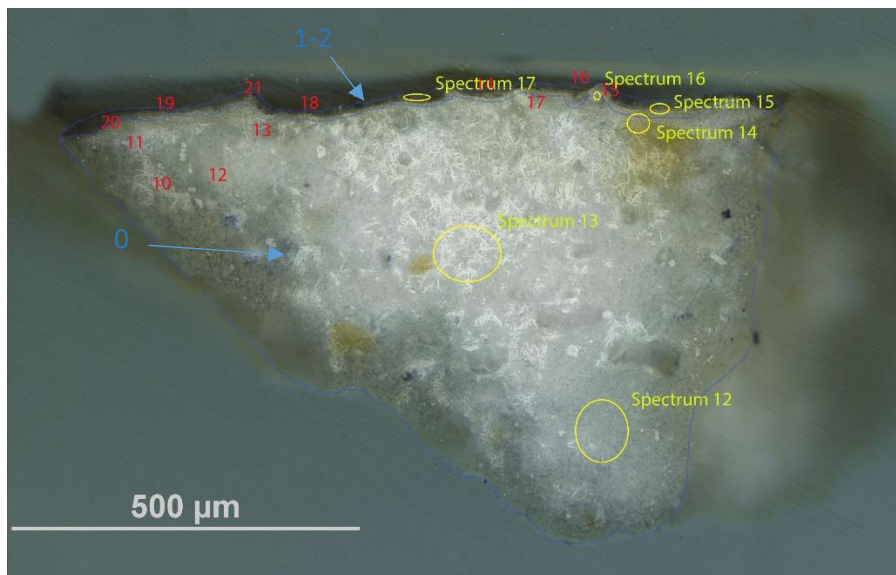
**FT-IR (FPA) image** (left). The different reflectance of the layers can be observed FPA image.

Spectrum	Layer	peaks (cm-1)						
		Casting Resin	Gypsum	Carbonate	Wax/resin	C=O ester carbonyl	SO overtone	Unknown
1	0	1328, 1760	1632		832, 928, 1040, 1232, 1280, 1488, 2896, 2928		2288	
2	0			748	848, 912, 960, 1232, 1568, 1712			
3	1	1328, 1760	1600		992, 1200, 1408, 1472, 2928		2256	
4	1	1312, 1760	1600	800	864, 976, 1088, 1184, 2960		2352	
5	1	1328, 1760	1600		768, 1088, 1200, 1392, 1504, 2832, 2944			
6	1	1312, 1760	1632		848, 1024, 1152, 1504, 2928, 2992		2512	
7	1	1312, 1760			784, 880, 976, 1088, 1152, 1584, 2912			
8	1	1312, 1760	1600		768, 928, 1088, 1152, 2944		2320	
9	1	1312, 1760	1600		784, 1088, 1152		2352	

## Sample 2



**Sampling.** This sample consists of a fragment taken from an area of loss along a crack, PL side.



Left: Overlapped (OM and BSE) cross-section image showing the stratigraphy (blue indicators).

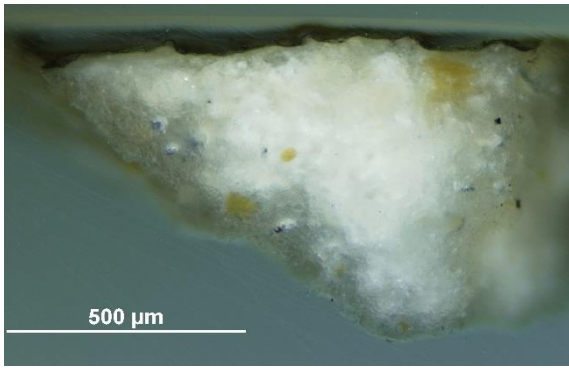
- 2. Dark layer**
- 1. Yellow layer**
- 0. Plaster bulk**

**Analysis spots.**

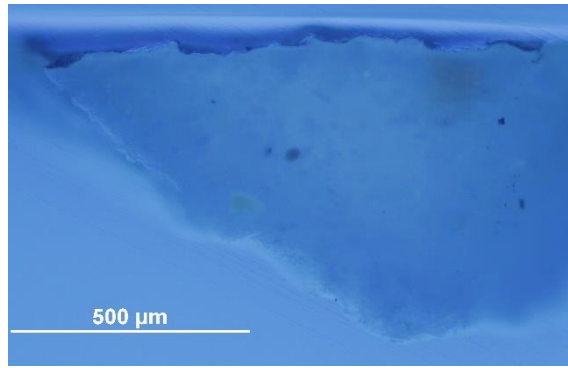
EDS analysis (yellow): Spectra 12-17

FT-IR analysis (red): nos. 10-21

**Summary.** The substrate (layer 0) is made of plaster (**calcium sulfate**,  $\text{CaSO}_4$ , confirmed by EDS, XRD and by the peak at  $1600\text{ cm}^{-1}$  and overtones in the FT-IR spectra). The tabular crystalline structure typical of gypsum plaster can be seen in layers 0 and 1. Layer 1, which appears grey under the microscope, consists of a portion of the lower layer soaked with the surface coating, showing characteristics of both layer 0 and layer 2. The BSE image shows that layer 1 appears thicker than layer 0, which resulted in less casting resin penetrated in this layer pores. Si, Mg and Al are the main elements of the inclusions present in all the layers. A **wax or resin** (FT-IR peaks at  $1200\text{-}1500$  and  $2800\text{-}3000\text{ cm}^{-1}$ ) was detected in all the layers.

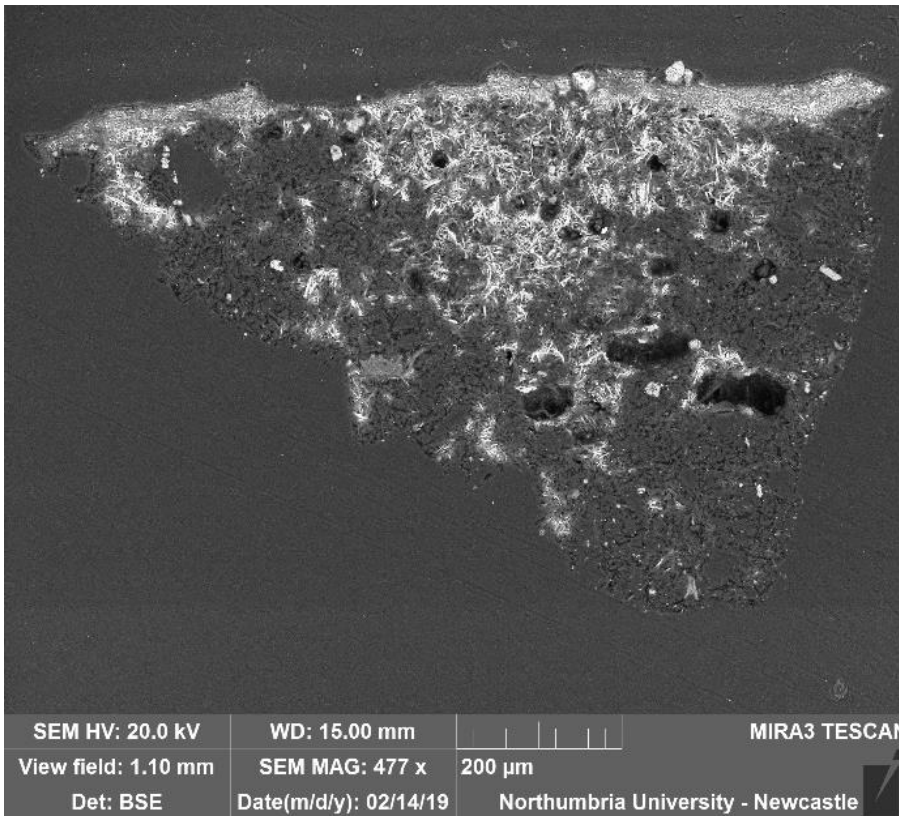


VLR OM (above)



UVf OM (above)

A fragment of this sample was pulverised and analysed by XRD. It was possible to identify the profile of gypsum (calcium sulfate) and the diffractogram was compared to references from the Rigaku SmartLab Database and the most significant peaks were at  $2\theta = 11.63, 20.75, 29.10, 31.10, 33.36, 40.64, 43.30, 48.34, 50.34$ .



BSE image (left).

The tabular crystalline structure typical of gypsum plaster can be seen in layers 0 and 1. Layer 1 seems thicker than layer 0.

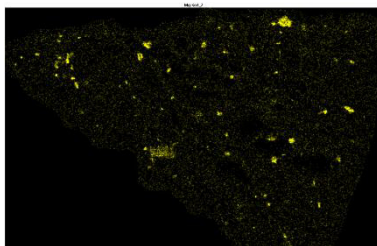
**EDS spectra**

suggest that the sample is made of calcium sulfate (C, O, Ca, S) and that Si, Al, Mg and traces of Na were also present.

**EDS mapping**

(below) shows that Mg, Al and Si inclusions are present in all the layers.

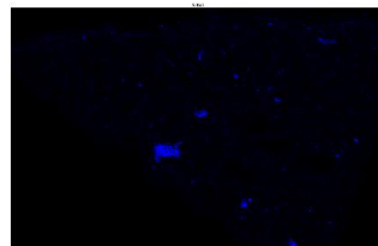
Magnesium (Mg)

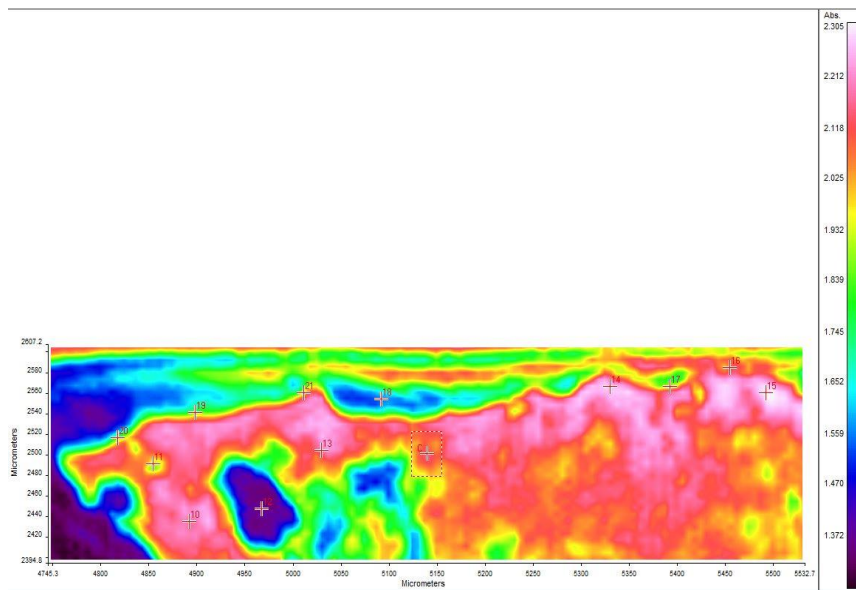
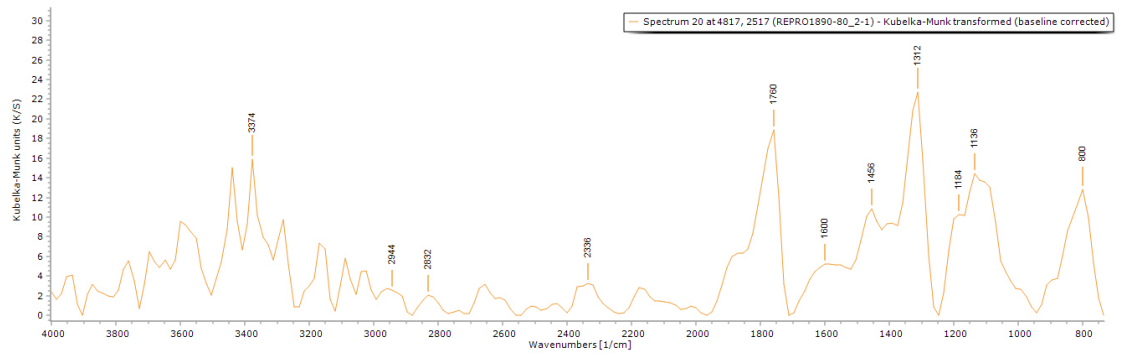


Aluminium (Al)



Silicon (Si)





**FT-IR spectrum 20** (above) of layers 1-2. Peaks for the casting resin (1312, 1760  $\text{cm}^{-1}$ ), gypsum (1600  $\text{cm}^{-1}$ , overtone 2200-2300  $\text{cm}^{-1}$ ) and a wax/resin (1136, 1456, 2800-3000  $\text{cm}^{-1}$ ). A summary of the peaks observed in the spectra 10-21 can be seen in the table below.

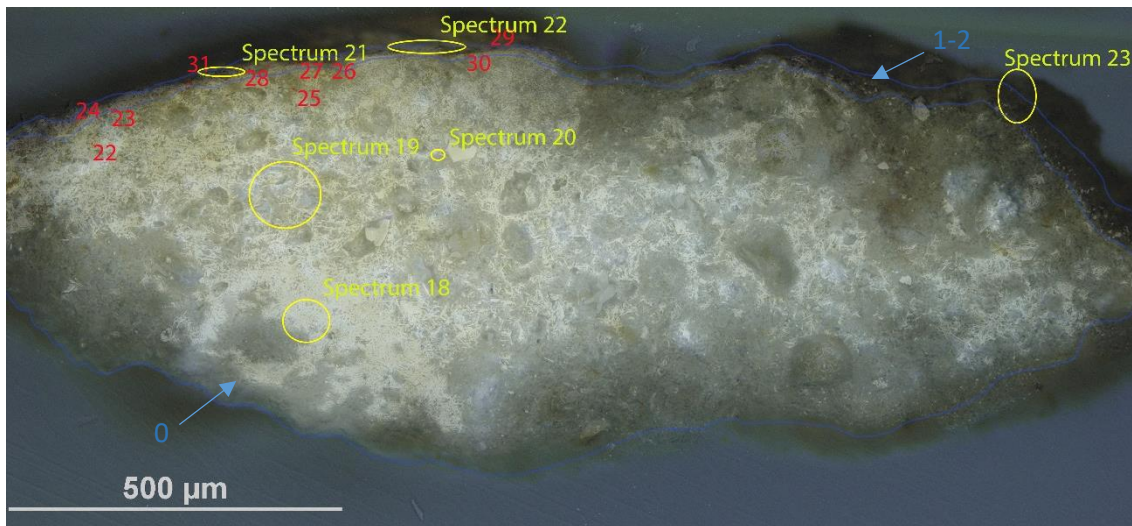
**FT-IR (FPA) image** (left). No clear layer definition can be observed in the FPA image.

Spectrum	Layer	peaks ( $\text{cm}^{-1}$ )						
		Casting Resin	Gypsum	Carbonate	Wax/resin	C=O ester carbonyl	SO overtone	Unknown
10	0	1328, 1760			784, 848, 928, 1008, 1072, 1232, 1296, 1392, 1584, 1680, 2864, 2992		2256	
11	0	1312			752, 880, 1072, 1232, 1456, 2880, 2992		2480	1792
12	0	1312, 1760	1600		784, 864, 992, 1088, 1152, 1488, 2848, 2960		2336	
13	0	1328, 1760	1600	800, 1769	880, 944, 1008, 1088, 1504, 1664, 2880, 2944		2272	
14	1-2	1312, 1760			912, 1088, 1568, 2816, 2880		2192	
15	1-2				768, 1008, 1072, 1296, 1424, 1584, 1792, 2784, 2896, 2976		2288	
16	1-2	1312, 1760			832, 992, 1088, 1136, 1200, 1392, 1504, 1568, 1648, 2816, 2896, 2992		2272	
17	1-2	1312			768, 912, 976, 1088, 1136, 1488, 1648, 1766, 2784, 2864, 2960		2304	
18	1-2	1312, 1760	1600		784, 1088, 1152, 1472, 2800		2352	
19	1-2	1312, 1760	1616	800	880, 992, 1088, 1152, 1456, 2848, 3008		2320	
20	1-2	1312, 1760	1600	800	1136, 1184, 1456, 2832, 2944		2336	
21	1-2	1312, 1760	1600		768, 880, 1088, 1200, 1488, 2880, 2976		2400	

## Sample 3



**Sampling.** This fragment taken from an area of loss on the PL edge.



Above: Overlapped (OM and BSE) cross-section image showing the stratigraphy (blue indicators).

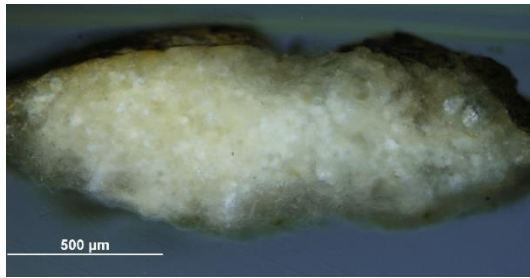
### 2. Varnish

#### 1. Dark layer

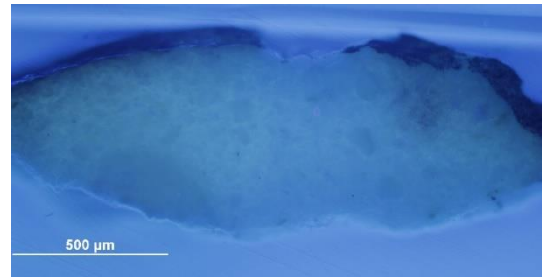
#### 0. Plaster bulk

**Analysis spots.** EDS analysis (yellow): Spectra 18-23; FT-IR analysis (red): nos. 22-31.

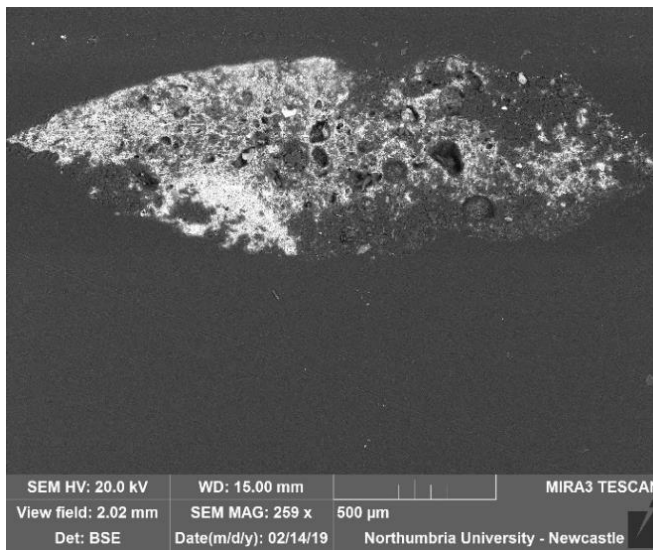
**Summary.** The sample is mostly made of C, O, S and Ca (**calcium sulfate**,  $\text{CaSO}_4$ , confirmed by EDS and by the peak at  $1600\text{-}1616\text{ cm}^{-1}$  in the FT-IR spectra). Al is overall present as used as a polishing agent, but could also, together with Si and Mg be present as part of silicate inclusions, which were observed in all the layers and are mostly localised in layers 1-2 (see EDS mapping). The structure typical of gypsum plaster can be seen in layer 0. Layer 1 appears dark under visible illumination and layer 2 fluoresces under UV illumination. A **wax or resin** is suggested by FT-IR (peaks at  $1000\text{-}1200$  and  $2800\text{-}3000\text{ cm}^{-1}$ ). Layer 2, fluorescing under UV illumination, might be consistent with a finishing varnish.



VLR OM (above)

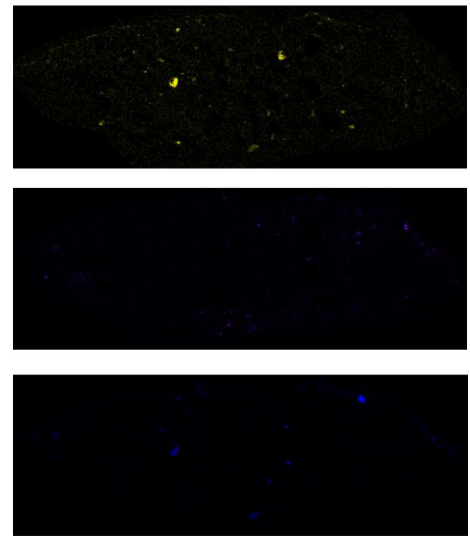


UVf OM (above)

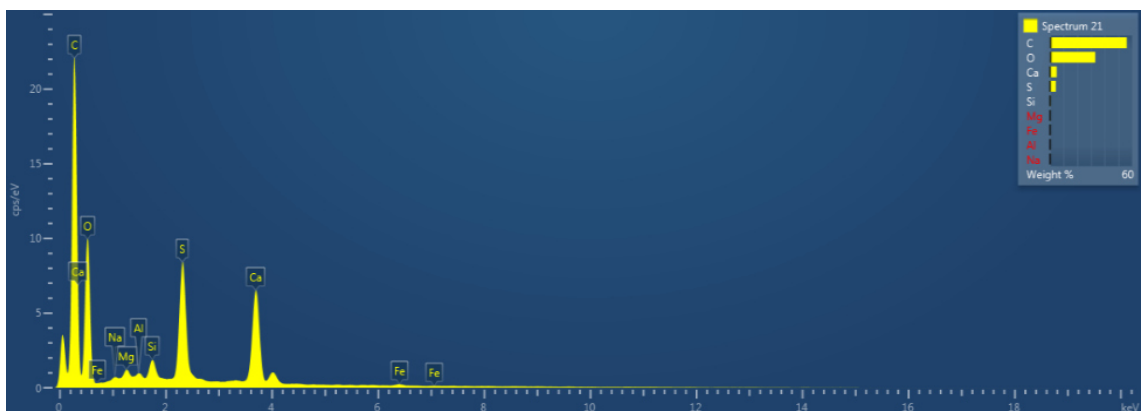


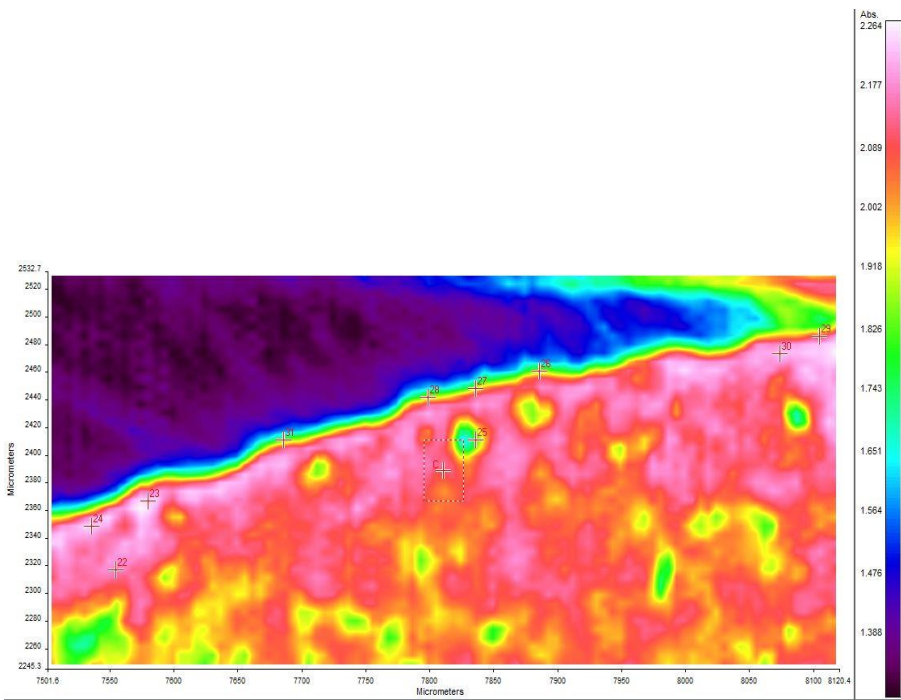
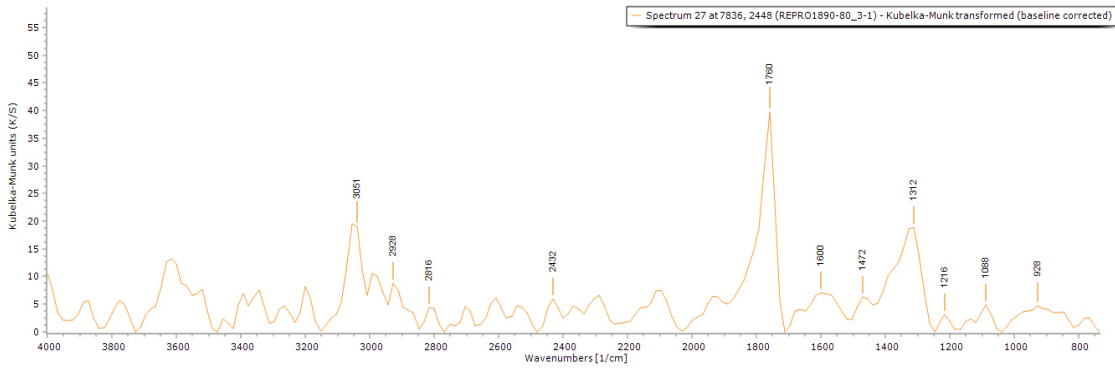
**BSE image** (above). The tabular crystalline structure typical of gypsum plaster can be seen in layers 0 and 1.

Calcium sulfate ( $\text{CaSO}_4$ ) and Al, Si and Mg were detected in all the layers. Traces of Fe and Sr were also detected in layers 1-2 (see **spectrum 21** below).



**EDS mapping** (above) shows that inclusions made of **magnesium** (Mg, top), **aluminium** (Al, middle) and **silicon** (Si, bottom) were detected in all the layers, but mostly localised in layer 2.





**FT-IR spectrum 27** (above) of layer 1. Peaks for the casting resin (1312, 1760  $\text{cm}^{-1}$ ), gypsum (1600  $\text{cm}^{-1}$ ), and a wax/resin (1472  $\text{cm}^{-1}$  and 2800-3000  $\text{cm}^{-1}$ ). A summary of the peaks observed in the spectra 22-31 can be seen in the table below.

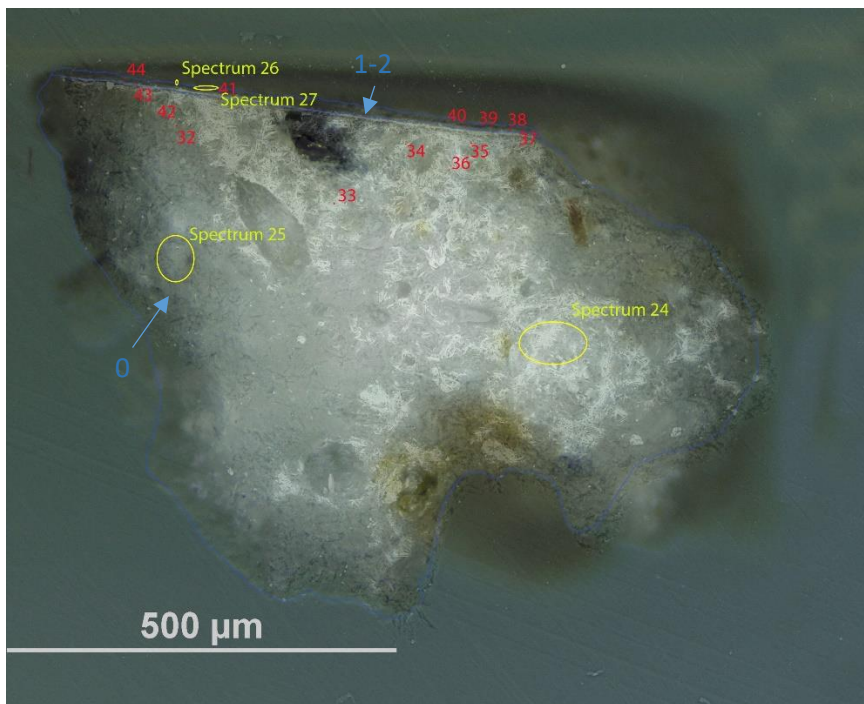
**FT-IR (FPA) image** (left). Indication of different reflectance of the layers can be observed in the Focal FPA image.

Spectrum	Layer	peaks ( $\text{cm}^{-1}$ )						
		Casting Resin	Gypsum	Carbonate	Wax/resin	C=O ester carbonyl	SO overtone	Unknown
22	0	1312, 1760	1600		864, 992, 1248, 1472, 1664, 2784, 2992		2192	1824
23	1	1312, 1760	1600		880, 992, 1488, 2784, 2992		2176	
24	1	1328, 1760	1600		768, 992, 1088, 1248, 1408, 1456, 1488, 2896, 2976		2270	
25	0	1328, 1760	1600		1232, 1376, 1504, 2864, 2976		2320	
26	1	1312, 1760	1600		912, 1008, 1088, 1184, 1472, 1520, 2800, 2921		2320	
27	1	1312, 1760	1600		768, 928, 1088, 1216, 1472, 2816, 2928		2288	
28	1	1328, 1760	1600		832, 1088, 2832, 2944		2304	
29	1	1312, 1760	1648		768, 992, 1088, 1200, 1392, 1488, 2880, 2944		2320	
30	1	1344, 1760			848, 1088, 1264, 1488, 1584, 1664, 2848, 2972		2288	
31	1	1312, 1760	1616		784, 992, 1072, 1184, 1520, 2832, 2989		2352	

## Sample 4



**Sampling.** This fragment taken from a large area of loss on the PL side, top rim.



Left: Overlapped (OM and BSE) cross-section image showing the stratigraphy (blue indicators).

### 2. Varnish layer

#### 1. Dark layer

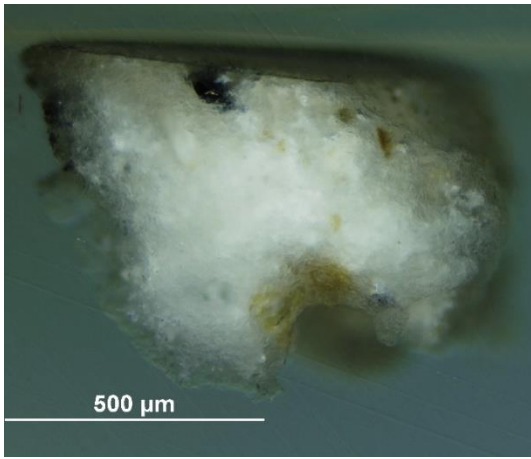
#### 0. Plaster bulk

### Analysis spots.

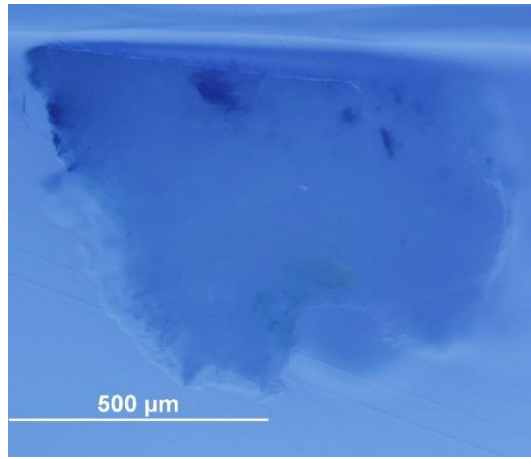
EDS analysis (yellow):  
Spectra 24-27

FT-IR analysis (red):  
nos. 32-44

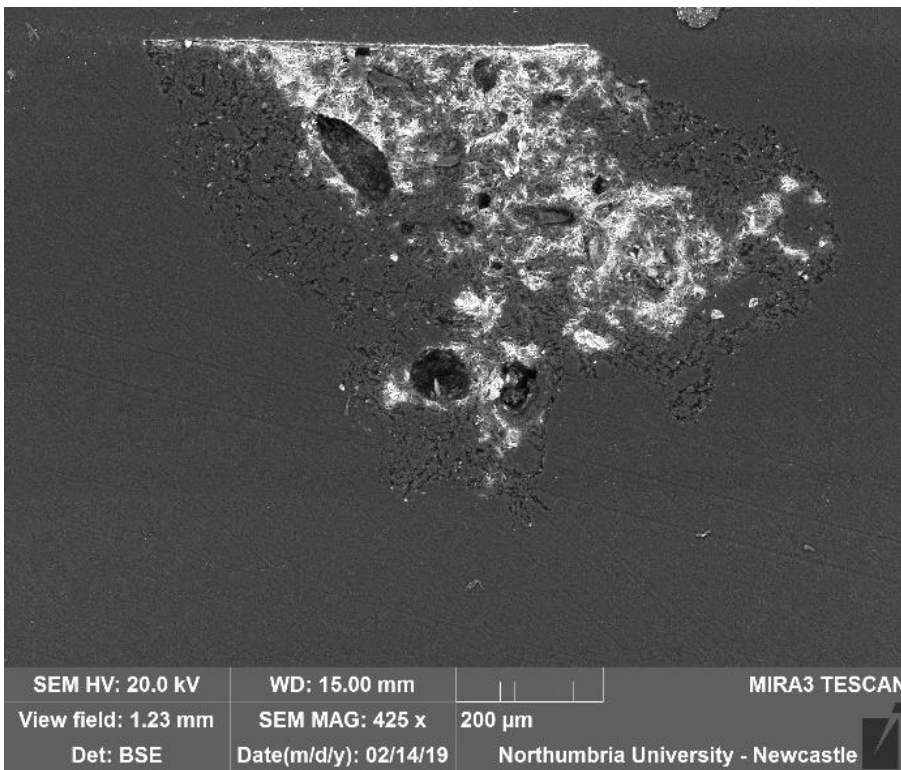
**Summary.** The sample is mostly made of C, O, S and Ca (**calcium sulfate**,  $\text{CaSO}_4$ , confirmed by EDS and by the peak at  $1600\text{-}1632\text{ cm}^{-1}$  in the FT-IR spectra). Al is overall present as used as a polishing agent, but could also, together with Si, K and Mg be present as part of silicate inclusions, which are present in all the layers and mostly localised in layer 1 (see EDS mapping). Layer 1 appears sark under visible illumination and layer 2 fluoresces under UV illumination. Traces of Pb, Cl, Na, P and Fe were also detected in the utmost layers. The structure typical of gypsum plaster can be seen in layer 0. A **wax or resin** is suggested by FT-IR (peaks at  $1000\text{-}1200$  and  $2800\text{-}3000\text{ cm}^{-1}$ ). py-TMAH-GC/MS shows markers characteristic of **oxidised colophony** mixed with **drying oil**. Amine fragments were also identified, as in the majority of natural 'non-protein binders' a minority of protein component is present too (Colombini & Modugno, 2009).



VLR OM (above)



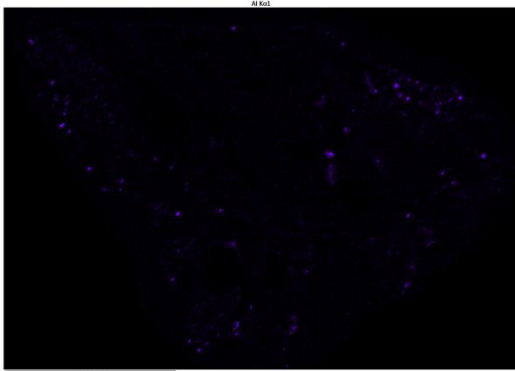
UVfOM (above)



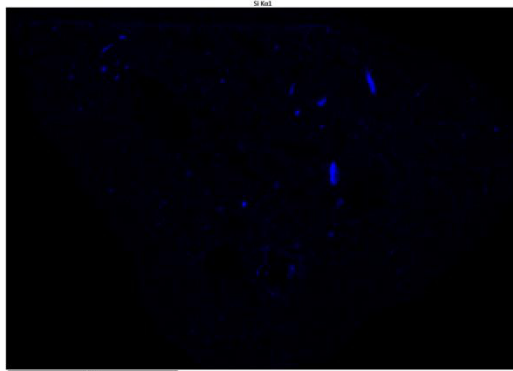
**BSE image (left).** The tabular crystalline structure typical of gypsum plaster can be seen in layer 0. Layer 1 consists mostly of Al and Si, which can be seen in the **EDS mapping (below)**.

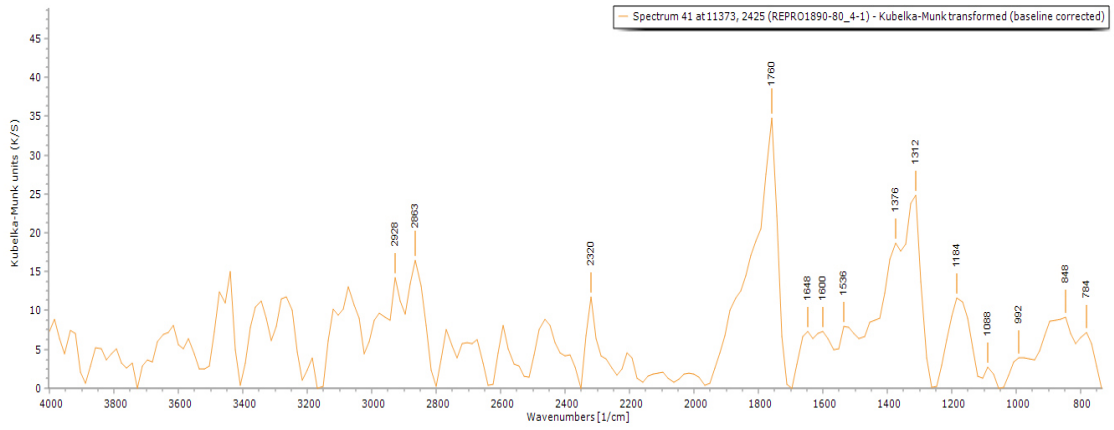
**EDS spectra** indicate that layers 0 and 1-2 consist of C, O, Ca, S, Al and Si. Traces of Pb, Cl, K, Na, P, and Fe were also detected in layers 1-2.

Aluminium (Al)

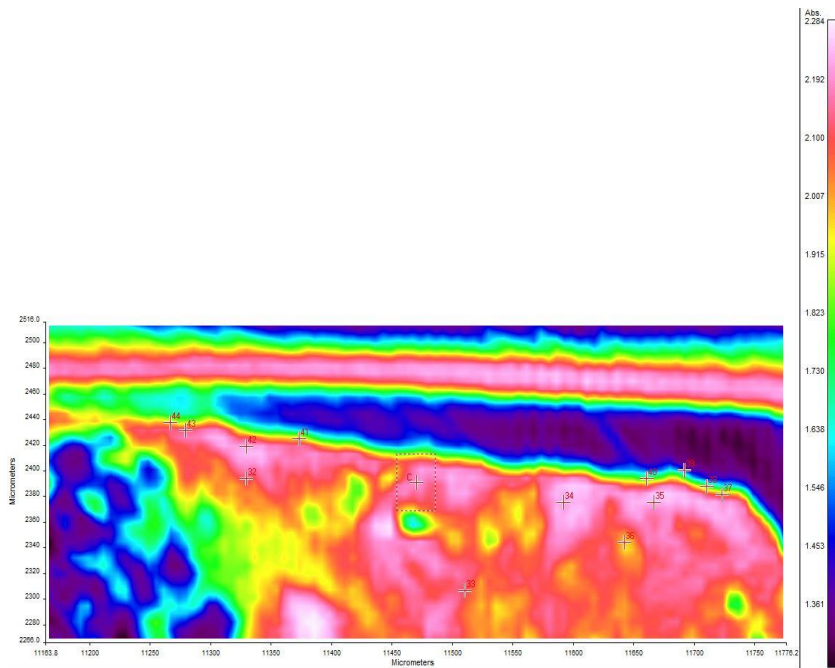


Silicon (Si)



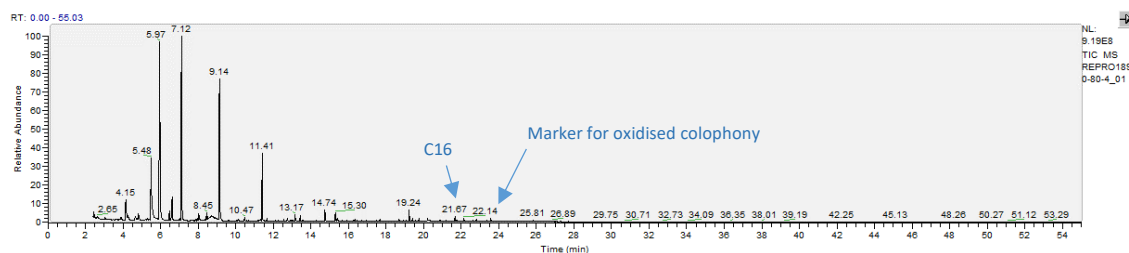


**FT-IR spectrum 41** (above) of layers 1-2. Peaks for the casting resin (1312, 1760  $\text{cm}^{-1}$ ), gypsum (1600  $\text{cm}^{-1}$ , overtone 2200-2300  $\text{cm}^{-1}$ ) and a wax/resin (1100-1500, 2863 and 2928  $\text{cm}^{-1}$ ). A summary of the peaks observed in the spectra 32-44 can be seen in the table below.



**FT-IR (FPA) image** (left). No clear layer definition can be observed in the FPA image.

Spectrum	Layer	peaks ( $\text{cm}^{-1}$ )							
		Casting Resin	Gypsum	Carbonate	Wax/resin	C=O ester carbonyl	SO overtone	Unknown	
32	0	1344, 1760	1632		848, 960, 1040, 1232, 1488, 2864, 2960			2224	
33	0			1776	752, 848, 992, 1056, 1280, 1376, 1568, 2880, 2960			2176	
34	0	1328, 1760	1616		816, 960, 1072, 1216, 1392, 1472, 1536, 1680, 2816, 2928			2218	
35	0	1312, 1760	1600		800, 944, 1056, 1232, 1360, 1392, 1472, 1664, 2912			2243	
36	0	1312	1632		752, 912, 1040, 1232, 1472, 2912	1744			
37	1-2	1312, 1760	1616		784, 1104, 1168, 1376, 1488, 2864, 2976			2320, 1824	
38	1-2	1312, 1760	1600	800	912, 1088, 1168, 1408, 2816, 2880			2336	
39	1-2	1312, 1760	1616		896, 1088, 1152, 1472, 1520			2336	
40	1-2	1312, 1760	1632	800	944, 1152, 1472, 2976			2336	
41	1-2	1312, 1760	1600		784, 848, 992, 1088, 1184, 1376, 1536, 1648, 2863, 2920			2320	
42	0	1328, 1760	1600		752, 960, 1088, 1216, 1296, 1408, 1456, 2880			2240	
43	1-2	1328, 1760			784, 928, 1024, 1072, 1200, 1392, 1440, 1568, 2848, 2948			2272	
44	1-2	1312, 1760			768, 880, 928, 992, 1088, 1184, 1488, 1584, 1648, 2800, 2896				



RT	m/z	Assignment	Formula
4.15	45(100), 58(12), 74(65)	Acetaldehyde, methoxy-	C3H6O2
5.48	42(9), 58(100), 88(3), 116(4)	1,2-Ethanediamine, N'-ethyl-N,N-dimethyl-	C6H16N2
5.97	42(13), 58(100), 117(17)	1,2-Ethanediamine, N'-ethyl-N,N-dimethyl-	C6H16N2
6.48	45(29), 58(54), 66(24), 79(20), 88(6), 95(100), 125(7)	Sulfuric acid, dimethyl ester	C2H6O4S
6.62	58(13), 65(16), 79(100), 95(11), 109(7), 128(5)	Methanesulfonic acid, methyl ester	C2H6O3S
7.12	44(7), 56(7), 72(100), 116(2), 131(2)	N,N'-Diisopropylethylenediamine	C8H20N2
9.14	44(100), 57(19), 86(65), 128(49)	Unidentified amine fragment	
11.41	42(6), 58(100), 70(9), 116(6)	1,2-Ethanediamine, N'-ethyl-N,N-dimethyl-	C6H16N2
11.66	42(34), 58(100), 72(20), 98(55), 127(63), 139(5)	FA fragment	
12.25	42(34), 58(100), 79(13), 91(22), 113(12), 135(55), 150(40)	Phenol, 2-methyl-5-(1-methylethyl)-	C10H14O
13.17	58(27), 88(22), 97(32), 116(40), 130(100), 152(5)	Unidentified amine fragment	
13.44	42(10), 58(21), 72(100), 101(7), 115(3), 130(6)	Unidentified amine fragment	
14.74	58(14), 84(7), 116(100), 139(15), 173(4)	Unidentified amine fragment	
15.3	42(6), 58(13), 116(100), 149(5), 173(4)	Unidentified amine fragment	
15.42	45(34), 58(100), 75(32), 85(43), 115(26), 119(79), 149(77), 165(58), 180(49)	FA fragment	
16.35	44(12), 58(39), 77(19), 92(6), 105(5), 133(6), 149(5), 163(100), 194(5)	Dimethyl phthalate	C10H10O4
17.5	44(32), 58(100), 74(20), 83(20), 111(17), 152(23), 192(10)	Nonanedioic acid, monomethyl ester	C10H18O4
18.7	44(37), 58(100), 77(17), 91(20), 105(5), 115(30), 149(20), 161(35), 175(17), 190(53), 224(5)	Unidentified terpenoid fragment	
19.24	45(81), 58(38), 75(100), 85(81), 101(68), 115(22), 139(25), 152(15), 161(35), 170(5), 183(20), 215(5), 228(5), 260(5)	Unidentified terpenoid fragment	
19.4	45(53), 58(100), 75(19), 85(29), 91(17), 109(25), 122(17), 137(40), 161(5), 182(27), 189(5), 204(5), 236(5)	Unidentified terpenoid fragment	
19.77	45(77), 58(100), 71(61), 84(41), 109(22), 116(31), 139(16), 152(5), 183(5), 193(5), 214(5), 228(5)	Unidentified terpenoid fragment	
21.67	58(46), 74(100), 87(65), 115(9), 129(9), 143(24), 161(10), 199(5), 227(11), 239(5), 270(5)	methyl palmitate	C17H34O2
22.8	45(51), 58(100), 75(29), 91(17), 117(16), 149(15), 163(14), 205(5), 237(5), 251(5), 270(5), 299(5), 331(5)	Unidentified oxidised tricyclic diterpenoid molecules	Marker for aged colophony
23.58	44(31), 58(74), 74(100), 87(60), 129(5), 143(24), 199(12), 241(5), 255(12), 298(5)	methyl stearate	C19H38O2
25.81	58(100), 71(27), 95(19), 109(10), 137(13), 159(12), 193(5), 207(19), 281(5)	Unidentified terpenoid fragment	

RT = retention time, m/z = mass/charge ratio

**Py-TMAH-GC/MS chromatogram** (top and described in the table above) shows small fragments due to derivatization (from  $t = 4.15$  to  $11.41$  min) and markers characteristic of **colophony** (several terpenoid fragments and marker at  $t = 22.80$  min) (Colombini & Modugno, 2009; Mills & White, 2012). The presence of **methyl azelate** ( $t = 17.50$ ), **methyl palmitate** ( $t = 21.67$ ) and **stearate** ( $t = 23.58$ ) suggests that the resin has been mixed with a **drying oil** ( $A/P = 0.92$ ,  $P/S = 1.75$ ), possibly **linseed oil**. Amine fragments were also identified, as in the majority of natural 'non-protein binders' a minority of protein component is present too (Colombini & Modugno, 2009).

## Experimental

The object was observed, and its conditions were documented. Samples from selected areas were taken by Valentina Risdonne. When possible, each sample was split into two parts: one fragment was embedded in polyester resin (Tiranti clear casting resin), polished and analysed under an optical microscope and the other was put aside for py-TMAH-GC/MS and XRD analysis.

The optical microscopy was performed with an Olympus BX51 Metallurgical Microscope equipped with four objectives (magnification of x5, x20, x50 and x100), and an x10 eyepiece. In many instances, a small amount of white spirit was applied on the surface of the cross-section to improve the saturation under the microscope. The microscope is equipped with a 6-cube filter turret which allows operating the system in reflected visible light (brightfield and darkfield mode) and reflected UV light (365 nm) using a 100 W mercury burner.

The SEM-EDS analysis was performed with a field emission TESCAN MIRA 3 with gigantic chamber. The SEM is equipped with: secondary electron detector (SE), secondary electron in-beam detector (In-beam SE), back-scatter detector (BSE), back-scatter in-beam detector (In-beam BSE), cathodoluminescence detector (without wavelength detection) (CL), plasma chamber/sample cleaner and software Alicona 3D imaging. For the EDS analytical part, it has an Oxford Instruments setup: Software: AztecEnergy, X-ray detector X-Max 150 mm<sup>2</sup> and X-ray detector X-Max Extreme, low energy detector for thin films, high resolution and low voltage. The samples were analysed by SEM-EDS Low Vacuum Mode (10-15 Pa). EDS Mapping and data processing were performed with Aztec Oxford software.

A Perkin Elmer Frontier FT-IR spectrometer (350 cm<sup>-1</sup> at the best resolution of 0.4 cm<sup>-1</sup>) was used, equipped with a germanium crystal for ATR measurements and combined with a Spectrum Spotlight 400 FT-IR microscope equipped with a 16×1 pixel linear mercury cadmium telluride (MCT) array detector standard with InGaAs array option for optimised NIR imaging. Spectral images from sample areas are possible at pixel resolutions of 6.25, 25, or 50 microns. The Perkin Elmer ATR imaging accessory consists of a germanium crystal for ATR imaging. These run with Perkin Elmer Spectrum 10™ software and with SpectrumIMAGE™ software. Baseline and Kubelka-Munk corrections were applied to the raw data acquired in diffuse reflectance.

The XRD analyses were performed with a Rigaku SmartLab SE equipped with a HyPix-400, a semiconductor hybrid pixel array detector and Cu source. The analyses were performed in Bragg-Brentano geometry mode, with 40 kV tube voltage and 50 mA tube current. The diffractograms were processed with a SmartLab II software. The data was compared to the RUFF database (Lafuente et al., 2016) and COD Database (Gražulis et al., 2009).

The instrument used for GC/MS is a Thermo Focus Gas Chromatographer with DSQ II single quadrupole mass spec. The column currently installed is a Agilent DB5-MS UI column (ID: 0.25 mm, length: 30 m, df: 0.25 µm, Agilent, Santa Clara, CA, USA). Carrier gas: helium. Detector temperature: 280 °C, Injector temperature: 250 °C. It can be used with the PyroLab 2000 Platinum filament pyrolyser (PyroLab, Sweden) attachment or in split/splitless mode. Detection: Total Ion monitoring (TIC). 1 µl of the sample with 1 µl of TMAH was placed on the Pt filament for the py-GC/MS. The inlet temperature to the GC was kept at 250 °C. The helium carrier gas flow rate was 1.5 ml/min with a split flow of 41 ml/min and a split ratio of 27. The MS transfer line was held at 260 °C and the ion source at 250 °C. The pyrolysis chamber was heated to 175 °C, and pyrolysis was carried out at 600 °C for 2 s. This run with Xcalibur™ and PyroLab™ software. The library browser supported NIST MS Version 2.0 (Linstrom & Mallard, 2014).

Valentina Risdonne, PhD student

[v.risdonne@vam.ac.uk](mailto:v.risdonne@vam.ac.uk) / [valentina.risdonne@northumbria.ac.uk](mailto:valentina.risdonne@northumbria.ac.uk)

Victoria and Albert Museum – Northumbria University

PhD project 'Materials and techniques for coating of the nineteenth-century plaster casts'

©V&A Museum

22 September 2020

## Notes

18 January 2019	Sampling	Valentina's PhD Lab book 1, page 149
29 January 2019	Casting	Valentina's PhD Lab book 1, page 158
5 February 2019	Microscopy	Valentina's PhD Lab book 1, page 163
14 October 2019	FT-IR	Valentina's PhD Lab book 1, page 175
3 December 2019	XRD	Valentina's PhD Lab book 2, page 4
18 March 2020	GC/MS	Valentina's PhD Lab book 2, page 50

A full record of analysis is available at <https://doi.org/10.25398/rd.northumbria.14040080>

## References

- Colombini, M. P., & Modugno, F. (2009). *Organic mass spectrometry in art and archaeology*. John Wiley & Sons.
- Gražulis, S., Chateigner, D., Downs, R. T., Yokochi, A. F. T., Quirós, M., Lutterotti, L., Manakova, E., Butkus, J., Moeck, P., & Le Bail, A. (2009). Crystallography Open Database—an open-access collection of crystal structures. *Journal of Applied Crystallography*, 42(4), 726–729.
- Lafuente, B., Downs, R. T., Yang, H., & Stone, N. (2016). The power of databases: the RRUFF project. In *Highlights in mineralogical crystallography* (pp. 1–29). Walter de Gruyter GmbH.
- Linstrom, P. J., & Mallard, W. G. (2014). *NIST Chemistry WebBook, NIST standard reference database number 69, National Institute of Standards and Technology, Gaithersburg MD, 20899*.
- Mills, J., & White, R. (2012). *Organic chemistry of museum objects*. Routledge.
- Price, B. A., Pretzel, B., & Lomax, S. Q. (2009). Infrared and Raman Users Group Spectral Database; 2007 ed. *IRUG: Philadelphia, PA, USA*.



**Northumbria  
University**  
NEWCASTLE

Analysis Report - Valentina Risdonne

Copy of a relief - The Coronation of the Virgin

(REPRO.1890-81)

Initiator: Charlotte Hubbard; Conservation Department

18 September 2020

© Victoria and Albert Museum



## Analysis Report - The Coronation of the Virgin (REPRO.1890-81)

### Contents

Contents.....	298
List of abbreviations.....	298
Summary.....	299
Sample 1.....	302
Sample 2.....	305
Sample 3.....	308
Sample 4.....	311
Experimental.....	315
Notes.....	316
References.....	316

### List of abbreviations

BSE	Back Scattered Electron
EDS	Energy Dispersive Spectrometry
FT-IR	Fourier-Transform Infra-Red
FPA	Focal Plane Array
GC/MS	Gas Chromatography-Mass Spectrometry
OM	Optical Microscopy
PL	Proper Left
PR	Proper Right
py	pyrolysis
SEM	Scanning Electron Microscopy
TMAH	tetramethylammonium hydroxide
UVf	Ultraviolet Fluorescence
VLR	Visible Light Reflectance
XRD	X-ray Diffraction
XRF	X-ray Fluorescence

## Summary

The bulk of the object is made of gypsum plaster, which contains several types of inclusions (including silicates and carbonates). By looking at the results, it is possible to hypothesise that in the surface layer, containing **magnesium**, **silicon** and **aluminium**, the organic medium is **shellac** and **linseed oil** or just one of these; in the case in which just one of them was present in the medium, the other was then applied as finishing. It is not possible to discriminate, due to the penetration of the coating into the plaster.



Figure 1. The copy of a relief.

The object, '**Copy of a relief - The Coronation of the Virgin (REPRO.1890-81)**' (Figure 1), is a plaster cast of a relief, with a representation of the Coronation of the Virgin executed under Pierre de Chelles (active about 1287; d. 1320). The original was carved in stone between 1296 and 1316, on the north side of the exterior of the apse of Notre Dame, Paris. The cast was made by Messrs Jean Pouzadoux, ca. 1890 and purchased for £12 (300 francs). The cast is now located in Gallery 46A (The Ruddock Family Cast Court), displayed upright. Its dimensions are 155.0x135.0 cm.

Conservation was carried out by the **conservator Sarah Healey** after the sampling procedure hereinafter discussed (**record from May 2019**). Alongside the treatment, two samples of paint from the front and a sample of plaster with horsehair at the back were

taken to identify lead or arsenic or any other hazardous materials present, or anything else that will be useful to identify before treatment. **XRF** analysis (in-house at the V&A by **Dr Lucia Burgio**) of samples showed no hazardous materials.

Samples from the plaster cast were taken from pre-existing areas of loss to investigate the stratigraphy and the method of manufacture (Figure 2). The samples were analyzed to provide data for the study of the objects of the Cast Courts collection within the PhD project 'Materials and techniques for coating of the nineteenth-century plaster casts'. Details on the experimental procedure are available in the Experimental section of this report. A selection of significant results is shown in the following pages and the relevant database of analysis (<https://doi.org/10.25398/rd.northumbria.14040182>).

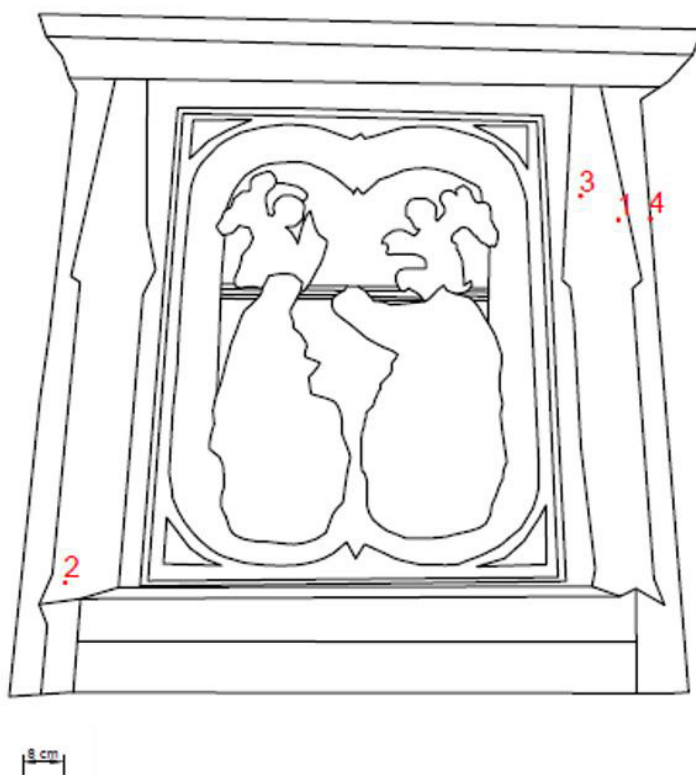


Figure 2. The relief outline with marked sampling sites.

**Sample 1:** fragment taken from an area of loss on the PL architectural element.

**Sample 2:** fragment taken from an area of loss on the PR, from the frame.

**Sample 3:** fragment taken from an area of loss on the PL, from the frame.

**Sample 4:** fragment taken from an area of loss on the PL, from the frame.

The **substrate** (layer 0 in all the samples) is made of gypsum plaster (**calcium sulfate**,  $\text{CaSO}_4$ , confirmed by EDS and by the peak at  $1600\text{-}1648\text{ cm}^{-1}$  in the FT-IR spectra, which also show the sulfate overtones in the  $2100\text{-}2300\text{ cm}^{-1}$  area). Al is overall present as used as a polishing agent, but could also, together with Mg and Si be present as part of **silicate** inclusions (confirmed EDS mapping). **Magnesium** (Mg) is present in the bulk of all the samples, possibly as an exchangeable element in the sulphate variety  $\text{MgSO}_4$  (more or less hydrated) (Cox et al., 1974). The crystalline structure typical of gypsum plaster (called *tabular* in mineralogy, see BSE images) can be seen in the bulk and the interface layer. The

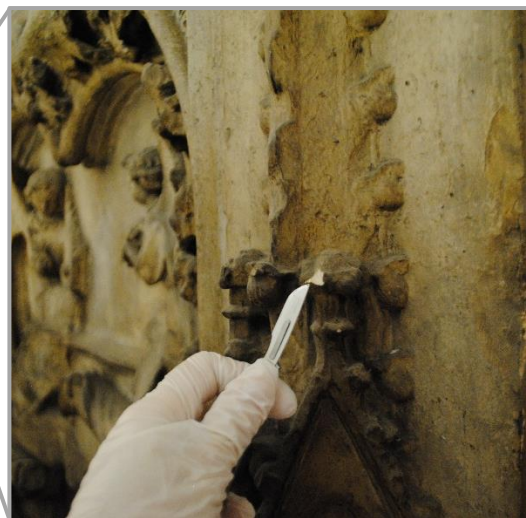
**interface layer** (layer 1 in all the samples) appears yellow under visible illumination and might consist of a portion of lower layer soaked with the surface coating(s), showing characteristics of both layers.

EDS mapping shows that in all the samples **layer 2**, dark under visible illumination, consists of **magnesium, silicon** and **aluminium**. Traces of Na, Fe, Pb, Mn, K, Ti and Cl were also detected. In samples 1 and 3 a **finishing layer**, fluorescent under UV illumination, was also observed. This can suggest either that a varnish was applied only on the projection areas or that the varnish was applied on all the surface, but it was differently adsorbed depending on the local variation of porosity.

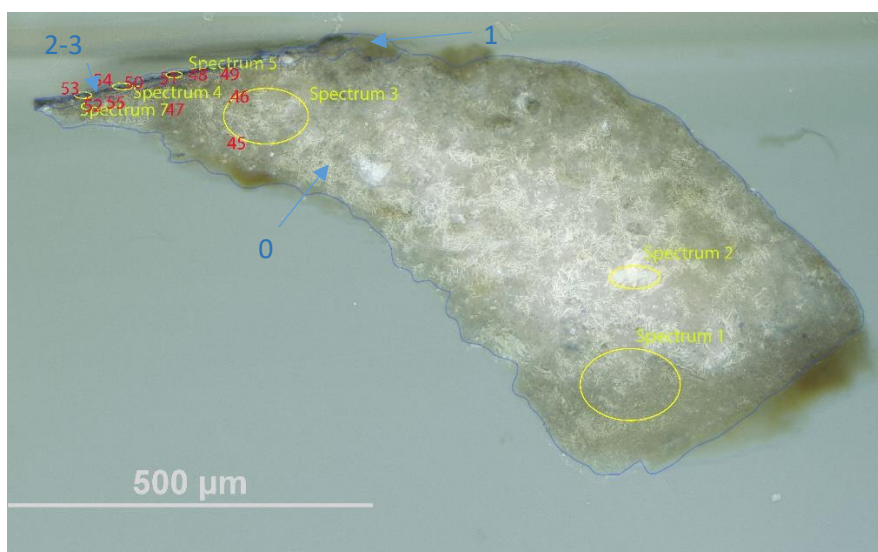
A **wax** or **resin** (FT-IR peaks at 1000-1200, 1472 and CH symmetric and asymmetric stretches in the 2800-3000  $\text{cm}^{-1}$ ) was detected in all the layers of all the samples, which indicates that either the material was added to the gypsum plaster wet admixture or that the coating has also penetrated in layer 0. The latter seems also possible as the average depth of the samples is about 0.5 mm. The additional presence of a **protein** cannot be excluded by interpreting the FT-IR spectra, due to the complexity of the admixture and also to the crowded pattern of the resins' FT-IR spectra (Price et al., 2009). Py-TMAH-GC/MS analysis of sample 4 suggests that the organic medium in this sample consists of **shellac** mixed with **linseed oil**. Amine fragments were also identified, as in the majority of natural 'non-protein binders' a minority of protein component is present too (Colombini & Modugno, 2009).

**NOTE:** casting in resin the fragments of plaster resulted in the fragments absorbing the resin when in the liquid state. This was visible in the BSE image as well as through the EDS mapping (Tiranti resin and catalyst are mainly made of organic compounds C, H and O). Aluminium (Al) traces are present in all the samples, due to the polishing chemical.

## Sample 1



**Sampling.** This fragment taken from an area of loss on the PL architectural element.



Left: Overlapped (OM and BSE) cross-section image showing the stratigraphy (blue indicators).

**3. Varnish layer**

**2. Dark layer**

**1. Yellowish and undefined layer**

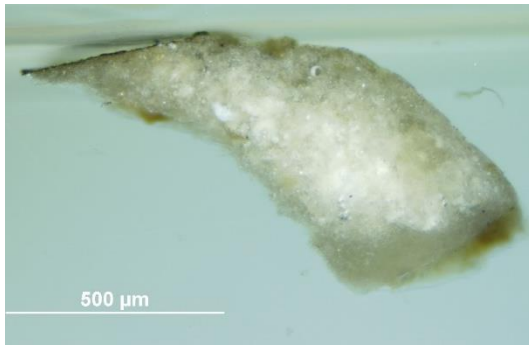
**0. Plaster bulk**

**Analysis spots.**

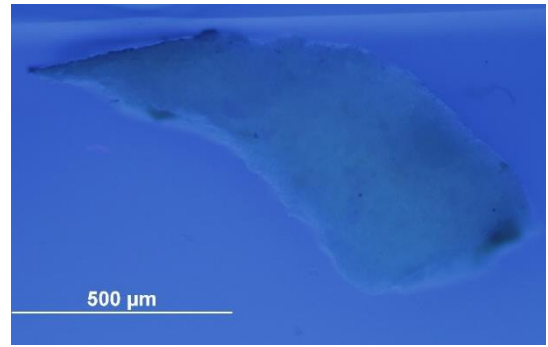
EDS analysis (yellow): Spectra 1-5 and 7

FT-IR analysis (red): nos. 45-55

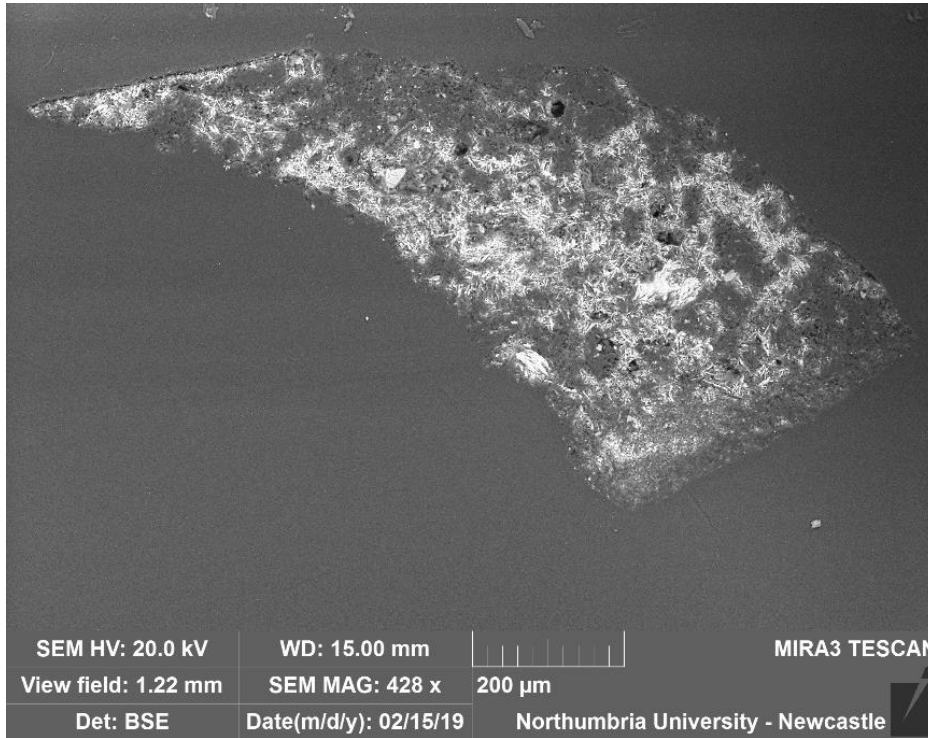
**Summary.** The substrate (layer 0) is made of plaster (**calcium sulfate**,  $\text{CaSO}_4$ , confirmed by EDS and by the peak at  $1600\text{ cm}^{-1}$  and overtones in the FT-IR spectra). The tabular crystalline structure typical of gypsum plaster can be seen in layers 0 and 1. Layer 1, which appears yellow under the microscope, consists of a portion of the lower layer soaked with the surface coating, showing characteristics of both layer 0 and layer 2. The surface dark layer (layer 2) is mostly made of silicon and traces of aluminium and magnesium, which are also present as inclusions in layers 0 and 1. Traces of Na, Fe, Ti and Cl were also detected. A **wax or resin** (FT-IR peaks at  $1472$  and  $2800\text{-}3000\text{ cm}^{-1}$ , and  $1744\text{ cm}^{-1}$  that suggests ester-containing wax or the additional presence of oil) was detected in all the layers. Layer 3, fluorescing under UV illumination, might be consistent with a finishing varnish.



VLR OM (above)



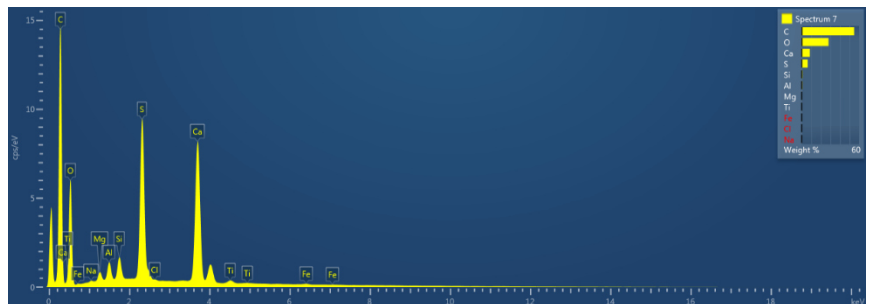
UVf OM (above)



BSE image (left).

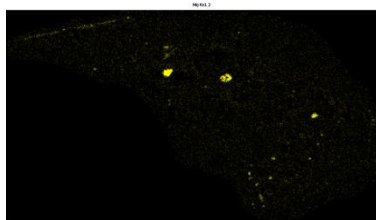
The tabular crystalline structure typical of gypsum plaster can be seen in layers 0 and 1.

Spectrum 7 (right) of layers 1-3 shows C, O, Ca, S, Si, Al, Mg and traces of Ti, Na, Cl and Fe.

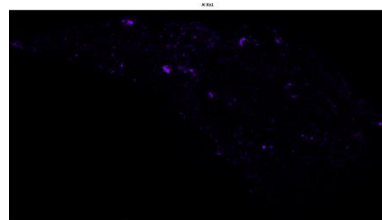


EDS mapping (below) shows that Mg, Al and Si inclusions are present in all the layers, but Si is mostly present in the utmost layers.

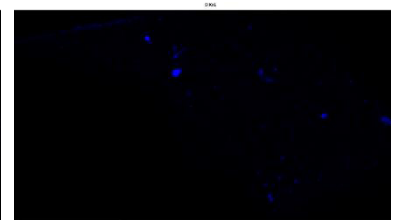
Magnesium (Mg)

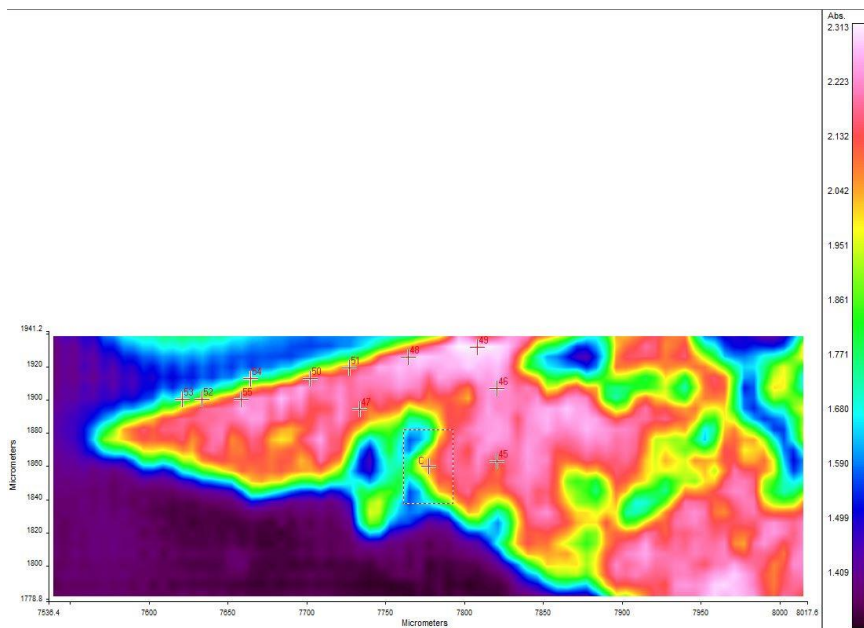
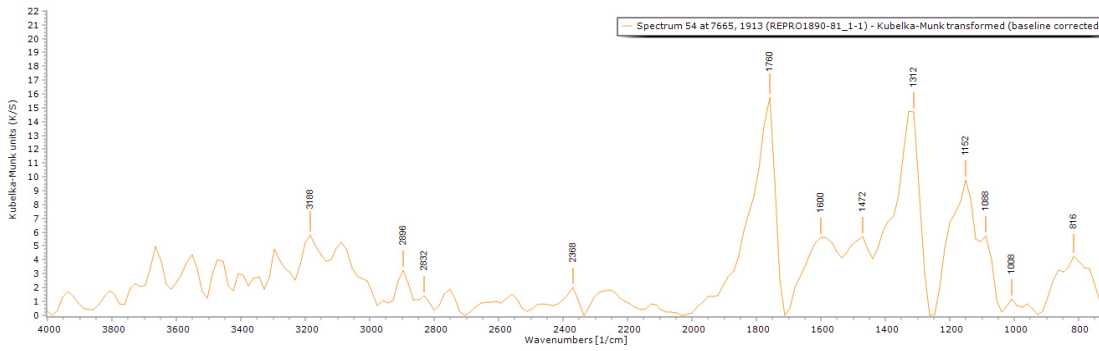


Aluminium (Al)



Silicon (Si)





**FT-IR spectrum 54** (above) of layers 2-3. Peaks for the casting resin (1312, 1760  $\text{cm}^{-1}$ ), gypsum (1600  $\text{cm}^{-1}$ ), overtone 2200-2300  $\text{cm}^{-1}$  and a wax/resin (1152, 1472, 2800-3000  $\text{cm}^{-1}$ ). A summary of the peaks observed in the spectra 45-55 can be seen in the table below.

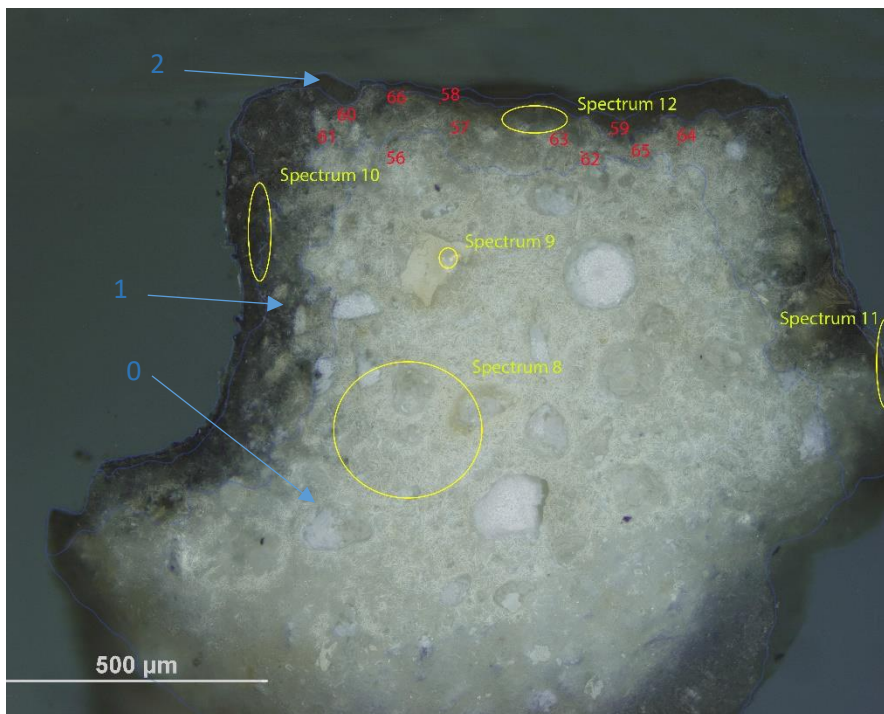
**FT-IR (FPA) image** (left). No clear layer definition can be observed in the FPA image.

Spectrum	Layer	peaks ( $\text{cm}^{-1}$ )						
		Casting Resin	Gypsum	Carbonate	Wax/resin	C=O ester carbonyl	SO overtone	Unknown
45	0	1760	1648		880, 992, 1104, 1216, 1296, 1408, 1456, 1584, 2896, 2976		2208	1968
46	0	1344	1600	800	768, 880, 1008, 1152, 1296, 1392, 1520, 2832, 2960	1744	2288	1808
47	0	1312, 1760			784, 912, 1072, 1408, 1472, 1536, 1680, 2832, 2992		2304	
48	0	1328	1632	1776	784, 880, 1072, 1168, 1488, 1536, 1584, 2880, 2928		2272	
49	0	1312	1600		912, 1088, 1216, 1376, 1408, 1504, 1664, 2896		2192	
50	1	1344, 1760	1632	800	896, 1008, 1088, 1152, 1488, 2816, 2896		2320	
51	0	1328, 1760			864, 1184, 1408, 1584, 2945		2384	
52	1	1312, 1760	1648		864, 1184, 1392, 1488, 2864, 2928		2384	
53	2-3	1312, 1760	1648		1008, 1200, 1408, 1472		2336	
54	2-3	1312, 1760	1600		816, 1008, 1088, 1152, 1472, 2832, 2896		2368	
55	1	1328	1600		784, 1152, 1216, 1408, 1472, 1520, 2832, 2912	1744	2272	

## Sample 2



**Sampling.** This sample consists of a fragment taken from an area of loss on the PR, from the frame.



**Left:** Overlapped (OM and BSE) cross-section image showing the stratigraphy (blue indicators).

**2. Dark layer**

**1. Grey and undefined layer**

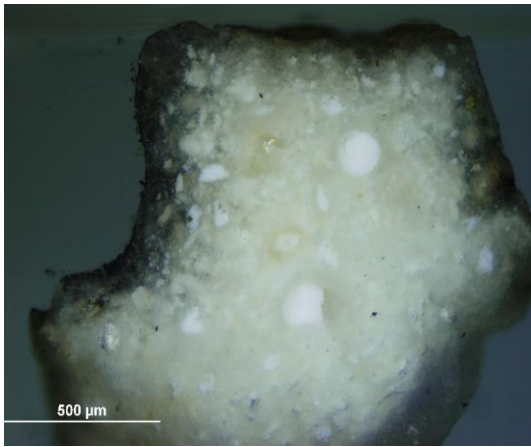
**0. Plaster bulk**

**Analysis spots.**

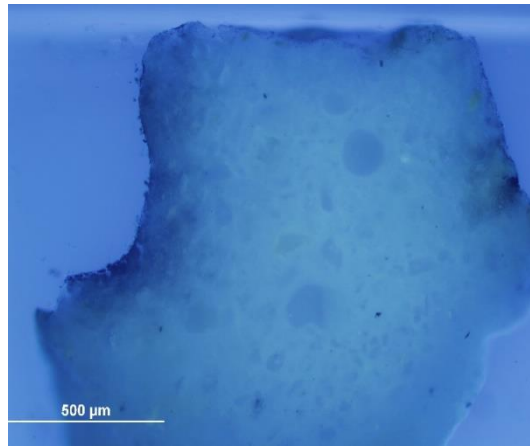
EDS analysis (yellow): Spectra 8-12

FT-IR analysis (red): nos. 56-66

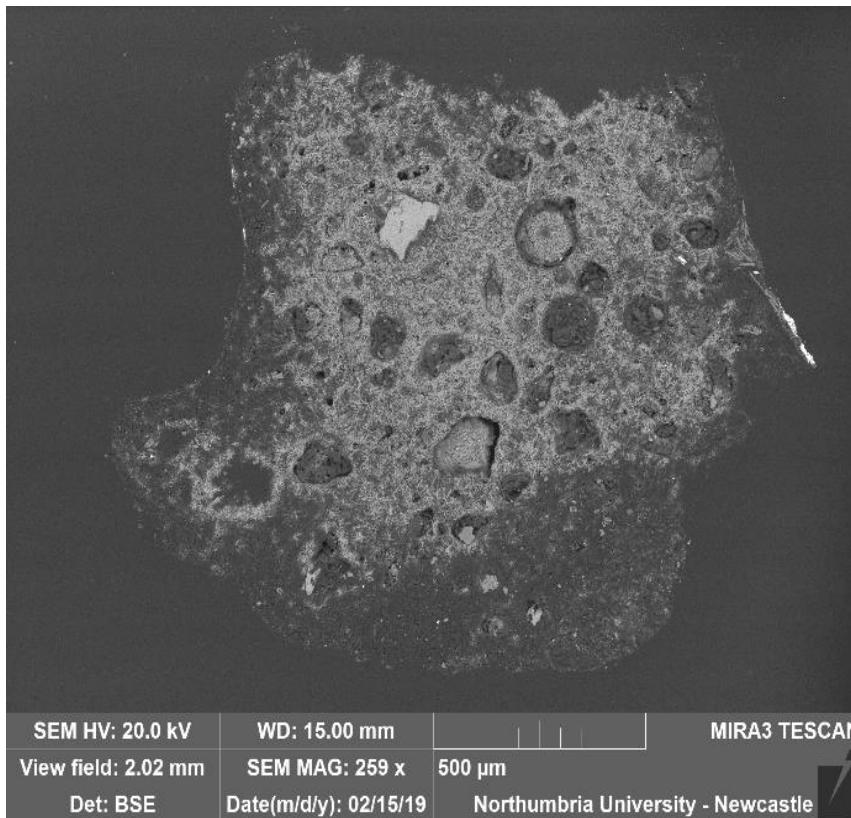
**Summary.** The substrate (layer 0) is made of plaster (**calcium sulfate**,  $\text{CaSO}_4$ , confirmed by EDS and by the peak at  $1600\text{ cm}^{-1}$  and overtones in the FT-IR spectra). The tabular crystalline structure typical of gypsum plaster can be seen in layers 0 and 1. Layer 1, which appears grey under the microscope, consists of a portion of the lower layer soaked with the surface coating, showing characteristics of both layer 0 and layer 2. The surface dark layer (layer 2) is mostly made of silicon and traces of aluminium and magnesium, which are also present as inclusions in layers 0 and 1. Traces of Ti, Pb, Mn, Mg, K, P, Na, Cl and Fe were also detected. A **wax or resin** (FT-IR peaks at  $1472$  and  $2800\text{-}3000\text{ cm}^{-1}$ ) was detected in all the layers.



VLR OM (above)



UVfOM (above)



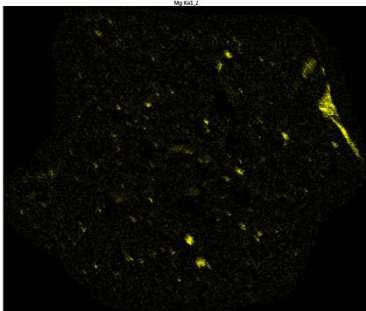
**BSE image** (left).

The tabular crystalline structure typical of gypsum plaster can be seen in layers 0 and 1.

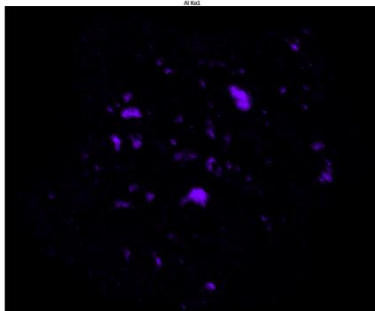
**EDS spectra** suggest that the sample is made of calcium sulfate (C, O, Ca, S) and that Si, Al, Mg and traces of Ti, Pb, Mn, Mg, K, P, Na, Cl and Fe are also present.

**EDS mapping** (below) shows that Mg, Al and Si inclusions are present in all the layers, but Si is mostly present in the utmost layers.

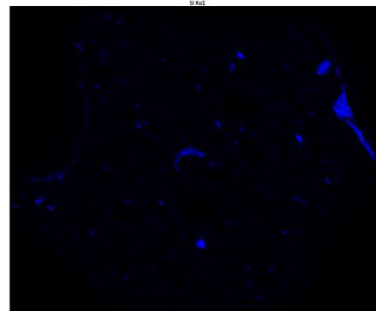
**Magnesium (Mg)**

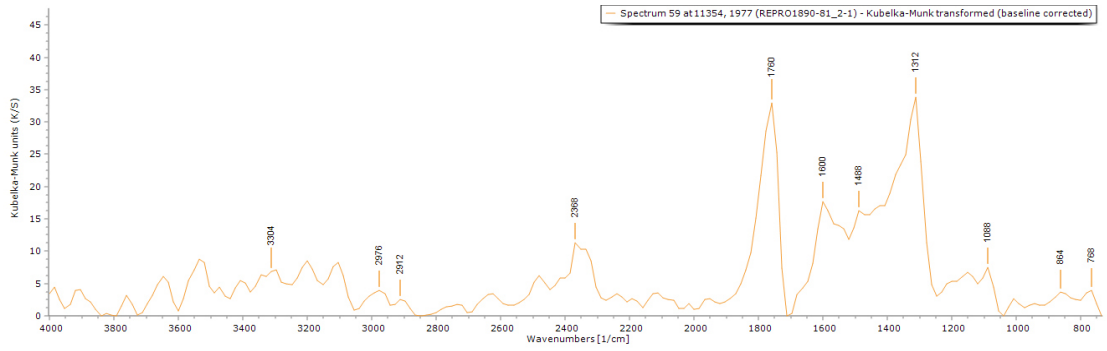


**Aluminium (Al)**

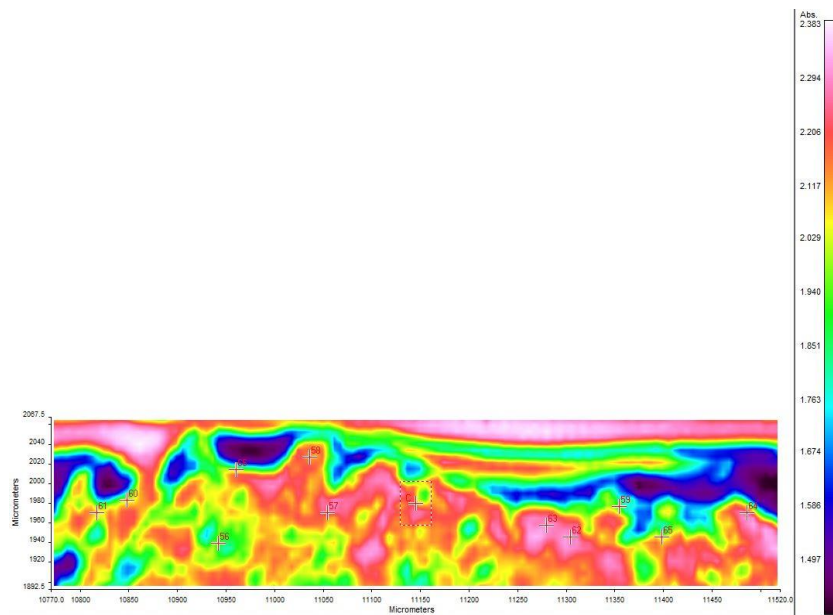


**Silicon (Si)**





**FT-IR spectrum 59** (above) of layer 2. Peaks for the casting resin (1312, 1760  $\text{cm}^{-1}$ ), gypsum (1600  $\text{cm}^{-1}$ ), overtone 2200-2300  $\text{cm}^{-1}$  and a wax/resin (1088, 1488, 2800-3000  $\text{cm}^{-1}$ ). A summary of the peaks observed in the spectra 56-66 can be seen in the table below.



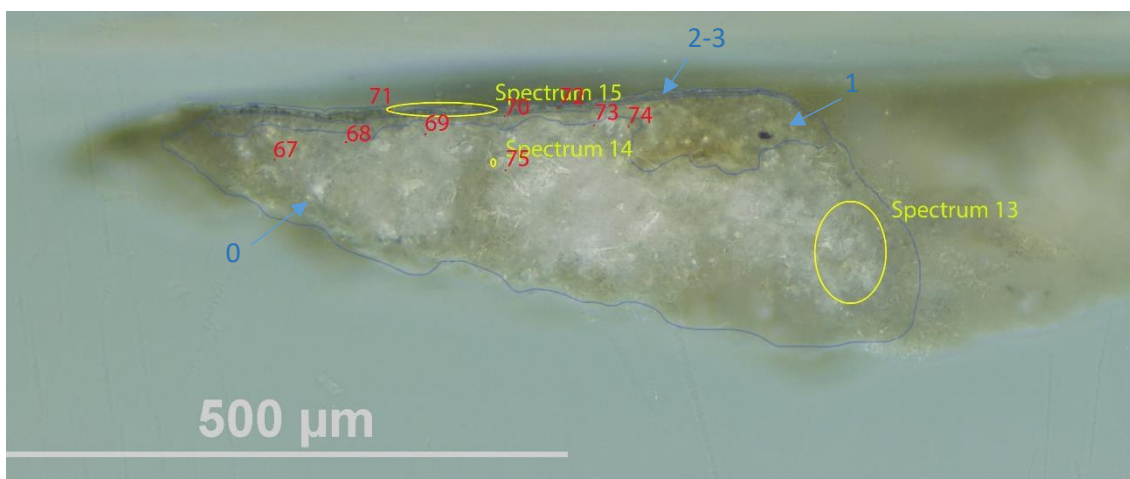
**FT-IR (FPA) image** (left). No clear layer definition can be observed in the FPA image.

Spectrum	Layer	peaks (cm-1)						
		Casting Resin	Gypsum	Carbonate	Wax/resin	C=O ester carbonyl	SO overtone	Unknown
56	1	1312, 1760			1200, 1392, 1664		2352	
57	1	1312, 1760			928, 1104, 1248, 1392, 1456, 1664, 2848, 2960		2304	
58	2	1312, 1760	1648		848, 1216, 1408, 1552		2240	
59	2	1312, 1760	1600		768, 864, 1088, 1488, 2912, 2976		2368	
60	1	1312, 1760	1600		880, 992, 1088, 1392, 1488, 1680, 2832, 2961		2288	
61	1	1328, 1760	1600		912, 1088, 1184, 2752, 2864		2336	
62	1	1760			752, 864, 1104, 1232, 1376, 1472, 1584, 1680, 2880		2224	
63	1	1312, 1760			896, 1088, 1376, 1488, 1584, 2864		2384	
64	1	1344, 1760			944, 1216, 1504, 1584, 2704, 2848		2256	
65	1	1344, 1760	1616		784, 880, 1008, 1088, 1184, 1472, 2896, 2960		2336	
66	1	1328, 1760			784, 1088, 1200, 1552, 2864, 3008		2336	

## Sample 3



**Sampling.** This fragment is taken from an area of loss on the PL, from the frame.



Above: Overlapped (OM and BSE) cross-section image showing the stratigraphy (blue indicators).

### 3. Varnish

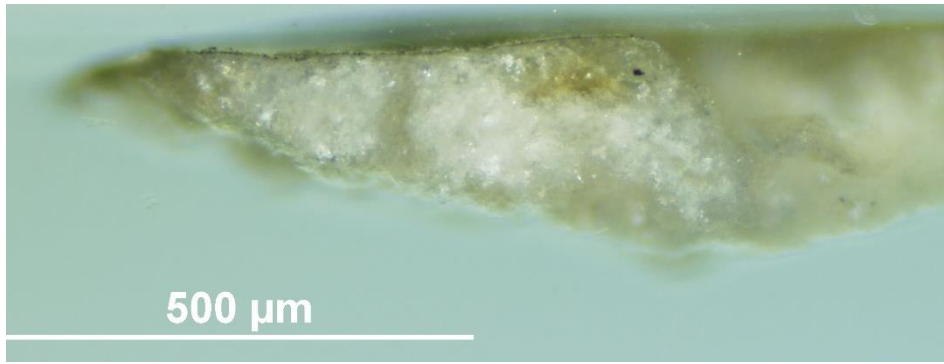
### 2. Dark layer

### 1. Yellowish and undefined layer

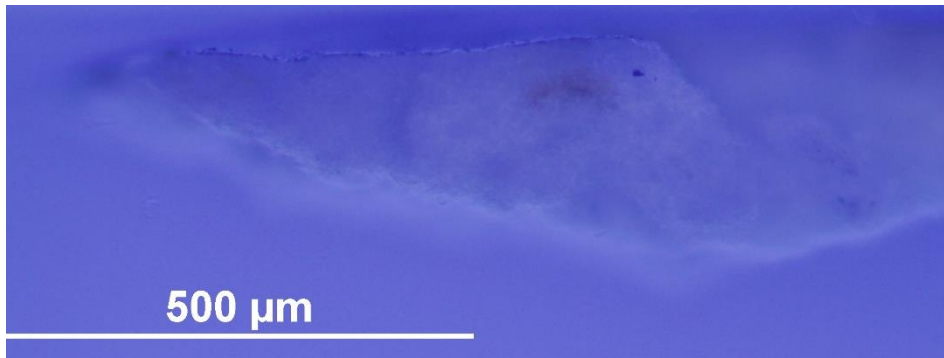
### 0. Plaster bulk

**Analysis spots.** EDS analysis (yellow): Spectra 13-15; FT-IR analysis (red): nos. 67-75.

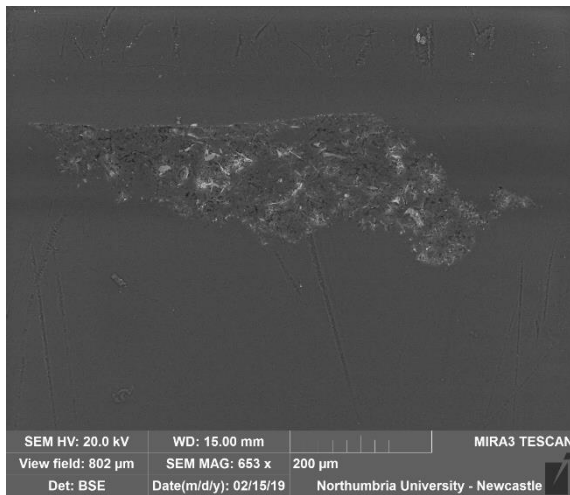
**Summary.** The sample is mostly made of C, O, S and Ca (**calcium sulfate**,  $\text{CaSO}_4$ , confirmed by EDS and by the peak at  $1600\text{-}1616\text{ cm}^{-1}$  in the FT-IR spectra). Al is overall present as used as a polishing agent, but could also, together with Si and Mg be present as part of silicate inclusions. Layers 2-3 consist mostly of Mg and Al (see EDS mapping) and traces of and traces of K, Fe, Cl and Ti were also detected in these layers. The structure typical of gypsum plaster can be seen in layers 0 and 1. Layer 1, which appears yellow under the microscope, consists of a small portion of the lower layer soaked with the surface coating, showing characteristics of both layer 0 and layer 2. A **wax or resin** is suggested by FT-IR (peaks at  $1000\text{-}1200$  and  $2800\text{-}3000\text{ cm}^{-1}$ ). Layer 3, fluorescing under UV illumination, might be consistent with a finishing varnish.



VLR OM (left)

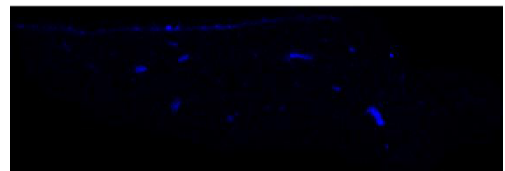
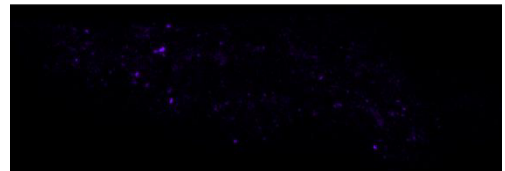
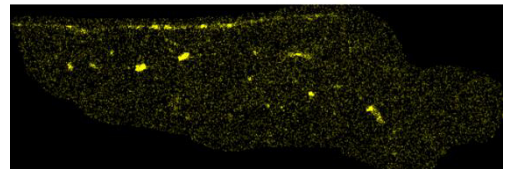


UVfOM (left)



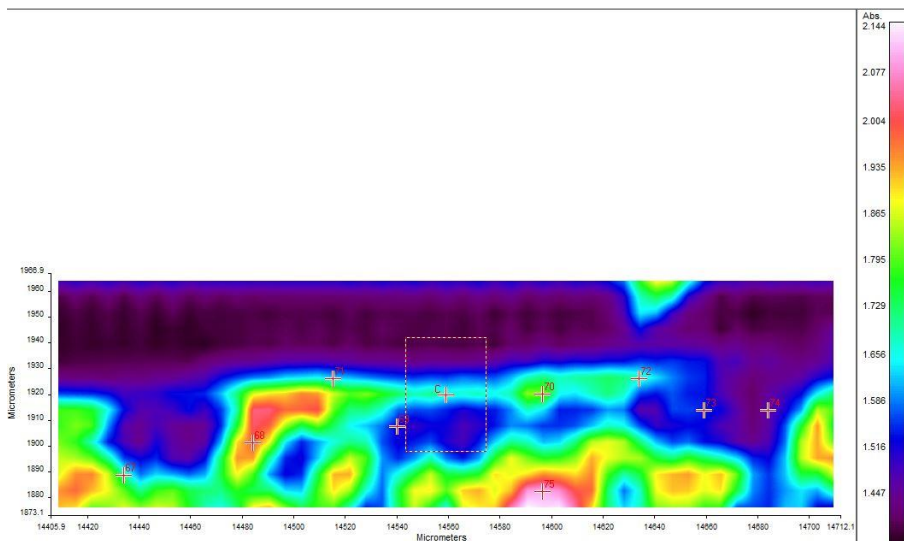
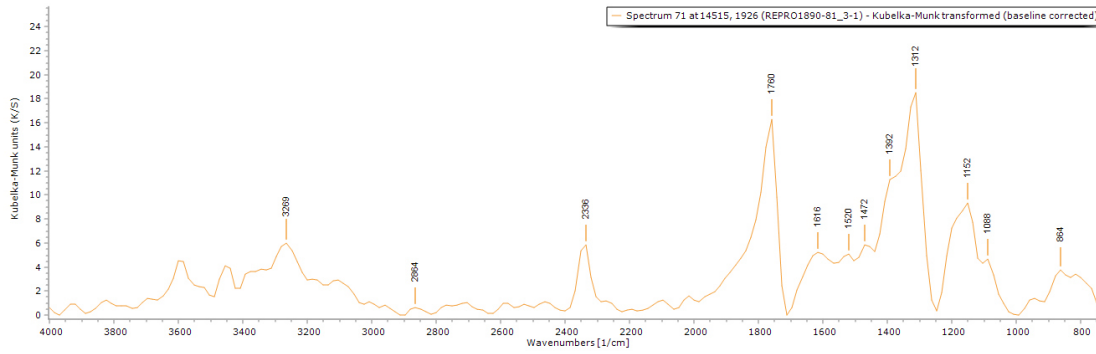
**BSE image** (above). The tabular crystalline structure typical of gypsum plaster can be seen in layers 0 and 1.

Calcium sulfate ( $\text{CaSO}_4$ ) and Mg were detected in all the layers. Si and Al are relevantly present in layers 2-3 (see **spectrum 15** below) and traces of Mg, K, Fe, Cl and Ti were also detected.



**EDS mapping** (above) shows that layer 2 is mostly made of magnesium (Mg, top), aluminium (Al, middle) and silicon (Si, bottom).





**FT-IR spectrum 71** (above) of layers 2-3. Peaks for the casting resin (1312, 1760  $\text{cm}^{-1}$ ), gypsum (1616  $\text{cm}^{-1}$ ), 1472  $\text{cm}^{-1}$  and a wax/resin (1000-1200 and 2800-3000  $\text{cm}^{-1}$ ). A summary of the peaks observed in the spectra 67-75 can be seen in the table below.

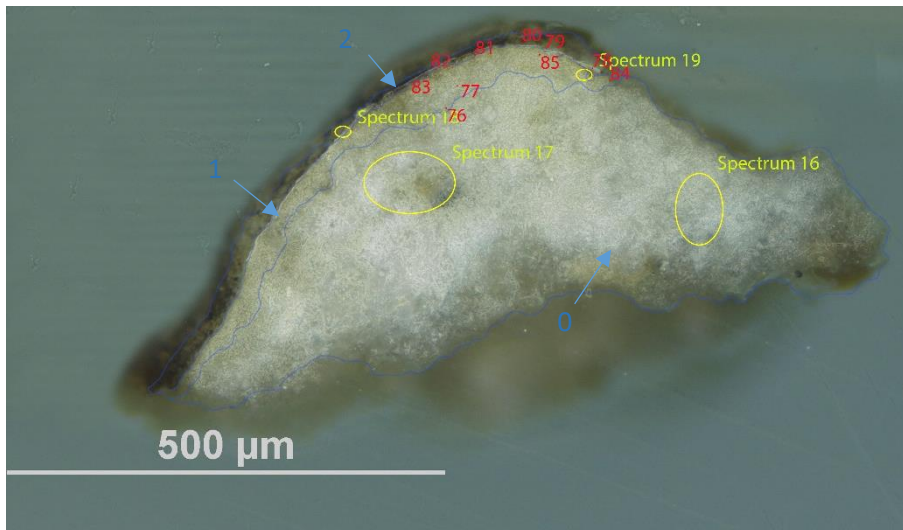
**FT-IR (FPA) image** (left). No clear layer definition can be observed in the FPA image.

Spectrum	Layer	peaks (cm-1)						
		Casting Resin	Gypsum	Carbonate	Wax/resin	C=O ester carbonyl	SO overtone	Unknown
67	0	1312, 1760			784, 880, 1168, 1392, 1472, 1568, 2832, 2960		2352	
68	0	1312, 1760	1600	800	880, 1152, 1392, 1472, 1664, 2864, 2945		2320	
69	0	1312, 1760	1616		784, 864, 1088, 1152, 1472, 2848, 2944		2352	
70	1	1312, 1760	1616		784, 1168, 1408		2336	
71	2-3	1312, 1760	1616		864, 1088, 1152, 1392, 1472, 1520, 2864		2336	
72	2-3	1312, 1760			784, 1088, 1184, 1392, 1472, 1536, 2960		2352	
73	0	1312, 1760	1648		784, 1088, 1168, 1472		2352	
74	0	1312, 1760	1600		784, 864, 1088, 1168, 1472,		2336	
75	0	1312, 1760			784, 1088, 1152, 1184, 1360, 1456, 1584, 1664, 2896, 2960		2224	

## Sample 4



**Sampling.** This fragment was taken from an area of loss on the PL, from the frame.



Left: Overlapped (OM and BSE) cross-section image showing the stratigraphy (blue indicators).

### 2. Dark layer

1. Yellowish and undefined layer

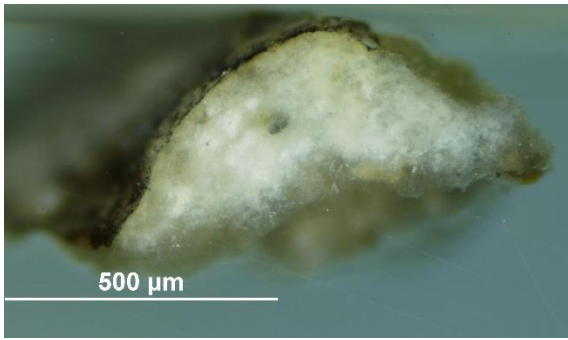
0. Plaster bulk

### Analysis spots.

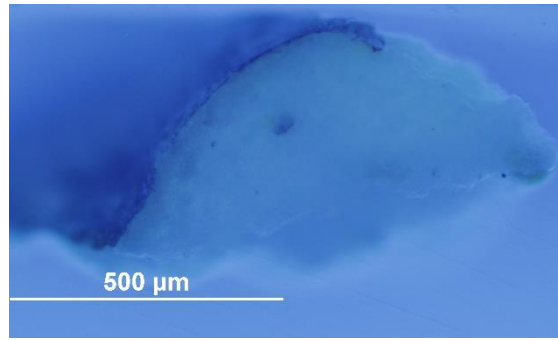
EDS analysis (yellow): Spectra 16-19

FT-IR analysis (red): nos. 76-85

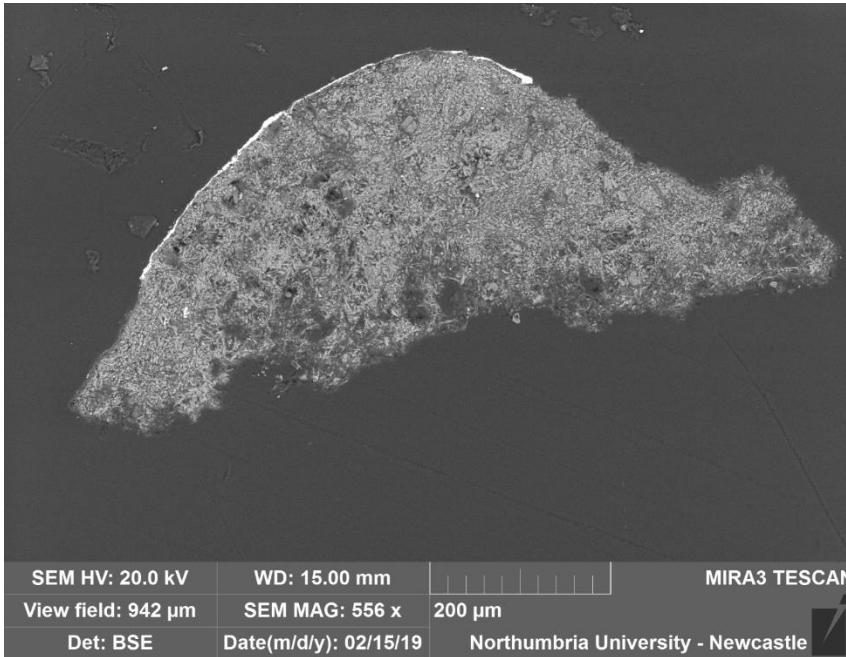
**Summary.** The sample is mostly made of C, O, S and Ca (**calcium sulfate**,  $\text{CaSO}_4$ , confirmed by EDS and by the peak at  $1600\text{-}1632\text{ cm}^{-1}$  in the FT-IR spectra). Al is overall present as used as a polishing agent, but could also, together with Si and Mg be present as part of silicate inclusions. Layer 2 consists mostly of Si, Mg and Al (see EDS mapping) and traces of Pb, Cl, Na, K and Fe. The structure typical of gypsum plaster can be seen in layers 0 and 1. Layer 1, which appears yellow under the microscope, consists of a small portion of the lower layer soaked with the surface coating, showing characteristics of both layer 0 and layer 2. A **wax or resin** is suggested by FT-IR (peaks at  $1000\text{-}1200$  and  $2800\text{-}3000\text{ cm}^{-1}$ ). py-TMAH-GC/MS shows markers characteristic of **shellac** mixed with **linseed oil**. Amine fragments were also identified, as in the majority of natural 'non-protein binders' a minority of protein component is present too (Colombini & Modugno, 2009).



VLR OM (above)



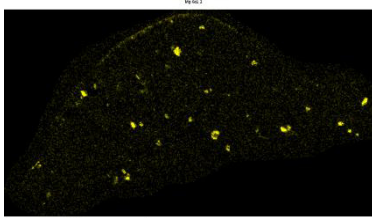
UVfOM (above)



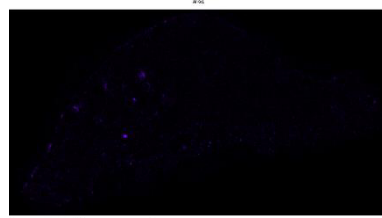
**BSE image (left).** The tabular crystalline structure typical of gypsum plaster can be seen in layers 0 and 1. Layer 2 consists of Mg, Al and Si, which can be seen in the **EDS mapping (below)**.

**EDS spectra** indicate that layers 0 and 1 consist of C, O, Ca, S, Al, Mg and Si. Layer 2 is mostly made of Mg, Si, Al and traces of Pb, Cl, Na, K and Fe (see **spectrum 18 below**).

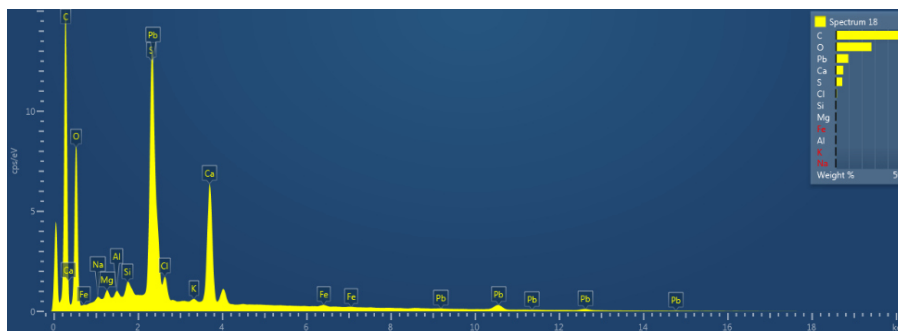
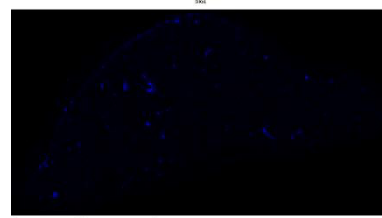
Magnesium (Mg)

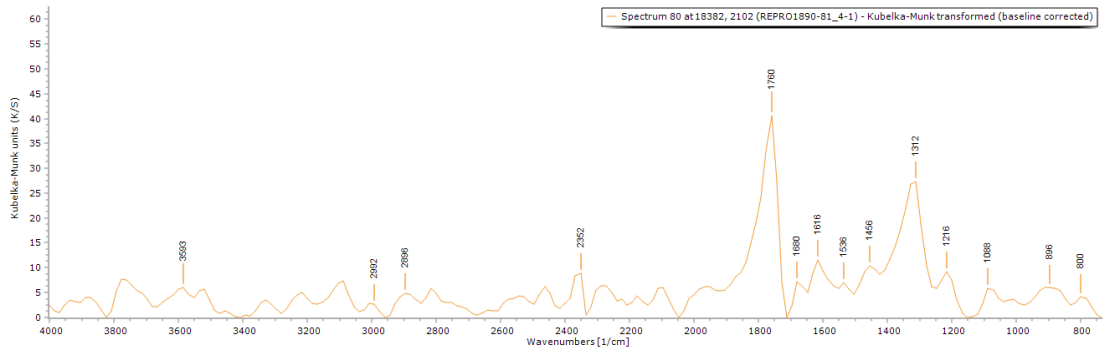


Aluminium (Al)

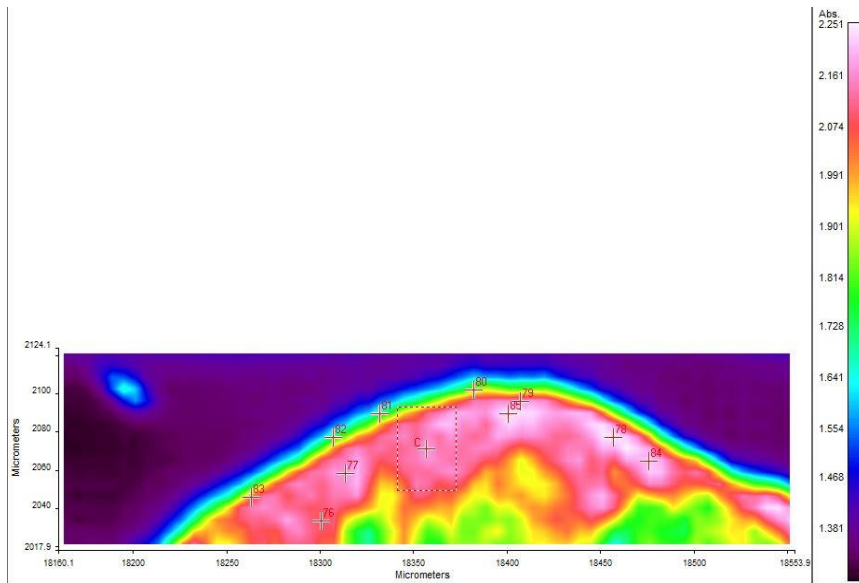


Silicon (Si)



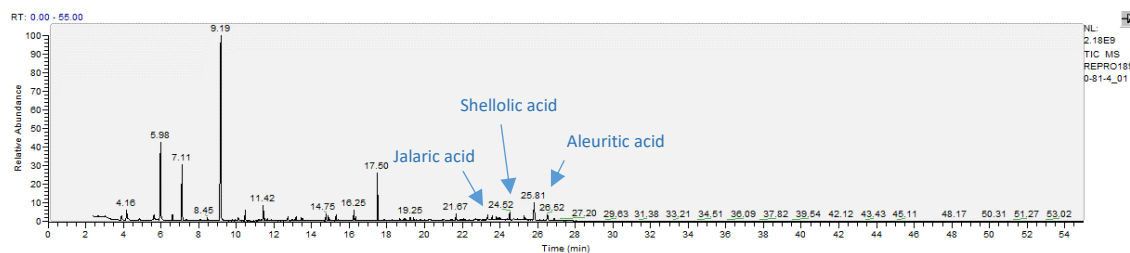


**FT-IR spectrum 80** (above) of layer 2. Peaks for the casting resin (1312, 1760  $\text{cm}^{-1}$ ), gypsum (1616  $\text{cm}^{-1}$ ), overtone 2200-2300  $\text{cm}^{-1}$  and a wax/resin (1216, 1456, 2896 and 2992  $\text{cm}^{-1}$ ). Peaks that might suggest the presence of a protein are also visible in the 1400-1600  $\text{cm}^{-1}$  area. A summary of the peaks observed in the spectra 76-85 can be seen in the table below.



**FT-IR (FPA) image** (left). No clear layer definition can be observed in the FPA image.

Spectrum	Layer	peaks ( $\text{cm}^{-1}$ )						
		Casting Resin	Gypsum	Carbonate	Wax/resin	C=O ester carbonyl	SO overtone	Unknown
76	1	1312	1616	1776	880, 960, 1040, 1232, 1472, 2896, 2970		2320	
77	1	1328, 1760	1616		960, 1232, 1520, 2864, 2961		2288	
78	2	1328, 1760	1632		1232, 1392, 1456, 1520, 2864, 2960		2208	
79	2	1312, 1760			912, 1008, 1072, 1216, 1488, 1552, 1664, 2832, 2952		2144	
80	2	1312, 1760	1616	800	896, 1088, 1216, 1456, 1536, 1680, 2896, 2992		2352	
81	2	1312, 1760	1616	800	1200, 1472, 1536, 2848		2320	
82	1	1328, 1760	1616		784, 1216, 1472, 2912		2336	
83	1	1328, 1760	1616		1168, 1504, 2816		2320	
84	1	1328		1776	880, 1040, 1232, 1568, 1680, 2800		2304	
85	1		1632	1776	896, 1008, 1072, 1216, 1296,		2304	



RT	m/z	Assignment	Formula
3.9	42(37), 58(100), 83(76)	2-Propanone, 1-(dimethylamino)-	C5H11NO
4.16	45(100), 58(35), 74(66), 91(4)	Ethanamine, 2-methoxy-	C3H9NO
5.63	45(42), 58(100), 72(6), 88(39), 119(3)	Ethanol, 2-[2-(2-methoxyethoxy)ethoxy]-	C7H16O4
5.98	42(13), 58(100), 117(15)	1,2-Ethanediamine, N'-ethyl-N,N-dimethyl-	C6H16N2
6.62	42(16), 58(43), 65(17), 79(100), 95(12), 109(7)	Methanesulfonic acid, methyl ester	C2H6O3S
7.11	42(8), 56(7), 72(100), 131(2)	N,N'-Diisopropylethylenediamine	C8H20N2
8.45	42(19), 58(42), 70(8), 86(100), 110(5), 128(51)	1,2-Ethanediamine, N,N-diethyl-N'-methyl-	C7H18N2
9.19	44(100), 57(18), 86(63), 128(47)	Unidentified amine fragment	
10.11	42(13), 59(40), 87(17), 115(100)	Gly-Gly-Gly	C6H11N3O4
10.46	44(99), 58(100), 86(25), 100(54), 142(65)	2-Nonanone	C9H18O
11.42	42(11), 58(100), 70(9), 89(5), 116(5)	1,2-Ethanediamine, N'-ethyl-N,N-dimethyl-	C6H16N2
12.73	42(11), 58(100), 128(3), 175(3)	Arginine	C6H14N4O2
13.18	58(34), 88(23), 99(30), 116(41), 130(100), 142(10)	Unidentified amine fragment	
13.44	55(12), 59(21), 72(100), 101(7), 114(14), 130(5), 143(6)	Unidentified amine fragment	
13.55	45(100), 58(58), 74(63), 83(33), 101(15), 110(47), 147(5), 162(5)	FA fragment	
14.75	58(12), 83(6), 99(4), 116(100), 139(5), 173(4)	Unidentified amine fragment	
14.89	42(41), 59(81), 74(89), 83(72), 87(33), 111(26), 115(100), 125(46), 157(33), 166(5), 180(5)	10-Undecenoic acid, methyl ester	C12H22O2
15.31	42(9), 58(21), 83(6), 99(4), 116(100), 149(4), 173(4)	Unidentified amine fragment	
16.25	41(30), 55(74), 69(77), 74(100), 83(51), 87(46), 97(58), 111(31), 129(77), 138(98), 171(60)	Tridecanoic acid	C13H26O2
16.35	44(5), 58(14), 77(18), 92(5), 104(4), 133(6), 149(5), 163(100), 194(4)	Dimethyl phthalate	C10H10O4
17.5	43(18), 55(59), 59(31), 74(62), 83(59), 87(26), 97(19), 111(56), 124(27), 143(30), 152(100), 185(38)	Nonanedioic acid, monomethyl ester	C10H18O4
18.69	44(41), 55(84), 58(100), 74(81), 87(35), 99(39), 115(38), 125(53), 138(40), 149(5), 157(5), 175(5), 190(42), 199(41)	FA fragment	
19.25	45(86), 58(74), 71(56), 75(100), 85(82), 101(64), 115(33), 139(29), 152(5), 161(37), 183(5), 193(5), 215(5)	Unidentified terpenoid fragment	
19.4	45(77), 58(96), 77(38), 85(78), 95(5), 109(44), 122(5), 137(58), 165(5), 182(43), 193(100), 224(5), 236(5)	Unidentified terpenoid fragment	
21.67	55(21), 74(100), 87(67), 115(7), 129(8), 143(20), 171(7), 185(7), 199(5), 227(11), 239(5), 270(5)	methyl palmitate	C17H34O2
23.35	41(57), 58(100), 69(64), 91(69), 105(5), 115(52), 121(63), 145(45), 155(5), 167(69), 179(50), 191(58), 203(61), 215(5), 231(5), 247(5), 262(94), 275(68), 307(5), 322(5)	jalaric acid	
23.58	43(23), 55(34), 74(100), 87(68), 115(5), 143(27), 199(14), 255(5), 298(5)	methyl stearate	C19H38O2
24.52	45(86), 58(100), 79(79), 91(85), 105(5), 115(64), 159(5), 169(60), 189(55), 201(60), 206(71), 238(69), 260(5), 288(5), 305(5), 320(94), 337(5)	shellolic acid	
25.3	45(77), 55(100), 74(62), 81(65), 95(53), 111(37), 121(5), 139(5), 155(49), 171(5), 187(5), 199(5), 215(5), 233(5), 247(5), 281(5), 306(5), 335(5)	Unidentified triterpenoid fragment	
25.81	45(33), 58(21), 71(100), 95(81), 109(25), 137(39), 159(49), 185(10), 201(77), 259(5)	aleuritic acid	
26.52	45(40), 55(36), 71(100), 81(26), 95(85), 109(31), 137(35), 159(38), 187(34), 201(43)	aleuritic acid	

RT = retention time, m/z = mass/charge ratio

**Py-TMAH-GC/MS chromatogram** (top and described in the table above) shows small fragments due to derivatization (from  $t = 3.90$  to  $11.42$  min) and markers characteristic of **shellac** (jalaric, shellolic and aleuritic acids at  $t = 23.35$ ,  $24.52$  and  $25.81$  min). The presence of **methyl azelate** ( $t = 17.50$  min), **methyl palmitate** ( $t = 21.67$ ) and **stearate** ( $t = 23.58$ ) suggest that the resin has been mixed with **linseed oil** ( $A/P = 3.9$  and  $P/S = 1.53$ ). Amine fragments were also identified, as in the majority of natural 'non-protein binders' a minority of protein component is present too (Colombini & Modugno, 2009).

## Experimental

The object was observed, and its conditions were documented. Samples from selected areas were taken by Valentina Risdonne. When possible, each sample was split into two parts: one fragment was embedded in polyester resin (Tiranti clear casting resin), polished and analysed under an optical microscope and the other was put aside for py-TMAH-GC/MS. Not enough material was available for XRD analysis.

The optical microscopy was performed with an Olympus BX51 Metallurgical Microscope equipped with four objectives (magnification of x5, x20, x50 and x100), and an x10 eyepiece. In many instances, a small amount of white spirit was applied on the surface of the cross-section to improve the saturation under the microscope. The microscope is equipped with a 6-cube filter turret which allows operating the system in reflected visible light (brightfield and darkfield mode) and reflected UV light (365 nm) using a 100 W mercury burner.

The SEM-EDS analysis was performed with a field emission TESCAN MIRA 3 with gigantic chamber. The SEM is equipped with: secondary electron detector (SE), secondary electron in-beam detector (In-beam SE), back-scatter detector (BSE), back-scatter in-beam detector (In-beam BSE), cathodoluminescence detector (without wavelength detection) (CL), plasma chamber/sample cleaner and software Alicona 3D imaging. For the EDS analytical part, it has an Oxford Instruments setup: Software: AztecEnergy, X-ray detector X-Max 150 mm<sup>2</sup> and X-ray detector X-Max Extreme, low energy detector for thin films, high resolution and low voltage. The samples were analysed by SEM-EDS Low Vacuum Mode (10-15 Pa). EDS Mapping and data processing were performed with Aztec Oxford software.

A Perkin Elmer Frontier FT-IR spectrometer (350 cm<sup>-1</sup> at the best resolution of 0.4 cm<sup>-1</sup>) was used, equipped with a germanium crystal for ATR measurements and combined with a Spectrum Spotlight 400 FT-IR microscope equipped with a 16×1 pixel linear mercury cadmium telluride (MCT) array detector standard with InGaAs array option for optimised NIR imaging. Spectral images from sample areas are possible at pixel resolutions of 6.25, 25, or 50 microns. The Perkin Elmer ATR imaging accessory consists of a germanium crystal for ATR imaging. These run with Perkin Elmer Spectrum 10™ software and with SpectrumIMAGE™ software. Baseline and Kubelka-Munk corrections were applied to the raw data acquired in diffuse reflectance.

The instrument used for GC/MS is a Thermo Focus Gas Chromatographer with DSQ II single quadrupole mass spec. The column currently installed is a Agilent DB5-MS UI column (ID: 0.25 mm, length: 30 m, df: 0.25 µm, Agilent, Santa Clara, CA, USA). Carrier gas: helium. Detector temperature: 280 °C, Injector temperature: 250 °C. It can be used with the PyroLab 2000 Platinum filament pyrolyser (PyroLab, Sweden) attachment or in split/splitless mode. Detection: Total Ion monitoring (TIC). 1 µl of the sample with 1 µl of TMAH was placed on the Pt filament for the py-GC/MS. The inlet temperature to the GC was kept at 250 °C. The helium carrier gas flow rate was 1.5 ml/min with a split flow of 41 ml/min and a split ratio of 27. The MS transfer line was held at 260 °C and the ion source at 250 °C. The pyrolysis chamber was heated to 175 °C, and pyrolysis was carried out at 600 °C for 2 s. This run with Xcalibur™ and PyroLab™ software. The library browser supported NIST MS Version 2.0 (Linstrom & Mallard, 2014).

Valentina Risdonne, PhD student

[v.risdonne@vam.ac.uk](mailto:v.risdonne@vam.ac.uk) / [valentina.risdonne@northumbria.ac.uk](mailto:valentina.risdonne@northumbria.ac.uk)

Victoria and Albert Museum – Northumbria University

PhD project 'Materials and techniques for coating of the nineteenth-century plaster casts'

©V&A Museum

18 September 2020

## Notes

18 January 2019	Sampling	Valentina's PhD Lab book 1, page 149
29 January 2019	Casting	Valentina's PhD Lab book 1, page 158
5 February 2019	Microscopy	Valentina's PhD Lab book 1, page 163
14 October 2019	FT-IR	Valentina's PhD Lab book 1, page 175
18 March 2020	GC/MS	Valentina's PhD Lab book 2, page 50

A full record of analysis is available at <https://doi.org/10.25398/rd.northumbria.14040182>

## References

- Colombini, M. P., & Modugno, F. (2009). *Organic mass spectrometry in art and archaeology*. John Wiley & Sons.
- Cox, K. G., Price, N. B., & Harte, B. (1974). *An introduction to the practical study of crystals, minerals, and rocks*. Halsted Press.
- Linstrom, P. J., & Mallard, W. G. (2014). *NIST Chemistry WebBook, NIST standard reference database number 69, National Institute of Standards and Technology, Gaithersburg MD, 20899*.
- Price, B. A., Pretzel, B., & Lomax, S. Q. (2009). *Infrared and Raman Users Group Spectral Database; 2007 ed. IRUG: Philadelphia, PA, USA*.



**Northumbria  
University**  
NEWCASTLE

Analysis Report - Valentina Risdonne

Copy of a relief - The Death of the Virgin

(REPRO.A.1916-3152)

Initiator: Charlotte Hubbard; Conservation Department

14 September 2020

© Victoria and Albert Museum



## Analysis Report - The Death of the Virgin (REPRO.A.1916-3152)

### Contents

Contents.....	318
List of abbreviations.....	318
Summary.....	319
Sample 1.....	322
Sample 2.....	325
Sample 3.....	328
Sample 4.....	332
Experimental.....	335
Notes.....	336
References.....	336

### List of abbreviations

BSE	Back Scattered Electron
EDS	Energy Dispersive Spectrometry
FT-IR	Fourier-Transform Infra-Red
FPA	Focal Plane Array
GC/MS	Gas Chromatography-Mass Spectrometry
OM	Optical Microscopy
PL	Proper Left
PR	Proper Right
py	pyrolysis
SEM	Scanning Electron Microscopy
TMAH	tetramethylammonium hydroxide
UVf	Ultraviolet Fluorescence
VLR	Visible Light Reflectance
XRD	X-ray Diffraction

## Summary

The bulk of the object is made of gypsum plaster, which contains several types of inclusions (including silicates and carbonates). Samples 1 and 2, taken from the front-facing side of the relief shows a significant concentration of lead, suggesting the possibility that these areas were highlighted with lead-based paint (contain aluminium and silicon too). Samples 3 and 4, taken from marginal and recess areas, show the same stratigraphy of samples 1 and 2 (a paint containing silicon and aluminium is possible), but do not contain lead. All the samples show a layer, fluorescing white-blue under UV illumination, that is consistent with a layer of varnish. Analysis suggests the presence of **diterpenic resin** (rosin or colophony) possibly mixed with a non-drying oil or a *tempera grassa*, that can be either been only applied onto the surface or also mixed with the paint.



Figure 1. The copy of a relief.

The object, '**Copy of a relief - The Death of the Virgin (REPRO.A.1916-3153)**' (Figure 1), is a plaster cast of a relief, with a representation of the Death of the Virgin executed under Pierre de Chelles (active about 1287; d. 1320). The original was carved in stone between 1296 and 1316, on the north side of the exterior of the apse of Notre Dame, Paris. The cast was made ca. 1850-1900 and given by the Architectural Association in 1916. The cast is now located in Gallery 46A (The Ruddock Family Cast Court), displayed upright. Its dimensions are 90.0x86.0 cm.

Conservation was carried out by the conservator **Sayuri Morio** after the sampling procedure hereinafter discussed (**record from May 2019**). The visual examination of the object showed that is structurally sound despite few straight joint lines and cracks are visible. The conservator described the entire surface of the object as covered with a 'brown and uneven paint' and very dusty. Salt efflorescent can be seen on the recessed areas; after the removal of the salt with a soft brush, the areas of salt left small white spots. There is some water damage on the lower quarter of the left-hand side; the water would have washed the paint and dissolved some gypsum, resulted in a very porous surface which collected dust and dirt. The object was examined under UV light. The surface fluoresces in mid-tone purple; small areas of overpaints and adhesive drips fluoresced in dull orange and greenish-white respectively. Sulfates were detected from the object's surface, which could be from the gypsum plaster itself, after analysis with Quantofix® salt strips. The object was dusted with brush and vacuum. Sturdier dirt was cleaned with Britzfix® sponge lightly dampened with deionised water or latex poultice method. Paint losses and chipped areas were retouched with acrylic paint.

Samples from the plaster cast were taken from pre-existing areas of loss to investigate the stratigraphy and the method of manufacture. The samples were analyzed to provide data for the study of the objects of the Cast Courts collection within the PhD project 'Materials and techniques for coating of the nineteenth-century plaster casts'. Details on the experimental procedure are available in the Experimental section of this report. A selection of significant results is shown in the following pages and the relevant database of analysis (<https://doi.org/10.25398/rd.northumbria.14040224>).

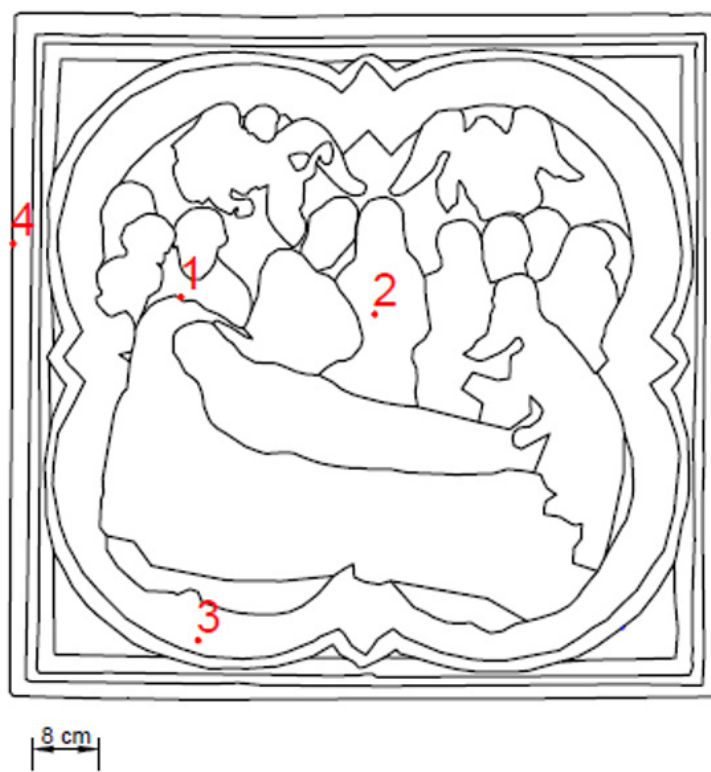


Figure 2. The relief outline with marked sampling sites.

**Sample 1:** fragment, already detached, taken from the PR, under two figures.

**Sample 2:** fragment and dust/salt taken from under the figure's hand.

**Sample 3:** fragment, already detached, taken from an area of crack, bottom PR edge.

**Sample 4:** fragment taken from an area of loss, PR edge.

The **substrate** (layer 0 in all the samples) is made of gypsum plaster (**calcium sulfate**,  $\text{CaSO}_4$ , confirmed by EDS, XRD and by peaks at  $1600\text{-}1648\text{ cm}^{-1}$  in the FT-IR spectra, which also show the sulfate overtones in the  $2100\text{-}2300\text{ cm}^{-1}$  area) and contains **Si-Al inclusions** (see EDS mapping). The *tabular* structure typical of gypsum plaster can be seen in layer 0 (BSE images) (Cox et al., 1974).

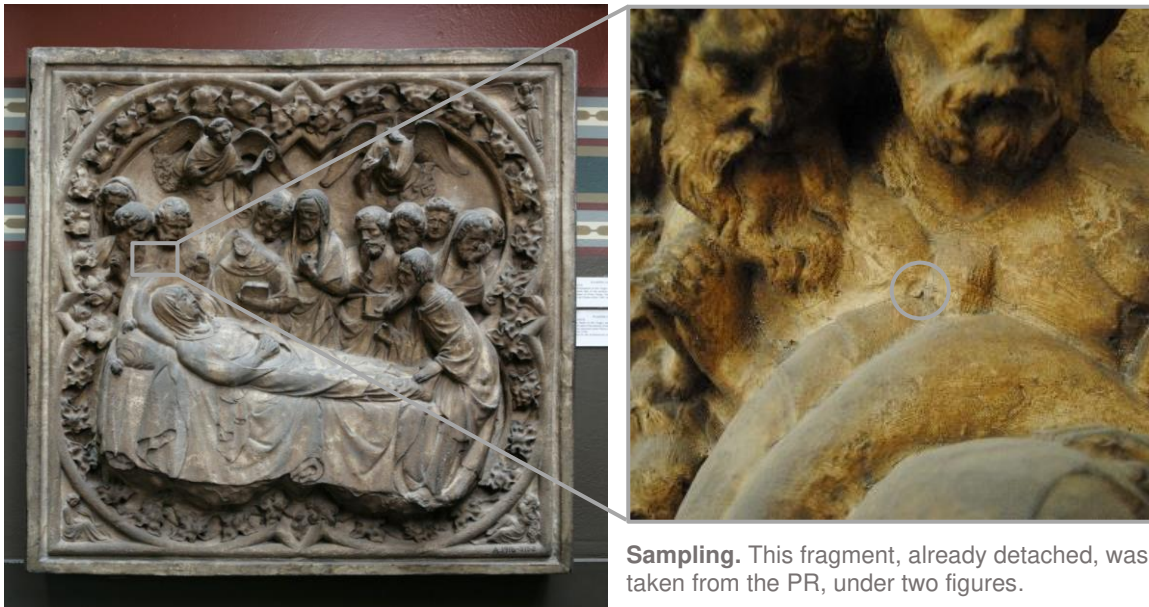
**Samples 1 and 2** shows a significant concentration of **lead** in the bulk but especially in the surface layers. A **white layer** (layer 1) is visible in sample 1 under visible illumination and EDS shows that layer 1 in samples 1 and 2 areas made of **lead** (Pb), **silicon** (Si) and **aluminium** (Al). Traces of Cl, Mg, Fe and K were also detected.

EDS mapping of **samples 3 and 4** indicate that the utmost layers in this samples are made mostly of **aluminium**, **silicon**, **strontium** and traces of **barium**. Traces of K, Na, Mg, Ti, Fe and Cl were also detected.

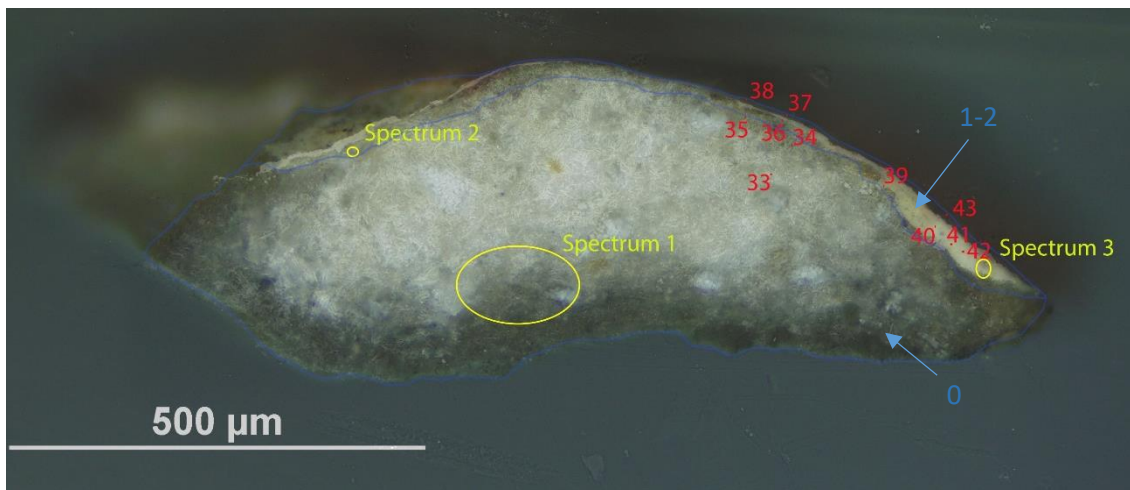
A **wax** or **resin** (FT-IR peaks at  $1000\text{-}1200$ ,  $1472$  and CH symmetric and asymmetric stretches in the  $2800\text{-}3000\text{ cm}^{-1}$ ) was detected in all the layers of all the samples, which indicates that either the material was added to the gypsum plaster wet admixture or that the coating has also penetrated in layer 0 (or both). The latter seems also possible as the average depth of the samples is about  $0.5\text{ mm}$ . The additional presence of a **protein** cannot be excluded by interpreting the FT-IR spectra, due to the complexity of the admixture and also to the crowded pattern of the resins' FT-IR spectra (Price et al., 2009). Py-TMAH-GC/MS analysis of sample 3 suggests that the organic medium in this sample consists of **diterpenic resin** (rosin or colophony) mixed with **linseed oil**. Protein indicators were also identified, as in the majority of natural 'non-protein binders' a minority of protein component is present too (Colombini & Modugno, 2009).

**NOTE:** casting in resin the fragments of plaster resulted in the fragments absorbing the resin when in the liquid state. This was visible in the BSE image as well as through the EDS mapping (Tiranti resin and catalyst are mainly made of organic compounds C, H and O). Aluminium (Al) traces are present in all the samples, due to the polishing chemical.

## Sample 1



**Sampling.** This fragment, already detached, was taken from the PR, under two figures.



Above: Overlapped (OM and BSE) cross-section image showing the stratigraphy (blue indicators).

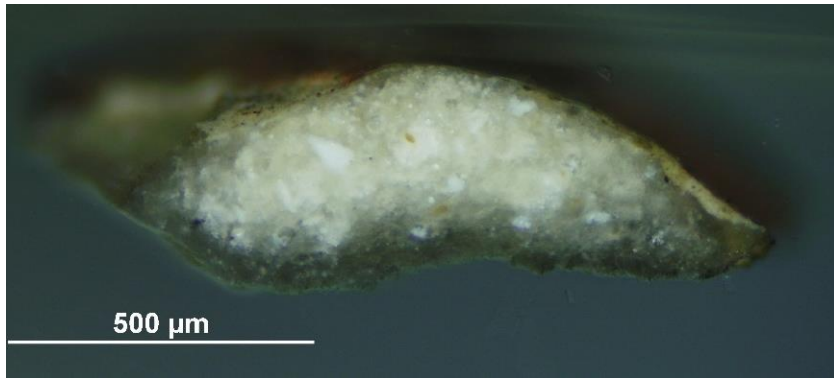
### 2. Varnish layer

#### 1. White layer

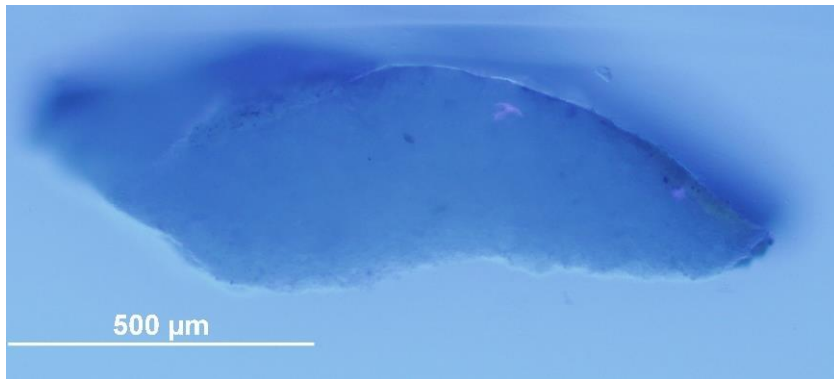
#### 0. Plaster bulk

**Analysis spots.** EDS analysis (yellow): Spectra 1-3; FT-IR analysis (red): nos. 33-43.

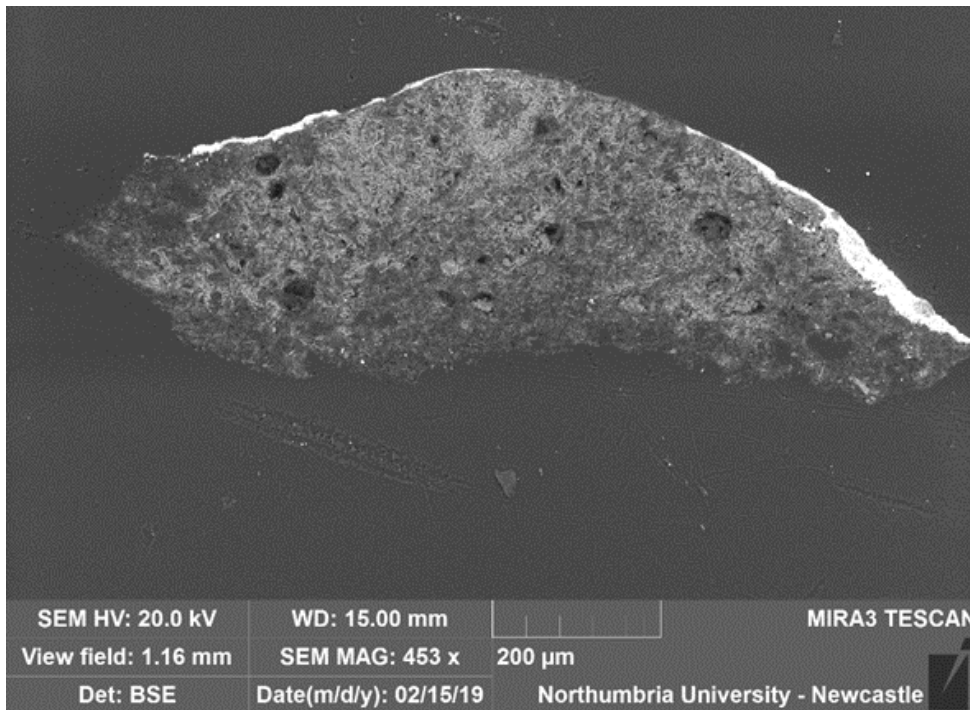
**Summary.** The substrate (layer 0) is made of plaster (**calcium sulfate**,  $\text{CaSO}_4$ , confirmed by EDS, XRD and by the peak at  $1600\text{ cm}^{-1}$  and overtones in the FT-IR spectra) and contains **Si-Al inclusions** (see EDS mapping). Layer 1, white under visible illumination, is mostly made of **lead (Pb)** and traces of Cl, Al, Si and Fe. Layer 3 is bright under UV illumination, suggesting that it might consist of a (synthetic) varnish. A **wax or resin** (FT-IR peaks at  $1472$  and  $2800\text{-}3000\text{ cm}^{-1}$ , and  $1744\text{ cm}^{-1}$  that suggests ester-containing wax or the additional presence of oil) was detected in all the layers.



VLR OM (left)



UVfOM (left)



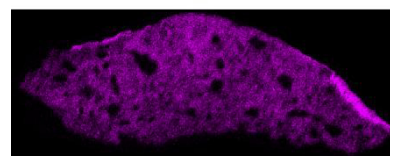
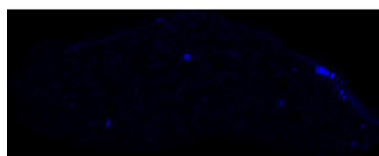
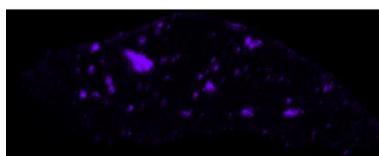
BSE image (left).

The tabular crystalline structure typical of gypsum plaster can be seen in layer 0. Inclusions made of Si and Al are present in layer 0 and layer 1 is mostly made of Pb and Si as shown in the EDS mapping (below).

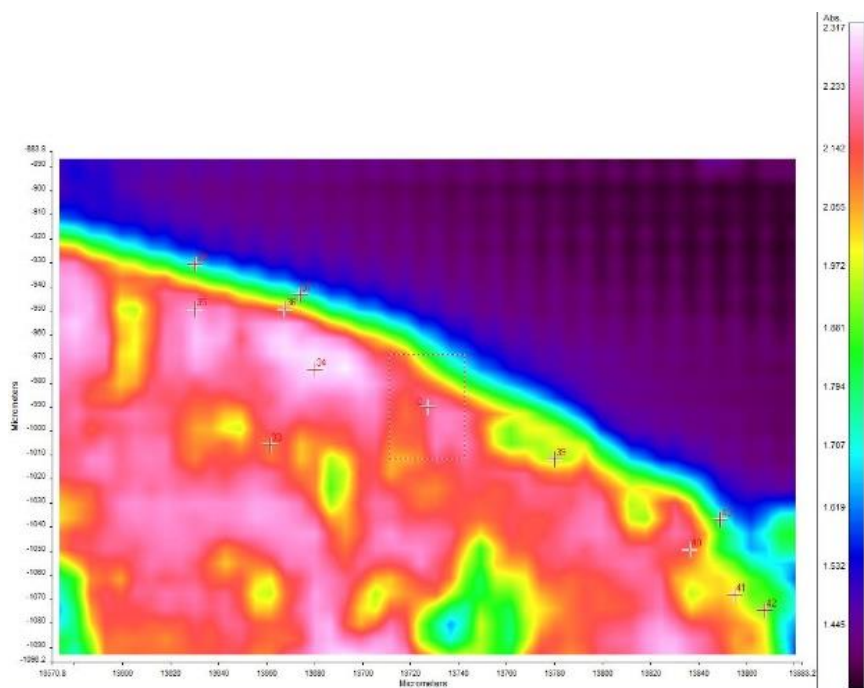
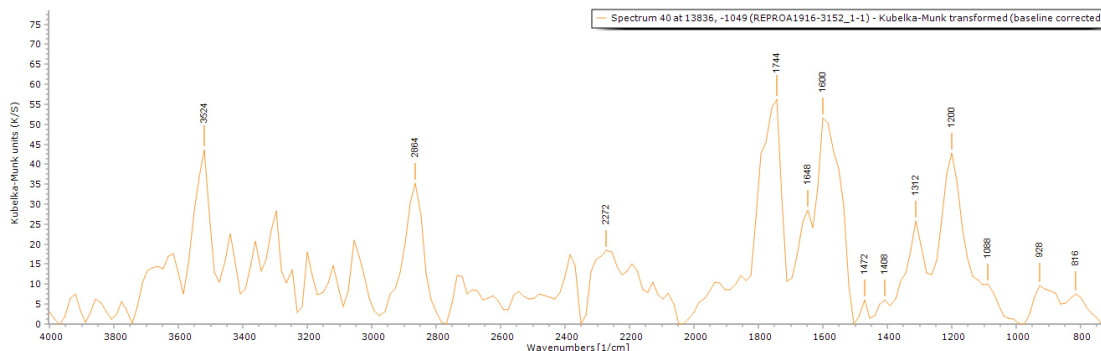
Aluminium (Al)

Silicon (Si)

Lead (Pb)



**XRD results.** A fragment of this sample was pulverised and analysed by XRD. It was possible to identify the partial profile of gypsum (calcium sulfate) and the diffractogram was compared to references from the Rigaku SmartLab Database and the most significant peaks were at  $2\theta = 29.34, 31.39, 33.63, 43.65$ . The partial match is due to the small quantity of sample available for the analysis and analysis settings.

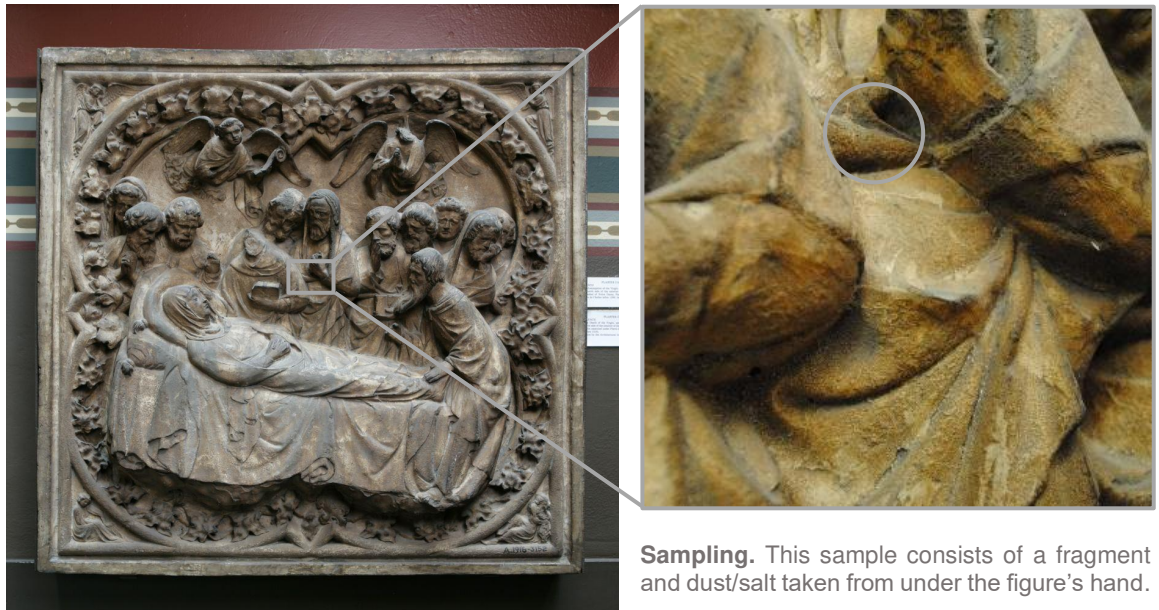


**FT-IR spectrum 40** (above) of layers 1-2. Peaks for the casting resin ( $1312, 1760\text{ cm}^{-1}$ ), gypsum ( $1600\text{ cm}^{-1}$ ), overtone  $2200\text{-}2300\text{ cm}^{-1}$  and a wax/resin ( $1200, 1408, 1472, 2864\text{ cm}^{-1}$ ) and the  $1744\text{ cm}^{-1}$  C=O ester carbonyl peak. A summary of the peaks observed in the spectra 33-43 can be seen in the table below.

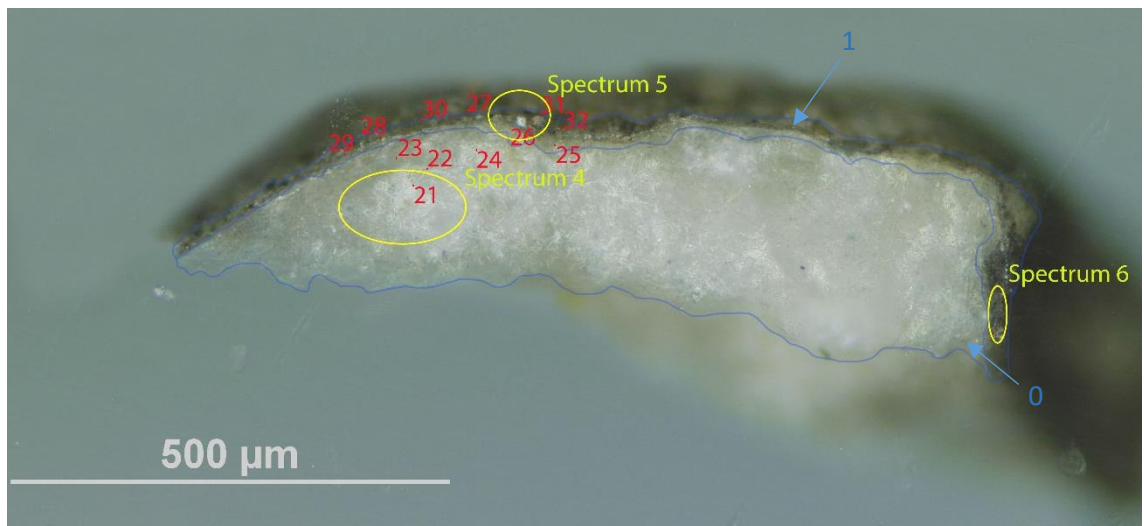
**FT-IR (FPA) image** (left) shows that the utmost layer is made of a material with a different reflectance.

Spectrum	Layer	peaks (cm-1)						
		Casting Resin	Gypsum	Carbonate	Wax/resin	C=O ester carbonyl	SO overtone	Unknown
33	0	1328	1600, 1680	800	880, 928, 1008, 1104, 1216, 1392, 1408, 1488, 2880, 2960	1744	2240	1968
34	0			800, 1776	860, 992, 1088, 1216, 1296, 1344, 1392, 1472, 1584, 1664, 2848, 2944		2240	1968
35	0	1760	1616		848, 912, 1008, 1088, 1248, 1344, 1472, 1568, 2864, 2912		2208	
36	1-2	1328, 1760	1616		880, 1024, 1088, 1200, 1472, 2848		2224	
37	1-2	1328, 1760	1616		784, 848, 1088, 1168, 1504, 2816, 2960		2368	
38	1-2	1312, 1760	1632		784, 848, 1008, 1088, 1168, 1472, 1536, 2880, 2960			
39	1-2	1312, 1760	1600	800	864, 1088, 1136, 1216, 1408, 1520, 2816, 2928		2320	1968
40	1-2	1312, 1760	1600, 1648		816, 928, 1088, 1200, 1408, 1472, 2864	1744	2272	
41	1-2	1328, 1760	1632		784, 912, 992, 1004, 1200, 1456, 1568, 2896, 2944		2288	
42	1-2	1328		800	896, 1008, 1088, 1184, 1504, 1584, 2800, 2880, 2928	1744		1856
43	1-2	1328, 1760	1616	800	1184, 1472, 1504, 2816, 2960		2304	

## Sample 2



**Sampling.** This sample consists of a fragment and dust/salt taken from under the figure's hand.



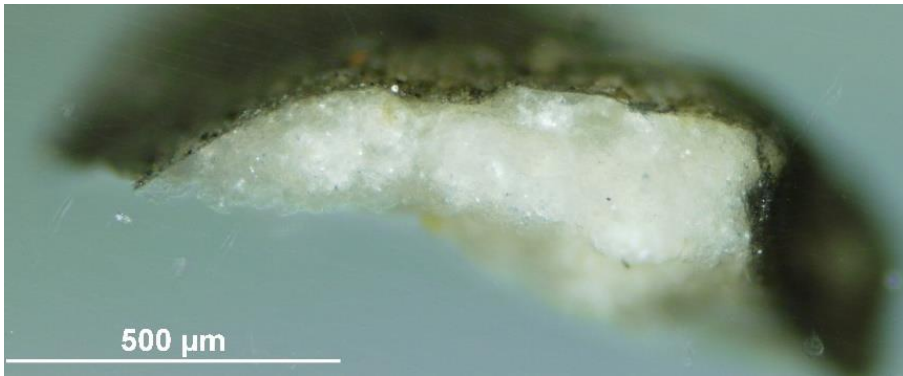
Above: Overlapped (OM and BSE) cross-section image showing the stratigraphy (blue indicators).

**1. Dark layer**

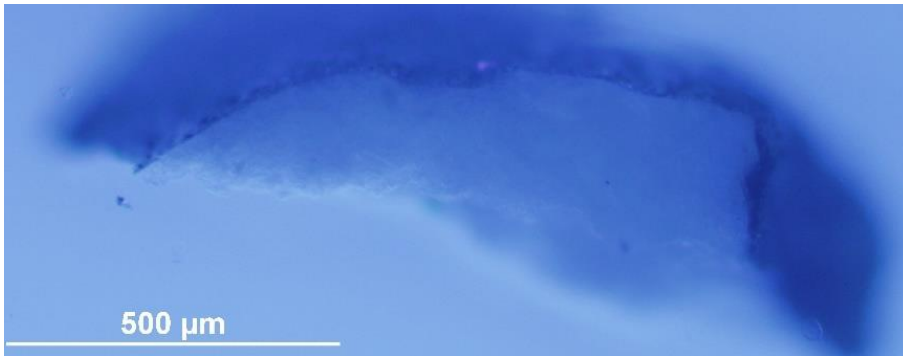
**0. Plaster bulk**

**Analysis spots.** EDS analysis (yellow): Spectra 4-6; FT-IR analysis (red): nos. 21-32.

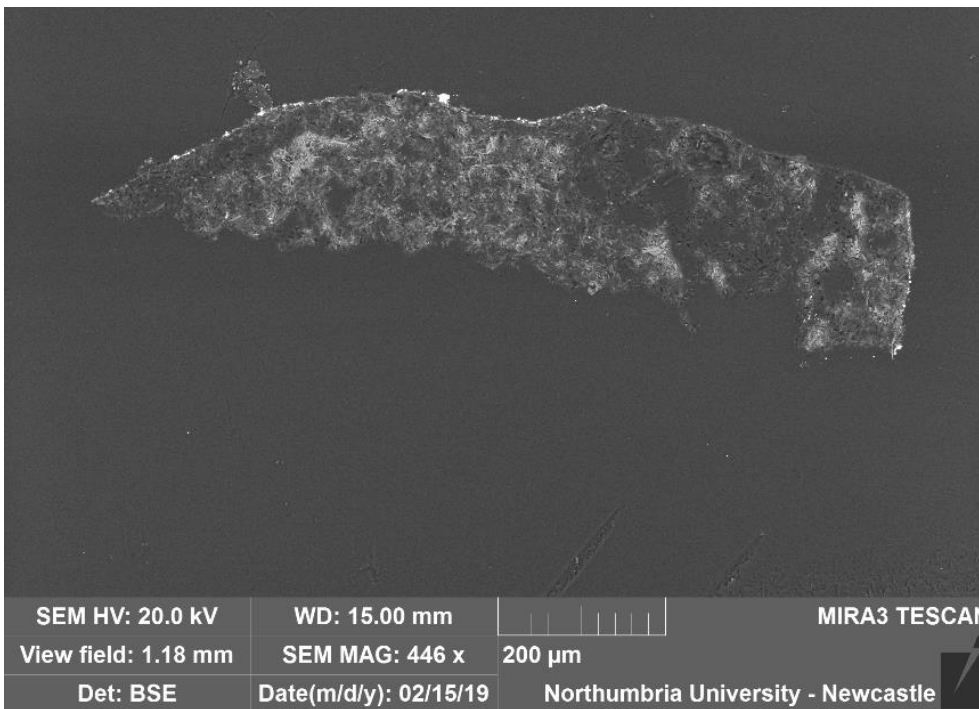
**Summary.** The substrate (layer 0) is made of plaster (**calcium sulfate**,  $\text{CaSO}_4$ , confirmed by EDS and by the peak at  $1600\text{-}1648\text{ cm}^{-1}$  and overtones in the FT-IR spectra). Si and Al are present in layers 0 and 1 and layer 1 also presents Pb, Cl, Mg, Fe and K. A **wax or resin** (FT-IR peaks at  $1200\text{-}1500$  and  $2800\text{-}3000\text{ cm}^{-1}$ ) was detected in all the layers.



VLR OM (left)



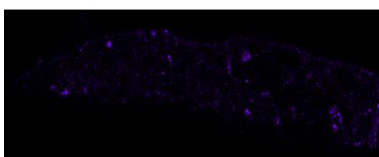
UVfOM (left)



BSE image (left).

The tabular crystalline structure typical of gypsum plaster can be seen in layer 0. Inclusions made of Si and Al are present in layer 0 and lead (Pb) is present in layers 0 and 1 (see EDS mapping below).

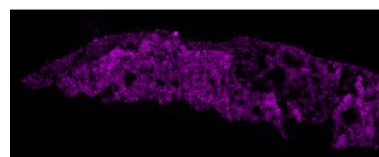
Aluminium (Al)

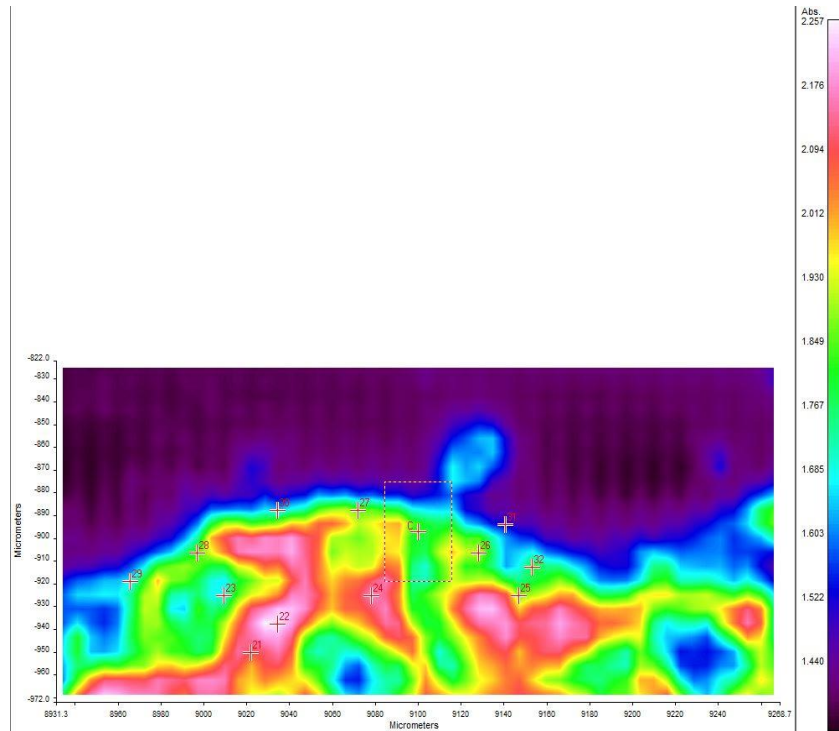
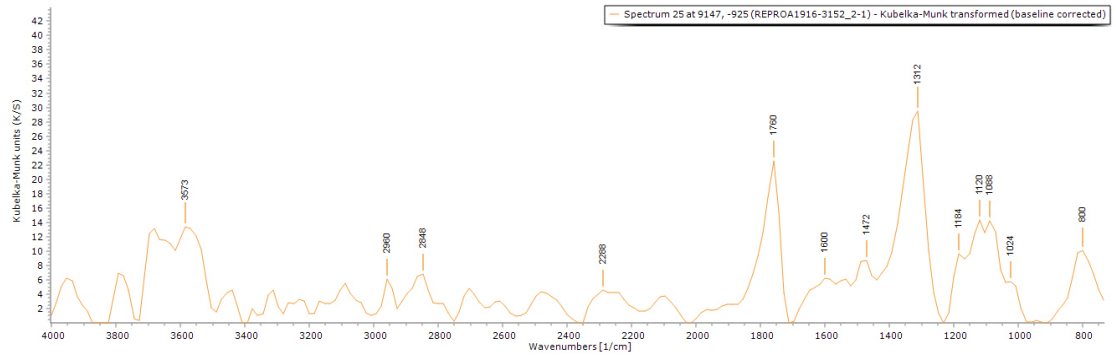


Silicon (Si)



Lead (Pb)





**FT-IR spectrum 25** (above) of layer 1. Peaks for the casting resin (1312, 1760  $\text{cm}^{-1}$ ), gypsum (1600  $\text{cm}^{-1}$ , overtone 2200-2300  $\text{cm}^{-1}$ ) and a wax/resin (1184, 1472, 2848 and 2960  $\text{cm}^{-1}$ ). A summary of the peaks observed in the spectra 21-32 can be seen in the table below.

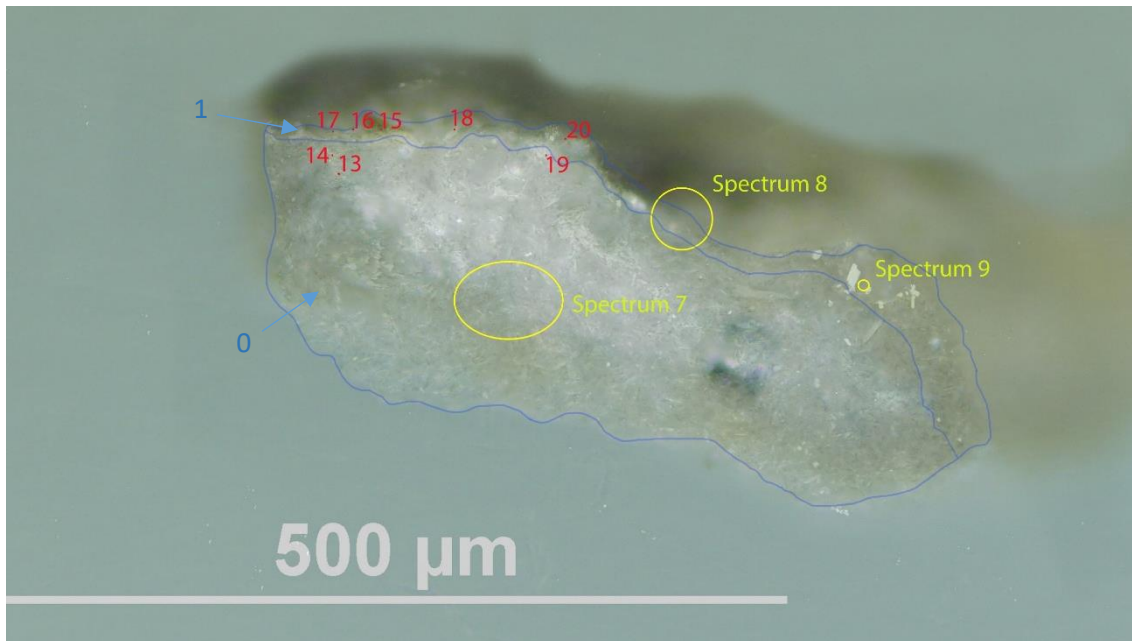
**FT-IR (FPA) image** (left) does not show differences in a layer fashion.

Spectrum	Layer	peaks (cm-1)						
		Casting Resin	Gypsum	Carbonate	Wax/resin	C=O ester carbonyl	SO overtone	Unknown
21	0	1312, 1760	1600, 1648		848, 1088, 1392, 1456, 2720, 2832, 2976			2224
22	0	1312		800, 1776	864, 1088, 1232, 1392, 1504, 1584, 2800, 2864		2144, 2240, 2416	
23	0	1312, 1760			768, 816, 1120, 1216, 1472, 1536, 2880		2464	
24	0	1312, 1760	1680	800	1024, 1088, 1216, 1376, 1440, 1536, 1584, 2864		2208	
25	1	1312, 1760	1600	800	1024, 1088, 1120, 1184, 1472, 2848, 2960		2288	
26	1	1312, 1760	1616	800	896, 1200, 1472, 1552, 2896		2368	1840
27	1	1312, 1760			784, 816, 1024, 1088, 1152, 1392, 1520, 1664, 2816, 2928		2288	
28	1	1312, 1760	1648	800	1136, 1520, 2944		2480	
29	1	1312, 1760	1648	800	1184, 1392, 1520, 2816, 2896		2224	
30	1	1312, 1760	1600		1168, 1392, 1504		2336	
31	1	1312, 1760	1616		784, 896, 1088, 1168, 1392, 1504		2224	
32	1	1312, 1760	1632		784, 1088, 1184, 1392, 1472, 1552, 2864		2336	

## Sample 3



**Sampling.** This fragment, already detached, was taken from an area of crack, bottom PR edge.



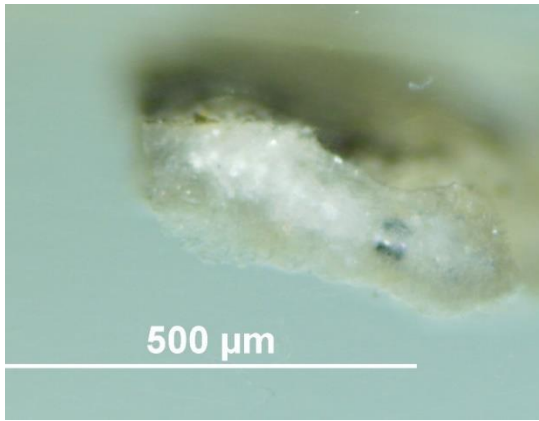
Above: Overlapped (OM and BSE) cross-section image showing the stratigraphy (blue indicators).

**1. Dark layer**

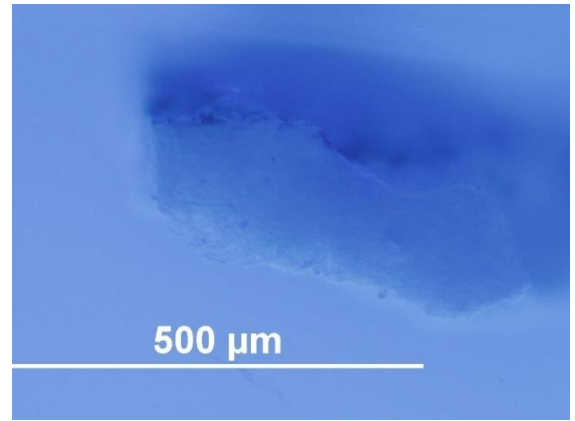
**0. Plaster bulk**

**Analysis spots.** EDS analysis (yellow): Spectra 7-9; FT-IR analysis (red): nos. 13-20.

**Summary.** The sample is mostly made of C, O, S and Ca (**calcium sulfate**,  $\text{CaSO}_4$ , confirmed by EDS and by the peak at  $1600\text{-}1648\text{ cm}^{-1}$  and overtones in the FT-IR spectra). Al is overall present as used as a polishing agent, but also relevantly present in the silicon inclusion, especially as the major component of layer 1 together with Si, Sr and traces of Ba (see EDS mapping). The structure typical of gypsum plaster can be seen in layer 0, which also shows Si, K and Sr inclusions. A **wax or resin** is suggested by FT-IR (peaks at  $1000\text{-}1200$  and  $2800\text{-}3000\text{ cm}^{-1}$ ) and py-TMAH-GC/MS shows markers characteristic of **diterpenoid resins**, possibly mixed with a non-drying oil or a *tempera grassa*. Amine fragments were also identified, as in the majority of natural 'non-protein binders' a minority of protein component is present too (Colombini & Modugno, 2009).



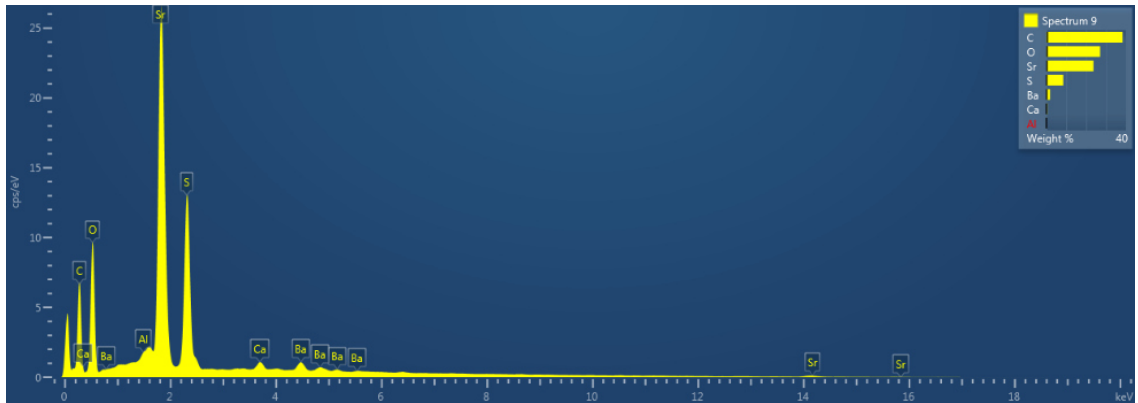
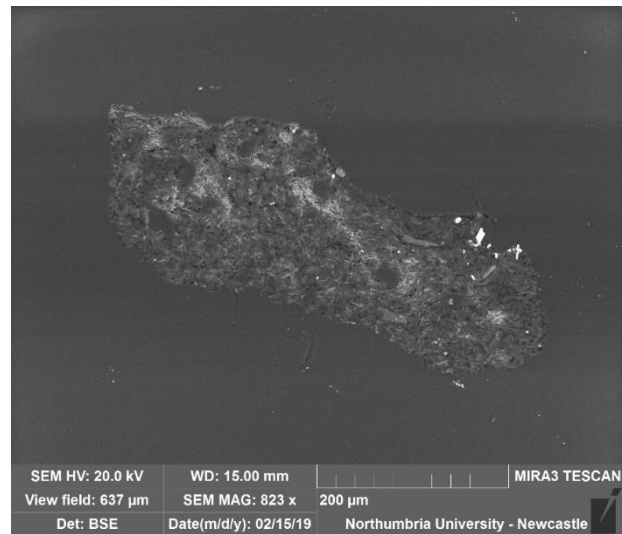
VLR OM (above)



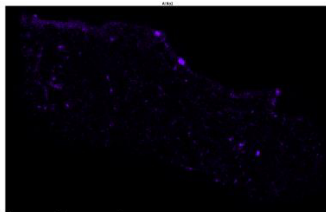
UVfOM (left)

**BSE image (right).** The tabular crystalline structure typical of gypsum plaster can be seen in layer 0. **Calcium sulfate** ( $\text{CaSO}_4$ ) was detected in all the layers and the brightest particles consist of **barium** and **strontium** as shown in spectrum 9 (below).

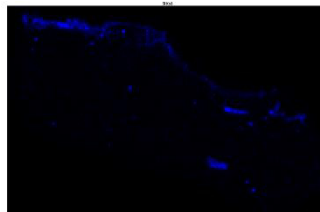
**EDS mapping (bottom)** shows that layer 1 is mostly made of aluminium (Al), silicon (Si) and strontium (Sr).



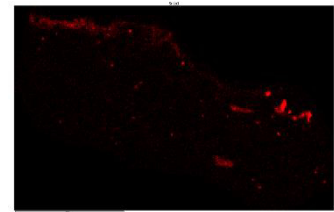
Aluminium (Al)

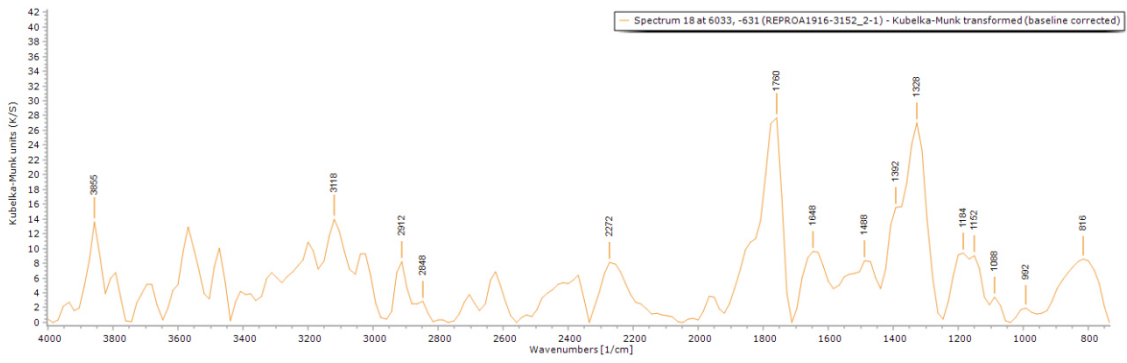


Silicon (Si)

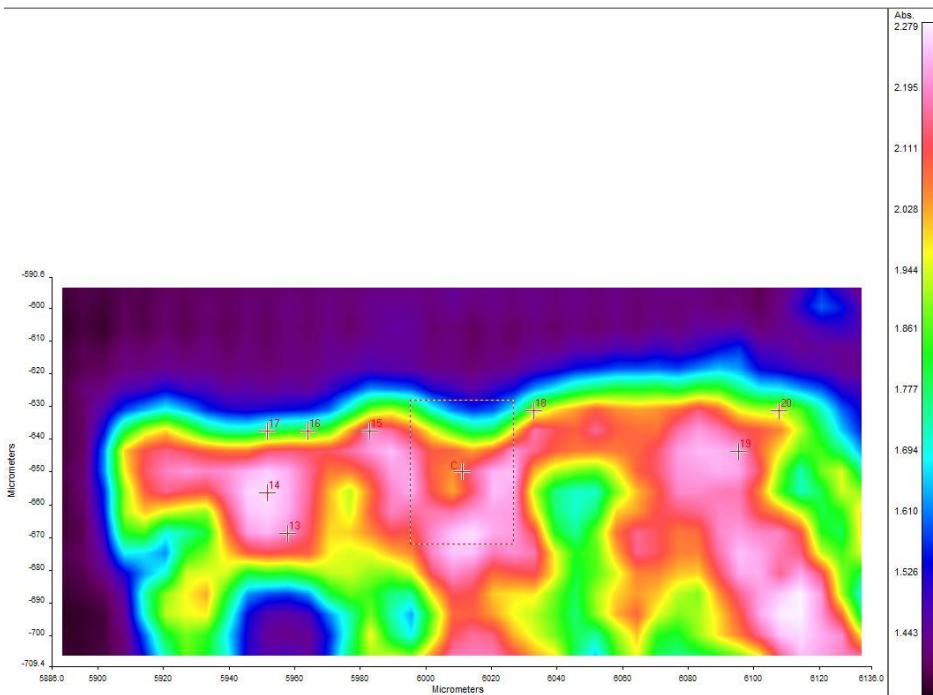


Strontium (Sr)



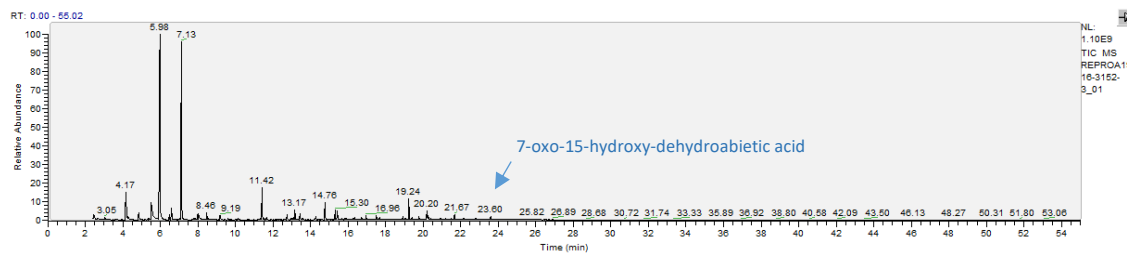


**FT-IR spectrum 18 (above) of layer 1.** Peaks for the casting resin (1328, 1760  $\text{cm}^{-1}$ ), gypsum (1648 $\text{cm}^{-1}$ ) and a wax/resin (1000-1200, 1488 and 2800-2900  $\text{cm}^{-1}$ ). A summary of the peaks observed in the spectra 13-20 can be seen in the table below.



**FT-IR (FPA) image (left).** No clear layer definition can be observed in the FPA image.

Spectrum	Layer	peaks (cm <sup>-1</sup> )						
		Casting Resin	Gypsum	Carbonate	Wax/resin	C=O ester carbonyl	SO overtone	Unknown
13	0	1312	1632		784, 896, 976, 1088, 1136, 1216, 1504, 1568, 2880, 2960	1744	2256	1824
14	0	1312		1776	784, 848, 944, 1104, 1216, 1392, 1488, 1568, 2864		2384	1824
15	1	1312, 1760	1600	800	1200, 1440, 1488, 2848, 2928		2384	1824
16	1	1312, 1760	1664	800	912, 1088, 1184, 1408, 1488, 2864, 2944		2256	
17	1	1312, 1760	1600		768, 832, 1088, 1184, 1472, 2800, 2896		2368	
18	1	1328, 1760	1648		816, 992, 1088, 1152, 1184, 1392, 1488, 2848, 2912		2272	
19	0	1328, 1760	1600		848, 944, 1072, 1136, 1200, 1392, 1472, 1552, 2864, 2992		2384	1808
20	1	1312, 1760	1616	800	1088, 1168, 1392, 1520, 2848, 2928		2384	



RT	m/z	Assignment	Formula
4.17	45(100), 59(7), 74(67)	Ethyl ether	C4H10O
4.85	44(9), 59(100), 73(14), 88(5)	3-Pentanol, 2-methyl-	C6H14O
5.53	42(10), 58(100), 72(9), 88(6), 116(5)	1,2-Ethanediamine, N'-ethyl-N,N-dimethyl-	C6H16N2
5.98	42(12), 58(100), 117(17)	N,N-dimethyl-	C6H16N2
6.47	45(23), 58(51), 66(22), 79(20), 95(100), 125(7)	Sulfuric acid, dimethyl ester	C2H6O4S
6.59	58(9), 65(16), 79(100), 95(11), 109(6)	Methanesulfonic acid, methyl ester	C2H6O3S
7.13	42(6), 58(100), 70(9), 116(6)	1,2-Ethanediamine, N'-ethyl-N,N-dimethyl-	C6H16N2
11.67	44(30), 58(100), 71(27), 74(18), 98(73), 108(16), 127(88), 139(14), 267(5), 355(5)	Monoacylglycerol fragment	
12.74	42(9), 58(100), 85(2), 113(2), 175(3)	Unidentified amine fragment	
13.17	56(15), 71(14), 88(24), 98(31), 116(41), 130(100), 141(6), 189(5)	Unidentified terpenoid fragment	
13.43	58(9), 72(100), 91(5), 115(5), 130(5), 147(40)	Unidentified amine fragment	
14.29	44(16), 58(43), 86(90), 91(21), 115(23), 133(54), 143(16), 161(100), 176(17)	Unidentified terpenoid fragment	
14.76	58(11), 84(7), 109(6), 116(100), 128(6), 139(13), 152(5), 173(5)	Unidentified amine fragment	
15.3	58(10), 84(4), 99(4), 116(100), 149(5), 173(5)	Unidentified amine fragment	
15.42	58(19), 75(5), 77(28), 91(40), 105(25), 119(100), 133(25), 149(81), 165(70), 180(57)	Unidentified terpenoid fragment	
16.96	45(100), 58(92), 75(36), 85(53), 91(25), 113(42), 125(38), 143(35), 171(40), 185(5), 194(5), 217(5)	Unidentified terpenoid fragment	
17.5	45(31), 55(83), 58(75), 74(79), 83(69), 87(32), 97(24), 111(61), 124(29), 143(38), 152(100), 177(5), 185(43)	methyl azelate	C10H18O4
19.24	45(77), 55(26), 71(44), 75(100), 85(76), 101(67), 115(22), 139(24), 152(15), 161(35), 170(5), 183(19), 215(5), 228(5), 260(5)	Unidentified terpenoid fragment	
20.2	45(99), 58(42), 71(64), 75(77), 85(85), 101(30), 115(34), 123(5), 139(31), 161(22), 183(5), 201(5), 215(5), 231(5), 246(5)	Unidentified terpenoid fragment	
21.67	55(19), 74(100), 87(63), 115(7), 129(8), 143(20), 171(6), 185(7), 199(7), 227(12), 239(5), 270(5)	methyl palmitate	C17H34O2
22.8	45(73), 58(100), 75(45), 91(28), 115(28), 149(24), 163(24), 177(5), 207(23), 251(5), 270(5), 299(5), 331(5)	7-oxo-15-hydroxy-dehydroabiatic acid	
23.6	58(41), 74(100), 87(65), 101(5), 115(10), 129(5), 143(25), 199(15), 255(13), 298(5)	methyl stearate	C19H38O2

RT = retention time, m/z = mass/charge ratio

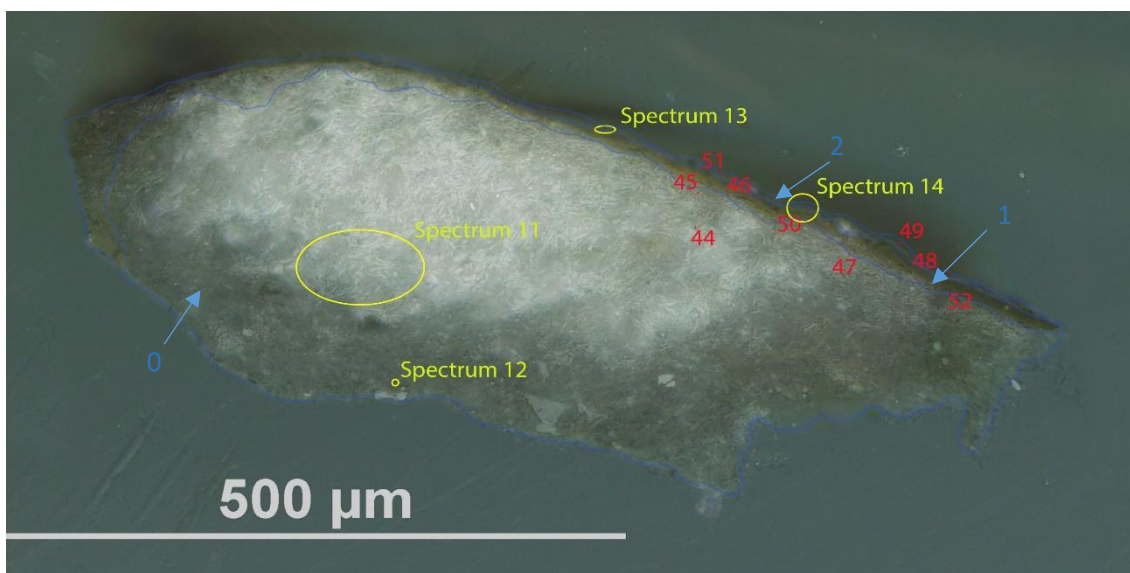
**Py-TMAH-GC/MS chromatogram**

(top and described in the table on the left) shows small fragments due to derivatization (from t = 4.21 to 7.13 min) and markers characteristic of **diterpenoid resins** (e.g. t = 22.80 min) and **pimarane** unidentified fragments (showing characteristic m/z = 133 and 161 peaks in the fragmentation pattern). The presence of **methyl azelate** (t = 17.50), **methyl palmitate** (t = 21.67) and **stearate** (t = 23.60) with **A/P = 0.55** and **P/S = 1.89** suggest that the resin has been mixed with a non-drying oil, a *tempera grassa* or that the FA detected are the ones naturally present in the natural resin. Amine fragments were also identified, as in the majority of natural 'non-protein binders' a minority of protein component is present too (Colombini & Modugno, 2009).

## Sample 4



**Sampling.** This fragment taken from an area of loss, PR edge.



Above: Overlapped (OM and BSE) cross-section image showing the stratigraphy (blue indicators).

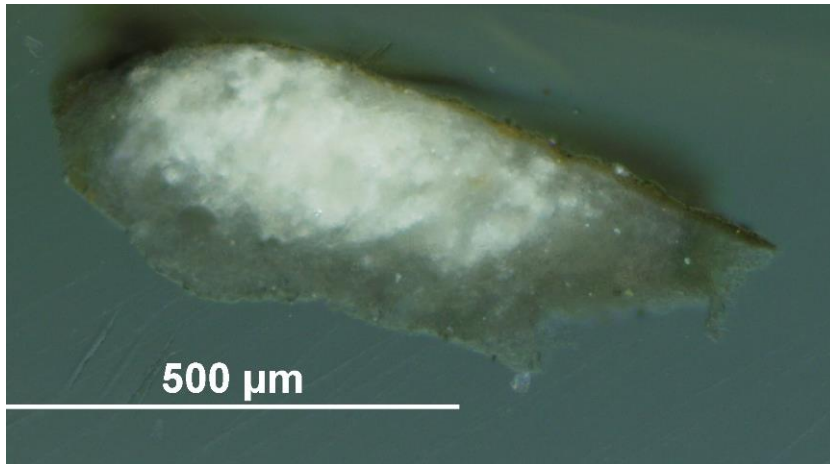
### 2. Varnish layer

### 1. Yellowish layer with dark inclusions

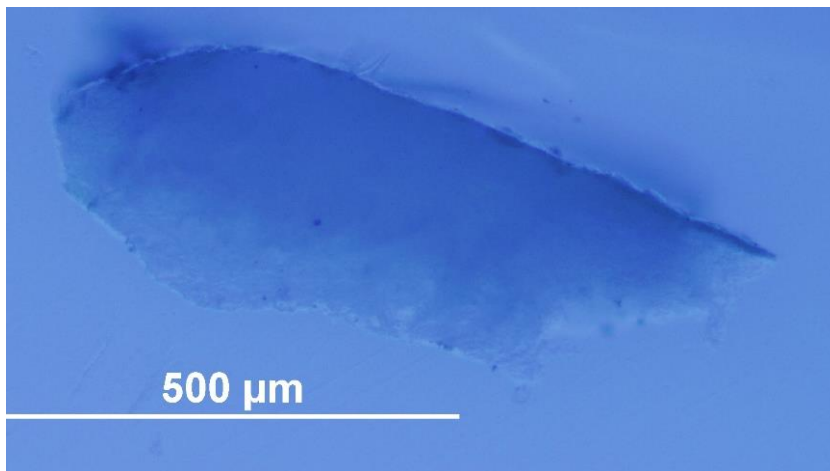
### 0. Plaster bulk

**Analysis spots.** EDS analysis (yellow): Spectra 11-14; FT-IR analysis (red): nos. 44-52.

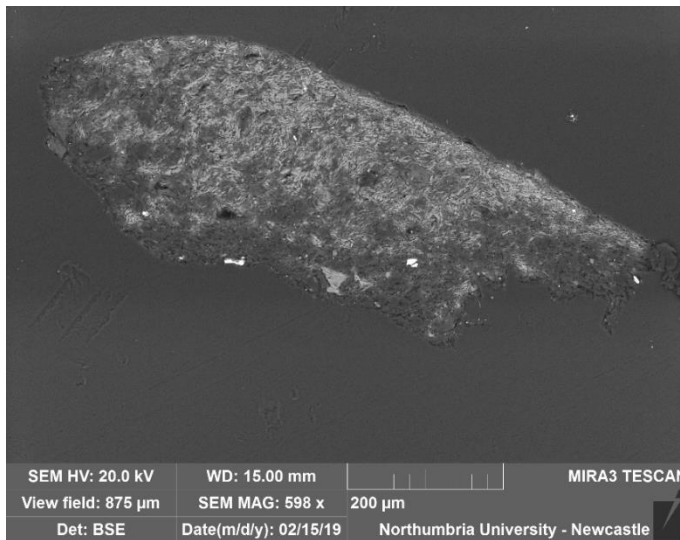
**Summary.** The sample is mostly made of C, O, S and Ca (**calcium sulfate**,  $\text{CaSO}_4$ , confirmed by EDS and by the peak at  $1600\text{-}1648\text{ cm}^{-1}$  and overtones area at  $200\text{-}2300\text{ cm}^{-1}$  in the FT-IR spectra). Al is overall present as used as a polishing agent, but could also, together with Sr and Si be present as part of silicate inclusions (confirmed by EDS mapping too). Traces of K, Na, Mg, Ti, Fe and Cl can be also seen in layers 1 and 2, which mostly consists of Sr. Al and Si as shown in the EDS mapping. The tabular structure typical of gypsum plaster can be seen in layer 0. Layer 1 appears dark yellow under the visible illumination and layer 2 fluoresces as a varnish under UV illumination; FT-IR peaks at  $1200\text{-}1400\text{ cm}^{-1}$  and  $2800\text{-}300\text{ cm}^{-1}$  suggests that it might be **wax or resin**, that was also detected in layers 0 and 1.



VLR OM ([left](#))



UVf OM ([left](#))



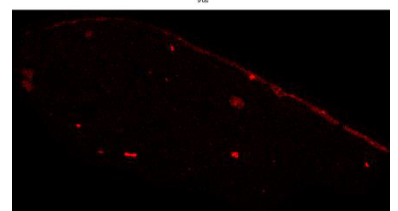
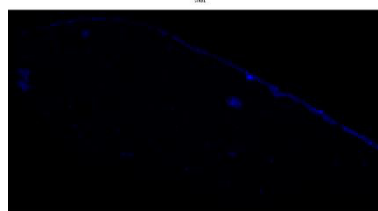
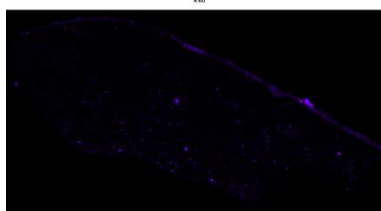
**BSE image** ([left](#)). The tabular crystalline structure typical of gypsum plaster can be seen in layer 0. The surface layers consist of Al, Si and Sr, which can be seen in the **EDS mapping** ([below](#)).

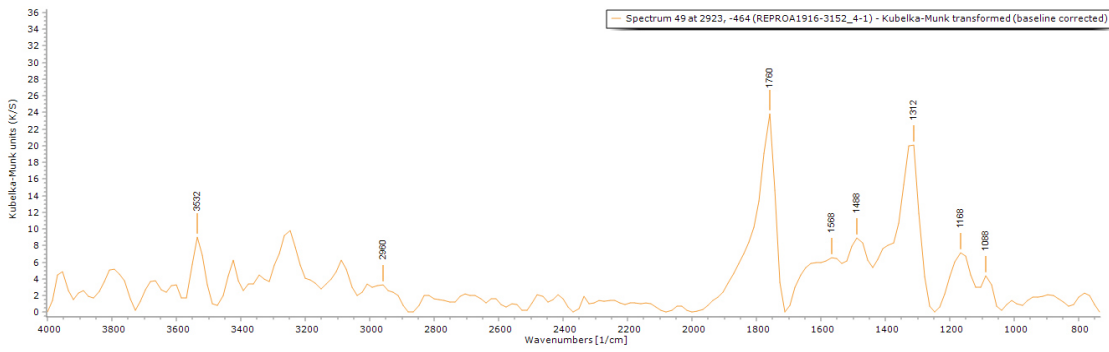
**EDS spectra** indicate that layers 0 and 1 consist of C, O, S, Ca, Al, Si and traces of K, Na, Mg, Ti, Fe, Cl can be also seen in layers 1 and 2.

Aluminium (Al)

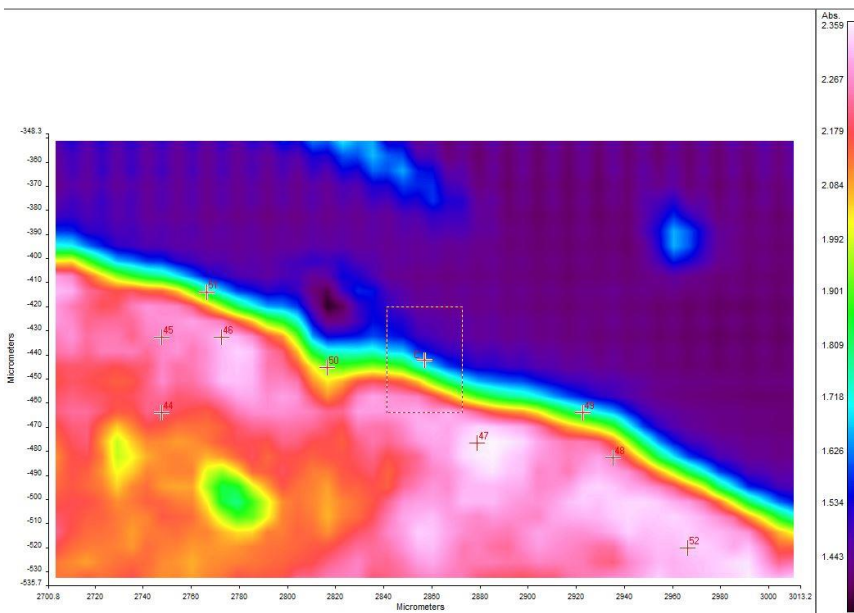
Silicon (Si)

Strontium (Sr)





**FT-IR spectrum 49** (above) of layer 2. Peaks for the casting resin (1312, 1760  $\text{cm}^{-1}$ ), gypsum (1600  $\text{cm}^{-1}$ ) and a wax/resin (1168, 1488, 1568 and 2960  $\text{cm}^{-1}$ ). A summary of the peaks observed in the spectra 44-52 can be seen in the table below.



**FT-IR (FPA) image** (left) shows that the utmost layer is made of a material with a different reflectance.

Spectrum	Layer	peaks ( $\text{cm}^{-1}$ )						
		Casting Resin	Gypsum	Carbonate	Wax/resin	C=O ester carbonyl	SO overtone	Unknown
44	0	1312, 1760	1616		864, 928, 1040, 1232, 1296, 1472, 2880, 2944		2240	1840
45	0	1344, 1761	1616		896, 1024, 1216, 1376, 1472, 1568, 2816, 2928		2272, 2448	
46	1	1328	1648	1776	784, 864, 928, 1072, 1232, 1376, 1424, 1568, 2880, 2944		2224	
47	0	1312		1776	864, 976, 1072, 1360, 1472, 2930		2396	
48	1	1312, 1760	1600, 1664		1104, 1216, 1376, 1424, 1488, 1552, 2832, 2880, 2944		2383	
49	2	1312, 1760			1088, 1168, 1488, 1568, 2960			
50	1	1328			870, 1216, 1408, 1552, 1680		2289	
51	2	1312, 1760	1600		784, 944, 1024, 1088, 1184, 1392, 1472, 2848		2368	
52	0	1328, 1760	1600		752, 848, 1008, 1104, 1232, 1376, 1424, 1488, 1696, 2800, 2992		2208	

## Experimental

The object was observed, and its conditions were documented. Samples from selected areas were taken by Valentina Risdonne. When possible, each sample was split into two parts: one fragment was embedded in polyester resin (Tiranti clear casting resin), polished and analysed under an optical microscope and the other was put aside for py-TMAH-GC/MS.

The optical microscopy was performed with an Olympus BX51 Metallurgical Microscope equipped with four objectives (magnification of x5, x20, x50 and x100), and an x10 eyepiece. In many instances, a small amount of white spirit was applied on the surface of the cross-section to improve the saturation under the microscope. The microscope is equipped with a 6-cube filter turret which allows operating the system in reflected visible light (brightfield and darkfield mode) and reflected UV light (365 nm) using a 100 W mercury burner.

The SEM-EDS analysis was performed with a field emission TESCAN MIRA 3 with gigantic chamber. The SEM is equipped with: secondary electron detector (SE), secondary electron in-beam detector (In-beam SE), back-scatter detector (BSE), back-scatter in-beam detector (In-beam BSE), cathodoluminescence detector (without wavelength detection) (CL), plasma chamber/sample cleaner and software Alicona 3D imaging. For the EDS analytical part, it has an Oxford Instruments setup: Software: AztecEnergy, X-ray detector X-Max 150 mm<sup>2</sup> and X-ray detector X-Max Extreme, low energy detector for thin films, high resolution and low voltage. The samples were analysed by SEM-EDS Low Vacuum Mode (10-15 Pa). EDS Mapping and data processing were performed with Aztec Oxford software.

A Perkin Elmer Frontier FT-IR spectrometer (350 cm<sup>-1</sup> at the best resolution of 0.4 cm<sup>-1</sup>) was used, equipped with a germanium crystal for ATR measurements and combined with a Spectrum Spotlight 400 FT-IR microscope equipped with a 16×1 pixel linear mercury cadmium telluride (MCT) array detector standard with InGaAs array option for optimised NIR imaging. Spectral images from sample areas are possible at pixel resolutions of 6.25, 25, or 50 microns. The Perkin Elmer ATR imaging accessory consists of a germanium crystal for ATR imaging. These run with Perkin Elmer Spectrum 10™ software and with SpectrumIMAGE™ software. Baseline and Kubelka-Munk corrections were applied to the raw data acquired in diffuse reflectance.

The XRD analyses were performed with a Rigaku SmartLab SE equipped with a HyPix-400, a semiconductor hybrid pixel array detector and Cu source. The analyses were performed in Bragg-Brentano geometry mode, with 40 kV tube voltage and 50 mA tube current. The diffractograms were processed with a SmartLab II software. The data was compared to the RUFF database (Lafuente et al., 2016) and COD Database (Gražulis et al., 2009).

The instrument used for GC/MS is a Thermo Focus Gas Chromatographer with DSQ II single quadrupole mass spec. The column currently installed is a Agilent DB5-MS UI column (ID: 0.25 mm, length: 30 m, df: 0.25 µm, Agilent, Santa Clara, CA, USA). Carrier gas: helium. Detector temperature: 280 °C, Injector temperature: 250 °C. It can be used with the PyroLab 2000 Platinum filament pyrolyser (PyroLab, Sweden) attachment or in split/splitless mode. Detection: Total Ion monitoring (TIC). 1 µl of the sample with 1 µl of TMAH was placed on the Pt filament for the py-GC/MS. The inlet temperature to the GC was kept at 250 °C. The helium carrier gas flow rate was 1.5 ml/min with a split flow of 41 ml/min and a split ratio of 27. The MS transfer line was held at 260 °C and the ion source at 250 °C. The pyrolysis chamber was heated to 175 °C, and pyrolysis was carried out at 600 °C for 2 s. This run with Xcalibur™ and PyroLab™ software. The library browser supported NIST MS Version 2.0 (Linstrom & Mallard, 2014).

Valentina Risdonne, PhD student

[v.risdonne@vam.ac.uk](mailto:v.risdonne@vam.ac.uk) / [valentina.risdonne@northumbria.ac.uk](mailto:valentina.risdonne@northumbria.ac.uk)

Victoria and Albert Museum – Northumbria University

PhD project 'Materials and techniques for coating of the nineteenth-century plaster casts'

©V&A Museum

14 September 2020

## Notes

18 January 2019	Sampling	Valentina's PhD Lab book 1, page 149
4 February 2019	Casting	Valentina's PhD Lab book 1, page 162
11 February 2019	Microscopy	Valentina's PhD Lab book 1, page 168
14 October 2019	FT-IR	Valentina's PhD Lab book 1, page 175
3 December 2019	XRD	Valentina's PhD Lab book 2, page 4
18 March 2020	GC/MS	Valentina's PhD Lab book 2, page 50

A full record of analysis is available at <https://doi.org/10.25398/rd.northumbria.14040224>

## References

- Colombini, M. P., & Modugno, F. (2009). *Organic mass spectrometry in art and archaeology*. John Wiley & Sons.
- Cox, K. G., Price, N. B., & Harte, B. (1974). *An introduction to the practical study of crystals, minerals, and rocks*. Halsted Press.
- Gražulis, S., Chateigner, D., Downs, R. T., Yokochi, A. F. T., Quirós, M., Lutterotti, L., Manakova, E., Butkus, J., Moeck, P., & Le Bail, A. (2009). Crystallography Open Database—an open-access collection of crystal structures. *Journal of Applied Crystallography*, 42(4), 726–729.
- Lafuente, B., Downs, R. T., Yang, H., & Stone, N. (2016). The power of databases: the RRUFF project. In *Highlights in mineralogical crystallography* (pp. 1–29). Walter de Gruyter GmbH.
- Linstrom, P. J., & Mallard, W. G. (2014). *NIST Chemistry WebBook, NIST standard reference database number 69, National Institute of Standards and Technology, Gaithersburg MD, 20899*.
- Price, B. A., Pretzel, B., & Lomax, S. Q. (2009). *Infrared and Raman Users Group Spectral Database; 2007 ed. IRUG: Philadelphia, PA, USA*.



**Northumbria  
University**  
NEWCASTLE

Analysis Report - Valentina Risdonne

Copy of a relief - The Entombment of the Virgin

(REPRO.A.1916-3153)

Initiator: Charlotte Hubbard; Conservation Department

9 September 2020

© Victoria and Albert Museum



## Analysis Report - The Entombment of the Virgin (REPRO.A.1916-3153)

### Contents

Contents .....	338
List of abbreviations.....	338
Summary .....	339
Sample 1 .....	342
Sample 2 .....	346
Sample 3 .....	347
Sample 4 .....	351
Experimental.....	354
Notes.....	355
References.....	355

### List of abbreviations

BSE	Back Scattered Electron
EDS	Energy Dispersive Spectrometry
FT-IR	Fourier-Transform Infra-Red
FPA	Focal Plane Array
GC/MS	Gas Chromatography-Mass Spectrometry
OM	Optical Microscopy
PL	Proper Left
PR	Proper Right
py	pyrolysis
SEM	Scanning Electron Microscopy
TMAH	tetramethylammonium hydroxide
UVf	Ultraviolet Fluorescence
VLR	Visible Light Reflectance
XRD	X-ray Diffraction

## Summary

The bulk of the object is made of gypsum plaster, which contains several types of inclusions (including silicates and carbonates). A layer of dust/dirt can be seen only in sample 4, which was likely taken from a repainted area, showing a different layer of zinc-barium white paint. The utmost layer of samples 1 and 3 are made of **aluminium**, **silicon** and **iron** and the organic medium consist of **diterpenic resin** (rosin or colophony) possibly mixed with **drying oil**.



Figure 1. The copy of a relief.

The object, '**Copy of a relief - The Entombment of the Virgin (REPRO.A.1916-3153)**' (Figure 1), is a plaster cast of a relief, with a representation of the Entombment of the Virgin executed under Pierre de Chelles (active about 1287; d. 1320). The original was carved in stone between 1296 and 1316, on the north side of the exterior of the apse of Notre Dame, Paris. The cast was made ca. 1850-1900 and given by the Architectural Association in 1916. The cast is now located in Gallery 46A (The Ruddock Family Cast Court), displayed upright. Its dimensions are 61.5x53.5 cm.

Conservation was carried out by the **conservator Sayuri Morio** after the sampling procedure hereinafter discussed (**record from May 2019**). The visual examination of the object showed that is structurally sound despite few straight joint lines and cracks are

visible. The conservator described the entire surface of the object as 'brown' and very dusty. The bottom of the object has a shiny waxy texture; a small area of flaky surface, a small amount of red paint and salt efflorescence can be also seen. There is a museum number written on the proper bottom left, and a star mark on the proper top right. The object was examined under UV light: the surface fluoresced in mid-tone purple and small areas of overpaints are visible on the proper top left corner. Samples from the reliefs were analysed by **XRF** (in-house at the V&A by **Dr Lucia Burgio**) to check if any hazardous material was present and none were detected. The dark colouration of the surface can be related to the presence of iron oxides. The object was dusted with brush and vacuum. Selected areas were cleaned with a smoke sponge to remove surface dirt, and sky-facing surfaces with Britzfix® sponge lightly dampened with deionised water. To remove the dark grim on the pronounced area, latex poultice method was used, applied with a nylon brush and followed by cleaning with a dampened Britzfix® sponge with deionised water. The red museum paint was removed with acetone on a cotton swab. Paint losses and chipped areas were sealed with Paraloid® B44 5% in acetone and IMS, then were retouched with acrylic paint.

Samples from the plaster cast were taken from pre-existing areas of loss to investigate the stratigraphy and the method of manufacture (Figure 2). The samples were analyzed to provide data for the study of the objects of the Cast Courts collection within the PhD project 'Materials and techniques for coating of the nineteenth-century plaster casts'. Details on the experimental procedure are available in the Experimental section of this report. A selection of significant results is shown in the following pages and the relevant database of analysis (<https://doi.org/10.25398/rd.northumbria.14040251>).

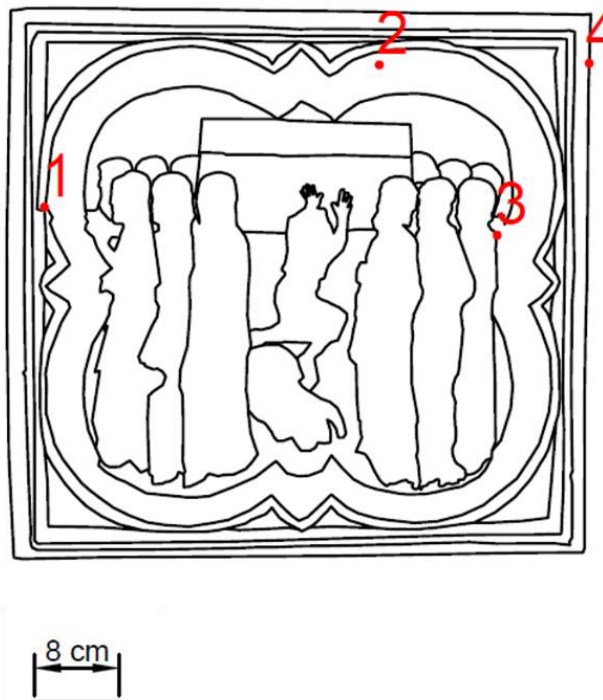


Figure 2. The relief outline with marked sampling sites.

**Sample 1:** fragment taken from an area of loss on the relief's PR.

**Sample 2:** dust taken from the top portion of the relief.

**Sample 3:** fragment taken from an undercut area on the PL of the relief.

**Sample 4:** fragment taken from an area of loss from the PL edge.

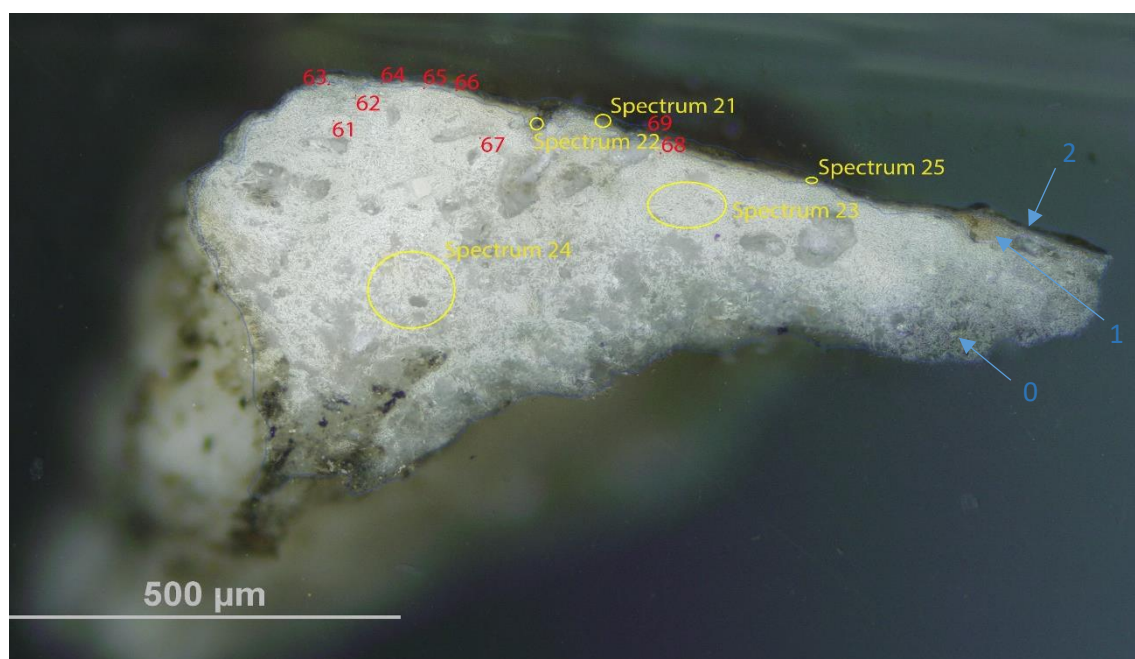
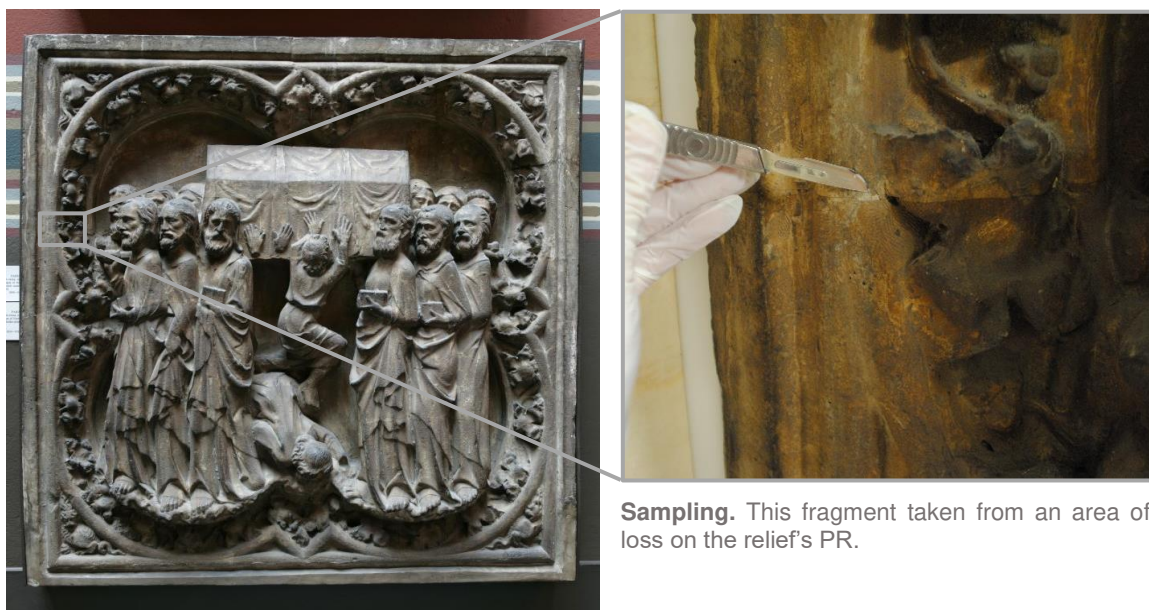
The **substrate** (layer 0 in samples 1, 3 and 4) is made of gypsum plaster (**calcium sulfate**,  $\text{CaSO}_4$ , confirmed by EDS and by the peak at  $1600\text{-}1648\text{ cm}^{-1}$  in the FT-IR spectra, which also show the sulfate overtones in the  $2100\text{-}2300\text{ cm}^{-1}$  area). Al is overall present as used as a polishing agent, but could also, together with K and Si be present as part of **silicate** inclusions (confirmed EDS mapping). Mg is present in the bulk of samples 1, 3 and 4, possibly as an exchangeable element in the sulphate variety  $\text{MgSO}_4$  (more or less hydrated) (Cox et al., 1974). **Barium** (Ba) was detected in all the layers of sample 3 and traces of titanium and were also detected in the surface layer. The crystalline structure typical of gypsum plaster (called *tabular* in mineralogy, see BSE images) can be seen in the bulk and the interface layer. The **interface layer** appears yellow under visible illumination and might consist of a portion of the lower layer soaked with the surface coating(s), showing characteristics of both layers.

EDS mapping shows that **layer 2**, dark under visible illumination, in samples 1 and 3 consists of **aluminium, silicon** and **iron**. Sample 4 shows the same substrate of samples 1 and 3 (layers 0 and 1) and a layer of **repaint** (layer 2, white under visible illumination, consisting of **barium, zinc** and **sodium** with traces of iron and chlorine) and a layer of dust (layer 4, dark under visible illumination and made of C, O, Ca, S and Si). Sample 2 was analysed with ATR-FT-IR and spectra consistent with sulfates and ammonium compounds (Catelli et al., 2016).

A **wax** or **resin** (FT-IR peaks at 928, 1472 and CH symmetric and asymmetric stretches in the  $2800\text{-}3000\text{ cm}^{-1}$ ) was detected in all the layers of samples 1, 3 and 4 which indicates that either the material was added to the gypsum plaster wet admixture or that the coating has also penetrated in layer 0. The latter seems also possible as the average depth of the samples is about 0.5 mm. The additional presence of a **protein** cannot be excluded by interpreting the FT-IR spectra, due to the complexity of the admixture and also to the crowded pattern of the resins' FT-IR spectra (Price et al., 2009). Py-TMAH-GCMS analysis of sample 3 suggests that the organic medium in this sample consists of **diterpenic resin** (rosin or colophony) possibly mixed with **drying oil**. Protein indicators were also identified, as in the majority of natural 'non-protein binders' a minority of protein component is present too (Colombini & Modugno, 2009).

**NOTE:** casting in resin the fragments of plaster resulted in the fragments absorbing the resin when in the liquid state. This was visible in the BSE image as well as through the EDS mapping (Tiranti resin and catalyst are mainly made of organic compounds C, H and O). Aluminium (Al) traces are present in all the samples, due to the polishing chemical.

## Sample 1



Above: Overlapped (OM and BSE) cross-section image showing the stratigraphy (blue indicators).

**2. Dark layer**

**1. Yellowish and undefined layer**

**0. Plaster bulk**

### **Analysis spots.**

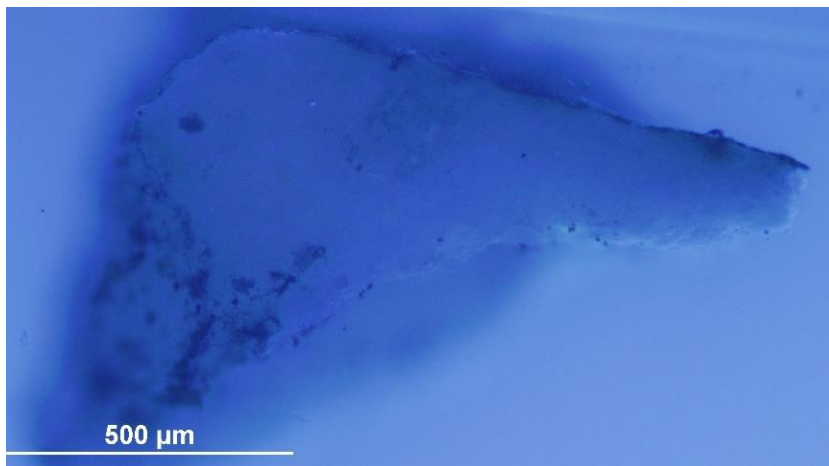
EDS analysis (yellow): Spectra 21-25

FT-IR analysis (red): nos. 61-69

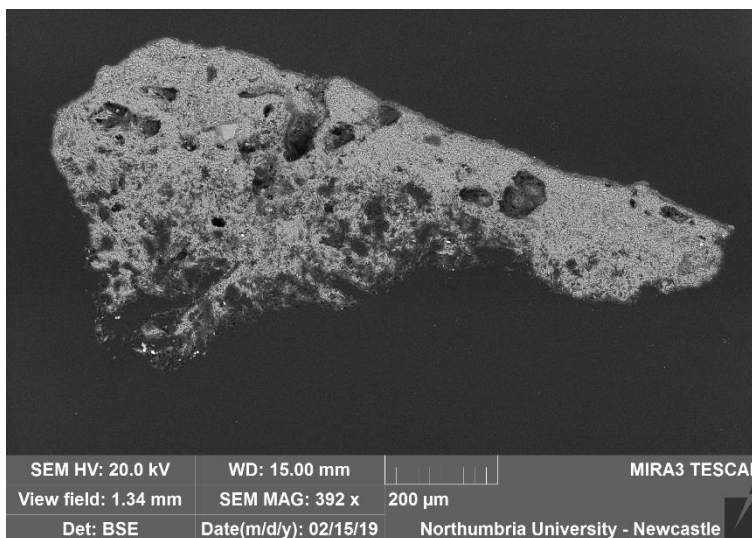
**Summary.** The substrate (layer 0) is made of plaster (**calcium sulfate**,  $\text{CaSO}_4$ , confirmed by EDS and by the peak at  $1632\text{ cm}^{-1}$  and overtones in the FT-IR spectra). Layer 1, which appears yellow under the microscope, consists of a portion of the lower layer soaked with the surface coating, showing characteristics of both layer 0 and layer 2. The surface dark layer (layer 2) is mostly made of silicon and aluminium and contains calcium sulfate and traces of Na, Fe, Ti, K, P and Cl (see EDS mapping and spectrum). Mg is relevantly present in all the layers. A **wax or resin** (FT-IR peaks at  $1472$  and  $2800\text{-}3000\text{ cm}^{-1}$ , and  $1744\text{ cm}^{-1}$  that suggests ester-containing wax or the additional presence of oil) was detected in all the layers.



VLR OM (left)

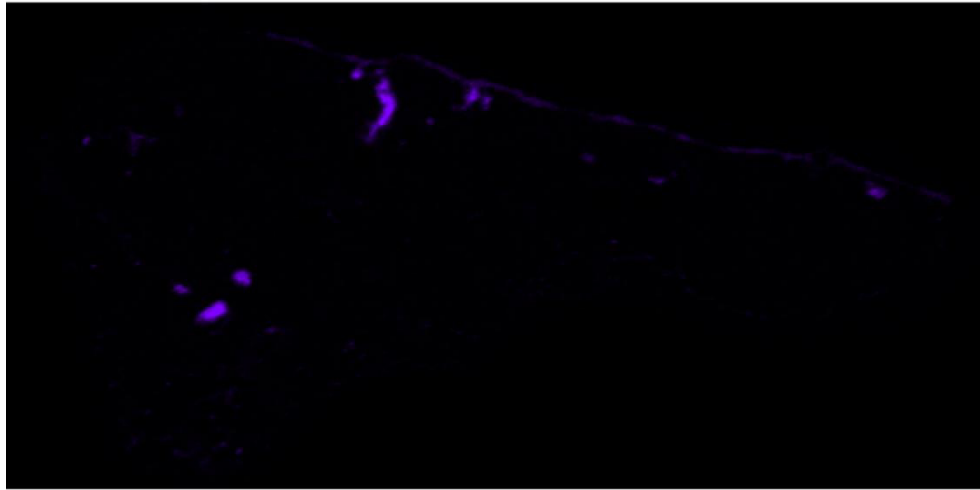


UVf OM (left)

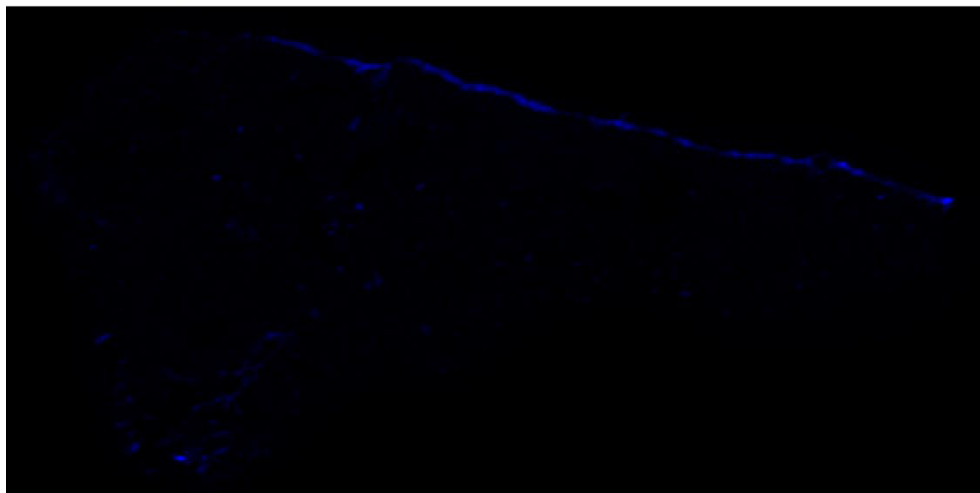


BSE image (left).

The tabular crystalline structure typical of gypsum plaster can be seen in layers 0 and 1.

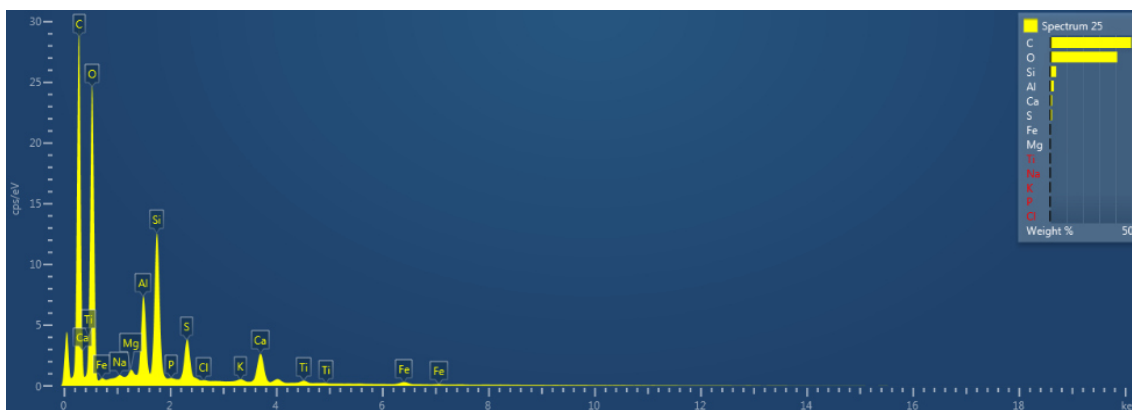


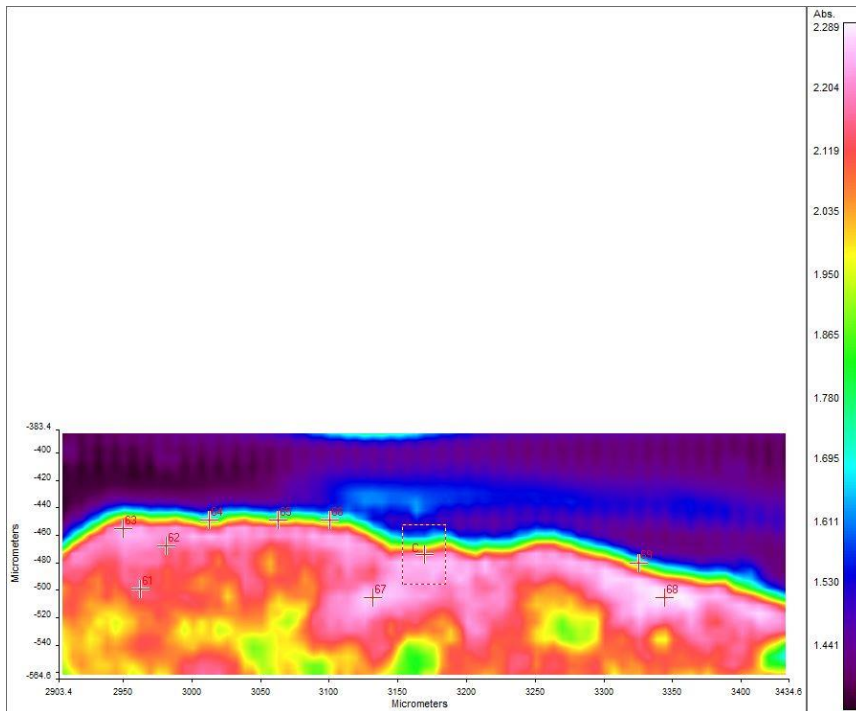
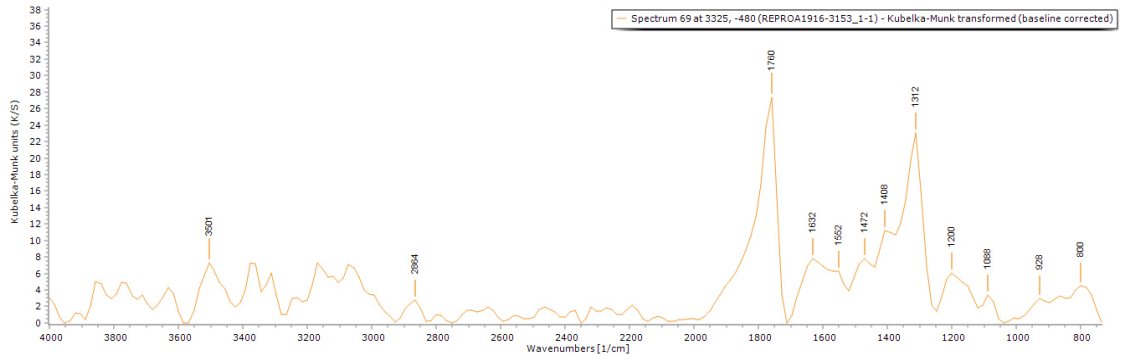
**EDS mapping** (left) shows that Al (top left) and Si (bottom left) are mostly present in layer 2.



500µm

**EDS spectrum** (below, spectrum 25) of layer 2 shows C, O, Ca and S, indicating calcium sulfates and carbonates. Si and Al are mostly present in layer 2 (as shown in the EDS mapping). Traces of Mg, Na, Fe, Ti, K, P and Cl were also detected.





**FT-IR spectrum 69** (above) of layer 2. Peaks for the casting resin (1312, 1760  $\text{cm}^{-1}$ ), gypsum (1632  $\text{cm}^{-1}$ ), overtone 2200-2300  $\text{cm}^{-1}$ ) and a wax/resin (1200, 1408, 1472, 2864  $\text{cm}^{-1}$ ). A summary of the peaks observed in the spectra 61-69 can be seen in the table below.

**FT-IR (FPA, Focal Plane Array) image** (left) shows that the utmost layer is made of a material with a different reflectance.

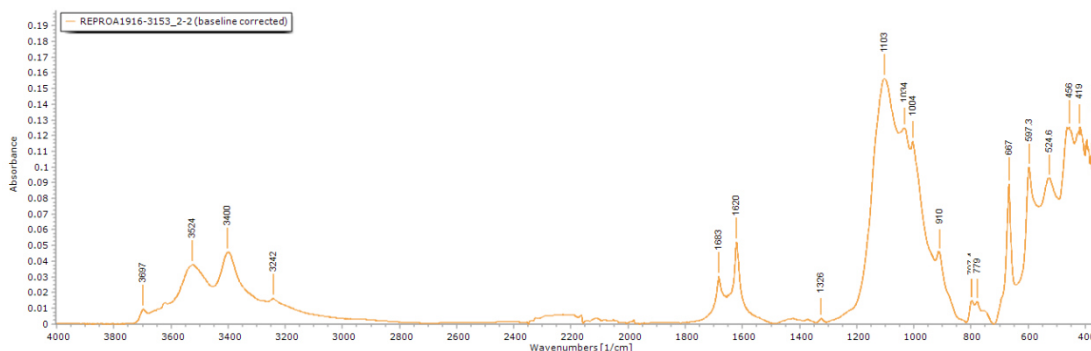
Spectrum	Layer	peaks (cm-1)						
		Casting Resin	Gypsum	Carbonate	Wax/resin	C=O ester carbonyl	SO overtone	Unknown
		1312	1040, 1648		960, 1248, 1408, 1488, 1584, 2960		1744	2198
61	0							
62	0	1312, 1760	1632		1008, 1248			2399
63	0	1312, 1760			1232, 1504			2485
64	1	1328, 1760	1632		864, 1088, 1200, 1504			
65	1	1328, 1760	1648		848, 1072, 1216, 1520, 2848, 2944			2336
66	1	1328, 1760	1632		784, 864, 1088, 1216, 1472, 1520, 2816			2352
67	0	1760	1040		944, 1296, 1360, 1504, 1584, 1664, 2960			2216, 1920
68	0	1328	1632		784, 1072, 1232, 1472, 1520, 1584, 2944	1744		2304
69	2	1312, 1760	1632	800	928, 1088, 1200, 1408, 1472, 1552, 2864			

## Sample 2



**Sampling.** This sample consists of dust taken from the top portion of the relief.

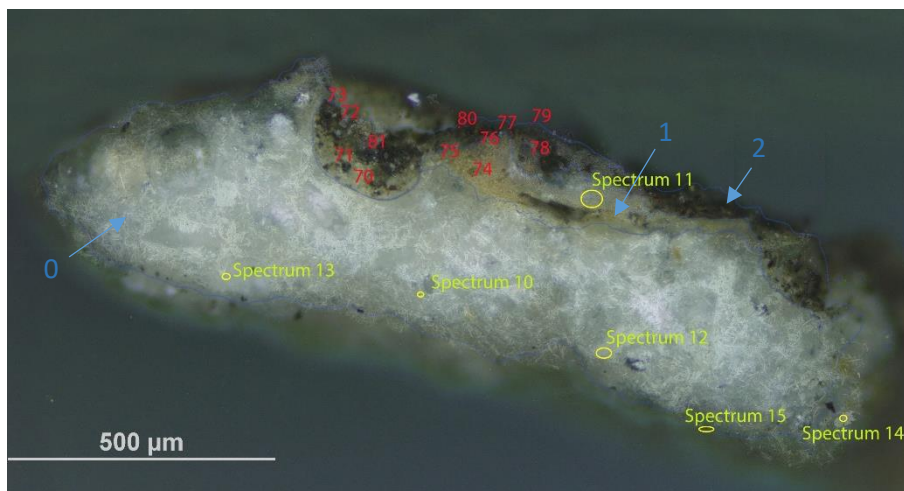
**Summary.** A small quantity of the dust/salt efflorescence collected because removing the salts would affect the surface: it was observed in other objects that light spotting was left behind after the removal of the efflorescence. Given that the purpose of the campaign was solely the sampling and not the treatment of the object, it was decided to remove as little material as possible. The small quantity allowed only one analysis to be carried on this sample. FT-IR-ATR was selected due to the simplicity and effectiveness of the analysis as related to the characteristics of the sample. The spectrum obtained (below) is consistent with sulfates and ammonium compounds (Catelli et al., 2016).



## Sample 3



**Sampling.** This fragment was taken from an undercut area on the PL of the relief.



Left: Overlapped (OM and BSE) cross-section image showing the stratigraphy (blue indicators).

**2. Dark layer**

**1. Yellowish and undefined layer**

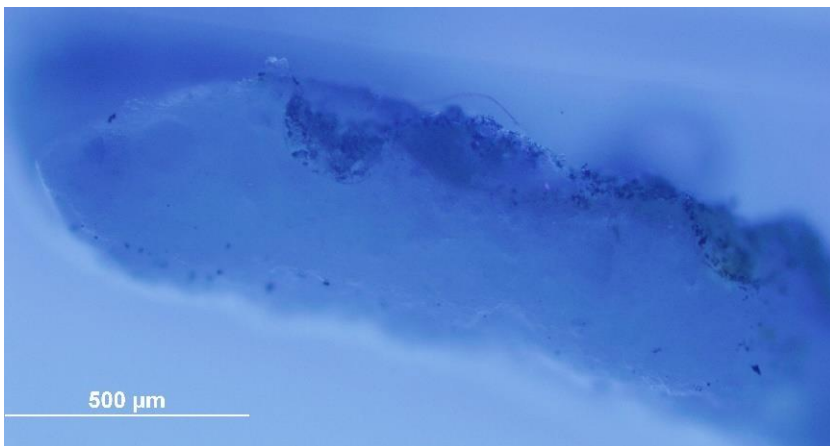
**0. Plaster bulk**

**Analysis spots.** EDS analysis (yellow): Spectra 10-15; FT-IR analysis (red): nos. 70-81.

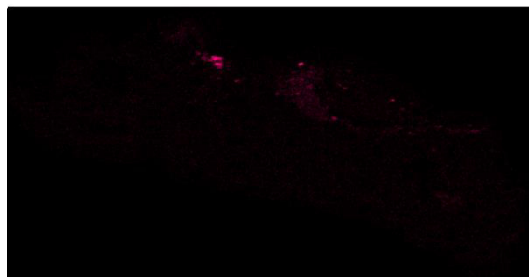
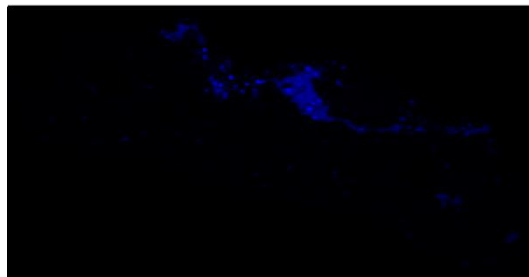
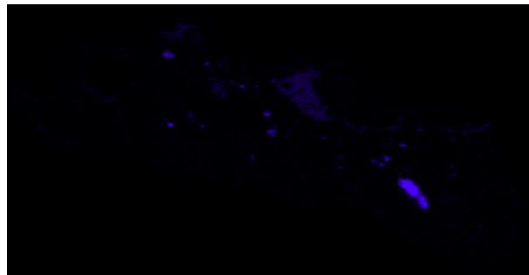
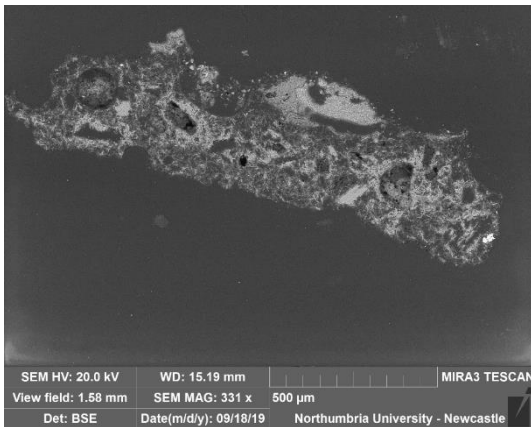
**Summary.** The sample is mostly made of C, O, S and Ca (**calcium sulfate**,  $\text{CaSO}_4$ , confirmed by EDS and by the peak at  $1600$  and  $1632\text{ cm}^{-1}$  in the FT-IR spectra). Al is overall present as used as a polishing agent, but could also, together with Si be present as part of silicate inclusions. Mg and Ba were detected in all the layers. Traces of Al, Ti, Sr and K were also detected. EDS mapping shows layer 2 is mostly made of aluminium (Al), silicon (Si) and iron (Fe). The structure typical of gypsum plaster can be seen in layers 0 and 1. Layer 1, which appears yellow under the microscope, consists of a small portion of the lower layer soaked with the surface coating, showing characteristics of both layer 0 and layer 2. A **wax or resin** is suggested by FT-IR (peaks at  $1000$ - $1200$  and  $2800$ - $3000\text{ cm}^{-1}$ ) and py-TMAH-GCMS shows markers characteristic of **diterpenoid resins** mixed with **linseed oil**. Amine fragments were also identified, as in the majority of natural 'non-protein binders' a minority of protein component is present too (Colombini & Modugno, 2009).



VLR OM (left)



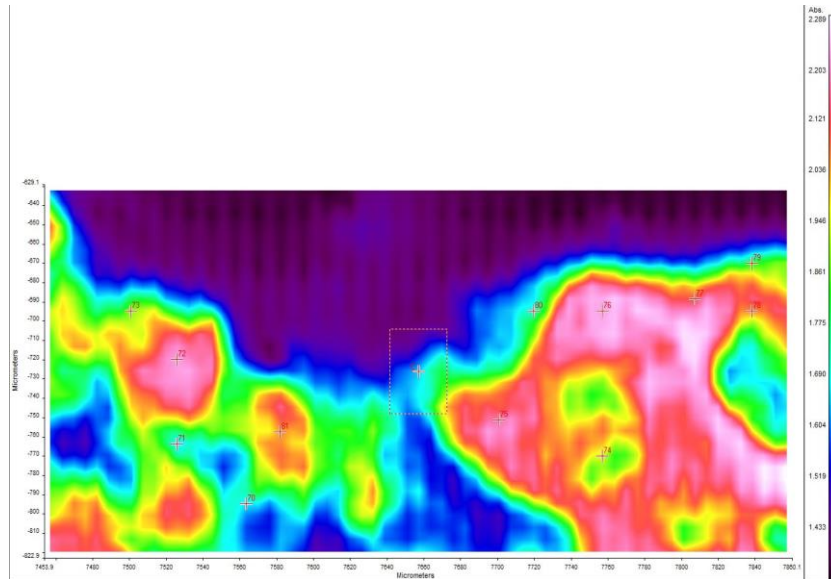
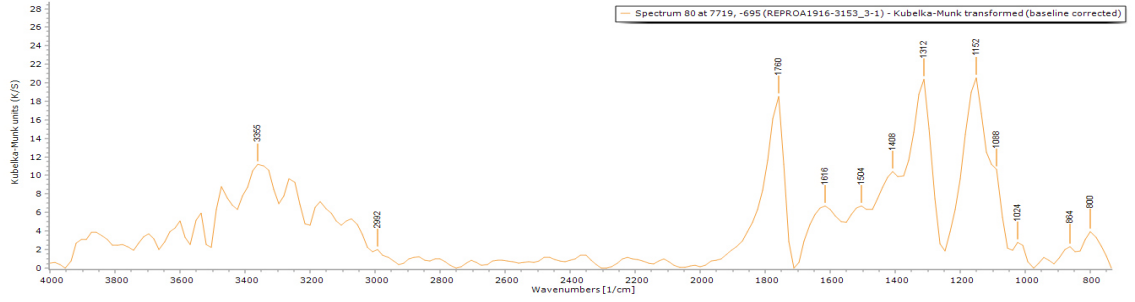
UVf OM (left)



**BSE image (above).** The tabular crystalline structure typical of gypsum plaster can be seen in layers 0 and 1.

Calcium sulfate ( $\text{CaSO}_4$ ) and Mg and Ba were detected in all the layers. Traces of Al, Ti, Sr and K were also detected.

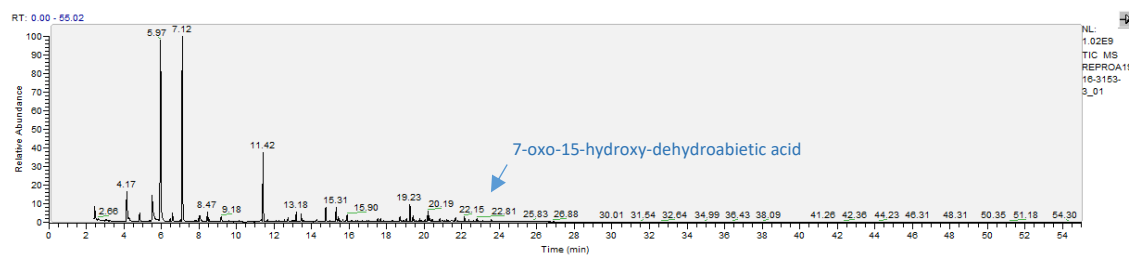
**EDS mapping (right)** shows that layer 2 is mostly made of aluminium (Al, top right), silicon (Si, middle right) and iron (Fe, bottom right).



**FT-IR spectrum 80** (above) of layer 2. Peaks for the casting resin (1312, 1760  $\text{cm}^{-1}$ ), gypsum (1616  $\text{cm}^{-1}$ ) and a wax/resin (100-1200 and 2992  $\text{cm}^{-1}$ ). A summary of the peaks observed in the spectra 70-81 can be seen in the table below.

**FT-IR (FPA) image** (left). No clear layer definition can be observed in the FPA image.

Spectrum	Layer	peaks (cm-1)						
		Casting Resin	Gypsum	Carbonate	Wax/resin	C=O ester carbonyl	SO overtone	Unknown
70	2	1312, 1760	1600		816, 992, 1104, 1168, 1504			
71	2	1312, 1760	1616	800	928, 1024, 1152, 1488			
72	2	1312, 1344, 1760	1648		784, 864, 944, 1168, 1200, 1504, 1552, 2880, 2944			
73	2	1312, 1760	1632		912, 1088, 1200, 1536, 2864		2176, 2336	
74	1	1312, 1760	1600	800	944, 1200, 1392, 1488, 2848, 2944		2240	1824
75	1	1312, 1760	1600	800	960, 1088, 1200, 1376, 1488, 1520, 1584, 2816, 2944		2320	
76	2	1312, 1760	1616		960, 1088, 1152, 1200, 1360, 1456, 1568, 2784		2208	
77	2	1328, 1760			880, 1024, 1152, 1216, 1424, 1488, 1584			
78	2	1328, 1760		800	912, 1200, 1456, 1584, 2832, 2912		2224	
79	2	1328, 1760			1088, 1200, 1504, 1552, 1648			
80	2	1312, 1760	1616	800	1024, 1088, 1152, 1408, 1504, 2992			
81	2	1312		1776	784, 928, 1072, 1136, 1184, 1376, 1520, 1648, 2944		2496	



RT	m/z	Assignment	Formula
2.44	42(12), 58(100), 102(2)	1,2-Ethanediamine, N,N,N'-trimethyl-	C5H14N2
4.17	45(100), 58(8), 74(67)	Ethyl ether	C2H8N2
4.85	43(6), 59(100), 73(7), 88(5)	3-Pentanol	C5H12O
5.51	42(10), 58(100), 72(6), 88(4), 116(4)	1,2-Ethanediamine, N'-ethyl-N,N-dimethyl-	C6H16N2
5.97	42(12), 58(100), 117(15)	1,2-Ethanediamine, N'-ethyl-N,N-dimethyl-	C6H16N2
7.12	44(7), 56(7), 72(100), 116(2), 131(3)	N,N'-Diisopropylethylenediamine	C8H20N2
9.18	44(100), 58(50), 86(64), 128(51)	Glycyl-dl-alanine	C5H10N2O3
11.42	42(6), 58(100), 70(9), 116(6)	1,2-Ethanediamine, N'-ethyl-N,N-dimethyl-	C6H16N2
12.74	42(10), 58(100), 72(3), 85(3), 175(3)	Unidentified amine fragment	
13.18	58(19), 71(14), 88(23), 98(31), 116(42), 130(100), 144(3)	Unidentified amine fragment	
13.44	42(9), 58(20), 72(100), 91(3), 119(5), 130(6), 147(6), 162(3)	Unidentified amine fragment	
14.77	58(12), 84(7), 109(6), 116(100), 128(5), 139(13), 152(3), 173(4)	Unidentified amine fragment	
15.31	58(12), 84(4), 99(4), 116(100), 149(13), 173(4), 180(4)	Unidentified amine fragment	
15.9	45(9), 58(20), 77(14), 91(17), 109(9), 139(10), 149(100), 165(18), 180(26)	Unidentified amine fragment	
18.71	45(32), 58(96), 77(28), 91(39), 105(10), 115(53), 161(75), 175(31), 190(100), 224(5)	Unidentified diterpenoid fragment	
19.23	45(81), 58(45), 75(100), 85(78), 101(66), 115(26), 123(18), 139(25), 152(16), 161(38), 170(10), 183(20), 215(5), 228(5), 261(5)	Unidentified diterpenoid fragment	
19.41	45(87), 58(100), 75(35), 85(52), 91(33), 99(5), 109(41), 115(32), 137(68), 161(34), 174(5), 182(48), 189(30), 205(5), 221(5), 236(29)	Unidentified diterpenoid fragment	
20.19	45(100), 58(68), 75(81), 85(88), 101(100), 115(34), 123(5), 139(32), 161(23), 183(5), 201(5), 215(5), 231(5)	Unidentified diterpenoid fragment	
21.68	44(27), 58(81), 74(100), 87(63), 91(16), 115(21), 129(16), 143(26), 161(31), 185(5), 189(25), 204(5), 227(5), 239(5), 264(5)	methyl palmitate	C17H34O2
22.15	45(57), 58(100), 75(32), 105(28), 119(35), 133(28), 147(25), 179(5), 193(25), 207(64), 238(5), 270(64)	Unidentified diterpenoid fragment	
22.81	45(56), 58(100), 75(31), 91(21), 115(19), 149(19), 179(17), 193(5), 207(5), 237(5), 250(5), 270(17), 299(5), 331(5)	7-oxo-15-hydroxy-dehydroabiatic acid	
23.59	44(35), 58(100), 74(84), 87(55), 91(5), 115(14), 129(5), 143(25), 185(5), 193(17), 207(5), 241(5), 255(15), 298(5)	methyl stearate	C19H38O2

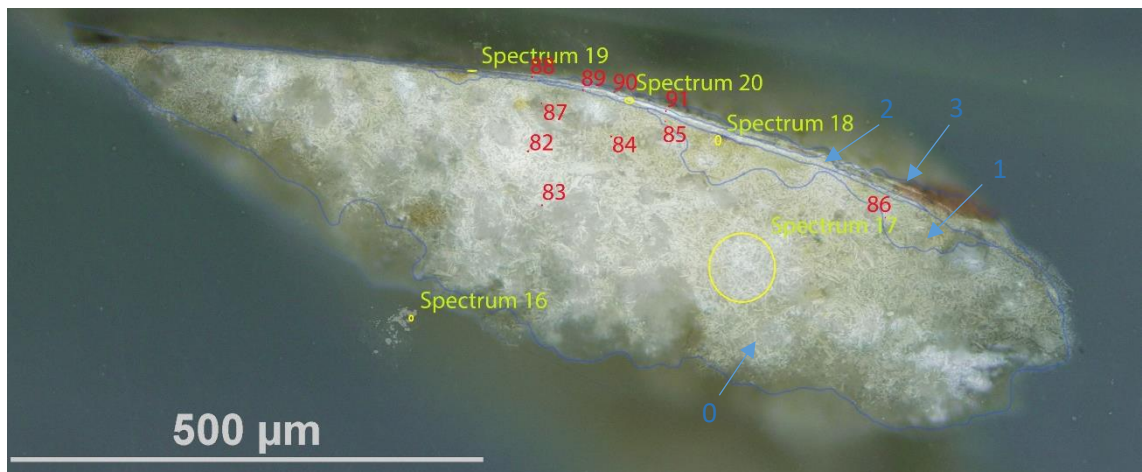
RT = retention time, m/z = mass/charge ratio

**Py-TMAH-GCMS chromatogram** ([top](#) and described in the table [above](#)) shows small fragments due to derivatization (from  $t = 4.21$  to  $7.12$  min) and markers characteristic of **diterpenoid resins** (e.g.  $t = 22.81$  min). The presence of **methyl palmitate** ( $t = 21.68$ ) and **stearate** ( $t = 23.59$ ) suggest that the resin has been mixed with **drying oil** ( $P/S = 1.44$ , likely **linseed oil**) or the FA is naturally present in the resin. Amine fragments were also identified, as in the majority of natural 'non-protein binders' a minority of protein component is present too (Colombini & Modugno, 2009).

## Sample 4



**Sampling.** This fragment was taken from an area of loss from the PL edge.



Left: Overlapped (OM and BSE) cross-section image showing the stratigraphy (blue indicators).

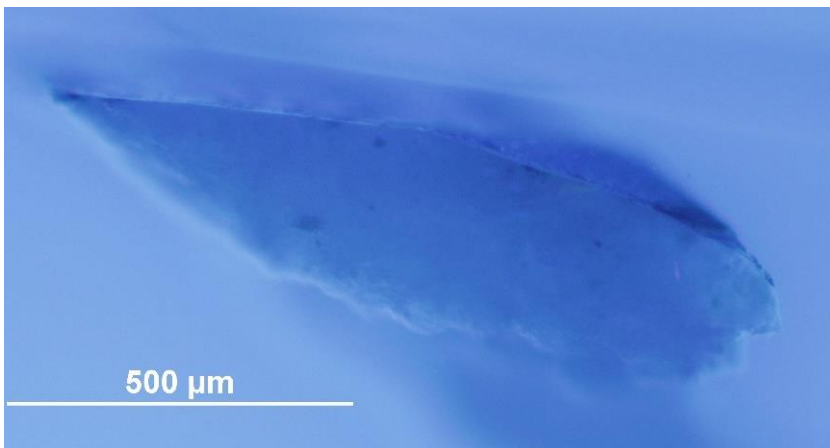
- 3. Dark layer
- 2. White layer
- 1. Yellowish layer with dark inclusions
- 0. Plaster bulk

**Analysis spots.** EDS analysis (yellow): Spectra 16-20; FT-IR analysis (red): nos. 82-91

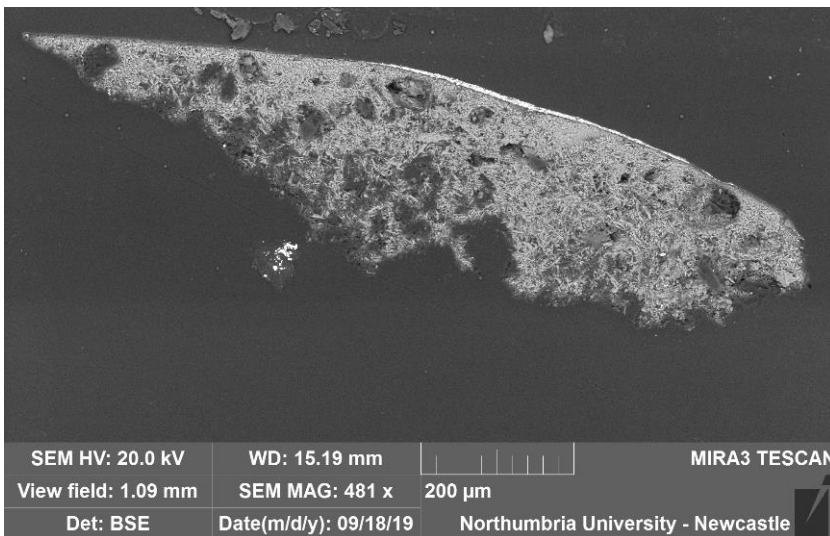
**Summary.** The sample is mostly made of C, O, S and Ca (**calcium sulfate**,  $\text{CaSO}_4$ , confirmed by EDS and by the peak at  $1600\text{-}1648\text{ cm}^{-1}$  and overtones area at  $200\text{-}2300\text{ cm}^{-1}$  in the FT-IR spectra). Al is overall present as used as a polishing agent, but could also, together with K and Si be present as part of silicate inclusions (confirmed by EDS mapping too). Mg is also relevantly present in the plaster bulk. The tabular structure typical of gypsum plaster can be seen in layers 0 and 1. Layer 1, which appears yellow under the microscope, consists of a small portion of the lower layer soaked with the surface coating. EDS mapping shows that layer 2, white under visible illumination, consists of **barium** (Ba), **zinc** (Zn) and **sodium** (Na) with traces of iron (Fe) and chlorine (Cl). Layer 3 is dark under visible illumination and its composition (C, O and gypsum plaster) is consistent with a layer of **dirt**. **Carbonates** and **silicates** are suggested by FT-IR peaks, and also a **wax or resin** and possibly a **protein** contribution (Price et al., 2009).



VLR OM (left)



UVf OM (left)



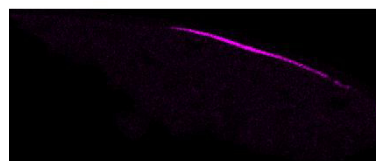
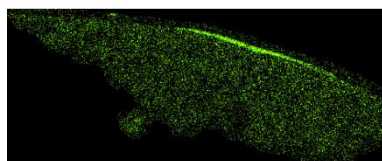
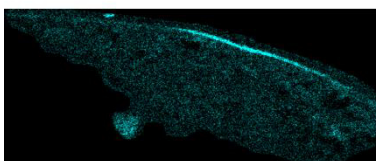
**BSE image (left).** The tabular crystalline structure typical of gypsum plaster can be seen in layers 0 and 1. Layer 2 consists of heavier elements, which can be seen in the **EDS mapping (below)**.

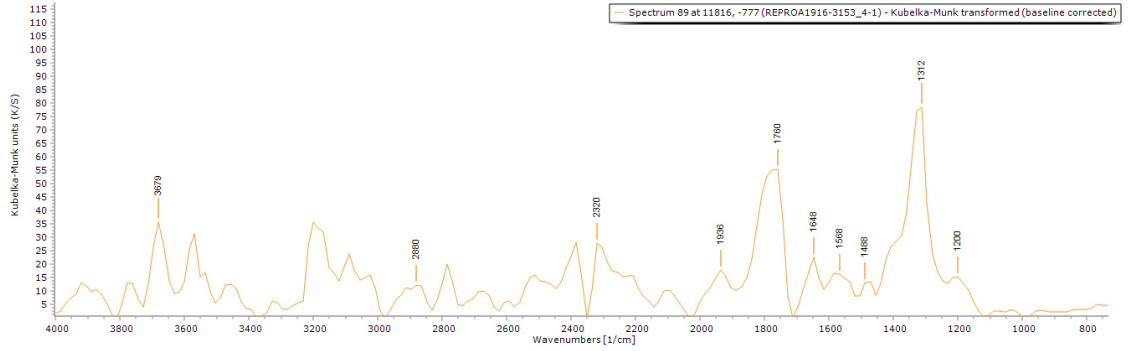
**EDS spectra** indicate that layers 0 and 1 consist of C, O, Ca, S, Si, Al, Mg and K. Layer 2 is made of Ba, Zn, Na and traces of Fe and Cl.

Sodium (Na)

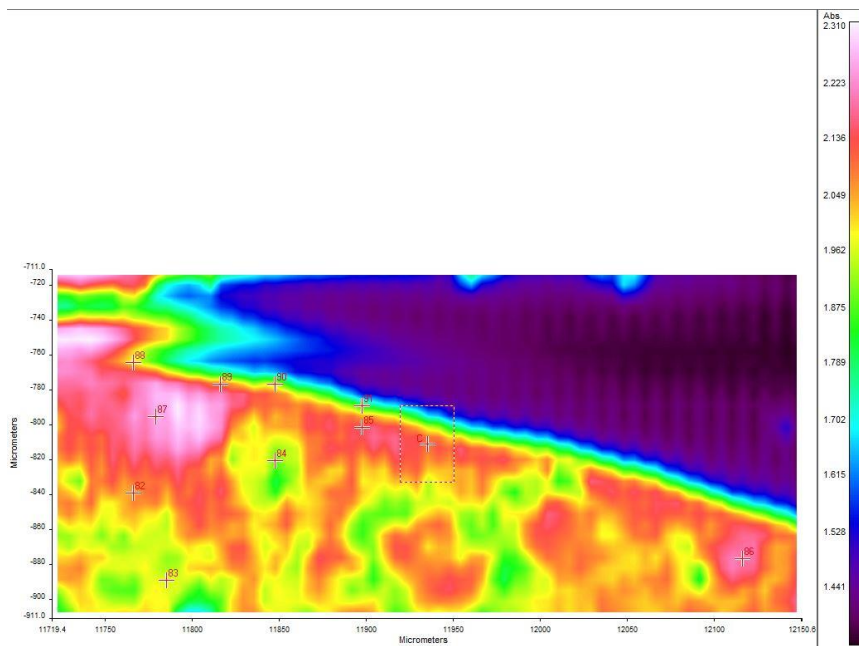
Zinc (Zn)

Barium (Ba)





**FT-IR spectrum 89** (above) of layer 2. Peaks for the casting resin (1312, 1760  $\text{cm}^{-1}$ ), gypsum (1600  $\text{cm}^{-1}$ , overtone 2200-2300  $\text{cm}^{-1}$ ), carbonate (800  $\text{cm}^{-1}$ ) and a wax/resin (1200, 2880, 1488 and 2988  $\text{cm}^{-1}$ ). Peaks that might suggest the presence of a protein are also visible in the 1400-1600  $\text{cm}^{-1}$  area. A summary of the peaks observed in the spectra 82-91 can be seen in the table below.



**FT-IR (FPA) image** (left). No clear layer definition can be observed in the FPA image.

Spectrum	Layer	peaks (cm-1)						
		Casting Resin	Gypsum	Carbonate	Wax/resin	C=O ester carbonyl	SO overtone	Unknown
82	0	1312, 1760		816	1024, 1376, 1520, 1664, 2864, 2944		2112, 2224	1952
83	0	1312, 1760	1632		784, 944, 1216, 1520, 2880, 2960		2224	
84	0	1344, 1760	1648	800	1024, 1232, 1296, 1472, 2832, 2928		2240	
85	1	1328, 1760	1648		1008, 1232, 1296, 1488, 1552, 2768, 2864		2224	
86	1	1344, 1760	1648		944, 1024, 1296, 1392, 1456, 1520, 1568, 2880, 2944		2256	
87	0			800, 1776	928, 1072, 1216, 1280, 1360, 1424, 1584, 1680, 2832, 2960		2112, 2209	
88	1	1328, 1760			784, 1104, 1200, 1552, 2864, 2944		2240	
89	2	1312, 1760	1648		1200, 1488, 1568, 2880		2320	1936
90	2	1328, 1760	1616	800	1072, 1200, 1472, 1536, 2864, 2960		2304	
91	2	1328, 1760		800	976, 1088, 1200, 1472, 1536, 2960		2272	1936

## Experimental

The object was observed, and its conditions were documented. Samples from selected areas were taken by Valentina Risdonne. When possible, each sample was split into two parts: one fragment was embedded in polyester resin (Tiranti clear casting resin), polished and analysed under an optical microscope and the other was put aside for py-TMAH-GCMS. Not enough material was available for XRD analysis. Sample 2 was analysed by ATR-FT-IR.

The optical microscopy was performed with an Olympus BX51 Metallurgical Microscope equipped with four objectives (magnification of x5, x20, x50 and x100), and an x10 eyepiece. In many instances, a small amount of white spirit was added to the surface of the cross-section to improve the saturation under the microscope. The microscope is equipped with a 6-cube filter turret which allows operating the system in reflected visible light (brightfield and darkfield mode) and reflected UV light (365 nm) using a 100 W mercury burner.

The SEM-EDS analysis was performed with a field emission TESCAN MIRA 3 with gigantic chamber. The SEM is equipped with: secondary electron detector (SE), secondary electron in-beam detector (In-beam SE), back-scatter detector (BSE), back-scatter in-beam detector (In-beam BSE), cathodoluminescence detector (without wavelength detection) (CL), plasma chamber/sample cleaner and software Alicona 3D imaging. For the EDS analytical part, it has an Oxford Instruments setup: Software: AztecEnergy, X-ray detector X-Max 150 mm<sup>2</sup> and X-ray detector X-Max Extreme, low energy detector for thin films, high resolution and low voltage. The samples were analysed by SEM-EDS Low Vacuum Mode (10-15 Pa). EDS Mapping and data processing were performed with Aztec Oxford software.

A Perkin Elmer Frontier FT-IR spectrometer (350 cm<sup>-1</sup> at the best resolution of 0.4 cm<sup>-1</sup>) was used, equipped with a germanium crystal for ATR measurements and combined with a Spectrum Spotlight 400 FT-IR microscope equipped with a 16×1 pixel linear mercury cadmium telluride (MCT) array detector standard with InGaAs array option for optimised NIR imaging. Spectral images from sample areas are possible at pixel resolutions of 6.25, 25, or 50 microns. The Perkin Elmer ATR imaging accessory consists of a germanium crystal for ATR imaging. These run with Perkin Elmer Spectrum 10™ software and with SpectrumIMAGE™ software. Baseline and Kubelka-Munk corrections were applied to the raw data acquired in diffuse reflectance.

The instrument used for GCMS is a Thermo Focus Gas Chromatographer with DSQ II single quadrupole mass spec. The column currently installed is a Agilent DB5-MS UI column (ID: 0.25 mm, length: 30 m, df: 0.25 µm, Agilent, Santa Clara, CA, USA). Carrier gas: helium. Detector temperature: 280 °C, Injector temperature: 250 °C. It can be used with the Pyrola 2000 Platinum filament pyrolyser (PyroLab, Sweden) attachment or in split/splitless mode. Detection: Total Ion monitoring (TIC). 1 µl of the sample with 1 µl of TMAH was placed on the Pt filament for the py-GC/MS. The inlet temperature to the GC was kept at 250 °C. The helium carrier gas flow rate was 1.5 ml/min with a split flow of 41 ml/min and a split ratio of 27. The MS transfer line was held at 260 °C and the ion source at 250 °C. The pyrolysis chamber was heated to 175 °C, and pyrolysis was carried out at 600 °C for 2 s. This run with Xcalibur™ and PyroLab™ software. The library browser supported NIST MS Version 2.0 (Linstrom & Mallard, 2014).

Valentina Risdonne, PhD student

[v.risdonne@vam.ac.uk](mailto:v.risdonne@vam.ac.uk) / [valentina.risdonne@northumbria.ac.uk](mailto:valentina.risdonne@northumbria.ac.uk)

Victoria and Albert Museum – Northumbria University

PhD project 'Materials and techniques for coating of the nineteenth-century plaster casts'

©V&A Museum

9 September 2020

## Notes

18 January 2019	Sampling	Valentina's PhD Lab book 1, page 149
4 February 2019	Casting	Valentina's PhD Lab book 1, page 162
11 February 2019	Microscopy	Valentina's PhD Lab book 1, page 168
14 October 2019	FT-IR	Valentina's PhD Lab book 1, page 175
18 March 2020	GCMS	Valentina's PhD Lab book 2, page 50

A full record of analysis is available at <https://doi.org/10.25398/rd.northumbria.14040251>

## References

- Catelli, E., Bănică, F.-G., & Bănică, A. (2016). Salt efflorescence in historic wooden buildings. *Heritage Science*, 4(1), 31. <https://doi.org/10.1186/s40494-016-0099-9>
- Colombini, M. P., & Modugno, F. (2009). *Organic mass spectrometry in art and archaeology*. John Wiley & Sons.
- Cox, K. G., Price, N. B., & Harte, B. (1974). *An introduction to the practical study of crystals, minerals, and rocks*. Halsted Press.
- Linstrom, P. J., & Mallard, W. G. (2014). *NIST Chemistry WebBook, NIST standard reference database number 69, National Institute of Standards and Technology, Gaithersburg MD, 20899*.
- Price, B. A., Pretzel, B., & Lomax, S. Q. (2009). *Infrared and Raman Users Group Spectral Database; 2007 ed. IRUG: Philadelphia, PA, USA*.





**Northumbria  
University**  
NEWCASTLE

Analysis Report - Valentina Risdonne

Copy of a relief - The Raising of Lazarus

(REPRO.1864-56)

Initiator: Charlotte Hubbard; Conservation  
Department

3 September 2020

© Victoria and Albert Museum



## Analysis Report - The Raising of Lazarus (REPRO.1864-56)

### Contents

Contents .....	358
List of abbreviations.....	358
Summary .....	359
Sample 1 .....	362
Sample 2 .....	366
Sample 3 .....	371
Sample 4 .....	374
Sample 5 .....	377
Experimental.....	380
Notes.....	381
References.....	381

### List of abbreviations

BSE	Back Scattered Electron
EDS	Energy Dispersive Spectrometry
FT-IR	Fourier-Transform Infra-Red
FPA	Focal Plane Array
GC/MS	Gas Chromatography-Mass Spectrometry
OM	Optical Microscopy
PL	Proper Left
PR	Proper Right
py	pyrolysis
SEM	Scanning Electron Microscopy
TMAH	tetramethylammonium hydroxide
UVf	Ultraviolet Fluorescence
VLR	Visible Light Reflectance
XRD	X-ray Diffraction

## Summary

The bulk of the object is made of gypsum plaster, which contains several types of inclusions (including Sr-K-Al silicates). A layer of dust/dirt can be seen in all the samples. Two samples were taken from the areas of repair (samples 1 and 2) and appear significantly different, possibly belonging to two different conservation campaigns. Sample 1 is made of gypsum plaster and toned with a **barium** (Ba), **zinc** (Zn) and **strontium** (Sr) paint. Sample 2 is made of gypsum plaster containing **lead** (Pb) and toned with **drying oil modified alkyd paint** containing **iron** (Fe), **barium** (Ba) and **chlorine** (Cl). The **wax** or **resin** applied on all the object did not form a film (no visible layer is present on samples 2, 3 and 4) but it is visible as it penetrated in the plaster bulk. The presence of a wax or resin was detected by FT-IR, but no unique assignation could be done, due to the complexity of the admixture.



Figure 1. The copy of a relief.

The object, '**Copy of a relief - The Raising of Lazarus (REPRO.1864-56)**' (Figure 1), is a plaster cast of a relief, in stone, with a representation of the Raising of Lazarus, made for the Chichester Cathedral (UK) in the second quarter of the twelfth century. The plaster cast was made by Giovanni Franchi and Son in London possibly in 1851. The cast was acquired in 1864, bought from Messrs Franchi & Son together with museum no. 1864-57 for £30.

The cast is now located in Gallery 46A (The Ruddock Family Cast Court), displayed upright. Its dimensions are 122.0x117.0 cm.

Samples from the plaster cast were taken from pre-existing areas of loss to investigate the stratigraphy and the method of manufacture (Figure 2). The samples were analyzed to provide data for the study of the objects of the Cast Courts collection within the PhD project 'Materials and techniques for coating of the nineteenth-century plaster casts'. Details on the experimental procedure are available in the Experimental section of this report. A selection of significant results is shown in the following pages and the relevant database of analysis (<https://doi.org/10.25398/rd.northumbria.14040281>).

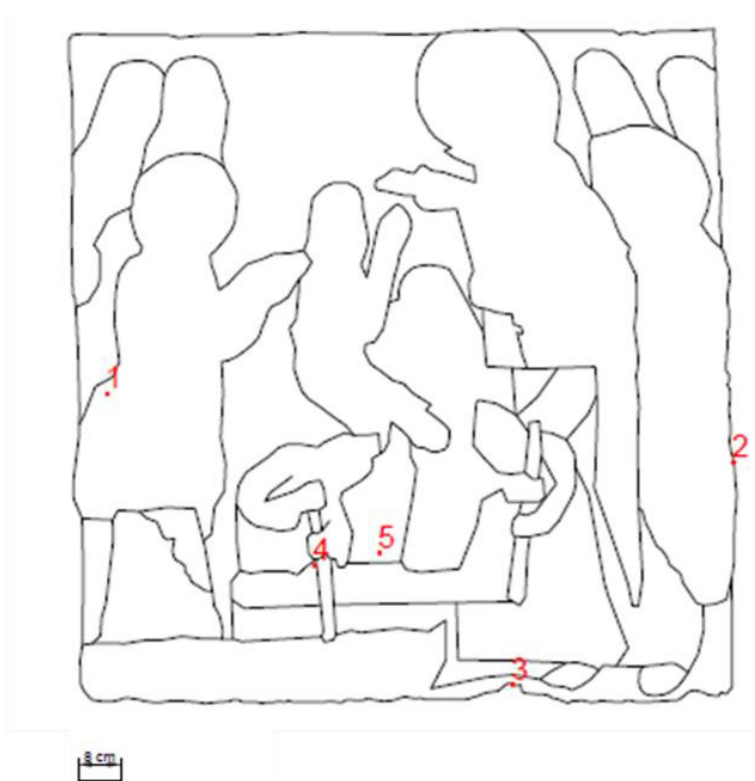


Figure 2. The relief outline with marked sampling sites.

**Sample 1:** fragment taken from an area of retouch, PR, from the vest of the Saint.

**Sample 2:** fragment taken from an area of loss, from the PL rim.

**Sample 3:** fragment taken from an area of loss located on the bottom edge.

**Sample 4:** fragment taken from a hole behind the figure's walking stick.

**Sample 5:** fragment taken from an area of loss from the centre of the relief, at the feet of the figure.

The **substrate** (layer 0 in all the samples) is made of gypsum plaster (**calcium sulfate**,  $\text{CaSO}_4$ , confirmed by EDS, XRD and by the peak at 1600, 1616 and 1632  $\text{cm}^{-1}$  in the FT-IR spectra, which also show the sulfate overtones in the 2100-2300  $\text{cm}^{-1}$  area). Sr, Na, K, Si, Al, Cl and Mg were detected in all the samples and EDS mapping confirmed that the large mineral inclusion visible in the BSE image of sample 1 are made of mineral gypsum. The presence of **silicates** in all the samples is confirmed by the EDS (C and Si; Al traces are present in all the layers due to the polishing medium or indicating Sr-K-Al silicates, also

visible in the EDS mapping). Mg is known as an exchangeable element in the sulfate variety  $\text{MgSO}_4$  (more or less hydrated) and Na can be also an exchangeable element in the sulfate or indicate the presence of sodium chloride (NaCl, possibly present in the quarry or derived by the source of water used to produce the plaster). EDS mapping does not show a specific difference in the elements' distribution in the layers in samples 3, 4 and 5. The crystalline structure typical of gypsum plaster (called *tabular* in mineralogy, see BSE images) can be seen in the bulk and the interface layer (layer 1 in samples 1, 2, 3, 5) (Cox et al., 1974).

The **interface layer** appears yellow under visible illumination and might consist of a portion of the lower layer soaked with the surface coating(s), showing characteristics of both layers.

A **black line** seems consistent with a layer of dirt and is present in all the samples (layer 2 in all the layers apart from sample 4, where it is layer 1, as the interface layer cannot be seen).

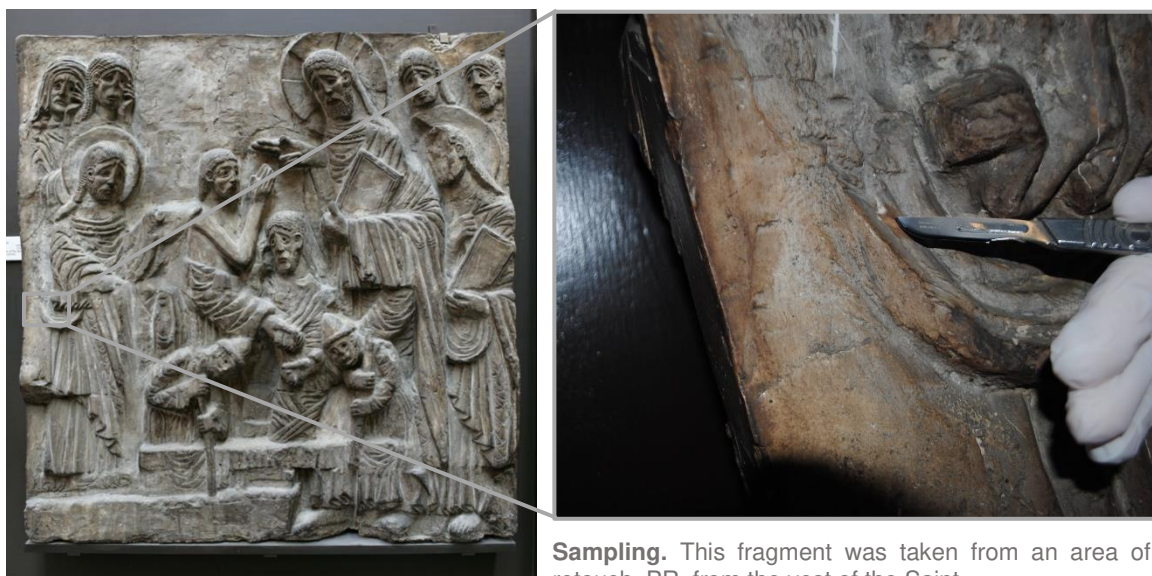
Layers 0, 1 and 2 are present and similar in samples 1, 3 and 5. Sample 2 appears different from all the other samples: it consists of **calcium sulfate** and presents all the trace elements detected in the other samples, but **lead** (Pb) is relevantly present in all the layers, suggesting that, although the area was not visually identified as an **area of repair**, that was likely to be the case. The utmost layer in this sample presents particles made of **iron** (Fe), **barium** (Ba) and **chlorine** (Cl). Sample 1 was identified as an **area of repair** during the sampling procedure and presents two additional layers, above the already described plaster substrate, interface layer and black line: a **white layer** under visible illumination - layer 3, consisting of heavy elements such as **barium** (Ba), **zinc** (Zn) and **strontium** (Sr), detected by EDS and shown in the mapping and BSE image, and a greyish/transparent under visible illumination (layer 4, most likely a varnish).

Traces of other elements can be seen especially in the top layers of samples 2, 3 and 5 (Fe, P, Na and Cl). Layer 2 in sample 2 appears greyish under visible illumination and shows several inclusions. By looking at the EDS mapping, these inclusions seem to consist of Fe, Ba and Cl. Traces of Ti, Pb, K and Mn are also present in layer 2. Ba, Sr and Mn were also detected in layers 2 and 3 of sample 3.

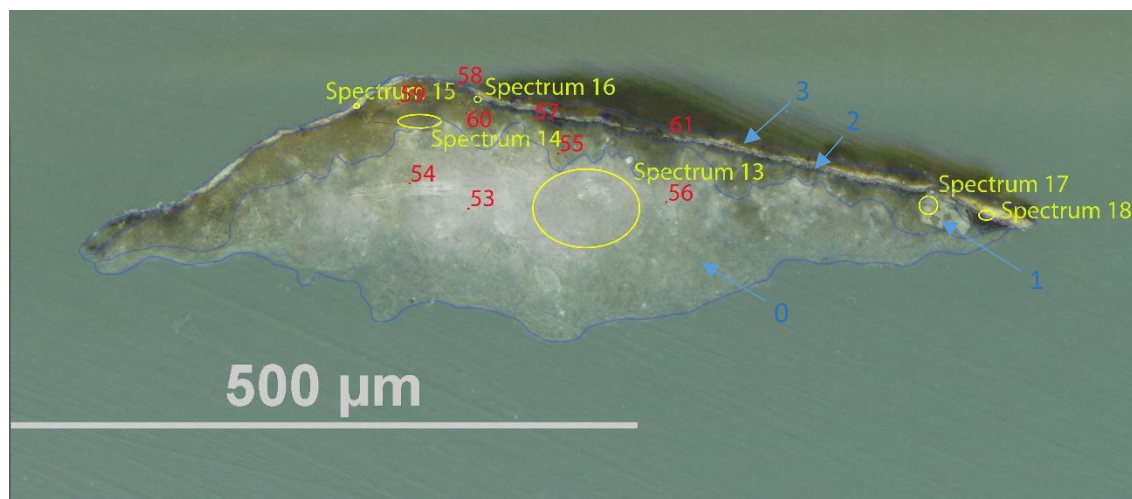
A **wax** or **resin** (FT-IR peaks at 800-1100, 1472 and CH symmetric and asymmetric stretches in the 2800-3000  $\text{cm}^{-1}$ ) was detected in all the layer of all the samples and due to the complexity of the spectra, the presence of a protein cannot be excluded in these samples. This indicates that either the material was added to the gypsum plaster wet admixture or that the coating has also penetrated in layer 0. The latter seems also possible as the average depth of the samples is about 0.5 mm. py-TMAH-GC/MS analysis of sample 2 indicated the presence of a **drying oil modified alkyd resin** (esters contributions cannot be seen in the FT-IR spectra, but this could be due to the complexity of the admixture and overall small concentration of the oil) (Colombini & Modugno, 2009; Price et al., 2009).

**NOTE:** casting in resin the fragments of plaster resulted in the fragments absorbing the resin when in the liquid state. This was visible in the BSE image as well as through the EDS mapping (Tiranti resin and catalyst are mainly made of organic compounds C, H and O). Aluminium (Al) traces are present in all the samples, due to the polishing chemical.

## Sample 1



**Sampling.** This fragment was taken from an area of retouch, PR, from the vest of the Saint.



Above: Overlapped (OM and BSE) cross-section image showing the stratigraphy (blue indicators).

3. White layer

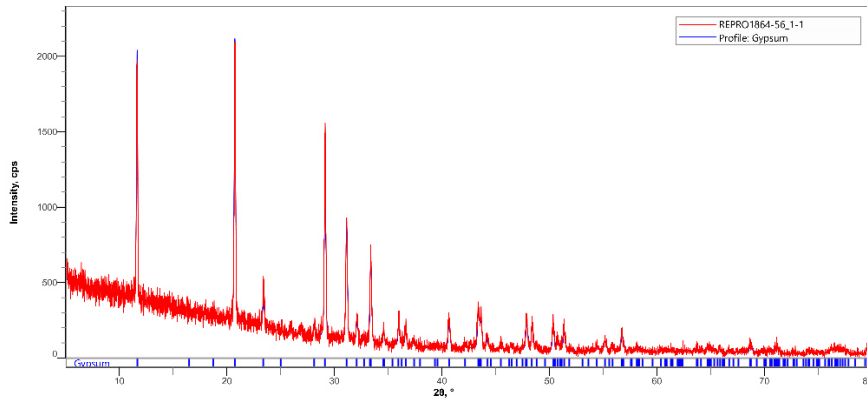
2. Dark line

1. Yellowish and undefined layer

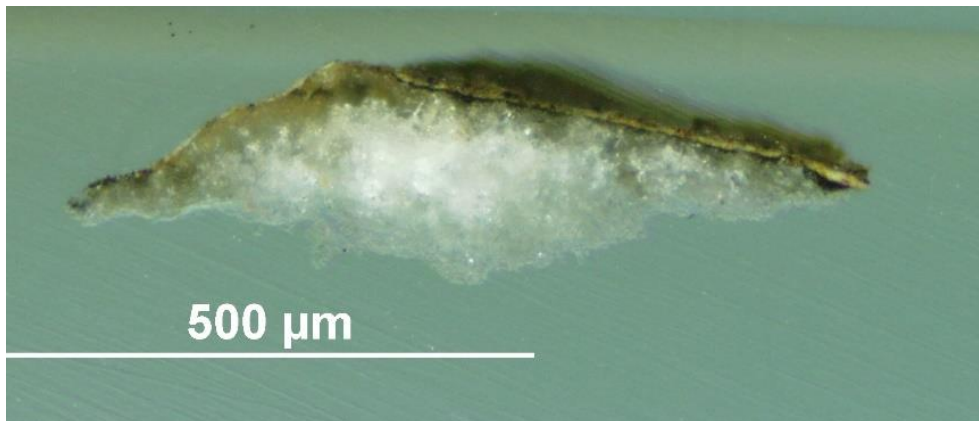
0. Plaster bulk

**Analysis spots.** EDS analysis (yellow): Spectra 13-18 FT-IR analysis (red): nos. 53-61

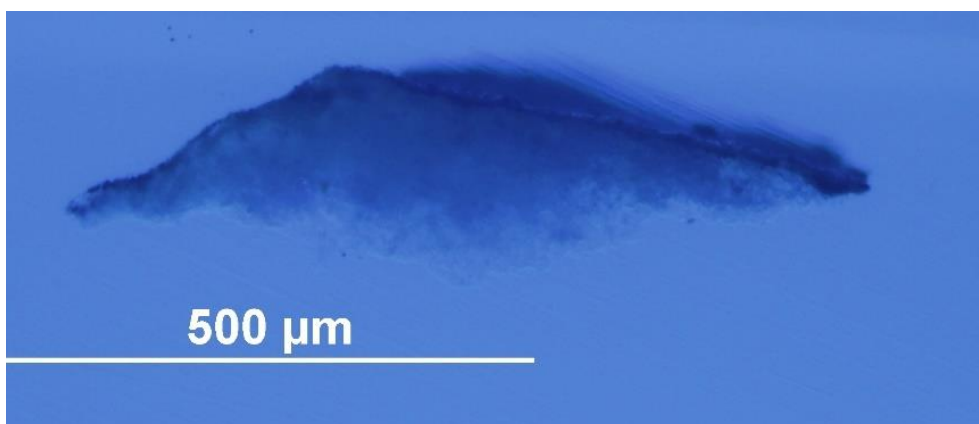
**Summary.** The substrate (layer 0) is made of gypsum plaster (**calcium sulfate**,  $\text{CaSO}_4$ , confirmed by EDS, XRD and by the peak at  $1600\text{ cm}^{-1}$  in the FT-IR spectra) and contains inclusions made of Sr, Na, Si, Al and Mg. EDS mapping confirmed that the large mineral inclusions visible in the BSE image are made of mineral gypsum. Layer 1, which appears yellow under the microscope, consists of a portion of lower layer soaked with the surface coating, showing characteristics of both layer 0 and layers 2-3. A dark line (layer 2) seems consistent with a layer of dirt. Layer 3 is white under visible illumination and, as observed in the BSE image and indicated by EDS mapping, consists of heavy elements such as Ba, Zn and Sr. A **wax or resin** (FT-IR peaks at  $1472$  and  $2800\text{-}3000\text{ cm}^{-1}$ ) was detected in all the layer and due to the complexity of the spectra, the presence of a protein cannot be excluded in this sample. Traces of Al are present in all the layers due to the polishing solution and traces of other elements can be seen especially in the top layers (Ba, Zn, Fe, P, Na and Cl).



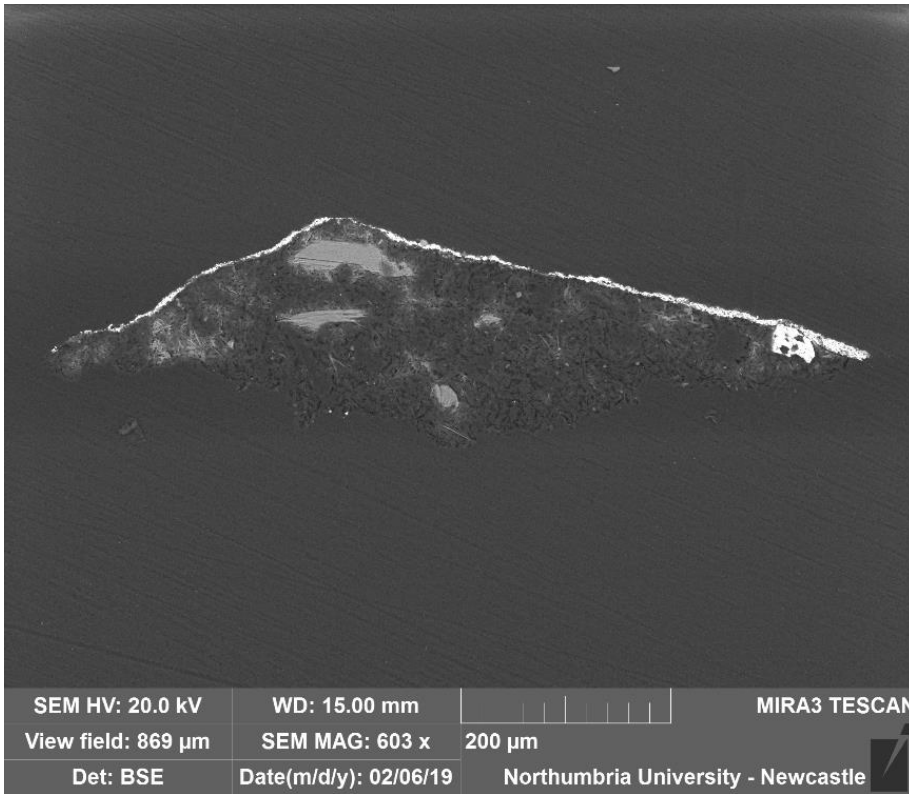
**XRD diffractogram (left):** a fragment of this sample was pulverised revealed the profile of gypsum (calcium sulfate) and the diffractogram was compared to references from the Rigaku SmartLab Database. The most significant peaks were at  $2\theta = 11.62, 20.75, 29.14, 33.36, 34.57, 47.82$ .



**VLR (left)**



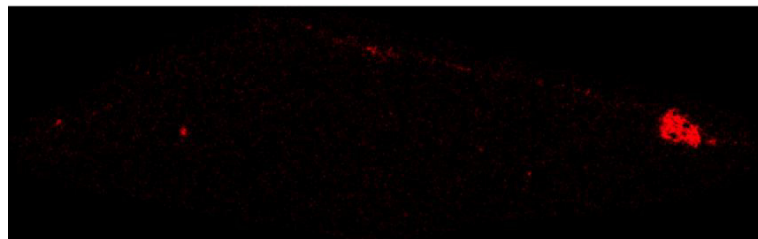
**UVfOM (left)**



**BSE image (left).** The tabular crystalline structure typical of gypsum plaster can be seen in layers 0 and 1. Large mineral gypsum inclusions are visible in the bulk (confirmed by EDS mapping)

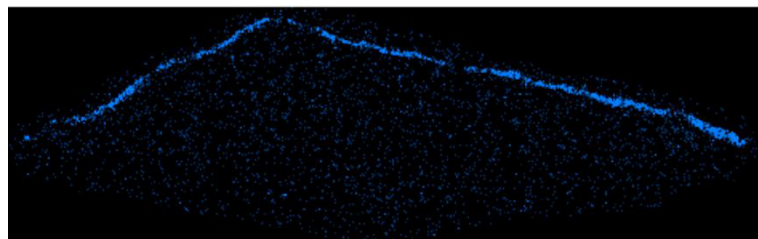
**EDS spectra** indicate that calcium sulfates and carbonates are present in all the layers. Sr is a typical contaminant in mineral gypsum. Fe, Ba, Zn, Na, Si, Ca, Al, Cl, K and P were detected in layers 2-3.

**Strontium (Sr)**

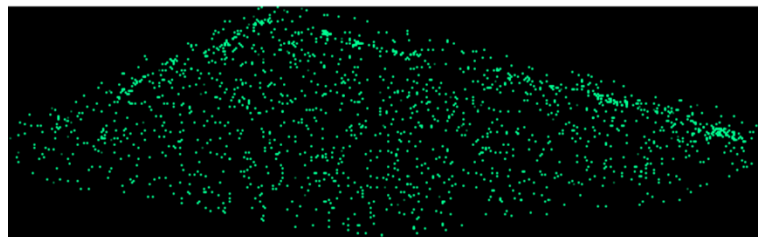


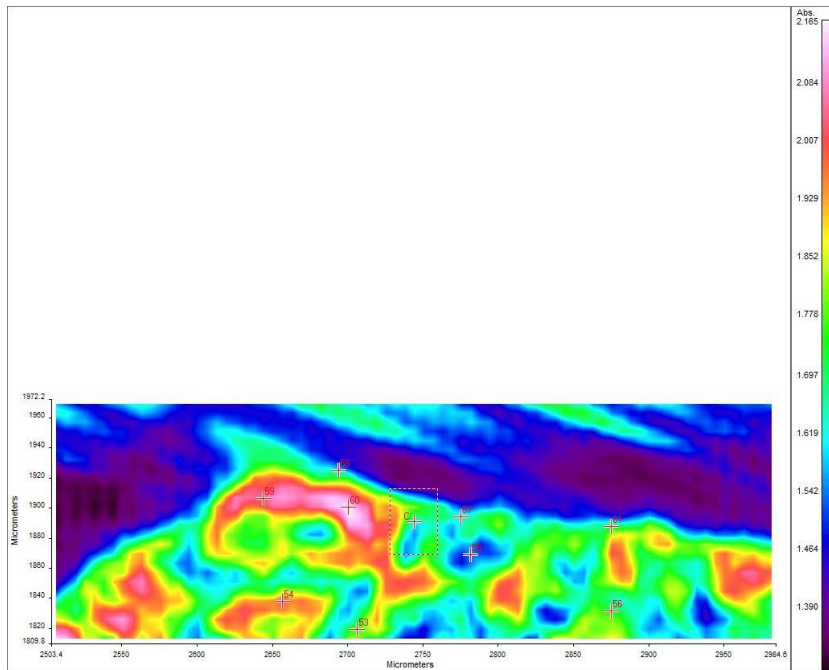
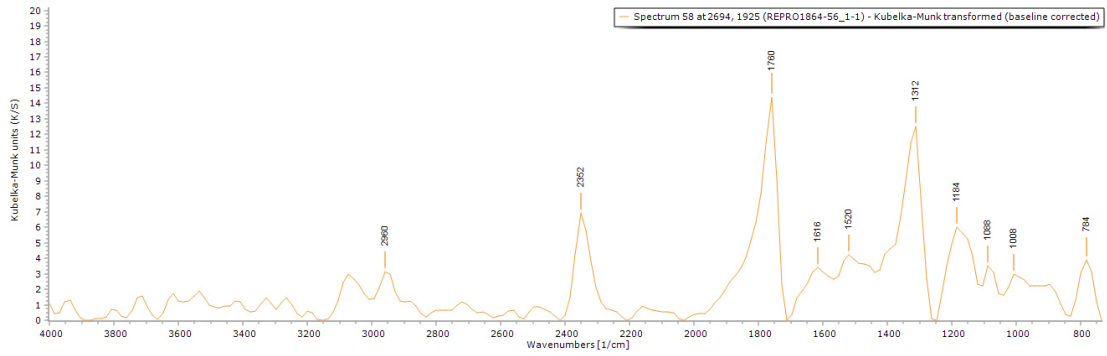
**EDS mapping (right)** shows that Sr (top), Ba (middle) and Zn (bottom) are mostly present in layer 3.

**Barium (Ba)**



**Zinc (Zn)**





**FT-IR spectrum 58** (above) of layer 3. Peaks for the casting resin (1312, 1760  $\text{cm}^{-1}$ ), gypsum (1616  $\text{cm}^{-1}$ , overtone 2200-2300  $\text{cm}^{-1}$ ) and a wax/resin (bands around 1000-1100  $\text{cm}^{-1}$  and 1500  $\text{cm}^{-1}$ , 2960  $\text{cm}^{-1}$ ). A summary of the peaks observed in the spectra 53-61 can be seen in the table below.

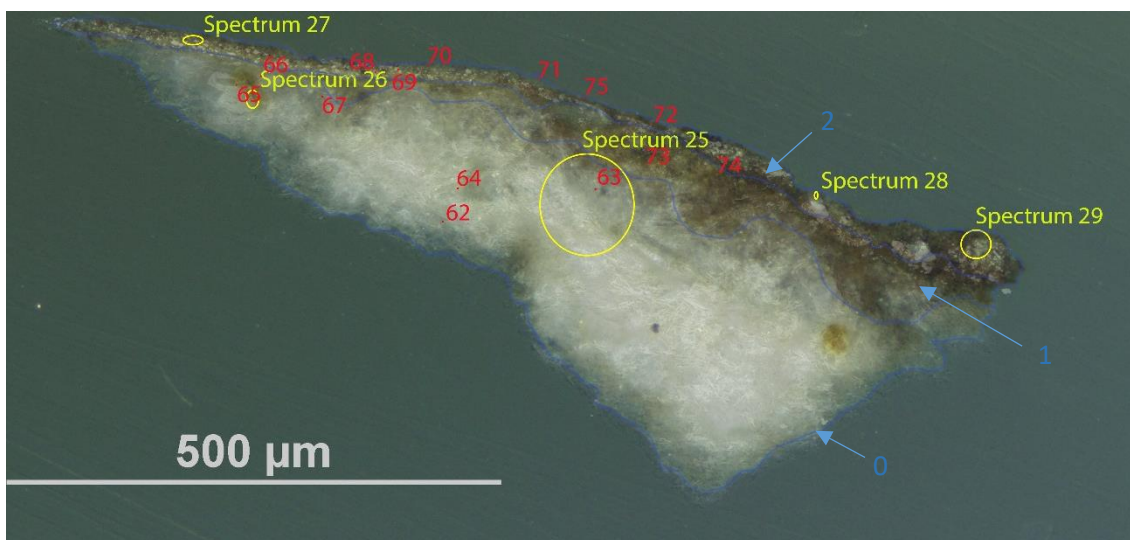
**FT-IR (FPA) image** (left). No clear layer definition can be observed in the FPA image.

Spectrum	Layer	peaks ( $\text{cm}^{-1}$ )						
		Casting Resin	Gypsum	Carbonate	Wax/resin	C=O ester carbonyl	SO overtone	Unknown
53	0	1312, 1760	1568, 1616		768, 1200, 1472, 2928		2128, 2192, 2304	
54	0	1312, 1760	1584, 1680		816, 1008, 1072, 1424, 2864, 2976		2144, 2224	
55	1	1312, 1760	1600		768, 1088, 1184, 1472, 2960		2096, 2352	
56	0	1312, 1760	1588, 1632		928, 1184, 1472, 2832, 2959		2464	
57	2	1312, 1760	800, 1632		1168, 1408, 2896, 2976		2336, 2480	1536
58	3	1312, 1760	1616		784, 1008, 1088, 1184, 2960		2352	1520
59	1	1312, 1760	1584, 1664		1040, 1232, 1408, 1472, 2848, 2944		2304	1280
60	1	1344	1600, 1664	800, 1776	928, 1008, 1248, 1296, 1408, 2832, 2959		2256, 2397	1520, 1856
61	3	1328, 1760	1600, 1664		992, 1152, 1504, 2960		2336	

## Sample 2



**Sampling.** This fragment was taken from an area of loss, from the PL rim.



Above: Overlapped (OM and BSE) cross-section image showing the stratigraphy (blue indicators).

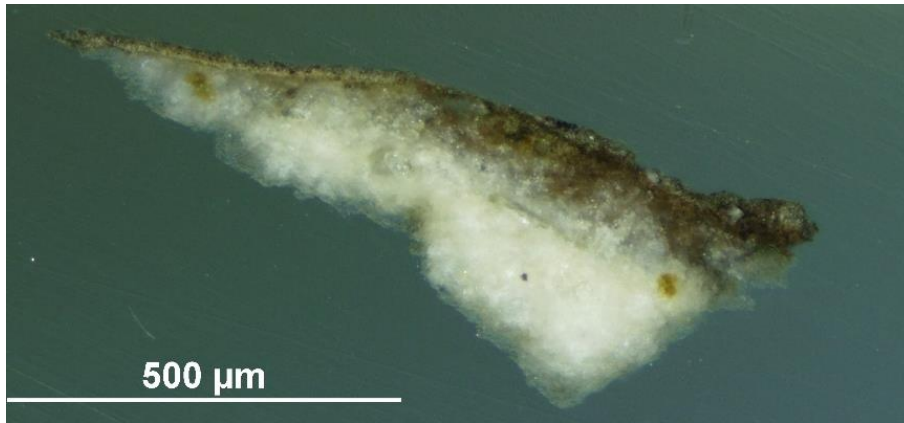
### 2. Layer with dark inclusions

### 1. Yellowish and undefined layer

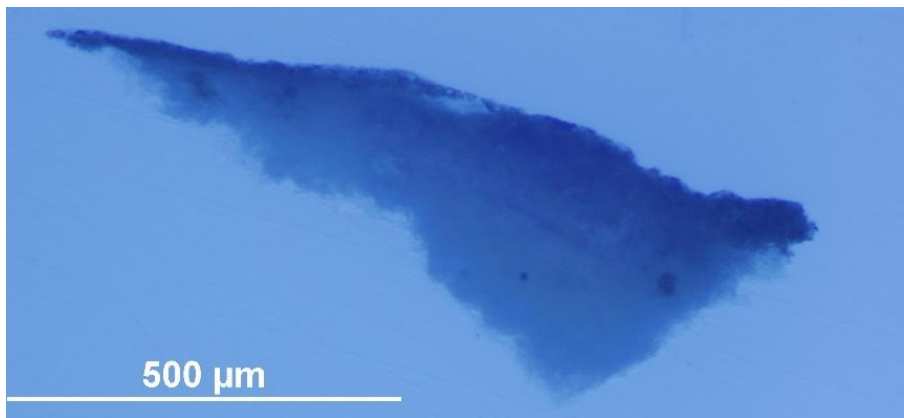
### 0. Plaster bulk

**Analysis spots.** EDS analysis (yellow): Spectra 25-29. FT-IR analysis (red): nos. 62-75

**Summary.** The substrate (layer 0) is made of plaster (**calcium sulfate**,  $\text{CaSO}_4$  and **lead**, Pb, confirmed by EDS and by the peak at  $1600$ ,  $1632$  and  $1760\text{ cm}^{-1}$  and overtones in the FT-IR spectra). EDS mapping shows that inclusions made of Al, Si and Sr are present in layer 0 and 1. Layer 1, which appears yellow under the microscope, consists of a portion of the lower layer soaked with the surface coating, showing characteristics of both layer 0 and layer 2. Layer 2 appears greyish under visible illumination and shows several inclusions. By looking at the EDS mapping, these inclusions seem to consist of Fe, Ba and Cl. Traces of Si, Al, Ti, Pb, K and Mn are also present in layer 2. A **wax or resin** (FT-IR peaks at  $800$ - $1100$ ,  $1472$ ,  $2800$ - $3000\text{ cm}^{-1}$ ) was detected in all the layers and GC/MS indicated the presence of a linseed oil modified alkyd resin (esters contributions cannot be seen in the FT-IR spectra, but this could be due to the complexity of the admixture and overall small concentration of the oil). Al is overall present as used as a polishing agent or part of the Si-Sr inclusions.

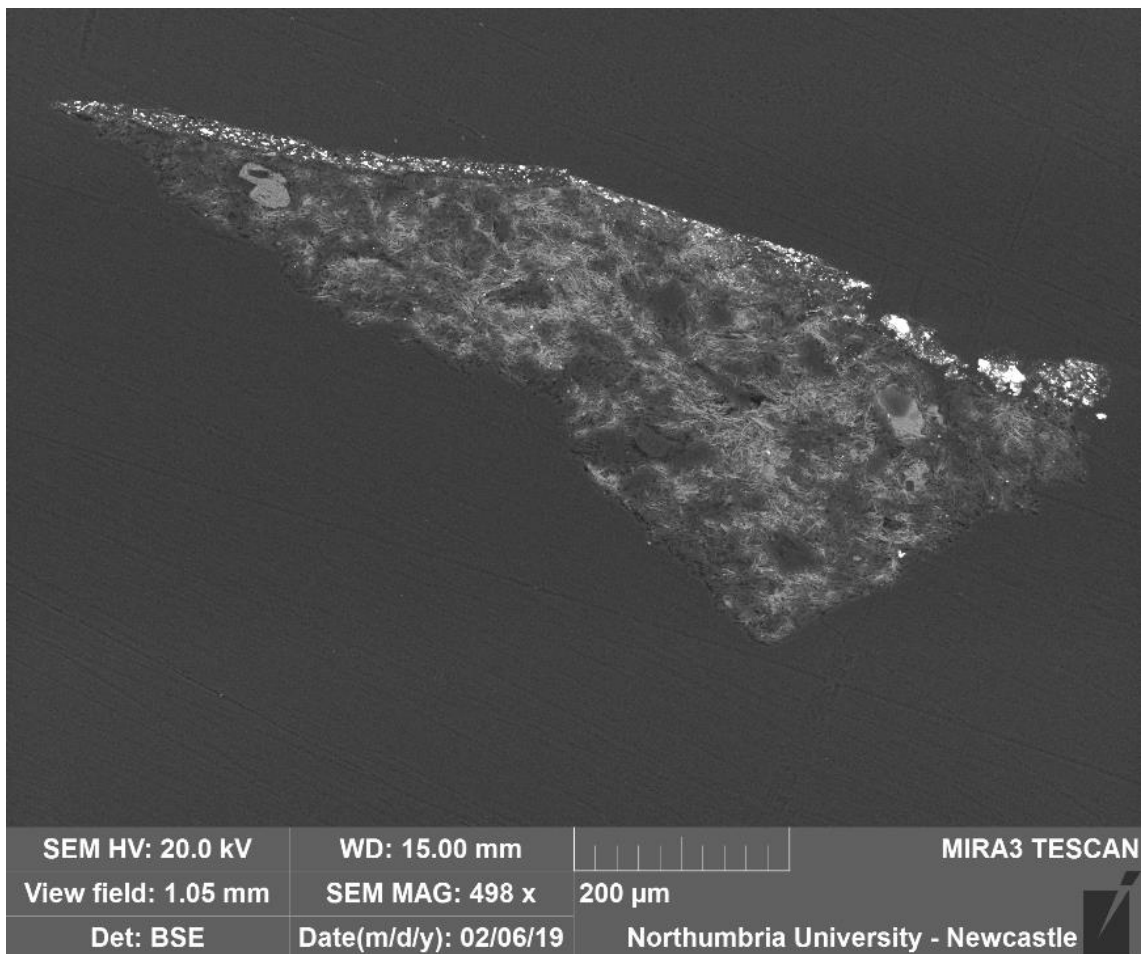


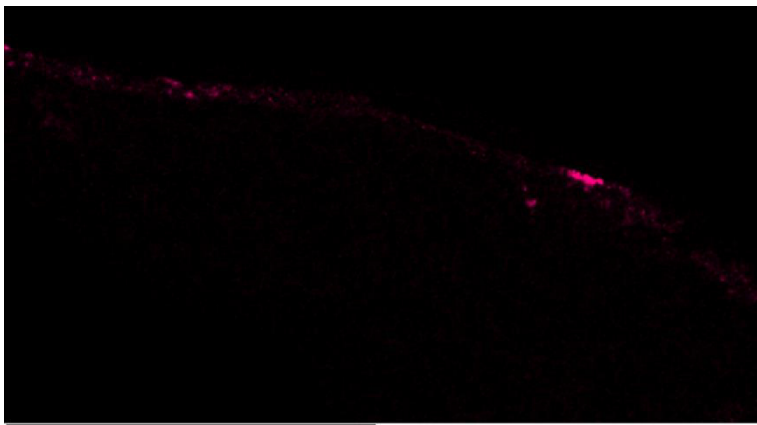
VLR OM (left)



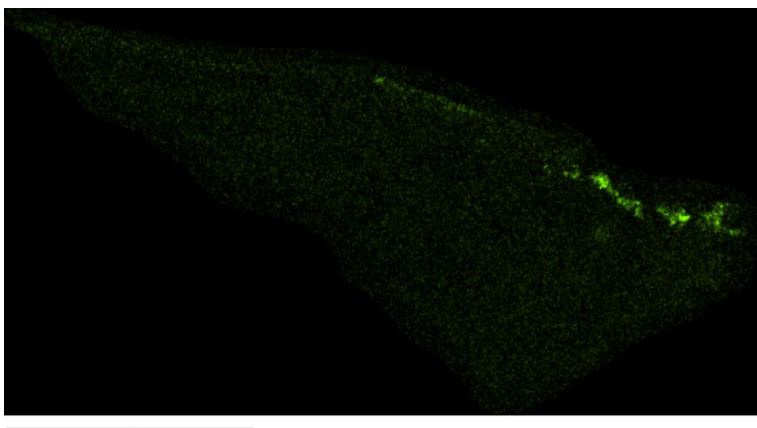
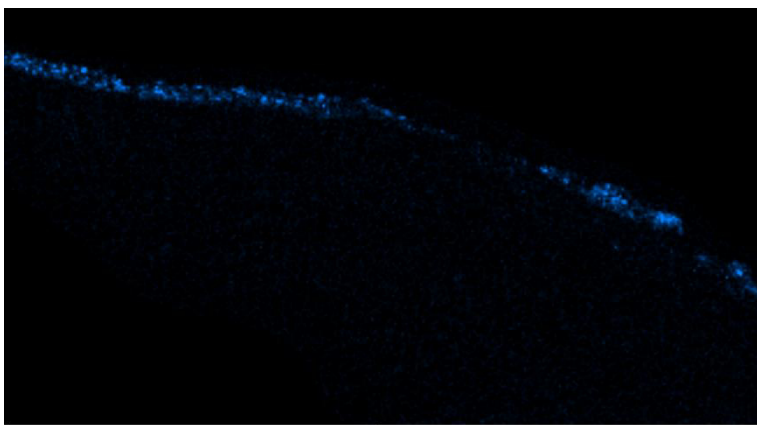
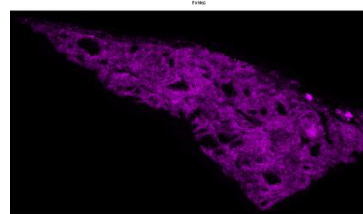
UVfOM (left)

**BSE image** (below). The tabular crystalline structure typical of gypsum plaster can be seen in layers 0 and 1. Inclusions are also visible in layer 2.

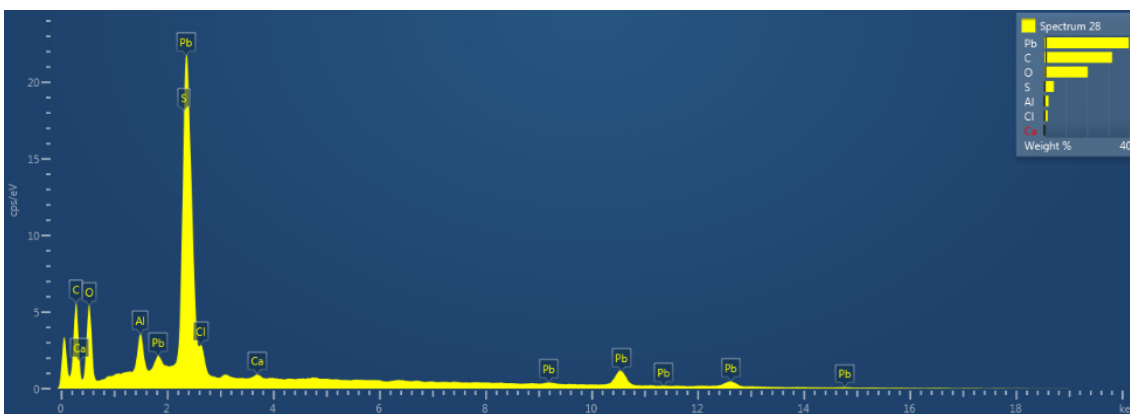


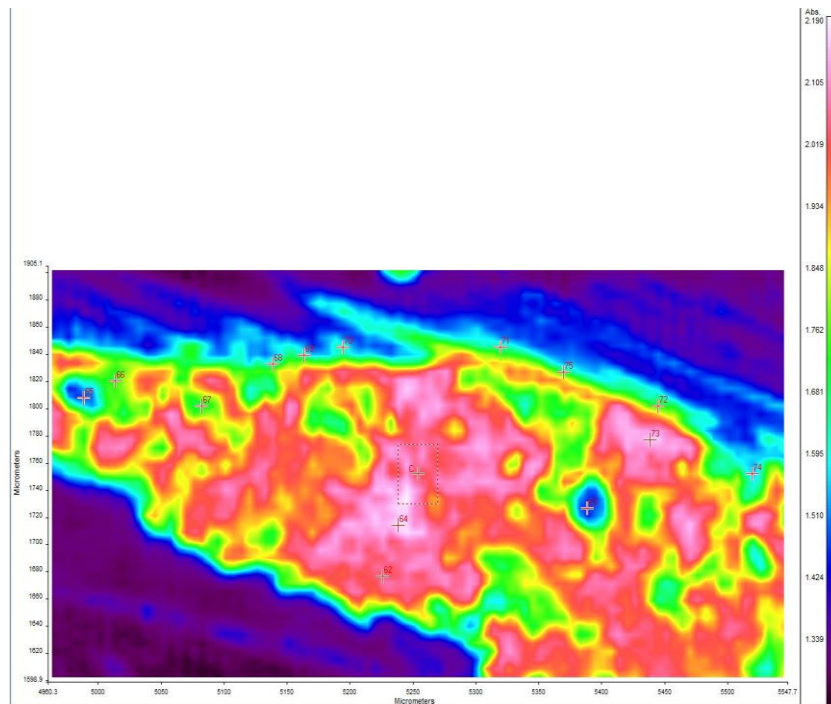
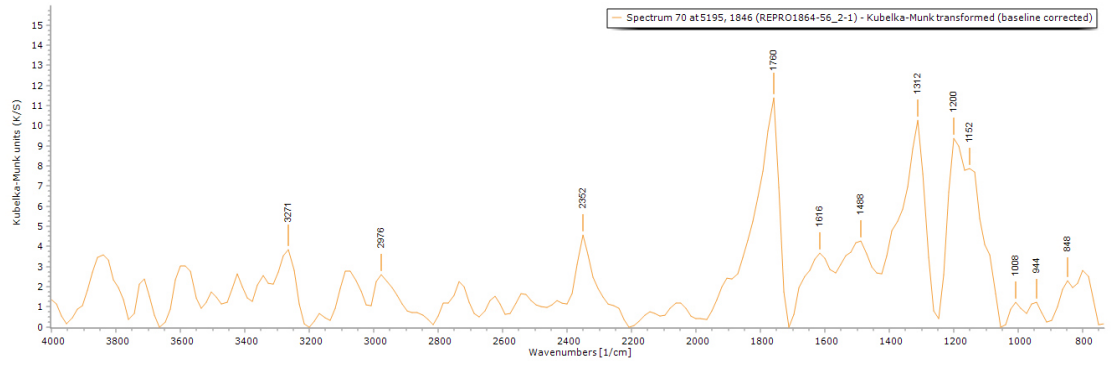


**EDS mapping** shows that Fe (top left), Ba (centre left) and Cl (bottom left) are mostly located in layer 2. Pb (below) is significantly present in all the layers.



**EDS spectrum** (below, spectrum 28) of layer 2 shows C, O, Ca and S, indicating calcium sulfates. This spectrum also shows the presence of lead Pb. Al traces are present in all the layers (polishing medium), or as part of Si-Sr inclusion.

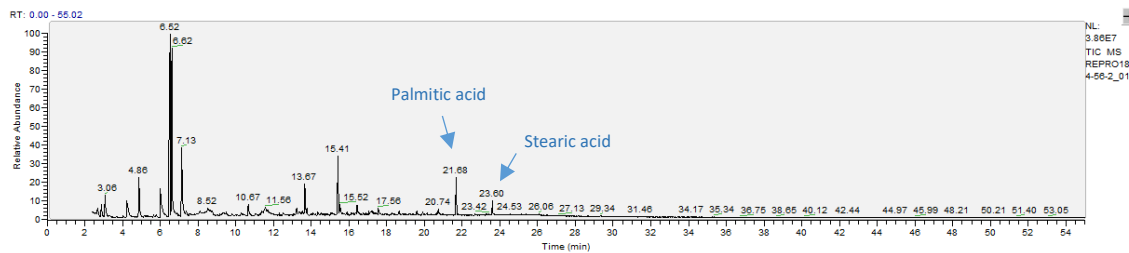




**FT-IR spectrum 70** (above) of layer 2. Peaks for the casting resin (1312, 1760  $\text{cm}^{-1}$ ), gypsum (1616  $\text{cm}^{-1}$ , overtone 2200-2300  $\text{cm}^{-1}$ ) and a wax/resin (1088, 1152, 1200, 1488, 2976  $\text{cm}^{-1}$ ). A summary of the peaks observed in the spectra 62-75 can be seen in the table below.

**FT-IR (FPA) image** (left). No clear layer definition can be observed in the FPA image.

Spectrum	Layer	peaks (cm-1)						
		Casting Resin	Gypsum	Carbonate	Wax/resin	=O ester carbonyl	SO overtone	Unknown
62	0	1312, 1760	832, 1616		768, 1072, 1472, 2784, 2983		2272	1856
63	0	1328, 1760	1632		768, 1088, 1184, 1472		2352	
64	0	1328, 1760	1600, 1680		944, 1024, 1088, 1232, 1440, 2832, 2912		2272, 2384	
65	0	1312, 1760			768, 1184, 1472		2352	
66	0	1312, 1760	816, 1616		1200, 1488, 2880, 2992		2352	
67	0	1312, 1760	1600		768, 848, 992, 1072, 1200, 1504, 2944		2208, 2368	1920
68	2	1312, 1760	1616		768, 1088, 1184, 1392, 1472		2320	1840
69	2	1312, 1760	1600, 1664		784, 944, 1152, 1488, 2960		2048, 2336	
70	2	1312, 1760	1616		848, 944, 1008, 1152, 1200, 1488, 2976		2352	
71	2	1312, 1760	1600		784, 1008, 1168, 1392, 1472, 2816		2320	
72	2	1328, 1760	1632		848, 1008, 1136, 1520, 2864, 2928		2352	1856
73	1	1312, 1760	1568		1040, 1376, 1488		2256	1872
74	1	1312, 1760	1600		1152, 1392, 2832		2336	
75	2	1312, 1760	1632		784, 848, 960, 992, 1136, 1200, 1392, 1472, 1552, 2928		2336	

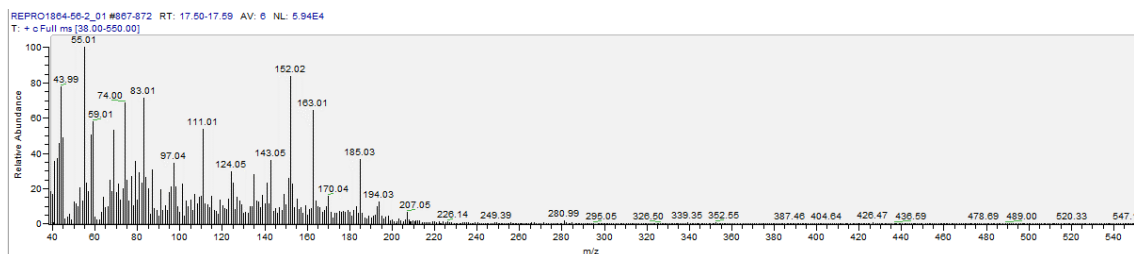
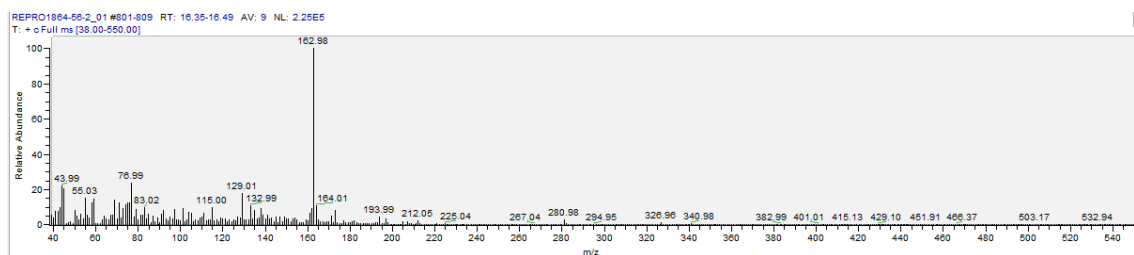


RT	m/z	Assignment	Formula
4.21	45(100), 58(4), 74(42)	Diethyl ether	C4H10O
4.86	43(9), 59(100), 88(5)	C6 fragment	
5.99	42(17), 58(100), 117(9)	1,2-Ethanediamine	C2H8N2
6.52	45(21), 48(11), 66(25), 79(17), 95(100), 125(6)	Sulfuric acid, dimethyl ester	C2H6O4S
6.62	45(11), 65(23), 80(100), 95(14), 109(6)	Methanesulfonic acid, methyl ester	C2H6O3S
7.13	44(9), 56(8), 72(100), 131(2)	1,2-Ethanediamine, N,N'-diethyl-N,N'-dimethyl-	C8H20N2
10.67	45(100), 58(15), 71(23), 73(15), 75(7), 103(49), 130(5)	Phthalic anhydride	C8H4O3
13.67	45(39), 55(14), 71(100), 85(19), 101(10), 111(10), 142(18), 147(10), 156(5)	Phthalic anhydride	C8H4O3
15.41	45(59), 55(21), 59(10), 75(67), 85(100), 101(11), 115(39), 127(20), 143(7), 154(12), 168(11), 186(8)	Alkyd Resin fragment	
16.44	44(22), 55(15), 77(24), 83(10), 115(10), 129(18), 133(11), 163(100), 194(5), 212(5), 281(5)	Dimethyl phthalate	C10H10O4
17.56	44(77), 55(100), 59(58), 74(69), 83(71), 97(34), 111(54), 124(30), 143(36), 152(84), 163(64), 170(10), 185(37), 194(10), 207(10)	Dimethyl phthalate	C10H10O4
19.6	44(100), 58(43), 74(52), 79(40), 91(25), 115(19), 135(31), 153(10), 163(23), 193(52), 207(10), 224(5), 281(5)	FA fragment	
21.68	44(33), 55(31), 69(19), 74(100), 87(64), 101(10), 129(10), 143(24), 171(10), 185(10), 207(10), 227(12), 239(10), 270(10)	methyl palmitate	C17H34O2
23.6	44(67), 55(37), 69(25), 74(100), 87(72), 101(10), 129(10), 143(28), 155(10), 185(10), 199(10), 207(29), 241(10), 255(14), 281(10), 298(10)	methyl stearate	C19H38O2

**Py-TMAH-GC/MS chromatogram** (above and described in the table, left) shows small fragments due to derivatization (from t = 4.21 to 7.13 min) and markers characteristic of **alkyd resins** (t = 10.67, 13.67, 15.41, 16.44 and 17.56 min). The presence of fatty acids fragments (t = 19.60) and **methyl palmitate** (t = 21.68) and **stearate** (t = 23.60) suggest that the resin has been modified with a **drying oil** (P/S = 1.30, possibly linseed oil).

RT = retention time, m/z = mass/charge ratio

Mass spectra assigned to dimethyl phthalate at t = 16.44 and 17.56 (fragmentation patterns, below)

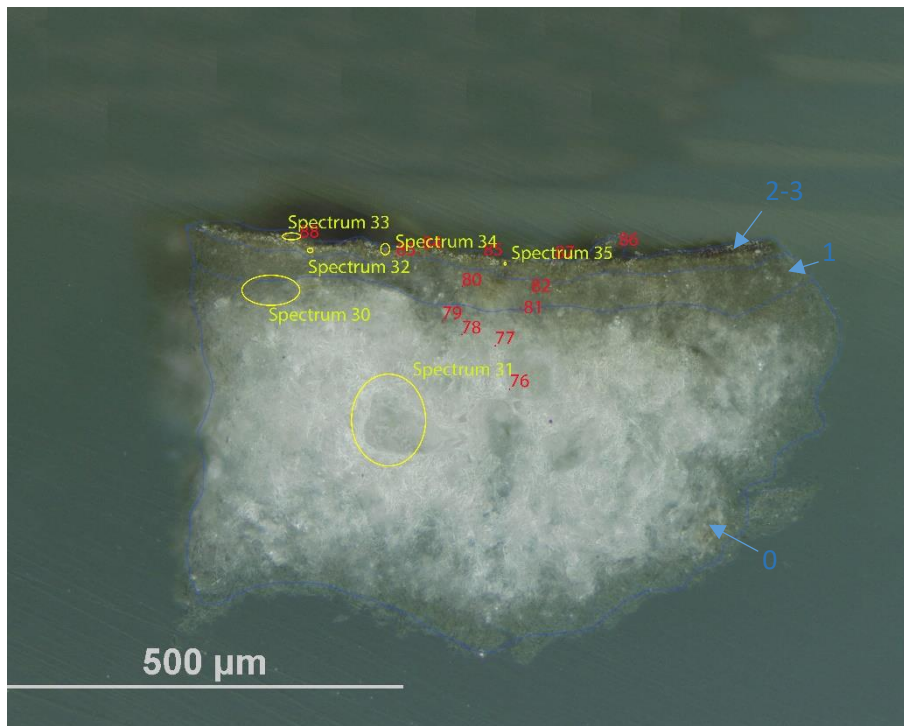


Diagnostic peaks, such as the phthalic anhydride and dimethyl phthalate indicates the presence of an alkyd resin. The fragmentation patterns of such derivatives can be complex and variate, depending on the derivated block from the polymeric structure but can be uniquely assigned by identifiable fragments such as m/s = 77, 92, 133, 163, 194 amongst the others (Cappitelli et al., 2004).

## Sample 3



**Sampling.** This fragment was taken from an area of loss located on the bottom edge.

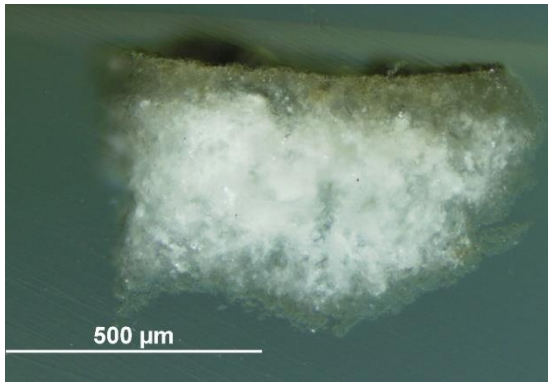


Left: Overlapped (OM and BSE) cross-section image showing the stratigraphy (blue indicators).

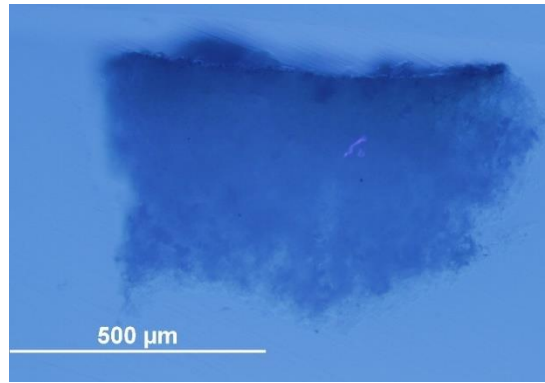
- 3. Varnish**
- 2. Dark layer**
- 1. Yellowish layer**
- 0. Plaster bulk**

**Analysis spots.**  
EDS analysis (yellow): Spectra 30-35; FT-IR analysis (red): nos. 76-88.

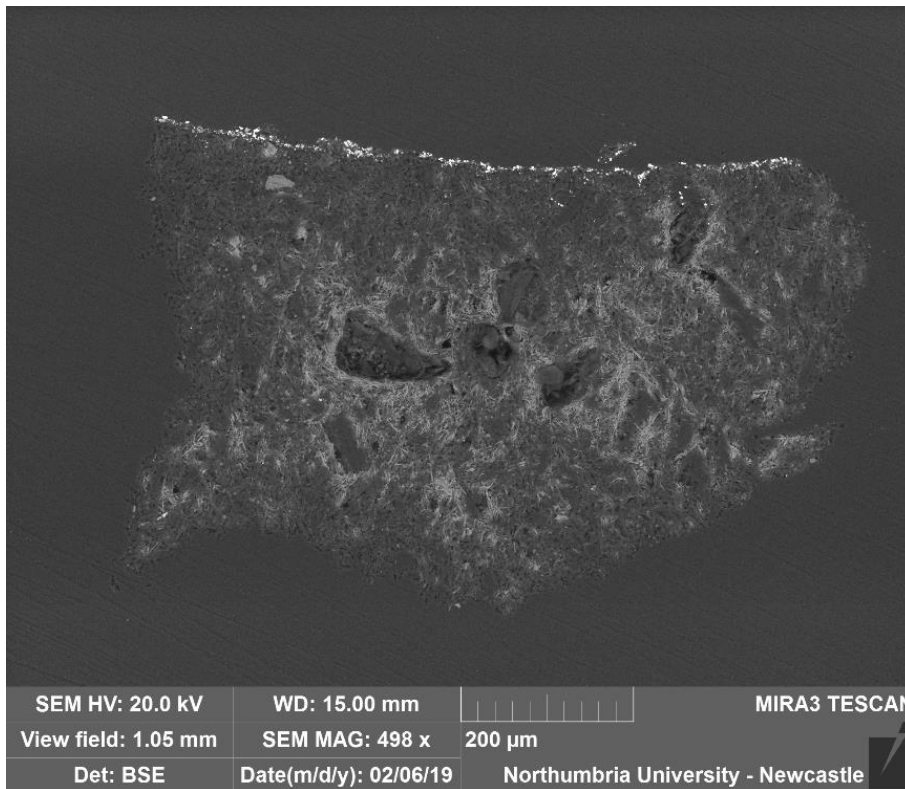
**Summary.** The sample is mostly made of C, O, S and Ca (**calcium sulfate**,  $\text{CaSO}_4$ , confirmed by EDS and by the peak at  $1600$  and  $1616\text{ cm}^{-1}$  in the FT-IR spectra). Al is overall present as used as a polishing agent, but could also, together with K and Si be present as part of silicate inclusions. C, O, S, Ca, Al, Cl, Na, K, Si were detected in all the layers and Ba, Fe, Sr and Mn were also detected in layers 2 and 3. The structure typical of gypsum plaster can be seen in layers 0 and 1. Layer 1 consists of a small portion of the lower layer soaked with the surface coating, showing characteristics of both layer 0 and layer 2. Layer 2, under visible illumination, seems to be made of a yellowish medium and includes several dark particles. The fluorescence colour suggests that layer 3 is made of a different medium from layer 2. A **wax or resin** (FT-IR peaks at  $1100\text{-}1300$ ,  $2800\text{-}3000\text{ cm}^{-1}$ ) was detected in all the and due to the complexity of the spectra, the presence of a protein cannot be excluded in this sample.



VLR OM (above)



UVfOM (left)

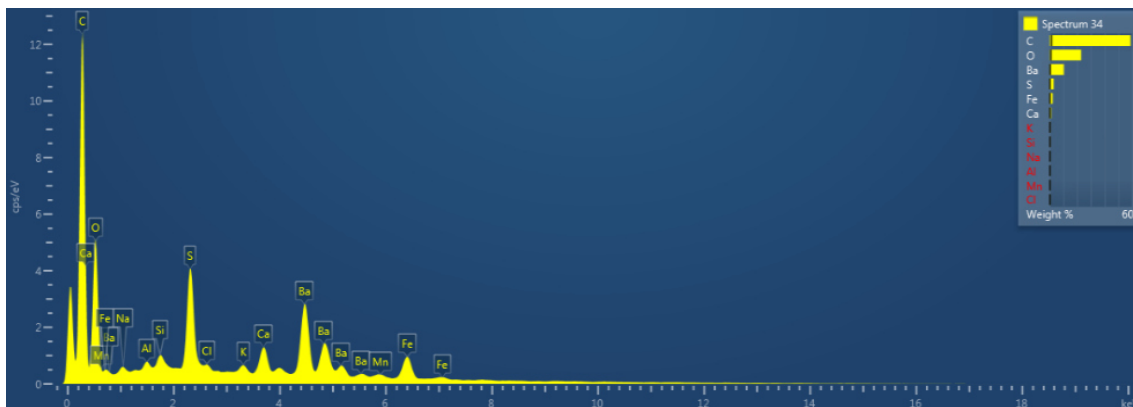


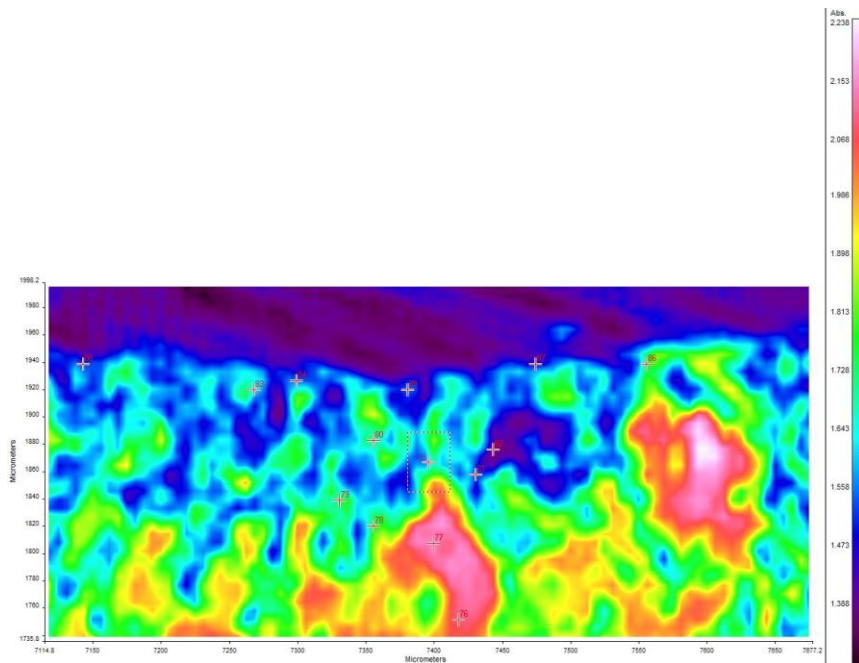
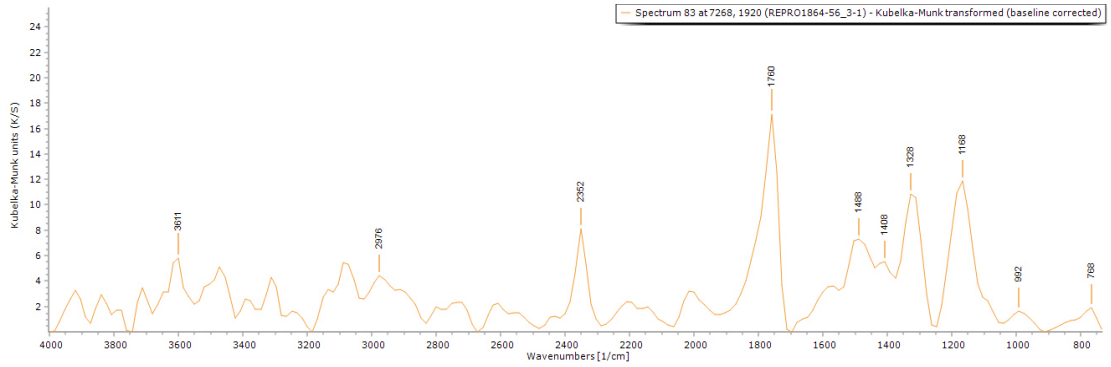
**BSE image (left).**

The tabular crystalline structure typical of gypsum plaster can be seen in layers 0 and 1.

**EDS mapping** did not indicate any notable elements distribution in a layer fashion.

C, O, S, Ca, Al, Cl, Na, K, Si were detected in all the layers and Ba, Fe, Sr and Mn were also detected in layers 2 and 3 (spectrum 34, below).





**FT-IR spectrum 83** (above) of layers 2-3. Peaks for the casting resin (1328, 1760  $\text{cm}^{-1}$ ), gypsum (1600  $\text{cm}^{-1}$ , overtone 2200-2300  $\text{cm}^{-1}$ ) and a wax/resin (1168, 2976  $\text{cm}^{-1}$ ). A summary of the peaks observed in the spectra 76-88 can be seen in the table [below](#).

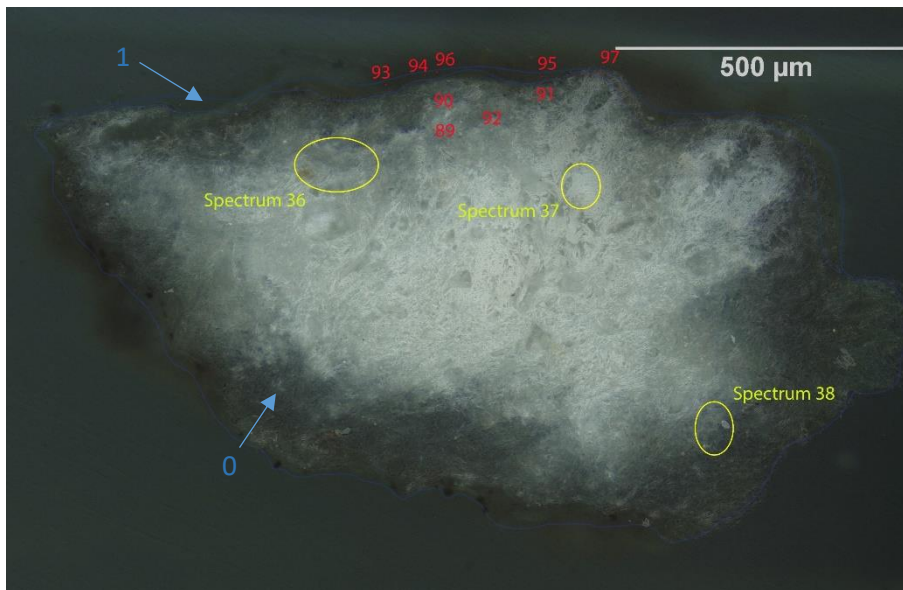
**FT-IR (FPA) image** (left). No clear layer definition can be observed in the FPA image.

Spectrum	Layer	peaks (cm-1)						
		Casting Resin	Gypsum	Carbonate	Wax/resin	C=O ester carbonyl	SO overtone	Unknown
76	0	1312, 1360, 1760	832, 1600		784, 976, 1072, 1200, 1456, 1696, 2928			2208
77	0	1312, 1360, 1760	1600		784, 896, 976, 1072, 1216, 1408, 1472, 1536, 2896, 2976			2224
78	0	1312, 1760	1616		784, 1072, 1216, 1488, 2784, 2951			2336
79	0	1312, 1760			784, 1088, 1200, 1536, 1584, 2886			2352
80	1	1312, 1760	1600		784, 864, 1088, 1200, 1472, 2960			2320
81	1	1312, 1760			768, 1184, 1584			2352
82	1	1312, 1760	1648	800	864, 976, 1088, 1168, 1408, 1584, 2912			2352
83	2-3	1328, 1760			768, 992, 1168, 1408, 1488, 2976			2352
84	2-3	1312, 1760			784, 1184, 1472, 1584, 2960			2352
85	2-3	1312, 1760			784, 848, 1008, 1088, 1168, 1472, 1584, 2912, 2960			2336
86	2-3	1312, 1760			1008, 1184, 1424, 1488, 2929			2352
87	2-3	1312, 1760	1616		784, 1184, 1392, 1504			2336
88	2-3	1312, 1760	1616		784, 1088, 1152, 1472, 2992			2336

## Sample 4



**Sampling.** This fragment was taken from a hole behind the figure's walking stick.



**Left:** Overlapped (OM and BSE) cross-section image showing the stratigraphy (blue indicators).

**1. Layer with dark inclusions**

**0. Plaster bulk**

**Analysis spots.**

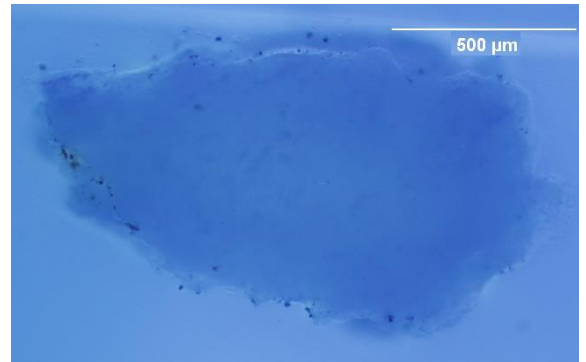
EDS analysis (yellow): Spectra 36-38

FT-IR analysis (red): nos. 89-97

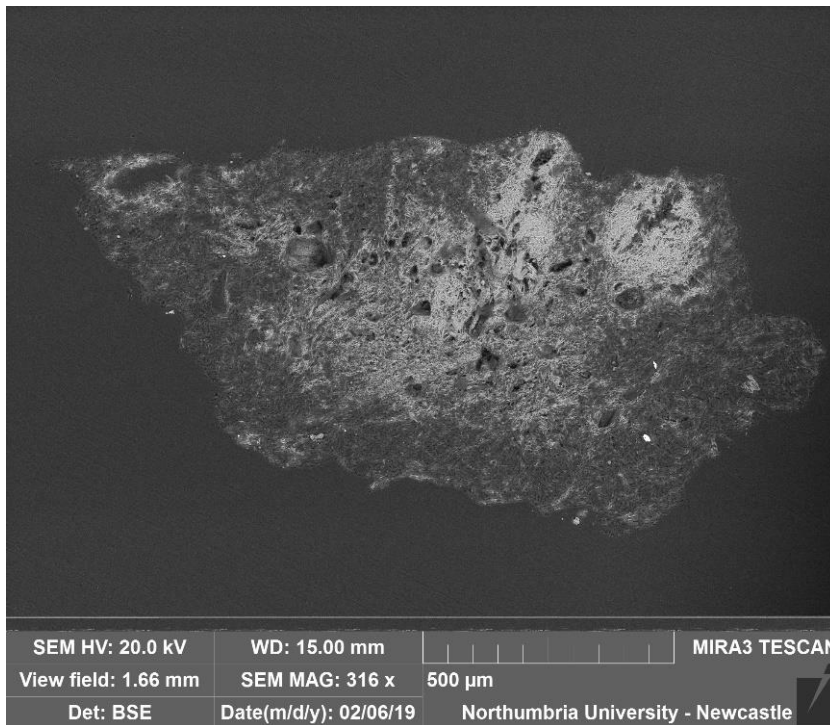
**Summary.** The sample is mostly made of C, O, S and Ca (**calcium sulfate**,  $\text{CaSO}_4$ , confirmed by EDS and by the peak at  $1600$  and  $1632\text{ cm}^{-1}$  and overtones in the FT-IR spectra). Al is overall present as used as a polishing agent but could also be present as part of silicate inclusions. EDS mapping does not show a specific difference in the elements' distribution in the layers. Traces of Sr, Na and Mg were also detected. The tabular structure typical of gypsum plaster can be seen in layers 0 and 1. Layer 1 includes several dark inclusions and is milky-white under UV illumination. A **wax or resin** is suggested by FT-IR spectra ( $1000\text{-}1200\text{ cm}^{-1}$ ,  $1472$  and  $2800\text{-}3000\text{ cm}^{-1}$ ) and due to the complexity of the spectra, the presence of a protein cannot be excluded in this sample.



VLR OM (above)



UVf OM (above)

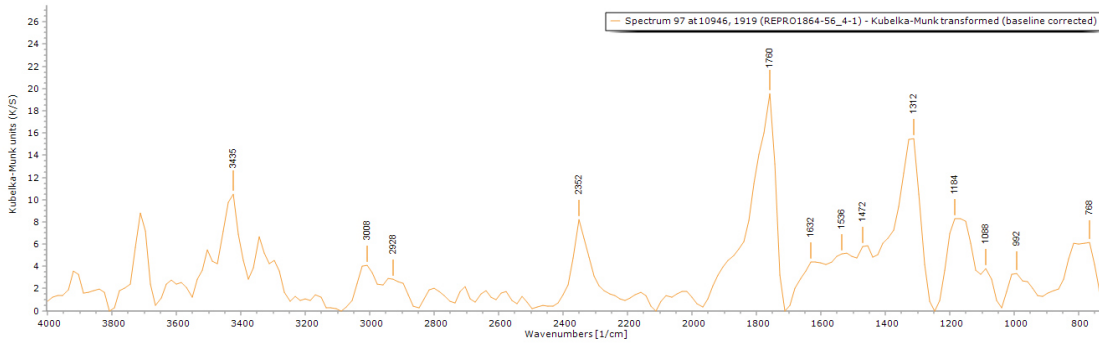


**BSE image (left).** The tabular crystalline structure typical of gypsum plaster can be seen in layers 0 and 1.

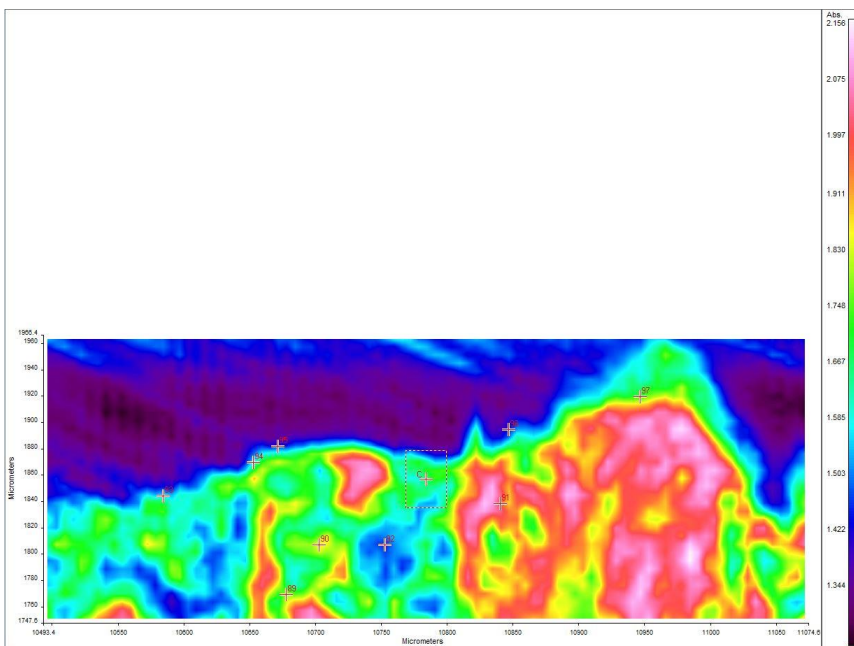
**EDS spectrum 38 (below)** from layer 0 indicates that it consists of C, O, Ca, S, and traces of Sr and Al. Na and Mg were also detected in other spectra in layer 0.

**EDS mapping** did not indicate any notable elements distribution in a layer fashion.





**FT-IR spectrum 97** (above) of layer 1. Peaks for the casting resin (1312, 1760  $\text{cm}^{-1}$ ), gypsum (1632  $\text{cm}^{-1}$ , overtone 2200-2300  $\text{cm}^{-1}$ ) and a wax/resin (1184, 1472, 2928  $\text{cm}^{-1}$ ). A summary of the peaks observed in the spectra 89-97 can be seen in the table below.



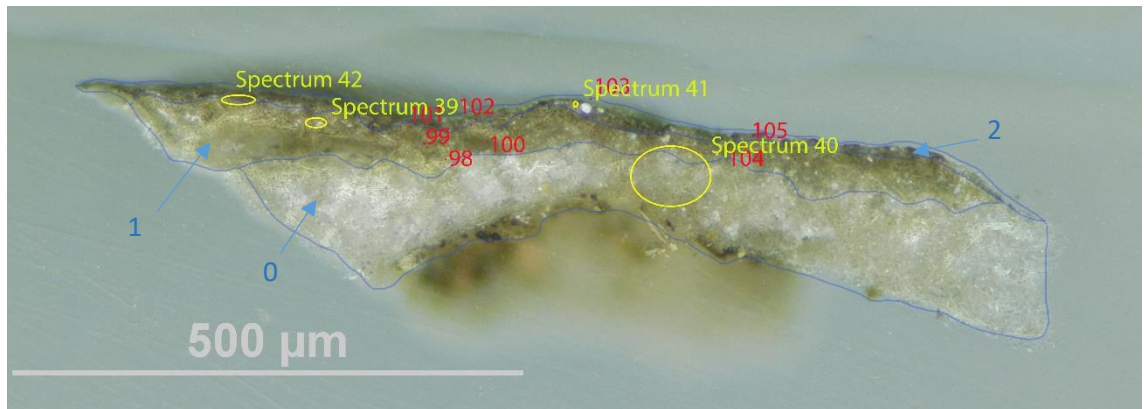
**FT-IR (FPA) image** (left). No clear layer definition can be observed in the FPA image.

Spectrum	Layer	peaks (cm-1)						
		Casting Resin	Gypsum	Carbonate	Wax/resin	C=O ester carbonyl	SO overtone	Unknown
89	0	1312, 1760	1600	1776	784, 864, 1088, 1216, 1472, 2880, 2944		2320	
90	0	1312, 1760	1616		944, 992, 1088, 1216, 1472, 2896, 2992		2352	
91	0	1312, 1760	832, 1600		784, 896, 976, 1024, 1088, 1232, 1360, 1472, 2848, 2944		2368	
92	0	1312, 1760	1616		768, 992, 1088, 1136, 1200, 1504, 2880		2352	
93	1	1312, 1760	1616		784, 1184, 1392, 1488, 2992		2320	
94	1	1312, 1760	1600		784, 1088, 1184, 1504, 2992		2336	
95	1	1312, 1760	1616		784, 992, 1088, 1168, 1392, 1456, 1536		2352	
96	1	1328, 1760	1616		784, 992, 1088, 1152, 1472, 2992		2352	
97	1	1312, 1760	1632		768, 992, 1088, 1184, 1472, 1536, 2928		2352	

## Sample 5



**Sampling.** This fragment was taken an area of loss from the centre of the relief, at the feet of the figure.



Left: Overlapped (OM and BSE) cross-section image showing the stratigraphy (blue indicators).

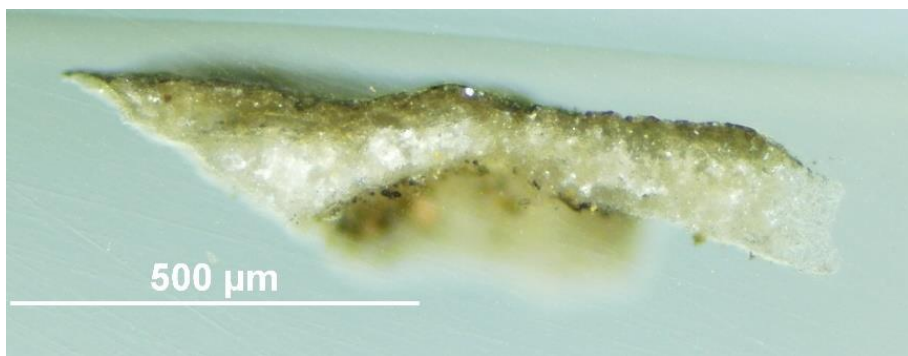
### 2. Dark layer

### 1. Yellowish layer

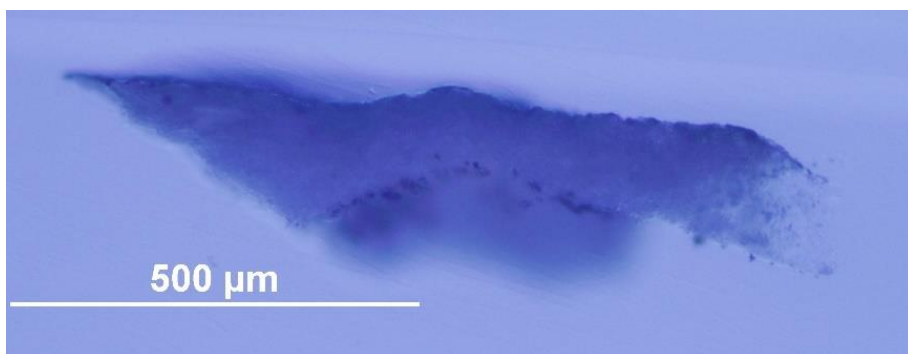
### 0. Plaster bulk

**Analysis spots.** EDS analysis (yellow): Spectra 39-42; FT-IR analysis (red): nos. 98-105.

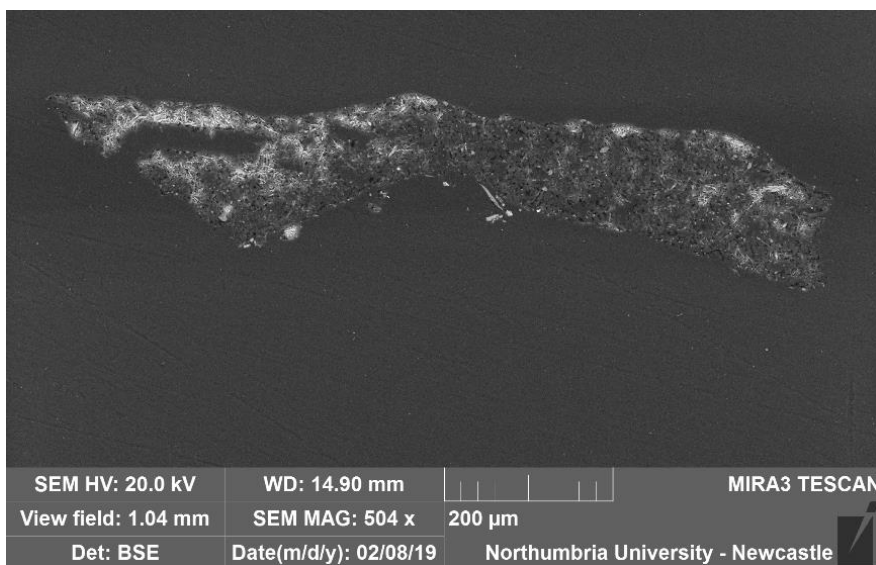
**Summary.** The sample is mostly made of C, O, S and Ca (**calcium sulfate**,  $\text{CaSO}_4$ , confirmed by EDS and by the peak at  $1600$  and  $1632\text{ cm}^{-1}$  in the FT-IR spectra). Al is overall present as used as a polishing agent, but could also, together with K and Si be present as part of silicate inclusions. EDS mapping does not show a specific difference in the elements' distribution in the layers. K, Na and Cl were found evenly distributed in all the layers. Traces of Mg and P were detected in layer 2. The tabular structure typical of gypsum plaster can be seen in layers 0 and 1. Layer 1, which appears yellow under the microscope, consists of a small portion of the lower layer soaked with the surface coating. A **wax or resin** is suggested by FT-IR spectra ( $1000\text{-}1200\text{ cm}^{-1}$ ,  $1472$  and  $2800\text{-}3000\text{ cm}^{-1}$ ) and due to the complexity of the spectra, the presence of a protein cannot be excluded in this sample.



VLR OM (left)



UVf OM (left)

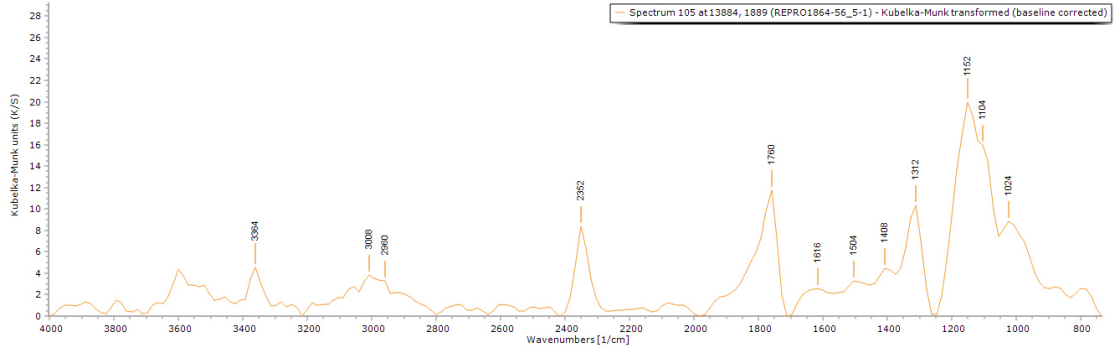


**BSE image (left)**. The tabular crystalline structure typical of gypsum plaster can be seen in layers 0 and 1.

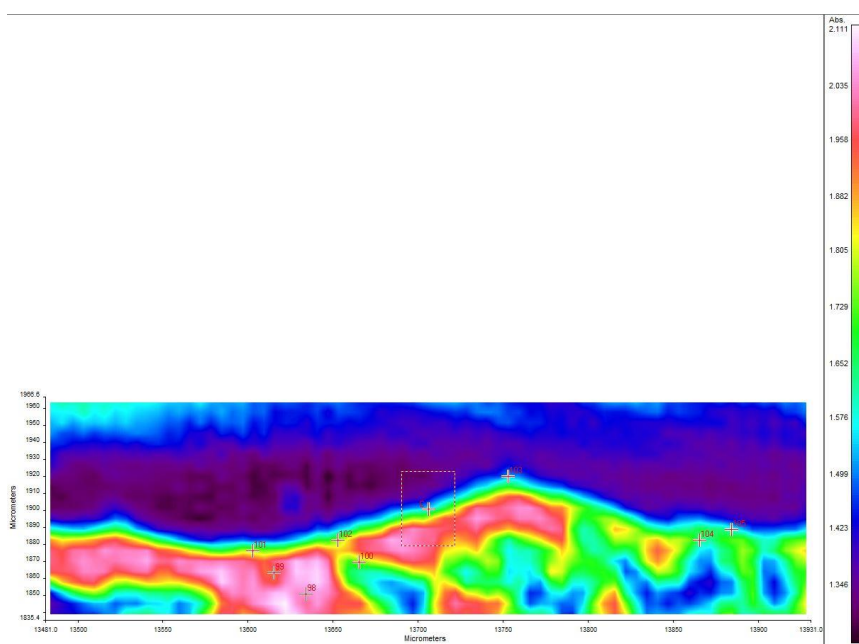
**EDS spectrum 42 (below)** from layer 2 shows C, O, S, Ca, Al, Na, Si, K, Cl, Mg.

**EDS mapping** did not indicate any notable elements distribution in a layer fashion. K, Na and Cl appear spread evenly in the layers and Si and Al are clustered in inclusions.





**FT-IR spectrum 105** (above) of layer 2. Peaks for the casting resin (1312, 1760  $\text{cm}^{-1}$ ), gypsum (1616  $\text{cm}^{-1}$ , overtone 2200-2300  $\text{cm}^{-1}$ ) and a wax/resin (1408, 2960  $\text{cm}^{-1}$ ). A summary of the peaks observed in the spectra 98-105 can be seen in the table [below](#).



**FT-IR (FPA) image** (left). No clear layer definition can be observed in the FPA image.

Spectrum	Layer	peaks (cm-1)						
		Casting Resin	Gypsum	Carbonate	Wax/resin	C=O ester carbonyl	SO overtone	Unknown
98	1	1328, 1760	1680		768, 864, 1072, 1216, 1456, 1584, 2960			2272
99	1	1312, 1760	1616		784, 1072, 1216, 1472, 2880			2280
100	1	1312, 1760			784, 864, 1088, 1200, 1392, 1504, 1568, 2704, 2944			2352
101	1	1312, 1760	1648		784, 1088, 1488, 2816, 2965			2384 1920
102	2	1312, 1760	1616	800	848, 1008, 1088, 1168, 1392, 1472, 2864, 2960			2352
103	2	1312, 1760	1600		784, 1008, 1088, 1408, 1488, 2816, 2960			2336
104	1	1312, 1760			1088, 1168, 1392, 1472, 1584, 2928			2368 1664
105	2	1312, 1760	1616		1024, 1104, 1152, 1408, 1504, 2960			2352

## Experimental

The object was observed, and its conditions were documented. Samples from selected areas were taken by Valentina Risdonne. When possible, each sample was split into two parts: one fragment was embedded in polyester resin (Tiranti clear casting resin), polished and analysed under an optical microscope and the other was put aside for py-TMAH-GC/MS.

The optical microscopy was performed with an Olympus BX51 Metallurgical Microscope equipped with four objectives (magnification of x5, x20, x50 and x100), and an x10 eyepiece. In many instances, a small amount of white spirit was applied on the surface of the cross-section to improve the saturation under the microscope. The microscope is equipped with a 6-cube filter turret which allows operating the system in reflected visible light (brightfield and darkfield mode) and reflected UV light (365 nm) using a 100 W mercury burner.

The SEM-EDS analysis was performed with a field emission TESCAN MIRA 3 with gigantic chamber. The SEM is equipped with: secondary electron detector (SE), secondary electron in-beam detector (In-beam SE), back-scatter detector (BSE), back-scatter in-beam detector (In-beam BSE), cathodoluminescence detector (without wavelength detection) (CL), plasma chamber/sample cleaner and software Alicona 3D imaging. For the EDS analytical part, it has an Oxford Instruments setup: Software: AztecEnergy, X-ray detector X-Max 150 mm<sup>2</sup> and X-ray detector X-Max Extreme, low energy detector for thin films, high resolution and low voltage. The samples were analysed by SEM-EDS Low Vacuum Mode (10-15 Pa). EDS Mapping and data processing were performed with Aztec Oxford software.

A Perkin Elmer Frontier FT-IR spectrometer (350 cm<sup>-1</sup> at the best resolution of 0.4 cm<sup>-1</sup>) was used, equipped with a germanium crystal for ATR measurements and combined with a Spectrum Spotlight 400 FT-IR microscope equipped with a 16×1 pixel linear mercury cadmium telluride (MCT) array detector standard with InGaAs array option for optimised NIR imaging. Spectral images from sample areas are possible at pixel resolutions of 6.25, 25, or 50 microns. The Perkin Elmer ATR imaging accessory consists of a germanium crystal for ATR imaging. These run with Perkin Elmer Spectrum 10™ software and with SpectrumIMAGE™ software. Baseline and Kubelka-Munk corrections were applied to the raw data acquired in diffuse reflectance.

The XRD analyses were performed with a Rigaku SmartLab SE equipped with a HyPix-400, a semiconductor hybrid pixel array detector and Cu source. The analyses were performed in Bragg-Brentano geometry mode, with 40 kV tube voltage and 50 mA tube current. The diffractograms were processed with a SmartLab II software. The data was compared to the RUFF database (Lafuente et al., 2016) and COD Database (Gražulis et al., 2009).

The instrument used for GC/MS is a Thermo Focus Gas Chromatographer with DSQ II single quadrupole mass spec. The column currently installed is a Agilent DB5-MS UI column (ID: 0.25 mm, length: 30 m, df: 0.25 µm, Agilent, Santa Clara, CA, USA). Carrier gas: helium. Detector temperature: 280 °C, Injector temperature: 250 °C. It can be used with the Pyrola 2000 Platinum filament pyrolyser (PyroLab, Sweden) attachment or in split/splitless mode. Detection: Total Ion monitoring (TIC). 1 µl of the sample with 1 µl of TMAH was placed on the Pt filament for the py-GC/MS. The inlet temperature to the GC was kept at 250 °C. The helium carrier gas flow rate was 1.5 ml/min with a split flow of 41 ml/min and a split ratio of 27. The MS transfer line was held at 260 °C and the ion source at 250 °C. The pyrolysis chamber was heated to 175 °C, and pyrolysis was carried out at 600 °C for 2 s. This run with Xcalibur™ and PyroLab™ software. The library browser supported NIST MS Version 2.0 (Linstrom & Mallard, 2014).

Valentina Risdonne, PhD student

[v.risdonne@vam.ac.uk](mailto:v.risdonne@vam.ac.uk) / [valentina.risdonne@northumbria.ac.uk](mailto:valentina.risdonne@northumbria.ac.uk)

Victoria and Albert Museum – Northumbria University

PhD project 'Materials and techniques for coating of the nineteenth-century plaster casts'

©V&A Museum

3 September 2020

## Notes

17 January 2019	Sampling	Valentina's PhD Lab book 1, page 146
29 January 2019	Casting	Valentina's PhD Lab book 1, page 158
5 February 2019	Microscopy	Valentina's PhD Lab book 1, page 163
14 October 2019	FT-IR	Valentina's PhD Lab book 1, page 175
3 December 2019	XRD	Valentina's PhD Lab book 2, page 4
18 March 2020	GC/MS	Valentina's PhD Lab book 2, page 50

A full record of analysis is available at <https://doi.org/10.25398/rd.northumbria.14040281>

## References

- Cappitelli, F., Zanardini, E., & Sorlini, C. (2004). The biodeterioration of synthetic resins used in conservation. *Macromolecular Bioscience*, *4*(4), 399–406.
- Colombini, M. P., & Modugno, F. (2009). *Organic mass spectrometry in art and archaeology*. John Wiley & Sons.
- Cox, K. G., Price, N. B., & Harte, B. (1974). *An introduction to the practical study of crystals, minerals, and rocks*. Halsted Press.
- Gražulis, S., Chateigner, D., Downs, R. T., Yokochi, A. F. T., Quirós, M., Lutterotti, L., Manakova, E., Butkus, J., Moeck, P., & Le Bail, A. (2009). Crystallography Open Database—an open-access collection of crystal structures. *Journal of Applied Crystallography*, *42*(4), 726–729.
- Lafuente, B., Downs, R. T., Yang, H., & Stone, N. (2016). The power of databases: the RRUFF project. In *Highlights in mineralogical crystallography* (pp. 1–29). Walter de Gruyter GmbH.
- Linstrom, P. J., & Mallard, W. G. (2014). *NIST Chemistry WebBook, NIST standard reference database number 69, National Institute of Standards and Technology, Gaithersburg MD, 20899*.
- Price, B. A., Pretzel, B., & Lomax, S. Q. (2009). Infrared and Raman Users Group Spectral Database; 2007 ed. *IRUG: Philadelphia, PA, USA*.





**Northumbria  
University**  
NEWCASTLE

Analysis Report - Valentina Risdonne

Copy of a relief - Christ at Bethany

(REPRO.1864-57)

Initiator: Charlotte Hubbard; Conservation Department

28 August 2020

© Victoria and Albert Museum



## Analysis Report - Christ at Bethany (REPRO.1864-57)

### Contents

Contents.....	384
List of abbreviations.....	384
Summary.....	385
Sample 1.....	388
Sample 2.....	392
Sample 3.....	396
Sample 4.....	399
Experimental.....	403
Notes.....	404
References.....	404

### List of abbreviations

BSE	Back Scattered Electron
EDS	Energy Dispersive Spectrometry
FT-IR	Fourier-Transform Infra-Red
FPA	Focal Plane Array
GC/MS	Gas Chromatography-Mass Spectrometry
OM	Optical Microscopy
PL	Proper Left
PR	Proper Right
py	pyrolysis
SEM	Scanning Electron Microscopy
TMAH	tetramethylammonium hydroxide
UVF	Ultraviolet Fluorescence
VLR	Visible Light Reflectance
XRD	X-ray Diffraction

## Summary

The bulk of the object is made of gypsum plaster, which contains several types of inclusions (including silicates and carbonates). A layer of dust/dirt can be seen underneath the coating layers suggesting that the coatings were applied sometime after the manufacturing of the cast. The samples taken from the reverse or the edge of the object (samples 1 and 2) show a coating containing silicon and aluminium and barium (sample 1) or strontium (sample 2). Two different coatings, one of which was not uniquely identified and the other shellac-based, are visible in sample 3 but overall detected in all the samples. This suggests that the application of the coatings might have created a film in some area of the casts, whereas in others it might only have soaked the plaster. This would have been dependent on several factors during the application, such as the slightly different porosity in different areas of the cast and the quantity of material applied in each brush application.



Figure 1. The copy of a relief.

The object, '**Copy of a relief - Christ at Bethany (REPRO.1864-57)**' (Figure 1), is a plaster cast of a relief, in stone, with a representation of Christ at Bethany, made for the Chichester Cathedral (UK) in the second quarter of the twelfth century. The plaster cast was made by Giovanni Franchi and Son in London possibly in 1851. The cast was acquired in 1864, bought from Messrs Franchi & Son together with museum no. 1864-56 for £30. The cast is

now located in Gallery 46A (The Ruddock Family Cast Court), displayed upright. Its dimensions are 135.0x112.0 cm.

Samples from the plaster cast were taken from pre-existing areas of loss to investigate the stratigraphy and the method of manufacture (Figure 2). The samples were analyzed to provide data for the study of the objects of the Cast Courts collection within the PhD project 'Materials and techniques for coating of the nineteenth-century plaster casts'. Details on the experimental procedure are available in the Experimental section of this report. A selection of significant results is shown in the following pages and the relevant database of analysis (<https://doi.org/10.25398/rd.northumbria.14040305>).

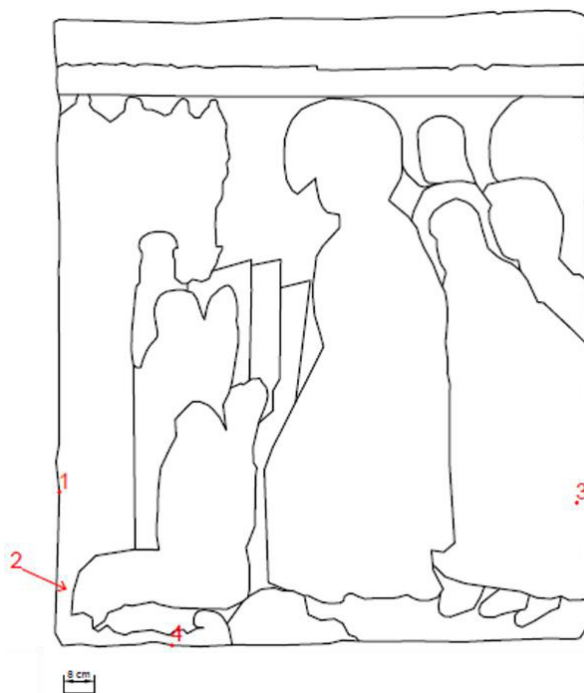


Figure 2. The relief outline with marked sampling sites.

**Sample 1:** fragment taken from the PR rim, from an area of loss.

**Sample 2:** fragment taken from the reverse, PR, from an area of loss.

**Sample 3:** fragment taken from an area of loss, PL.

**Sample 4:** fragment taken from the bottom edge.

The **substrate** (layer 0 in all the samples) is made of gypsum plaster (**calcium sulfate**,  $\text{CaSO}_4$ , confirmed by EDS, XRD and by the peak at 1600, 1632 and 1680  $\text{cm}^{-1}$  in the FT-IR spectra, which also show the sulfate overtones in the 2100-2300  $\text{cm}^{-1}$  area). The presence of **carbonates** and **silicates** in all the samples is confirmed by the EDS (C and Si; Al traces are present in all the layers due to the polishing medium or indicating K-Al silicates) and FT-IR (carbonates peaks at 800, 1056, 1088, 1792  $\text{cm}^{-1}$  and also overtones in the 2100-2300  $\text{cm}^{-1}$  area). Traces of **strontium** (Sr) were also detected as common inclusion in mineral gypsum and, in samples 2 and 3, the EDS mapping suggests that K-Al-Sr silicate inclusions are present in all the layers. The crystalline structure typical of gypsum plaster (called *tabular* in mineralogy, see BSE images) can be seen in the bulk and the interface layer (layer 1 in all the samples) (Cox et al., 1974). The **interface layer** appears yellow under visible illumination and might consist of a portion of the lower layer soaked

with the surface coating(s), showing characteristics of both layers. It can be observed in the BSE images that the tabular structure of the sulfate appears denser in layer 1 than in layer 0, suggesting that the presence of some of the coating in layer 1 might have improved the cohesion of this layer and/or filled the pores, preventing to a certain degree the penetration of the casting resin in the layer. Layers 1 and 0 are present and similar in all the four samples. Traces of other elements can be seen especially in the top layers of all the samples (Cl, Na, Mg, Ba and Fe in sample 1; Fe, Mn, Na, Cl and Mg in samples 2 and 3). Mg is known as an exchangeable element in the sulfate variety  $\text{MgSO}_4$  (more or less hydrated) and  $\text{BaSO}_4$  can be also naturally present in the gypsum mineral. Fe is also a common inclusion in many minerals. Na can be also an exchangeable element in the sulfate or indicate the presence of sodium chloride ( $\text{NaCl}$ , possibly present in the quarry or derived by the source of water used to produce the plaster) (Cox et al., 1974).

A **black line** is present in samples 1 (layer 2, underneath the coatings), 3 (layer 4, above the coatings) and 4 (layer 2, underneath the coatings) and is likely to be dust/dirt as carbonates were detected in this layer, without constituting a coherent application.

A **wax** or **resin** (FT-IR peaks at 928, 1472 and CH symmetric and asymmetric stretches in the 2800-3000  $\text{cm}^{-1}$ , and 1728-1744  $\text{cm}^{-1}$  that suggests ester-containing wax or the additional presence of oil) was detected in all the layers, which indicates that either the material was added to the gypsum plaster wet admixture or that the coating has also penetrated in layer 0. The latter seems also possible as the average depth of the samples is about 0.5 mm. A **protein** contribution is suggested by the FT-IR spectra of samples 3 and 4. The presence of **shellac** was confirmed by py-TMAH-GC/MS on sample 4, but no protein derivatives were observed (Colombini & Modugno, 2009; Mills & White, 2012). This suggests that either a very small quantity of a protein material was used in the admixture or that no protein material was added and the FT-IR peaks that might be assigned to amines of proteins are instead part of the complex shellac FT-IR spectrum (Price et al., 2009). Indication of the presence of **drying oil**, possibly **linseed oil**, was found by py-TMAH-GC/MS.

**Sample 1** was taken from an edge and **two coatings** can be observed: layer 3 is present only on the top of the sample (front of the object) and consist of gypsum plaster and resin/wax; layer 4, greyish under visible illumination, consists of Ba, Si and Al and seems to have been applied on the front and side surface of the object.

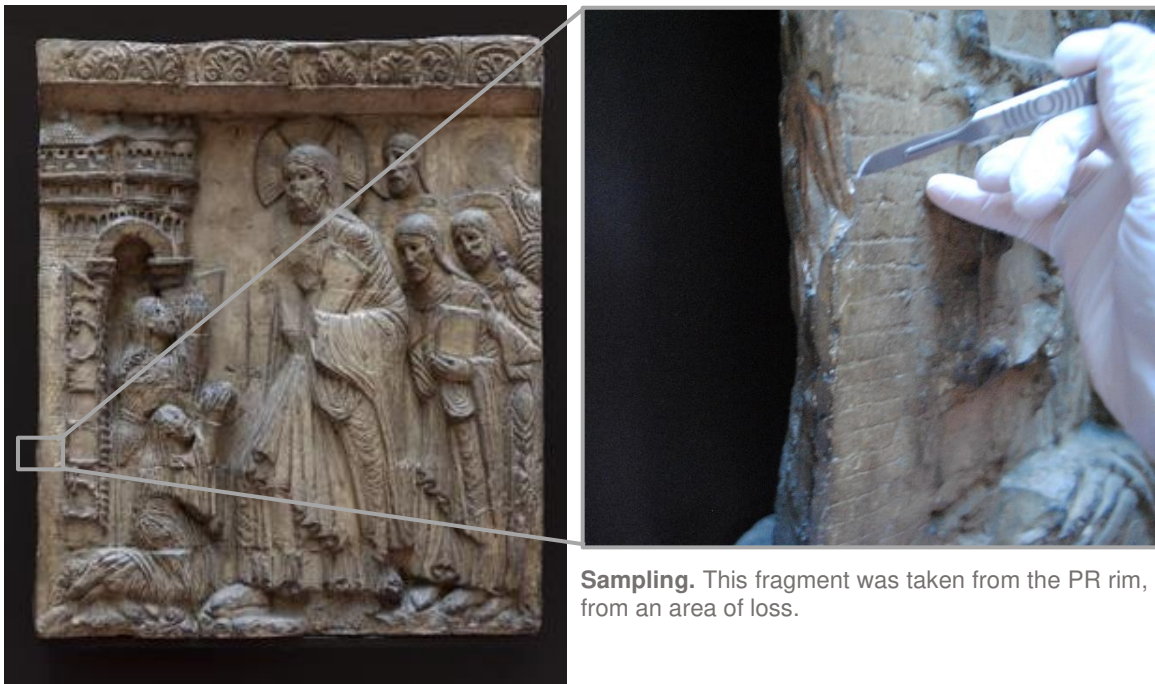
In **sample 2**, taken from the reverse of the cast, a coating containing aluminium (Al), strontium (Sr) and silicon (Si) can be observed. The wax/resin was also detected in this layer, suggesting that it was either the medium of the coating or that the wax/resin was applied onto the Al-Sr-Si coating and soaked it without creating a film.

**Sample 3** shows **two coatings**, both dark under visible illumination. Layer 2 is milky-white and layer 3 is pink-orange under UV illumination. These characteristics suggest that layer 2 consists either of an inorganic material or a varnish (not detected by FT-IR), and layer 3 contains **shellac**.

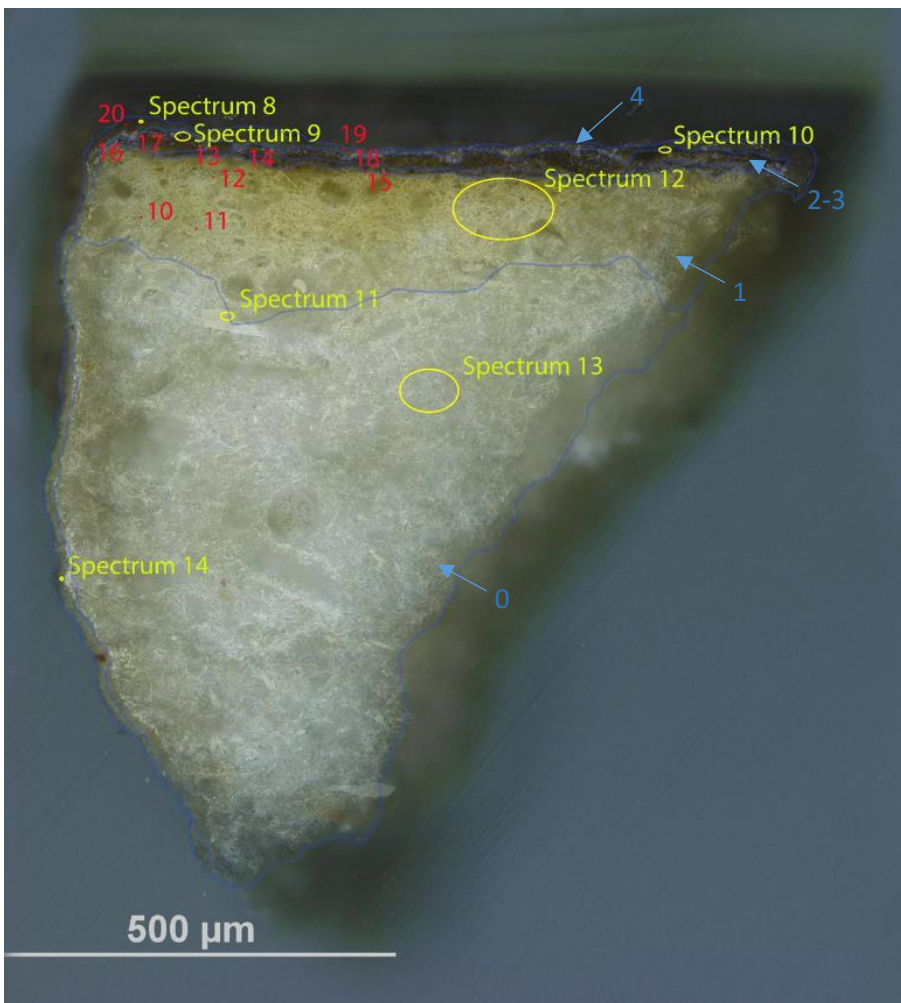
**Sample 4** shows a coating, dark under visible illumination, milky-white under UV illumination. This suggests that layer 3 consists either of inorganic material, a varnish or oil (not detected by FT-IR). Nonetheless, **shellac** was confirmed by py-TMAH-GC/MS, suggesting that this material penetrated the layers without forming a film.

**NOTE:** casting in resin the fragments of plaster resulted in the fragments absorbing the resin when in the liquid state. This was visible in the BSE image as well as through the EDS mapping (Tiranti resin and catalyst are mainly made of organic compounds C, H and O). Aluminium (Al) traces are present in all the samples, due to the polishing chemical.

## Sample 1



**Sampling.** This fragment was taken from the PR rim, from an area of loss.



Left: Overlapped (OM and BSE) cross-section image showing the stratigraphy (blue indicators).

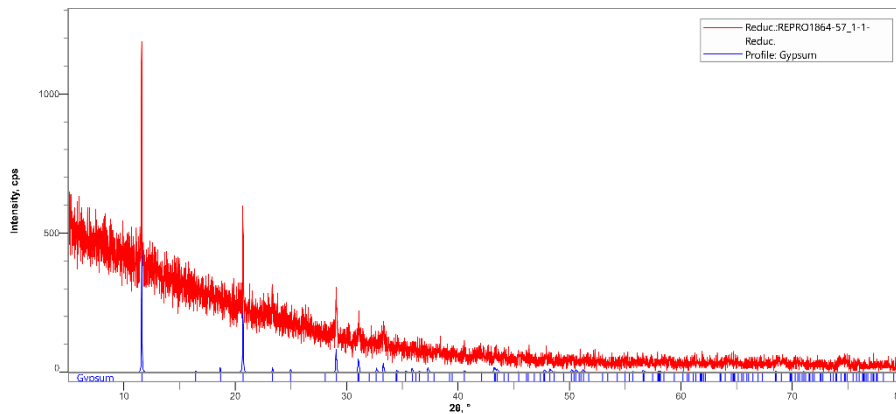
- 4. Grey layer
- 3. Dark layer
- 2. Black line
- 1. Yellowish and undefined layer
- 0. Plaster bulk

**Analysis spots.**

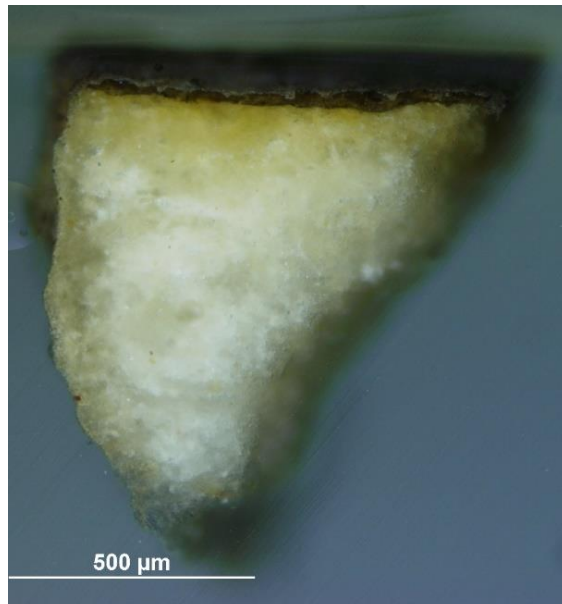
EDS analysis (yellow): Spectra 8-14

FT-IR analysis (red): nos. 10-20

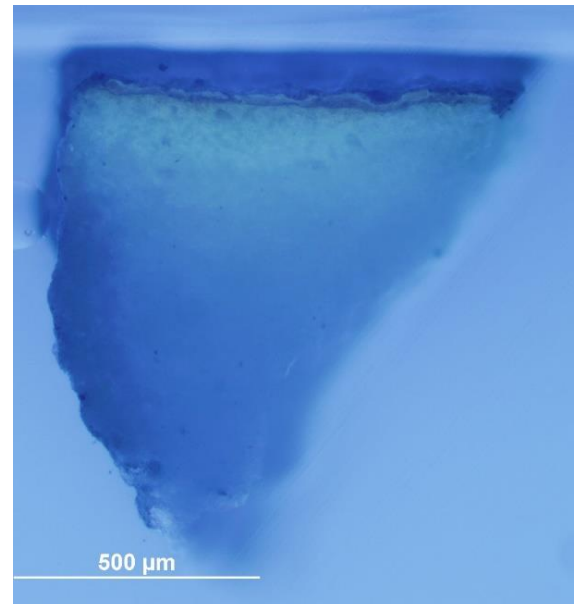
**Summary.** The substrate (layer 0) is made of plaster (**calcium sulfate**,  $\text{CaSO}_4$ , confirmed by EDS, XRD and by the peak at  $1600\text{ cm}^{-1}$  in the FT-IR spectra). Layer 1, which appears yellow under the microscope, consists of a portion of lower layer soaked with the surface coating, showing characteristics of both layer 0 and layers 2 and 3. A black line (layer 2), a dark layer (layer 3) and the utmost layer, lighter in colour under visible illumination (layer 4) constitute the coating layers. These seem to be mostly made of Al, Ba and Si are relevantly present in layer 4 (see EDS mapping and spectrum), contain a **carbonate** (suggested by FT-IR peaks at  $800$ ,  $1088$ ,  $1792\text{ cm}^{-1}$ , and mostly detected in layer 4, possibly suggesting that layer 4 consists of dust), calcium sulfate and a **wax or resin** (FT-IR peaks at  $1472$  and  $2976\text{ cm}^{-1}$ , and  $1728\text{ cm}^{-1}$  that suggests ester-containing wax or the additional presence of oil). Traces of Al are present in all the layers due to the polishing solution and traces of other elements can be seen especially in the top layers (Cl, Al, Na, K and Fe). Traces of **Sr** were also detected as common inclusion in mineral gypsum.



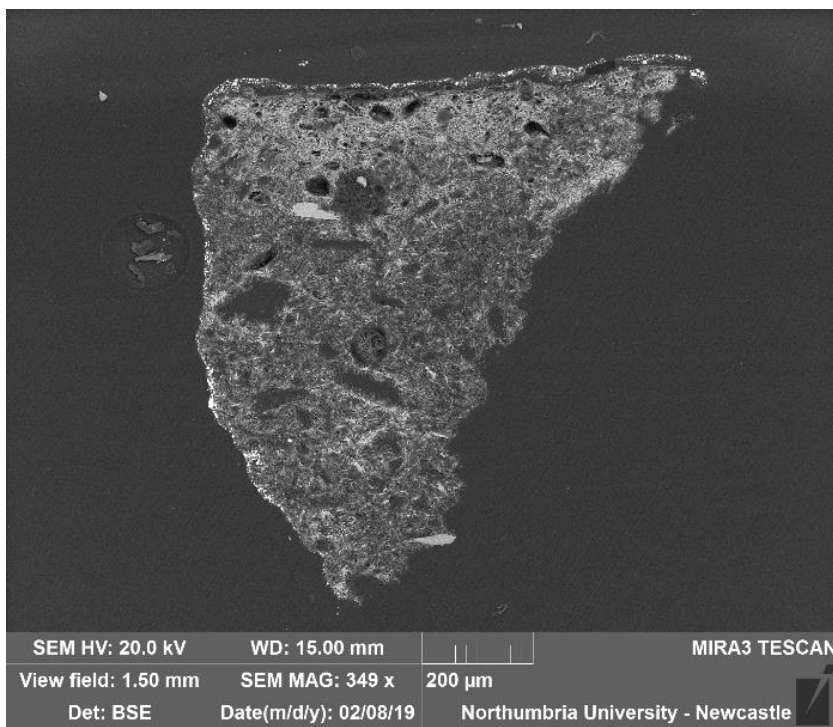
**XRD diffractogram (left):** a fragment of this sample was pulverised revealed the profile of gypsum (calcium sulfate) and the diffractogram was compared to references from the Rigaku SmartLab Database. The most significant peaks were at  $2\theta = 11.60$ ,  $20.69$ ,  $29.07$ ,  $33.32$ ,  $34.55$ ,  $47.91$ ,  $64.20$



VLR OM



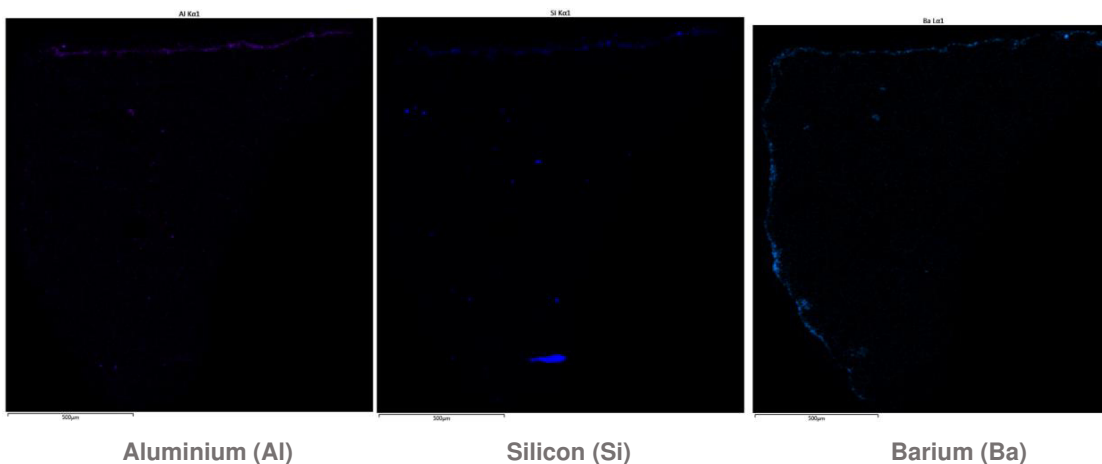
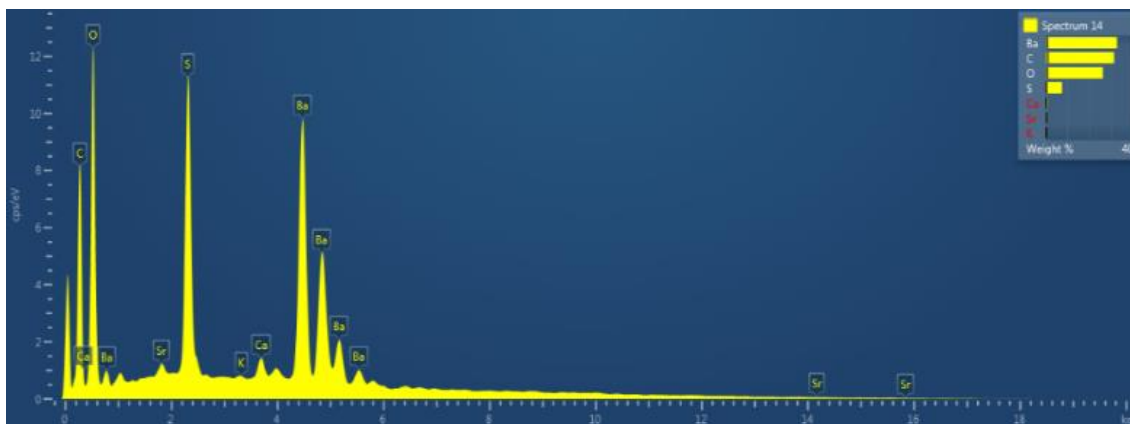
UVf OM

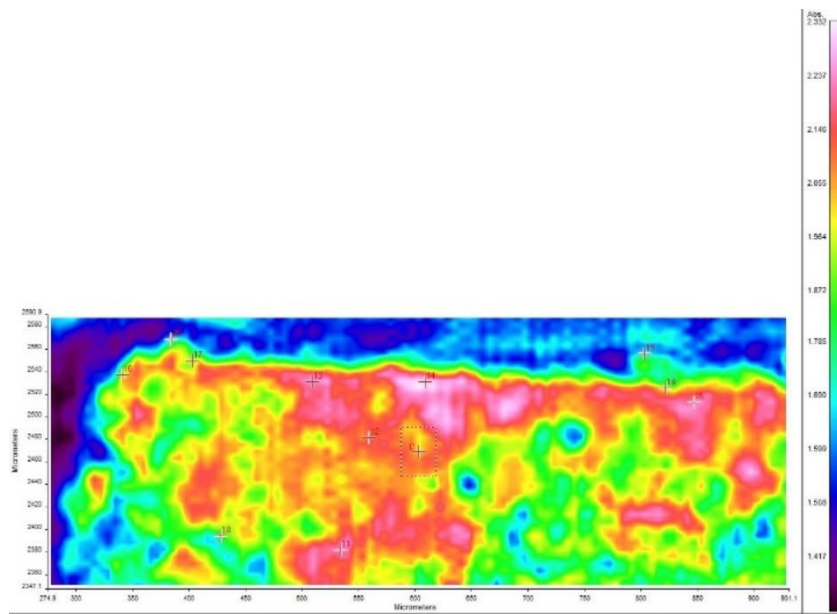
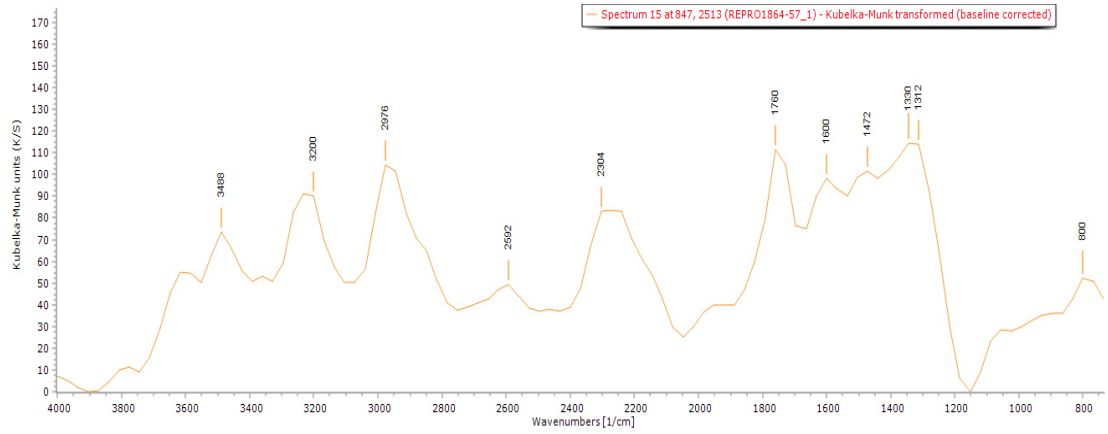


**BSE image** (left). The tabular crystalline structure typical of gypsum plaster can be seen in layers 0 and 1.

**EDS spectrum** (below, spectrum 14) of layer 4 shows C, O, Ca and S, indicating calcium sulfates and carbonates. Sr is a typical contaminant in mineral gypsum and Ba seems to be added on the object surface (as shown in the EDS mapping).

**EDS mapping** (below) shows that Al (left), Si (centre) and Ba (right) are mostly present in layer 4.





**FT-IR spectrum 15** (above) of layers 2-3. Peaks for the casting resin (1312, 1344, 1760  $\text{cm}^{-1}$ ), gypsum (1600  $\text{cm}^{-1}$ , overtone 2200-2300  $\text{cm}^{-1}$ ) and a wax/resin (1472, 2960  $\text{cm}^{-1}$ ). A summary of the peaks observed in the spectra 10-20 can be seen in the table below.

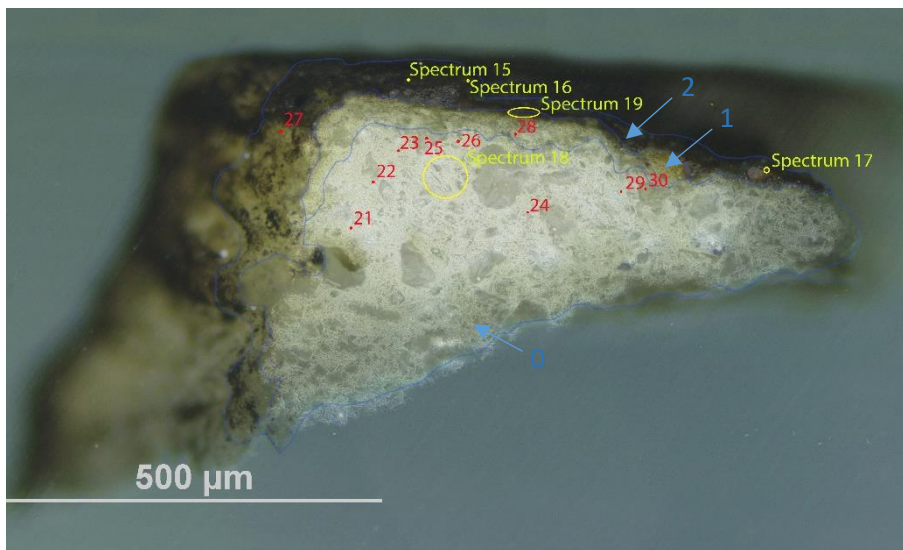
**FT-IR (FPA) image** (left). No clear layer definition can be observed in the FPA image.

Spectrum	Layer	peaks (cm-1)						
		Casting Resin	Gypsum	Carbonate	Wax/resin	C=O ester carbonyl	SO overtone	Unknown
10	1	1341, 1760			1472, 2976		2208	
11	1	1312	1600		1472, 2976	1728	2208	
12	1	1312	896, 1684		2912, 2944		2240	
13	2-3		1684	1408	2944	1735	2240	
14	2-3	1312, 1344, 1769	1588		2848		2080, 2304	
15	2-3	1312, 1344, 1760	1600		1472, 2960		2304	
16	4	1312, 1330, 1760	1600	800	2976		2304	
17	4	1312, 1344, 1760		800, 1088, 1792	2959		2272	1504
18	2-3	1312, 1344		800, 1088, 1792	2959		2112, 2272	1504
19	4	1312, 1344, 1760		800, 1786	1472, 2976		2240	
20	4	1321, 1760		1088, 1792			2048	1504

## Sample 2



**Sampling.** This fragment was taken from the reverse, PR, from an area of loss.



Left: Overlapped (OM and BSE) cross-section image showing the stratigraphy (blue indicators).

**2. Dark layer**

**1. Yellowish and undefined layer**

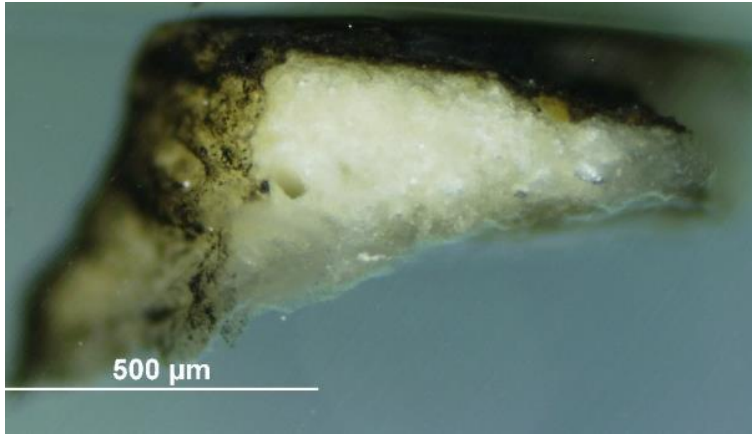
**0. Plaster bulk**

**Analysis spots.**

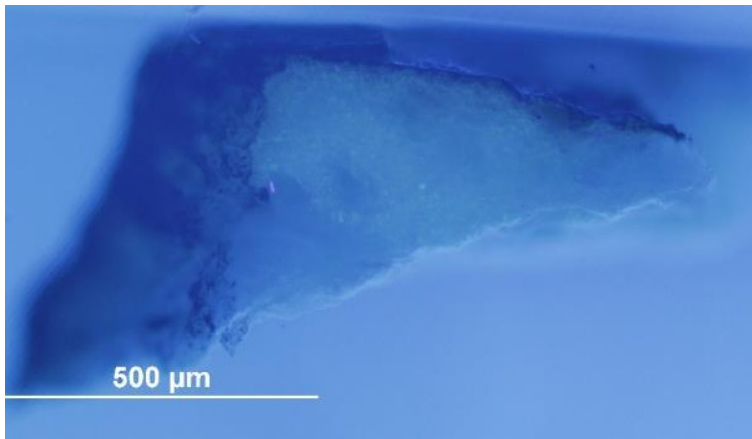
EDS analysis (yellow): Spectra 15-19

FT-IR analysis (red): nos. 21-30

**Summary.** The substrate (layer 0) is made of plaster (**calcium sulfate**,  $\text{CaSO}_4$ , confirmed by EDS and by the peak at  $1600$  and  $1632\text{ cm}^{-1}$  in the FT-IR spectra). Layer 1, which appears yellow under the microscope, consists of a portion of the lower layer soaked with the surface coating, showing characteristics of both layer 0 and layer 2. A dark layer (layer 2) clearly shows large inclusions under OM and in BSE image. By looking at the EDS mapping, these inclusions seem to consist of Al, Si and Sr. EDS shows that all the layers contain **calcium sulfate** (confirmed by FT-IR), a **carbonate** (suggested by FT-IR peaks at  $800$ ,  $1056$ ,  $1792\text{ cm}^{-1}$ ), and a **wax or resin** (FT-IR peaks at  $928$ ,  $1472$ ,  $2816$  and  $2944\text{ cm}^{-1}$ , and  $1728\text{ cm}^{-1}$  that suggests ester-containing wax or the additional presence of an oil). Al is overall present as used as a polishing agent or part of the Si-Sr inclusions. Traces of Fe, Mn, Na, Cl and Mg were also detected.

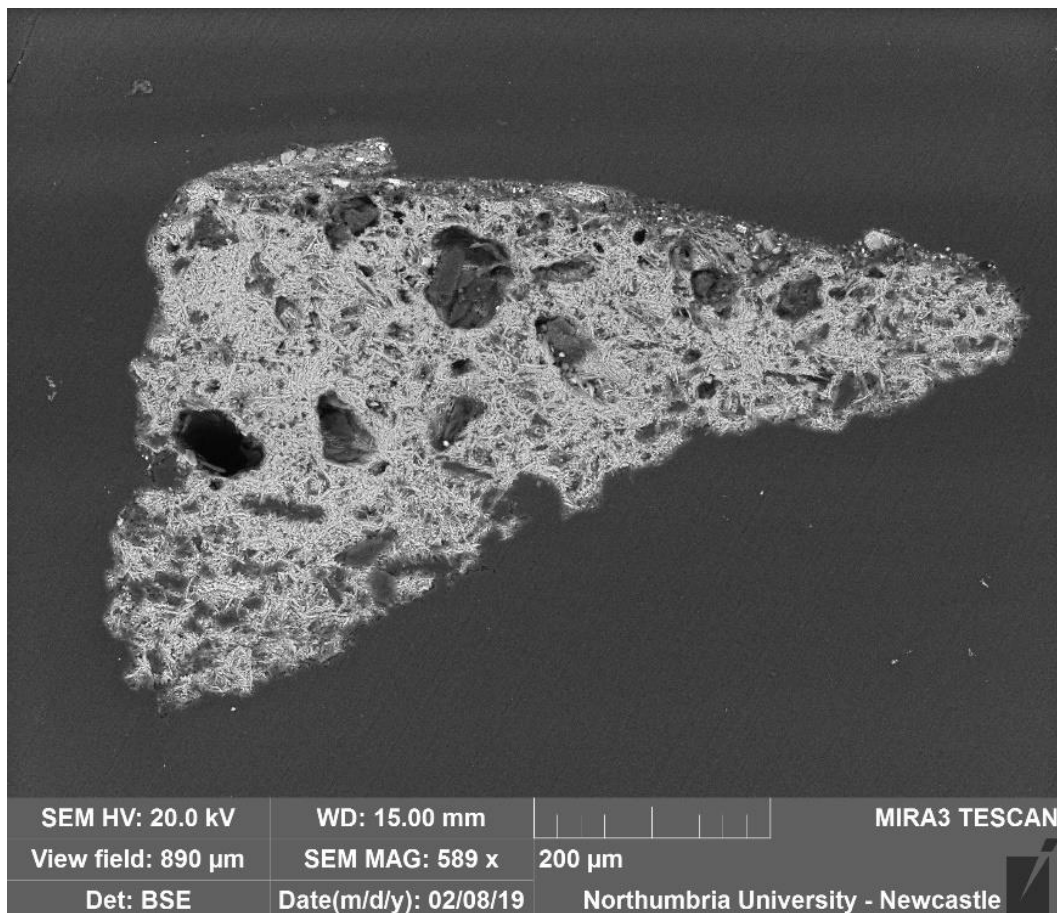


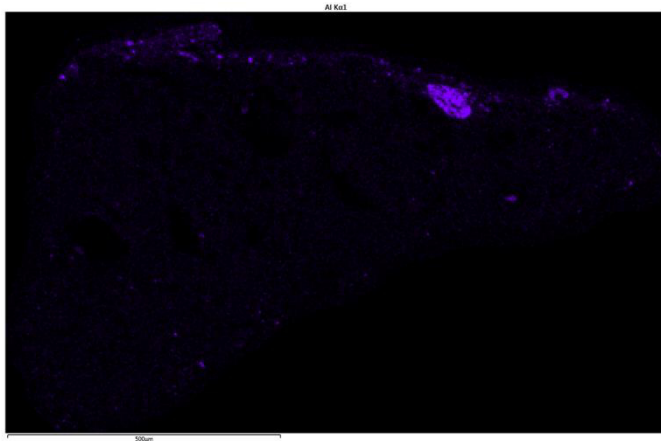
VLR OM (left)



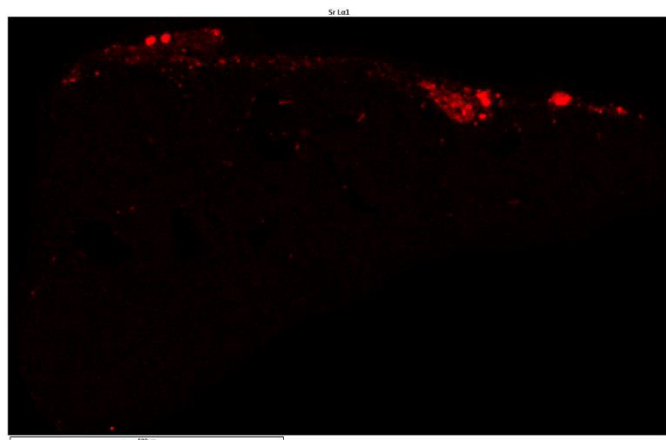
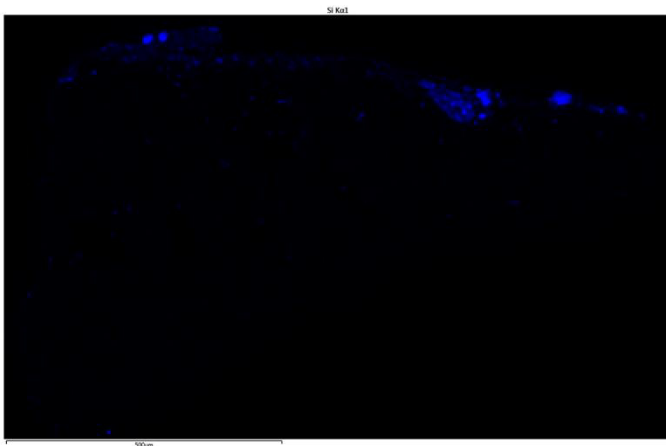
UVfOM (left)

**BSE image (below).** The tabular crystalline structure typical of gypsum plaster can be seen in layers 0 and 1. Large inclusions are also visible.

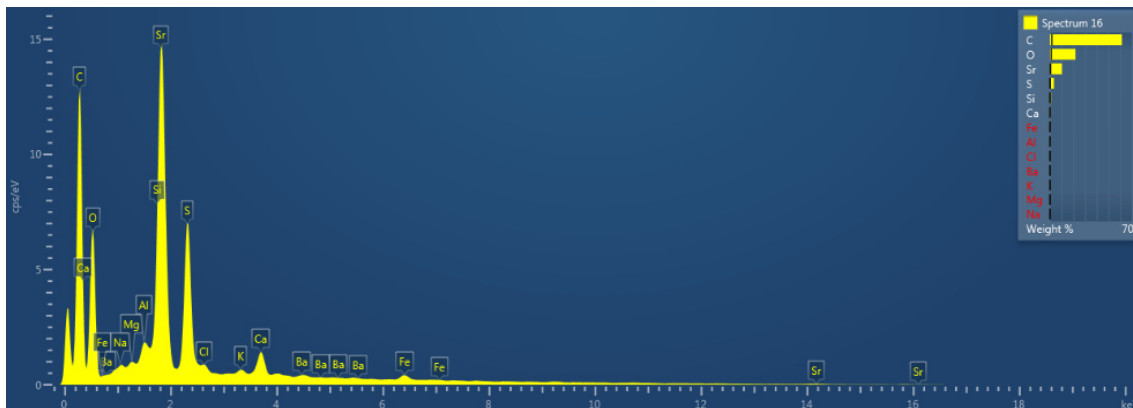


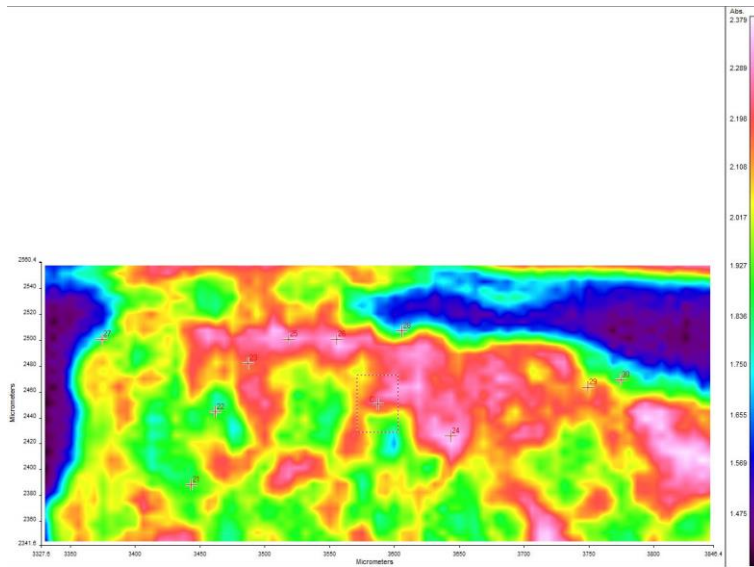
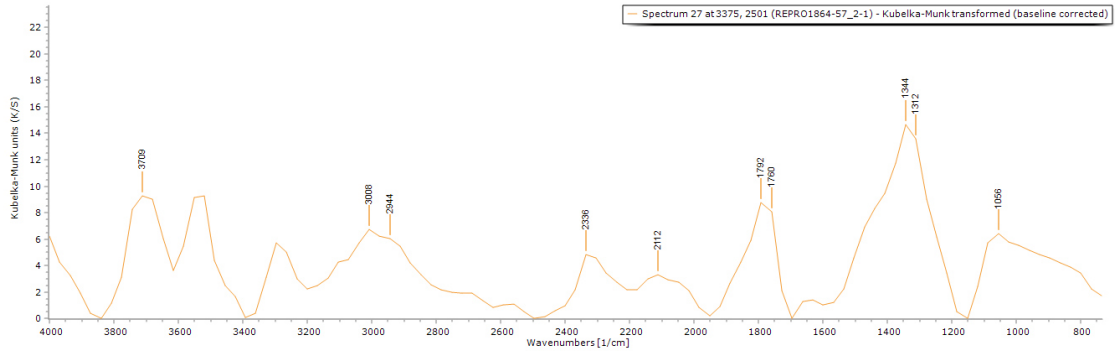


EDS mapping shows that Al (top left), Si (centre left) and Sr (bottom right) are mostly located in layer 2.



EDS spectrum (below, spectrum 16) of layer 2 shows C, O, Ca and S, indicating calcium sulfates and carbonates. Sr is a typical contaminant in mineral gypsum, but in this sample appears to have been present in large inclusions (as shown in the EDS mapping). Al traces are present in all the layers (polishing medium), or as part of Si-K inclusion. Ba is present too. Mg, Fe, Na and Cl were also detected.



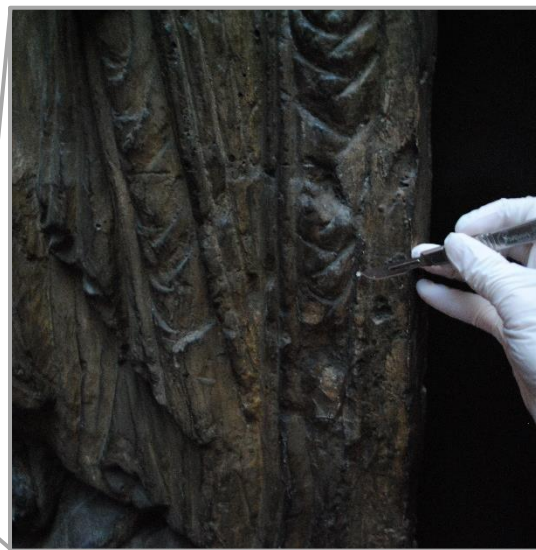


**FT-IR spectrum 27** (above) of layer 2. Peaks for the casting resin (1312, 1344, 1760  $\text{cm}^{-1}$ ), gypsum (1600  $\text{cm}^{-1}$ , overtone 2200-2300  $\text{cm}^{-1}$ ), carbonate (1056, 1792  $\text{cm}^{-1}$ ) and a wax/resin (2944  $\text{cm}^{-1}$ ). A summary of the peaks observed in the spectra 21-30 can be seen in the table below.

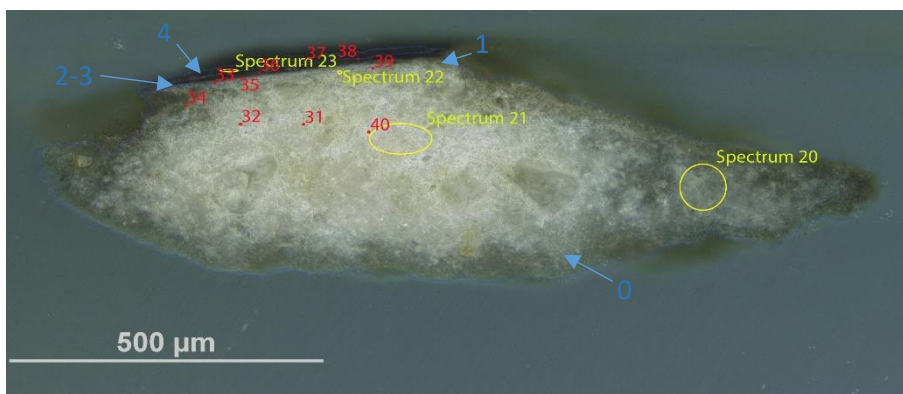
**FT-IR (FPA) image** (left). No clear layer definition can be observed in the FPA image.

Spectrum	Layer	peaks (cm-1)						
		Casting Resin	Gypsum	Carbonate	Wax/resin	C=O ester carbonyl	SO overtone	Unknown
21	0				1292, 1664, 2944		2208	
22	0				1285, 1664, 1696,		2240	
23	0	1312, 1760	1568		2912	1728	2240	
24	0	1317			1664, 1696, 2944	1728	2176, 2272	
24	0	1312	832	1056	1536, 1568, 1664,	1728	2208	1280
25	0				2944, 2976			
25	0	1312, 1344,	896, 1600		1472, 2868		2240	
26	0	1760						
26	0	1312, 1344,	1600	1056, 1792	2944		2112, 2336	
27	2	1760						
27	2	1312, 1344,	1600, 1632	800, 1792	2784, 2816	1184	2304	
28	1	1760						
28	1	1312, 1344,		1056	928, 2720, 2944		2272	
29	0	1760						
29	0	1344	896, 1632	1792	928, 1472, 2912		2240, 2368	
30	0							

## Sample 3



**Sampling.** This fragment was taken from an area of loss, PL.

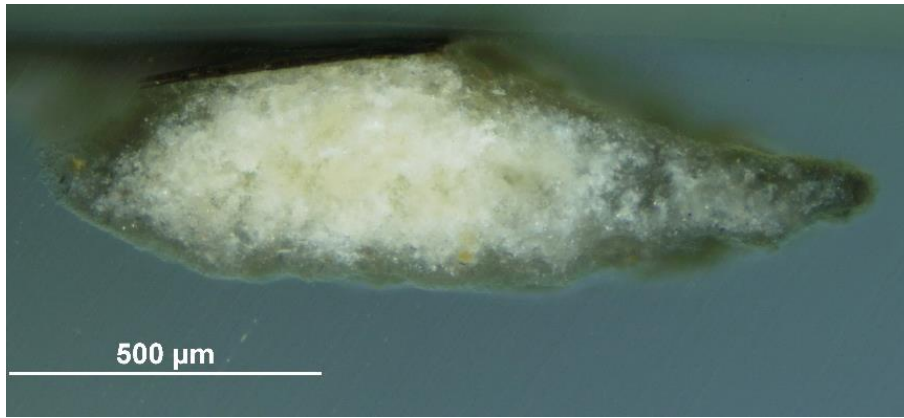


Left: Overlapped (OM and BSE) cross-section image showing the stratigraphy (blue indicators).

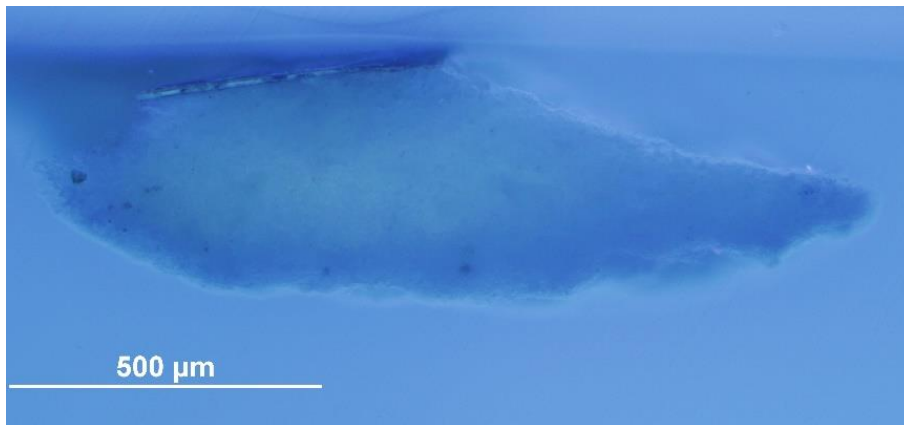
- 4. Black line**
- 3. Dark layer (shellac medium)**
- 2. Dark layer**
- 1. Yellowish and undefined layer**
- 0. Plaster bulk**

**Analysis spots.** EDS analysis (yellow): Spectra 20-23; FT-IR analysis (red): nos. 31-40.

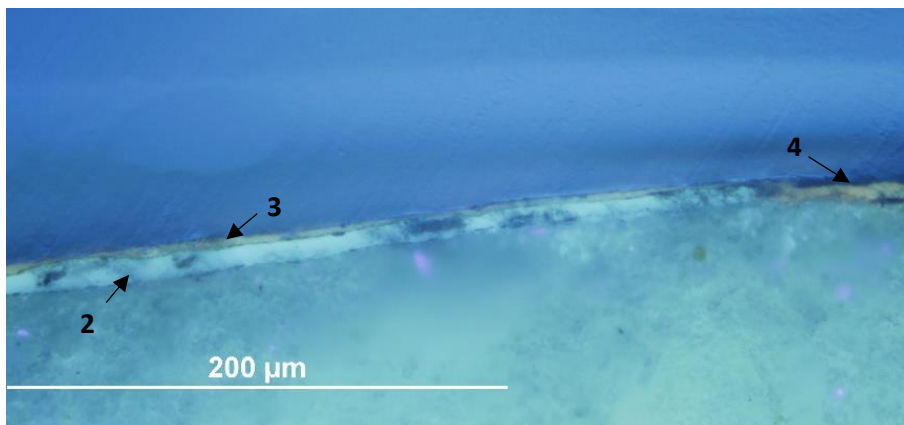
**Summary.** The sample is mostly made of C, O, S and Ca (**calcium sulfate**,  $\text{CaSO}_4$ , confirmed by EDS and by the peak at  $1600$  and  $1632\text{ cm}^{-1}$  in the FT-IR spectra). Al is overall present as used as a polishing agent, but could also, together with K and Si be present as part of silicate inclusions. EDS mapping shows that inclusions made of Sr, Al and Si are present in all the layers. The structure typical of gypsum plaster can be seen in layers 0 and 1. Layer 1, which appears yellow under the microscope, consists of a small portion of the lower layer soaked with the surface coating, showing characteristics of both layer 0 and layer 2. The fluorescence colour suggests that layers 2 and 3 are two different coatings and that layer 3 contains **shellac**. **Carbonates** and **silicates** are suggested by FT-IR peaks at  $800$ ,  $1056$ ,  $1792\text{ cm}^{-1}$ , and also a **wax or resin** (FT-IR peaks at  $928$ ,  $1232$ ,  $2854$  and  $2928\text{ cm}^{-1}$ , and  $1744\text{ cm}^{-1}$  that suggests ester-containing wax or the additional presence of an oil). Traces of K, Na, Cl and Mg were also detected by EDS and indication of a **protein** can be seen in some of the FT-IR spectra.



VLR OM (left)

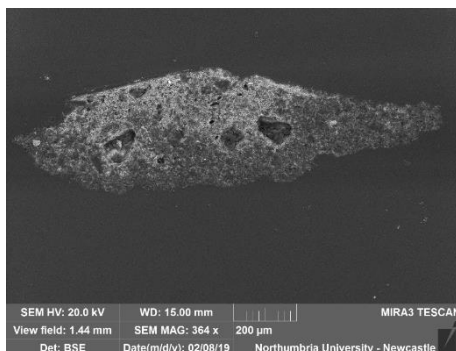


UVfOM (left)



UVfOM (detail, left)

The colour of fluorescence (orange-pinkish) suggests that layer 3 contains shellac.

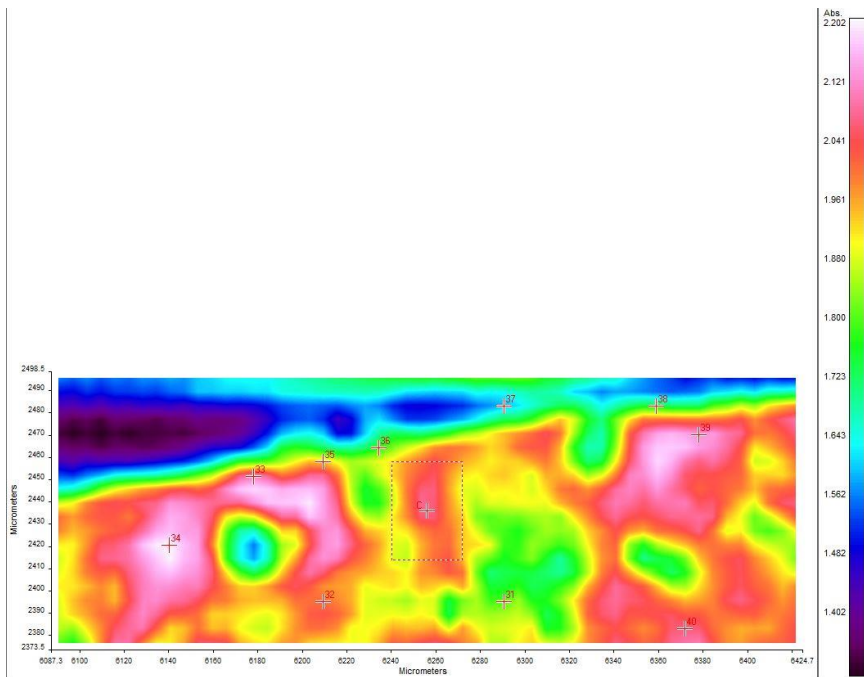
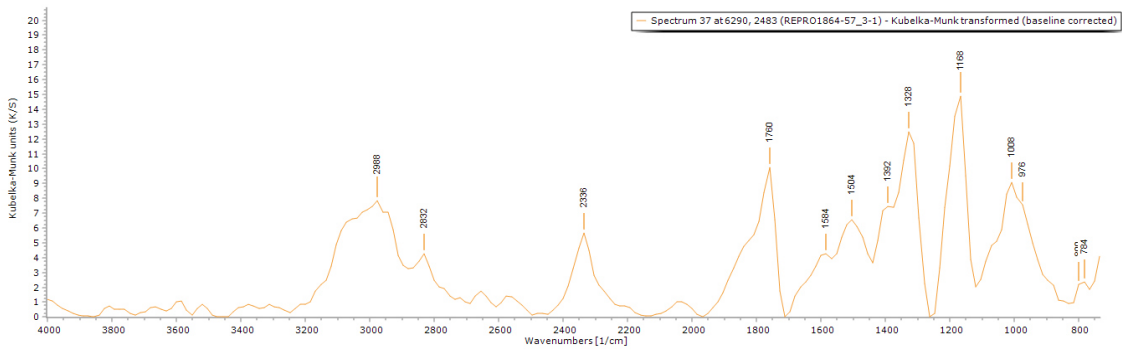


Sr (below) inclusions were detected and this element is usually detected as natural inclusion in mineral gypsum.

EDS mapping did not indicate any notable elements distribution in a layer fashion, but Sr, Al and Si appear in the same spots, suggesting that they constitute the same inclusions.



**BSE image (above).** The tabular crystalline structure typical of gypsum plaster can be seen in layers 0 and 1.

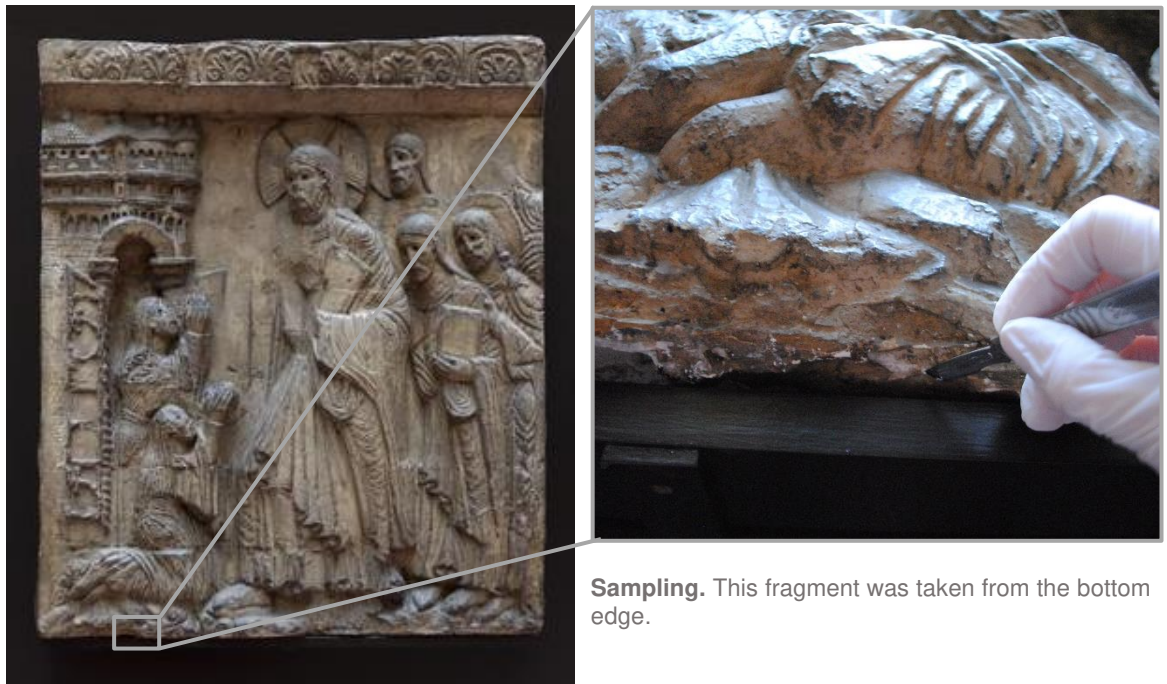


**FT-IR spectrum 37** (above) of layer 4. Peaks for the casting resin (1328, 1760  $\text{cm}^{-1}$ ), gypsum (1600  $\text{cm}^{-1}$ , overtone 2200-2300  $\text{cm}^{-1}$ ), carbonate (800  $\text{cm}^{-1}$ ) and a wax/resin (2832, 2988  $\text{cm}^{-1}$ ). A summary of the peaks observed in the spectra 31-40 can be seen in the table below.

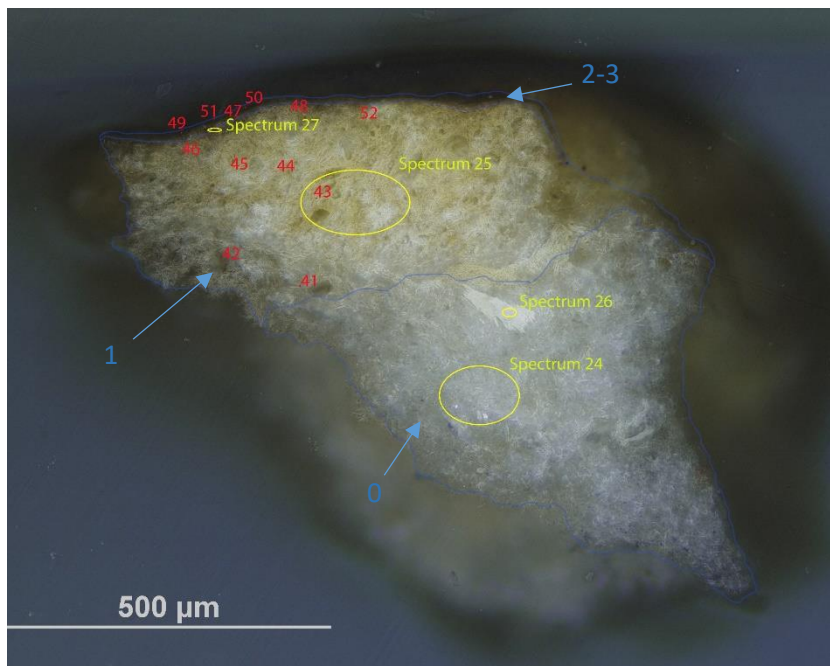
**FT-IR (FPA) image** (left). No clear layer definition can be observed in the FPA image.

Spectrum	Layer	peaks (cm-1)							
		Casting Resin	Gypsum	Carbonate	Protein	Wax/resin	C=O ester carbonyl	SO overtone	Unknown
31	0	1344, 1760	1632	800		1008, 1024, 1216, 1568, 1776, 2864, 2944		2184, 2240	
32	0	1312, 1344		1440, 1776		768, 1008, 1232, 2784,	1744		2256
33	1	1760	1616			1472, 2848, 2949			2208
34	0	1312, 1760		1088	1456, 1584, 1680	928, 1024, 1360, 2848,	1712		2262
35	1	1312, 1760		1088	1456, 1536, 1680	768, 1232, 1360, 2864,			2016
36	2-3	1312		1088	1408, 1504, 1584	1216, 1776, 2864, 2928			2080
37	4	1328, 1760		800	1392, 1504, 1584	976, 1008, 2832, 2988			2336
38	2-3	1328, 1760	1152	864, 1792, 1504, 1568, 1648		784, 1008, 2880, 2984			2240
39	1	1312, 1760	1616	880, 1072	1456, 1568	768, 1232, 2916			2240
40	0	1312		896	1456, 1584	1024, 1744, 2800, 2936			2205

## Sample 4



**Sampling.** This fragment was taken from the bottom edge.



Left: Overlapped (OM and BSE) cross-section image showing the stratigraphy (blue indicators).

### 3. Coating

### 2. Black line

1. Yellowish layer with dark inclusions

0. Plaster bulk

### Analysis spots.

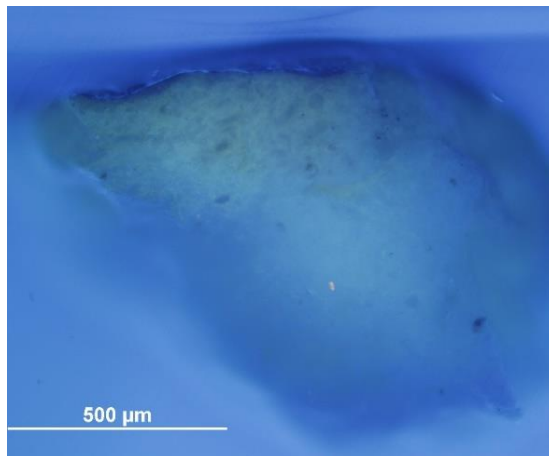
EDS analysis (yellow):  
Spectra 24-27

FT-IR analysis (red): nos.  
41-52

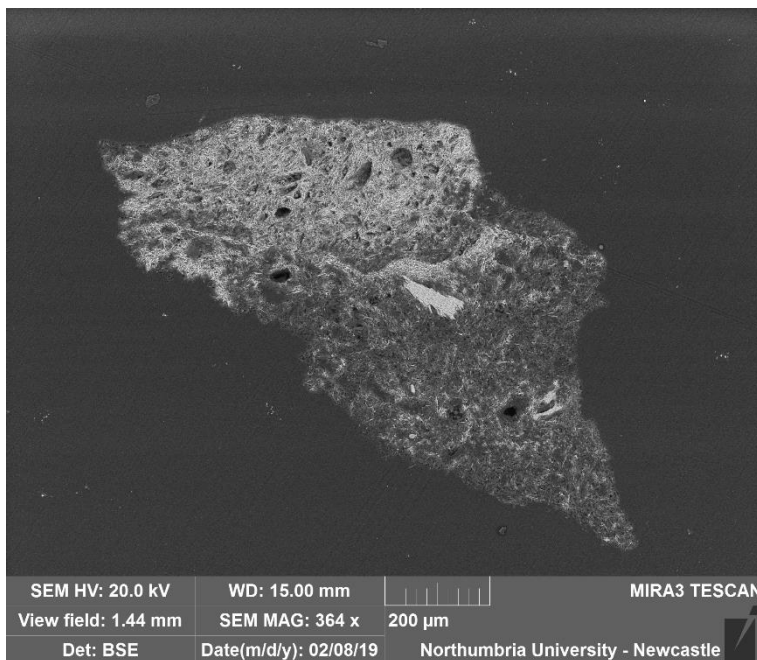
**Summary.** The sample is mostly made of C, O, S and Ca (**calcium sulfate**,  $\text{CaSO}_4$ , confirmed by EDS and by the peak at  $1600$  and  $1632\text{ cm}^{-1}$  in the FT-IR spectra). Al is overall present as used as a polishing agent, but could also, together with K and Si be present as part of silicate inclusions. EDS mapping does not show a specific difference in the elements' distribution in the layers. Traces of Na, Cl, Mg, Fe and Ba were detected in all the layers. The tabular structure typical of gypsum plaster can be seen in layers 0 and 1. Layer 1, which appears yellow under the microscope, consists of a small portion of the lower layer soaked with the surface coating. **Carbonates** and **silicates** are suggested by FT-IR peaks, and also a **wax or resin** and possibly a **protein** contribution. The presence of **shellac** was confirmed by Py-TMAH-GC/MS, but no protein derivatives were observed. This suggests that either a very small quantity of a protein material was used in the admixture or that no protein material was added and the FT-IR peaks that might be assigned to amines of proteins are instead part of the complex shellac FT-IR spectrum (Price et al., 2009). A **drying oil**, possibly **linseed oil**, is also suggested by py-TMAH-GC/MS (Colombini & Modugno, 2009).



VLR OM (above)



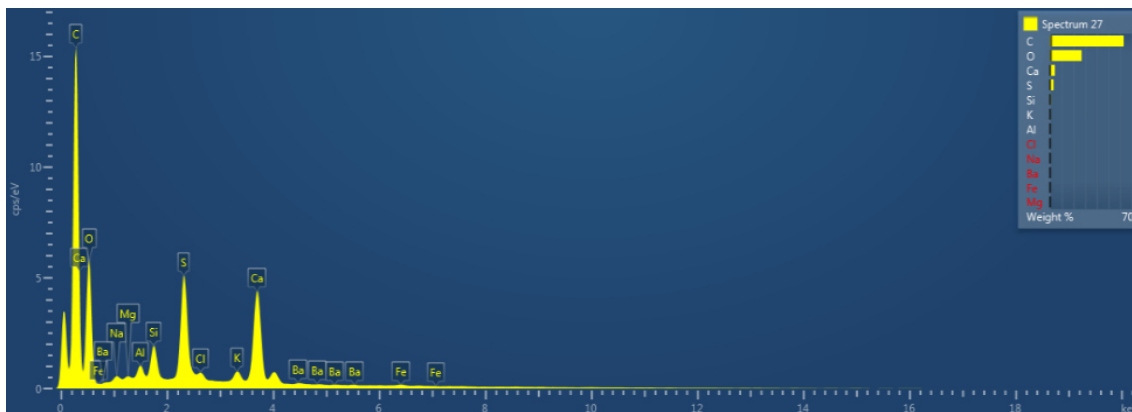
UVfOM (above)

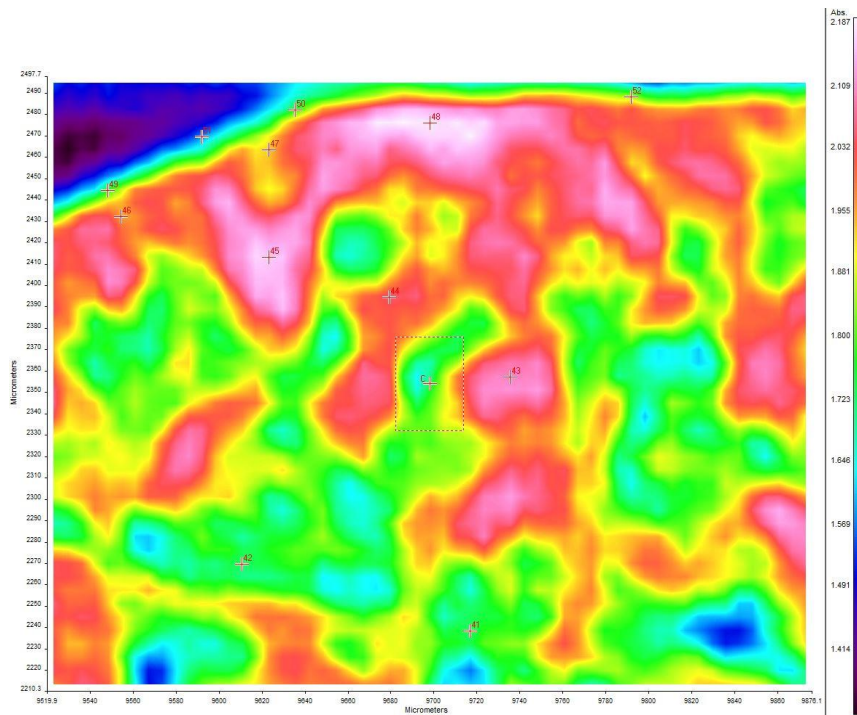
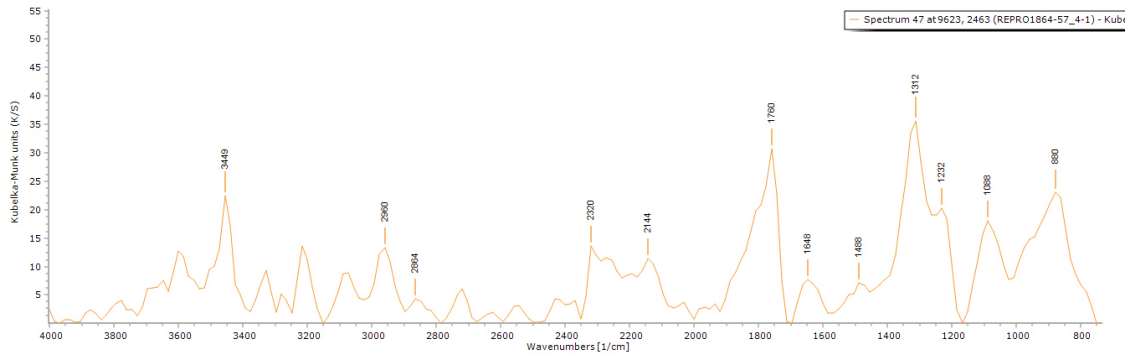


**BSE image (left)**. The tabular crystalline structure typical of gypsum plaster can be seen in layers 0 and 1.

**EDS spectrum 27 (below)** from layers 2-3 indicate that it consists of C, O, Ca, S, and Si. Traces of Al, K, Na, Cl, Mg, Fe and Ba were also detected. Sr was also detected in layer 0.

**EDS mapping** did not indicate any notable elements distribution in a layer fashion.

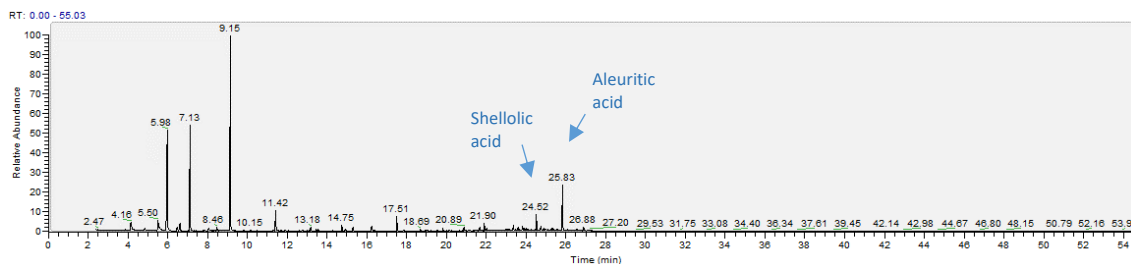




**FT-IR spectrum 47** (above) of layers 2-3. Peaks for the casting resin (1312, 1760  $\text{cm}^{-1}$ ), gypsum (1600  $\text{cm}^{-1}$ , overtone 2200-2300  $\text{cm}^{-1}$ ), carbonate (800  $\text{cm}^{-1}$ ) and a wax/resin (2832, 2988  $\text{cm}^{-1}$ ). Peaks that might suggest the presence of a protein are also visible in the 1400-1600  $\text{cm}^{-1}$  area. A summary of the peaks observed in the spectra 41-52 can be seen in the table below.

**FT-IR (FPA) image** (left). No clear layer definition can be observed in the FPA image.

Spectrum	Layer	peaks (cm-1)							
		Casting Resin	Gypsum	Carbonate	Protein	Wax/resin	C=O ester carbonyl	SO overtone	Unknown
41	1	1312, 1760	1680	896		768, 1008, 1216, 1472, 2848,		2336	
42	1	1312, 1760	800, 1616,	896	1456, 1536, 1680	1024, 1136, 1216, 2912,		2224	
43	1	1328	1392, 1632			928, 1008, 1072, 1232, 2864,	1728	2144, 2240	
44	1	1328, 1760	1392, 1680			944, 1216, 1488, 2864, 2928		2208, 2256	
45	1	1328, 1760	1616, 1680	800, 864, 1088, 1424		944, 992, 1264, 2896, 2960		2277	1808
46	1	1312, 1760	1616	800	1456, 1552	912, 992, 1072, 1216, 2912,		2336	
47	2-3	1312, 1760	1648	1088		880, 1232, 1488, 2864, 2960		2144, 2320	
48	1	1344			1392, 1488, 1584, 1664	832, 944, 1072, 1216, 1280, 2848, 2928		2288, 2432	1776
49	2-3	1312, 1760	1632			848, 928, 1088, 1472, 1552		2240	
50	2-3	1312, 1760		896	1456, 1588	992, 1216, 1376		2205	
51	2-3	1328, 1760	1632		1392, 1488	768, 992, 1088, 1136, 1200		2320	
52	1	1312, 1760	1616			992, 1136, 1552, 2800, 2928		2336	

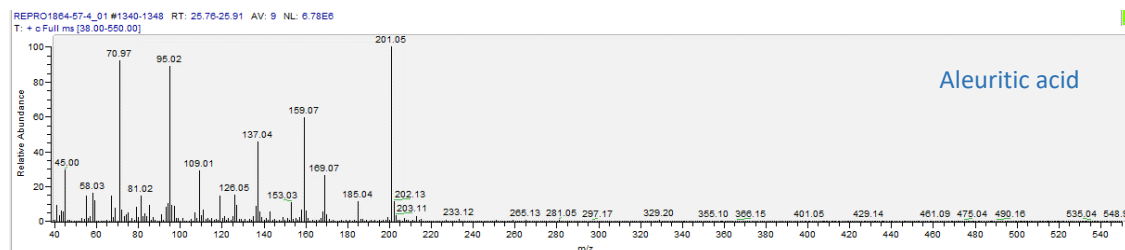
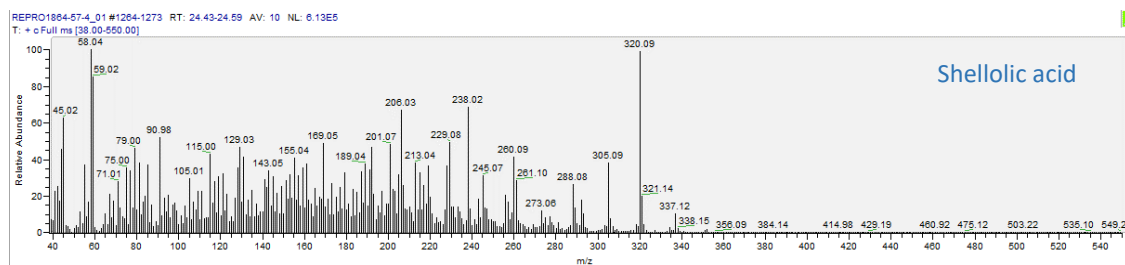


**Py-TMAH-GC/MS chromatogram** (above and described in the table below) shows small fragments due to derivatization ( $t = 5.98, 7.13, 9.15, 11.42$  min), Fatty Acids fragments ( $t = 13.18, 14.75, 16.25, 21.9$  min) and compounds characteristic of **shellac** ( $t = 24.52, 25.83, 26.88$  min). The complete pattern of derivatives of shellac was not found, possibly due to the small percentage of this material in the sample. The presence of **methyl azelate** ( $t = 17.50$ ), **methyl palmitate** ( $t = 21.67$ ) and **stearate** ( $t = 23.59$ ) might suggest that the resin has been mixed with an **oil** (**A/P = 3.70** and **P/S = 0.93**), possibly **linseed oil** (Colombini & Modugno, 2009).

RT	m/z	Assignment	Formula
4.16	45(100), 58(28), 74(48)	Diethyl ether	C <sub>4</sub> H <sub>10</sub> O
5.5	42(13), 58(100), 72(5), 88(5), 116(4)	1,2-Ethanediamine	C <sub>2</sub> H <sub>8</sub> N <sub>2</sub>
5.98	42(13), 58(100), 117(16)	1,2-Ethanediamine	C <sub>2</sub> H <sub>8</sub> N <sub>2</sub>
7.13	56(7), 72(100)	Propenoic acid	C <sub>3</sub> H <sub>4</sub> O <sub>2</sub>
9.15	42(47), 44(100), 57(19), 86(73), 128(58)	1-Butanamine, N-butyl-	C <sub>8</sub> H <sub>19</sub> N
11.42	42(10), 58(100), 70(10), 116(5)	1,2-Ethanediamine	C <sub>2</sub> H <sub>8</sub> N <sub>2</sub>
13.18	44(30), 58(81), 71(13), 74(12), 87(8), 88(25), 98(31), 116(41), 119(10), 130(100), 150(8)	FA fragment	
14.75	42(7), 58(21), 116(100), 128(6), 173(5)	FA fragment	
16.25	44(39), 58(100), 74(73), 83(44), 87(39), 97(53), 111(26), 129(73), 138(89), 171(52)	FA fragment	
17.51	43(20), 55(68), 59(55), 74(65), 83(62), 87(28), 111(57), 124(31), 143(34), 151(100), 185(43)	Nonanedioic acid, monomethyl ester	C <sub>10</sub> H <sub>18</sub> O <sub>4</sub>
21.67	55(29), 74(100), 87(82), 115(10), 129(13), 143(27), 171(11), 185(11), 199(6), 227(17), 239(5), 270(5)	methyl palmitate	C <sub>17</sub> H <sub>34</sub> O <sub>2</sub>
21.9	44(30), 55(75), 58(70), 74(88), 84(65), 98(100), 112(40), 149(41), 167(40), 199(31), 241(40)	Tridecanedioic acid, dimethyl ester	C <sub>15</sub> H <sub>28</sub> O <sub>4</sub>
23.59	43(23), 58(48), 74(100), 87(82), 97(5), 129(14), 143(32), 157(5), 185(5), 199(16), 255(17), 275(27), 298(5)	methyl stearate	C <sub>19</sub> H <sub>38</sub> O <sub>2</sub>
24.52	45(63), 58(100), 79(46), 91(52), 115(43), 129(47), 155(41), 169(49), 192(47), 206(67), 238(68), 260(41), 320(98), 337(10)	Shellolic acid	C <sub>15</sub> H <sub>20</sub> O <sub>6</sub>
25.83	153(11), 159(60), 169(27), 185(11), 201(100)	Aleuritic acid	C <sub>17</sub> H <sub>34</sub> O <sub>5</sub>
26.88	137(44), 141(63), 153(10), 169(22), 173(37), 185(10), 201(66) 207(20),	C <sub>15</sub> fragment	

RT = retention time, m/z = mass/charge ratio

Mass spectra (fragmentation patterns, below)



## Experimental

The object was observed, and its conditions were documented. Samples from selected areas were taken by Valentina Risdonne. When possible, each sample was split into two parts: one fragment was embedded in polyester resin (Tiranti clear casting resin), polished and analysed under an optical microscope and the other was put aside for XRD and py-TMAH-GC/MS.

The optical microscopy was performed with an Olympus BX51 Metallurgical Microscope equipped with four objectives (magnification of x5, x20, x50 and x100), and an x10 eyepiece. In many instances, a small amount of white spirit was applied on the surface of the cross-section to improve the saturation under the microscope. The microscope is equipped with a 6-cube filter turret which allows operating the system in reflected visible light (brightfield and darkfield mode) and reflected UV light (365 nm) using a 100 W mercury burner.

The SEM-EDS analysis was performed with a field emission TESCAN MIRA 3 with gigantic chamber. The SEM is equipped with: secondary electron detector (SE), secondary electron in-beam detector (In-beam SE), back-scatter detector (BSE), back-scatter in-beam detector (In-beam BSE), cathodoluminescence detector (without wavelength detection) (CL), plasma chamber/sample cleaner and software Alicona 3D imaging. For the EDS analytical part, it has an Oxford Instruments setup: Software: AztecEnergy, X-ray detector X-Max 150 mm<sup>2</sup> and X-ray detector X-Max Extreme, low energy detector for thin films, high resolution and low voltage. The samples were analysed by SEM-EDS Low Vacuum Mode (10-15 Pa). EDS Mapping and data processing were performed with Aztec Oxford software.

A Perkin Elmer Frontier FT-IR spectrometer (350 cm<sup>-1</sup> at the best resolution of 0.4 cm<sup>-1</sup>) was used, equipped with a germanium crystal for ATR measurements and combined with a Spectrum Spotlight 400 FT-IR microscope equipped with a 16×1 pixel linear mercury cadmium telluride (MCT) array detector standard with InGaAs array option for optimised NIR imaging. Spectral images from sample areas are possible at pixel resolutions of 6.25, 25, or 50 microns. The Perkin Elmer ATR imaging accessory consists of a germanium crystal for ATR imaging. These run with Perkin Elmer Spectrum 10™ software and with SpectrumIMAGE™ software. Baseline and Kubelka-Munk corrections were applied to the raw data acquired in diffuse reflectance.

The XRD analyses were performed with a Rigaku SmartLab SE equipped with a HyPix-400, a semiconductor hybrid pixel array detector and Cu source. The analyses were performed in Bragg-Brentano geometry mode, with 40 kV tube voltage and 50 mA tube current. The diffractograms were processed with a SmartLab II software. The data was compared to the RUFF database (Lafuente et al., 2016) and the COD Database (Gražulis et al., 2009).

The instrument used for GC/MS is a Thermo Focus Gas Chromatographer with DSQ II single quadrupole mass spec. The column currently installed is a Agilent DB5-MS UI column (ID: 0.25 mm, length: 30 m, df: 0.25 µm, Agilent, Santa Clara, CA, USA). Carrier gas: helium. Detector temperature: 280 °C, Injector temperature: 250 °C. It can be used with the Pyrola 2000 Platinum filament pyrolyser (PyroLab, Sweden) attachment or in split/splitless mode. Detection: Total Ion monitoring (TIC). 1 µl of the sample with 1 µl of TMAH was placed on the Pt filament for the py-GC/MS. The inlet temperature to the GC was kept at 250 °C. The helium carrier gas flow rate was 1.5 ml/min with a split flow of 41 ml/min and a split ratio of 27. The MS transfer line was held at 260 °C and the ion source at 250 °C. The pyrolysis chamber was heated to 175 °C, and pyrolysis was carried out at 600 °C for 2 s. This run with Xcalibur™ and PyroLab™ software. The library browser supported NIST MS Version 2.0 (Linstrom & Mallard, 2014).

Valentina Risdonne, PhD student

[v.risdonne@vam.ac.uk](mailto:v.risdonne@vam.ac.uk) / [valentina.risdonne@northumbria.ac.uk](mailto:valentina.risdonne@northumbria.ac.uk)

Victoria and Albert Museum – Northumbria University

PhD project 'Materials and techniques for coating of the nineteenth-century plaster casts'

©V&A Museum

28 August 2020

## Notes

17 January 2019	Sampling	Valentina's PhD Lab book 1, page 146
29 January 2019	Casting	Valentina's PhD Lab book 1, page 158
5 February 2019	Microscopy	Valentina's PhD Lab book 1, page 163
14 October 2019	FT-IR	Valentina's PhD Lab book 1, page 175
3 December 2019	XRD	Valentina's PhD Lab book 2, page 4
18 March 2020	GC/MS	Valentina's PhD Lab book 2, page 50

A full record of analysis is available at <https://doi.org/10.25398/rd.northumbria.14040305>

## References

- Colombini, M. P., & Modugno, F. (2009). *Organic mass spectrometry in art and archaeology*. John Wiley & Sons.
- Cox, K. G., Price, N. B., & Harte, B. (1974). *An introduction to the practical study of crystals, minerals, and rocks*. Halsted Press.
- Gražulis, S., Chateigner, D., Downs, R. T., Yokochi, A. F. T., Quirós, M., Lutterotti, L., Manakova, E., Butkus, J., Moeck, P., & Le Bail, A. (2009). Crystallography Open Database—an open-access collection of crystal structures. *Journal of Applied Crystallography*, 42(4), 726–729.
- Lafuente, B., Downs, R. T., Yang, H., & Stone, N. (2016). The power of databases: the RRUFF project. In *Highlights in mineralogical crystallography* (pp. 1–29). Walter de Gruyter GmbH.
- Linstrom, P. J., & Mallard, W. G. (2014). *NIST Chemistry WebBook, NIST standard reference database number 69, National Institute of Standards and Technology, Gaithersburg MD, 20899*.
- Mills, J., & White, R. (2012). *Organic chemistry of museum objects*. Routledge.
- Price, B. A., Pretzel, B., & Lomax, S. Q. (2009). Infrared and Raman Users Group Spectral Database; 2007 ed. *IRUG: Philadelphia, PA, USA*.

The charm of the Cast Courts does not lie only in the collection, but also in the purpose-made spaces. The west court is now redecorated in its original colours, as it was originally painted in purple-red below the balcony and olive-green above while immediately below the brackets was a band of strapwork containing 'names of cities celebrated in the history of art arranged alphabetically from Ahmedabad to Zurich'. The combination of colours was however defined as 'utterly inharmonious' by some of the contemporary critics (Baker, 1982). The original decoration was recovered after the refurbishment work<sup>1</sup>, which has also included extensive research into the original decorative architectural scheme of the gallery, established by Josephine Darrah in the 1980s and recently extended by Crick-Smith et al. (2012).

The needs of the museum environment in the case of a mixed collection, as in the Victoria and Albert Museum, can be rather complicated. The aim is to regulate air conditioning, energy efficiency and environmental control, which can be achieved to a degree and with difficulty. The general purpose is to obtain the best visibility of the objects in their environment while minimising photo-degradation where this is important. This can be achieved by providing the minimum exposure at the lowest levels at which they can be seen reasonably well. Moreover, the thermal environment in museums and galleries has to satisfy the preservation and display of the objects, the human comfort and the well-being of the building (Cassar, 1994; Garside et al., 2017). In an outdoor environment, the hazard for the preservation comes mostly from natural sources (dirt, pollution, heat, cold and moisture) whereas in a museum environment, often the real hazard is caused by people: the crowds of people impose wildly fluctuating conditions, bringing dirt and generating heat and moisture while they demand warmth and light. Isella et al. (2017), for example, report finding a thick layer of different exogenic material (including pigeon dropping and solid particles coming both from soil and pollution) and, as a result of the contact with human hands, a greasy, grey layer had been formed on the lower part of the plaster casts; moreover, the artworks were damaged by different acts of vandalism, which caused the fracture of exposed extremities. The natural factors that influence the deterioration of an object in a museum are radiation (UV, VIS and near-IR), high and low temperatures and their

---

<sup>1</sup> The original decorative scheme (colours and some details) are documented in a watercolour also including glass mosaic floor panels designed by F. W. Moody and executed by Powell and Sons of Whitefriars. These and the mosaic floor do not survive. The mosaic of the central corridor executed by the women prisoners of Woking prison (named by Cole *opus criminale*) has recently been conserved and cleaned (Baker, 1982).

changes/cycles, moisture (relative air humidity), gases and particles in air (pollution), microorganisms, oxygen and time (determining the effect for all the factors above to work) (Brokerhof, 2006; Jelle, 2012). All the degradation processes influence each other. For example, the wet and dry deposition of CO<sub>2</sub>, SO<sub>x</sub> and NO<sub>x</sub> can promote the formation of salts (Maguregui et al., 2009). The extent of the photodeterioration depends upon several factors: the intensity of light, time exposure, the spectral characteristic of the light, the intrinsic capacity of individual organic substances to absorb and be affected by light. High temperature and high relative humidity speed up the process of photodecomposition as well as causing the more generally recognised forms of physical deterioration. At normal temperatures and humidity, however, the rate of change of temperature and humidity is usually of more concern.

The V&As environmental monitoring system, OCEAN (Object Centred Environmental Analysis Network, *Figure A7.1*), continually gathers climate data from over 650 sensors measuring primarily temperature, humidity and light. Data is recorded every 15 minutes, generating over 40 million time-stamped data points a year. Once the data is collected decisions are made on how the climate could be a risk to the collections and what actions can be undertaken by the Estate team to manage the conditions. The challenge is finding a way to process and concisely present the data to key stakeholders (Lima, 2017).

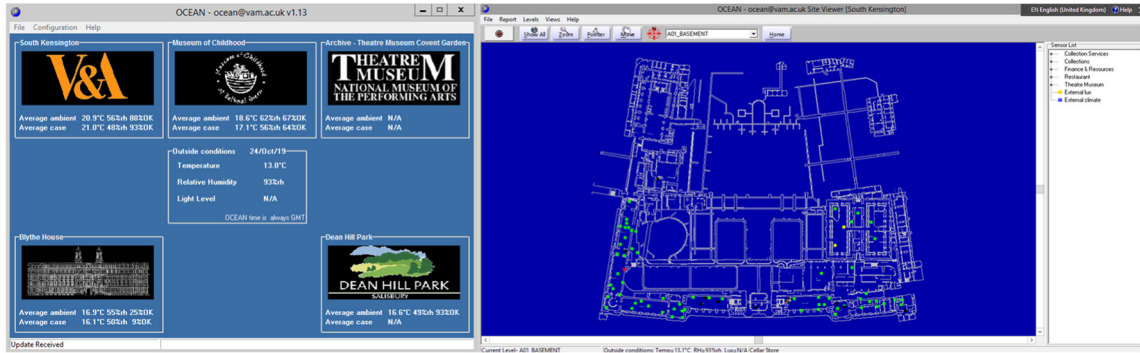
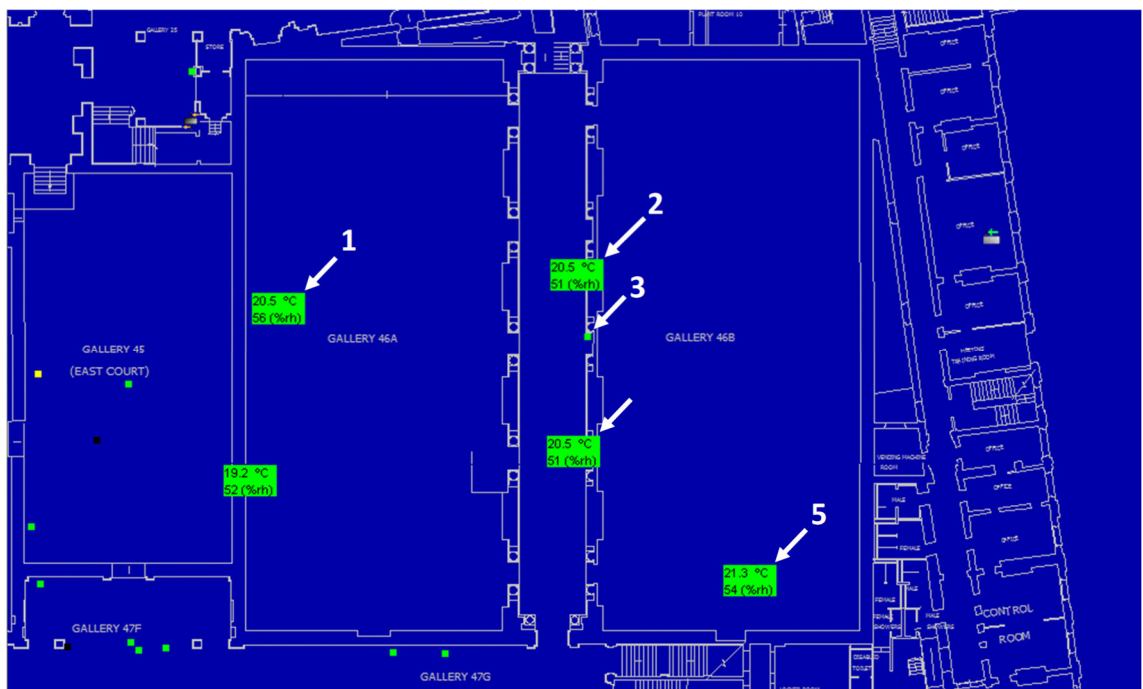


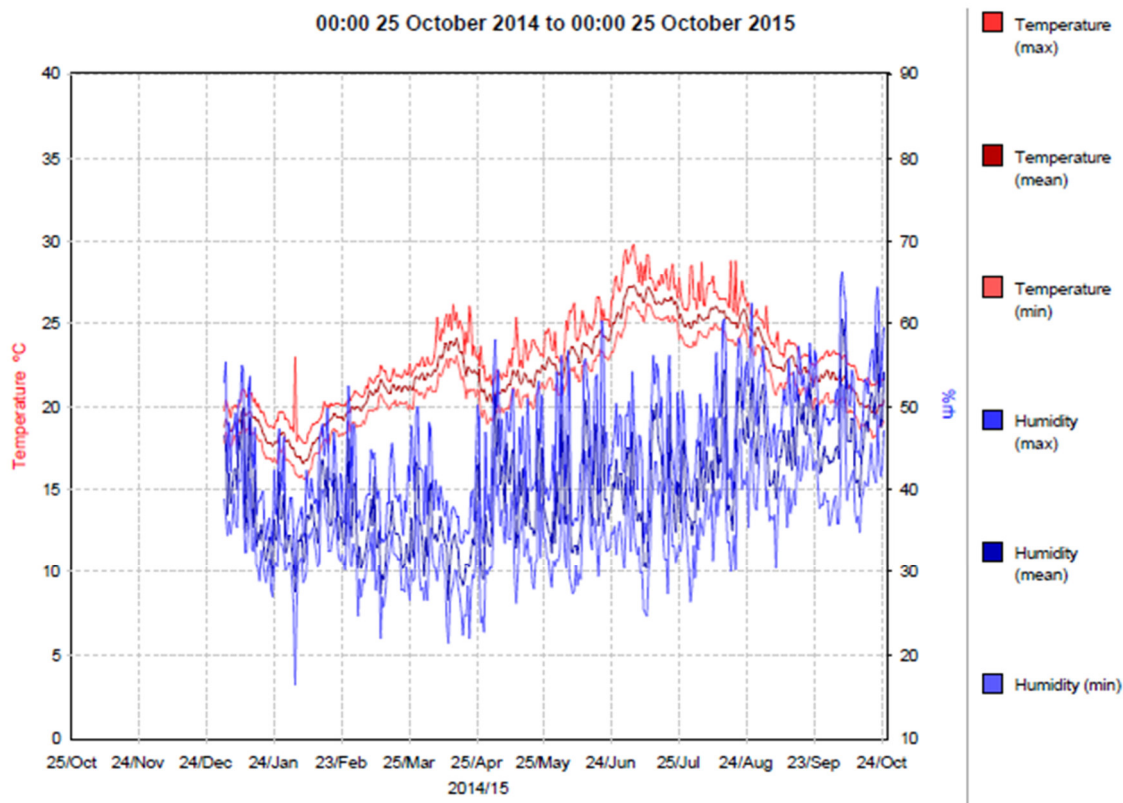
Figure A7.1. OCEAN is the software that allows the live monitoring of the environmental conditions in the V&A's premises. The map on the right shows the galleries and the location of the data logs.



DATA LOG	LOCATION
1	G46A(low). Room 4322: Gallery 46A
2	G46 C2(low). Room 4323: Gallery 46
3	G46. Room 4323: Gallery 46
4	G46 C3(low). Room 4323: Gallery 46
5	G46B(low). Room 4324: Gallery 46B

Figure A7.2. Image and table showing the data logs located on the ground level of the Cast Courts. There are two located in Gallery 46A, one in Galley 46B and three in the corridor in between them.

## TEMPERATURE AND HUMIDITY OCT 2014-OCT 2015

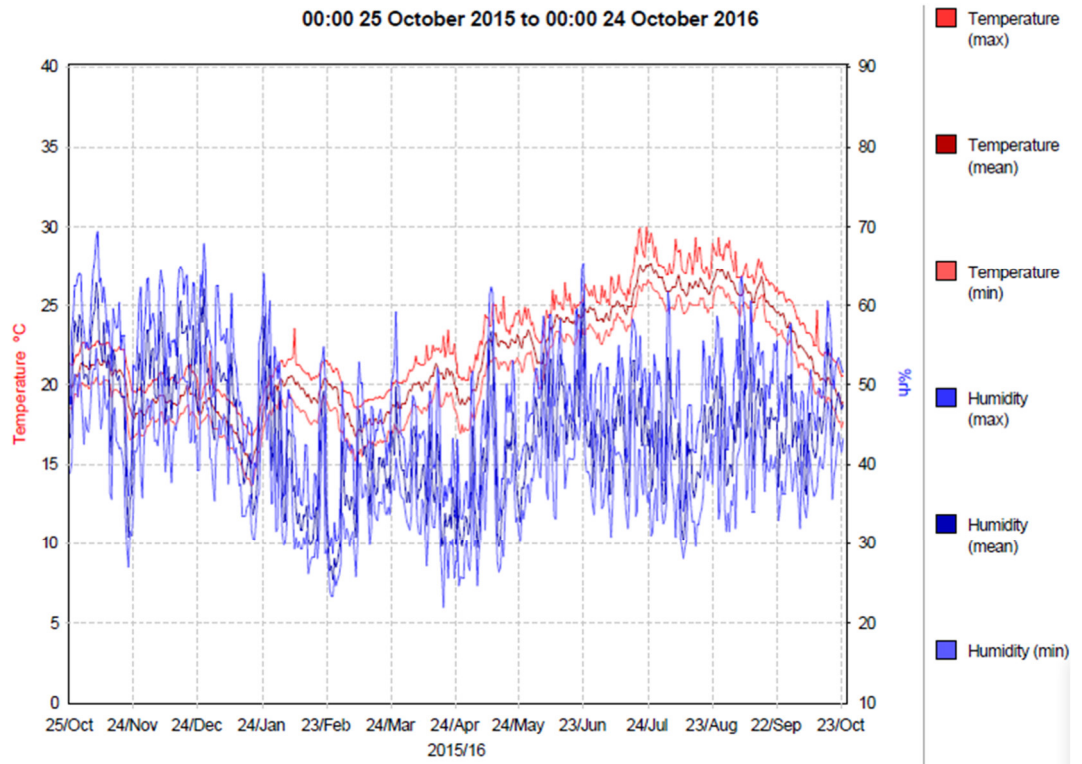


The graph represents the spread of data over all sensors included in the report

No. of sensors	Temperature			Humidity			Time within limits %		
	Mean	Min	Max	Mean	Min	Max	Temperature	Humidity	Overall
5	22.2	15.6	29.8	40	16	66	78	49	39

Sensor Data Summary: 00:00 25 October 2014 to 00:00 25 October 2015										
Sensor Name	Space No.	Temperature			Humidity			Time within limits %		
		Mean	Min	Max	Mean	Min	Max	Temperature	Humidity	Overall
G46	4323	22.6	16.9	27.7	39	24	57	75	45	32
G46A (high)	4322	22	15.6	29.8	40	22	66	74	48	38
G46A (low)	4322	21.5	15.6	27.6	41	21	64	81	55	47
G46B (high)	4324	22.8	16.1	28.1	39	16	64	74	45	33
G46B (low)	4324	22.1	16.5	28	41	23	63	83	53	42

TEMPERATURE AND HUMIDITY OCT 2015-OCT 2016

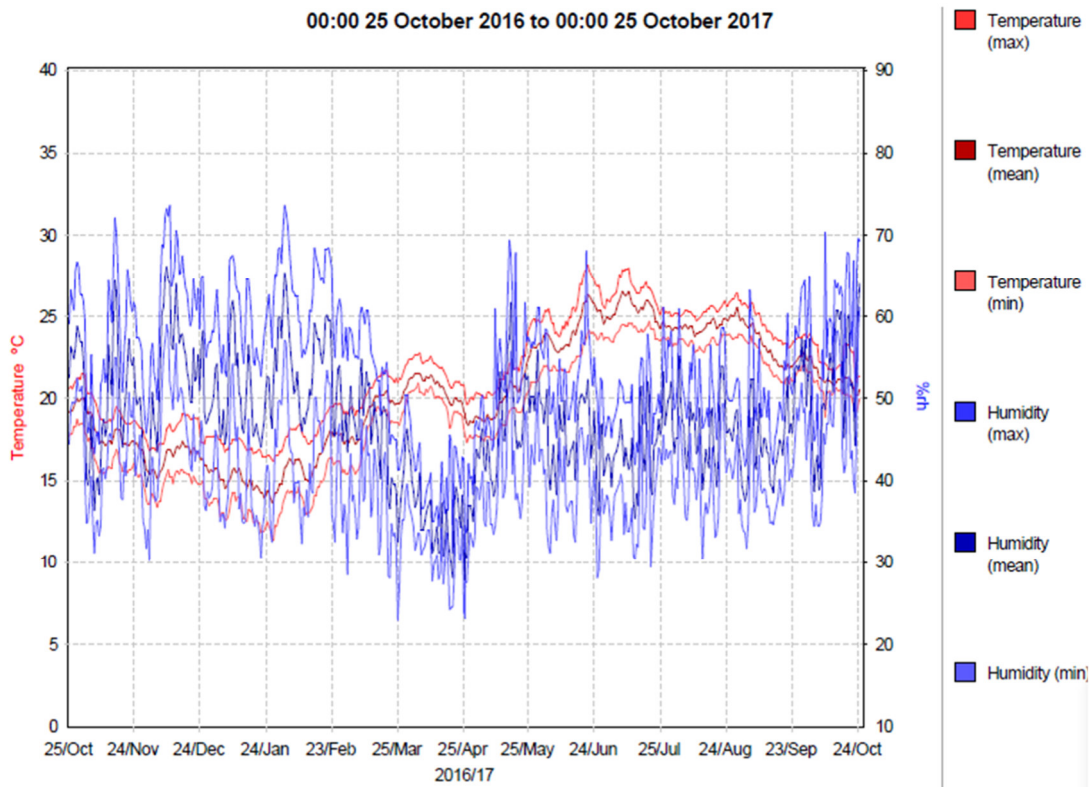


The graph represents the spread of data over all sensors included in the report

No. of sensors	Temperature			Humidity			Time within limits %		
	Mean	Min	Max	Mean	Min	Max	Temperature	Humidity	Overall
5	21.6	13.7	30	44	22	69	70	70	48

Sensor Data Summary: 00:00 25 October 2015 to 00:00 24 October 2016											
Sensor Name	Space No.	Temperature			Humidity			Time within limits %			
		Mean	Min	Max	Mean	Min	Max	Temperature	Humidity	Overall	
G46	4323	22.2	16.1	28	42	24	63	75	65	48	
G46A (high)	4322	21.2	13.7	30	44	22	68	63	71	45	
G46A (low)	4322	20.9	13.7	28	46	24	69	65	76	49	
G46B (high)	4324	21.7	14.4	28.5	42	23	66	69	65	44	
G46B (low)	4324	21.8	15.1	28.4	44	23	65	79	71	55	

## TEMPERATURE AND HUMIDITY OCT 2016-OCT 2017

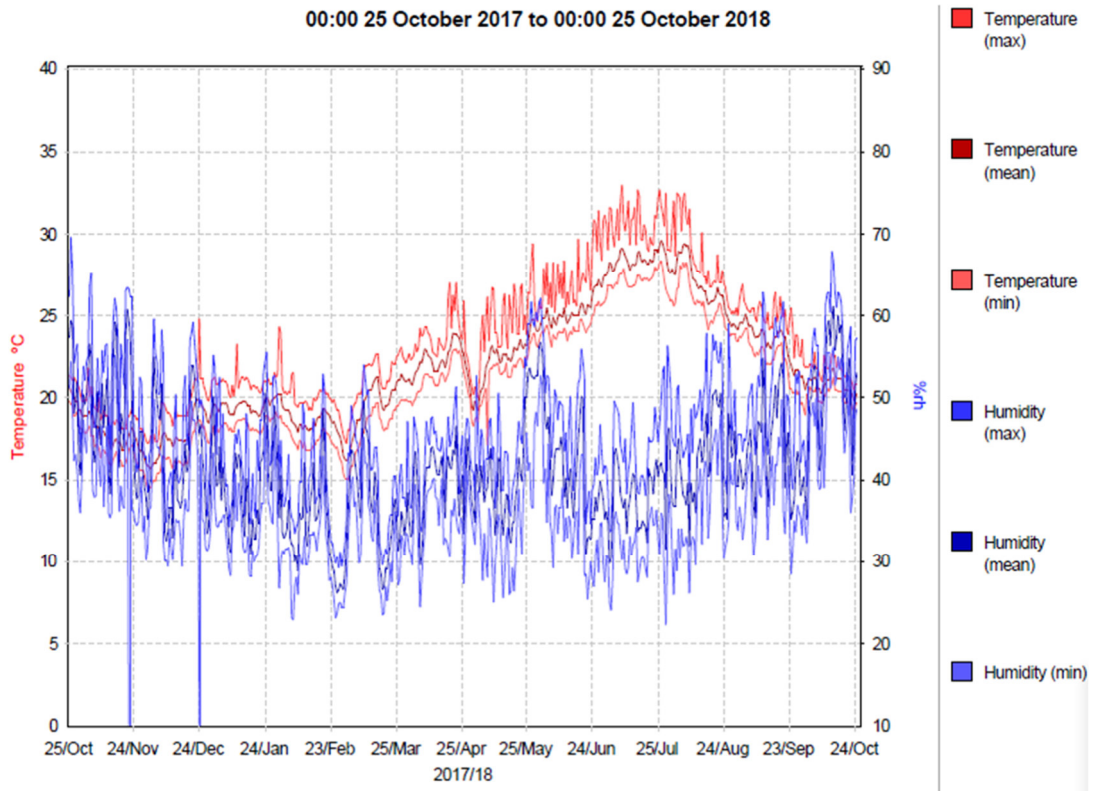


The graph represents the spread of data over all sensors included in the report

No. of sensors	Temperature			Humidity			Time within limits %		
	Mean	Min	Max	Mean	Min	Max	Temperature	Humidity	Overall
5	20.3	11.4	28.2	47	23	74	61	83	49

Temperature Distribution Data: 00:00 25 October 2016 to 00:00 25 October 2017											
Sensor Name	Space No.	Temperature			Humidity			Time within limits %			
		Mean	Min	Max	Mean	Min	Max	Temperature	Humidity	Overall	
G46	4323	21.2	15	26.9	44	24	70	65	79	48	
G46A (high)	4322	19.6	11.4	26.8	50	28	72	56	90	50	
G46A (low)	4322	19.3	11.5	25.2	51	23	74	62	89	56	
G46B (high)	4324	20.9	14	28.2	44	23	70	60	72	41	
G46B (low)	4324	20.5	13.4	27.8	47	23	68	64	85	52	

TEMPERATURE AND HUMIDITY OCT 2017-OCT 2018

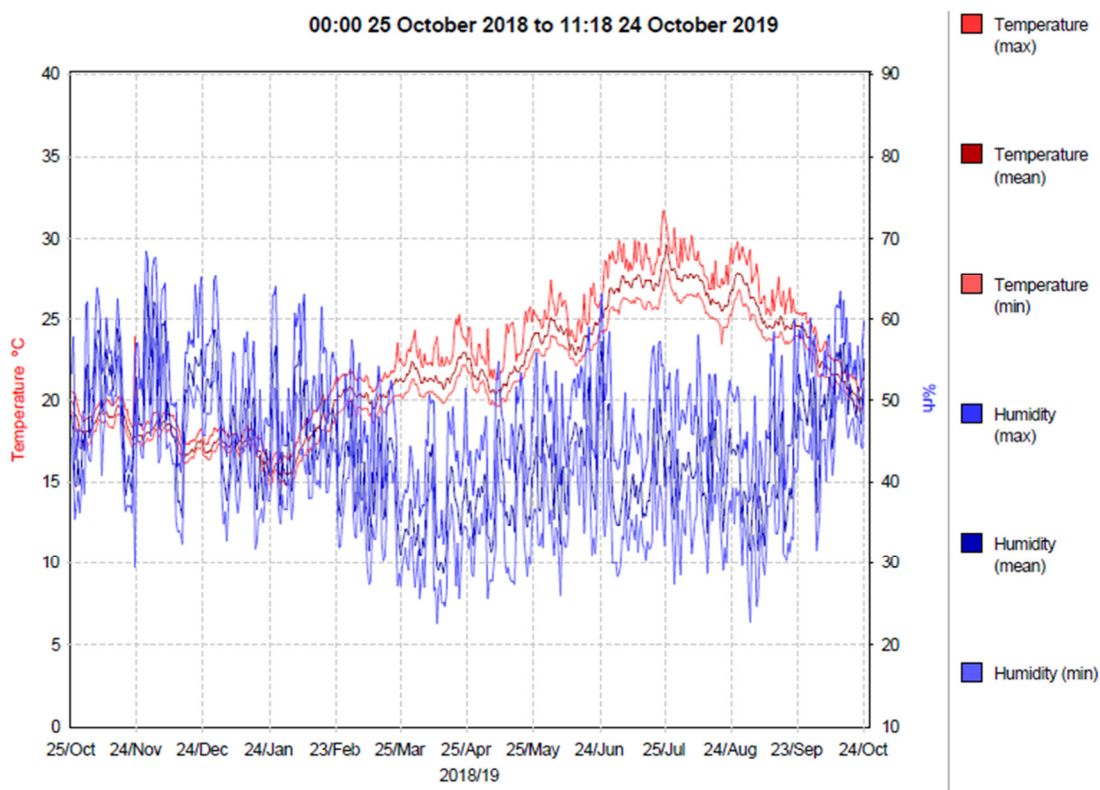


The graph represents the spread of data over all sensors included in the report

No. of sensors	Temperature			Humidity			Time within limits %		
	Mean	Min	Max	Mean	Min	Max	Temperature	Humidity	Overall
5	21.8	14.5	33	42	7	70	67	58	40

Sensor Data Summary: 00:00 25 October 2017 to 00:00 25 October 2018											
Sensor Name	Space No.	Temperature				Humidity			Time within limits %		
		Mean	Min	Max	Mean	Min	Max	Temperature	Humidity	Overall	
G46	4323	19.6	18.2	24.8	40	7	70	54	100	57	57
G46A (high)	4322	21.7	14.6	33	41	22	65	59	54	34	34
G46A (low)	4322	21.3	14.5	29.8	42	25	68	61	63	41	41
G46B (high)	4324	22.4	16.3	30.4	42	24	70	71	56	41	41
G46B (low)	4324	22.1	15.9	29.8	42	23	65	76	59	44	44

### TEMPERATURE AND HUMIDITY OCT 2018-OCT 2019



The graph represents the spread of data over all sensors included in the report

No. of sensors	Temperature			Humidity			Time within limits %		
	Mean	Min	Max	Mean	Min	Max	Temperature	Humidity	Overall
5	21.7	14.8	31.7	43	23	69	59	68	39

Temperature Distribution Data: 00:00 25 October 2018 to 11:18 24 October 2019										
Sensor Name	Space No.	Temperature			Humidity			Time within limits %		
		Mean	Min	Max	Mean	Min	Max	Temperature	Humidity	Overall
G46	4323	21.4	15	28.8	46	28	69	59	83	47
G46A (high)	4322	21.7	14.9	31.7	42	23	64	58	62	36
G46A (low)	4322	21.5	14.8	29.6	43	25	64	60	67	39
G46B (high)	4324	22.1	15.4	30.1	43	27	66	60	64	37
G46B (low)	4324	22	15.1	30.8	43	26	65	60	65	38

## REFERENCES

- Baker, Malcolm. (1982). *The History of the Cast Courts*. V&A Masterpieces Series. <http://www.vam.ac.uk/content/articles/t/the-cast-courts/> (last accessed: 27/03/2021)
- Brokerhof, A. W. (2006). The deterioration processes of organic objects in museum, historic house and archive environments. *EU MASTER Final Workshop, UCL, London, 10*.
- Cassar, M. (1994). *Museums environment energy*. Her Majesty's Stationery Office. ISBN-13: 978-0112905196
- Crick-Smith, I., Crick-Smith, M., Faulding, R., & Croft, P. (2012). *The Cast Courts, Victoria and Albert Museum: architectural paint research archive report*.
- Garside, D., Curran, K., Korenberg, C., MacDonald, L., Teunissen, K., & Robson, S. (2017). How is museum lighting selected? An insight into current practice in UK museums. *Journal of the Institute of Conservation, 40*(1), 3–14.
- Isella, E., Bonelli, D., Cerea, S., Mancini, F., Ruppen, V., Botteon, A., & Sansonetti, A. (2017). Experiences at the Academy of Fine Arts of Brera in Milan, Italy: the application of laser-technology on three case studies of the historical heritage. (P. Targowsk Ed.), *Lasers in the Conservation of Artworks XI, Proceedings of LACONA XI*. NCU Press. <https://doi.org/10.12775/3875-4.16>
- J Jelle, B. P. (2012). Accelerated climate ageing of building materials, components and structures in the laboratory. *Journal of Materials Science, 47*(18), 6475–6496. <http://dx.doi.org/10.1007/s10853-012-6349-7>
- Lima, C. R. (2017). *Partícula (rizando) o V&A: conservação preventiva em ação*. MSc Thesis.
- Maguregui, M., Sarmiento, A., Escribano, R., Martinez-Arkarazo, I., Castro, K., & Madariaga, J. M. (2009). Raman spectroscopy after accelerated ageing tests to assess the origin of some decayed products found in real historical bricks affected by urban polluted atmospheres. *Analytical and Bioanalytical Chemistry, 395*(7), 2119–2129. <https://doi.org/10.1007/s00216-009-3153-6>



THE PHYSICAL MODELS AND THE ACCELERATION FACTORS

The **thermal model** applied for this study is based on the relationship proposed by Arrhenius (*Equation A8.1*), which is based on the thermal distribution of electronic, vibrational, and rotational energies. If to react molecules need to have energy above a certain level (the activation energy  $E_a$ ), as Arrhenius proposed, then a change in reaction rates will occur with increased temperature. The Arrhenius equation has been traditionally used in accelerated thermal ageing tests (Nelson, 2009) and states that:

$$k = A \cdot e^{(-E_a/RT)} \quad (\text{A8.1})$$

Where  $k$  is the reaction rate,  $A$  is the Arrhenius factor (a reaction-specific constant),  $E_a$  is the activation energy for the reaction,  $R = 8.314 \text{ J/Kmol}$  is the gas constant and  $T$  is the temperature in degrees Kelvin (Erhardt & Mecklenburg, 1995; Mills & White, 2012). This equation implies that the chemical degradation processes, defined by the reaction rate, increases asymptotically when  $T$  increases.

A **temperature acceleration factor  $AF_T$**  may then be calculated as the ratio between the reaction rate in the laboratory ageing apparatus  $k_{lab}$  and the 'actual' ageing  $k_{act}$ :

$$AF_T = k_{lab}/k_{act} = \frac{A_{lab}e^{-E_{a,lab}/(RT_{lab})}}{A_{act}e^{-E_{a,act}/(RT_{act})}} \approx \frac{e^{-E_{a,lab}/(RT_{lab})}}{e^{-E_{a,act}/(RT_{act})}} \quad (\text{A8.2})$$

where  $T_{lab}$  and  $T_{act}$  denote the temperature in the thermal chamber and the temperature in the real scenario, respectively. It is here assumed that the pre-exponential factor  $A$  is temperature independent which gives  $A_{lab} \approx A_{act}$ . Furthermore, it is also assumed that the activation energy  $E_a$  is temperature independent and  $E_{a,lab} = E_{a,act}$ .

The rate of a reaction, or stage in a reaction, is proportional to the reciprocal of the time of the reaction. This would imply that, if the degradation processes occurred constantly over the period in which the studied material have been naturally ageing ( $t_{act}$ ), then:

$$t_{lab} = t_{act}/AF_T \quad (\text{A8.3})$$

After setting the values of equations in *Equation A8.2*, it is, therefore, possible to define a relationship between the time of the experiment  $t_{lab}$  and the time in which the target material has been ageing in the real scenario  $t_{act}$ . The Arrhenius equation is also widely employed to extrapolate the so-measured rates of deterioration and to estimate thereby the rate at the moderate temperature of ordinary usage (Nelson, 2009).

To define the **irradiation model** for the light component of the accelerated ageing, it is possible to define the *relative damage factor* (D) caused by the radiation (Cassar, 1994) as described by:

$$D = k_1 \cdot (I \cdot t) \quad (A8.4)$$

D is an adimensional relative factor that can be used to compare the effects of any light source, in terms of its radiant power, on a material.  $k_1$  is a constant factor depending on the material characteristics, I and t are the intensity of the radiant exposure and its time, respectively. D being a relative factor, the intensity of the exposure could be expressed by using several photometric and radiometric dimensions that describe the energetic characteristics of the light, as long as they remain constant between the terms of the comparison. More precisely, the selected unit must present the same spectral distribution across the terms of the comparison. It was therefore decided to use the irradiance  $E(\lambda)$  [ $W/m^2$ ] in *Equation A8.4*, which, as described in *Section 2.4.1*, is a radiometric dimension (Oleari, 1998).

The *radiant exposure* H of a surface is the amount of light per unit area, irradiance  $E(\lambda)$ , in a time  $t$  and measured in  $J/m^2$ :

$$H = E \cdot t \quad (A8.5)$$

To approximate in the laboratory (lab) the same light-driven damage or ageing that occurred in a real-life scenario (act=actual),  $D_{lab}$  must be equal to  $D_{act}$ .  $k_1$  is a constant and  $k_{1,lab}=k_{1,act}$  when working with the same material (Cassar, 1994). Therefore:

$$E(\lambda)_{lab} \cdot t_{lab} = E(\lambda)_{act} \cdot t_{act} \quad (A8.6)$$

In other words, the accelerated ageing aims to equal the radiant exposure. *Equation A8.6* represents the *principle of reciprocity* or *total exposure theory*: by increasing the intensity of the exposure in the laboratory, it is possible to achieve the same radiant exposure or degree of deterioration (*Equation 2.7*) in a shorter time. However, it is important to remember that a higher intensity does imply a shorter test period, but test samples must not be exposed to conditions and strains which may induce reactions that will never occur during actual

ageing<sup>1,2</sup> (Jelle, 2012). Moreover, caution must be used when photometric dimensions are used to describe the intensity of exposure: it is not intensity but the frequency (inverse of wavelength) that determines the energy of electromagnetic radiation and its tendency to be absorbed by specific chemical structures (Feller, 1994). As reported in *Equation A8.7*, the relative damage factor  $D$  has been found inversely proportional to the log of the wavelength  $\lambda$ , due to the higher energy of photons at shorter wavelengths (Cassar, 1994).

$$D = k_2 \cdot \log_{10} (1/\lambda) \quad (\text{A8.7})$$

where  $k_2$  is a constant factor depending on the type of material feller. This suggests that *Equation A8.6* is only applicable when the exposure 'lab' and 'act' have the same wavelength if a photometric dimension is used instead of the irradiance  $E(\lambda)$ . A measure of such property is the spectral sensitivity of a material, which express how the amount of damage, caused by a unit of light energy, varies according to the wavelength of light and may vary greatly from material to material (McKeen, 2015; Quill et al., 2004). The photodegradation potential of a light source can be understood by reviewing its Spectral Power Distribution (SPD), defined as the intensity of a light source as a function of the individual wavelength (Quill et al., 2004).

The light acceleration factor  $AF_{UV}$  is therefore defined by Cassar (1994) as:

$$AF_{UV} = P_{lab}/P_{act} \quad (\text{A8.8})$$

Where  $P_{lab}$  and  $P_{act}$  are the radiant flux, measured in Watt, in the laboratory and in the real scenario. Being the irradiance  $E(\lambda)$  also defined by *Equation 2.1* in *Section 2.4.1*, and  $A_{lab}=A_{act}$ , then:

$$AF_{UV} = (E(\lambda)_{lab} \cdot A_{lab}) / (E(\lambda)_{act} \cdot A_{act}) = E(\lambda)_{lab} / E(\lambda)_{act} \quad (\text{A8.9})$$

---

<sup>1</sup> The principle is often misinterpreted and criticized: the theory, in fact, does not claim that exaggerating the condition in laboratory is possible to reproduce what would happen in a real scenario in a longer period of time, but states that by increasing the intensity of the exposure, the time of exposure reduces. To a scientist, this would naturally suggest that the principle is valid under certain experimental conditions, limitation and approximations.

<sup>2</sup> Accelerated ageing should not cause any changes or chemical reactions in the materials and components which would not occur upon the longer actual ageing process. For example, in the case that radiation initiates photodegradation, the subsequent chemical degradation processes will have exponentially increasing kinetic reaction rates with respect to increasing temperatures (Arrhenius relationship); however, if the temperature increases from 60° to 70° C, the increase in chemical reaction rate will be much larger than the ones occurring when increasing from 30° to 40° C, even if the increase in temperature is 10° C in both cases Jelle, B. P. (2012) 'Accelerated climate ageing of building materials, components and structures in the laboratory', *Journal of materials science*, 47(18), pp. 6475-6496.. A higher ageing temperature is therefore causing a higher reaction rate for the ageing processes and thus leading to an acceleration of the climate ageing.

By assuming that the aim is to fulfil the reciprocity principle (*Equation A8.6*), then  $AF_{UV}$  is also equal to the ratio  $t_{act}/t_{lab}$ , and it is possible to calculate the time of the light ageing, under the defined conditions as:

$$t_{lab} = t_{act}/AF_{UV} \quad (\text{A8.10})$$

Practically, to calculate the thermal acceleration factor  $AF_T$  (*Equation A8.2*) and consequently the  $t_{lab}$  (*Equation A8.3*), the time of the sample in the thermal chamber at the selected temperature, it is necessary to define the activation energy  $E_{a,lab}=E_{a,act}$ .  $E_a$  is specific to every reaction, implying that, for every reaction happening in the mixture, a different  $E_a$  should be considered resulting in different  $AF_T$ . There is no  $E_a$  reference value in the literature for any of the many reactions that could be expected during the deterioration of the surfaces of the plaster casts. Moreover, if this value had to be retrieved from the literature, it should have been specific not only of the individual deterioration reaction of the substrate and the coating but of the overall substrate-coating system. An experimental method to calculate the  $E_a$  is based on the theory of Modulated Thermogravimetry (MTGA™) on activation energy (Moropoulou et al., 1995; Schulman, 2020). Studies that are based on this theory demonstrated, for example, that the activation energy for the deterioration processes of paraffin, white and yellow beeswax is in the range of 115 kJ/mol to 123 kJ/mol (Schulman, 2020). The values of the overall activation energies corresponding to the decomposition process of wood lie within 146–112 kJ/mol (Popescu et al., 2010). Hudson-Lamb et al. (1996) found that the four stages of dehydration of natural gypsum are characterised by activation energy ranging from 88 kJ/mol to 98 kJ/mol. Symoniuk et al. (2016) reported that activation energy of oxidation reaction for the selected linseed oils ranged from 93.14 to 94.53 kJ/mol or between 74.03 and 77.76 kJ/mol depending on the method selected. Jelle (2012), on the other hand, in his experiment of accelerated climate ageing of building materials arbitrarily set the activation energy at 70 kJ/mol. By replacing the values defined in *Sections 2.4.1* and *5.2.1.3* of  $T_{act} = 21.52$  °C and  $T_{lab} = 40$  °C in the  $AF_T$  equation based on the Arrhenius equation, it is easy to calculate that for a lower value of  $E_a = 70$  kJ/mol,  $AF_T = 5.40$  and for a higher value of  $E_a = 150$  kJ/mol,  $AF_T = 37.09$ . Another factor that should be considered for the definition of the  $E_a$  is that this value is variable as dependent on the reaction progress, in particular for multistage reactions (Roduit & Odlyha, 2006). Defining the value of  $E_a$  as a constant during the stages of the reaction is a significant approximation, however necessary in lack of scientific literature that investigate the specific values.

As for the determination of radiation acceleration factor  $AF_{UV}$  (*Equation A8.9*), it is necessary to calculate the irradiation produced by the Q-Sun Xenon Xe-1 Test Chamber. The Spectral Power Distribution (SPD, *Glossary*) of the chamber was integrated with the

Simpson method (Abdel-Baset et al., 2019; Clenshaw & Curtis, 1960) and a total of 496.92 W/m<sup>2</sup> was calculated. The radiation arriving on the samples was also measured by a sensor including the IR region, although it is commonly recognised that most of the photodegradation happens in the UV area (Cassar, 1994; Thomson, 2013). As the SPD of the chamber is designed to approximate the SPD of the daylight, the differences in the intensity of the light at different wavelength can be dismissed in our considerations. By using a pyrometer (Thorlabs® S120VC - Standard Photodiode Si Power Sensor, Wavelength Range 200 - 1100 nm, Optical Power Range up to 50 mW) the irradiance of the Q-sun chamber was measured equal to 300 W/m<sup>2</sup>, which seems consistent with the calculated theoretical value of 496.92 W/m<sup>2</sup>, after power losses. Considering the aimed 117 W/m<sup>2</sup> average annual irradiance and the measured actual value of the chamber, the AF<sub>UV</sub> was calculated as equal to 2.56 (Risdonne & Theodorakopoulos, 2021).

The acceleration factors calculated suggest that to achieve 150 years of ageing according to the simplified methodology outlined in *Section 2.4.1*, the characteristics of the equipment described in *Section 5.2.1.3* and the calculations herein detailed, it would be necessary to perform a minimum thermal accelerated ageing of 4.04 years (corresponding to the higher acceleration factor based on the lower E<sub>a, act</sub>) and a light accelerated ageing of 58.34 years.

## GRAVIMETRY

The weight of the three control plaster cubes (C1, C2 and C3) was measured throughout the experiments. For every cube 30 weight measurements (nos. 0-29) were taken, so that each measurement was assigned a weight ( $w_{C,j}$ ) at a time ( $t_{C,j}$ ) ( $j= 0 \dots 29$ ). The error of these weight measurements is given by the resolution ( $r$ ) of the JJ-BC Series Electronic Analytical Balance and equal to 0.1 mg. The average values of the weights of the cubes (C1, C2 and C3) at  $t_{C,j}$  were calculated and, as the error of the weight measurements is equal to  $r$  for C1, C2 and C3, the error ( $er$ ) of the average is given by:

$$er_{\overline{w_{C,j}}} = \sqrt{(r/3)^2 + (r/3)^2 + (r/3)^2} \quad (\text{A8.11})$$

and therefore, equal to  $5.77 \cdot 10^{-5}$  for all the measurements., The weight loss % ( $\Delta w_{C,0-j}\%$ ) of the cubes at  $t_{C,j}$ , relative to the initial weight  $w_{C,0}$  at  $t_{C,0}$ , represents the water loss during the drying process and was measured as follows:

$$\Delta w_{C,0-j}\% = \frac{(w_{C,0} - w_{C,j})}{w_{C,0}} \cdot 100 \quad (\text{A8.12})$$

The error for  $\Delta w_{C,0-j}\%$  is equal to:

$$er_{\Delta w_{C,0-j}\%} = \sqrt{\left(\frac{100w_{C,j}}{w_{C,0}^2} \cdot s_{w_{C,0}}\right)^2 + \left(\frac{100}{w_{C,0}} \cdot s_{w_{C,j}}\right)^2} \quad (\text{A8.13})$$

Where  $w_{C,0}$  and  $s_{w_{C,0}}$  are the weight and standard deviation of the cubes at  $t_{C,0}$  and  $w_{C,j}$  and  $s_{w_{C,j}}$  are the weight and standard deviation of the cubes at  $t_{C,j}$ .

The weight loss % ( $\Delta w_{C,0-j}$ ) of the cubes for each  $t_{C,i}$  was used to apply a correction to the gravimetry measurements  $w_z$  taken from the twelve plaster plates (P1 to 12) at  $t_z$  ( $z= 0 \dots 38$ ). Such correction was applied to observe the effects of ageing on the weight of the coatings only. The differences in the shape and size of the plates and the cubes (and therefore the different surface area-volume ratio) would have suggested that the rate of weight loss is different between the plates and cubes, but by looking at the plates and cubes gravimetry data, it was possible to assume that the rate is very similar.

As the  $w_{C,j}$  at  $t_{C,j}$  of the cubes has a unique correspondence to the  $w_z$  at  $t_z$  measured on the plates, a point by point correction was applied and calculated as follows:

$$w'_z = w_z - \left(\frac{w_z \cdot \Delta w_{C,0-j}\%}{100}\right) \quad (\text{A8.14})$$

Where  $w'_z$  is the weight of the plate, at time  $t_z$ , after the correction,  $w_z$  is the weight of the plate, at time  $t_z$  without correction and the weight loss % ( $\Delta w_{C,0-j}\%$ ) of the cubes at  $t_{C,j}$  correspondent to  $t_j$ .

As the error for the measured  $w_z$  is given by the resolution of the JJ-BC Series Electronic Analytical Balance and equal to 0.1 mg and the error for  $\Delta w_{C,0-j}\%$  is described in equation A8.13, the error for equation A8.14 is:

$$er_{w'_i} = \sqrt{\left(\frac{100 - \Delta w_{C,0-j}\%}{100} \cdot er_{w_z}\right)^2 + \left(\frac{w_z}{100} \cdot s_{\Delta w_{C,0-j}\%}\right)^2} \quad (\text{A8.15})$$

The data for the gravimetry of the plates were then normalised to the initial value  $w_0$  and 100 by defining:

$$w''_z = \frac{w'_z}{w'_0} \cdot 100 \quad (\text{A8.16})$$

Where  $w'_z = (w'_1 \dots w'_{38})$  and  $w''_z$  is the zth normalised data.

## COLOURIMETRY

For each measurement taken with the spectrophotometer CM-2600d (Konica Minolta) (*Section 5.2.11*) two sets of data were acquired in Specular Component Included (SCI) and Specular Component Excluded (SCE) modes. Three measurements of  $L^*$ ,  $a^*$ ,  $b^*$  (CIELAB 1976 colour space) (Oleari, 1998) and  $R(\lambda)$  ( $\lambda = 360\text{-}740\text{ nm}$ ) for each area analysed were obtained. The spectrophotometer supplier defines the standard deviation  $s$  for spectral reflectance  $R(\lambda)$  and chromatic values  $L^*$ ,  $a^*$ ,  $b^*$  as within 0.1%.

The standard deviation of the measured mean  $L^*$ ,  $a^*$ ,  $b^*$  and  $R(\lambda)$  was calculated and is, for example for  $L^*$ , given by:

$$s_{L^*} = \sqrt{\frac{\sum(L_i^* - \bar{L}^*)^2}{n - 1}} \quad (\text{A8.17})$$

where  $i = 1, 2, 3$ ,  $L^*$  takes on each value in the set,  $\bar{L}^*$  is the average (statistical mean) of the set of values and  $n = 3$  is the number of values. *Equation A8.16* conveniently corresponds to the STDEV.P Excel® Formula to calculate the standard deviation of population, using the "n" method.

The error of the averaged values due to the propagation of the 0.1% instrumental error will be then given, for example for  $L^*$ , by:

$$\text{er}_{\bar{L}^*} = \sqrt{\left(\frac{L_1^* \cdot 0.001}{3}\right)^2 + \left(\frac{L_2^* \cdot 0.001}{3}\right)^2 + \left(\frac{L_3^* \cdot 0.001}{3}\right)^2} \quad (\text{A8.18})$$

The **colour difference  $\Delta E_{ab}^*$  CIELAB 1976**, between two points 1 and 2, is defined by:

$$\Delta E_{ab}^* = \sqrt{(L_1^* - L_2^*)^2 + (a_1^* - a_2^*)^2 + (b_1^* - b_2^*)^2} \quad (\text{A8.19})$$

where the difference is calculated between two colours with coordinates  $(L_1^*, a_1^*, b_1^*)$  and  $(L_2^*, a_2^*, b_2^*)$ .  $L^*$  is the lightness,  $a^*$  defines the red/green value and  $b^*$  the blue/yellow value. Once the error of the mean values of  $L^*$ ,  $a^*$  and  $b^*$  are calculated (*Equation A8.18*), it is also possible to calculate the error of  $\Delta E_{ab}^*$ , which is:

$$\begin{aligned}
 er_{\Delta E_{ab}^*} = & \{ \{ [(L_2^* - L_1^*)^2 + (a_2^* - a_1^*)^2 + (b_2^* - b_1^*)^2]^{-0.5} \cdot (L_2^* - L_1^*) er_{L_2} \}^2 \\
 & + \{ 1 - [(L_2^* - L_1^*)^2 + (a_2^* - a_1^*)^2 + (b_2^* - b_1^*)^2]^{-0.5} \cdot (L_2^* - L_1^*) er_{L_1} \}^2 \\
 & + \{ [(L_2^* - L_1^*)^2 + (a_2^* - a_1^*)^2 + (b_2^* - b_1^*)^2]^{-0.5} \cdot (a_2^* - a_1^*) er_{a_2} \}^2 \\
 & + \{ 1 - [(L_2^* - L_1^*)^2 + (a_2^* - a_1^*)^2 + (b_2^* - b_1^*)^2]^{-0.5} \cdot (a_2^* - a_1^*) er_{a_1} \}^2 \\
 & + \{ [(L_2^* - L_1^*)^2 + (a_2^* - a_1^*)^2 + (b_2^* - b_1^*)^2]^{-0.5} \cdot (b_2^* - b_1^*) er_{b_2} \}^2 \\
 & + \{ 1 - [(L_2^* - L_1^*)^2 + (a_2^* - a_1^*)^2 + (b_2^* - b_1^*)^2]^{-0.5} \cdot (b_2^* - b_1^*) er_{b_1} \}^2 \}^{0.5}
 \end{aligned} \tag{A8.20}$$

Equations A8.19 and A8.20 were applied to evaluate the differences of colour and errors on the plaster surfaces before (UA) and after (A) accelerated ageing.

The **colour difference CIEDE2000,  $\Delta E_{00}$** , (Oleari, 1998) is defined by the coordinates ( $L'$ ,  $a'$ ,  $b'$ ,  $C'$ ,  $h'$ ) that can be calculated from the CIELAB coordinates as follows:

$$L' = L^* \tag{A8.21}$$

$$a' = (1 + G)a^* \quad \text{where} \quad G = 0.5 \left( 1 - \sqrt{\frac{\overline{C_{ab}^*}^7}{\overline{C_{ab}^*}^7 + 25^7}} \right) \tag{A8.22}$$

$$b' = b^* \tag{A8.23}$$

$$C' = \sqrt{a'^2 + b'^2} \tag{A8.24}$$

$$h' = \tan^{-1} \frac{b'}{a'} \tag{A8.25}$$

The errors for  $L'$  and  $b'$  are defined by the error of the mean value of  $L^*$  and  $b^*$  (Equation A8.18). The error of  $C_{ab}^* = \sqrt{a^{*2} + b^{*2}}$  is:

$$er_{C_{ab}^*} = \sqrt{(a \cdot (a^{*2} + b^{*2})^{-0.5} \cdot er_a)^2 + (b \cdot (a^{*2} + b^{*2})^{-0.5} \cdot er_b)^2} \tag{A8.26}$$

$\overline{C_{ab}^*}$  is defined by the mean value of the  $C_{ab}^*$  of the compared set of values (before and after ageing in this work, UA and A) and the error was calculated as:

$$er_{\overline{C_{ab}^*}} = \sqrt{\left( \frac{er_{C_{ab}^*,UA}}{2} \right)^2 + \left( \frac{er_{C_{ab}^*,A}}{2} \right)^2} \tag{A8.27}$$

The standard deviation relevant to Equation A8.22 are:

$$er_G = \sqrt{\left( \frac{7\bar{C}_{ab}^{*-6} \cdot (\bar{C}_{ab}^{*-7} + 6103515625) - 7\bar{C}_{ab}^{*-13}}{2(\bar{C}_{ab}^{*-7} + 6103515625)^2} \cdot \frac{1}{2} \left( \frac{\bar{C}_{ab}^{*-7}}{(\bar{C}_{ab}^{*-7} + 6103515625)} \right)^{-0.5} \cdot er_{\bar{C}_{ab}^*} \right)^2} \quad (\text{A8.28})$$

and

$$er_{a'} = \sqrt{(a^* \cdot er_G)^2 + ((G + 1) \cdot er_{a^*})^2} \quad (\text{A8.29})$$

The error for *Equation A8.24* is calculated similarly to the formula described in *Equation A8.26*. The error of *Equation A8.25* is defined as:

$$er_{h'} = \sqrt{\left( \frac{er_{b'}}{a' \left( \left( \frac{b'}{a'} \right)^2 + 1 \right)} \right)^2 + \left( -er_{a'} \frac{b'}{a'^2 \left( \left( \frac{b'}{a'} \right)^2 + 1 \right)} \right)^2} \quad (\text{A8.30})$$

The colour difference  $\Delta E_{00}$  is equal to:

$$\Delta E_{00} = \sqrt{\left( \frac{\Delta L'}{k_L S_L} \right)^2 + \left( \frac{\Delta C'}{k_C S_C} \right)^2 + \left( \frac{\Delta H'}{k_H S_H} \right)^2 + R_T \left( \frac{\Delta C'}{k_C S_C} \right) \left( \frac{\Delta H'}{k_H S_H} \right)} \quad (\text{A8.31})$$

where

$$S_L = 1 + \frac{0.015(\bar{L}' - 50)^2}{\sqrt{20 + (\bar{L}' - 50)^2}} \quad (\text{A8.32})$$

$$S_C = 1 + 0.045\bar{C}' \quad (\text{A8.33})$$

$$T = 1 - 0.17(\bar{h}' - 30^\circ) + 0.24 \cos(2\bar{h}') + 0.32 \cos(3\bar{h}' + 6^\circ) - 0.20 \cos(4\bar{h}' - 63^\circ) \quad (\text{A8.34})$$

$$S_H = 1 + 0.015\bar{C}'T \quad (\text{A8.35})$$

$$R_C = 2 \sqrt{\frac{\bar{C}'^7}{\bar{C}'^7 + 25^7}} \quad (\text{A8.36})$$

$$\Delta\theta = 30e^{-[(\bar{h}' - 275^\circ)/25]^2} \quad (\text{A8.37})$$

$$R_T = -\sin(2\Delta\theta)R_C \quad (\text{A8.38})$$

$$\Delta L' = L'_A - L'_{UA} \quad (\text{A8.39})$$

$$\Delta C' = C'_A - C'_{UA} \quad (\text{A8.40})$$

$$\Delta h' = h'_A - h'_{UA} \quad (\text{A8.41})$$

$$\Delta H' = 2\sqrt{C'_A \cdot C'_{UA}} \cdot \sin\left(\frac{\Delta h'}{2}\right) \quad (\text{A8.42})$$

$\bar{L}'$ ,  $\bar{C}'$ ,  $\bar{h}'$  are the mean of the values between the compared set of data and the relevant errors are determined similarly as shown in Equation A.27. The errors for Equations A8.31 to A.42 deviations were calculated as follows:

$$er_{S_L} = \sqrt{\left(\frac{(0.03(\bar{L}' - 50)((\bar{L}' - 50)^2 + 20)^{0.5} - 0.015(\bar{L}' - 50)^3((\bar{L}' - 50)^2 + 20)^{-0.5}}{(\bar{L}' - 50)^2 + 20} er_{L'}\right)^2} \quad (\text{A8.43})$$

$$er_{S_C} = \sqrt{(0.045 er_{\bar{C}'})^2} \quad (\text{A8.44})$$

$$er_T = \sqrt{\left(\left(\left(0.17 \cdot \sin(\bar{h}' - 30^\circ)\right) - \left(0.48 \cdot \sin 2\bar{h}'\right) - \left(0.96 \sin(3\bar{h}' + 6^\circ)\right) + \left(0.8 \sin(4\bar{h}' - 63^\circ)\right)\right) \cdot er_{\bar{h}'}}\right)^2} \quad (\text{A8.45})$$

$$er_{S_H} = \sqrt{(0.015T er_{\bar{C}'})^2 + (0.015\bar{C}' er_T)^2} \quad (\text{A8.46})$$

$$er_{R_C} = \sqrt{\left(\frac{7R_T^6 \cdot (R_T^7 + 6103515625) - 7R_T^{13}}{(R_T^7 + 6103515625)^2} \cdot \left(\frac{R_T^7}{(R_T^7 + 6103515625)}\right)^{-0.5} \cdot er_{R_T}\right)^2} \quad (\text{A8.47})$$

$$er_{\Delta\theta} = \sqrt{\left(-\left(60 \cdot \left(\frac{1}{25}\right)^2 \cdot (\bar{h}' - 275) \cdot e^{-[(\bar{h}' - 275^\circ)/25]^2}\right) \cdot er_{\bar{h}'}\right)^2} \quad (\text{A8.48})$$

$$er_{S_H} = \sqrt{(-2R_C \cdot \cos 2\Delta\theta \cdot er_{\Delta\theta})^2 + (-\sin 2\Delta\theta \cdot er_{R_C})^2} \quad (\text{A8.49})$$

$$er_{\Delta L'} = \sqrt{(er_{L'A})^2 + (-er_{L'UA})^2} \quad (\text{A8.50})$$

$$er_{\Delta C'} = \sqrt{(er_{C'A})^2 + (-er_{C'UA})^2} \quad (\text{A8.51})$$

$$er_{\Delta h'} = \sqrt{(er_{h'A})^2 + (er_{h'UA})^2} \quad (\text{A8.52})$$

$$er_{\Delta H'} = \left( \left( C'_{UA} \cdot \sqrt{C'_{A'} \cdot C'_{UA}} \cdot \sin\left(\frac{\Delta h'}{2}\right) \cdot er_{C'A} \right)^2 + \left( C'_{A'} \cdot \sqrt{C'_{A'} \cdot C'_{UA}} \cdot \sin\left(\frac{\Delta h'}{2}\right) \cdot er_{C'UA} \right)^2 + \left( \sqrt{C'_{A'} \cdot C'_{UA}} \cdot \cos\left(\frac{\Delta h'}{2}\right) \cdot er_{\Delta h'} \right)^2 \right)^{0.5} \quad (\text{A8.53})$$

$$er_{\Delta E_{00}} = \left( \left( \frac{\Delta L'}{S_L} \cdot er_{\Delta L'} \cdot \sqrt{\left( \left( \frac{\Delta L'}{S_L} \right)^2 + \left( \frac{\Delta C'}{S_C} \right)^2 + \left( \frac{\Delta H'}{S_H} \right)^2 + \frac{R_T \Delta C' \Delta H'}{S_C S_H} \right)} \right)^2 + \left( -\frac{\Delta L'^2 er_{S_L}}{S_L^3} \cdot \sqrt{\left( \left( \frac{\Delta L'}{S_L} \right)^2 + \left( \frac{\Delta C'}{S_C} \right)^2 + \left( \frac{\Delta H'}{S_H} \right)^2 + \frac{R_T \Delta C' \Delta H'}{S_C S_H} \right)} \right)^2 + \left( \frac{\Delta C' \Delta H' R_T er_{\Delta C'}}{S_C^3 S_H} \cdot \sqrt{\left( \left( \frac{\Delta L'}{S_L} \right)^2 + \left( \frac{\Delta C'}{S_C} \right)^2 + \left( \frac{\Delta H'}{S_H} \right)^2 + \frac{R_T \Delta C' \Delta H'}{S_C S_H} \right)} \right)^2 + \left( -0.5 er_{S_C} \left( \frac{2 \Delta C'^2}{S_C^3} + \frac{R_T \Delta C' \Delta H'}{S_C^2 S_H} \right) \cdot \sqrt{\left( \left( \frac{\Delta L'}{S_L} \right)^2 + \left( \frac{\Delta C'}{S_C} \right)^2 + \left( \frac{\Delta H'}{S_H} \right)^2 + \frac{R_T \Delta C' \Delta H'}{S_C S_H} \right)} \right)^2 + \left( -0.5 er_{\Delta H'} \left( \frac{2 \Delta H'}{S_H^2} + \frac{R_T \Delta C'}{S_C S_H} \right) \cdot \sqrt{\left( \left( \frac{\Delta L'}{S_L} \right)^2 + \left( \frac{\Delta C'}{S_C} \right)^2 + \left( \frac{\Delta H'}{S_H} \right)^2 + \frac{R_T \Delta C' \Delta H'}{S_C S_H} \right)} \right)^2 + \left( -0.5 er_{S_H} \left( \frac{2 \Delta H'^2}{S_H^3} + \frac{R_T \Delta C' \Delta H'}{S_H^2 S_C} \right) \cdot \sqrt{\left( \left( \frac{\Delta L'}{S_L} \right)^2 + \left( \frac{\Delta C'}{S_C} \right)^2 + \left( \frac{\Delta H'}{S_H} \right)^2 + \frac{R_T \Delta C' \Delta H'}{S_C S_H} \right)} \right)^2 + \left( \frac{0.5 er_{R_T \Delta C' \Delta H'}}{S_C S_H} \cdot \sqrt{\left( \left( \frac{\Delta L'}{S_L} \right)^2 + \left( \frac{\Delta C'}{S_C} \right)^2 + \left( \frac{\Delta H'}{S_H} \right)^2 + \frac{R_T \Delta C' \Delta H'}{S_C S_H} \right)} \right)^2 \right)^{0.5} \quad (\text{A8.54})$$

The **Yellowness Index for ASTM Method E313** (Oleari, 1998; Steven, 2005), for D65/10°, is calculated from:

$$YI_{E313} = \frac{100(1.3013X - 1.1498Z)}{Y} \quad (\text{A8.55})$$

X, Y and Z are the CIE Tristimulus values. Conversion equations to obtain X, Y, Z values from CIELAB coordinates, are particularly complicated, but several codes for such conversion are available online as provided by spectrophotometers suppliers. The

conversion codes used here are provided by HutchColor (Copyright © 1995 - endoftime HutchColor, LLC).

The **Whiteness Index (CIE 2004)** (Kotwaliwale et al., 2007; Oleari, 1998), for D65/10°, is defined as:

$$WI = Y + 800(0.3138 - x) + 1700(0.3310 - y) \quad (\text{A8.56})$$

where  $x = X/(X+Y+Z)$  and  $y = Y/(X+Y+Z)$ , calculated from the CIE Tristimulus values (Oleari, 1998) and based on the CIE (Y, x, y) coordinates. The WI values were calculated for all the areas of the plates, which were not white enough to provide values falling within the limits of the index validity.

The equations described above for the colour differences  $\Delta E_{ab}^*$  and  $\Delta E_{00}$  and the Yellowness Index 313  $YI_{313}$  and Whiteness Index **WI** values, before and after ageing (UA-A), were similarly applied to the measured areas before and after cleaning (S-C, soiled and cleaned).

## GLOSSIMETRY

After evaluating the gloss with 20/60/85° mode, as described in *Section 5.2.12*, the 85° was selected. Three gloss (85°) measurements were taken from the same sample area with a Rhopoint IQ™ Glossmeter. The mean value was calculated, and its standard deviation  $s$  (for example of spot P1a) was defined as:

$$s_{Gloss_{P1a}} = \sqrt{\frac{\sum (Gloss_{P1a,i} - \overline{Gloss_{P1a}})^2}{n - 1}} \quad (A8.57)$$

The change of gloss at 85° was calculated as the percentage difference between the mean value calculated on the unaged (UA) sample's area and the aged (A) value (in a before/after fashion), as follows:

$$\Delta Gloss \% = \frac{(Gloss_A - Gloss_{UA})}{Gloss_{UA}} \cdot 100 \quad (A8.58)$$

And the error was defined as:

$$er_{\Delta Gloss \%} = \sqrt{\left(\frac{100}{Gloss_{UA}} \cdot s_{Gloss_A}\right)^2 + \left[\left(-\frac{Gloss_A}{Gloss_{UA}^2} \cdot 100\right) \cdot s_{Gloss_{UA}}\right]^2} \quad (A8.59)$$

The change of gloss at 85° was also calculated as the percentage difference between the mean value calculated on the soiled (S) sample's area and the cleaned (C) value (in a before/after fashion), as follows:

$$\Delta Gloss \% = \frac{(Gloss_C - Gloss_S)}{Gloss_S} \cdot 100 \quad (A8.60)$$

And the error was defined as:

$$s_{\Delta Gloss \%} = \sqrt{\left(\frac{100}{Gloss_S} \cdot s_{Gloss_C}\right)^2 + \left[\left(-\frac{Gloss_C}{Gloss_S^2} \cdot 100\right) \cdot s_{Gloss_S}\right]^2} \quad (A8.61)$$

## REFERENCES

- Abdel-Baset, M., Zhou, Y., & Hezam, I. (2019). Use of a sine cosine algorithm combined with Simpson method for numerical integration. *International Journal of Mathematics in Operational Research*, 14(3), 307–318.  
<http://dx.doi.org/10.1504/IJMOR.2019.099381>
- Cassar, M. (1994). *Museums environment energy*. Her Majesty's Stationery Office. ISBN-13: 978-0112905196
- Clenshaw, C. W., & Curtis, A. R. (1960). A method for numerical integration on an automatic computer. *Numerische Mathematik*, 2(1), 197–205.  
<https://doi.org/10.1007/BF01386223>
- Erhardt, D., & Mecklenburg, M. F. (1995). Accelerated vs natural aging: Effect of aging conditions on the aging process of cellulose. *MRS Online Proceedings Library Archive*, 352.
- Feller, R. L. (1994). *Accelerating aging—photochemical and thermal aspects*. The Getty Conservation Institute. Los Angeles: Getty Publications.
- Hudson-Lamb, D. L., Strydom, C. A., & Potgieter, J. H. (1996). The thermal dehydration of natural gypsum and pure calcium sulphate dihydrate (gypsum). *Thermochimica Acta*, 282, 483–492.
- Jelle, B. P. (2012). Accelerated climate ageing of building materials, components and structures in the laboratory. *Journal of Materials Science*, 47(18), 6475–6496.
- Kotwaliwale, N., Bakane, P., & Verma, A. (2007). Changes in textural and optical properties of oyster mushroom during hot air drying. *Journal of Food Engineering*, 78(4), 1207–1211.
- McKeen, L. W. (2015). *Fluorinated coatings and finishes handbook: The definitive user's guide*. William Andrew.
- Mills, J., & White, R. (2012). *Organic chemistry of museum objects*. Routledge.
- Moropoulou, A., Bakolas, A., & Bisbikou, K. (1995). Characterization of ancient, byzantine and later historic mortars by thermal and X-ray diffraction techniques. *Thermochimica Acta*, 269, 779–795.
- Nelson, W. B. (2009). *Accelerated testing: statistical models, test plans, and data analysis* (Vol. 344). John Wiley & Sons.
- Oleari, C. (1998). *Misurare il colore: spettrofotometria, fotometria e colorimetria: fisiologia e percezione*. Milano: Hoepli Editore. ISBN: 9788820341268
- Popescu, C.-M., Lisa, G., Manoliu, A., Gradinariu, P., & Vasile, C. (2010). Thermogravimetric analysis of fungus-degraded lime wood. *Carbohydrate Polymers*, 80(1), 78–83.
- Quill, J., Fedor, G., Brennan, P., & Everett, E. (2004). Quantifying the indoor light environment: testing for light stability in retail and residential environments. *NIP & Digital Fabrication Conference, 2004(2)*, 689–698.
- Risdonne, V., & Theodorakopoulos, C. (2021). *Database of results. Materials and techniques for coating of the nineteenth-century plaster casts. A scientific and archival investigation of the Victoria & Albert Museum cast collection*. Northumbria University. <https://doi.org/https://doi.org/10.25398/rd.northumbria.14053985>

- Roduit, B., & Odlyha, M. (2006). Prediction of thermal stability of fresh and aged parchment. *Journal of thermal analysis and calorimetry*, 85(1), 157-164.  
<https://doi.org/10.1007/s10973-005-7410-4>
- Schulman, Y. (2020). *Advanced Thermal Analysis of Phase Change Materials - Three Organic Waxes using Modulated TGA and Modulated DSC*.  
<https://www.tainstruments.com/pdf/literature/TA406.pdf>
- Steven, H. (2005). White gold alloys: Colour measurement and grading. *Gold Bulletin*, 38(2), 55–67.
- Symoniuk, E., Ratusz, K., & Krygier, K. (2016). Comparison of the oxidative stability of linseed (*Linum usitatissimum* L.) oil by pressure differential scanning calorimetry and Rancimat measurements. *Journal of Food Science and Technology*, 53(11), 3986–3995.
- Thomson, G. (2013). *The museum environment*. Amsterdam: Elsevier. ISBN: 9781483102719

## APPENDIX 9. ADDITIONAL TABLES AND FIGURES

### X-RAY DIFFRACTION ANALYSIS

Table A9.1. XRD peaks ( $2\theta$ , °) of the plaster samples analysed for this study and relevant references R040029 and R060509 from the RRUFF database.

$2\theta$ [°]												
REPRO.1873-380_2	REPRO.1873-380_3	REPRO.1873-561_1	REPRO.1874-29_1	REPRO.1874-45_1	REPRO.1875-16_1	REPRO.1875-17_2	REPRO.1890-80_2	REPRO.A.1916-3152_1	REPRO.1865-56_1	REPRO.1865-57_1	R040029	R060509
11.63	11.67	11.59	11.59	11.63	11.64	11.63	11.63		11.62	11.60	11.66	11.69
20.69	20.75	20.69	20.67	20.77	20.82	20.71	20.75		20.74	20.69	20.77	20.79
23.38	23.37	23.36	23.35						23.43			
26.87												
29.12	29.11	29.06	29.04	29.13	29.18	29.09	29.10	29.34	28.11	29.07	28.15	28.16
31.10	31.12	31.06	31.05	31.16	31.21	31.10	31.10	31.39	29.14		29.14	29.16
	32.09	32.07		32.15					31.11			
33.46	33.35	33.32	33.30	33.47	33.48	33.32	33.36	33.62	32.10			
	34.54								33.36	33.32		
	35.94	35.91	35.94	36.04					34.57	34.55	34.62	
	36.66	36.58							36.01		36.00	36.01
	37.34								36.65		36.65	
40.57	40.63	40.59	40.59	40.71	40.74		40.64		37.32		37.41	37.42
43.47	43.38	43.30	43.28	43.49		43.58	43.31		40.63		42.21	
								43.65	43.39			
	44.16	44.14							43.64		44.23	
45.83	45.52								44.16		45.53	45.55
	46.49										46.46	
47.87	47.86	47.81	47.79	47.94	47.96		47.82		47.82	47.91	47.88	47.90
	48.36	48.34	48.33	48.45	48.47		48.34		48.36		48.40	48.42
	48.73	48.74										
	50.33	50.29	50.24	50.31	50.44		50.34		50.36			
	50.73	50.75		50.89					50.74			
	51.34	51.31	51.31				51.37		51.39			
	54.41					54.00			54.43		54.47	
	55.15	55.12	55.09			55.08			55.14		55.19	55.22
	55.81			55.91					55.85		55.86	
56.68	56.73	56.67	56.71	56.76	56.86				56.77			
58.21	58.19					57.57					60.36	
	64.75									64.20		
	65.82											
	66.73										66.71	
67.02												
68.95	68.67	68.61	68.80									
	70.66											
71.47	71.23						71.78					
	74.12											
	76.57											
	77.40											
	79.61											

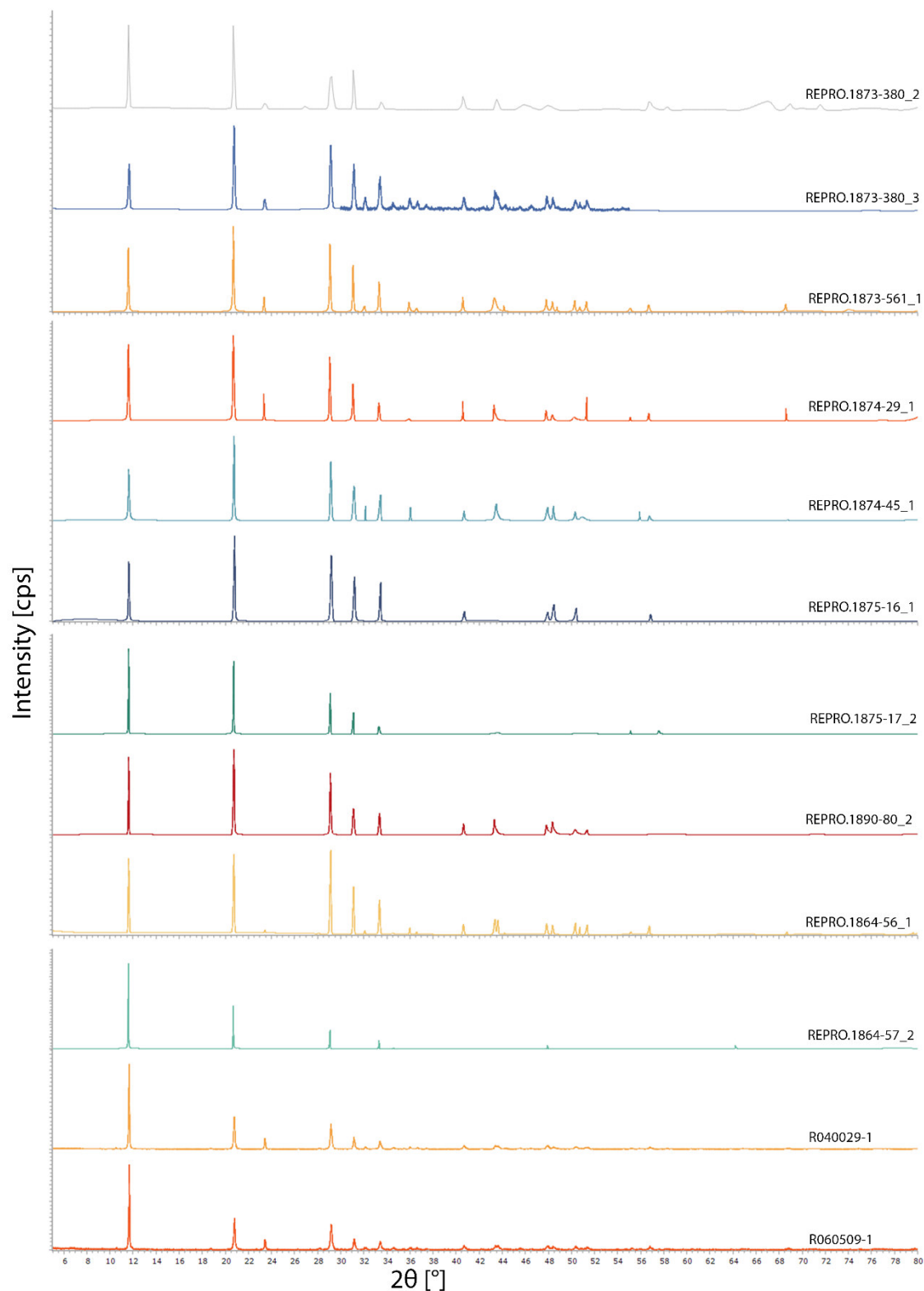


Figure A9.1. XRD diffractograms of samples analysed for this study showed that, despite a few additional peaks that can be seen in some samples, the pattern of gypsum plaster is consistently present. The relevant peaks are provided in Table A9.1. The diffractograms were compared to the references in the databases (Gražulis et al., 2009; Lafuente et al., 2016), for example, R040029 and R060509 from the RRUFF database.

## CROSS-SECTION IMAGES OF AREAS OF REPAIR

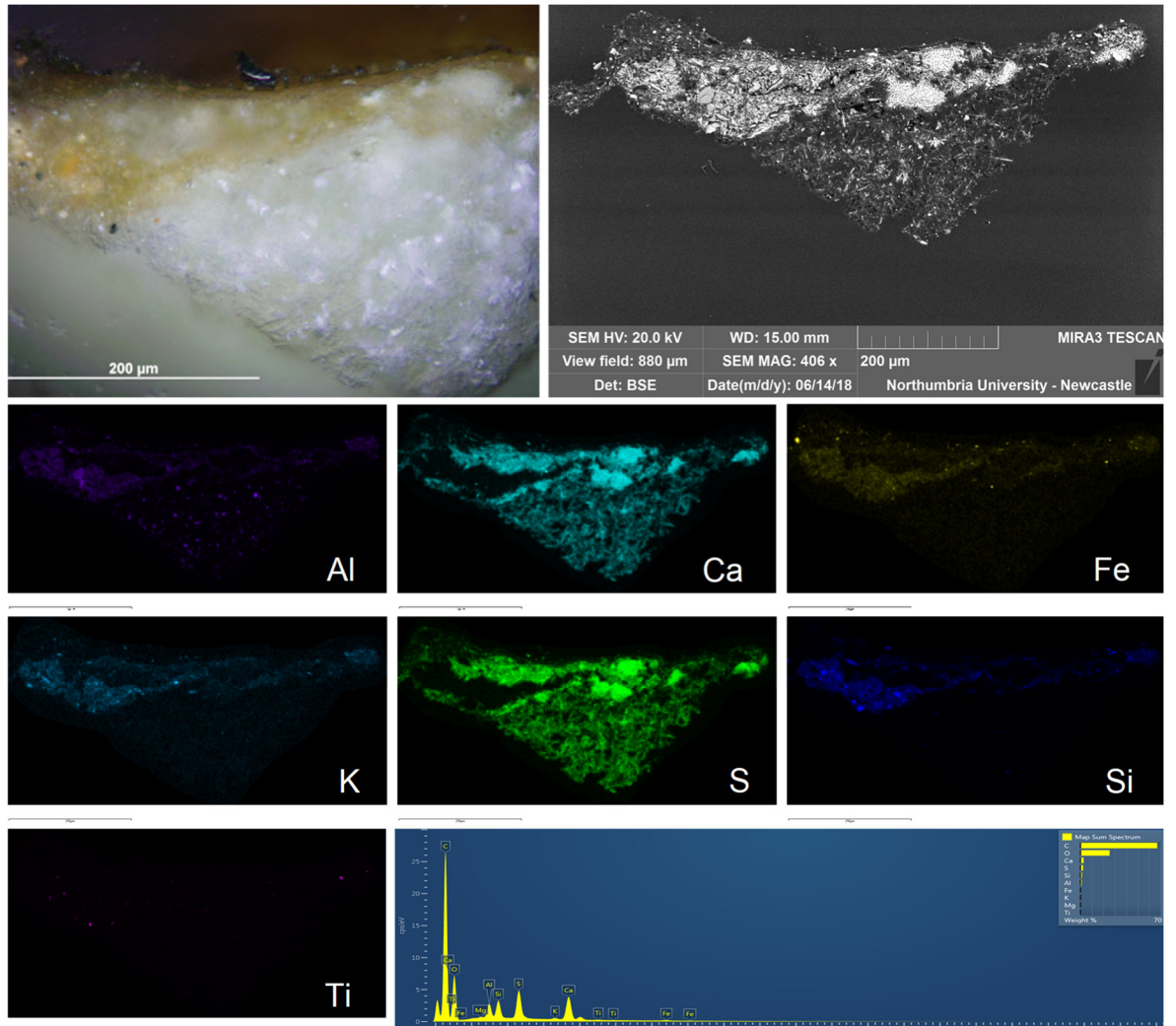


Figure A9.2. REPRO.1873-380\_6. VLR OM (top left) and BSE (top right) images. EDS mapping (bottom) showing aluminium (Al), calcium (Ca), iron (Fe), potassium (K), sulfur(S), silicon (Si) and titanium (Ti). EDS spectrum (bottom right).

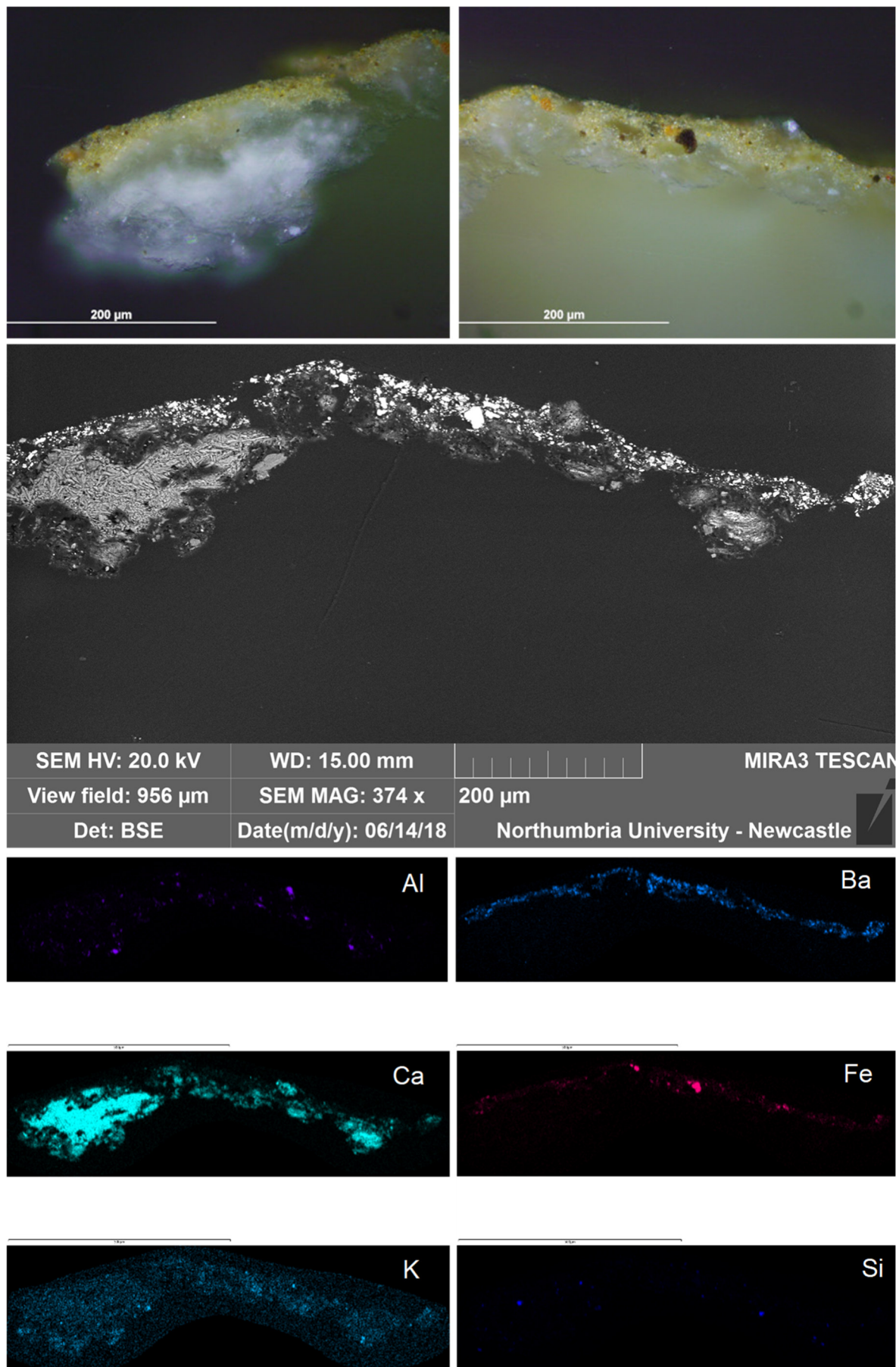


Figure A9.3. REPRO.1873-380\_7. VLR OM (top) and BSE (middle) images. EDS mapping (bottom) showing aluminium (Al), barium (Ba), calcium (Ca), iron (Fe), potassium (K) and silicon (Si).

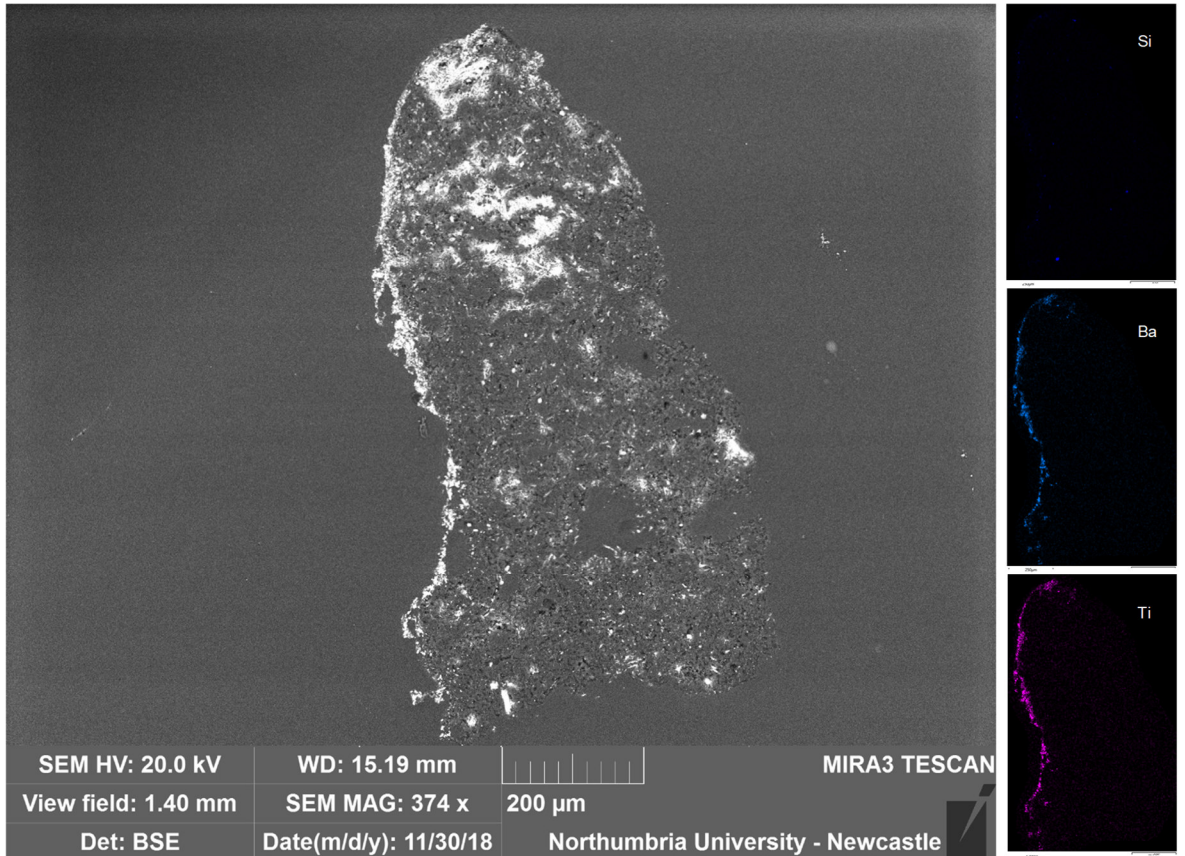


Figure A9.4. REPRO.1873-561\_6. BSE (left) image and EDS mapping (right) showing silicon (Si), barium (Ba) and titanium (Ti).

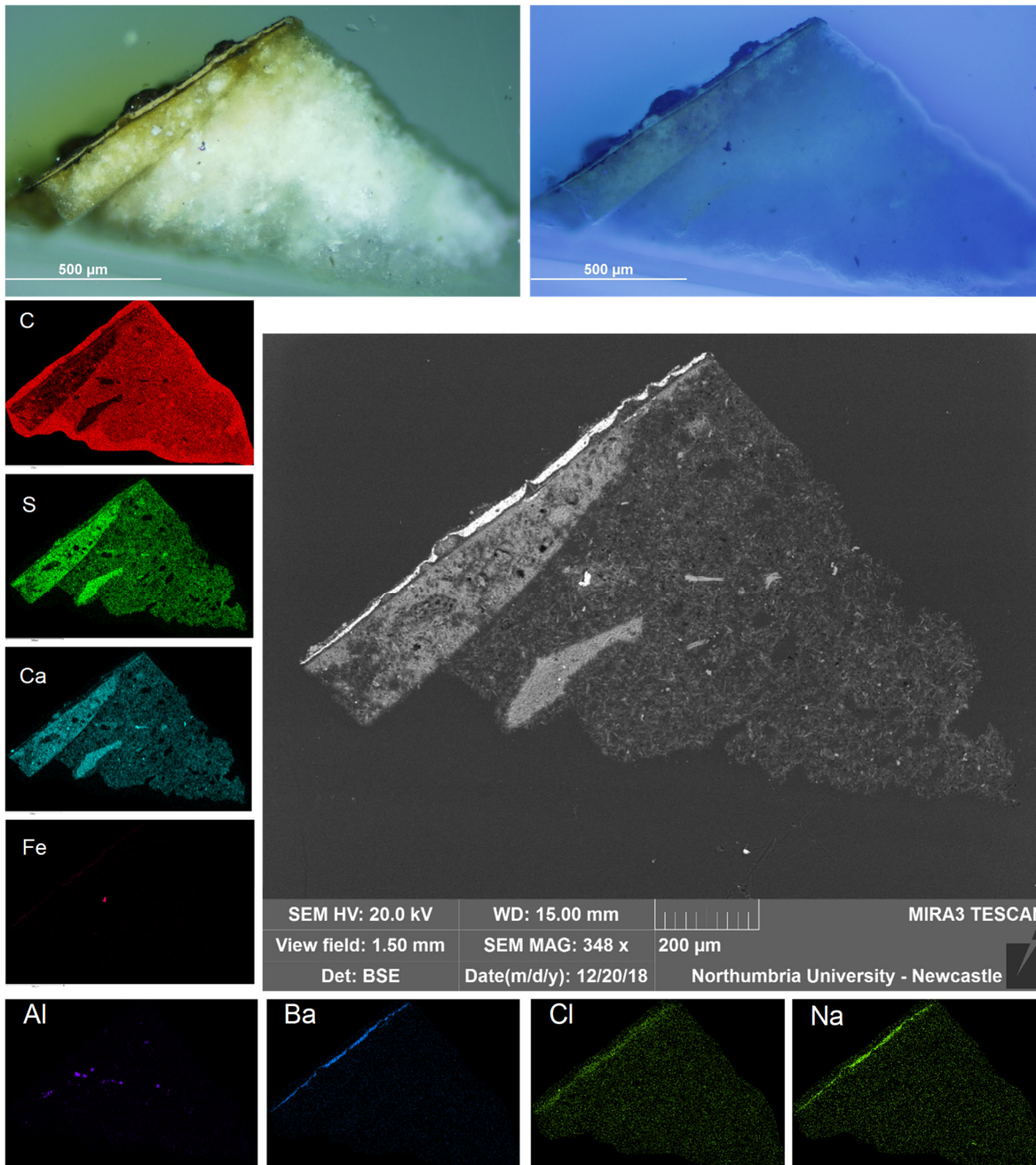


Figure A9.5. REPRO.1875-16\_1. VLR (top left) and UVf (top right) OM and BSE (centre) images. EDS mapping (left and bottom) showing carbon (C), sulfur (S), calcium (Ca), iron (Fe), aluminium (Al), barium (Ba), chlorine (Cl) and sodium (Na).

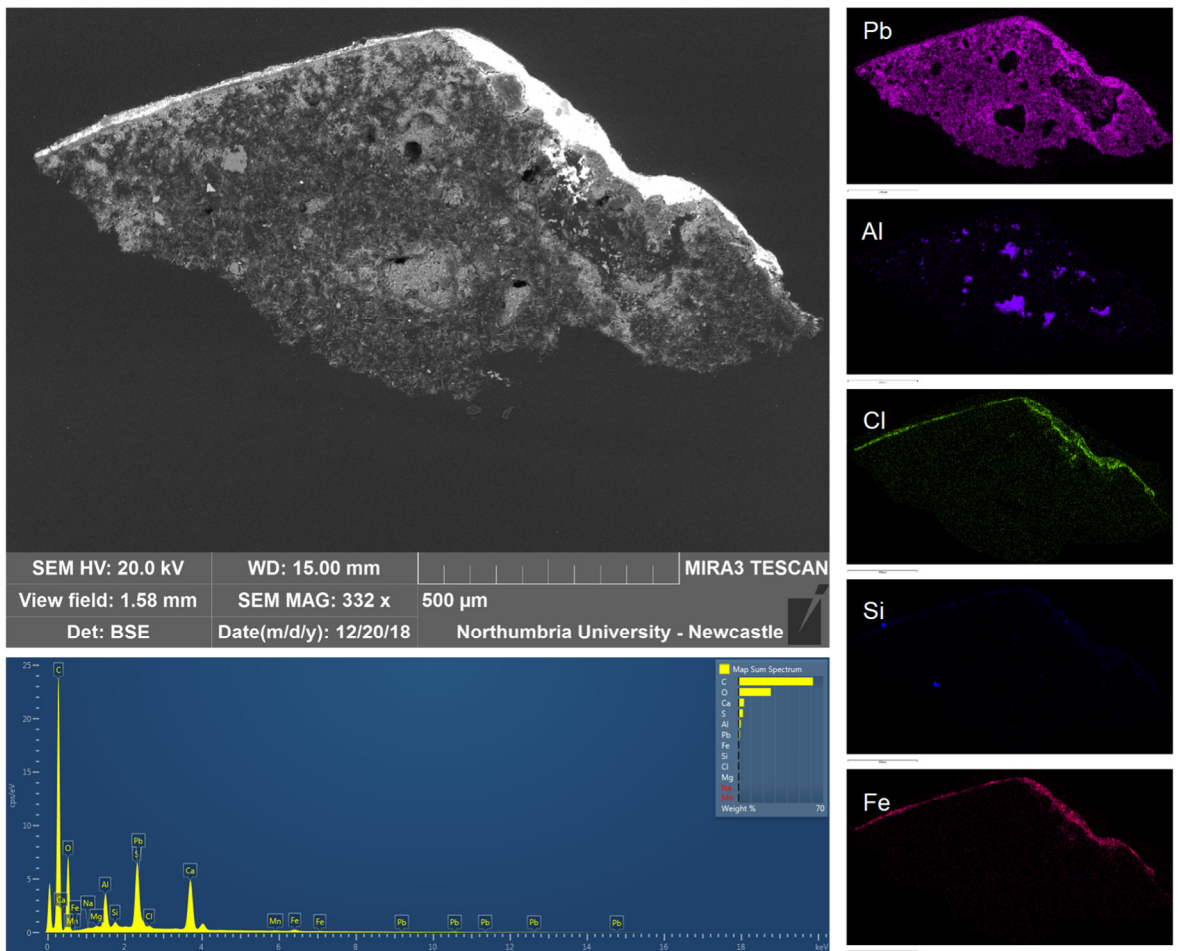


Figure A9.6. REPRO.1875-17\_2. BSE (top left) image, EDS spectrum (bottom left) and EDS mapping (right) showing lead (Pb), aluminium (Al), chlorine (Cl), silicon (Si) and iron (Fe).

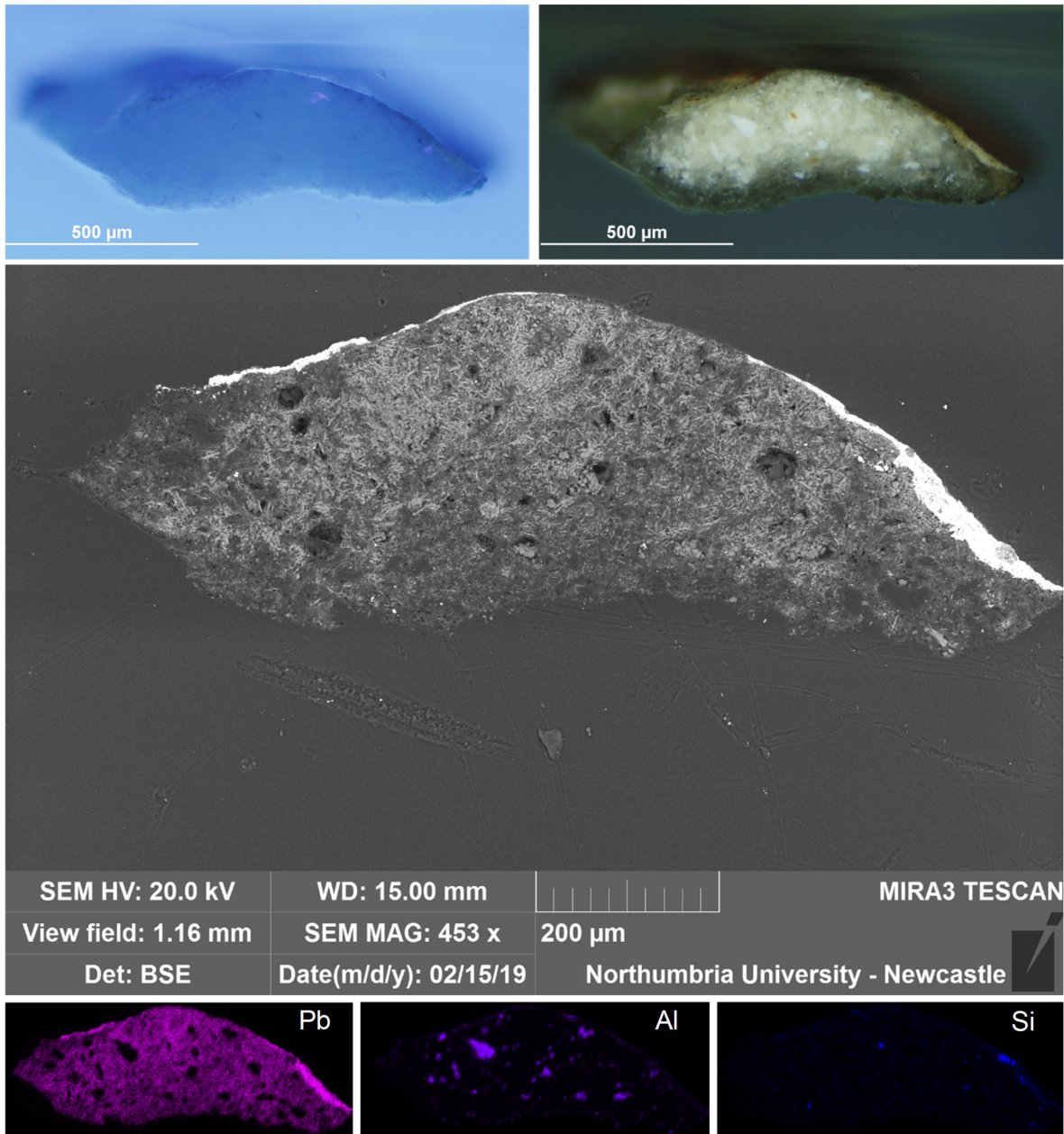


Figure A9.7. REPRO.A.1916-3152\_1. VLR (top left) and UVf (top right) OM and BSE (centre) images. EDS mapping (bottom) showing lead (Pb), aluminium (Al) and silicon (Si).

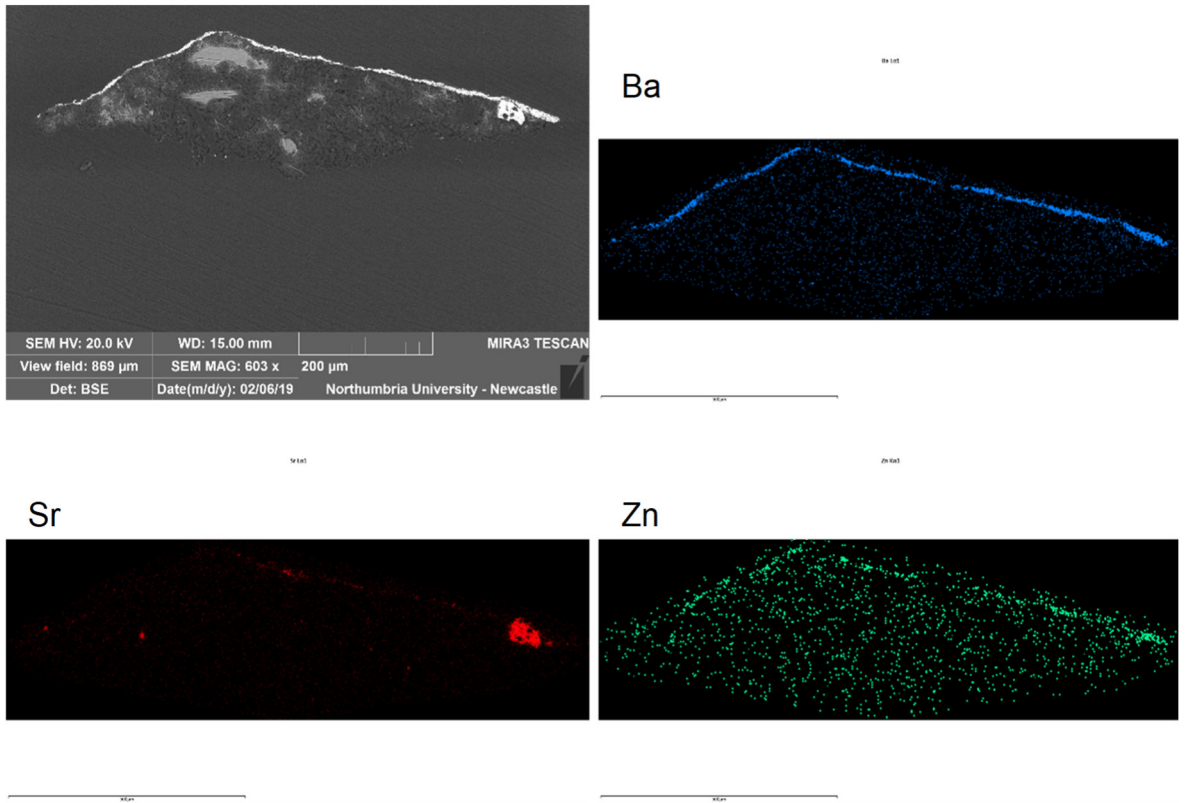


Figure A9.8. REPRO.1864-56\_1. BSE image (top left) and EDS mapping (top right and bottom) showing barium (Ba), strontium (Sr) and zinc (Zn).

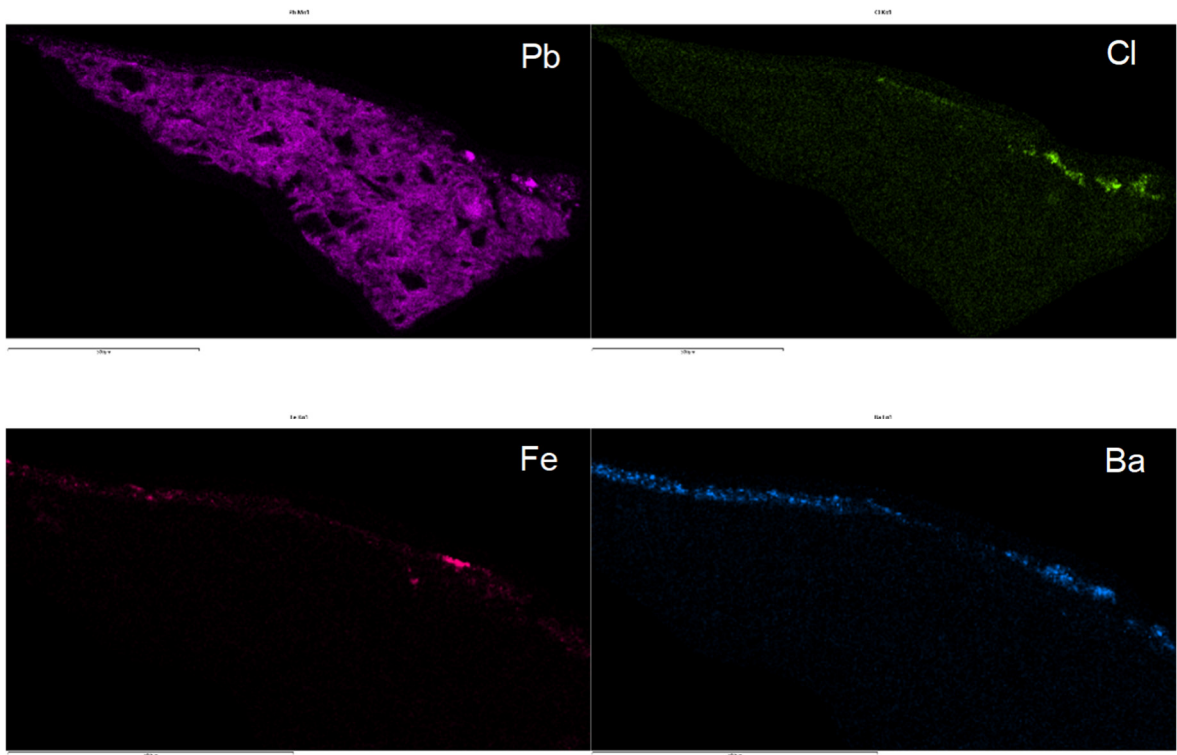
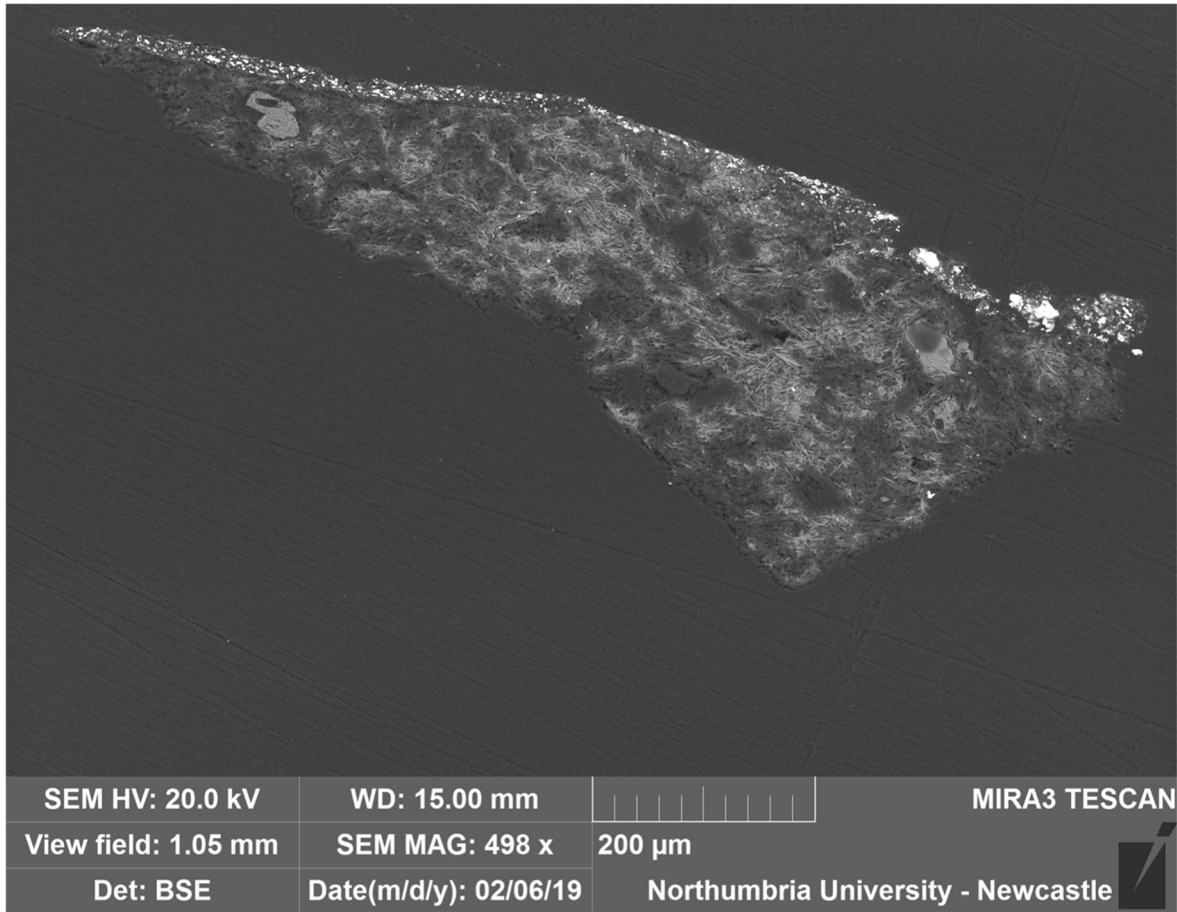


Figure A9.9. REPRO.1864-56\_2. BSE image (top) and EDS mapping (bottom) showing lead (Pb), chlorine (Cl), iron (Fe) and barium (Ba).

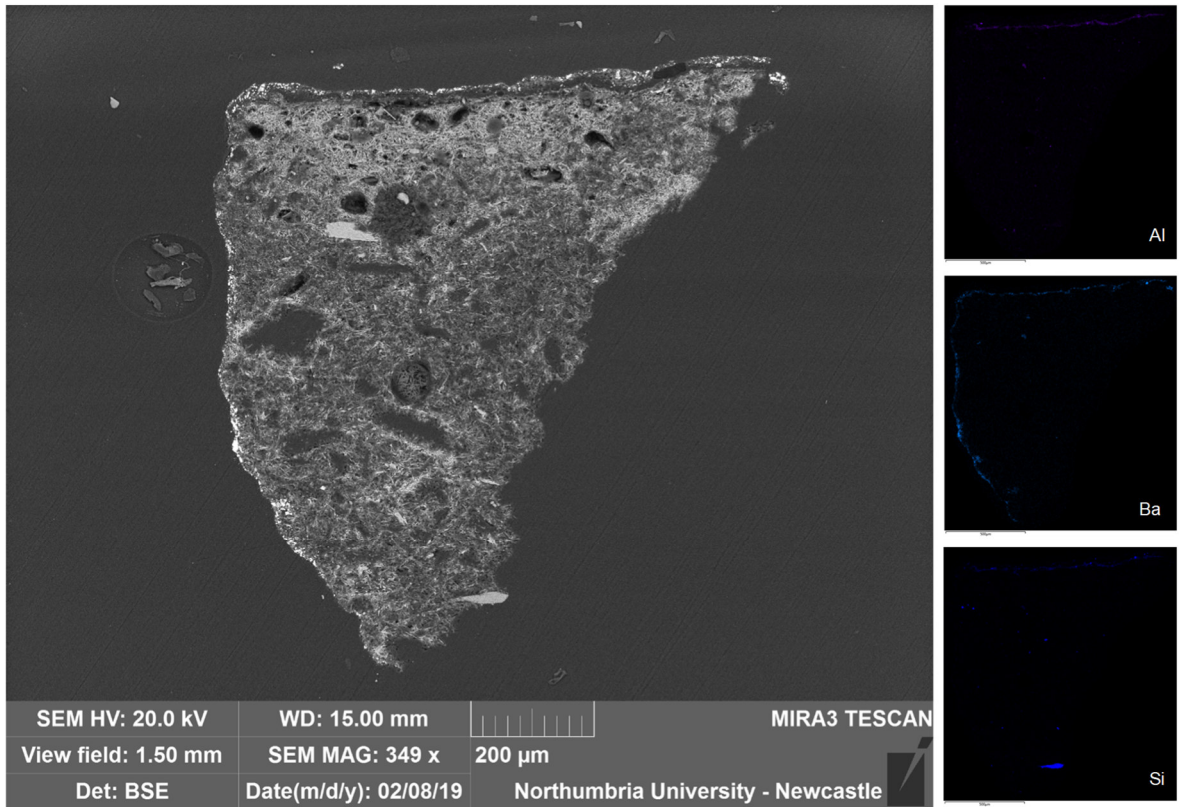
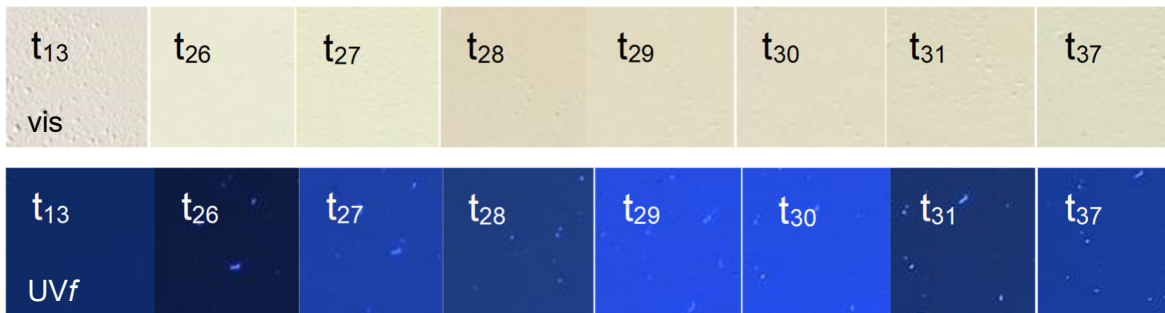


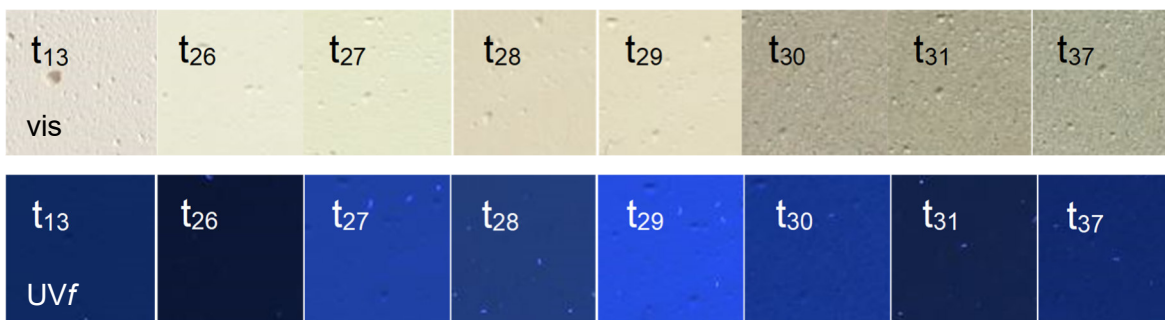
Figure A9.10. REPRO.1864-57\_1. BSE image (left) and EDS mapping (right) showing aluminium (Al), barium (Ba) and silicon (Si).

## COATED PLASTER SURFACES AGEING AND CLEANING

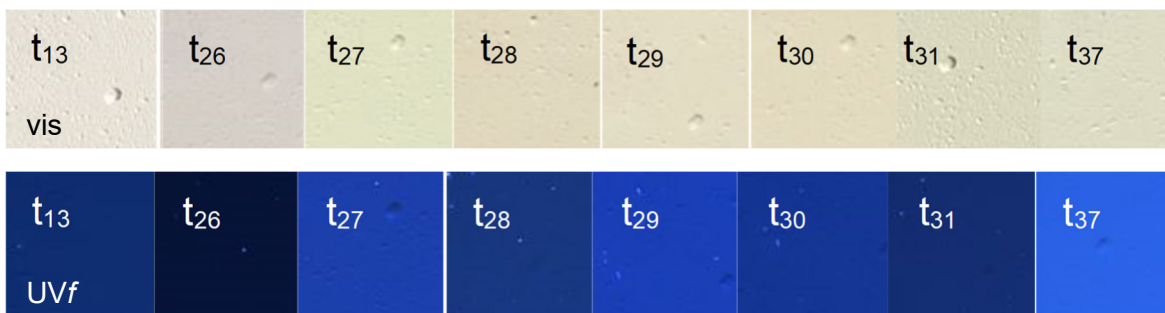
*P1d*



*P1a*



*P3d*



*P3a*

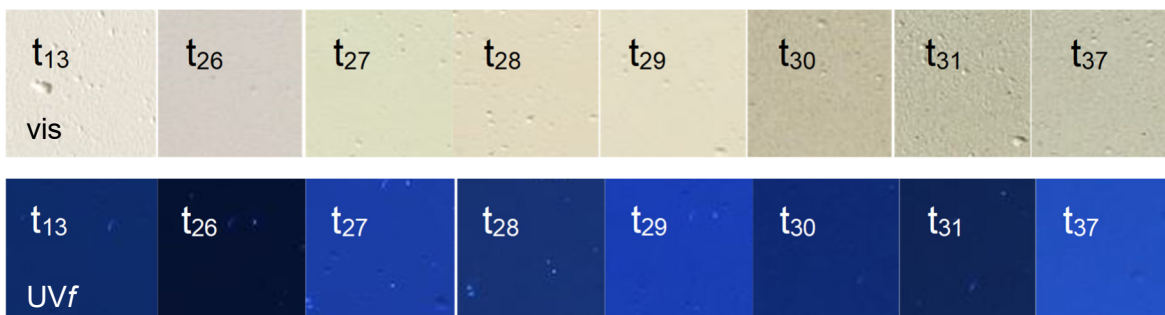
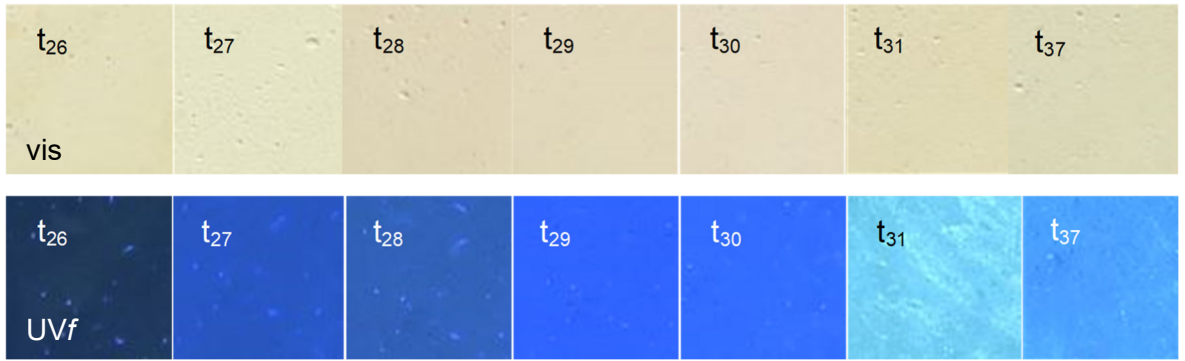
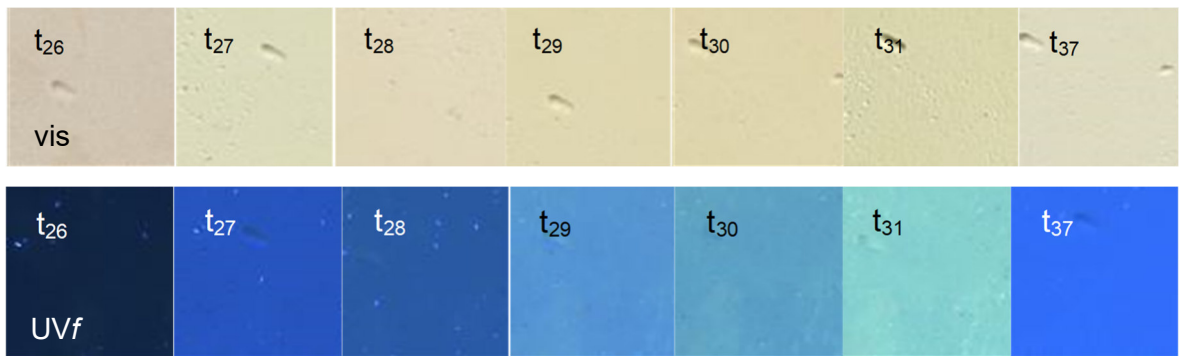


Figure A9.11. Vis and UVf images of control sections P1d (US, UA), P1d (S, UA) P3d (US, A) and P3d (S, A) from t<sub>13</sub> to t<sub>37</sub>. Each square corresponds approximately to a 1x1 cm portion of the section.

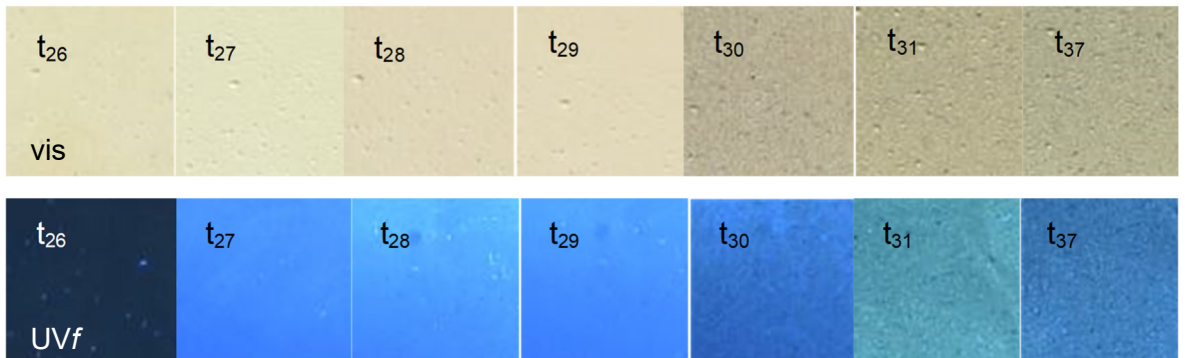
P1e



P3e



P1b



P3b

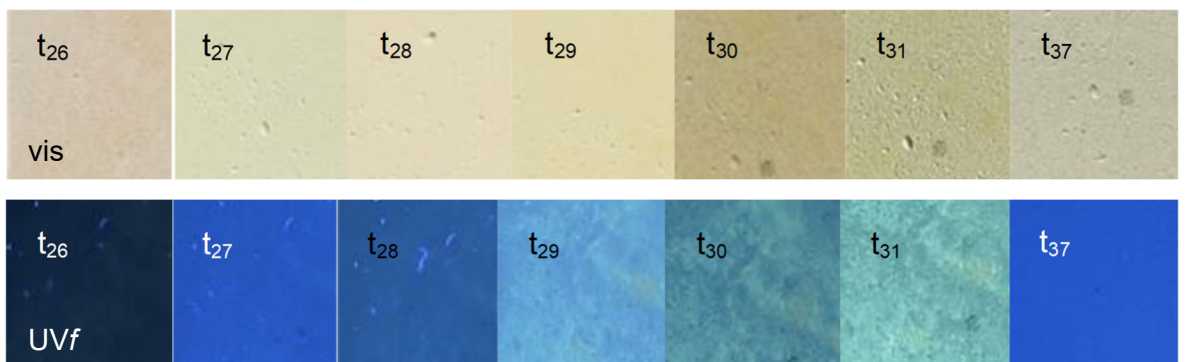
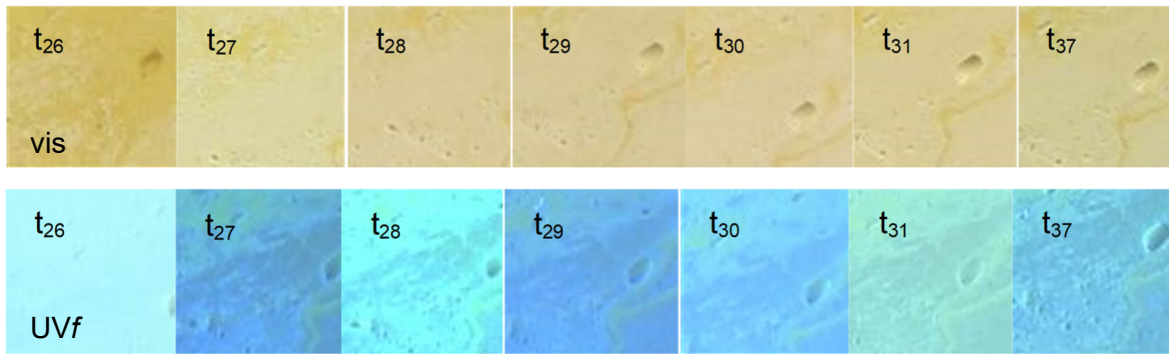
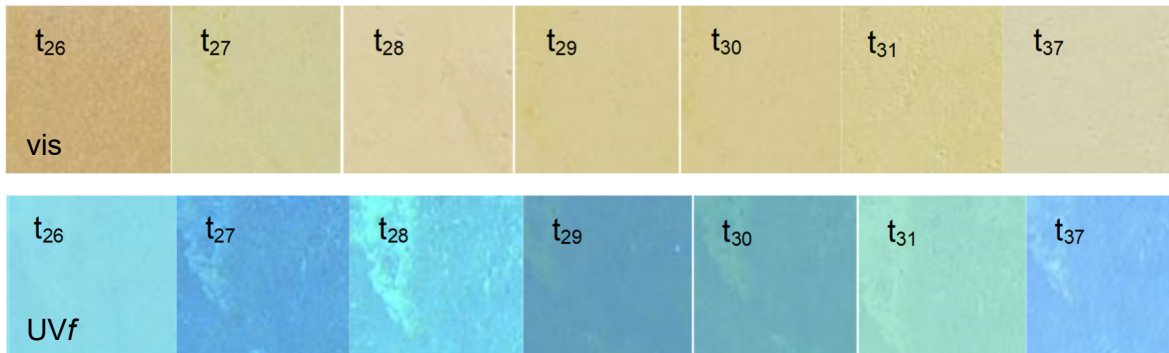


Figure A9.22. Vis and UVf images cold-pressed linseed oil (1-1) coated plates, sections P1e and P3e (US, UA and A) and P1b and P3b (S, UA and A) from t<sub>26</sub> to t<sub>37</sub>. Each square corresponds approximately to a 1x1 cm portion of the section.

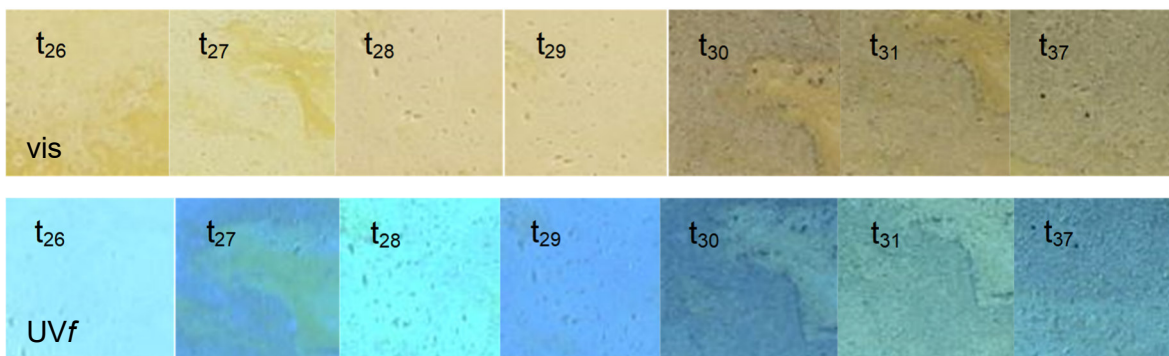
P1f



P3f



P1c



P3c

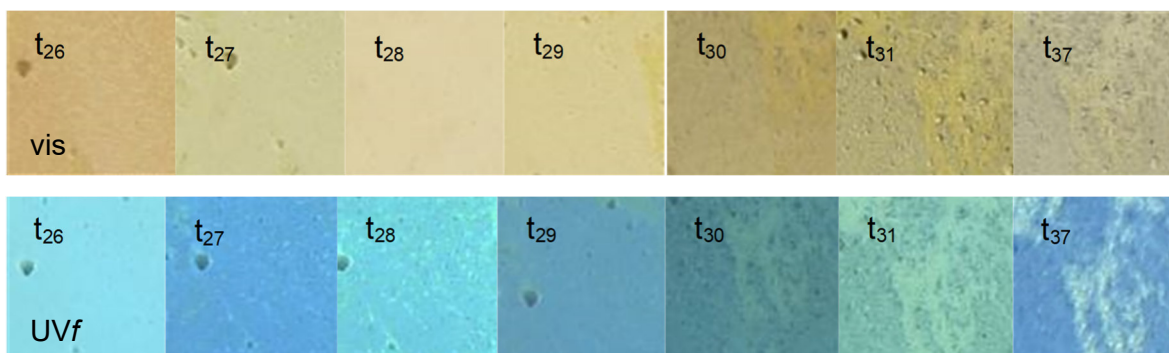
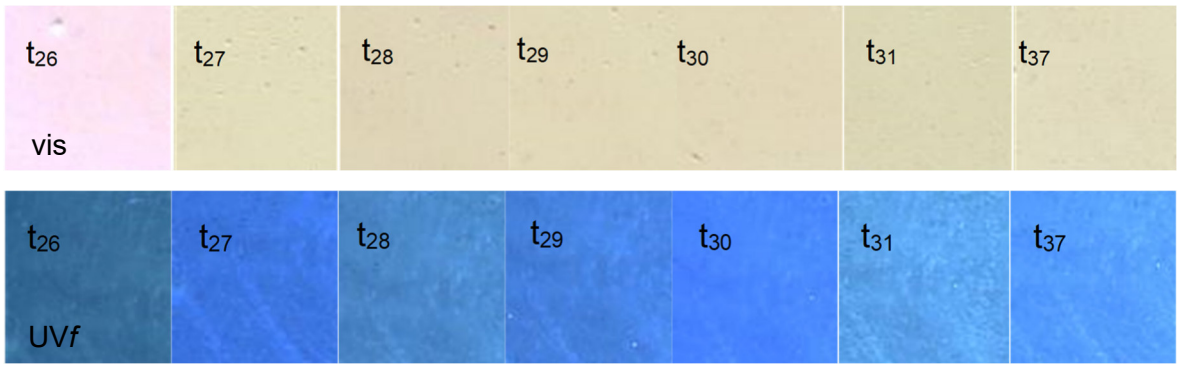
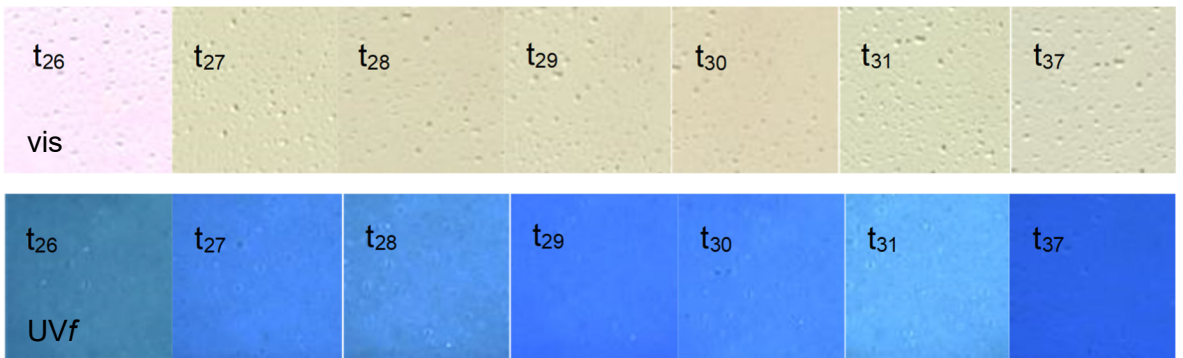


Figure A9.33. Vis and UVf images boiled linseed oil (1-2) coated plates, sections P1f and P3f (US, UA and A) and P1c and P3c (S, UA and A) from t<sub>26</sub> to t<sub>37</sub>. Each square corresponds approximately to a 1x1 cm portion of the section.

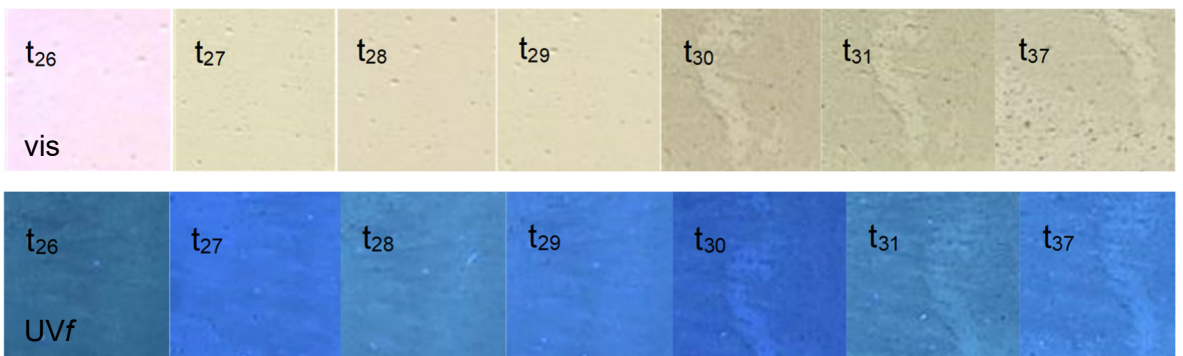
P5e



P7e



P5b



P7b

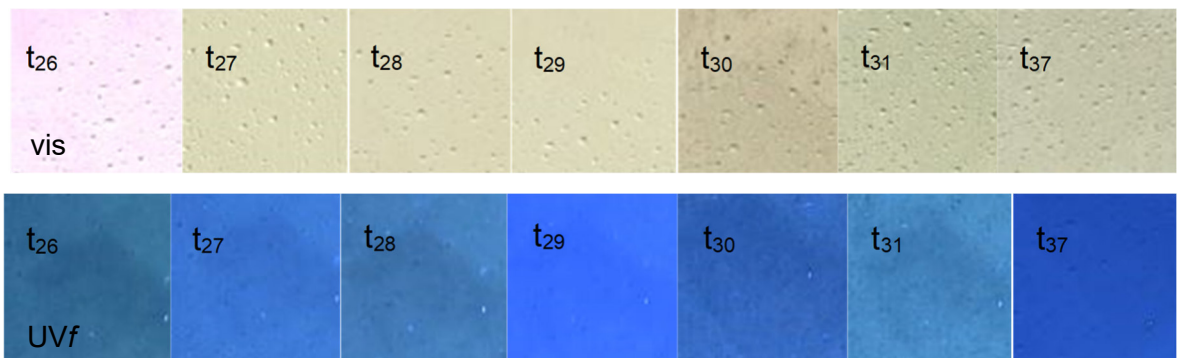
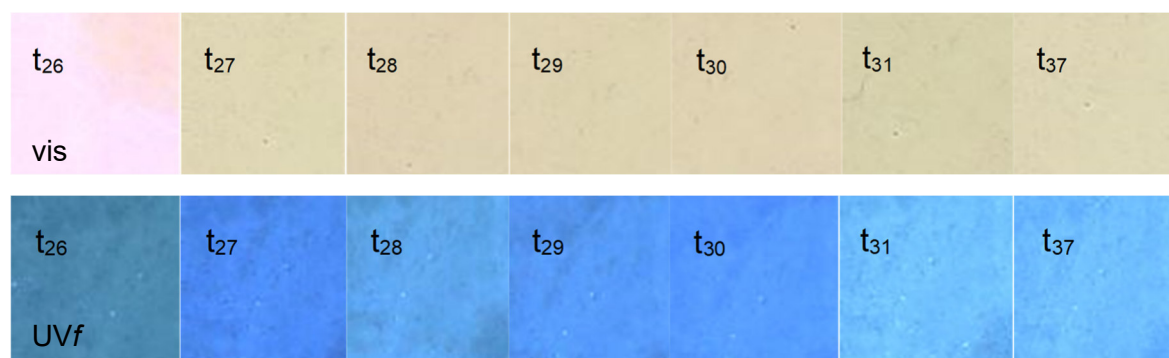
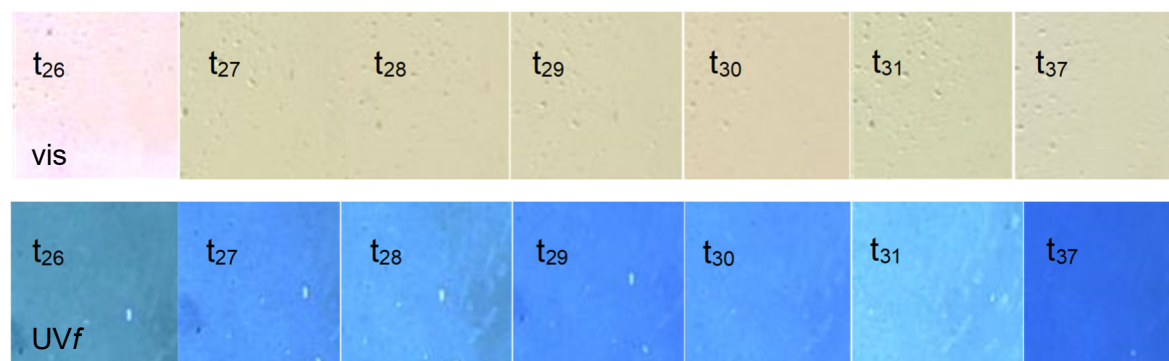


Figure A9.14. Visible and UVf images shellac6% (2-1) coated plates, sections P5e and P7e (US, UA and A) and P5b and P7b (S, UA and A) from t<sub>26</sub> to t<sub>37</sub>. Each square corresponds approximately to a 1x1 cm portion of the section.

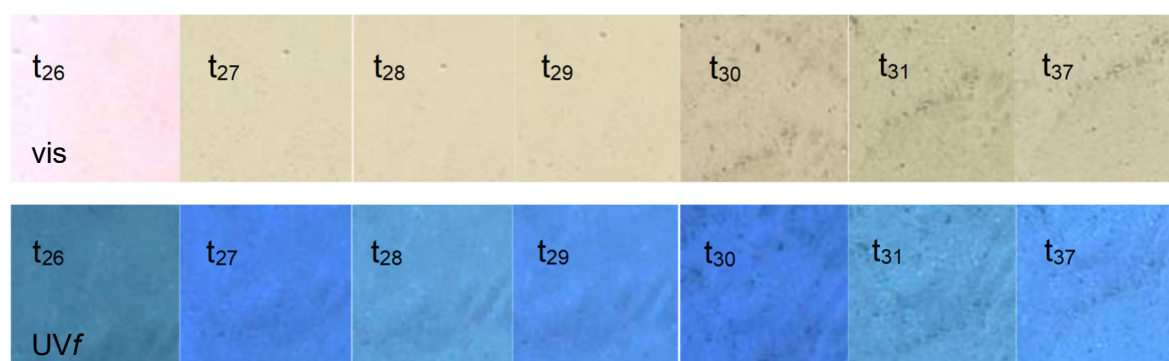
P5f



P7f



P5c



P7c

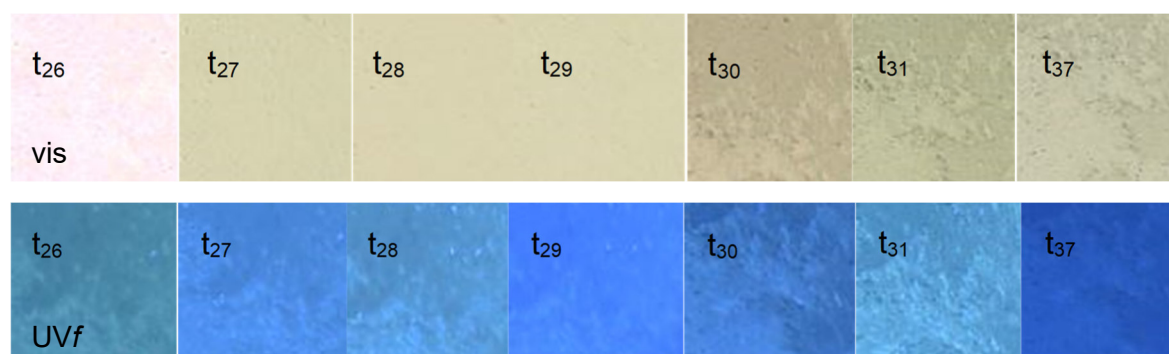
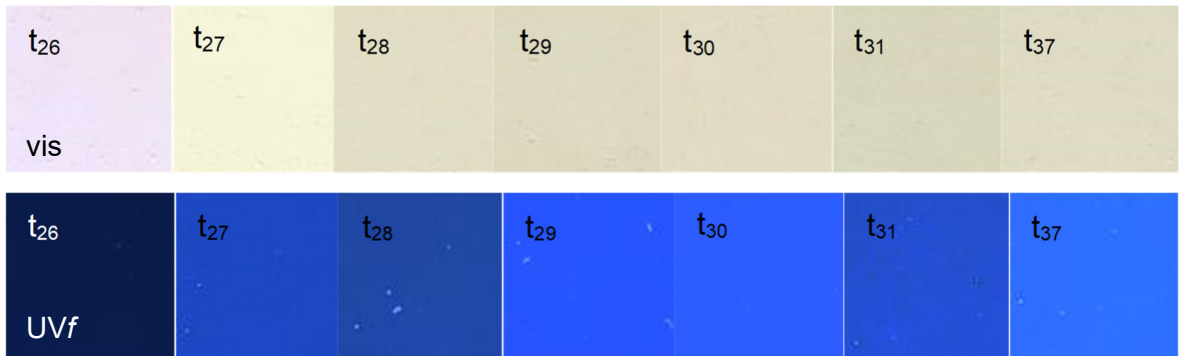
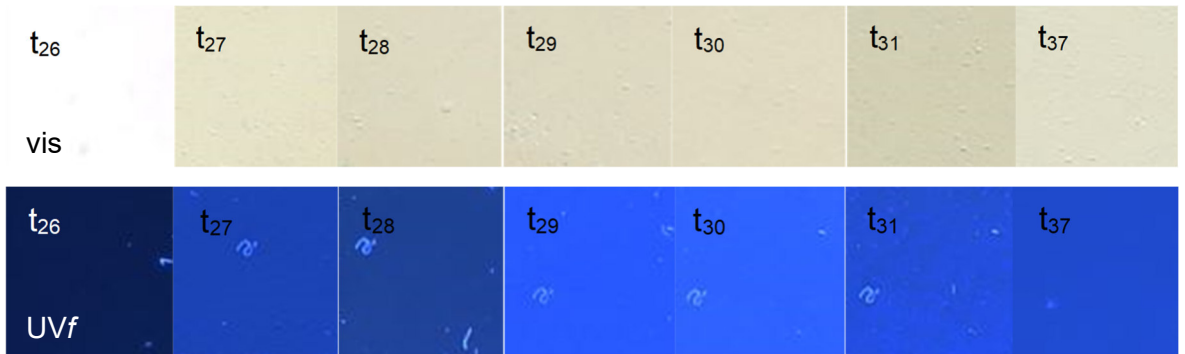


Figure A9.15. Visible and UVf images shellac18% (2-2) coated plates, sections P5f and P7f (US, UA and A) and P5c and P7c (S, UA and A) from t<sub>26</sub> to t<sub>37</sub>. Each square corresponds approximately to a 1x1 cm portion of the section.

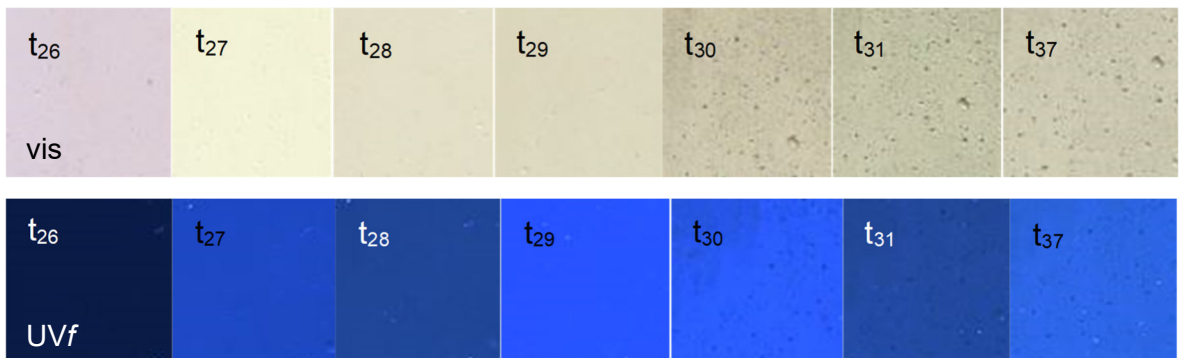
P9e



P11e



P9b



P11b

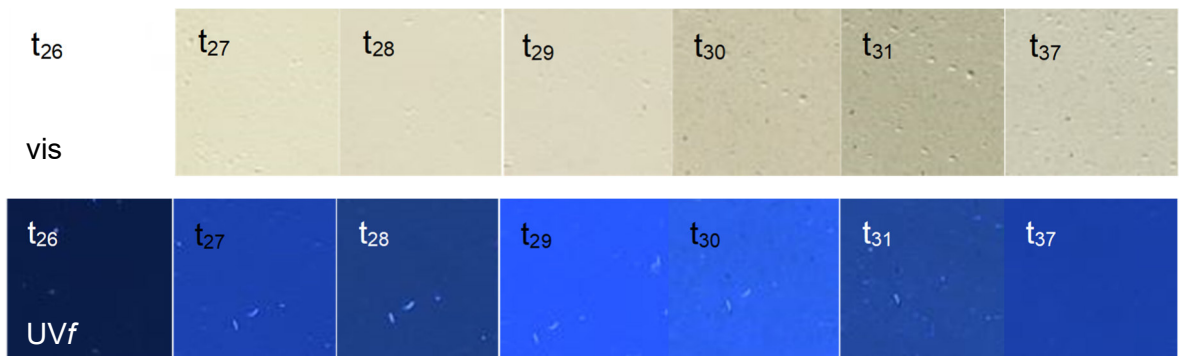
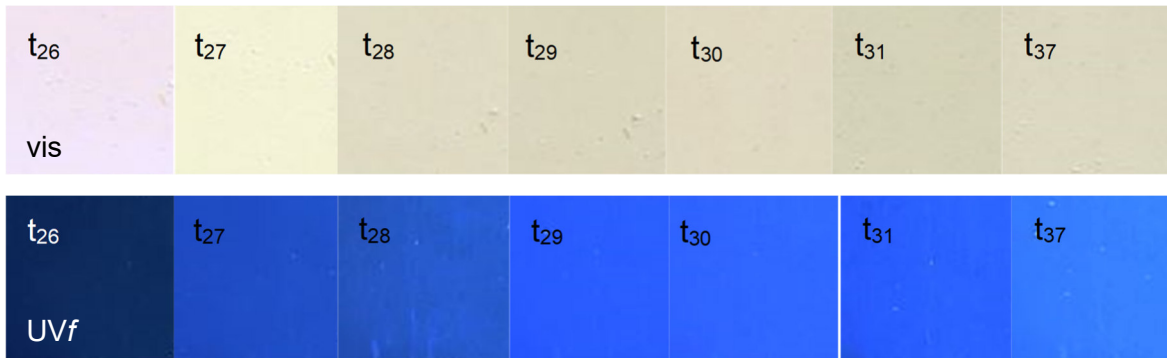
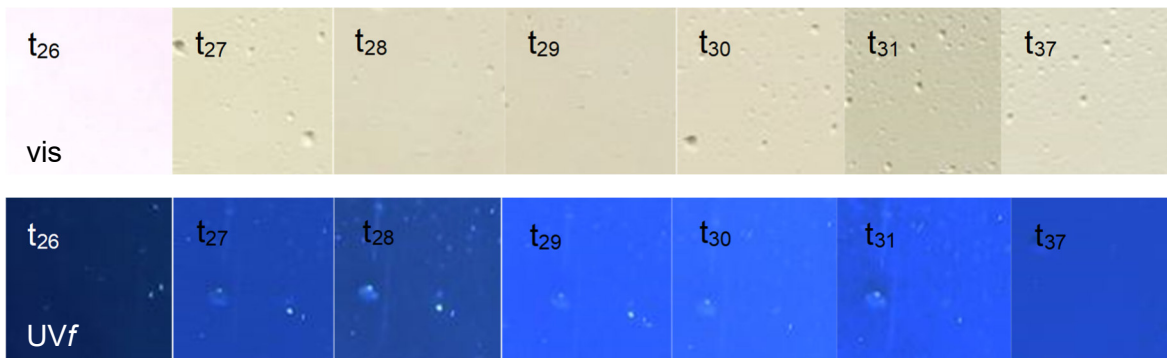


Figure A9.46. Visible and UVf images barite20° (3-1) coated plates, sections P9e and P11e (US, UA and A) and P9b and P11b (S, UA and A) from t<sub>26</sub> to t<sub>37</sub>. Each square corresponds approximately to a 1x1 cm portion of the section.

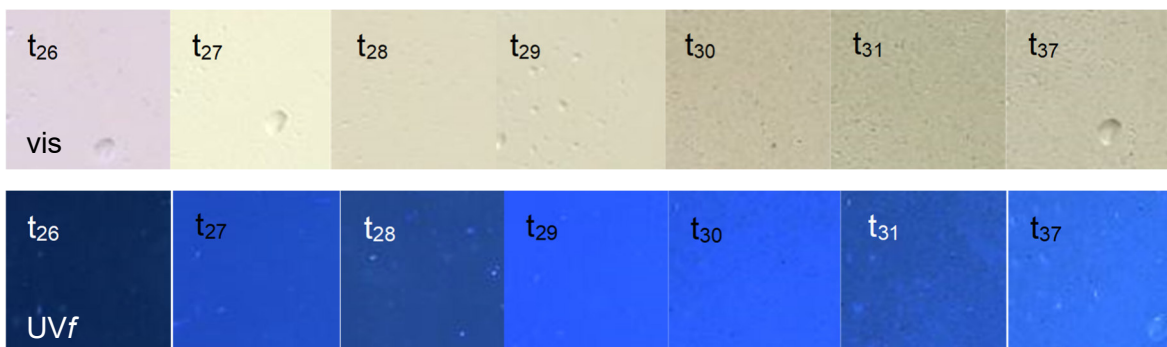
P9f



P11f



P9c



P11c

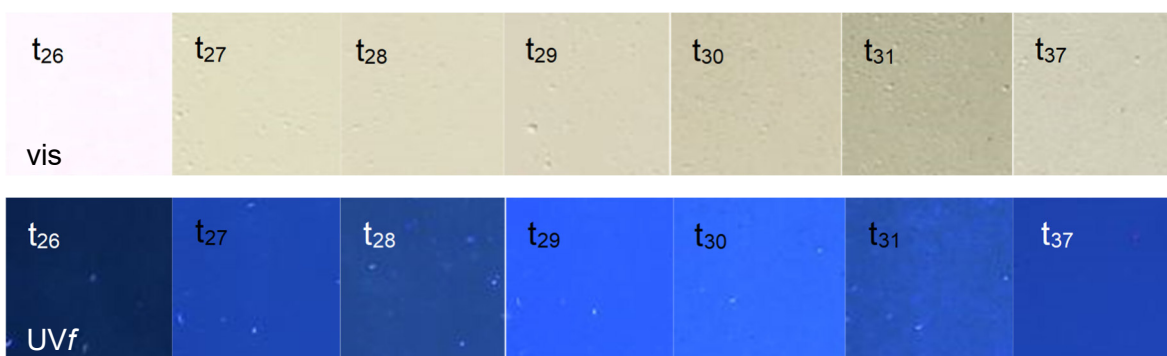
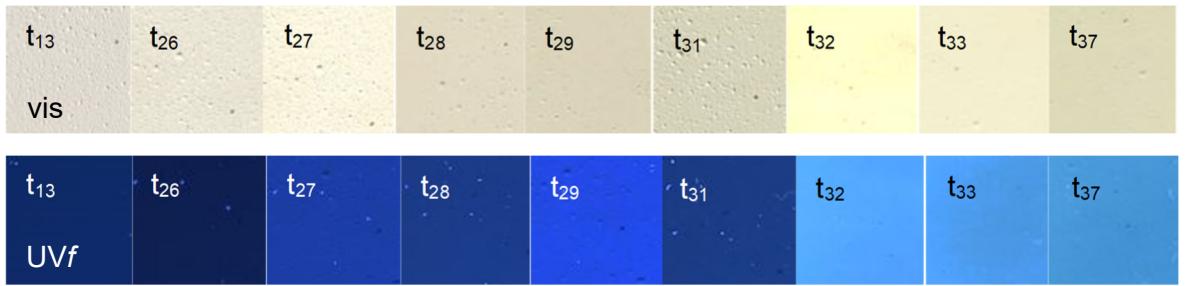
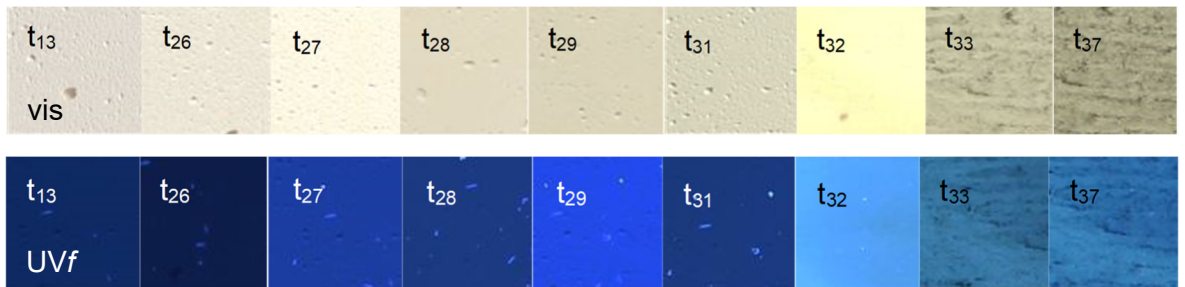


Figure A9.57. Visible and UVf images barite60° (3-2) coated plates, sections P9f and P11f (US, UA and A) and P9c and P11c (S, UA and A) from t<sub>26</sub> to t<sub>37</sub>. Each square corresponds approximately to a 1x1 cm portion of the section.

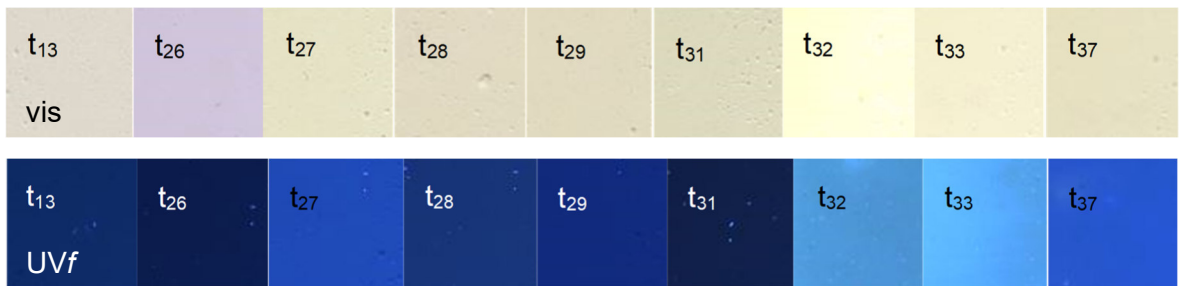
P2d



P2a



P4d



P4a

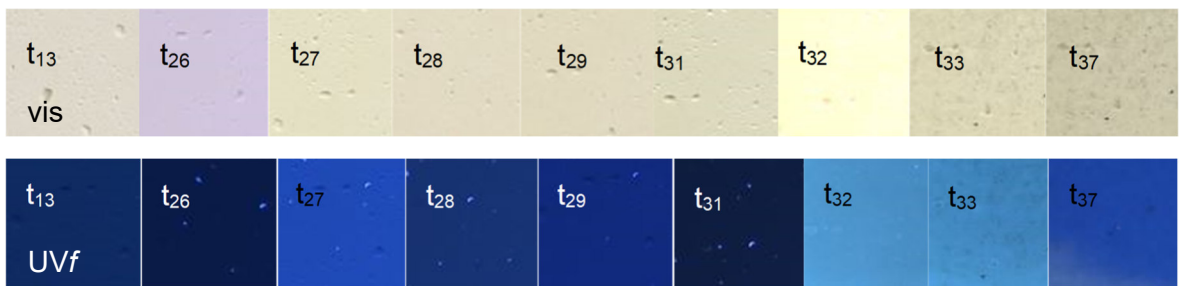
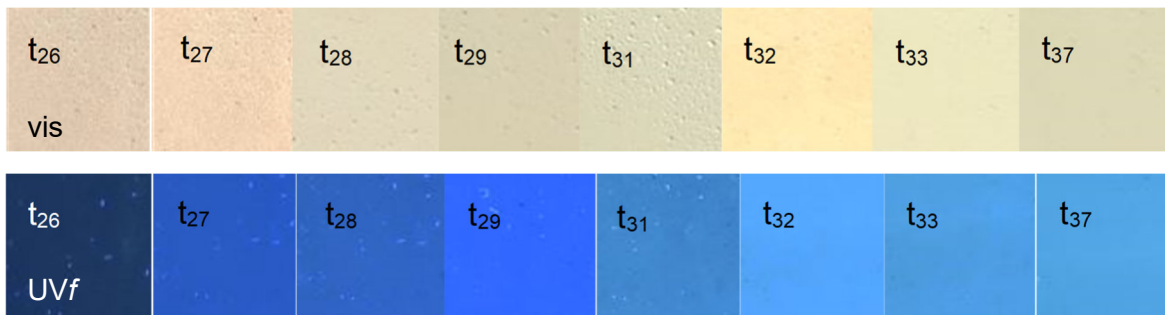
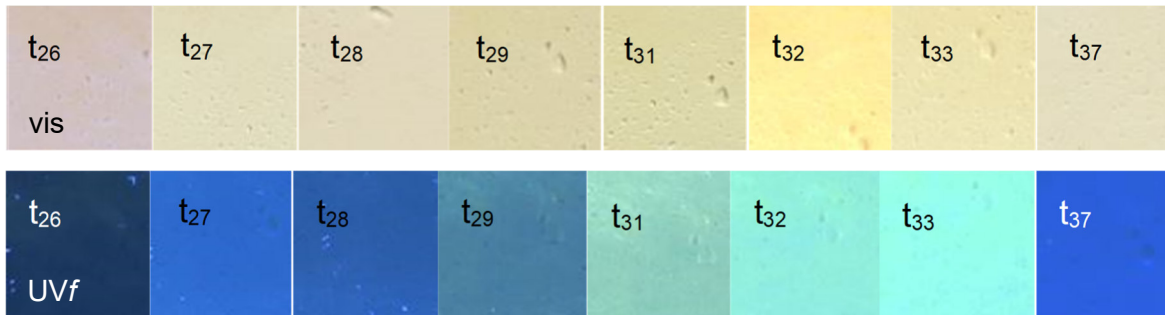


Figure A9.68. Vis and UVf images of plaster and beeswax sections P2d (US, UA), P2d (S, UA), P4d (US, A) and P4a (S, A) from t<sub>13</sub> to t<sub>37</sub>. Each square corresponds approximately to a 1x1 cm portion of the section.

P2e



P4e



P2b



P4b

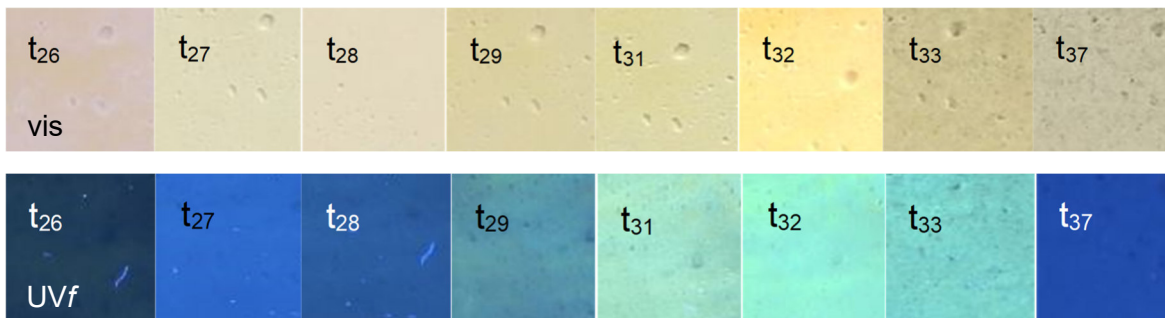
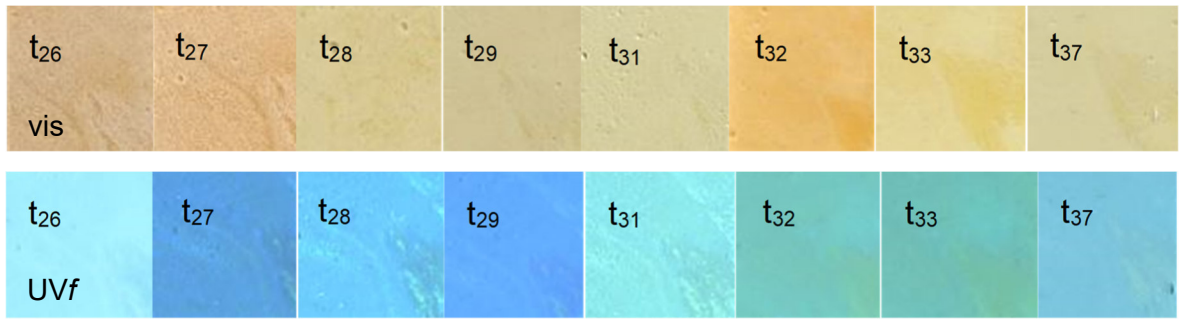
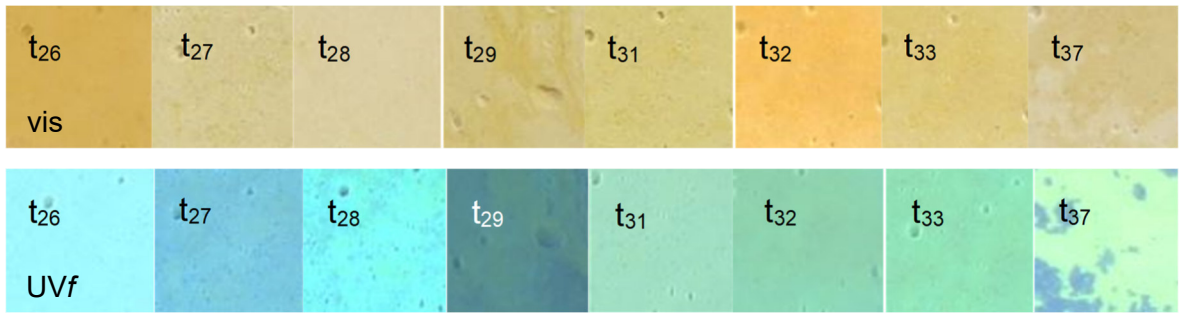


Figure A9.79. Visible and UVf images of cold-pressed linseed oil (1-1) and beeswax (4) coated plates, sections P2e and P4e (US, UA and A) and P2b and P4b (S, UA and A) from t<sub>26</sub> to t<sub>37</sub>. Each square corresponds approximately to a 1x1 cm portion of the section.

*P2f*



*P4f*



*P2c*



*P4c*

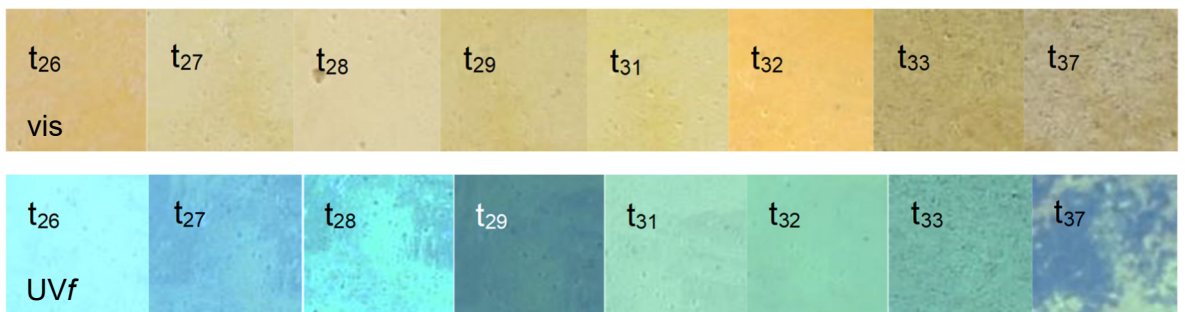
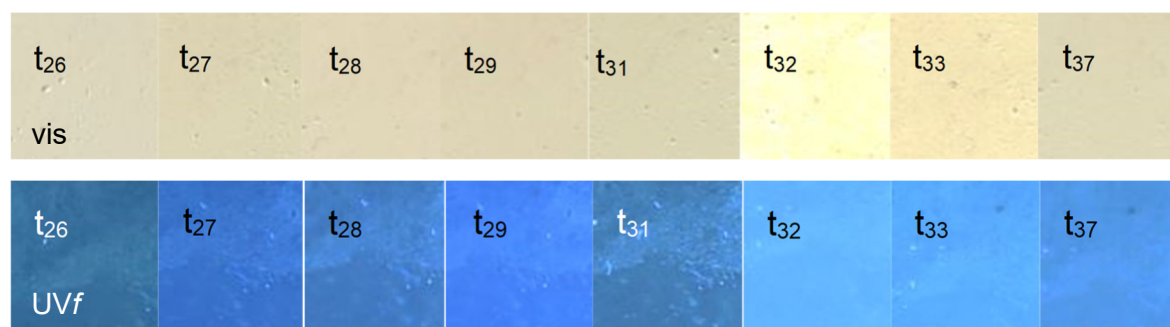
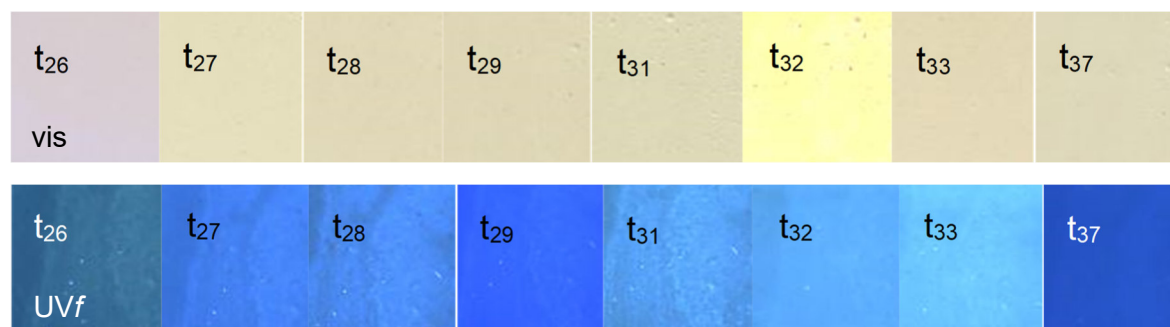


Figure A9.20. Visible and UVf images of boiled linseed oil (1-2) and beeswax (4) coated plates, sections P2f and P4f (US, UA and A) and P2c and P4c (S, UA and A) from t<sub>26</sub> to t<sub>37</sub>. Each square corresponds approximately to a 1x1 cm portion of the section.

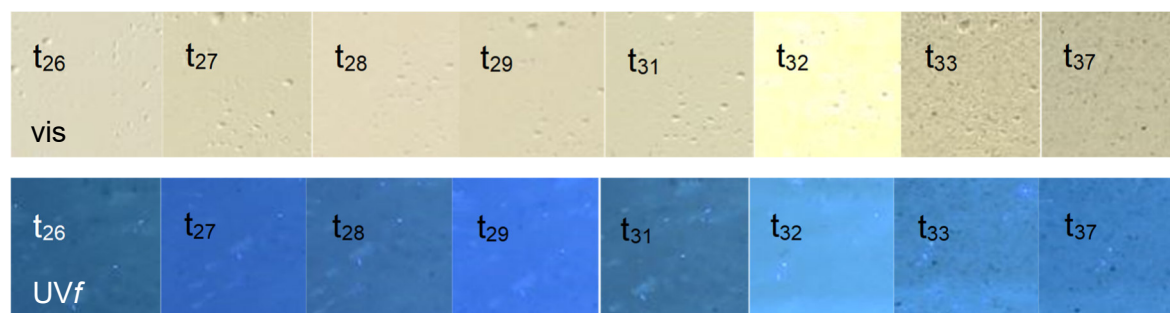
P6e



P8e



P6b



P8b

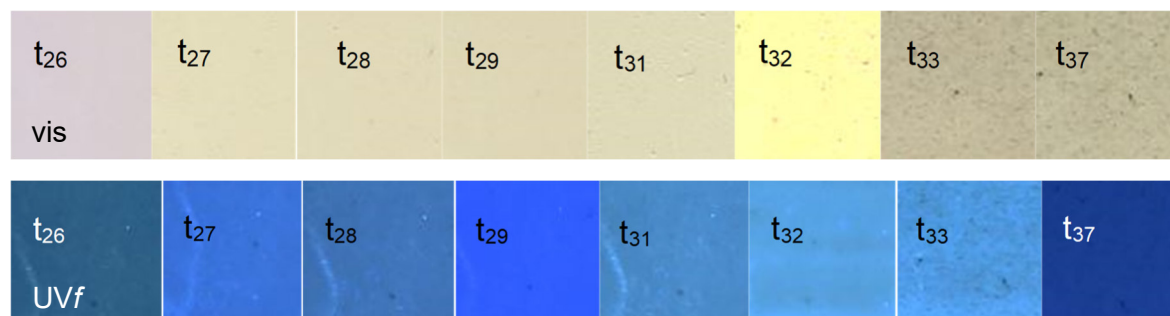
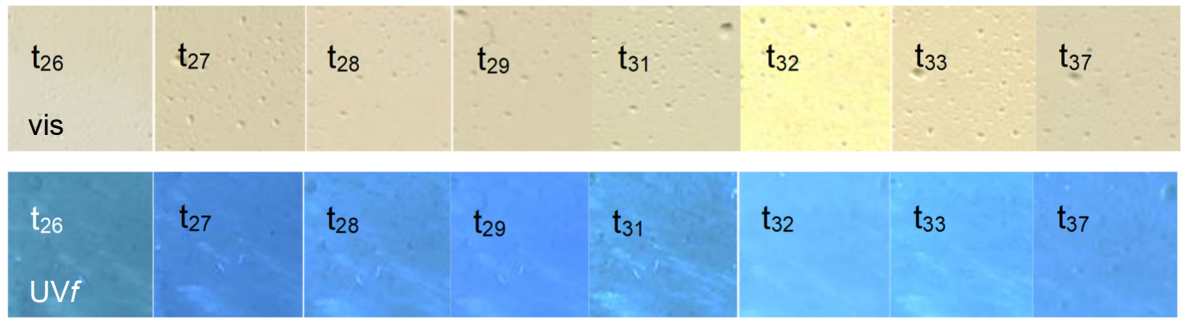
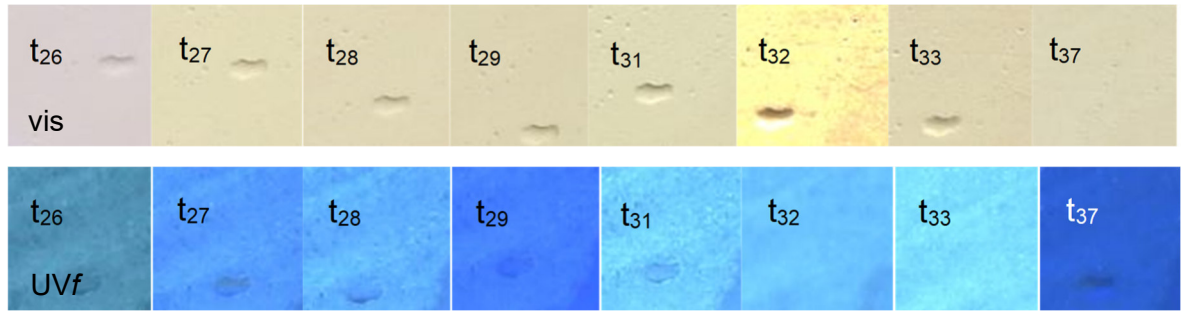


Figure A9.21. Visible and UVf images of shellac6% (2-1) and beeswax (4) coated plates, sections P6e and P8e (US, UA and A) and P6b and P8b (S, UA and A) from t<sub>26</sub> to t<sub>37</sub>. Each square corresponds approximately to a 1x1 cm portion of the section.

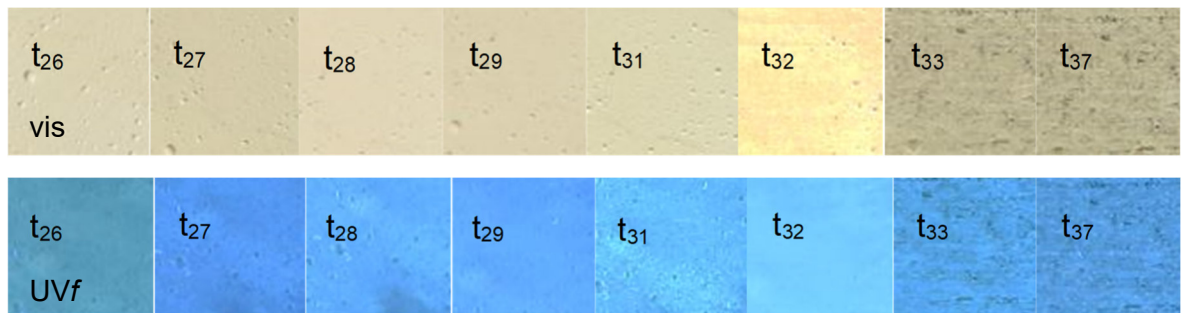
*P6f*



*P8f*



*P6c*



*P8c*

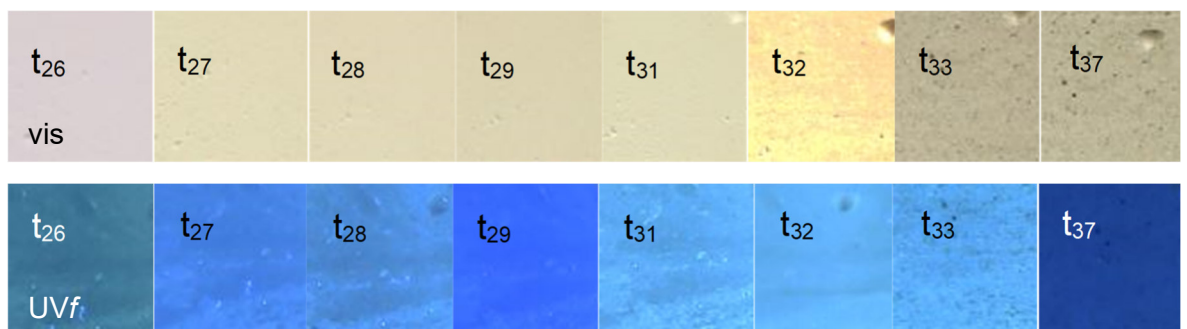
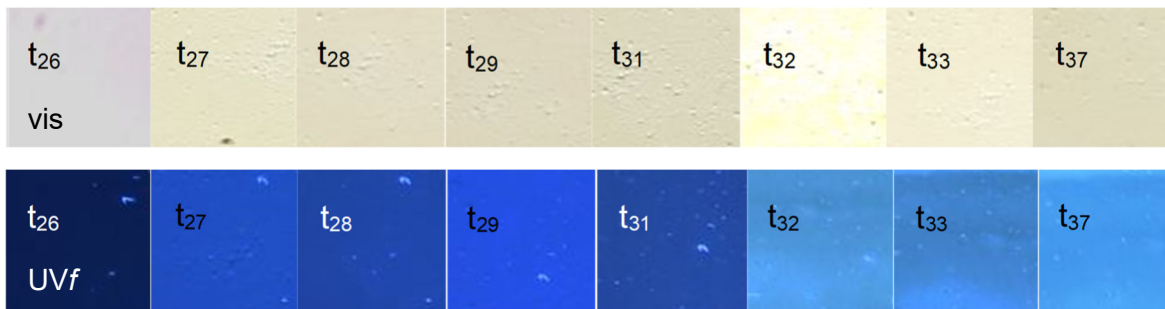
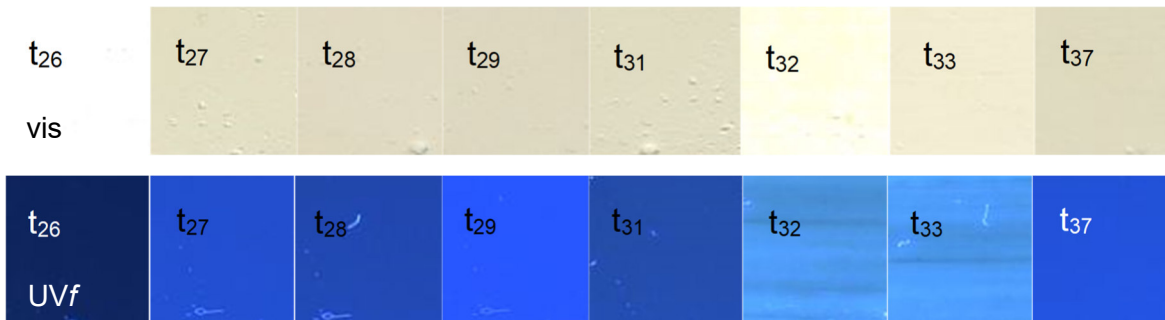


Figure A9.22. Visible and UVf images of shellac18% (2-2) and beeswax (4) coated plates, sections P6f and P8f (US, UA and A) and P6c and P8c (S, UA and A) from  $t_{26}$  to  $t_{37}$ . Each square corresponds approximately to a 1x1 cm portion of the section.

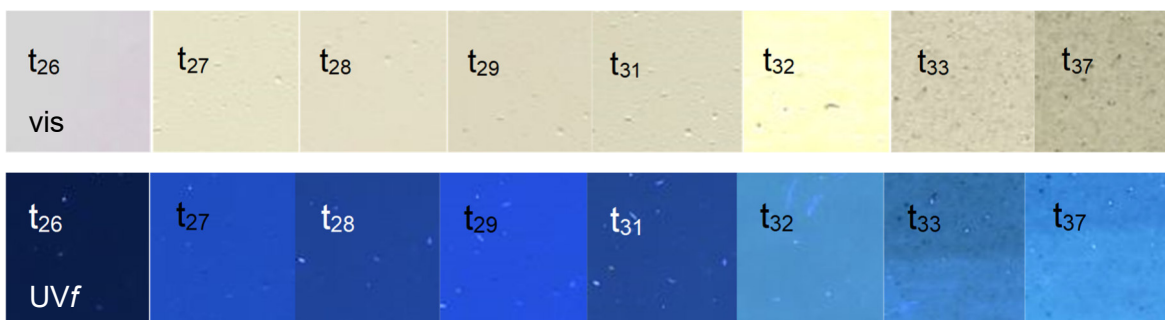
P10e



P12e



P10b



P12b

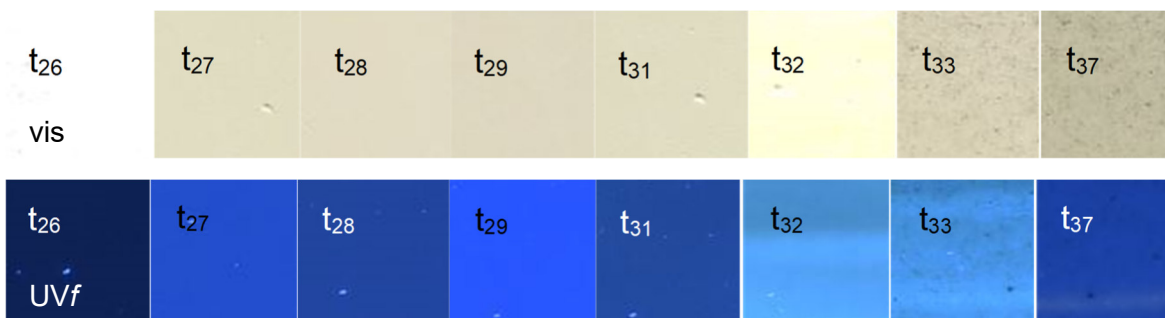
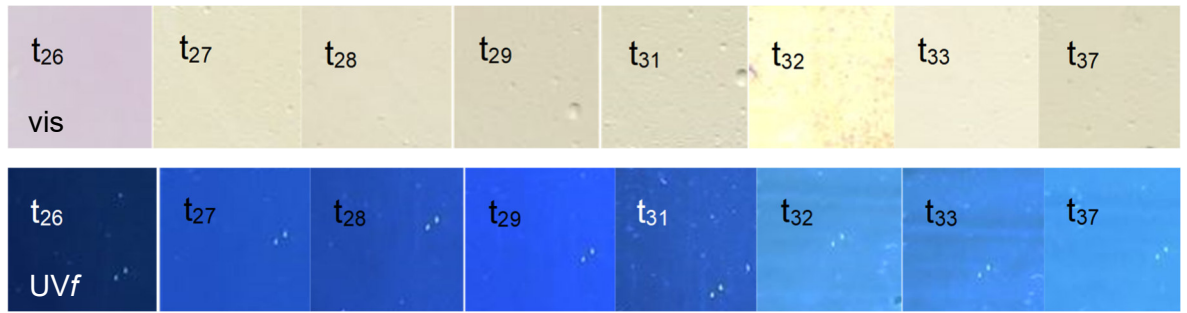
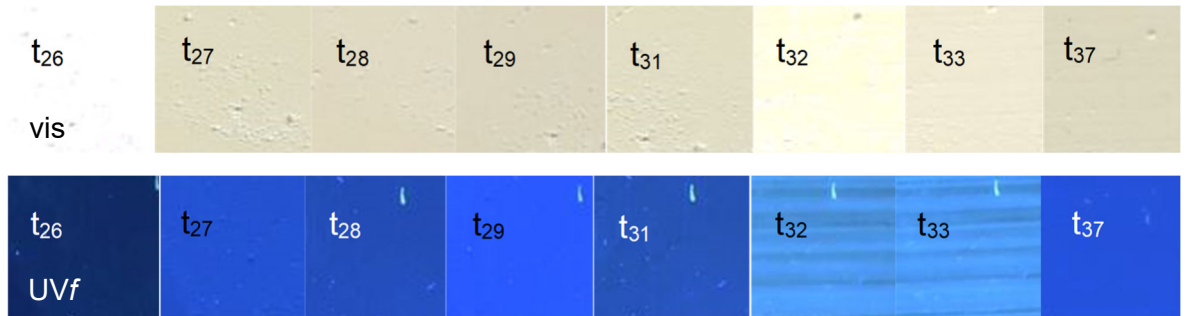


Figure A9.23. Visible and UVf images of barite<sub>20°</sub> (3-1) and beeswax (4) coated plates, sections P10e and P12e (US, UA and A) and P10b and P12b (S, UA and A) from t<sub>26</sub> to t<sub>37</sub>. Each square corresponds approximately to a 1x1 cm portion of the section.

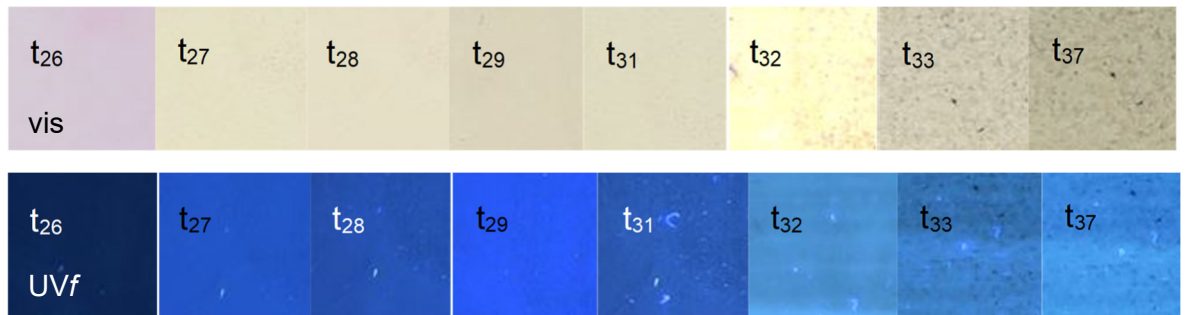
*P10f*



*P12f*



*P10c*

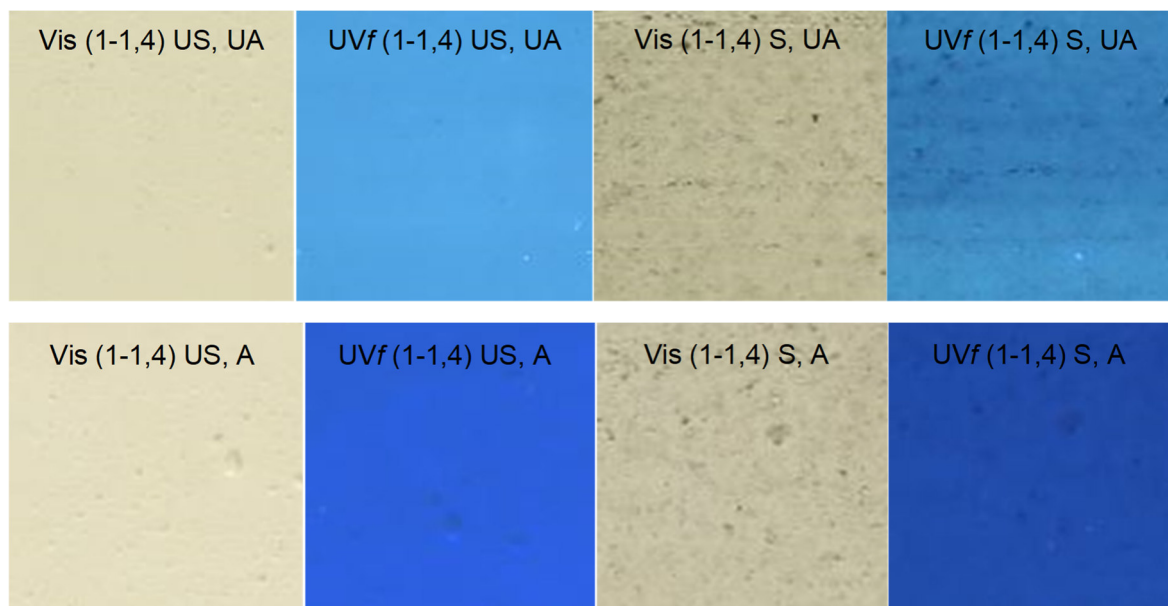


*P12c*



Figure A9.24. Visible and UVf images of boiled linseed oil (3-2) and beeswax (4) coated plates, sections *P10f* and *P12f* (US, UA and A) and *P10c* and *P12c* (S, UA and A) from t<sub>26</sub> to t<sub>37</sub>. Each square corresponds approximately to a 1x1 cm portion of the section.

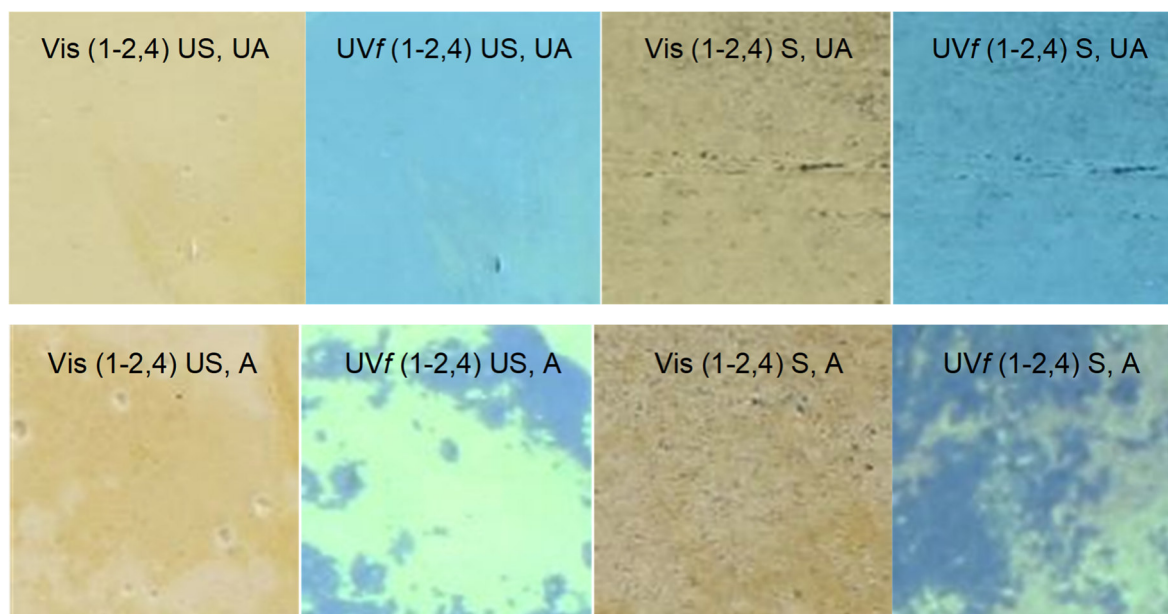
*Cold-pressed linseed oil (1-1) and beeswax (4)*



*P2e → P4e*  
 Discoloration (S100%, I1)  
 Reduced fluorescence under UVf

*P2b → P4b*  
 Discoloration (S100%, I1)  
 Reduced fluorescence under UVf

*Boiled linseed oil (1-2) and beeswax (4)*

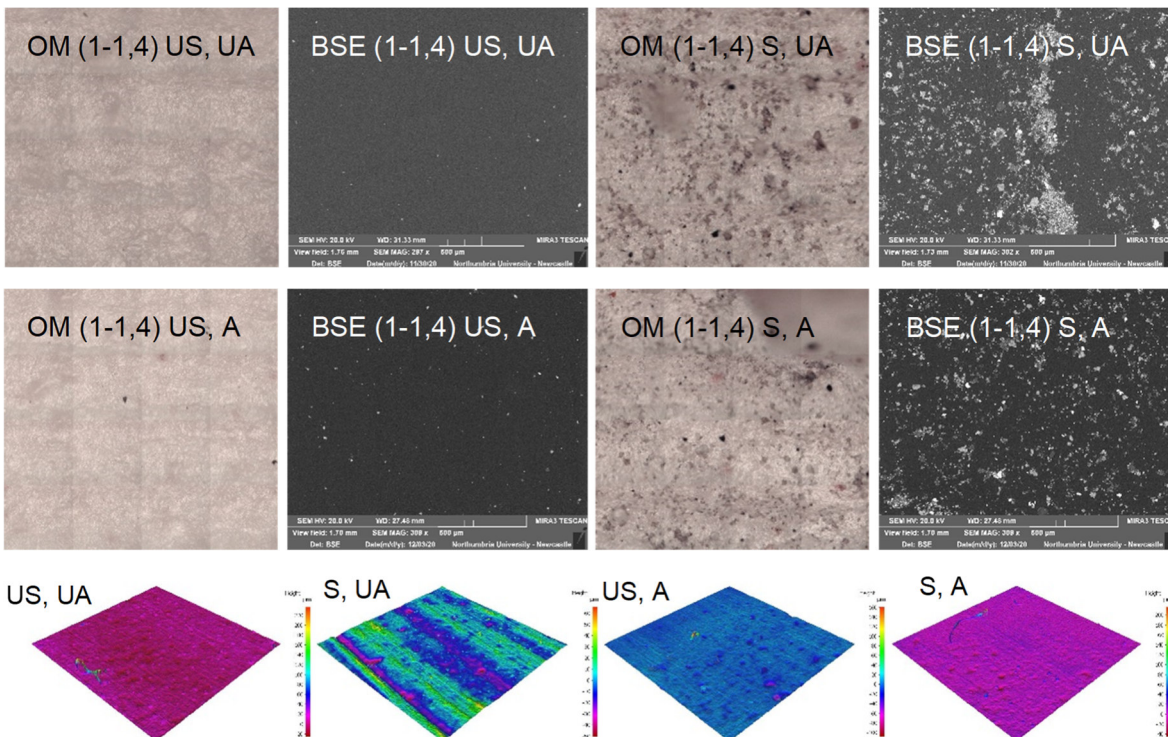


*P2f → P4f*  
 Discoloration (S100%, I1)  
 Varied absorption of the coating  
 Brighter fluorescence under UVf

*P2c → P4c*  
 Discoloration (S100%, I2)  
 Brighter fluorescence under UVf

Figure A9.25. Visible and UVf images of the unaged (UA) and aged (A) sections coated with cold-pressed linseed oil + beeswax (1-1,4) and boiled linseed oil + beeswax (1-2,4) at  $t_{37}$  and relevant visual examination notes. Each square corresponds approximately to a 1x1 cm portion of the section.

*Cold-pressed linseed oil (1-1) and beeswax (4)*



*Boiled linseed oil (1-2) and beeswax (4)*

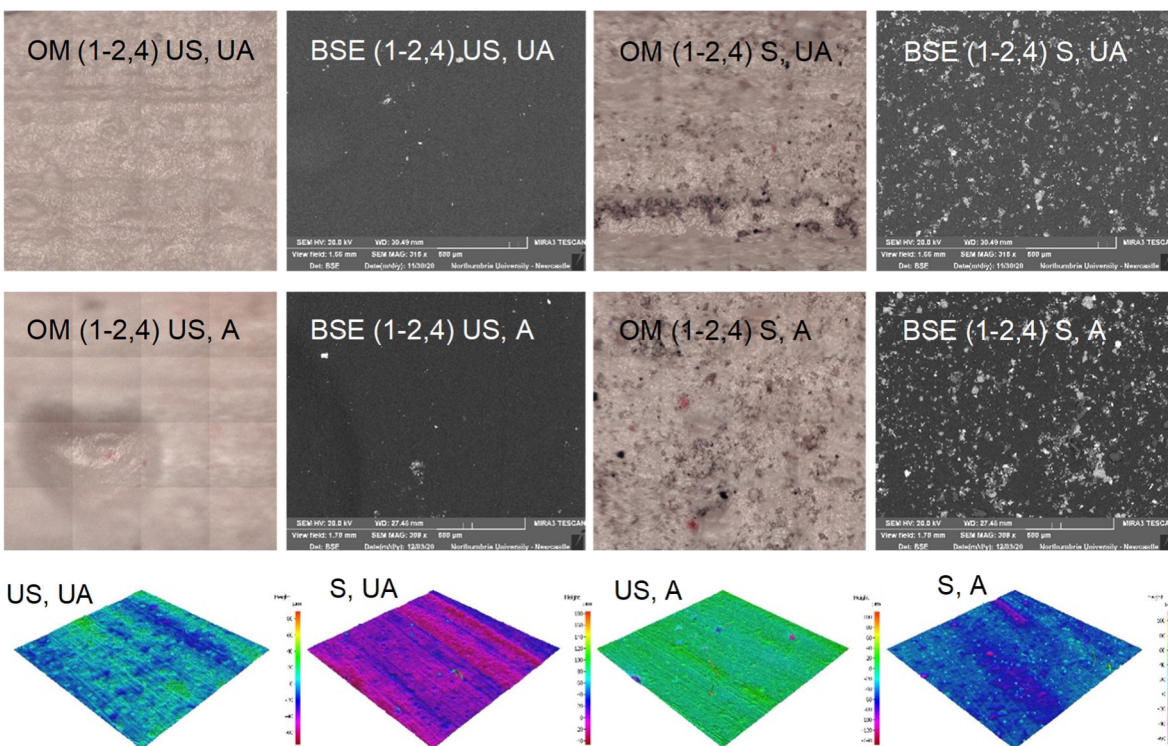
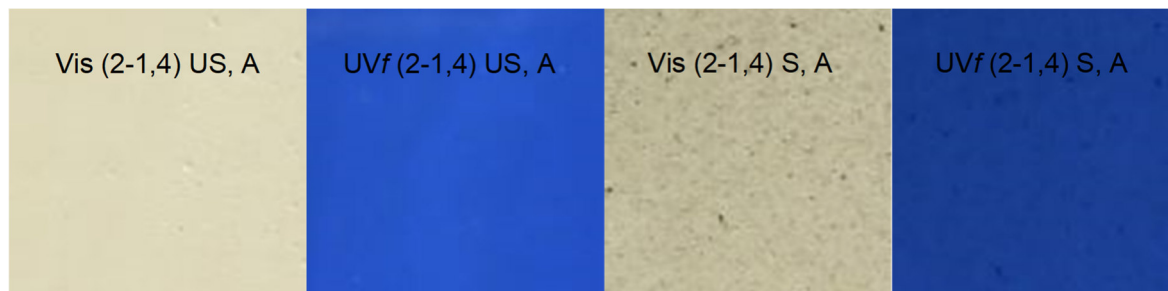
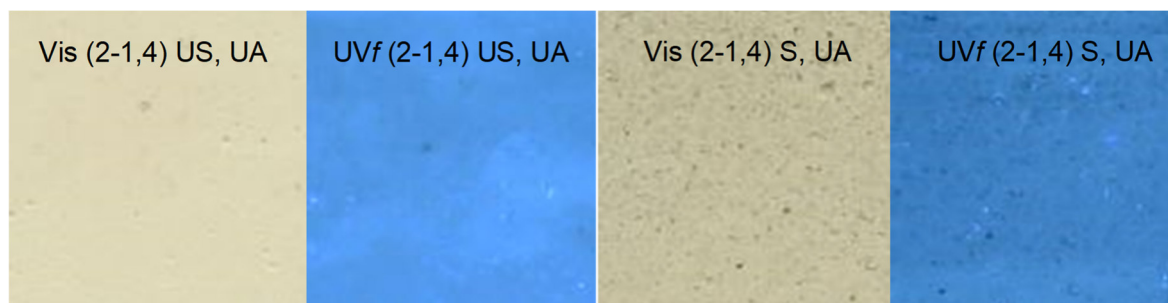


Figure A9.26. FT-IR microscope survey images (1x1 mm), BSE images and high-resolution 3D images (5.3x5.3 mm) of the unaged (UA) and aged (A) sections coated with cold-pressed linseed oil + beeswax (1-1,4) and boiled linseed oil + beeswax (1-2,4) at  $t_{37}$ .

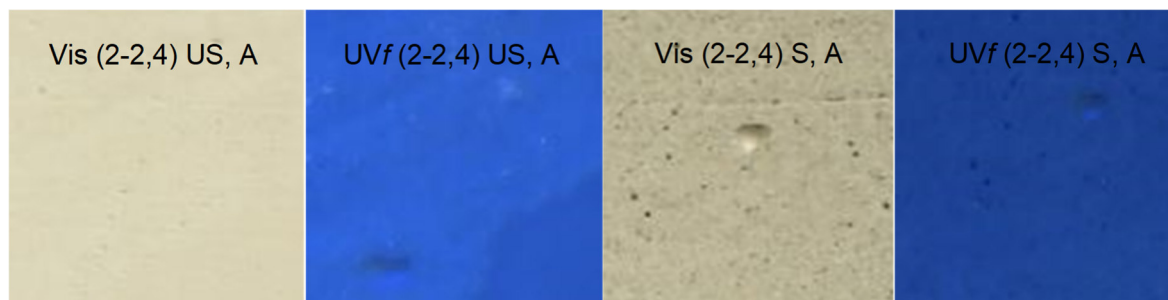
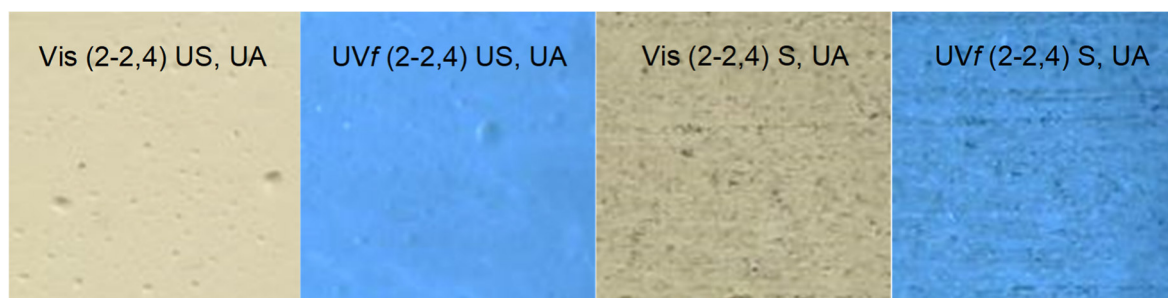
*Shellac6% (2-1) and beeswax (4)*



*P6e → P8e*  
 Discoloration (S100%, I2)  
 Reduced fluorescence under UVf

*P6b → P8b*  
 Discoloration (S100%, I2)  
 Reduced fluorescence under UVf

*Shellac18% (2-2) and beeswax (4)*

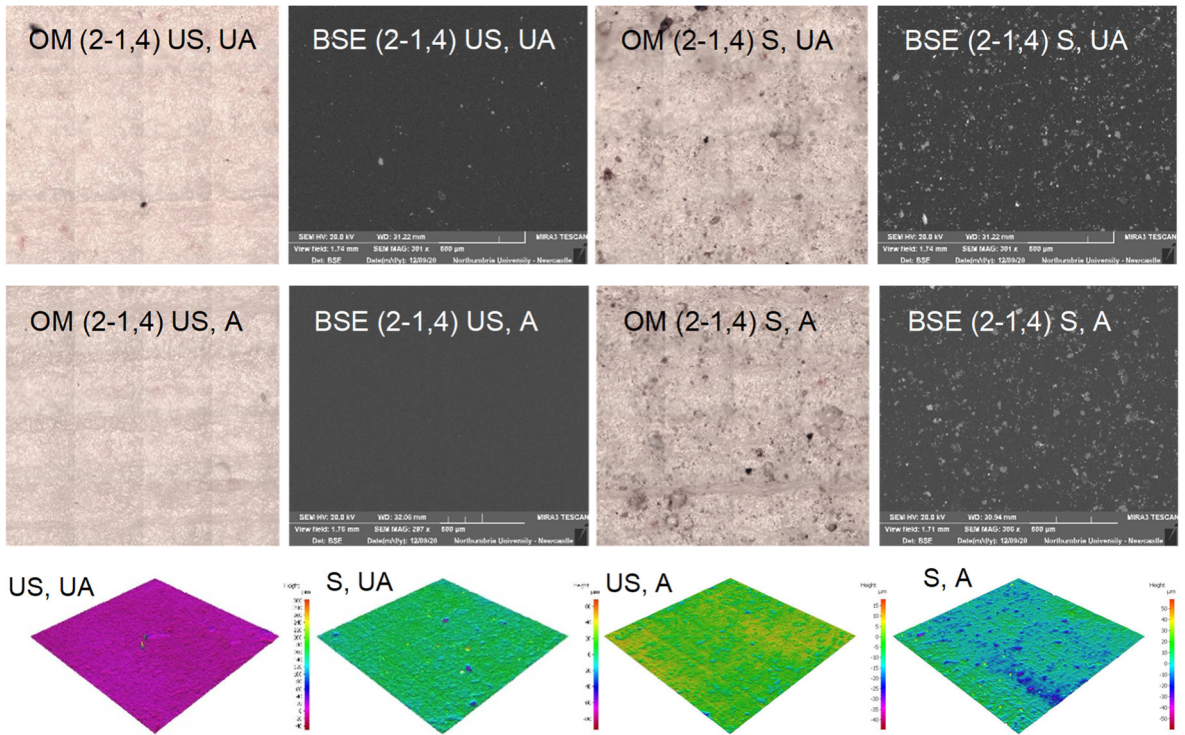


*P6f → P8f*  
 Discoloration (S100%, I2)  
 Reduced fluorescence under UVf

*P6c → P8c*  
 Discoloration (S100%, I2)  
 Reduced fluorescence under UVf

Figure A9.27. Visible and UVf images of the unaged (UA) and aged (A) sections coated with shellac6% + beeswax (2-1,4) and shellac18% + beeswax (2-2,4) at  $t_{37}$  and relevant visual examination notes. Each square corresponds approximately to a 1x1 cm portion of the section.

Shellac6% (2-1) and beeswax (4)



Shellac18% (2-2) and beeswax (4)

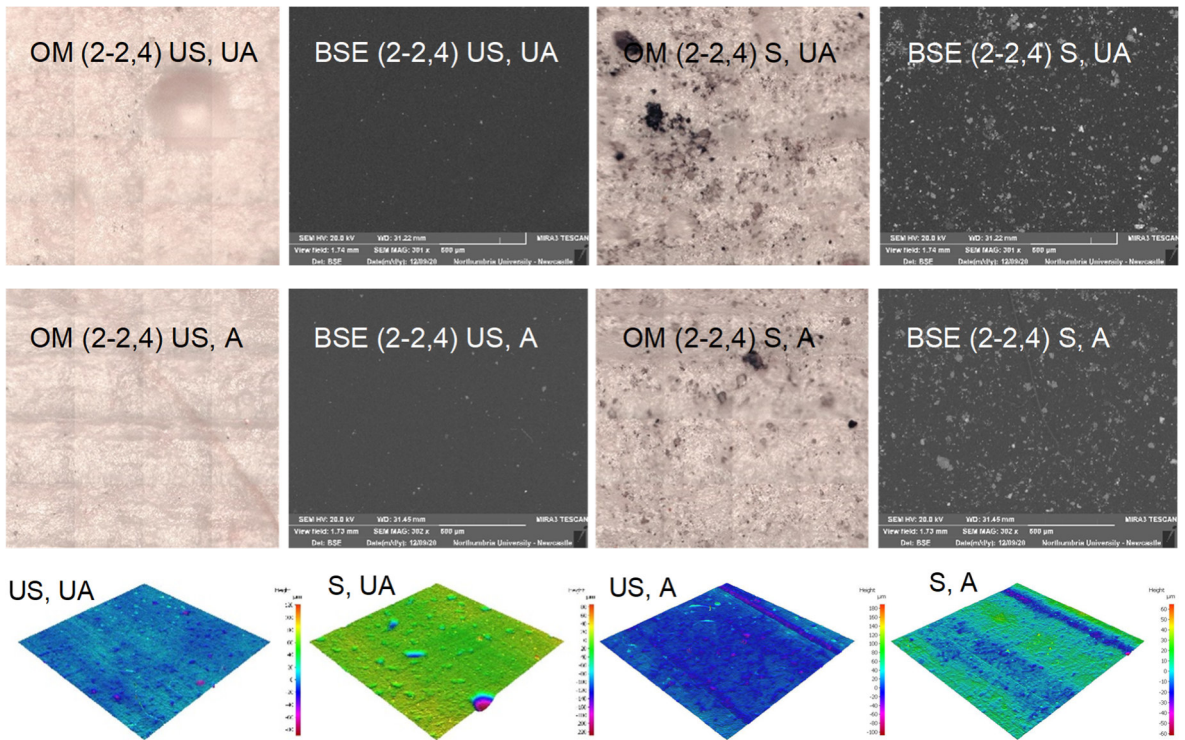
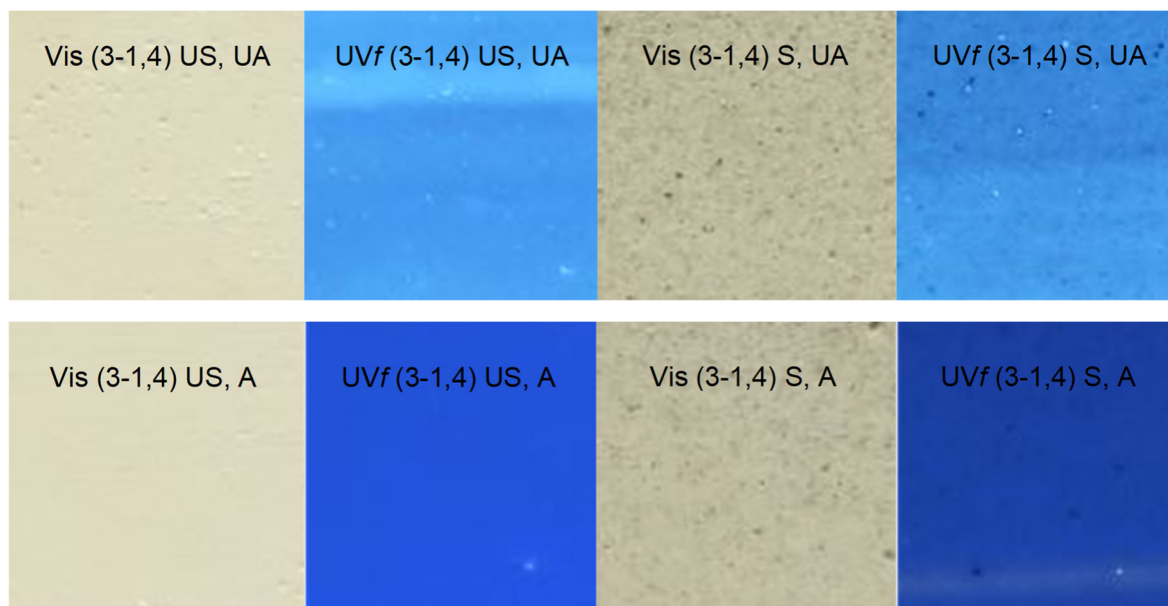


Figure A9.28. FT-IR microscope survey images (1x1 mm), BSE images and high-resolution 3D images (5.3x5.3 mm) of the unaged (UA) and aged (A) sections coated with shellac6% + beeswax (2-1,4) and shellac18% + beeswax (2-2,4) at  $t_{37}$ .

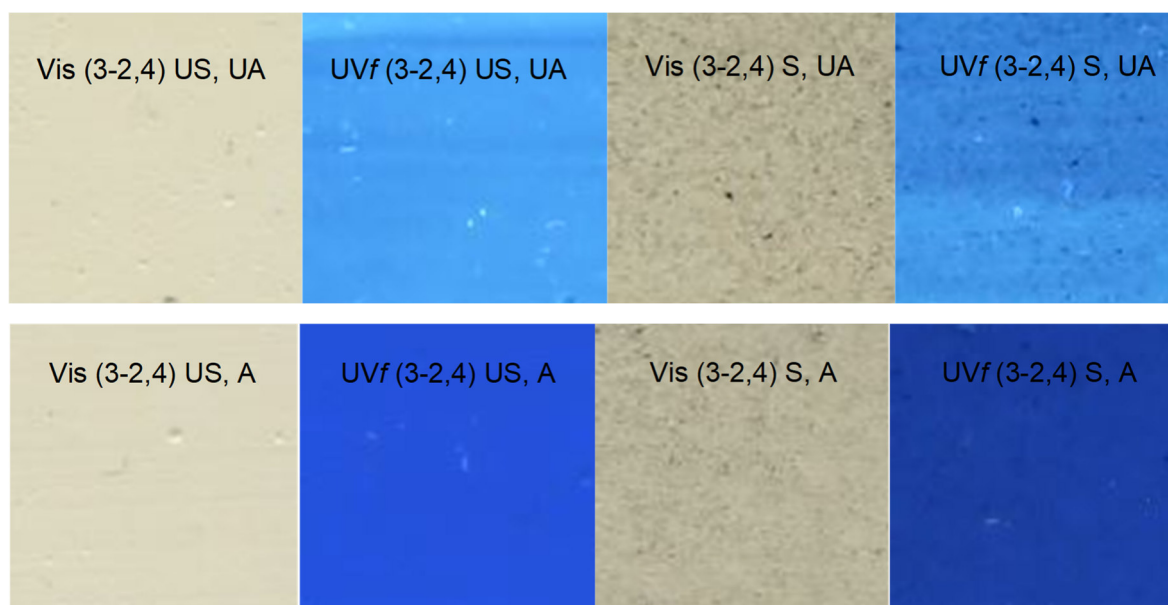
*Barite20° (3-1) and beeswax (4)*



*P10e → P12e*  
Whitening (S100%, I1)  
Reduced fluorescence under UVf

*P10b → P12b*  
Whitening (S100%, I1)  
Reduced fluorescence under UVf

*Barite60° (3-2) and beeswax (4)*

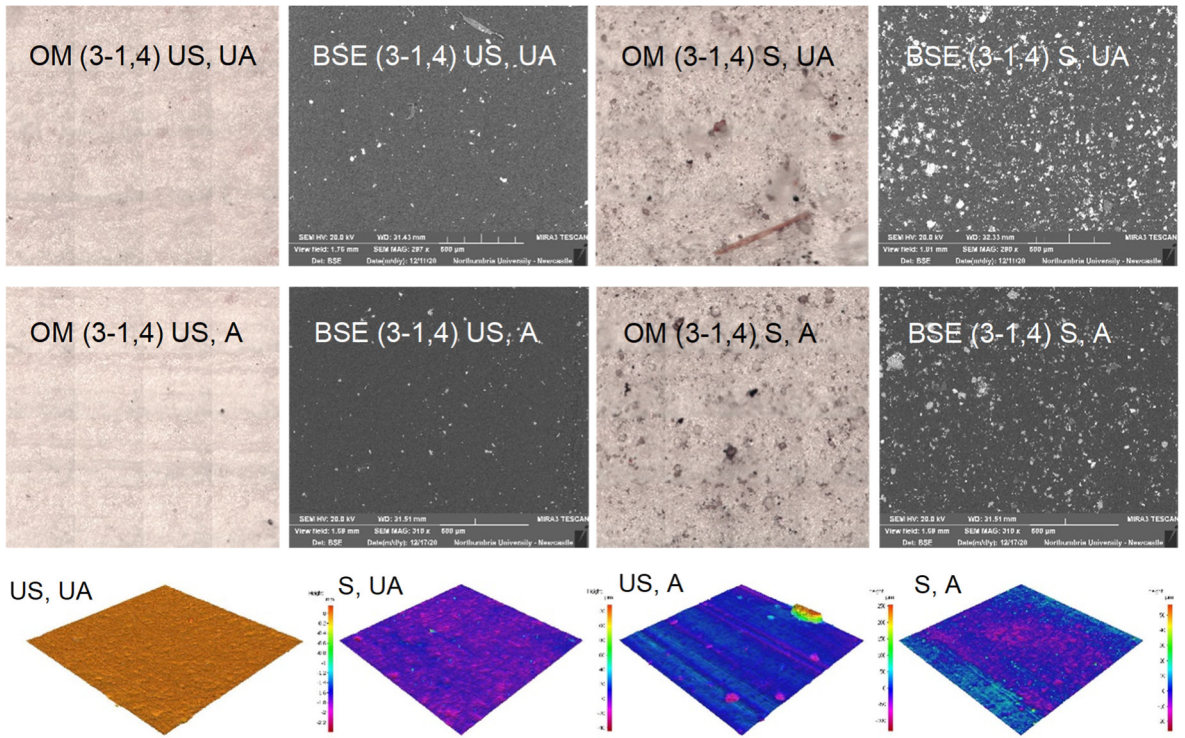


*P10f → P12f*  
Whitening (S100%, I1)  
Reduced fluorescence under UVf

*P10c → P12c*  
Whitening (S100%, I1)  
Reduced fluorescence under UVf

Figure A9.29. Visible and UVf images of the unaged (UA) and aged (A) sections coated with barite20° + beeswax (3-1,4) and barite20° + beeswax (3-2,4) at *t*<sub>37</sub> and relevant visual examination notes. Each square corresponds approximately to a 1x1 cm portion of the section.

*Barite20° (3-1) and beeswax (4)*



*Barite60° (3-2) and beeswax (4)*

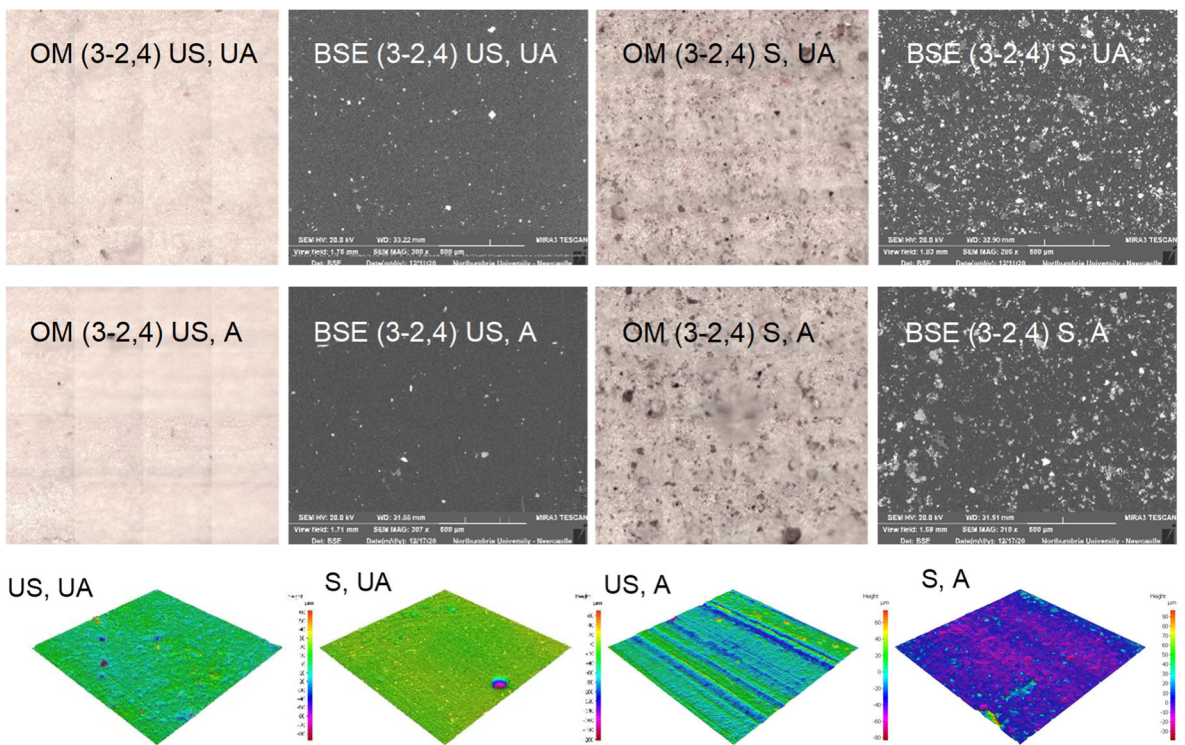


Figure A9.30. FT-IR microscope survey images (1x1 mm), BSE images and high-resolution 3D images (5.3x5.3 mm) of the unaged (UA) and aged (A) sections coated with barite20° + beeswax (3-1,4) and barite20° + beeswax (3-2,4) at  $t_{37}$ .

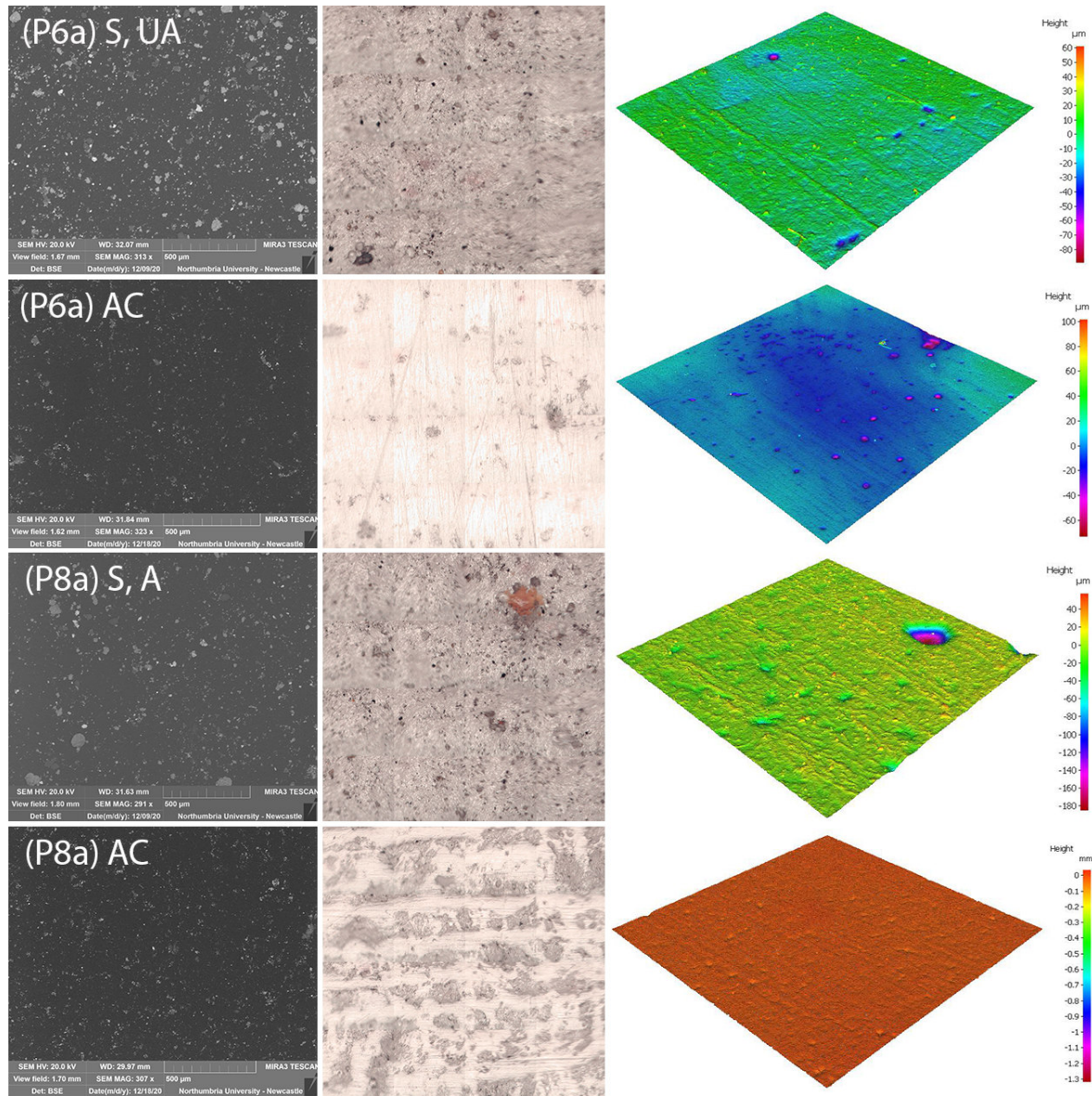


Figure A9.31. From left to right: BSE images, FT-IR survey micrographs (1x1 mm) and the and the HR 3D images (5.3x5.3 mm) of the plaster surfaces coated with beeswax (4) (P6a and P8a) before (S) and after (AC) cleaning with PE-PAM-IMS solution (Sol I).

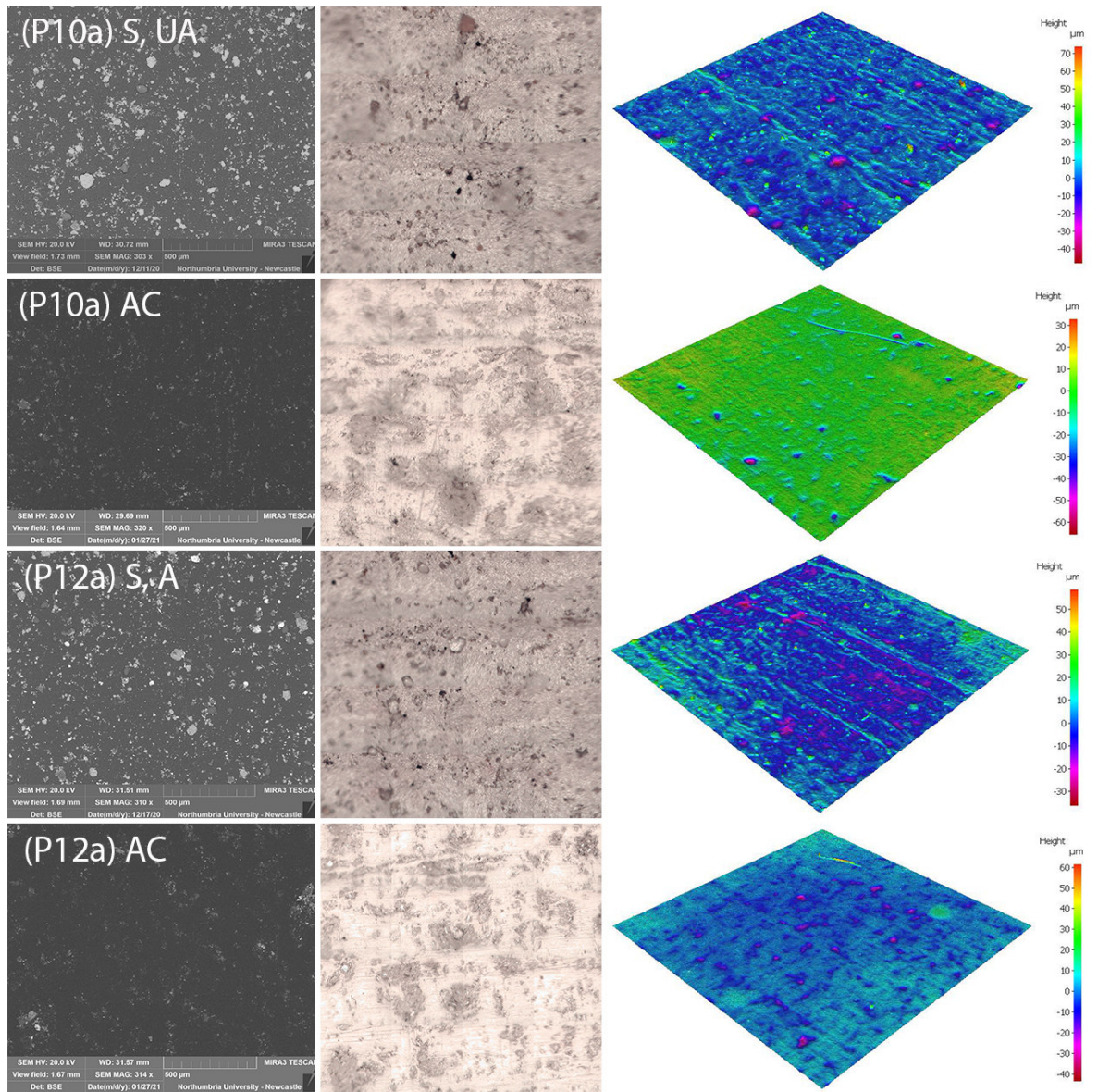


Figure A9.32. From left to right: BSE images, FT-IR survey micrographs (1x1 mm) and the HR 3D images (5.3x5.3 mm) of the plaster surfaces coated with beeswax (4) (P10a and P12a) before (S) and after (AC) cleaning with PE-PAM-IMS solution (Sol I).

## FT-IR SPECTRA AND FIGURES

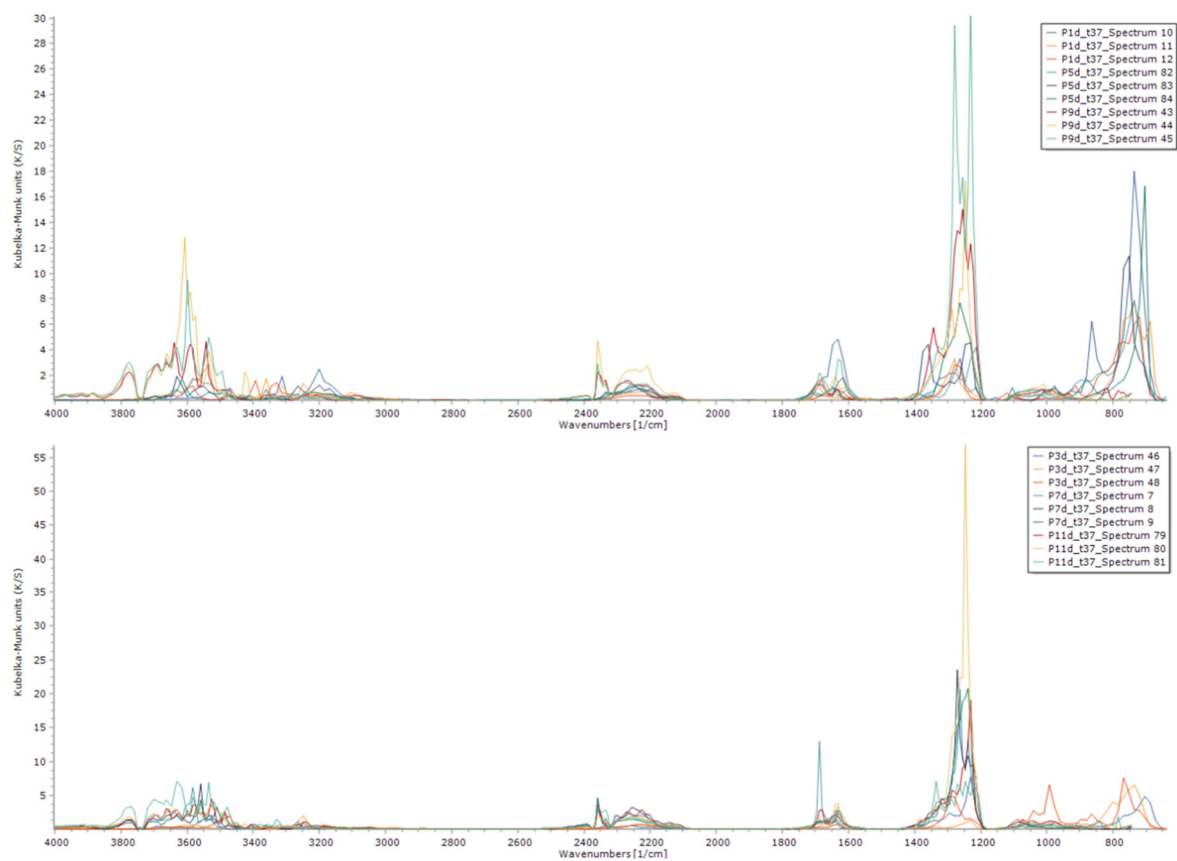


Figure A9.33. Top. FT-IR spectra acquired from the unaged, unsoiled areas (d of P1, 5 and 9) at  $t_{37}$ . Bottom. FT-IR spectra acquired from the aged, unsoiled areas (d of P3, 7 and 11) at  $t_{37}$ .

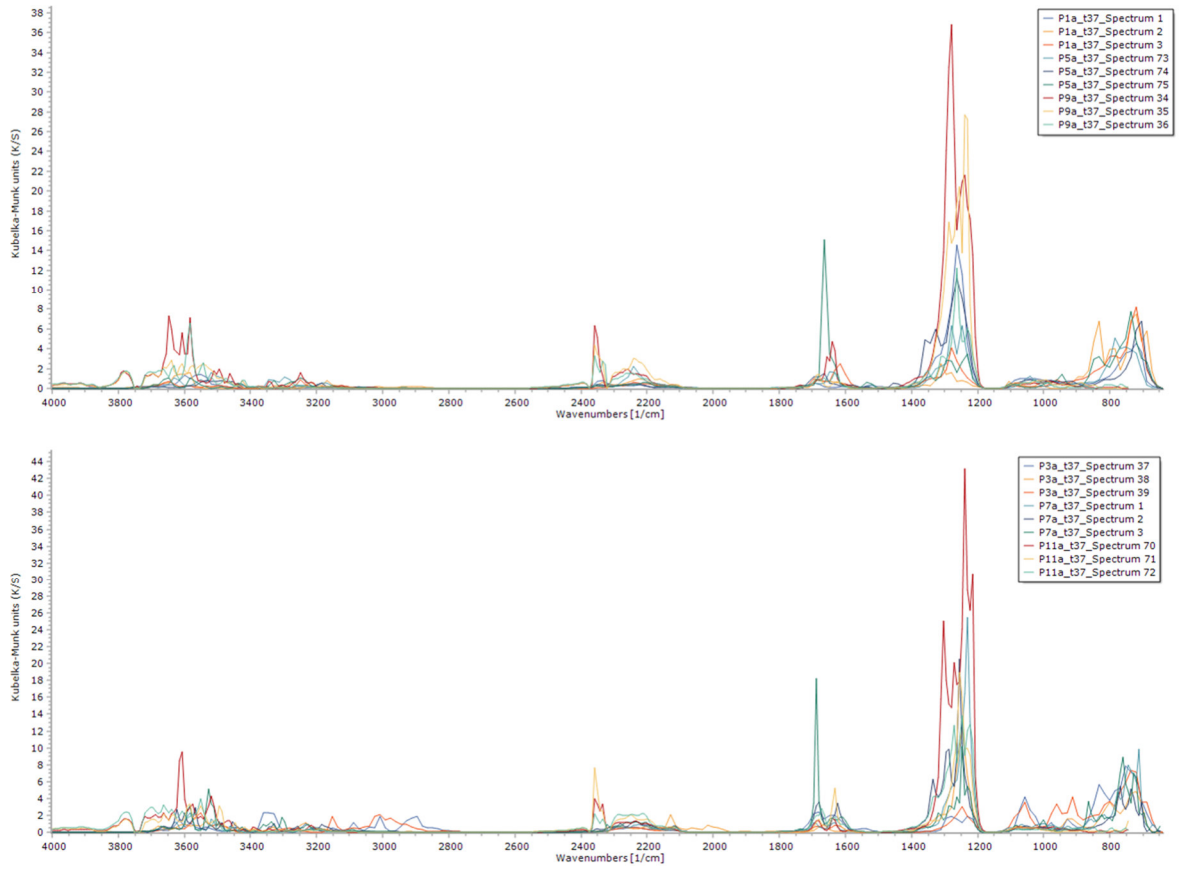


Figure A9.34. Top. FT-IR spectra acquired from the unaged, soiled areas (a of P1, 5 and 9) at  $t_{37}$ . Bottom. FT-IR spectra acquired from the aged, soiled areas (a of P1, 5 and 9) at  $t_{37}$ .

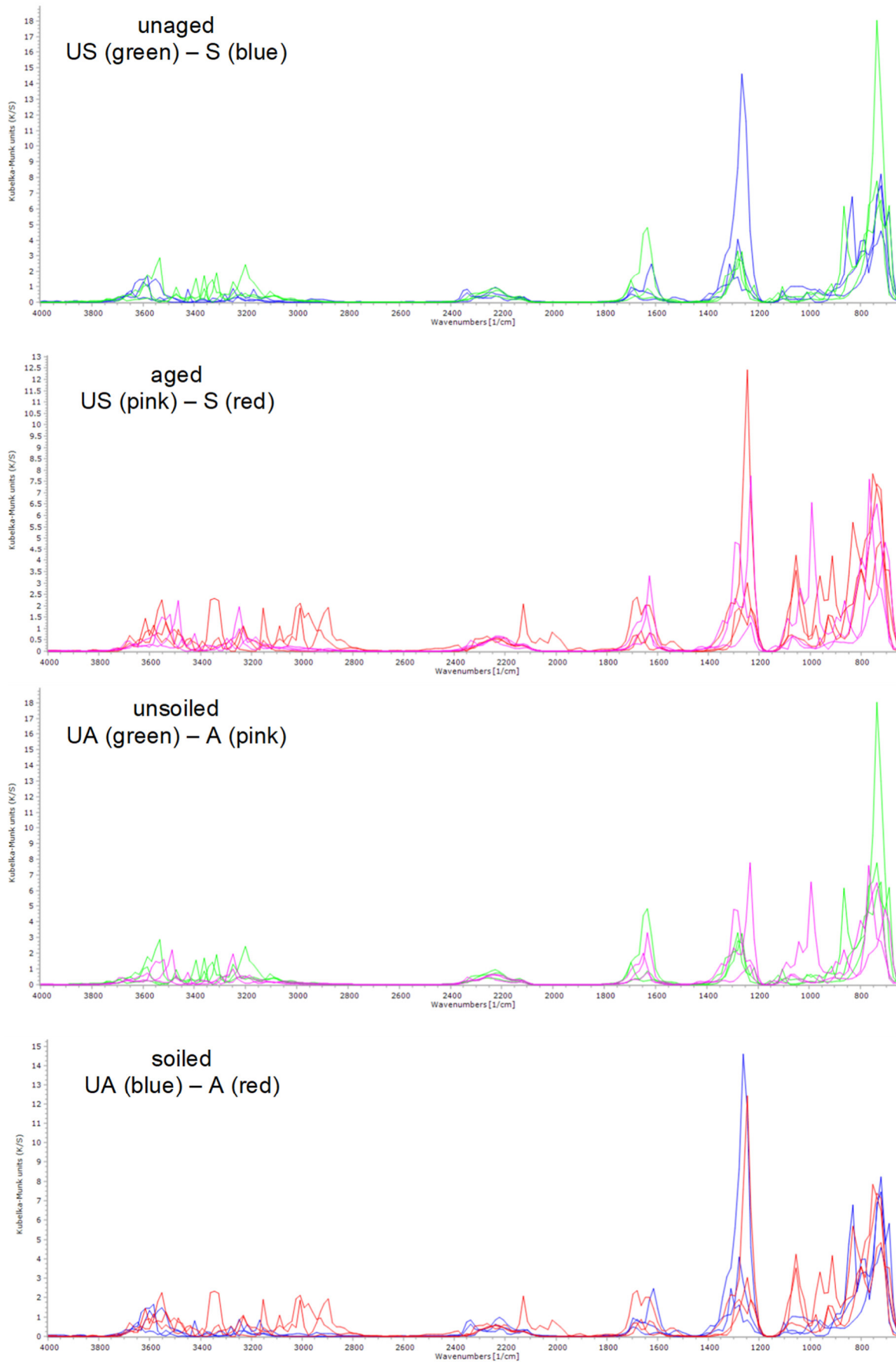


Figure A9.35. Diffuse reflectance FT-IR spectra acquired from the unaged (UA) P1 control sections (US d, and S a) and aged P3 control sections (US d, and S a).

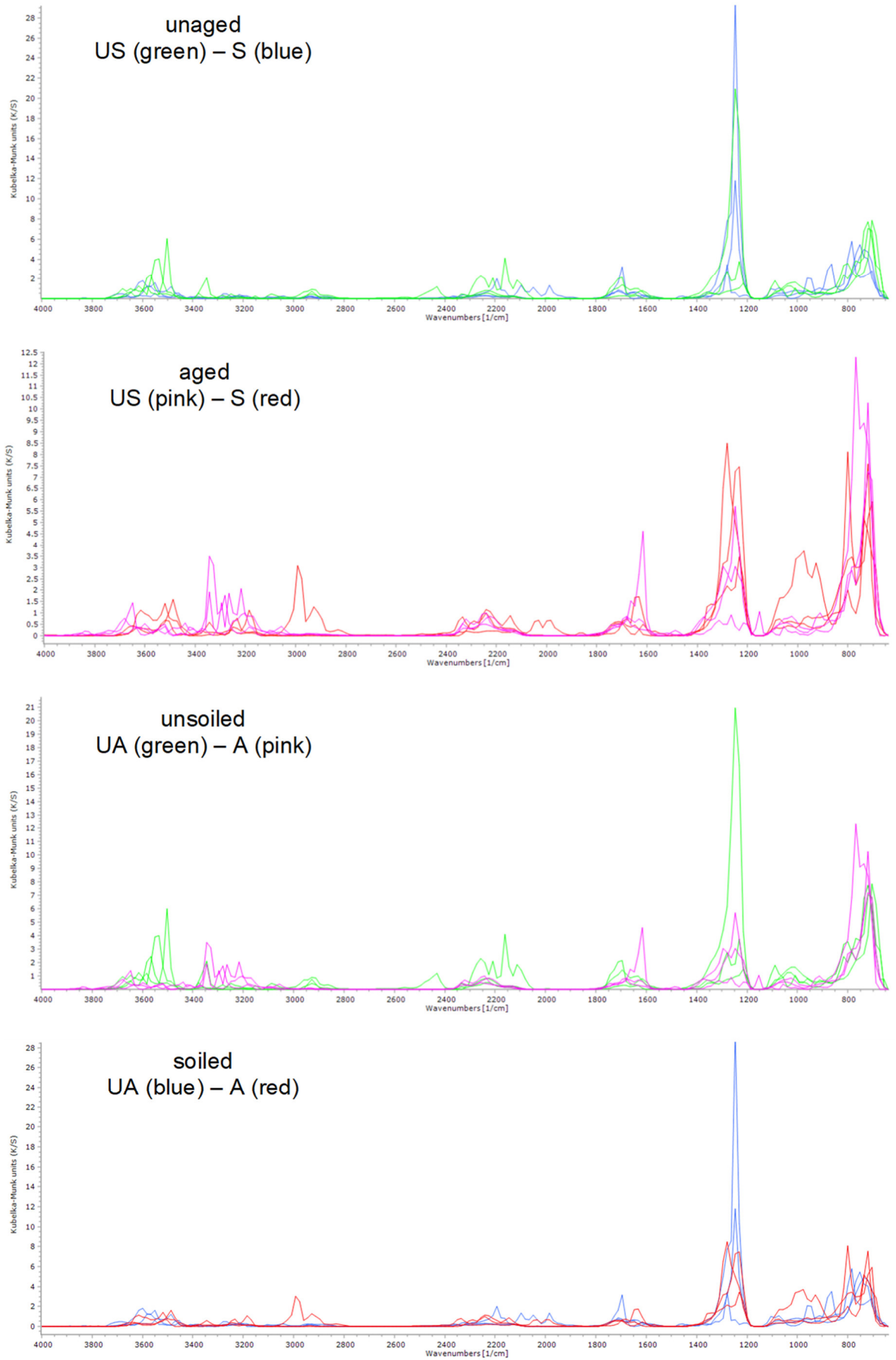


Figure A9.36. FT-IR spectra acquired from unsoiled (unaged P1e and aged P3e) and soiled (unaged P1b and aged P3b) areas of the plaster surface coated with cold-pressed linseed oil (1-1) at  $t_{37}$ .

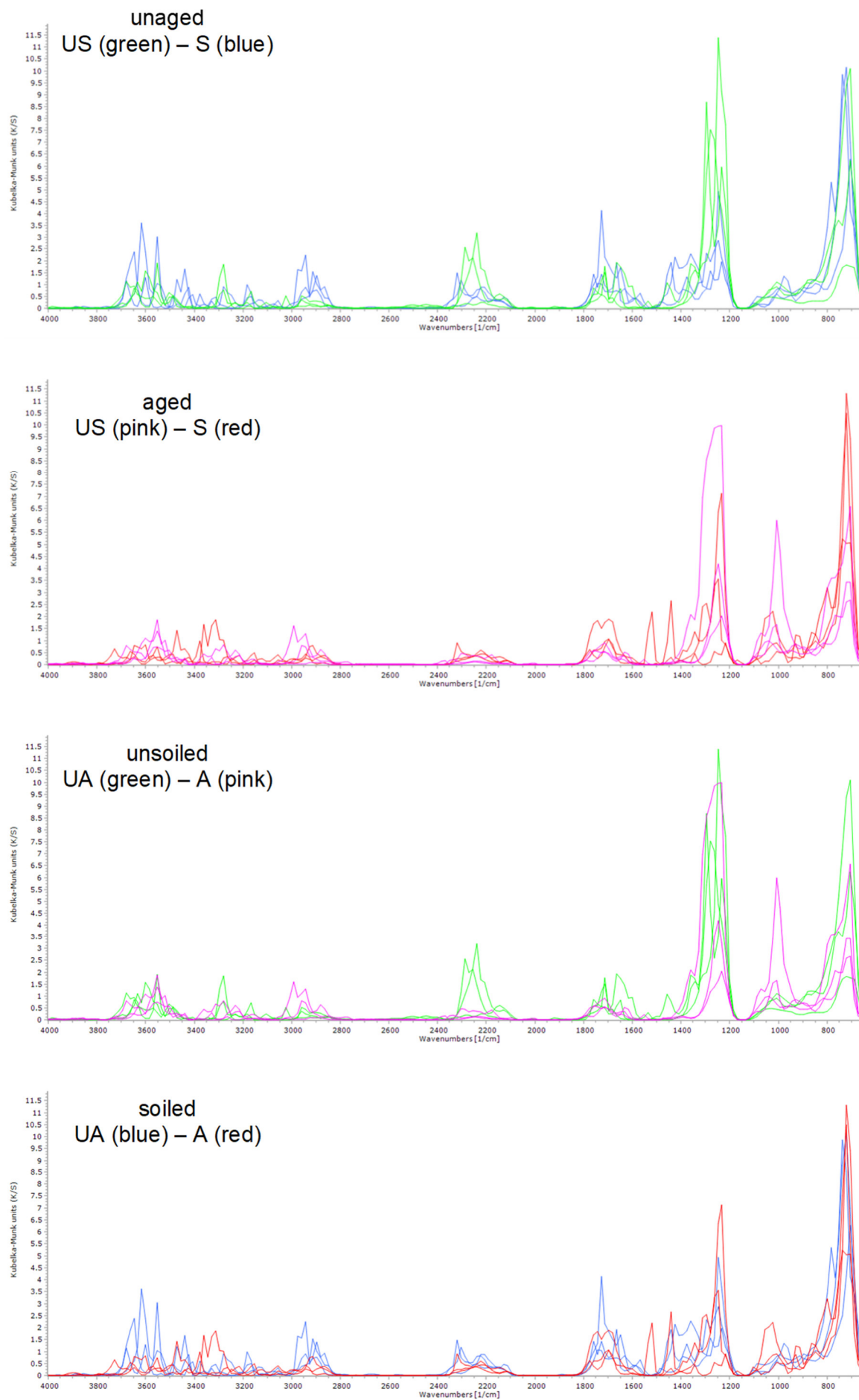


Figure A9.37. FT-IR spectra acquired from unsoiled (unaged P1f and aged P3f) and soiled (unaged P1c and aged P3c) areas of the plaster surface coated with boiled linseed oil (1-2) at  $t_{37}$ .

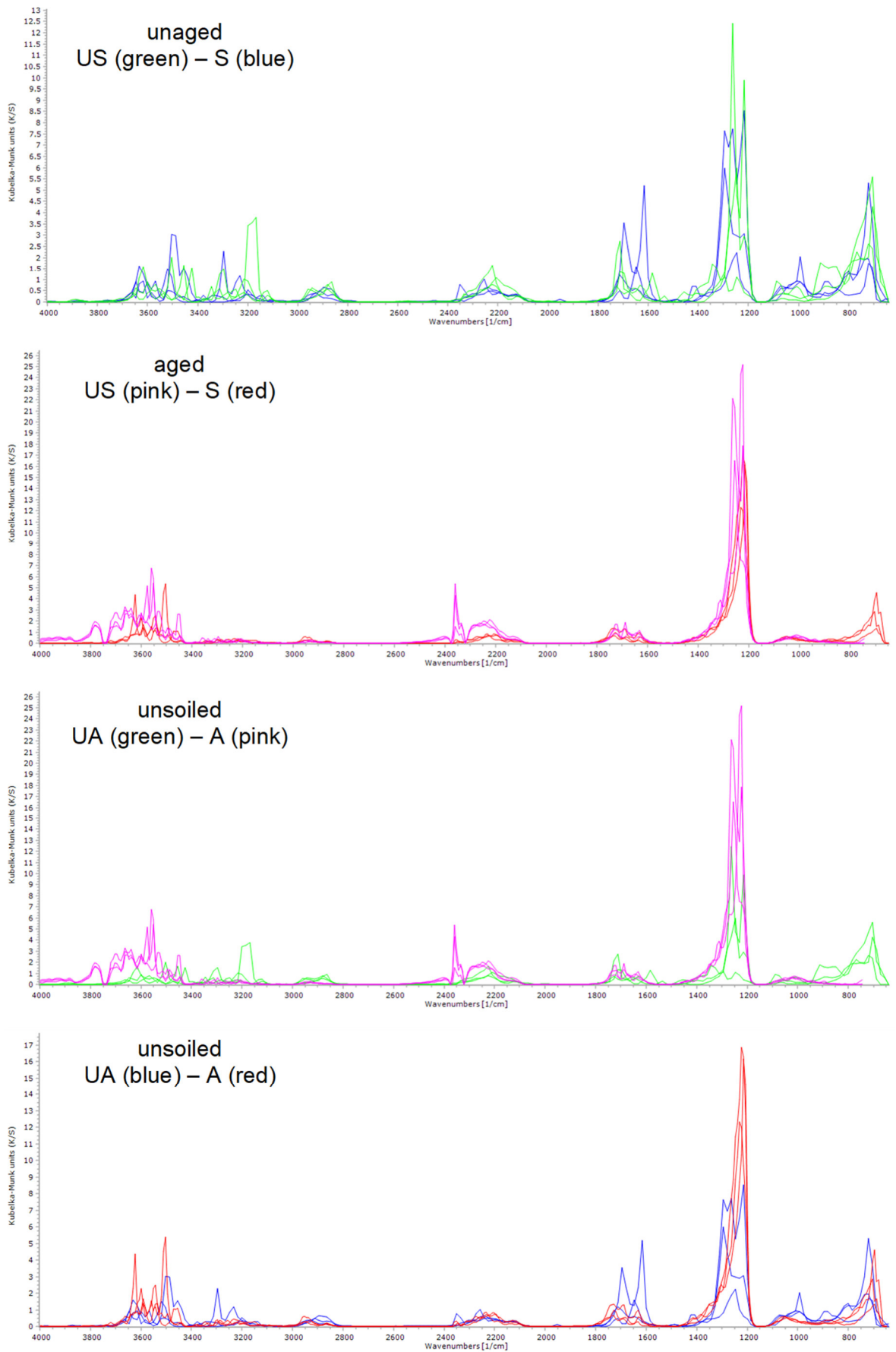


Figure A9.38. FT-IR spectra acquired from unsoiled (unaged P5e and aged P7e) and soiled (unaged P5b and aged P7b) areas of the plaster surface coated with shellac6% (2-1) at  $t_{37}$ .

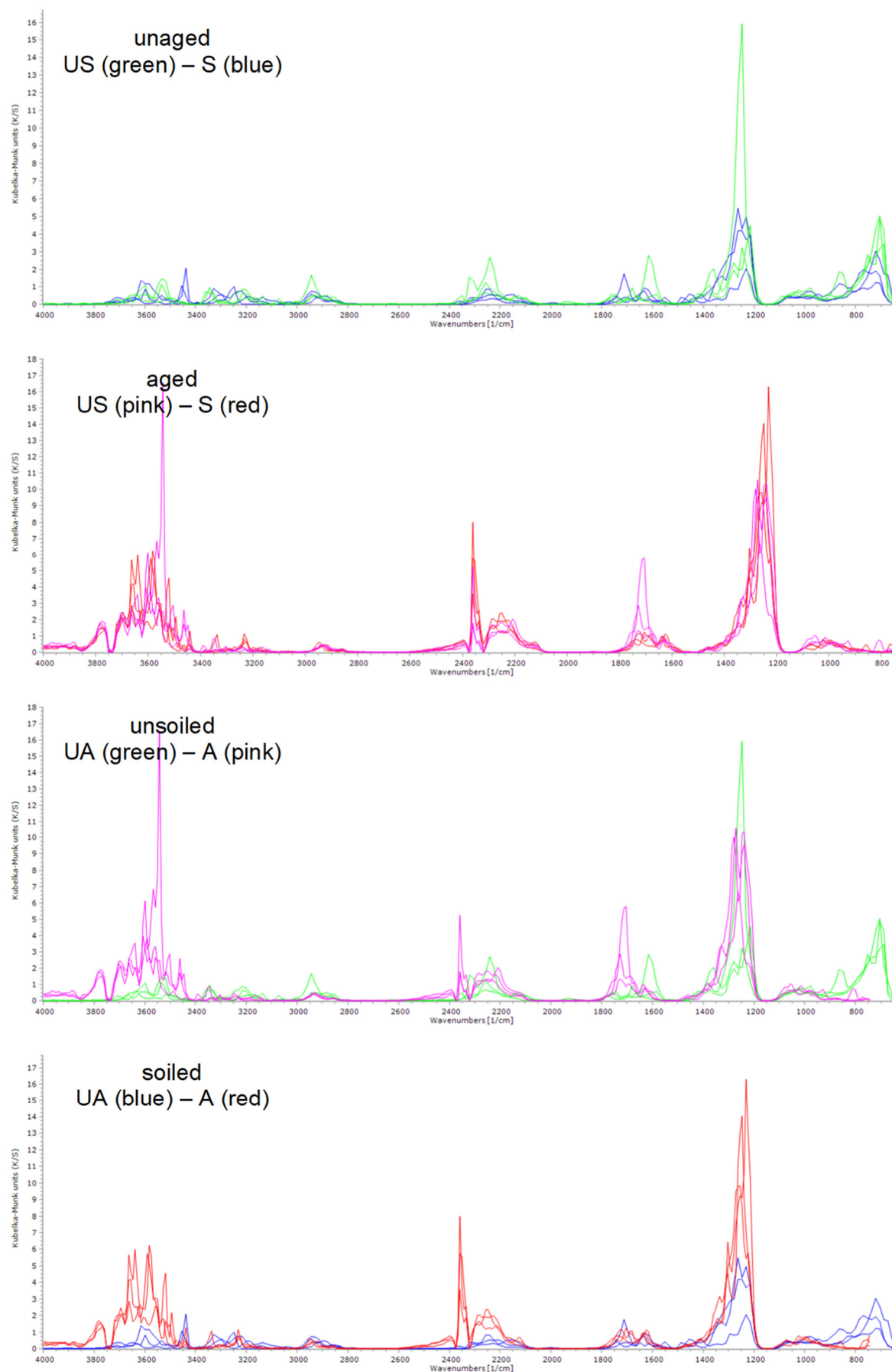


Figure A9.39. FT-IR spectra acquired from unsoiled (unaged P5f and aged P7f) and soiled (unaged P5c and aged P7c) areas of the plaster surface coated with shellac18% (2-2) at t<sub>37</sub>.

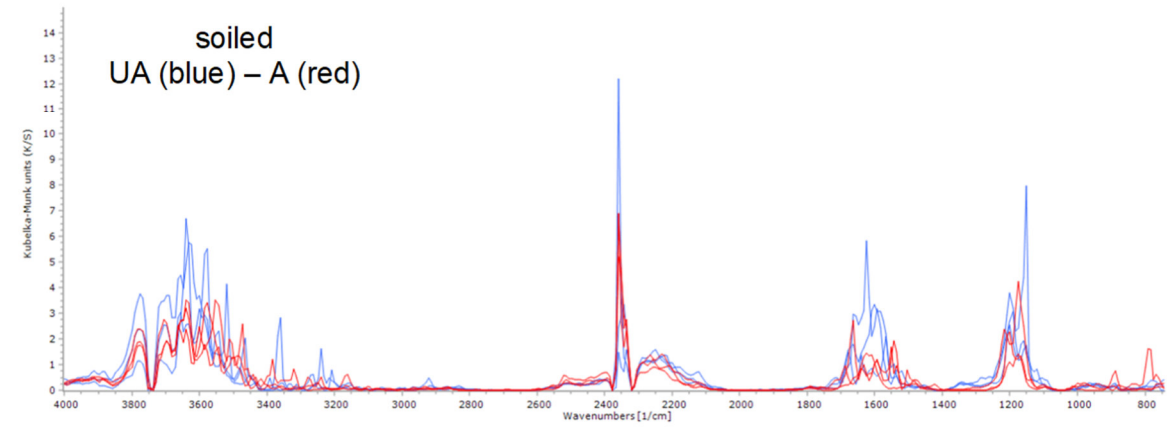
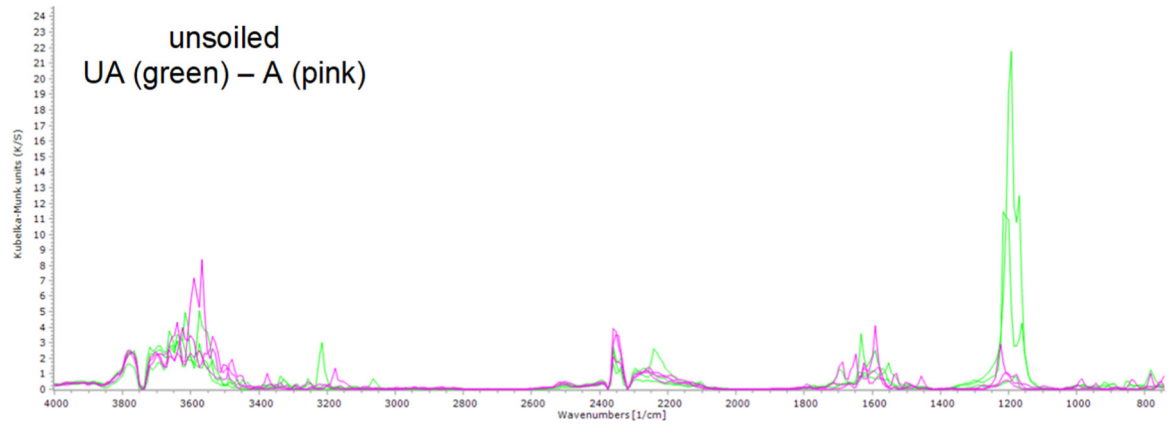
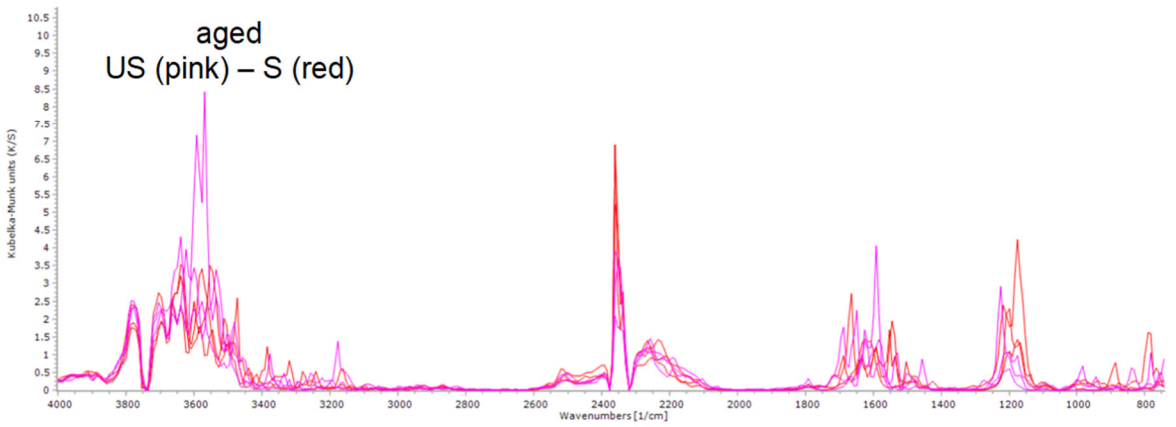
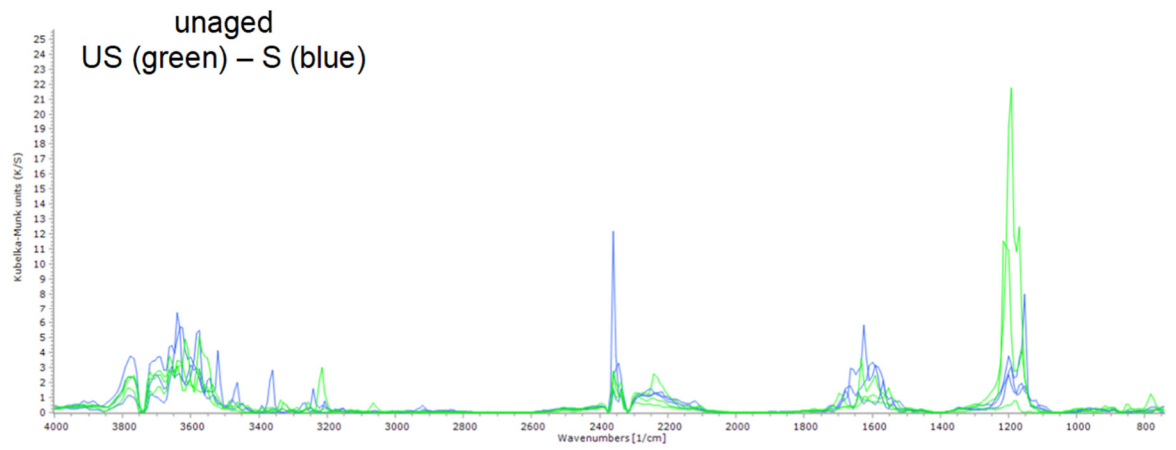


Figure A9.40. FT-IR spectra acquired from unsoiled (unaged P9e and aged P11e) and soiled (unaged P9b and aged P11b) areas of the plaster surface coated with barite<sup>20</sup> (3-1) at  $t_{37}$ .

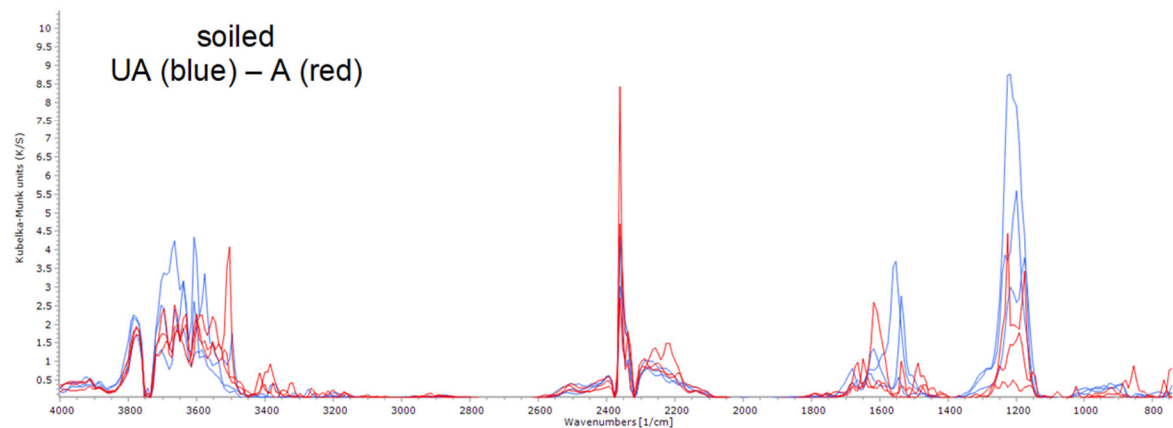
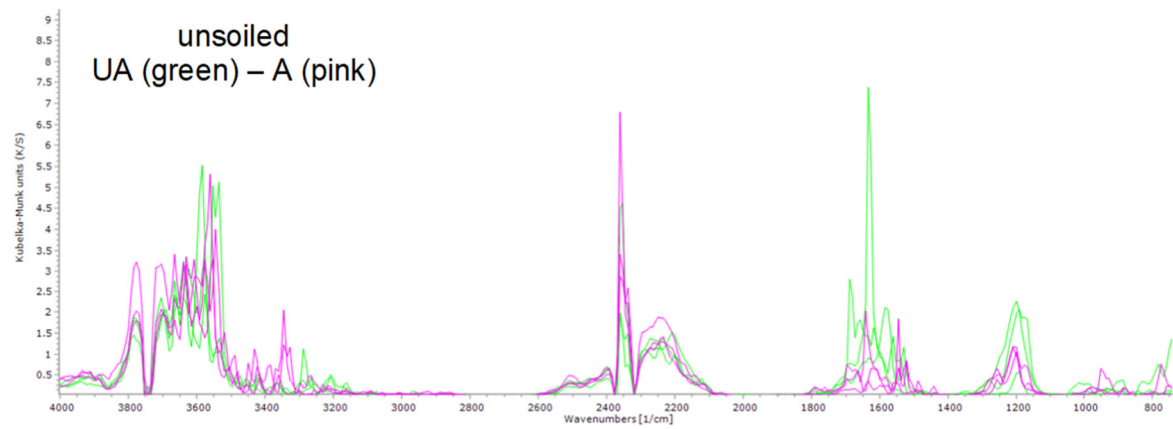
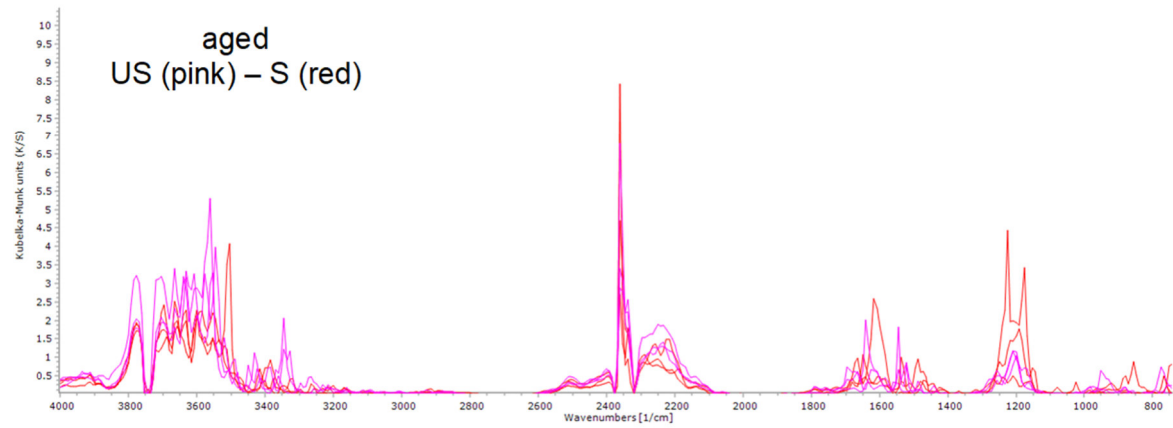
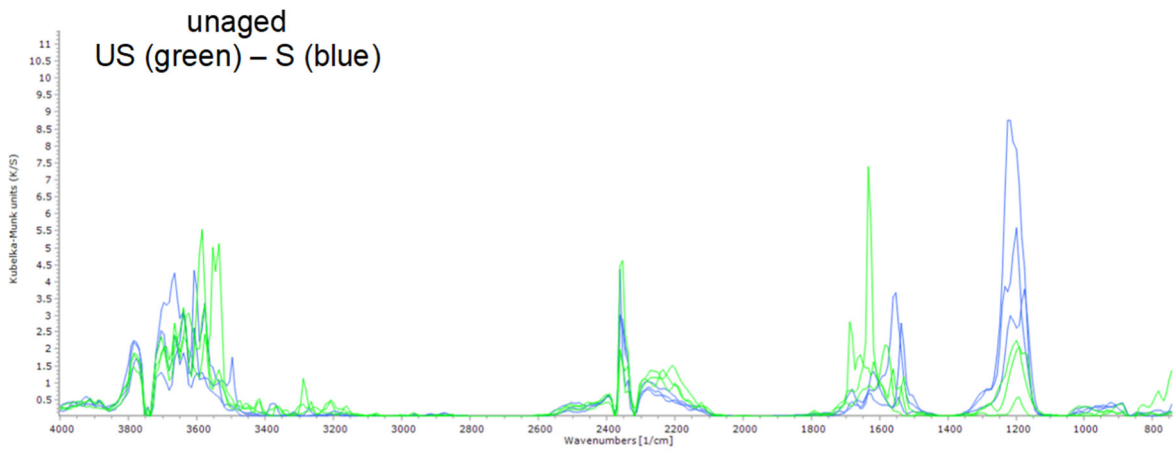


Figure A9.41. FT-IR spectra acquired from unsoiled (unaged P9f and aged P11f) and soiled (unaged P9c and aged P11c) areas of the plaster surface coated with barite60° (3-2) at  $t_{37}$ .

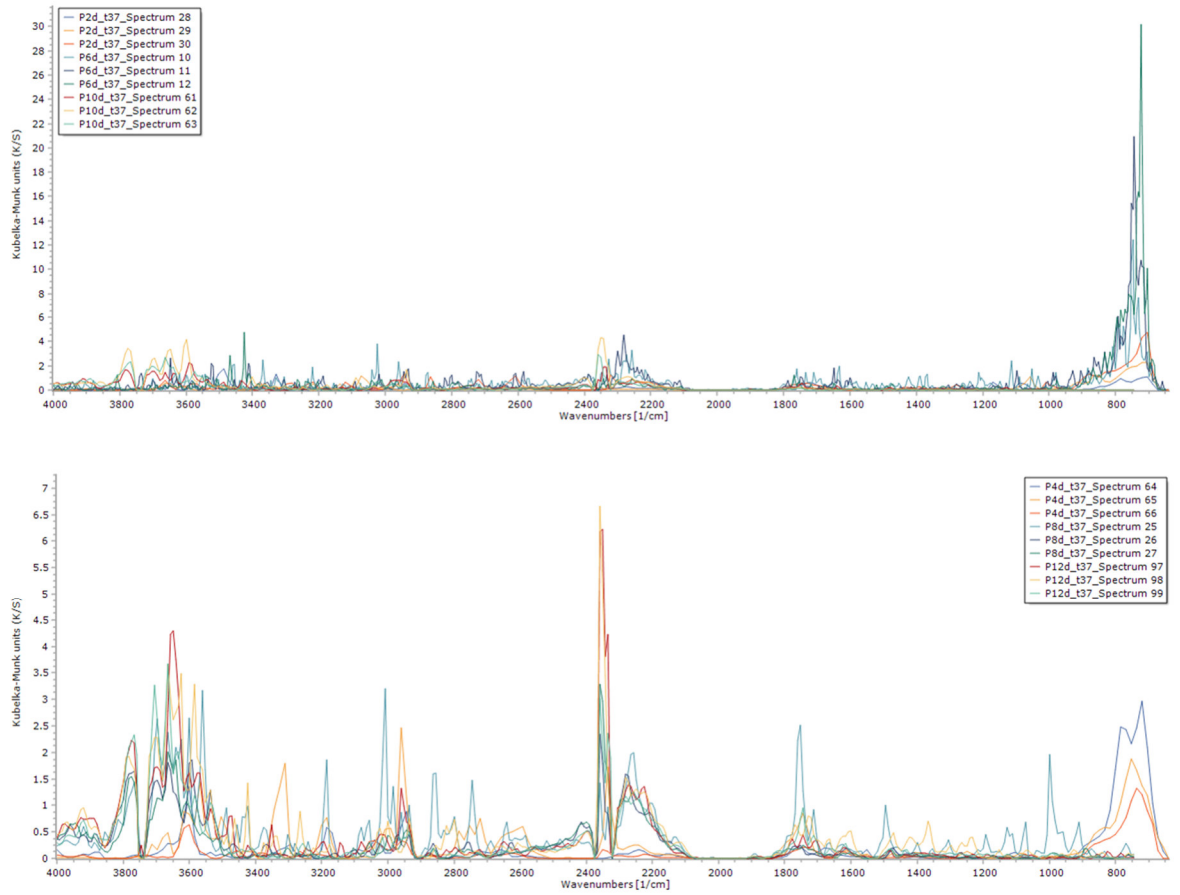


Figure A9.42. Top. FT-IR spectra acquired from the unaged, unsoiled areas (d of P2, 6 and 10) at  $t_{37}$ . Bottom. FT-IR spectra acquired from the aged, unsoiled areas (d of P4, 8 and 12) at  $t_{37}$ .

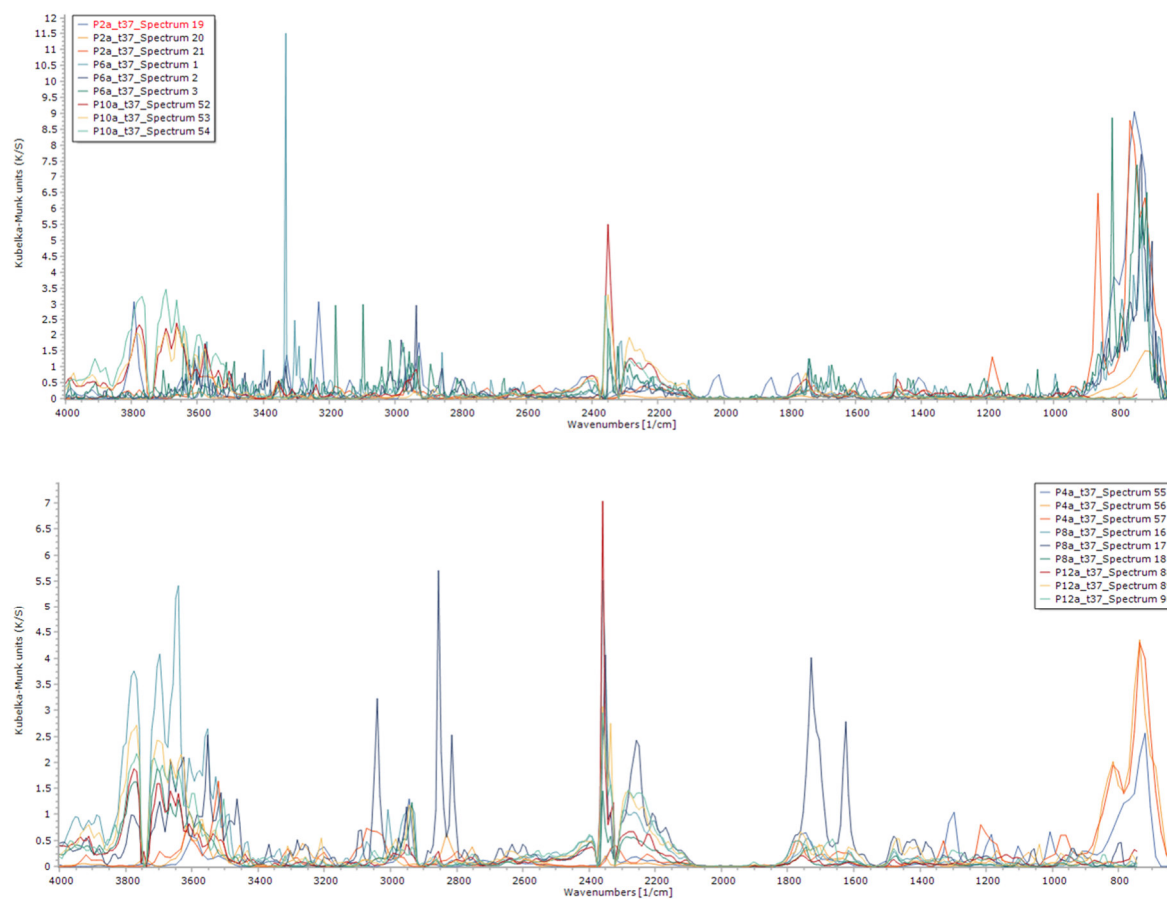


Figure A9.43. Top. FT-IR spectra acquired from the unaged, soiled areas (a of P2, 6 and 10) at  $t_{37}$ . Bottom. FT-IR spectra acquired from the aged, soiled areas (a of P4, 8 and 12) at  $t_{37}$ .

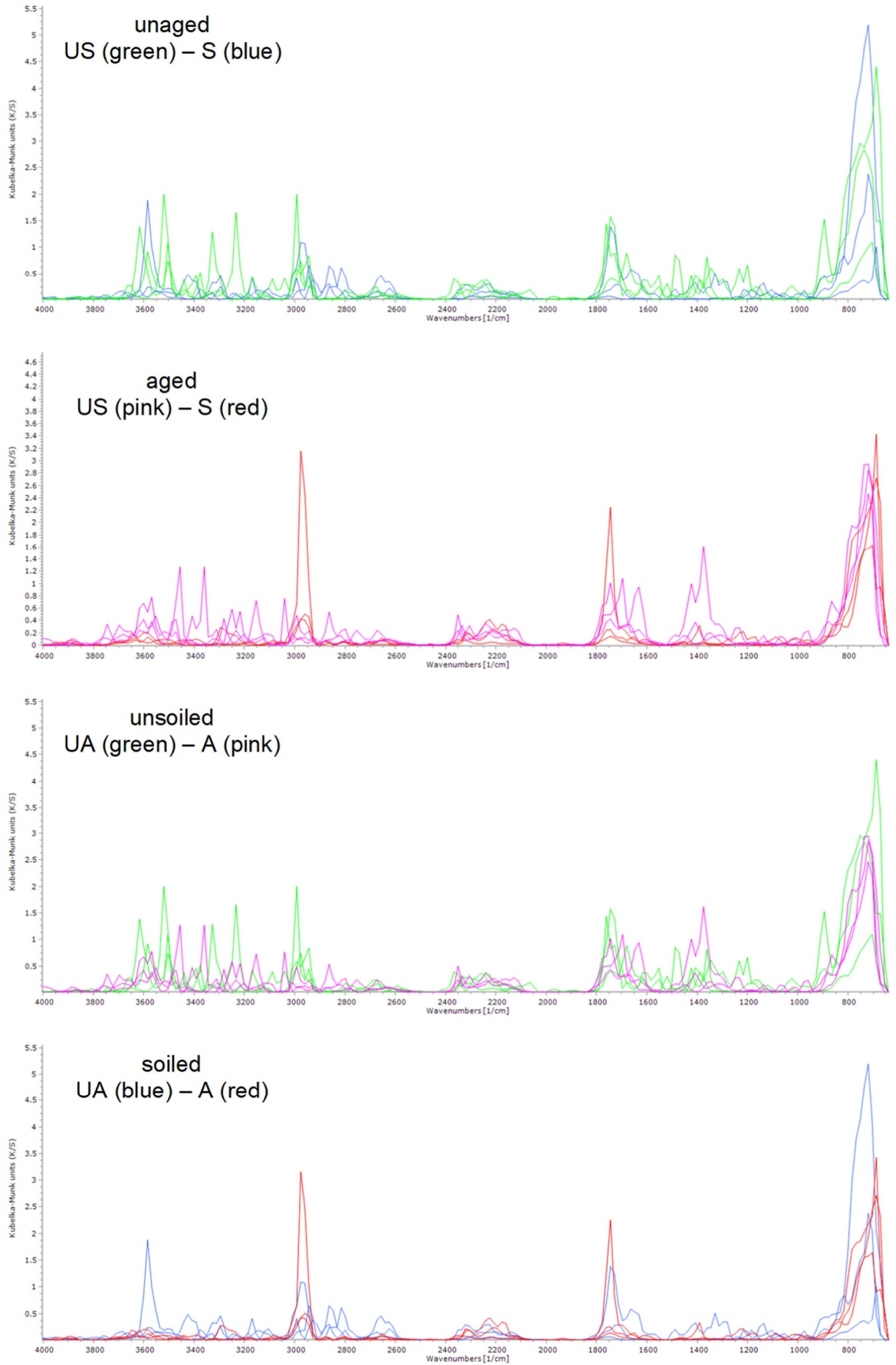


Figure A9.44. FT-IR spectra acquired from unsoiled (unaged P2e and aged P4e) and soiled (unaged P2b and aged P4b) areas of the plaster surface coated with cold-pressed linseed oil (1-1) and beeswax (4) at  $t_{37}$ .

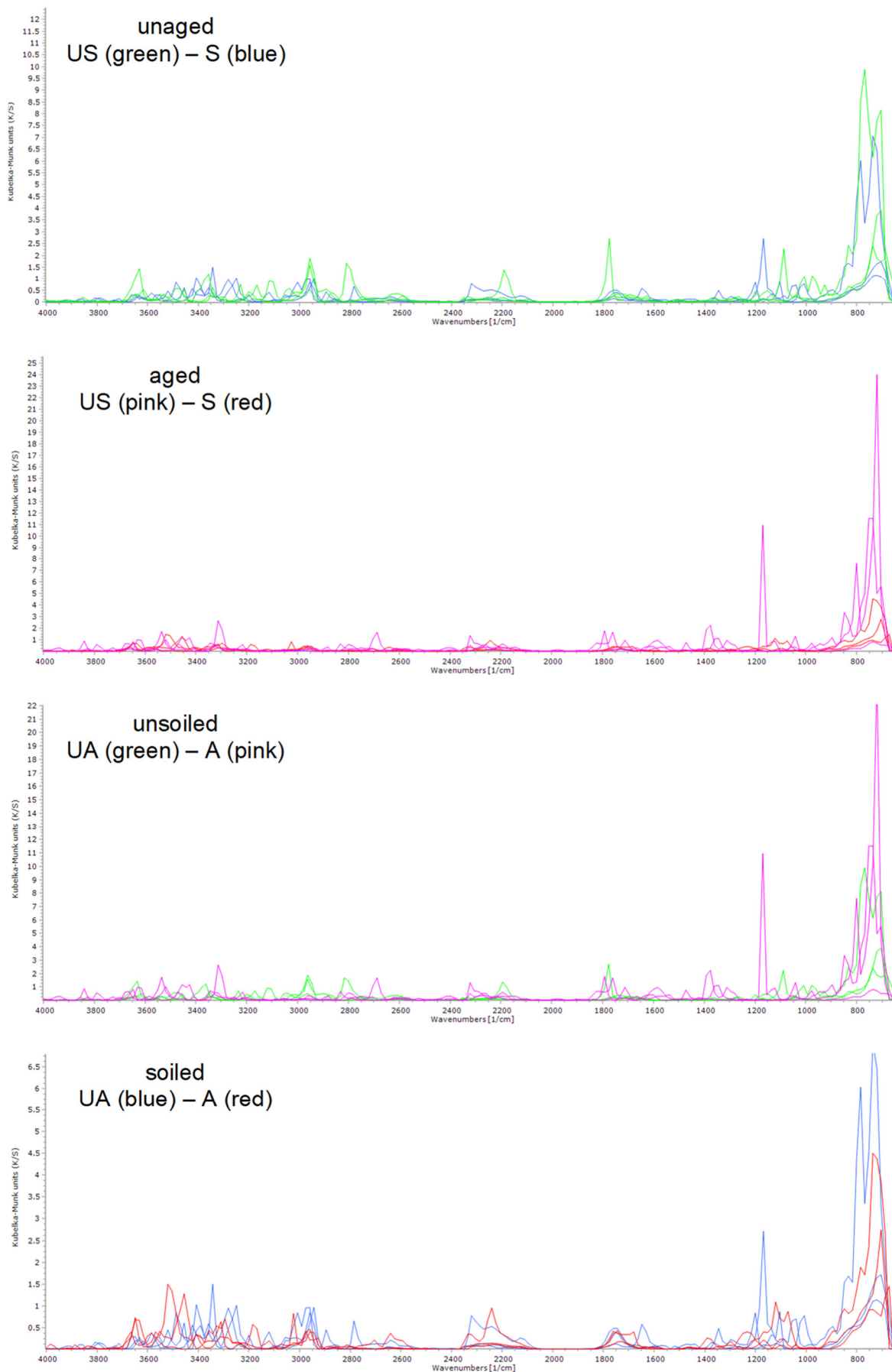


Figure A9.45. FT-IR spectra acquired from unsoiled (unaged P2f and aged P4f) and soiled (unaged P2c and aged P4c) areas of the plaster surface coated with boiled linseed oil (1-2) and beeswax (4) at  $t_{37}$ .

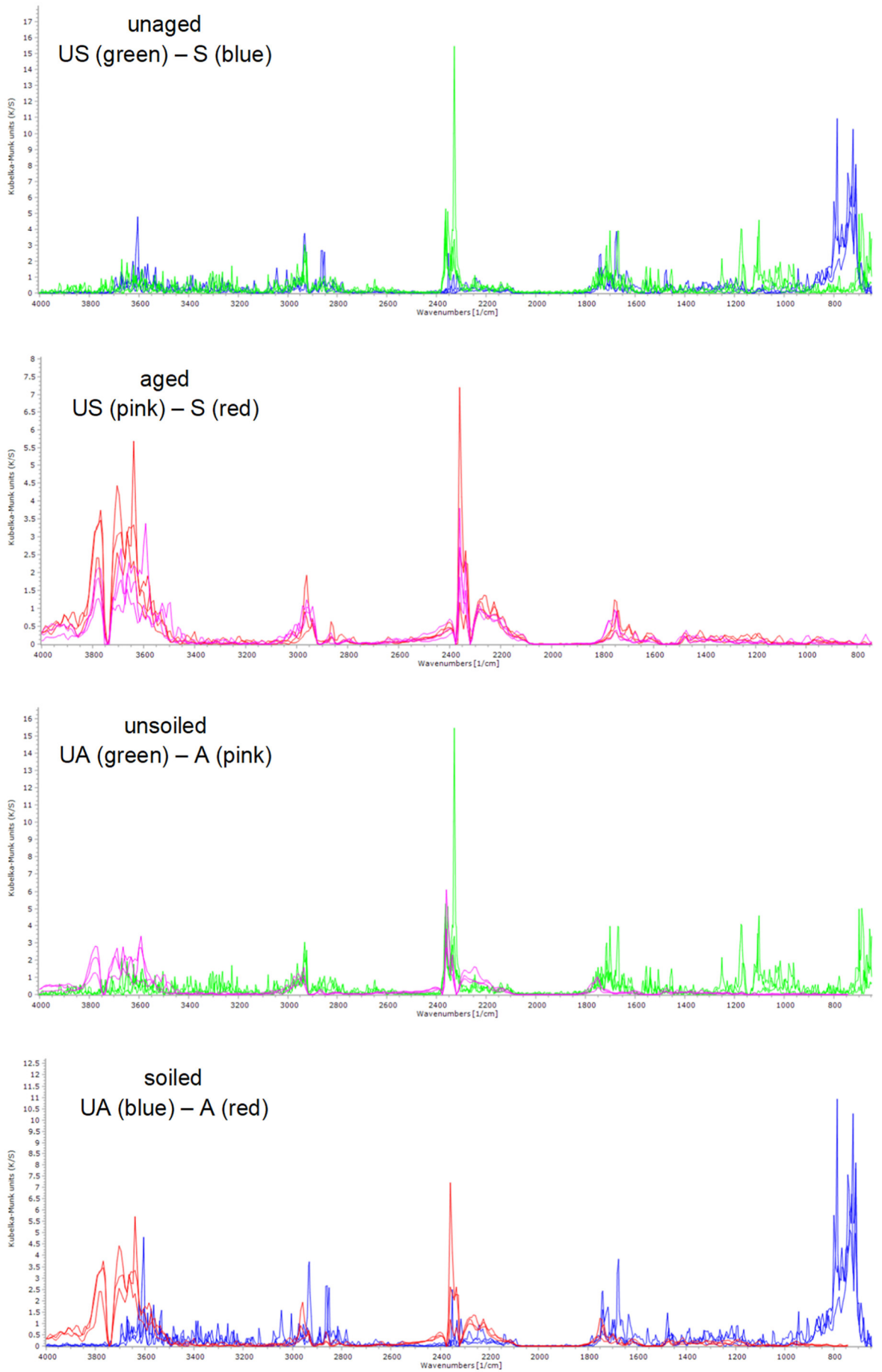


Figure A9.46. FT-IR spectra acquired from unsoiled (unaged P6e and aged P8e) and soiled (unaged P6b and aged P8b) areas of the plaster surface coated with shellac6% (2-1) and beeswax (4) at  $t_{37}$ .

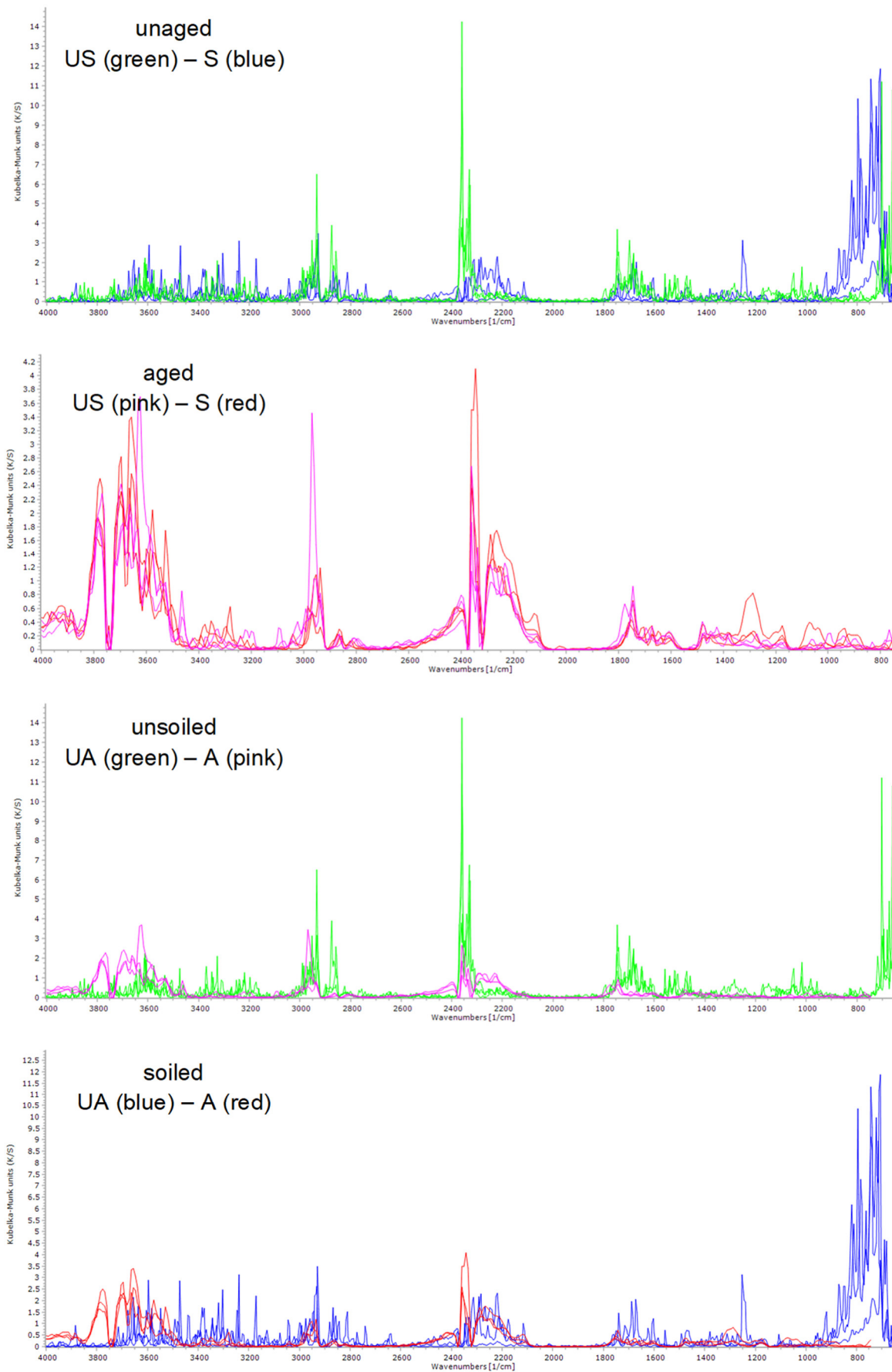


Figure A9.47. FT-IR spectra acquired from unsoiled (unaged P6f and aged P8f) and soiled (unaged P6c and aged P8c) areas of the plaster surface coated with shellac18% (2-2) and beeswax (4) at  $t_{37}$ .

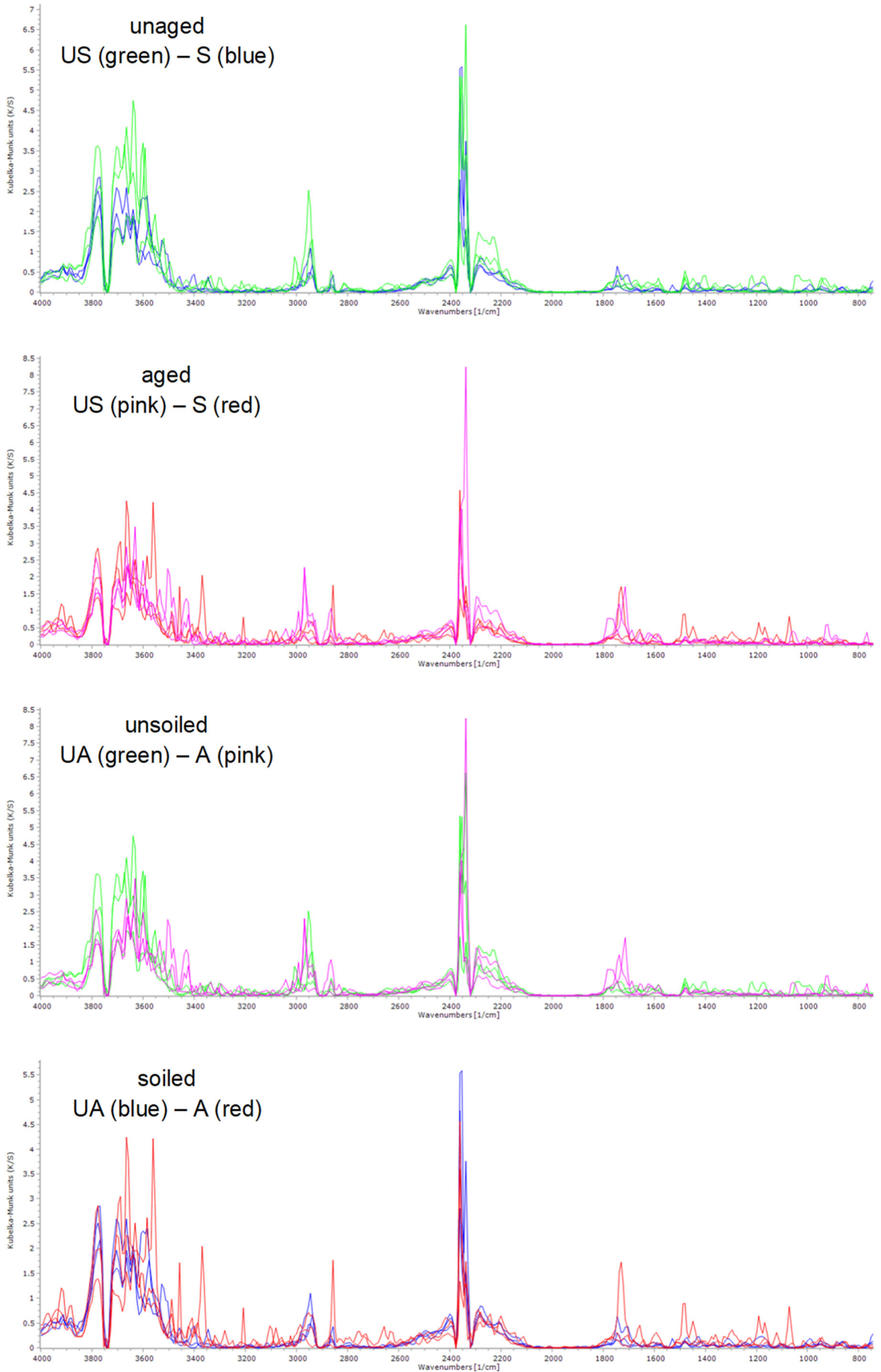


Figure A9.48. FT-IR spectra acquired from unsoiled (unaged P10e and aged P12e) and soiled (unaged P10b and aged P12b) areas of the plaster surface coated with barite20° (3-1) and beeswax (4) at  $t_{37}$ .

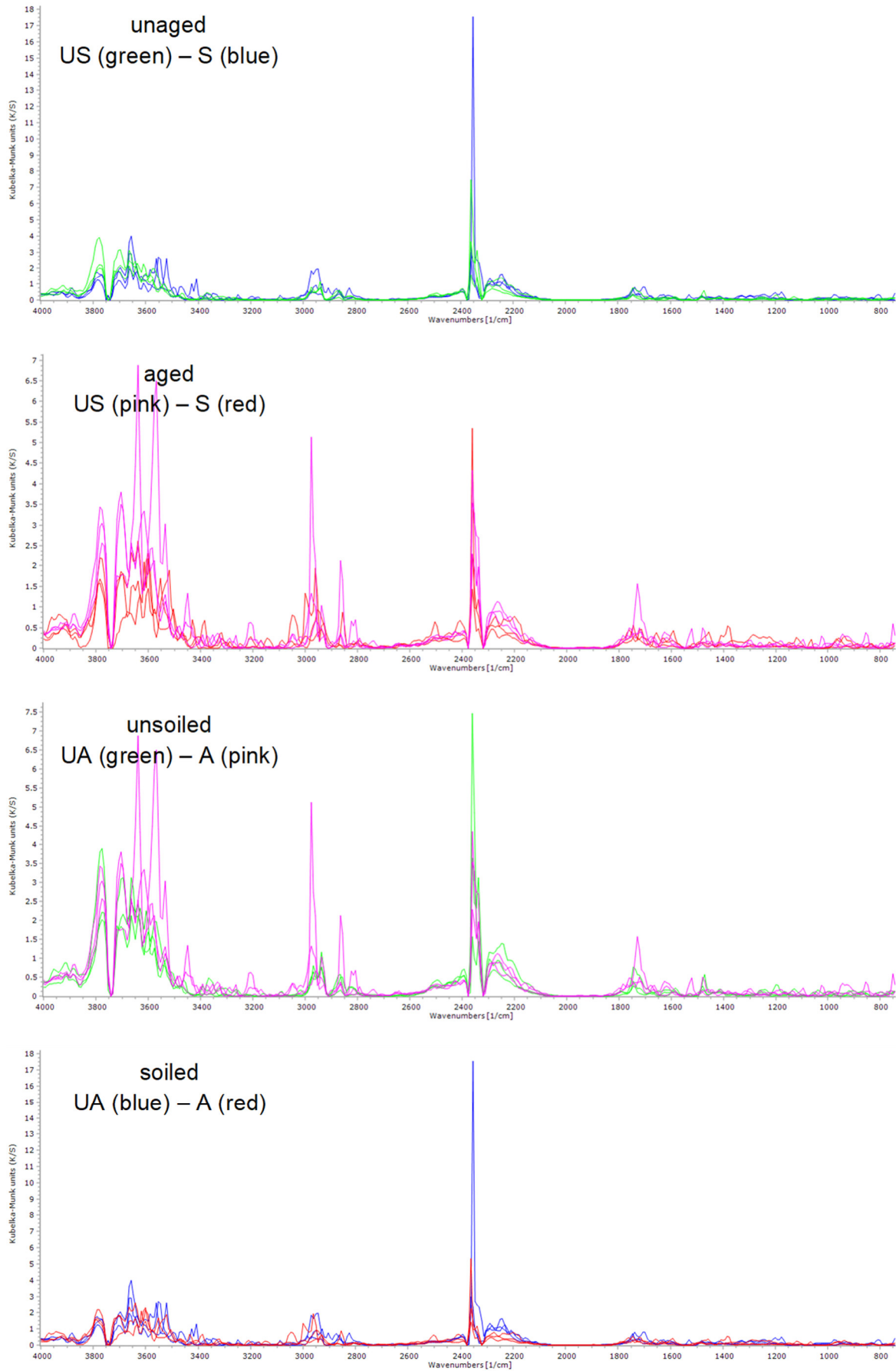


Figure A9.49. FT-IR spectra acquired from unsoiled (unaged P10f and aged P12f) and soiled (unaged P10c and aged P12c) areas of the plaster surface coated with barite<sup>60°</sup> (3-2) and beeswax (4) at  $t_{37}$ .

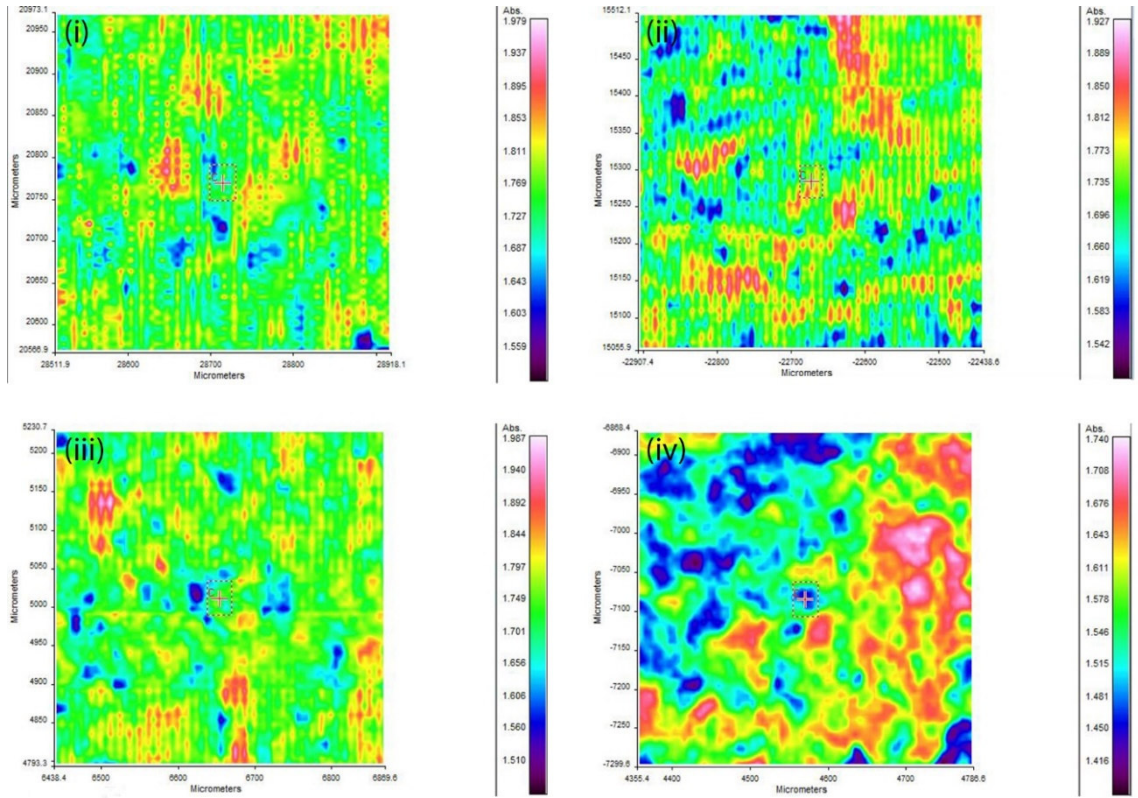


Figure A9.50. Focal Plane Array (FPA) full range absorbance images of the uncoated gypsum plaster unaged and unsoiled (P1d) (i), aged and unsoiled (P3d) (ii), aged and soiled (P3a) (iii) and aged and cleaned (P3a, AC) (iv). Although differences can be seen, no consistent observations can be made.

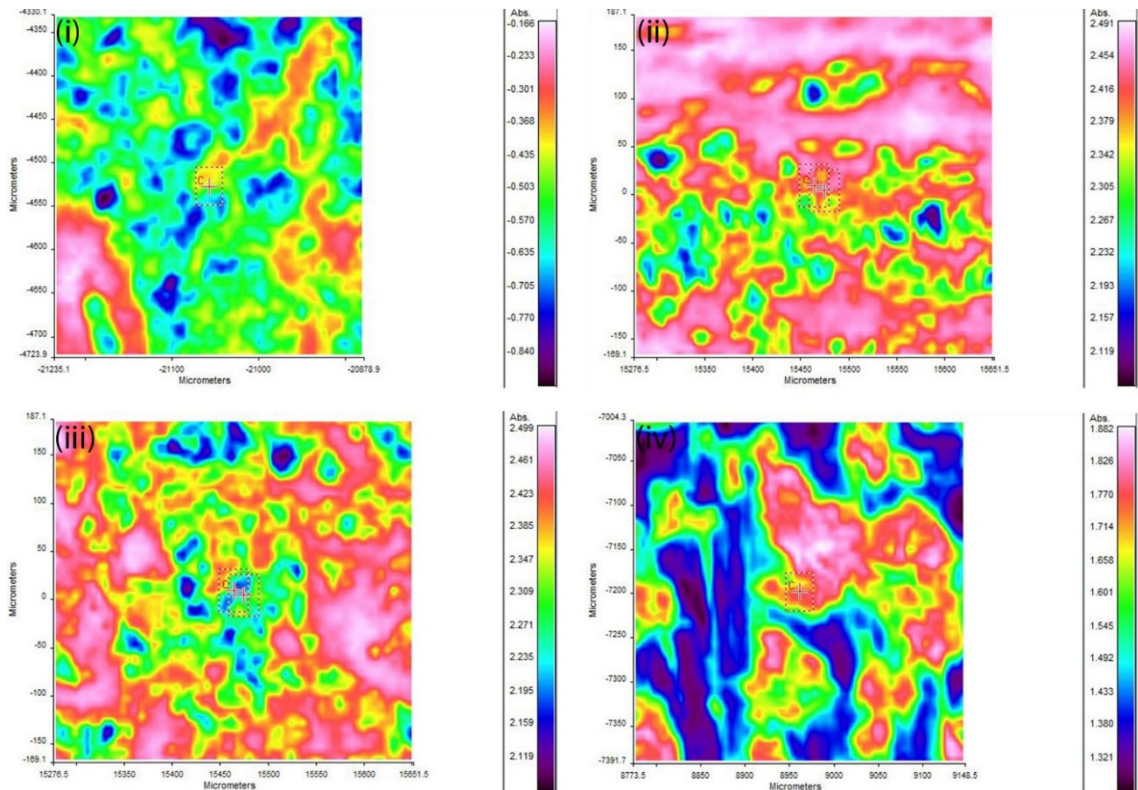


Figure A9.51. Focal Plane Array (FPA) full range absorbance images of the gypsum plaster coated with shellac18% and beeswax unaged and unsoiled (P6f) (i), aged and unsoiled (P8f) (ii), aged and soiled (P8c) (iii) and aged and cleaned (P8c, AC) (iv). Although differences can be seen, no consistent observations can be made.

